

# **Deutsche Gesellschaft für Experimentelle und Klinische Pharmakologie und Toxikologie e.V.**

## **Abstracts**

of the 80<sup>th</sup> Annual Meeting  
April 1 – 3, 2014 Hannover, Germany

This supplement was not sponsored by outside commercial interests.  
It was funded entirely by the publisher.



001

### Re-evaluation of the clinical data on *Eleutherococcus senticosus*, radix, with respect to its safety in hypertensive patients

Schmidt, Mathias<sup>1</sup>; Kelber, Olat<sup>2</sup>; Abdel-Aziz, Heba<sup>2</sup>; Kraft, Karin<sup>3</sup>

<sup>1</sup>Herbsearch Germany, Mattsies, Germany

<sup>2</sup>Steigerwald Arzneimittelwerk GmbH, Scientific Department, Darmstadt, Germany

<sup>3</sup>Chair of Natural Medicine, University of Rostock, Germany

*Eleutherococcus senticosus* radix is indicated for symptoms of asthenia such as fatigue and weakness, an indication common especially in elderly patients. However, most reviews and monographs including the HPMC monograph [1] state the contraindication „arterial hypertension“. This excludes many elderly patients from therapy with *Eleutherococcus*, as the prevalence of arterial hypertension in this age group is high. We therefore reviewed all available data on the use of *Eleutherococcus* by hypertensive patients in order to evaluate whether the gain of safety created by the contraindication would outweigh the exclusion of a large proportion of patients potentially benefiting from the use of *Eleutherococcus*.

A systematic database search was conducted in Embase and Medline. Key words were ((*Eleutherococcus*) or (*Acanthopanax*) or (*Eleutherococci*) or (Siberian ginseng)). The results were further narrowed down by hand-searching.

A large number of clinical and preclinical studies as well as reviews and monographs was identified and evaluated systematically. It was found that all sources directly or indirectly refer to only two Russian publications presented in a review from 1985 [2]. Mikunis et al. (1966) published a trial on 55 patients with rheumatic heart disease treated with *Eleutherococcus* [3]. They report an increase in blood pressure in two of them. However, in consideration of the disease treated, this is not necessarily an adverse effect caused by *Eleutherococcus*. The observation of hypertension also contradicts findings reported in a review on various clinical observations [2], and the results of a double-blind clinical trial in which hypertension was defined as an indication [4]. Dalinger (1966) even recommended the use of *Eleutherococcus* for patients with blood pressure values below 180/90 mm Hg, based on the results of his small study [5]. He mentioned no adverse effects. Later citations of these two studies [3, 5] tended to mix up their results, frequently indicating secured adverse effects in hypertensive patients. They are neither in accordance with the original data, nor are they supported by other published data, which rather point to potential antihypertensive effects.

The contraindication „arterial hypertension“ is not evidence-based and should be carefully re-evaluated for not unnecessarily excluding a large patient group from the benefits of *Eleutherococcus*.

1. HPMC (2008) Monograph. EMEA/HPMC/244569/2006; 2. Farnsworth NR et al. (1985) Economic and Medicinal Plant Research. Wagner H et al. (Ed.), London, Academic Press 1: 155.; 3. Mikunis RI et al. (1966) Lek Sredstva Dal'nego Vostoka 7: 221; 4. Cicero AF et al. (2004) Arch. Gerontol Geriatr Suppl 9: 69; 5. Dalinger OI (1966) Stimulatory tsentral'noi nervnoy sistemi. Tomsk Univ: 112

002

### Velocity of the release of free cyanide from foods containing high levels of cyanogenic glycosides after tissue destruction as important factor determining their toxicity

Schneider, Lidia; Buhrke, Thorsten; Lampen, Alfonso; Abraham, Klaus

Bundesinstitut für Risikobewertung, Lebensmittelsicherheit, Berlin, Germany

**Background:** The acute toxicity of cyanide after its enzymatic release from cyanogenic glycosides in plants eaten as food (e.g. bitter almonds) is well-known and triggered by the peak level of cyanide in the body. In this regard, not only the content of bound cyanide in foods is relevant, but also the velocity of the release after chewing of the food and the following surge of free cyanide in the body. This was demonstrated in a human study regarding the bioavailability of cyanide after consumption of 100 g persipan, 30.9 g linseed and 6 bitter apricot kernels (dose of bound cyanide: 6.8 mg), showing mean peak cyanide levels in blood of 1.3 µM ( $t_{max}$  105 min), 5.7 µM ( $t_{max}$  40 min), and 14.3 µM ( $t_{max}$  20 min), respectively (Abraham et al., Naunyn-Schmiedeberg's Arch Pharmacol 2013, 386 Suppl 1: S3). Additional in-vitro investigations were performed to confirm the velocity of the enzymatic release (by plant β-glucosidase) of free cyanide after tissue destruction as important factor determining the toxicity of cyanogenic foods.

**Methods:** Food samples containing 1 mg of cyanide equivalent were homogenized using mortar and pestle, and were suspended in 100 ml PBS buffer. The suspension was gently stirred at room temperature, and the release of free cyanide was determined in samples taken from the suspension at different times using a GC/MS method with  $K^{13}C^{15}N$  as internal standard.

**Results:** Release of cyanide was much slower in case of linseed compared to bitter apricot kernels. Mean proportion (n=4-5) of the total amount released within 10 min after tissue destruction was 2.3 % and 23.7 %, respectively.

**Conclusion:** Toxicity of cyanogenic foods is determined not only by its content of bound cyanide, but also by the velocity of the release of free cyanide after tissue destruction by chewing. The effectiveness of this process depends on the two plant-specific partners of the chemical reaction, the cyanogenic glycoside and the β-glucosidase (specificity? content?), and can be investigated using the in-vitro method described. From current knowledge, only bitter fruit kernels and (unprocessed) cassava have high contents of bound cyanide as well as effective β-glucosidase activity to cause severe toxicity in humans after consumption of a typical amount of these foods. The hazard of other foods also containing high levels of cyanogenic glycosides (e.g. linseed) may be overestimated if risk assessment is based on the equivalent content of cyanide only.

003

### SLC10A5 is involved in the intracellular conjugation of bile acids in the liver

Aretz, Julia Silke<sup>1</sup>; Herebian, Diran<sup>2</sup>; Geyer, Joachim<sup>1</sup>

<sup>1</sup>Institut für Pharmakologie und Toxikologie, Justus-Liebig-Universität Gießen, Germany

<sup>2</sup>Klinik für Allgemeine Pädiatrie, Neonatologie und Kinderkardiologie, Universitätsklinikum Düsseldorf, Germany

The Solute Carrier Family SLC10, also known as the sodium-bile acid co-transporter family, includes the well-characterized transport proteins NTCP (Na<sup>+</sup>/Taurocholate Cotransporting Polypeptide, SLC10A1), ASBT (Apical Sodium-dependent Bile acid Transporter, SLC10A2), and SOAT (Sodium-dependent Organic Anion Transporter, SLC10A6), and four orphan carriers, SLC10A3-SLC10A5 as well as SLC10A7. One of these, SLC10A5, is regarded as potential bile acid transporter due to its high expression level in liver, kidney and gastrointestinal tract and its close sequence similarity to NTCP and ASBT. In contrast to them, SLC10A5 does not localize to the cell membrane in several transfected cell lines, but shows an intracellular vesicular expression pattern. Extensive in vitro transport studies with different <sup>3</sup>H-labelled bile acids in stably SLC10A5-transfected HEK293 cells failed to show bile acid transport function for SLC10A5. Therefore, we established a knockout mouse model for phenotypic analysis. The B6.S5-Slc10a5<sup>tm1.1lox</sup> mouse (Slc10a5 ko mouse) is a constitutive knockout that lacks the whole coding sequence of the Slc10a5 gene. Under standard housing conditions no phenotype deviation occurred between the Slc10a5 ko and wild-type (wt) mice. However, 1 week feeding of 0.5 % cholic acid revealed significant differences between both strains. In these experiments, bile composition and plasma levels were examined by UPLC-MS/MS. Under control diet no differences in total quantity, bile acid composition and amount of cholesterol and phospholipids were found in bile of Slc10a5 ko and wt mice. Cholic acid feeding increased the total quantity of bile, the bile acid concentration and the amount of cholesterol and phospholipids in both genotypes. But Slc10a5 ko mice excreted 20-fold more unconjugated bile acids into bile than the wt control group, though the overall bile acid concentration of the bile was identical between both strains, pointing to limited bile acid conjugation or transport under cholic acid feeding. In order to analyze, if this effect was due to dysregulation of any bile acid transporter or enzymes involved in bile acid biosynthesis and conjugation, we performed a whole genome expression analysis of liver mRNA, but found no significant differences between the Slc10a5 ko mice and the wt mice. In conclusion: Slc10a5 seems to be involved in the mechanism of intracellular bile acid transport and conjugation, but its molecular transport function needs further elucidation.

004

### TRPM7 proteins contribute to preimplantation embryo development in mice

Bach, Aline<sup>1</sup>; Weißgerber, Petra<sup>2</sup>; Cavalié, Adolfo<sup>2</sup>; Buchholz, Stefanie<sup>2</sup>; Matka, Christin<sup>1</sup>; Flockerzi, Veit<sup>2</sup>; Freichel, Marc<sup>1</sup>

<sup>1</sup>Universität Heidelberg, Pharmakologisches Institut, Germany

<sup>2</sup>Universität des Saarlandes, Experimentelle und Klinische Pharmakologie und Toxikologie, Homburg, Germany

The transient receptor potential-melastatin-like 7 gene (*Trpm7*) encodes a bifunctional channel-kinase that is known to be essential for cellular survival in avian lymphocytes. The channel is permeable for divalent cations including Ca<sup>2+</sup> and Mg<sup>2+</sup>. TRPM7 is ubiquitously expressed in humans and we identified *Trpm7* transcripts in various murine cell types including embryonic stem cells using Northern blot analysis. Mice homozygous for a *Trpm7* null allele generated by insertion of β-geo cassette into the first intron of *Trpm7* die before E7.5 (ref. 1). We observed that removal of exon 2 resulting in a frameshift mutation causes that embryos at embryonic day 3.5 (E3.5) are strongly degenerated with the blastomeres being detached from the zona pellucida (ref. 2). Thus, we systematically investigate key processes of embryonic development before implantation including compaction, tight junction formation and maintenance, intracellular polarization of blastomeres and the formation of the trophectoderm lineage (ref. 3). Compaction was demonstrated in *Trpm7*-deficient embryos by staining for zonula occludens-1 between E2.5 and E3.0 to identify tight junction formation. Interestingly, tight junctions are still detectable until E3.5 when a fluid filled cavity usually forms. Concomitant with the increase in cell adhesion and tight junction formation all cells rapidly polarize along the axis perpendicular to cell contact leading to formation of distinct apical and basolateral domains that can be distinguished by detection of PKCζ and E-Cadherin, respectively. No difference was observed in the apical arrangement of PKCζ or the basolateral arrangement of E-Cadherin in *Trpm7*-deficient embryos. Furthermore there is no mislocalization or disruption of the microtubule network or f-actin. We conclude that TRPM7-deficient embryos undergo compaction, build tight junctions and reach blastomere polarity via an intact cytoskeleton suggesting that loss of TRPM7 evokes defective development thereafter, e.g. during specification of distinct cell lineages which is currently analysed by staining cells of the trophoctoderm and the inner cell mass. Alternatively TRPM7 inactivation may affect processes that determine cavity formation.

1. Jin J. et al., Science 322: 756-60 (2008)

2. Weissgerber P., et al. Naunyn-Schmiedeberg's Arch Pharmacol 377, Suppl. 1: 35 (2008)

3. Cockburn & Rossant, J. Clin. Invest. 120: 995-1003 (2010)

## 005

**Characterization of the focal kainate model in mice as a model for difficult-to-treat seizures****Bankstahl, Marion;** Klein, Sabine; Löscher, Wolfgang

Tierärztliche Hochschule Hannover, Institut für Pharmakologie, Toxikologie und Pharmazie, Germany

**Rationale:**

Despite introduction of numerous third-generation antiepileptic drugs (AEDs) in recent decades, seizure control by medication still fails in about 30% of epilepsy patients. Including animal models with a high frequency of difficult-to-treat seizures in the AED development process might facilitate the identification of new drug candidates not affected by mechanisms of pharmacoresistance, like overexpression of P-glycoprotein (Pgp). Aim of the present study was to evaluate the focal kainate model in mice as a model for pharmacoresistant epilepsy.

**Methods:**

Female FVB/N-wild type and Pgp-knockout (*mdr1a/b*<sup>-/-</sup>) mice were injected with kainic acid into the right dorsal hippocampus to initiate a non-convulsive status epilepticus, which led to the occurrence of spontaneous recurrent seizures. Chronic epileptic mice (n=6-14 per drug and dose) were treated with vehicle and clinically effective doses of diazepam (2 and 5 mg/kg), phenobarbital (25 and 50 mg/kg), phenytoin (20 mg/kg), carbamazepine (20 and 40 mg/kg), levetiracetam (400 and 800 mg/kg), and valproate (300 mg/kg). Seizures frequency was assessed by continuous EEG-/video-monitoring before and after injections and visual analysis of the EEG. According to individual treatment effects, mice were categorized as responders or nonresponders. Responders were defined by peak reduction of seizures by 75% compared to predrug (basal) seizure frequency.

**Results:**

Basal seizure frequency of individual mice ranged from 20 to 300 seizures per hour. Significant anticonvulsant group effects in wild-type mice were only found with 5 mg/kg diazepam. No differences in anticonvulsant drug action were observed between wild-type and *mdr1a/b*<sup>-/-</sup> mice except for 2 mg/kg diazepam and 50 mg/kg phenobarbital. Responders occurred after every drug treatment except for 20 and 40 mg/kg carbamazepine. The amount of responders was comparable between wild-type and *mdr1a/b*<sup>-/-</sup> mice.

**Conclusion:**

The focal kainate mouse model is characterized by seizures pharmacoresistant to a broad range of AEDs. However, Pgp has no major impact on AED response in this model. Further studies have to reveal whether the focal kainate model might be suitable for identification of drug candidates targeting new anticonvulsant mechanisms.

## 006

**TRPC channels are involved in glial Ca<sup>2+</sup> signaling and migration****Belkacemi, Thabet;** Philipp, Stefan E.; Weißgerber, Petra; Flockerzi, Veit; Beck, Andreas

Universität des Saarlandes, Institut für Pharmakologie und Toxikologie, Universitätsklinikum, Homburg, Germany

After an acute brain injury a severe astrogliosis, i.e. increased proliferation and migration of astrocytes, occurs in the injured brain region. Proliferation and migration are triggered by cytosolic Ca<sup>2+</sup> signals, due to intracellular Ca<sup>2+</sup> release and/or Ca<sup>2+</sup> influx. Canonical transient receptor potential channels (TRPCs) and TRPA1 channels are non-selective Ca<sup>2+</sup> permeable ion channels, and suggested to be expressed in astrocytes. They might be involved in the glial Ca<sup>2+</sup> signaling and thereby in migration and proliferation.

Using a fluorescence-labeled antibody against the astrocyte-specific surface marker glutamate aspartate transporter (GLAST), we sorted mouse cortical astrocytes, derived from 1-3 days old pups and cultured for two weeks, by fluorescence-activated cell sorting (FACS). From 5 independent cell preparations RNA was prepared to perform RT-PCR for TRPC transcripts. Consistently, TRPC1-, TRPC2-, TRPC3- and TRPC4 cDNA fragments were amplified. Next we used various agonists to induce Ca<sup>2+</sup> entry. Calcium imaging experiments, using the Ca<sup>2+</sup>-sensitive fluorescent dye Fura-2, revealed OAG-mediated Ca<sup>2+</sup> entry and intracellular Ca<sup>2+</sup> oscillations in astrocytes isolated from wild-type mice. OAG, an analogue of diacylglycerol (DAG), is known to activate TRPC2, TRPC3, TRPC6 and TRPC7. We used astrocytes from various TRPC-deficient mouse strains to delineate the TRPC channel responsible for OAG-induced Ca<sup>2+</sup> signaling. In addition we performed *in vitro* migration assays of wild-type and TRPC-deficient astrocytes, and studied glial scar formation after inducing cortical stab lesions. The results presented show that TRPC-dependent Ca<sup>2+</sup> signaling is important in astrocyte migration, and probably in astrogliosis after severe brain injury.

## 007

**Titanium(IV)-Salan Complexes: A New Tool in Tumor Therapy?**Pesch, Theresa<sup>1</sup>; Schuhwerk, Harald<sup>2,3</sup>; Debiak, Malgorzata<sup>2</sup>; Immel, Timo<sup>4</sup>; Bürkle, Alexander<sup>2</sup>; Huhn, Thomas<sup>4</sup>; **Beneke, Sascha**<sup>2</sup><sup>1</sup>Universität Zürich, vet. Pharmakologie & Toxikologie, Switzerland<sup>2</sup>Universität Konstanz, Molekulare Toxikologie, Germany<sup>3</sup>Fritz-Lipmann Institut, Genomische Stabilität, Jena, Germany<sup>4</sup>Universität Konstanz, Fachbereich Chemie, Germany

Two decades ago, titanium(IV) complexes entered clinical trials in tumor therapy. Despite promising activity in cell culture and mouse models, human therapy failed due to rapid degradation in aqueous solutions. Recently, titanium(IV) complexes gained new attention due to diminished hydrolysis of salan-derivatives. Some of these compounds showed toxicity at concentrations similar to cisplatin. We investigated now in more detail a compound called Tc52 and compared it with the structurally very similar but non-toxic Tc53. As expected, Tc52 showed loss of viability in different cell lines at similar concentrations. Deduced from the DNA damaging activity of the early titanium(IV) complexes, we speculated that Tc52 would also elicit genotoxic stress. To our surprise, we could not detect the induction of any DNA damage, although we tested for DNA breaks and crosslinks as well as for indirect markers like poly(ADP-ribose) and phosphorylation of H2AX. FACS analysis revealed that Tc52 induced apoptosis in HeLa tumor cells, but not in Vh7 normal fibroblasts. This was supported by data from western-blotting. In order to test if this effect was dependent on p53 status, we treated non-tumorigenic early-passage HEK293 cells with impaired p53 function and p53-positive U2OS tumor cells with Tc52 and monitored the impact on cell death. Similar to HeLa, tumorigenic U2OS cells underwent apoptosis, whereas HEK293 did not. A more detailed investigation revealed in Vh7 fibroblasts signs of senescence, i.e. chromatin restructuring and expression of senescence-associated  $\beta$ -galactosidase.

In summary, the titanium complex Tc52 induces a concentration dependent loss of viability in tested cell lines, but whereas tumor cells showed an apoptotic response, non-tumor cells such as fibroblasts underwent senescence. This effect of Tc52 was independent of p53 status and did not involve DNA damage. Thus, Tc52 and derivatives may represent a new tool for tumor treatment, specifically inducing apoptosis in cancer cells but not in non-tumorigenic cells.

Currently, we analyze the impact of Tc52 together with other cytotoxic compounds acting independently from DNA damage in order to determine the underlying mechanism of action.

## 008

**Cyclin-dependent kinase 6 (CDK6) serves as a nuclear cofactor for p65 NF- $\kappa$ B-driven transcription****Handschick, Katja**<sup>1</sup>; **Beuerlein, Knut**<sup>1</sup>; Jurida, Liane<sup>1</sup>; Bartkuhn, Marek<sup>2</sup>; Müller, Helmut<sup>1</sup>; Soelch, Johanna<sup>1</sup>; Weber, Axel<sup>1</sup>; Dittich-Breiholz, Oliver<sup>3</sup>; Schneider, Heike<sup>3</sup>; Scharfe, Maren<sup>4</sup>; Jarek, Michael<sup>4</sup>; Stellzig, Julia<sup>5</sup>; Schmitz, M. Lienhard<sup>5</sup>; Kracht, Michael<sup>1</sup><sup>1</sup>Rudolf-Buchheim-Institute of Pharmacology, Justus-Liebig-University, Giessen, Germany<sup>2</sup>Institute for Genetics, Justus-Liebig-University, Giessen, Germany<sup>3</sup>Institute of Physiological Chemistry, Medical School, Hannover, Germany<sup>4</sup>Helmholtz Centre for Infection Research, Braunschweig, Germany<sup>5</sup>Institute of Biochemistry, Justus-Liebig-University, Giessen, Germany

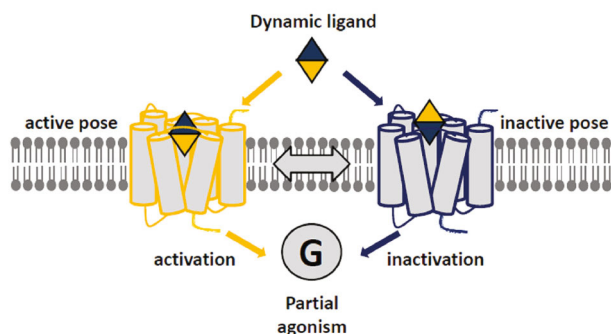
Chronic inflammation and dysregulated cell proliferation in cancer are intimately linked, but the underlying cellular and molecular mechanisms are incompletely understood. Two major players of these pathways are the cyclin-dependent kinases CDK4 and CDK6, which control cell cycle progression in G1 during aberrant proliferation, and the transcription factor nuclear factor kappa B (NF- $\kappa$ B), which regulates the expression of inflammatory and tumor-promoting genes. We, therefore, investigated cytokine-triggered gene expression in different cell cycle stages. Transcriptome analysis revealed that G1 release through CDK6 and CDK4 primes and cooperates with the cytokine-driven gene response. CDK6 physically and functionally interacts with the NF- $\kappa$ B subunit p65 in the nucleus and is found at promoters of many transcriptionally active NF- $\kappa$ B target genes. CDK6 recruitment to distinct chromatin regions of inflammatory genes was essential for proper loading of p65 to its cognate binding sites and for the function of p65 coactivators, such as TRIP6. Furthermore, cytokine-inducible nuclear translocation and chromatin association of CDK6 depends on the kinase activity of TAK1 and p38. This study identifies CDK6 as a molecular link between inflammatory microenvironment and permanent cell cycle progression, two major hallmarks of cancer, and predicts that inhibiting CDK activity by the widely used compound PD332991 will not only affect uncontrolled tumor cell proliferation, but also have an impact on innate immune functions arising from stroma or tumor cells. These results have widespread biological implications, as aberrant CDK6 expression or activation that is frequently observed in human tumors modulates NF- $\kappa$ B to shape the cytokine and chemokine repertoires in chronic inflammation and cancer.

## 009

**Dynamic ligand binding: A new route to fine-tune GPCR signalling****Bock, Andreas**<sup>1,2</sup>; de Amici, Marco<sup>3</sup>; Holzgrabe, Ulrike<sup>4</sup>; Hoffmann, Carsten<sup>5</sup>; Kostenis, Evi<sup>1</sup>; Tränkle, Christian<sup>1</sup>; Mohr, Klaus<sup>1</sup><sup>1</sup>University of Bonn/Institute of Pharmacy, Pharmacology & Toxicology Section, Germany<sup>2</sup>University of Würzburg/Institute of Pharmacology and Toxicology, Germany<sup>3</sup>Università degli Studi di Milano/Dipartimento di Scienze Farmaceutiche, Sezione di Chimica Farmaceutica "Pietro Pratesi", Italy<sup>4</sup>University of Würzburg/Institute of Pharmacy, Department of Pharmaceutical Chemistry, Germany<sup>5</sup>University of Würzburg/Bio-Imaging-Center/Rudolf-Virchow-Zentrum and Institute of Pharmacology and Toxicology, Germany<sup>6</sup>University of Bonn/Institute of Pharmaceutical Biology, Molecular-, Cellular-, and Pharmacobiology Section, Germany

G protein-coupled receptors (GPCRs) induce intracellular responses upon binding agonist ligands. Agonists are subclassified as full and partial agonists depending on whether they trigger a maximal biological response or induce a submaximal effect, respectively. The current explanation for different agonist efficacies includes an impaired engagement of receptor epitopes used by full agonists, a weaker stabilisation of the contracted agonist binding cavity or, more generally, an induction of different receptor conformations. In any case, this concept is based on the assumption that an agonist is bound to the receptor exclusively in one orientation. We expand this concept by demonstrating that bipharmacophoric partial agonists at the muscarinic  $M_2$  receptor dynamically switch between two distinct binding orientations referred to as *dynamic ligand binding*. By co-stabilizing both an active and an inactive receptor subpopulation, the ratio of orientations dictates the resulting response of the system. The fractional size of receptor subpopulations can be precisely set by chemical design. Therefore, the new conceptual framework of ligand efficacy presented here allows rationally generating libraries of *tailor-made* partial agonists with predictable efficacy. Consequently, the therapeutically most efficient and safest level of receptor activation can for the first time be systematically elucidated.

Bock *et al.* Dynamic ligand binding dictates partial agonism at a G protein-coupled receptor. *Nat. Chem. Biol.* 10, 18-20 (2014).



#### Dynamic ligand binding:

Dynamic ligand binding dictates partial agonism at a G protein-coupled receptor

## 010

### Effects of Galialacton on the Pathogenesis of Atherosclerosis— Results in Two Mouse Models

**Bollmann, Franziska**<sup>1,2</sup>; Jäckel, Sven<sup>2</sup>; Jurk, Kerstin<sup>2</sup>; Reinhardt, Christoph<sup>2</sup>; Wu, Zhixiong<sup>2</sup>; Xia, Ning<sup>2</sup>; Li, Huige<sup>2</sup>; Pautz, Andrea<sup>1</sup>; Kleinert, Hartmut<sup>1</sup>

<sup>1</sup>Medical Center of the Johannes Gutenberg University Mainz, Department of Pharmacology, Germany

<sup>2</sup>Medical Center of the Johannes Gutenberg University Mainz, Centre of Thrombosis and Hemostasis, Germany

Atherosclerotic events are one of the major courses for cardiovascular mortality in patients suffering from chronic inflammatory diseases like rheumatoid arthritis (RA). Compared to the general population RA-patients have an increased risk (50 %) of cardiovascular events. This elevated risk is independent of the traditional factors as age, gender, smoking, or hypertension. Today, it is believed that the systemic inflammation confers a significant and independent factor for the morbidity in those patients.

Apolipoprotein E-deficient mice (ApoE<sup>-/-</sup>) fed with western-type diet are a well-established model of atherosclerosis, as they develop hypercholesterolemia and fibrotic plaque progression. One disadvantage of this model is the lack of spontaneous plaque ruptures; thrombotic events have to be induced in those mice. ApoE<sup>-/-</sup>-mice heterozygous for the inactivation of the tissue factor pathway inhibitor (TFPI) were shown to have a higher risk for thrombotic and atherosclerotic events as traditional ApoE<sup>-/-</sup>-mice.

In this study the anti-inflammatory and anti-atherosclerotic capacity of the fungal compound Galialacton (Gal) was evaluated in ApoE<sup>-/-</sup>- and ApoE<sup>-/-</sup>TFPI<sup>+/-</sup> mice using intra-vital microscopy and qPCR analysis. To induce atherosclerosis, all mice were fed with western-type diet for 18 weeks. Gal was applied for the last 6 weeks every other day with 10mg/kg *i.p.*

Gal-treatment reversed the nutrition-dependent increase of platelet adhesion to the endothelium after injury of the common carotid artery in ApoE<sup>-/-</sup>-mice to the level of normal diet mice. qPCR analysis revealed a significant decrease of the mRNA expression of pro-atherosclerotic and pro-inflammatory markers as S100A8, osteopontin, and IL-6. Endothelium-activation markers were significantly reduced in atherosclerotic ApoE<sup>-/-</sup>TFPI<sup>+/-</sup>-mice after Gal-treatment when compared to control mice. Our results indicate a reduced disease progression in both ApoE<sup>-/-</sup>- and ApoE<sup>-/-</sup>TFPI<sup>+/-</sup>-mice after Gal-treatment when analysing platelet-endothelium-interaction and marker gene expression.

## 011

### Discovery and promotion of a new class of chemosensitizer reversibly inhibiting protein disulfide isomerase

**Braig, Simone**<sup>1</sup>; Eirich, Jürgen<sup>2</sup>; Kazmaier, Uli<sup>3</sup>; Sieber, Stephan<sup>2</sup>; Vollmar, Angelika<sup>1</sup>

<sup>1</sup>LMU München, Pharmazeutische Biologie, Germany

<sup>2</sup>TU München, Organic Chemistry, Garching, Germany

<sup>3</sup>Universität des Saarlandes, Institut für Organische Chemie, Saarbrücken, Germany

A major drawback in cancer therapy is the development of resistance to anti-neoplastic drugs. Due to deregulation of intracellular signaling pathways, cancer cells continue to proliferate and became insensitive to apoptotic signals. Hence, understanding and circumventing apoptosis resistance mechanisms is crucial to abrogate uncontrolled growth of tumors.

Since cancer cells proliferate rapidly, increased synthesis of proteins and thus enhanced endoplasmic reticulum (ER) function and capacity is inevitable. Upon treatment with chemotherapeutics, cancer cells are under ER stress characterized by upregulation of ER chaperones such as protein disulfide isomerase (PDI) in order to maintain ER homeostasis and support cancer cell survival. Targeting PDI might thus be a feasible approach to fight chemoresistance.

Here we introduce the first reversible and highly specific PDI inhibitors that were discovered by the search for substances, which are able to sensitize tumor cells towards classical chemotherapeutic agents. Using a commercially available compound library we found a small molecule (T8) that strongly increased the sensitivity of various tumor cell lines to different chemotherapeutics without being cytotoxic itself up to 100µM. To identify

direct targets of T8 being responsible for its chemosensitizing action we used the activity-based protein profiling (ABPP) approach (1,2): employing a specially designed photo probe (JP04) which mimicked the mother compound (T8) proteome analysis using SILAC revealed protein disulfide isomerase as a binding partner of JP04. The identification of PDI as an almost exclusive target of JP04 was followed by rounds of chemical optimizing of T8, structure activity relationship studies and in depth pharmacological characterization and validation of PDI as a promising novel target for chemosensitization.

#### References:

(1) Nodwell MB, Sieber SA. ABPP methodology: introduction and overview. *Top Curr Chem.* 2012;324:1-41.

(2) Böttcher T, Pitscheider M, Sieber SA. Natural products and their biological targets: proteomic and metabolomic labeling strategies. *Angew Chem Int Ed Engl.* 2010 Apr 1;49(15):2680-98.

## 012

### Impact of the NO/cGMP pathway on the sympathetic activity

**Broekmans, Kathrin**; Koesling, Doris; Mergia, Evanthia

Ruhr-Universität Bochum, Pharmakologie und Toxikologie, Germany

Because of its vasodilating properties, the impact of the NO/cGMP pathway on blood pressure is well established, whereas its role in the sympathetic nervous system is controversial. The key enzyme of the NO/cGMP pathway is the NO-stimulated guanylyl cyclase which exists in two isoforms, NO-GC1 and NO-GC2. In the vasculature, NO-GC1 is responsible for the major part of cGMP formation. Deletion of NO-GC1 leads to a reduction of the vascular relaxation which results in an increased vascular tone as measured in perfused hind limb experiments. However, NO-GC1 KO mice did not have elevated blood pressure. Further analysis of cardiac parameters, revealed a reduced heart rate in the NO-GC1 KO mice (NO-GC1 KO 575 ± 9 bpm vs. WT 612 ± 10 bpm).

In contrast to the vascular system, both NO-GC isoforms are equally responsible for the cGMP formation in the central nervous system and are required for synaptic transmission in the CA1 region of the hippocampus. Occurrence of both isoforms has also been detected in regions responsible for blood pressure regulation. In the Medulla oblongata, the NO-GC2 isoform was found to account for ~70 % and the NO-GC1 for ~30 % of the cGMP formation. These results suggest that the NO-GC isoforms might be involved in regulation of blood pressure not only at vascular but also at neuronal sites. Therefore we developed an experimental approach to examine the impact of the NO-GC isoforms on vascular and central blood pressure regulation. Furthermore, we evaluate the status of the sympathetic activity of the NO-GC KO mice by determining the norepinephrine content in the plasma.

## 013

### Cool-temperature-mediated activation of phospholipase C-gamma 2 in PLAID, a novel form of human hereditary antibody deficiency and immune dysregulation

**Bühler, Anja**<sup>1</sup>; Walliser, Claudia<sup>1</sup>; Haas, Jennifer<sup>1</sup>; Kraus, Johann M.<sup>2</sup>; Fillingner, Davide<sup>3</sup>; Havenith, George<sup>3</sup>; Kestler, Hans A.<sup>2</sup>; Milner, Joshua D.<sup>4</sup>; Gierschik, Peter<sup>1</sup>

<sup>1</sup>Ulm University Medical Center, Institute of Pharmacology and Toxicology, Germany

<sup>2</sup>Ulm University, Medical Systems Biology, Germany

<sup>3</sup>Loughborough University, Environmental Ergonomics Research Centre, Leicestershire, Great Britain

<sup>4</sup>NIH, Allergic Inflammation Unit, Laboratory of Allergic Diseases, NIAID, Bethesda, United States

Deletions in the gene encoding signal-transducing inositol phospholipid-specific phospholipase C- $\gamma_2$  (PLC $\gamma_2$ ) are associated with the novel human hereditary disease PLAID (PLC $\gamma_2$ -associated antibody deficiency and immune dysregulation) characterized by a rather puzzling concurrence of augmented and diminished functions of the immune system, such as cold urticaria triggered by only minimal decreases in temperature, autoimmunity, and immunodeficiency. Understanding of the functional effects of the genomic alterations at the level of the affected enzyme, PLC $\gamma_2$ , is currently lacking. PLC $\gamma_2$  is critically involved in coupling various cell surface receptors to regulation of important functions of immune cells such as mast cells, B cells, monocytes/macrophages, and neutrophils. PLC $\gamma$  is unique by carrying three Src (SH) and one split pleckstrin homology domain (spPH) between the two catalytic subdomains. Prevailing evidence suggests that activation of PLC $\gamma$  is primarily due to loss of SH-domain-mediated autoinhibition and/or enhanced plasma membrane translocation. Here, we show that the two PLAID PLC $\gamma_2$  mutants lacking portions of the SH tandem are strongly (> 100-fold), rapidly, and reversibly activated by cooling by only a few degrees. We found that the underlying mechanism is distinct from a mere loss of SH-tandem-mediated autoinhibition and dependent on both the integrity and the pliability of the spPH domain. The results suggest a new mechanism of PLC $\gamma$  activation with unique thermodynamic features and assign a novel, less submissive role to its spPH domain. Involvement of this mechanism in other human disease states associated with cooling such as exertional asthma and certain acute coronary events appears an intriguing possibility.

## 014

### The orphan drug carbaglu is a substrate of the sodium dicarboxylate cotransporter 3 (NaDC3) and of the organic anion transporter 1 (OAT1)

**Burckhardt, Birgitte C.**; Schwob, Elisabeth; Hagos, Yohannes; Burckhardt, Gerhard  
Universitätsmedizin Göttingen, Institut für Vegetative Physiologie und Pathophysiologie, Germany

Inborn defects in the carbamoylphosphate synthase 1 (CPS1) cause a reduction of *N*-acetylglutamate (NAG), an essential cofactor for the function of the urea cycle. As a consequence, blood levels of ammonia are elevated leading to hepatic encephalopathy, severe neurotoxic symptoms, lethargy, coma, and death - if untreated. Besides protein restriction to reduce production of ammonia, the orphan drug *N*-carbamoylglutamate (carbagluic acid, carbaglu, NCG) is used to treat hyperammonemia. NCG substitutes for NAG on CPS1, thereby reactivating the urea cycle and finally reducing blood ammonia levels. The renal clearance of NCG exceeds its glomerular filtration rate, suggesting active secretion of NCG in kidney proximal tubules. The first step in secretion is the uptake of a compound across the basolateral membrane of proximal tubule cells. There, the organic anion transporters (OATs) are working in cooperation with the sodium-dependent dicarboxylate cotransporter 3 (NaDC3). These transporters are known to be uptake transporters. To demonstrate interaction of NCG with the OATs, the impact of NCG on human OAT1, 2, and 3 stably transfected in HEK293 cells was tested. Whereas OAT2 and 3 did not interact with NCG, the uptake of the lead substrate of OAT1, *p*-aminohippurate, was inhibited by NCG with an IC<sub>50</sub> of 228 ± 41 µM. Because NaDC3 is an electrogenic transporter, the two-electrode voltage clamp technique was used to monitor sodium- and concentration-dependent NCG-mediated currents in *Xenopus laevis* oocytes expressing NaDC3. NCG was identified as a high affinity substrate of NaDC3 with a K<sub>M</sub> of 27 ± 7 µM. This value is in the order of the K<sub>M</sub> for succinate, the lead substrate of NaDC3. The K<sub>M</sub> for NCG equals the plasma concentration of patients treated with NCG. Below K<sub>M</sub>, succinate- and NCG-induced currents were additive, a further proof that both substances are substrates of NaDC3. We propose that NaDC3 and - to a lesser extent - OAT1 are involved in renal secretion of carbaglu.

## 015

### Phase I metabolism and mutagenicity of phenylpropenes occurring in food: Implications for their carcinogenic mode of action

**Cartus, Alexander**<sup>1</sup>; Bischoff, Roland<sup>1</sup>; Berg, Kerstin<sup>1</sup>; Valliotti, Sabrina<sup>1</sup>; Glatt, Hansruedi<sup>2</sup>; Esselen, Melanie<sup>3</sup>; Schrenk, Dieter<sup>1</sup>

<sup>1</sup>TU Kaiserslautern, Lebensmittelchemie und Toxikologie, Germany

<sup>2</sup>Deutsches Institut für Ernährungsforschung, Ernährungstoxikologie, Nuthetal, Germany

Phenylpropenes (PP) are naturally occurring plant constituents present in many foodstuffs. Some are genotoxic carcinogens in rodents, e.g. methyleugenol (ME), safrole or estragole. The activation occurs via a cytochrome P450 (CYP)-catalyzed oxidation leading to a 1'-alcohol which is sulfonated afterwards. Upon loss of sulfate, a carbocation is formed, which can react with DNA.

The majority of PP with a propenyl side chain e.g. anethole, methylisoeugenol (MIE) or isosafrole are not genotoxic or carcinogenic in rodents. Exceptions are alpha- and beta-asarone (aA, bA), which caused liver tumors in mice (gamma-asarone, gA, has not been tested so far). The molecular mechanism(s) responsible for the carcinogenicity of aA and bA is (are) still not understood.

We investigated the phase I metabolism of different PP, including the allylic PP ME and gA, as well as the propenyl MIE, aA, and bA using human liver microsomes (HLM) and Supersomes<sup>TM</sup> (expressing human CYP1A2, 2A6, 2C19, 2D6, 2E1 or 3A4) and determined (apparent) kinetic parameters for the formation of different metabolites. The contribution of different CYPs in HLM was investigated applying the 'relative activity factor'-approach. Furthermore, we tested the parent compounds and selected phase I

metabolites in the fluctuation Ames test using different *Salmonella typhimurium* strains, including human SULT-expressing strains and in the comet assay using V79 cells.

Based on  $v_{max}/K_M$  ratios, side-chain hydroxylation is the predominant pathway of aA and gA phase I metabolism at very low concentrations more relevant for human exposure, whereas ME, MIE and bA are mostly metabolized to side-chain epoxides/dihydrodiols. Although the dihydrodiols of all tested PP were quantifiable in HLM, the precursor epoxides were only detectable in incubations with aA and bA. This suggests that these epoxides are poor substrates for the microsomal epoxide hydrolases and exert limited reactivity.

aA and bA were genotoxic in the fluctuation Ames test only with metabolic activation. However, all side-chain alcohols of asarones (1'-OH, (E)-3'-OH and (Z)-3'-OH) were negative. Furthermore, the parent compounds aA, bA and gA significantly induced DNA-damage in V79 cells, whereas the contribution of phase I metabolites to the observed DNA-strand breaking effects is still under investigation.

The results imply that the epoxides of aA and bA may act as genotoxic metabolites of those compounds.

## 016

### PolH is p53 dependently induced and involved in protection against chloroethylating anticancer drugs

**Tomcic, Maja**; Aasland, Dorthe; Kaina, Bernd; **Christmann, Markus**  
Universitätsmedizin Mainz, Institut für Toxikologie, Germany

The transcription factor p53 plays an important role in the response of tumor cells to anticancer drugs. Previously we showed that melanoma cells deficient in p53 are hypersensitive to the chloroethylating drug fotemustine (1). Here we identified the translesion polymerase eta (PolH) as a p53 regulated target involved in the protection against this drug. Upon fotemustine treatment, induction of PolH was observed in p53 proficient but not p53 deficient melanoma cell lines and this induction was abrogated by the use of pifithrin- $\alpha$ , an inhibitor of p53. Furthermore, binding of p53 to the PolH promoter was shown by ChIP. Induction of PolH was also observed in primary human PBMCs, lymphoblastoid cells and in a mouse model xenograft. To analyze the role of PolH in the protection against fotemustine, PolH deficient XPV cells and PolH specific siRNA were utilized. Both, PolH deficient XPV cells and melanoma cells transfected with PolH specific siRNA showed increased sensitivity to fotemustine. *Vice versa*, overexpression of PolH in melanoma cells protected these cells. PolH seems to be directly involved in the bypass of fotemustine adducts since PolH knockdown reduced the repair of these lesions as measured by host cell reactivation assays. Moreover a strong accumulation of PolH in the nucleus of fotemustine treated cells and binding to the damaged DNA was observed by immunofluorescence. The data show that PolH is a genotoxic stress-inducible repair factor, which is involved in the repair of DNA damage induced by chloroethylating drugs and thus represents a potential marker of cancer cell resistance.

[1] Naumann et al., Br J Cancer. 2009 100(2), 322-33.

## 017

### Toxic Effects of Various Modifications of a Nanoparticle Following Inhalation

**Creutzenberg, Otto**; Voss, Jens-Uwe; Mangelsdorf, Inge; Tillmann, Thomas; Pohlmann, Gerhard; Hansen, Tanja; Kock, Heiko; Schaudien, Dirk

Fraunhofer-Institut für Toxikologie und Experimentelle Medizin - ITEM, Toxikologie und Umwelthygiene, Hannover, Germany

The toxic effects of the dust triple TiO<sub>2</sub> UV TITAN M262, TiO<sub>2</sub> UV TITAN M212 and TiO<sub>2</sub> P25 (coded NM-103, NM-104 and NM-105, respectively, in the JRC repository) were compared in a 28-day inhalation test. Differences in crystal structure (rutile vs. anatase) or surface modification (hydrophobic vs. hydrophilic) suggested a different toxic potential after uptake in lungs. Wistar rats were exposed to aerosol concentrations of 3, 12 and 48 mg/m<sup>3</sup> mimicking exposure scenarios at workplaces (6 hours/day, 5 days/week for 28 days). This dosing scheme induced a non-, partial, and complete lung overload, respectively. Endpoints investigated after end of exposure (3 days, 1.5 and 3 months of recovery) were i.) analysis of bronchoalveolar lavage fluid (BALF); ii.) histopathology; iii.) transmission electron microscopy (TEM) analysis; and iv.) chemical analysis of test item retention in lungs, liver, and brain. - PMN in BALF as inflammation indicator resulted in the low dose groups for NM-105 at control levels, whereas NM-103 and NM-104 induced approx. 10% PMN. After 45 and 94 days of recovery in clean air, NM-103-treated animals also returned to normal; in contrast, NM-104-treated animals remained in the significant 5-8% range. In the mid and high dose groups, NM-105 showed a weaker inflammatory effect than NM-103 and NM-104. - Test item retention analysis data reflected well the different grades of clearance retardation due to the various lung loads and fitted to the values predicted by the MPPD model. A very low translocation potential of particles from lungs was detected. - Histopathology revealed a similar dose-dependent character of changes between NM-103, NM-104 and NM-105. - TEM analysis showed intraalveolar macrophages as the most prominent compartment of particle detection. - Experimental and predicted NOAEL values (according to Pauluhn, 2011) were 3 and 5 mg/m<sup>3</sup>, respectively. A preliminary toxicity ranking on the basis of the induction of PMN influx and other endpoints is: NM-104 > NM-103 > NM-105.

However, pronounced differences in toxicity were not observed between the three test items.

**The project was funded by the Federal Institute for Occupational Safety and Health (BAuA), Dortmund, Germany.**

Pauluhn J (2011). Poorly soluble particulates: searching for a unifying denominator of nanoparticles and fine particles for DNEL estimation. *Toxicology* 279, 176-188

## 018

### Effects of Triazole Fungicides on Vitamin D Metabolism and Selected Carrier Proteins

**Dabrowski, Alexander;** Knebel, Constanze; Heise, Tanja; Niemann, Lars; Pfeil, Rudolf; Marx-Stoelting, Philip; Kneuer, Carsten

Bundesinstitut für Risikobewertung, Chemikaliensicherheit, Berlin, Germany

**Background:** A 28-day feeding study with the triazole fungicides cyproconazole, epoxiconazole, propiconazole, tebuconazole, as well as the imidazole prochloraz was performed in male Wistar rats. Screening with low-density RT-PCR arrays had suggested effects on gene expressions of the vitamin D (VitD) receptor, VitD-related enzymes and carrier proteins in adrenals, testis, prostate as well as in liver [1-3]. The aim of this study was to clarify these findings and describe possible influences on VitD metabolism and carrier proteins included their dose dependency.

**Methods:** Quantitative real-time PCR analysis was performed with liver and kidney from treated rats as well as HepG2 and MDCKII cells exposed *in vitro*. Target genes included those directly related to VitD, metabolic enzymes of phase I & II relevant to VitD as well as selected transporters. Parathyroid hormone (PTH) levels in blood serum were analysed by ELISA, determination of vitamin D<sub>3</sub> levels is ongoing. Dose levels tested *in vivo* were based on NOAELs from regulatory studies and ranged from NOAEL/100 to NOAEL x10.

**Results:** All azoles increased gene expression of Abcb1a, Abcb1b and Slco1a2 in liver more than 2-fold from a dose corresponding to the NOAEL. In kidneys, significant changes in mRNA levels for these genes were also observed, but without clear dose-response relationship. *In vitro*, ABCB1 expression was reduced at 160 µM of propiconazol, epoxiconazol and prochloraz in MDCKII cells, but not clearly dose dependent for the azoles. In HepG2 cells, there was an induction of ABCB1 by epoxiconazole. Modulation of VitD related genes could be confirmed: significant changes in transcript levels were observed for Cyp2r1 (25-hydroxylase), Gc (VitD binding protein) and Vdr (VitD receptor) in rat liver. Indications for changes in Cyp24a1 and Cyp27b1 in kidneys of treated rats could not be confirmed. However, several Cyp3a and Ugt1a enzymes, which can unspecifically metabolise VitD, were induced at dose level corresponding to the NOAEL and . The concentration of PTH was affected significantly by the treatment with cyproconazole and a combination of cyproconazole, epoxiconazole and prochloraz. Potential cumulative effects resulting from the combination of cyproconazole, epoxiconazole and prochloraz could be illustrated.

**Conclusion:** The results suggest that carrier proteins and VitD related targets may play a role in the mechanism of toxicity of azole fungicides and their toxicological interaction.

[1] Heise T., Rieke S., Schmidt F., Ladwig M., Haider W., Sommerfeld C., Pfeil R., Niemann L., Marx-Stoelting P., *Hepatotoxic effects of five (triazole) fungicides in a broad dose range*, Naunyn-Schmiedeberg's Arch Pharmacol (2013) 386 (Suppl 1):S1-S104.

[2] Rieke S., Schmidt F., Heise T., Pfeil R., Niemann L., Marx-Stoelting P., *Triazole fungicide effects on the adrenal gland in vivo in a broad dose range*, Naunyn-Schmiedeberg's Arch Pharmacol (2013) 386 (Suppl 1):S1-S104.

[3] Schmidt F., Rieke S., Heise T., Niemann L., Pfeil R., Marx-Stoelting P., *Toxic effects of triazole fungicides on rat male reproductive system in prostate gland and testis*, Naunyn-Schmiedeberg's Arch Pharmacol (2013) 386 (Suppl 1):S1-S104.

## 019

### Doxorubicin- and etoposide-driven transcriptional repression affects highly expressed genes which are characterized by topoisomerase IIα enrichment at promoters

**Deng, Shiwei;** Yan, Tiandong; Gödtel-Armbrust, Ute; Wojnowski, Leszek

Department of Pharmacology, University Medical Center of the Johannes Gutenberg University Mainz, Germany

Antitumor drugs such as doxorubicin (DOX) and etoposide (VP16) result, among others, in a topoisomerase IIα (Top2α)-mediated downregulation of specific gene sets. The contribution of this downregulation to these drugs' antitumor effects is unknown. We investigated the molecular characteristics of genes susceptible to Top2α-mediated transcriptional shutdown using cells with conditional expression of this enzyme. DNA damage, cell survival, apoptosis and global gene expression changes were more Top2α-dependent following VP16 than DOX exposure. Chromatin immunoprecipitation assays revealed an enrichment of Top2α binding to promoters, which was particularly pronounced for highly expressed genes. Conditional depletion of Top2α resulted in subtle gene repression which was accompanied by reduced RNA pol II binding to gene promoters. VP16 and DOX treatments, respectively, attenuated (VP16) and eliminated (DOX) the aforementioned Top2α promoter enrichment. This was caused not by Top2α promoter displacement but by the increased binding of the enzyme to non-promoter regions. The formation of γ-H2AX at promoter regions was enhanced by drug treatments in a Top2α-dependent manner. The RNA pol II was depleted from gene promoters by

either drug irrespective of the initial Top2α binding status. Strikingly, genes with higher pre-treatment expression levels and promoter Top2α binding were preferentially repressed by drug treatments. In conclusion, transcription of highly expressed genes may rely on promoter Top2α binding. These genes are more susceptible to transcription repression mediated by Top2α poisoning.

## 020

### Transient CAR and PXR activation results in multigenerational gene expression changes

**Dietrich, Karin;** Mathäs, Marianne; Wojnowski, Leszek

Universitätsmedizin der Johannes Gutenberg-Universität Mainz, Institut für Pharmakologie, Germany

The exposure to environmental or human-made xenobiotics including drugs induces the hepato-intestinal transcription of metabolizing enzymes and transporters. The time-span of this so-called induction is assumed not to exceed xenobiotic exposure, as this would minimize disturbances of endobiotic metabolism. We investigated if induction mediated via the major mammalian xenosensors PXR and CAR may be transmitted via the germline. Newborn and adult F<sub>0</sub> mice were given single injections of the PXR activator PCN and of the CAR activator TCPOBOP. Three months (newborn injection) or one week later (adult injection) they were mated with untreated mice of the opposite sex and gene expression changes were assessed in F<sub>1</sub> and F<sub>2</sub> mice. Both injection time-points resulted in multigenerational (F<sub>0</sub> → F<sub>1</sub>) gene expression changes. Thus, the CAR target Cyp2b10 was induced 91- (females) and 120-fold (males) in livers of newborn, and 2.4- (females) and 7-fold (males) in adult F<sub>1</sub> mice born by F<sub>0</sub> females treated as newborns with TCPOBOP. High throughput sequencing of livers of newborn F<sub>1</sub> mice born by F<sub>0</sub> females treated as newborns with TCPOBOP revealed expression changes in genes related to lipid metabolism (Cyp2b9, Mup1) and to immunological diseases. Cyp2b10 was also induced 748- (females) and 539-fold (males) in livers of newborn F<sub>1</sub> mice born by F<sub>0</sub> females treated as adults with TCPOBOP. New-born and 3-month-old F<sub>1</sub> descendants of F<sub>0</sub> female mice treated as newborns with the PXR ligand PCN showed expression changes in genes with a role in energy homeostasis and glucose metabolism. To investigate if Cyp2b10 induction by TCPOBOP undergoes transgenerational transmission (F<sub>0</sub> → F<sub>2</sub>...), we mated either-sex F<sub>1</sub> offspring of females treated as newborns with TCPOBOP with untreated mice of the opposite sex. The Cyp2b10 gene expression was unchanged in F<sub>2</sub> mice. The above results demonstrate that maternal exposure to CAR and PXR activators prior to pregnancy changes in the F<sub>1</sub> mice the expression of genes implicated in drug metabolism and in energy homeostasis. The mechanism of this multigenerational transmission and its relevance to humans, many of whom undergo treatments with CAR and PXR activators, are currently under investigation.

## 021

### A Novel Tirucallic Acid Derivative Induces Inhibition of the Akt/mTOR Pathway, G<sub>2</sub> Cell Cycle Arrest, and Apoptosis in Chemoresistant Prostate Cancer Cells

**El Gafaary, Menna;** Syrovets, Tatiana; Büchele, Berthold; Simmet, Thomas

Institute of Pharmacology of Natural Products & Clinical Pharmacology, Ulm, Germany

Three tirucallic acid derivatives (3-oxo-tirucallic acid - OTA, 3-α-acetoxy-tirucallic acid - α-ATA (7,8) and its positional isomer α-ATA(8,9)) were isolated to chemical homogeneity from the acetylated resin of *Boswellia serrata* Roxb. using HPLC techniques and their molecular identity was confirmed by mass spectrometry and nuclear magnetic resonance spectroscopy. All compounds inhibited proliferation of androgen-insensitive prostate cancer cells *in vitro* and induced their apoptosis as shown by disruption of the mitochondrial membrane potential, exposure of phosphatidylserine on the outer leaflet of the plasma membrane, and DNA fragmentation. Interestingly α-ATA(8,9) showed higher potency and activity toward androgen refractory prostate adenocarcinoma cells, when compared to its positional isomer α-ATA(7,8). All tirucallic acids derivatives exhibited either no or only little effect on normal peripheral blood mononuclear cells. OTA and α-ATA(8,9) initially arrest the cancer cells in the G<sub>1</sub> phase, followed by a simultaneous curtailing in the S and G<sub>2</sub> phase, and finally cell death. At the molecular level, the compounds were found to inhibit the Akt/mammalian target of rapamycin (mTOR) pathway, which is often constitutively active in human prostate cancer. The compounds downregulated the activity of PDK1 and S6 kinase, inhibited expression of eukaryotic initiation factor 4 (EIF4) and phosphorylation of GSK3β on serine 9. Moreover, the downregulation of the Akt/mTOR pathway was associated with a remarkably decreased expression of the cell cycle regulators, cyclin D1, cyclin E, cyclin B1, cyclin-dependent kinases CDK4 and CDK2, and the phosphorylation of Rb protein. On the other hand, the compounds induced expression of the cell-cycle inhibitor p21<sup>Cip1</sup>. In an *in vivo* model, the tirucallic acid derivatives were strong proliferation inhibitors and triggered apoptosis in prostate cancers xenografted onto chick chorioallantoic membranes. The ability of tirucallic acids to control the growth of androgen-insensitive prostate cancer cells without affecting the viability of normal cells or the chick embryo suggests that they could serve as lead compounds for the development of novel antitumor therapeutics with a low profile of toxic side effects.

## 022

**Randomized comparison of aliskiren and amlodipine on RAAS biomarkers and metabolism in obese hypertensive patients**

**Engeli, Stefan**<sup>1</sup>; May, Marcus<sup>1</sup>; Nussberger, Juerg<sup>2</sup>; Danser, Jan<sup>3</sup>; Dole, William<sup>4</sup>; Prescott, Margaret<sup>4</sup>; Dahlke, Marion<sup>4</sup>; Stitah, Sylvie<sup>3</sup>; Parasar, Pal<sup>4</sup>; Jordan, Jens<sup>1</sup>

<sup>1</sup>Medizinische Hochschule Hannover, Institut für Klinische Pharmakologie, Germany

<sup>2</sup>Centre Hospitalier Universitaire Vaudois, Department of Internal Medicine, Lausanne, Switzerland

<sup>3</sup>Erasmus MC, Department of Internal Medicine, Rotterdam, Netherlands

<sup>4</sup>Novartis Pharma, Basel, Switzerland

**Introduction**

The direct renin inhibitor, aliskiren, reaches adipose and skeletal muscle tissues concentrations apparently sufficient to reduce tissue RAAS activity. The main objectives of the current study were to assess in obese hypertensive patients the effects of aliskiren on Angiotensin II concentrations in interstitial fluid of subcutaneous fat and skeletal muscle and on plasma RAAS biomarkers. We also determined the effects of aliskiren on lipid and carbohydrate metabolism in subcutaneous fat and skeletal muscle.

**Methods**

After 1-2 weeks wash-out and a single-blind run-in placebo period, 16 patients were randomized to either 300 mg aliskiren or 5 mg amlodipine once daily. Before randomization and after 12 weeks of treatment, we performed an insulin modified frequently sampled intravenous glucose tolerance test (FSIGT), together with two microdialysis catheters placed each in abdominal subcutaneous adipose tissue and the *vastus lateralis* muscle. Blood and interstitial fluid samples were obtained at baseline and through the glucose tolerance test.

**Results**

Interstitial Ang II concentrations were highly variable. A *post-hoc* analysis excluding biological impossible values (Ang II >100 fmol/ml) demonstrated increased Ang II with amlodipine, and decreased Ang II with aliskiren. The difference was significant in skeletal muscle but not adipose tissue. Glucose/insulin injections at the beginning of the FSIGT significantly increased median Ang II concentrations from 0.86 to 2.65 fmol/mL ( $p=0.008$ ) in the aliskiren group and from 1.50 to 2.40 fmol/mL ( $p=0.102$ ) in the amlodipine group before treatment. Aliskiren treatment markedly attenuated the glucose/insulin-stimulated increase in plasma Ang II concentrations. Whereas insulin sensitivity (SI) was not changed by treatment, the acute insulin response to glucose (AIRG) was slightly enhanced by aliskiren (899±320 before vs. 1129±464 after treatment) but not amlodipine. Aliskiren elicited weak local hemodynamic effects with a trend towards increased blood flow in adipose tissue but not skeletal muscle. Aliskiren tended to decrease glycerol concentrations in adipose tissue but not skeletal muscle, suggesting a tissue-specific effect on lipolysis.

**Discussion**

Aliskiren effectively lowered blood pressure in obese hypertensive patients and reduced availability of Ang II in the circulation and in tissues. Tissue-specific metabolic effects were small. On the other hand, the influence on the insulin response to glucose suggests that beside being effective in lowering blood pressure, aliskiren treatment addresses some of the metabolic deteriorations characteristic for hypertensive patients with abdominal obesity.

## 023

**Agonist and mechanically induced receptor activations evoke distinct active receptor conformations**

**Erdoğan, Serap**<sup>1</sup>; Storch, Ursula<sup>1</sup>; Winter, Michaela<sup>1</sup>; Hoffmann, Carsten<sup>2</sup>; Gudermann, Thomas<sup>1</sup>; Mederos Y Schnitzler, Michael<sup>1</sup>

<sup>1</sup>LMU, Walther-Straub-Institut, München, Germany

<sup>2</sup>Julius-Maximilians-Universität Würzburg, Lehrstuhl für Pharmakologie, Germany

The FRET technique is widely used to monitor interactions between two proteins. Here, we insert two fluorochromes in one protein which allows detection of dynamic intramolecular conformational changes of G-protein coupled receptors. To analyze whether there are differences between agonist-induced and mechanically induced active receptor conformations we analyzed the G<sub>q/11</sub> protein coupled histamine H<sub>1</sub> receptor which showed the highest mechanosensitivity in previous studies. This receptor regulates many physiological processes like ileum contraction, modulation of circadian cycle, systemic vasodilatation, allergy-induced itching and bronchoconstriction. Therefore, the receptor was C-terminally linked to cerulean, a stable cyan fluorescent protein and in addition, a small tetracycline-binding motif was inserted at different positions at the beginning, the middle and the end of the third intracellular loop, which allows binding of the small fluorescent arsenical hairpin binder FIAsh, a yellow fluorophore. Agonist stimulations with histamine (100  $\mu$ M) and mechanical stimulations with hypotonic bath solutions (150-250 mOsmol) were performed using a focal pressurized perfusion system. Interestingly, mechanical stimulation resulted in a significantly greater decrease of the FRET signal than agonist stimulation with higher amplitudes and faster kinetics. Furthermore, the amplitude of mechanically induced FRET signals showed a concentration dependency since hypotonic solution with 150 mOsmol evoked higher FRET amplitudes than 250 mOsmol bath solution. Altogether, our results indicate that agonist stimulation induces a different active receptor conformation than mechanical stimulation.

## 024

**Photorhabdus luminescens ADP-ribosylating toxin requires Hsp90, Cyclophilins and FK506-binding proteins for membrane translocation**

**Ernst, Katharina**<sup>1</sup>; Lang, Alexander<sup>2</sup>; Aktories, Klaus<sup>2</sup>; Barth, Holger<sup>1</sup>

<sup>1</sup>Universitätsklinikum Ulm, Institut für Pharmakologie und Toxikologie, Germany

<sup>2</sup>Universität Freiburg, Institut für experimentelle und klinische Pharmakologie und Toxikologie, Germany

Several severe diseases e.g. anthrax or diphtheria are caused by bacterial AB-type protein toxins. These AB-type toxins employ an elaborate uptake mechanism to enter target cells where they achieve a cytotoxic effect. They consist of a binding/translocation component (B) that facilitates receptor-binding and membrane translocation and an A-component harboring enzymatic activity. In recent studies it has been shown by our group that toxins with an ADP-ribosyltransferase activity namely *Clostridium* (*C.*) *botulinum* C2 toxin, *C. perfringens* iota toxin and *C. difficile* CDT [1,2] require the host cell factors heat shock protein 90 (Hsp90) and peptidyl-prolyl-*cis/trans*-isomerases (PPIases) of the cyclophilin (Cyp) and FK506-binding protein (FKBP) families for their membrane translocation. In contrast, toxins with a different enzyme activity e.g. the lethal toxin of *Bacillus anthracis* which use a very similar uptake mechanism are independent of these host cell factors [3]. In addition, it was demonstrated that only recombinant fusion toxins that contain an ADP-ribosyltransferase domain require Hsp90, Cyps and FKBP. In this context we investigated the involvement of Hsp90, Cyps and FKBP in the uptake of the *P. luminescens* ADP-ribosylating PTC3 toxin. PTC3 is taken up into target cells similar to AB-type toxins regarding receptor-mediated endocytosis and translocation from acidified endosomes but nevertheless displays differences like a syringe-like microinjection machinery during membrane translocation [4,5]. Here we show that Hsp90, Cyps and FKBP are required for an efficient membrane translocation of the ADP-ribosyltransferase component TccC3 of PTC3 toxin [6]. Inhibition of the activity of Hsp90, Cyps and FKBP by specific pharmacological inhibitors led to a decreased intoxication demonstrated by cell rounding. In a toxin translocation experiment where the acidic endosomal conditions are mimicked at the cytoplasmic membrane we showed that the inhibitors of Hsp90 and PPIases inhibited exactly this step of toxin uptake into the target cell whereas other steps like receptor-binding and enzymatic activity were not impaired. Furthermore, the artificial translocation of the isolated ADP-ribosyltransferase domain TccC3hrv via the *B. anthracis* PA-pore was also delayed by the inhibitors and TccC3hrv interacted with Hsp90, FKBP51, Cyp40 and CypA in co-precipitation experiments. These results suggest a role of these host cell factors in membrane translocation and/or refolding of the *P. luminescens* PTC3 toxin and support our hypothesis that the requirement of Hsp90, Cyps and FKBP is a common characteristic for ADP-ribosylating toxins.

[1] Barth H (2011). Naunyn-Schmied Arch Pharmacol 383

[2] Kaiser et al. (2012) Cell. Microbiol. 14

[3] Dmochewitz et al. (2011) Cell. Microbiol. 13

[4] Lang et al. (2010) Science 327

[5] Gatsogiannis et al. (2013) Nature 495

[6] Lang, Ernst, Lee et al. (2013) Cell. Microbiol. Epub ahead of print doi:10.1111/cmi.12228

## 025

**Lipoic acid inhibits the DNA repair protein O<sup>6</sup>-methylguanine-DNA methyltransferase (MGMT) in vitro and in colorectal cancer cells**

**Göder, Anja**; Nagel, Georg; Kaina, Bernd; **Fahrer, Jörg**

Universitätsmedizin Mainz, Institut für Toxikologie, Germany

Alkylating agents occur in food and tobacco smoke, but are also used in cancer chemotherapy, inducing the cytotoxic and pre-mutagenic DNA lesion O<sup>6</sup>-methylguanine (O<sup>6</sup>-MeG). The DNA repair protein MGMT is responsible for the removal of O<sup>6</sup>-MeG adducts, by catalyzing the transfer of the methyl group from O<sup>6</sup>-MeG onto a cysteine residue in its catalytic cleft. This results in its inactivation and proteolytic degradation. Recent studies now provide evidence that MGMT is modulated by several natural compounds, including the disulfide-containing drug disulfiram.

In the present study, we analyzed the effects of the antioxidant lipoic acid (LA), an essential co-factor of pyruvate dehydrogenase and dietary supplement with disulfide structure, on MGMT *in vitro* and in colorectal tumor cells. First, recombinant MGMT was overexpressed in *E. coli* and purified to homogeneity, yielding highly active protein. Incubation of MGMT with LA *in vitro* led to a strong concentration-dependent inhibition of its activity with an IC<sub>50</sub> value of 35  $\mu$ M. This effect was partially reversible by pre-treatment with the antioxidant N-acetyl cysteine (NAC). Incubation of HCT116 colorectal cancer cells with LA suppressed cellular MGMT activity in a time- and concentration-dependent manner. Interestingly, this was mirrored on protein level by LA-induced depletion of cytoplasmic and nuclear MGMT, which was not observed after NAC treatment. Q-PCR analysis revealed no changes in MGMT mRNA levels in response to LA, suggesting a posttranslational mechanism of MGMT depletion. Strikingly, the decrease in MGMT protein levels coincided with LA-induced autophagy, a cellular mechanism involved in the lysosomal degradation of misfolded proteins. This was attested by Cyto-ID staining of autophagosomal vesicles and immunoblot analysis of the autophagy marker LC3B. siRNA knockdown of the crucial autophagy regulator Beclin-1 blocked LA-induced autophagy, but did not affect LA-mediated MGMT degradation. Chemical inhibition of autophagy by bafilomycin A1 had also no clear influence on LA-triggered MGMT depletion.

Taken together, our findings revealed the natural compound LA as a novel direct inhibitor of MGMT *in vitro* and in living cancer cells. The LA-dependent MGMT degradation was not attributable to autophagy induction and may rather involve the proteasomal pathway, which should be addressed in future studies.



## 026

**Do extremely low frequency magnetic fields have impact on adrenergic receptor binding in hematopoietic cells from rat spleen and bone marrow?**Fedrowitz, Maren<sup>1</sup>; Hass, Ralf<sup>2</sup>; Otte, Anna<sup>2</sup>; Löscher, Wolfgang<sup>1</sup><sup>1</sup>University of Veterinary Medicine, Dept. of Pharmacology, Toxicology, and Pharmacy, Hannover, Germany<sup>2</sup>Medical University, Dept. of Obstetrics and Gynecology, Biochemistry and Tumor Biology Lab, Gynecology Research Unit, Hannover, Germany

Extremely low frequency magnetic fields (ELF-MF) are ubiquitously distributed in our environment as they occur at higher field strengths near power lines and during use of electrical devices. There is evidence from epidemiological studies that ELF-MF exposure increase the risk for childhood leukemia, but the underlying mechanisms for ELF-MF effects on the hematopoietic system are still unclear. Recent studies suggest that adrenergic receptors are involved in cell proliferation and cancer development and are considered as new targets for tumor treatment (e.g. Cole & Sood, Clin Cancer Res, 2012 or Bruzzone et al. Brit J Pharmacol, 2008). In the present study, we investigated the binding to adrenergic receptors in primary spleen and bone marrow cells after *in vivo* ELF-MF exposure of rats from two inbred strains, Lewis and Fischer 344 (F344), with different sensitivities towards stress, carcinogens, and ELF-MF exposure. Female and male rats were exposed to 50 Hz ELF-MF at a field strength of 100  $\mu$ T for two weeks. Control groups were simultaneously sham-exposed in the same room. After preparation, cells were incubated with tritiated radioligands: prazosin (0.5 and 1 nM), yohimbine (2 and 5 nM), and CGP-12177 (2 and 10 nM) for alpha1-, alpha2, and beta1/2-receptors, respectively. In order to determine specific binding, concurrent incubations with radioligands and phentolamine (10  $\mu$ M) or propranolol (10  $\mu$ M) were performed for alpha- and beta-receptors, respectively. In Lewis spleen cells, a significantly increased alpha2-receptor binding was observed after *in vivo* ELF-MF exposure. In contrast, the beta-receptor binding was significantly enhanced in ELF-MF-exposed spleen cells from F344 but not Lewis. Investigations in bone marrow cells revealed a significantly decreased binding of yohimbine in cells from female Lewis. Cell cycle analysis showed no alterations in spleen and bone marrow cells from both strains after ELF-MF *in vivo*. The present investigations indicate that exposure to ELF-MF has impact on adrenergic receptor binding particularly in spleen cells. The observed effects were dependent on the rat strain and might be due to the different sensitivities of the strains concerning stress and the immune system. Further studies will concentrate on the role of ELF-MF exposure and the impact of adrenergic receptors on immune functions. This work is supported by the 7th Framework Program of the European Union (FP7-ENV-2011, Project ARIMMORA).

## 027

**C3 Rho-inhibitor for targeted pharmacological manipulation of osteoclast-like cells**Förtsch, Christina<sup>1</sup>; Tautzenberger, Andrea<sup>2</sup>; Zwerger, Christian<sup>1</sup>; Kreja, Ludwika<sup>2</sup>; Ignatius, Anita<sup>1</sup>; Barth, Holger<sup>1</sup><sup>1</sup>Universitätsklinikum Ulm, Institut für Pharmakologie und Toxikologie, Germany<sup>2</sup>Universitätsklinikum Ulm, Institut für Unfallchirurgische Forschung und Biomechanik, Germany

*Clostridium botulinum* and *Clostridium limosum* produce C3 toxins (C3bot1, and C3lim, respectively), which catalyze the ADP-ribosylation of Rho thereby inhibiting Rho-signalling in living cells [1]. We discovered earlier that C3bot1 and C3lim are selectively taken up into monocytes and macrophages by an endocytotic mechanism and cause typical morphological changes [2]. Therefore, C3bot1 and C3lim represent attractive molecular tools for a targeted pharmacological inhibition of Rho-dependent processes in monocytes/macrophages and derived cells. In comparison to C3bot1 and C3lim, the effects of the recombinant C2IN-C3lim fusion toxin [3] on RAW 264.7 macrophages was significantly stronger [3], suggesting that the C2IN portion of this protein might enhance the uptake of C3lim into the cytosol of these cells. Like the C3 toxins, C2IN-C3lim was not taken up into other cell types such as epithelial cells or fibroblasts.

Here, we investigated the effects of C2IN-C3lim on murine RAW 264.7 macrophages and osteoclast-like cells which were differentiated from RAW 264.7 cells by treatment with RANKL [4]. C2IN-C3lim was efficiently taken up into the cytosol of RAW 264.7 cells and inhibited their proliferation but did not induce cell death. C2IN-C3lim significantly decreased the RANKL-induced differentiation of RAW 264.7 cells into osteoclast-like cells *in vitro* [4]. This effect was concentration- and time-dependent and most effective when C2IN-C3lim was added at the early stage of differentiation. A single-dose application of C2IN-C3lim resulted in a decreased cell number, even when the toxin was removed after 24h while application of C2IN-C3lim at later time-points during osteoclast differentiation had no comparable effects. Control experiments with enzymatically inactive C3 toxin revealed that the C3-catalyzed ADP-ribosylation of Rho was essential for the observed effects. When applied to already differentiated osteoclasts, C2IN-C3lim was also taken up and inhibited their resorption activity *in vitro*. Other bone cell-types such as pre-osteoblastic cells were not affected by C2IN-C3lim. C3lim and C3bot1 showed overall comparable effects to C2IN-C3lim but were less efficient. Collectively, the results demonstrate that C3-treatment inhibits the Rho-dependent osteoclast differentiation and osteoclast activity *in vitro*, suggesting that C3 toxin and derived fusion toxins might be attractive lead compounds for development of novel therapeutic strategies against osteoclast-associated diseases.

[1] Vogelsang, M., Pautsch, A., & Aktories, K. C3 exoenzymes, novel insights into structure and action of Rho-ADP-ribosylating toxins. *Naunyn-Schmiedeberg's Arch. Pharmacol.* 374, 347-360 (2007).

[2] Fahrer, J. et al. Selective and specific internalization of clostridial C3 ADP-ribosyltransferases into macrophages and monocytes. *Cell Microbiol.* 12, 233-247 (2010).

[3] Barth, H., Hofmann, F., Olenik, C., Just, I., & Aktories, K. The N-terminal part of the enzyme component (C2I) of the binary *Clostridium botulinum* C2 toxin interacts with the binding component C2II and functions as a carrier system for a Rho ADP-ribosylating C3-like fusion toxin. *Infect. Immun.* 66, 1364-1369 (1998).

[4] Tautzenberger, Förtsch, Zwerger, Dmochewitz, Kreja, Ignatius and Holger Barth, PLOS ONE, in press

## 028

**PharmaSkills: a collaborative tool for clinical pharmacology**

Fensch, Isabelle; Wojnowski, Leszek

Johannes Gutenberg University, Department of Pharmacology, Mainz, Germany

Although drug prescribing constitutes a substantial part of physician activities and accounts for some 15% of healthcare costs, its teaching is frequently inadequate. Delivering clinical pharmacology curricula requires proficiency in a broad spectrum of clinical sciences, in addition to physiology, pathophysiology, chemistry, and pharmacology. Frequent changes in clinical guidelines and drug approval/availability status necessitate constant and time-consuming monitoring and updating. These challenges are particularly pronounced on the neighboring African continent, which suffers from faculty shortages, underdeveloped infrastructure, and over-crowding due to rapidly growing student enrolment. Since 2008, our Department has supported the development of an eLearning course in general and clinical pharmacology at the Kilimanjaro Christian Medical University College (KCMUCo) in Moshi, Tanzania. Based on this experience, in late 2012 we launched a collaborative Wiki tool PharmaSkills.org. PharmaSkills are pairs of questions and brief (<200 words) answers describing pharmacotherapeutic decisions in common clinical situations. PharmaSkills focus on practical drug prescribing competences according to current guidelines. Content of interest can be rapidly identified from a pop-down menu or using a search window. The individual PharmaSkills are linked to additional elements such as summaries of essential general and clinical information on relevant drugs and to current clinical guidelines. Users can comment on the content of the individual PharmaSkills, resulting in topic-specific discussion fora. Planned extensions include links to exemplary clinical vignettes and to self-assessment questions. The first 60 of the envisaged ~250 PharmaSkills have been developed with the active participation of our students and faculty and had 2500 visits in the first month. Taken together, PharmaSkills may provide a useful learning and reference tool for medical students and simultaneously they may help to define a consensus clinical pharmacology curriculum. The participation of interested clinical pharmacology teachers and their students from other medical faculties is encouraged.

## 029

**Testing mixtures *in vivo* at human-relevant exposure levels**Fussell, Karma Claire<sup>1</sup>; Schneider, Steffen<sup>1</sup>; Melching-Kollmuss, Stephanie<sup>1</sup>; Groeters, Sibylle<sup>1</sup>; Strauss, Volker<sup>1</sup>; Siddeek, Benazir<sup>2</sup>; Benahmed, Mohamed<sup>2</sup>; Frericks, Markus<sup>1</sup>; van Ravenzwaay, Bennard<sup>1</sup><sup>1</sup>BASF SE, Experimental Toxicology and Ecology, Ludwigshafen am Rhein, Germany<sup>2</sup>INSERM, U895/Centre Méditerranéen de Médecine Moléculaire (C3M), NICE Cedex 3, France

Endocrine disruption has become an important topic of public concern. Despite an increasing amount of attention, little is understood about whether environmentally relevant doses of endocrine disrupting chemicals (EDCs) affect homeostasis. Furthermore, knowledge gaps often exist in the studies used to assess EDCs. To address these concerns we performed pre-/post-natal reproductive toxicity studies to measure the developmental toxicity of low single- and mixture-doses of three anti-androgens. Doses were selected to mimic a low observed adverse effect level (LOAEL), the no observed adverse effect level (NOAEL) for endocrine effects, and the acceptable daily intake (ADI) for each compound, which were then additionally combined together into three mixtures of the LOAELs, NOAELs, and ADIs. The endocrine consequences of a larger effect dose of flutamide were also evaluated as a positive control.

While female offspring developed normally, the male offspring demonstrated anti-androgenic effects at the single and mixed LOAEL doses only. A significant decrease in anogenital distance on PND 1 and an increase in the number of nipples/areolas on PND 12 were noted in these animals. The latter effect was partially transient, as all had regressed by PND 20, except at the positive control dose. The male offspring in these dose groups which were reared to young adulthood displayed additional anti-androgenic effects including delayed sexual maturation and reduced sex organ sizes and weights; offspring from the positive control dose also had an increased incidence of developmental sexual defects. No adverse effects were noted at either the NOAEL or ADI dose levels. Assessment of molecular endpoints including the transcriptome, miRNome and metabolome (with hormone levels) is ongoing.

## 030

### **Clostridium difficile Toxin B induces programmed cell death independently of Rho GTPase glucosylation**

Gerhard, Ralf; Wohlan, Katharina; Tatge, Helma; Srivarahtarajan, Sangar; Goy, Sebastian; Genth, Harald; Just, Ingo  
Medizinische Hochschule Hannover, Institut für Toxikologie, Germany

Pathogenic *Clostridium difficile* produce two exotoxins, TcdA and TcdB, which glucosylate and thereby inactivate Rho GTPases. In consequence to Rho inhibition apoptosis is eventually induced in the cells. Cell death induced by high concentrations of TcdB is associated with cell shrinkage, chromatin condensation and loss of plasma membrane integrity, which are typical signs of pycnotic cell death. The glucosyltransferase deficient mutant TcdB D286/288N was also able to induce cell death with almost identical EC<sub>50</sub> values compared to wild type TcdB. Chromatin condensation was accompanied by ballooning of the nuclear envelope and an effect on the cell cycle was further investigated. In fact, phosphorylation of cell cycle associated proteins, i.e. Aurora B and C, and Histone H3 was affected by TcdB as well as by TcdB D286/288N. The EC<sub>50</sub> of Rho glucosylation and that of cytotoxic effect as measured by WST-test were 0.04 ng/ml and 140 ng/ml, respectively, for TcdB. Pycnotic cell death with specific phenotype of blister formation and chromatin condensation was specifically induced by TcdB from strain VPI10473 via the glucosyltransferase domain. A chimera of TcdB harbouring the glucosyltransferase domain of variant TcdB from cd1470 was unable to induce these effects. This newly discovered cytotoxic effect was not observed for TcdA and thus emphasizes the role of TcdB as cytotoxin and fertilizes discussion about the major human pathogen of *C. difficile*.

### **031**

#### **Integrated metabolic and spatial-temporal modelling identified a novel mechanism of ammonia detoxification**

Challab, Ahmed<sup>1,2</sup>; Henkel, Sebastian<sup>3</sup>; Driesch, Dominik<sup>3</sup>; Höhme, Stefan<sup>4</sup>; Zellmer, Sebastian<sup>5</sup>; Drasdo, Dirk<sup>6</sup>; Gebhardt, Rolf<sup>7</sup>; Hengstler, Jan G.<sup>1</sup>

<sup>1</sup>Leibniz Research Centre for Working Environment and Human Factors, Systems toxicology, Dortmund, Germany

<sup>2</sup>South Valley University, Faculty of Veterinary Medicine, Qena, Egypt

<sup>3</sup>Biocontrol, Jena, Germany

<sup>4</sup>Interdisziplinäres Zentrum für Bioinformatik, Leipzig, Germany

<sup>5</sup>German Federal Institute for Risk Assessment, Department of Product Safety, Berlin, Germany

<sup>6</sup>Institute National de Recherche en Informatique et en Automatique, Le Chesnay Cedex, France

<sup>7</sup>Universität Leipzig, Institut für Biochemie der Medizinischen Fakultät, Germany

Acute liver intoxication is life threatening due to the systemic impairment of metabolic homeostasis. Notably, hyperammonemia which develop following liver failure is the main player of hepatic encephalopathy. However, accurate calculation of metabolic alterations after hepatic intoxication is technically challenging. To improve the understanding of ammonia detoxification during liver damage and regeneration we established an integrated metabolic and spatial-temporal model. First a metabolic model involving all already known mechanisms of ammonia detoxification was established. We then integrated the metabolic model to a spatial-temporal model simulating the destruction and the regeneration process following CCl<sub>4</sub> intoxication. For model validation we used a mouse system where the hepatotoxic agent CCl<sub>4</sub> was injected. Metabolic parameters relevant for ammonia detoxification were measured in the portal vein "liver inflow", the hepatic vein "liver outflow" and in the right heart chamber "mixed venous blood" in a time dependent manner after CCl<sub>4</sub> intoxication. Interestingly, the model predicts much higher ammonia output compared to the experimental data. After iterative cycles of experiments and modelling we identified a so far unknown mechanism that can systemically detoxify ammonia. Upon acute liver damage glutamate dehydrogenase (GDH) is released into the systemic circulation. As soon as blood ammonia concentrations elevated this enzyme switches from the normal ammonia production into ammonia consumption. This occurs by consumption of ammonia plus alpha-ketoglutarate ( $\alpha$ -KG) and production of glutamate. However, this reaction is only limited by the depletion of  $\alpha$ -KG. This suggests that substitution of  $\alpha$ -KG in patients with acute liver failure might provide a systemic detoxification of ammonia via the reversed GDH reaction. These data show how the integrated metabolic and spatial-temporal modelling improved the understanding of ammonia detoxification and identified the necessity of  $\alpha$ -KG substitution upon acute liver damage.

### **032**

#### **Transgenic mice for real time visualization of cGMP in intact adult cardiomyocytes**

Götz, Konrad; Nikolaev, Viacheslav

Emmy Noether Gruppe der DFG, Universitätsmedizin Göttingen, Kardiologie und Pneumologie, Germany

cGMP is an important second messenger which is involved in the regulation of cardiac contractility and pathological hypertrophy. Signaling by cGMP is considered cardioprotective, but due to the lack of real-time imaging techniques, little is known about the spatio-temporal dynamics of cGMP in adult cardiomyocytes. Therefore, we generated a transgenic mouse model with cardiomyocyte-specific expression of the highly sensitive fluorescence resonance energy transfer (FRET)-based cGMP biosensor red cGES-DE5 to visualize cGMP dynamics in isolated adult mouse cardiomyocytes. Furthermore FRET experiments were performed in cardiomyocytes isolated from mice,

transgenically expressing the FRET-based cAMP sensor Epac1-camps to analyze cGMP/cAMP signaling crosstalk. We found relatively low basal cGMP levels (~10 nM), which can be increased by stimulation of particulate guanylyl cyclases with natriuretic peptides (CNP, ANP), especially CNP shows strongest signals (CNP>>ANP/BNP). This is in clear contrast to soluble guanylyl cyclase (sGC) activity, where stimulation with NO donors such as SNAP and DEA/NO could not increase cytosolic cGMP. However we could detect small FRET responses to NO donor in the presence of isoproterenol plus the PDE5 inhibitor tadalafil. In addition, constitutive activity of this cyclase is involved in basal cGMP production, since inhibition of sGC with ODC showed a decrease of cGMP levels. Interestingly, we found that PDE3 is the predominant cGMP-hydrolyzing PDE. Inhibition of PDE 1, 2 and 5 had only little effect, whereas PDE3 inhibitor cilostamide, even under stimulated conditions, showed strong responses, suggesting that PDE3 is the major cGMP-PDE family controlling cGMP levels at basal state and in the presence of cGMP/cAMP agonists. This was also the case in a model of cardiac hypertrophy after transverse aortic constriction model. In hypertrophied cells, we could also observe as significant increase in the PDE5 inhibitor response. In summary, we successfully generated a transgenic mouse model for cGMP-FRET measurements in adult cardiomyocyte and could show that cGMP pools produced by GC-B after CNP stimulation are mainly regulated by PDE3, so this receptor and PDE form one functional unit important for the regulation of cGMP/cAMP cross-talk.

### **033**

#### **Signaling mechanisms of cell in cell invasion**

Grosse, Robert

Universität Marburg, Pharmakologie, Germany

Non-apoptotic plasma membrane blebs, known as cancer cell blebbing, are actin-dependent dynamic cellular protrusions critically important for tumor cell invasiveness and metastasis. Here we exploited a model system for the investigation of sustained cancer cell blebbing using hydrogel-coated surfaces. Under these conditions, cells undergo active, bleb-dependent homotypic cell-in-cell invasion, a not well understood process frequently observed during cancer spread. Using systematic siRNA analysis we identified LPA receptor 2 (LPA2) and G $\alpha$ 12 signaling to be necessary for cell-in-cell invasion. We further found that during sustained blebbing, the SRF coactivator MAL (also known as MRTF-A or MKL1) localizes to the cell nucleus, whereas in non-blebbing cells MAL predominantly resides in the cytoplasm. Assuming that there is a functional role of nuclear MAL in blebbing, we investigated several genes known to be involved in non-apoptotic plasma membrane blebbing and identified the cortical actin linker Ezrin as a novel MAL/SRF target-gene. Together, these results identify G-protein-coupled receptor signaling as well as MAL/SRF transcriptional activity for productive membrane dynamics and cell in cell invasion.

### **034**

#### **Expression and function of TRPM3 proteins in mouse pituitary gland**

Hasan, Nouma<sup>1</sup>; Beck, Andreas<sup>1</sup>; Mannebach, Stefanie<sup>1</sup>; Weißgerber, Petra<sup>1</sup>; Freichel, Marc<sup>1</sup>; Philipp, Stephan

<sup>1</sup>Universität des Saarlandes, Institut für Experimentelle und Klinische Pharmakologie und Toxikologie, Homburg, Germany

<sup>2</sup>Rupprechts-Karls-Universität Heidelberg, Pharmakologisches Institut, Germany

TRPM3 proteins form Ca<sup>2+</sup>-permeable cation channels in the plasma membrane that are activated by the neurosteroid pregnenolone sulphate (PregS) and efficiently blocked by flavanones like hesperetin. TRPM3 channels are expressed in pancreatic  $\beta$ -cells and dorsal root ganglion neurons where they are involved in insulin secretion and pain perception, respectively. TRPM3 transcripts are also expressed in human hypophysis and a plethora of other cells and tissues. However, their function in these tissues is still unknown.

Northern and Western blots and RT-PCR analysis confirmed expression of TRPM3 transcripts and proteins in the whole pituitary gland of the mouse and indicated TRPM3 expression in both neuro and adenohypophysis. Accordingly, mice expressing the green fluorescent protein under the control of the TRPM3 promoter displayed prominent GFP-expression in the posterior lobe (PL), weaker expression in the intermediate lobe (IL) as well as expression in single cells of the anterior lobe (AL). Immunohistochemical analysis indicated TRPM3 expression in folliculostellate cells of the anterior lobe, pituicytes of the posterior lobe and finally in  $\alpha$ -melanocyte-stimulating hormone ( $\alpha$ -MSH)-releasing (melanotrope) cells.

Fura-2 imaging experiments uncovered PregS-inducible Ca<sup>2+</sup> entry in both AL and IL/PL cells that was blocked by hesperetin. Consistently, we detected PregS/hesperetin sensitive currents in melanotrope cells that largely resembled currents through recombinant TRPM3 channels and that were not detected in melanotropes from TRPM3-deficient mice. Our data demonstrate functional expression of TRPM3 channels in  $\alpha$ -MSH-secreting cells and provide the basis for a deeper understanding of their biological role in the pituitary gland.

## 035

**Increased lymphocyte-mediated tumor cell killing by cannabinoids via upregulation of ICAM-1 expression**Haustein, Maria<sup>1</sup>; Ramer, Robert<sup>1</sup>; Linnebacher, Michael<sup>2</sup>; Hinz, Burkhard<sup>1</sup><sup>1</sup>Institute of Toxicology and Pharmacology, University of Rostock, Germany<sup>2</sup>Section of Molecular Oncology and Immunotherapy, Department of General Surgery, University of Rostock, Germany

Cannabinoids have recently been shown to promote the expression of the intercellular adhesion molecule-1 (ICAM-1) on lung cancer cells as part of their anti-invasive and antimetastatic action. Using lung cancer cell lines (A549, H460) and metastatic cells derived from a lung cancer patient, the present study addressed the impact of cannabinoid-induced ICAM-1 upregulation on cancer cell adhesion to lymphokine-activated killer (LAK) cells and LAK cell-mediated cytotoxicity. Cannabidiol (CBD), a non-psychoactive cannabinoid, enhanced the susceptibility of cancer cells to adhesion to and subsequent lysis by LAK cells, with both effects being reversed by a neutralizing ICAM-1 antibody. Increased cancer cell lysis by CBD was likewise abrogated when CBD-induced ICAM-1 expression was blocked by specific siRNA or by antagonists to cannabinoid-activated receptors (CB<sub>1</sub>, CB<sub>2</sub>, transient receptor potential vanilloid 1). In addition, enhanced killing of CBD-treated cancer cells was reversed by preincubation of LAK cells with an antibody to lymphocyte function associated antigen-1 (LFA-1) suggesting intercellular ICAM-1/LFA-1 crosslink as crucial event for CBD-induced killing of lung cancer cells by LAK cells. An ICAM-1-dependent cancer cell killing by LAK cells could further be confirmed when lung cancer cells were treated with the phytocannabinoid  $\Delta^9$ -tetrahydrocannabinol or with R(+)-methanandamide, a stable endocannabinoid analogue. Altogether, our data demonstrate that cannabinoid-induced upregulation of ICAM-1 on lung cancer cells is responsible for increased cancer cell susceptibility to LAK-mediated cytotoxicity. These findings provide first-time proof for a novel mechanism within the diverse antitumorigenic effects of cannabinoids.

## 036

**Modulation of stress resistance and related signalling in cell culture and *Caenorhabditis elegans* by baicalein derivatives**

Wilke, Simone; Stolz, Stephan; Wätjen, Wim; Havermann, Susannah

Martin-Luther-Universität Halle-Wittenberg, Biofunktionalität sekundärer Pflanzenstoffe, Germany

Extracts derived from Baical Skullcap (*Scutellaria baicalensis* Lamiaceae) are used in Traditional Chinese Medicine (TCM) for the treatment of several diseases. One of the major compounds is the flavonoid baicalein (5,6,7-trihydroxyflavone) which may be responsible for the biological effects of the extracts. We have previously demonstrated that baicalein is an activator of the redox sensitive Nrf2/ARE-pathway both in Hct116 human colon carcinoma cells and the model organism *Caenorhabditis elegans* (Nrf2-homologue SKN-1). This pathway modulates oxidant response, stress resistance and ageing (SKN-1) by regulating the expression of a set of antioxidant and phase II drug metabolising enzymes. To elucidate the structural features responsible for the biological activity of baicalein, we studied effects of baicalein-6-methylether (oroxylin A), baicalein-7-methylether (negletein) and baicalein-5,6,7-trimethylether on Hct116 cells and *C. elegans*.

Baicalein, oroxylin A and negletein are potent direct antioxidants in a cell free system (TEAC-Assay), while the methylation of all three hydroxyl groups blocks this property. The influence on intracellular ROS accumulation was surveyed using the fluorescent probe dihydrofluorescein diacetate in the human colon carcinoma cell line Hct116 and *in vivo* in *C. elegans*. Baicalein and negletein further showed the beneficial effect of prolonging the life span of *C. elegans*. We therefore analysed the effect of the compounds on the localisation of the ageing-associated transcription factor using a transgenic strain expressing a SKN-1::GFP fusion protein. Further life span assays with knock-down of SKN-1 using RNAi were performed to reveal the role activation of SKN-1 plays concerning the observed positive effects. In comparison to these *in vivo* experiments the modulation of the Nrf2-pathway in Hct116 cells by the baicalein derivatives was analysed using western blot and a reporter gene assay. Baicalein and negletein activated Nrf2 while the other compounds did not.

This study showed that the OH-groups of baicalein are important for the activation of the mammalian transcription factor Nrf2 and its homologue SKN-1 (*C. elegans*). Our results indicate that the catechol moiety at positions 5 and 6 is sufficient for the activation. The potency of the compound is increased by an additional hydroxyl function.

## 037

**Influences of I(f)-channel blockade with ivabradine on heart rate and sympathetic vasoconstrictor activity**Heusser, Karsten<sup>1</sup>; Brinkmann, Julia<sup>1</sup>; Schroeder, Christoph<sup>1</sup>; Grossheppig, Anika<sup>2</sup>; Wenzel, Daniela<sup>2</sup>; Diedrich, André<sup>3</sup>; Sweep, Fred C.<sup>4</sup>; Mehling, Heidrun<sup>5</sup>; Luft, Friedrich C.<sup>5</sup>; Tank, Jens<sup>1</sup>; Jordan, Jens<sup>1</sup><sup>1</sup>Hannover Medical School, Institute of Clinical Pharmacology, Germany<sup>2</sup>Hannover Medical School, Institute of Biostatistics, Germany<sup>3</sup>Vanderbilt University School of Medicine, Autonomic Dysfunction Center, Nashville, United States<sup>4</sup>Radboud University Nijmegen Medical Centre, Department of Laboratory Medicine, Netherlands<sup>5</sup>Charité Medical Faculty and Max Delbrück Center for Molecular Medicine, Experimental Clinical Research Center, Berlin, Germany

**Background:** Hyperpolarization-activated and cyclic nucleotide-gated 4 (HCN4) channels produce the sinus node pacemaker current which is regulated through cAMP, thus, providing a common pathway for sympathetic and parasympathetic heart rate (HR) control. We hypothesized that HCN4 blockade affects baroreflex HR regulation such that HR is reduced at a given blood pressure. Furthermore, we assessed the effect on resting muscle sympathetic nerve activity (MSNA).

**Methods:** Twenty-one healthy male subjects (27±4 years) completed a double-blind, placebo-controlled, cross-over study. They ingested ivabradine (7.5 mg) or placebo 13 and 1 hour before measurements with ≥3 weeks washout between treatments. We continuously recorded EKG, finger blood pressure, impedance cardiograms, and MSNA. In addition, we assessed brachial blood pressures and cardiac output by foreign gas rebreathing. Incremental infusions of sodium nitroprusside and phenylephrine were used for pharmacologic baroreflex characterization. We applied the relationship between heart rate and systolic blood pressure obtained during drug infusions to individually normalize HR to mean resting systolic blood pressure of both visits (primary endpoint). Furthermore, we analyzed venous plasma catecholamine concentrations.

**Results:** I(f) blockade reduced normalized supine heart rate from 65.9±8.1 to 58.4±6.2 bpm (p<0.001). Likewise, there was a HR fall without normalization (61.9±7.0 vs 58.1±6.5 bpm, p=0.012). Systolic (123±8 vs 122±8 mmHg, p=0.649) and diastolic (68.5±5.3 vs 69.1±5.4 mmHg, p=0.582) blood pressure remained unchanged with ivabradine. Despite lowered HR, stroke volume was not increased (118±23 vs 118±18 ml, p=0.899). There was a trend towards reduced cardiac output (7.74±1.60 vs 7.19±1.15 l/min, ~-7.6%, p=0.071) and increased peripheral resistance (956±185 vs 1010±160 dyn\*s/cm<sup>5</sup>, ~5.6%, p=0.088). I(f) blockade did not affect MSNA (burst frequency: 28.4±7.9 vs 26.2±6.7 bursts/min, p=0.221; burst incidence: 46.0±11.3 vs 45.3±12.1 bursts/100 heart beats, p=0.575; total MSNA: 1.14±0.45 vs 1.26±0.76 au/min, p=0.892). Plasma catecholamine levels were not changed (noradrenaline: 1040±500 vs 910±210 pM, p=0.654; adrenaline: 135±84 vs 132±64 pM, p=0.553; dopamine: 69±25 vs 70±14 pM, p=0.520). Baroreflex heart rate regulation (16.8±8.4 vs 14.8±6.5 ms/mmHg, p=0.151) and sympathetic baroreflex sensitivity (-2.74±1.07 vs -2.53±0.83 bursts/min/mmHg, p=0.247) were similar with placebo and with ivabradine.

**Conclusion:** In healthy young men, HCN4 blockade with ivabradine reduces HR leaving physiological baroreflex HR regulation intact. The HR reduction is not associated with reflex sympathetic activation.

## 038

**Marine Sponge compounds Aaptamine and Agelasin D confer protection against genotoxic stress in the *in vivo* model organism *C. elegans***Honnen, Sebastian<sup>1</sup>; Jung, Alexander<sup>1</sup>; Pohl, Christin<sup>1</sup>; Dresler, Miriam<sup>1</sup>; Proksch, Peter<sup>2</sup>; Fritz, Gerhard<sup>1</sup><sup>1</sup>Heinrich Heine University, Toxicology, Düsseldorf, Germany<sup>2</sup>Heinrich Heine University, Pharmaceutical Biology and Biotechnology, Düsseldorf, Germany

Due to its short generation time, well-characterized developmental timing, transparency as well as easy genetic accessibility, the nematode *C. elegans* has become a model system to study both DNA damage response and effects of natural compounds *in vivo*. As in other multicellular organisms, a conserved set of DNA repair and apoptosis pathways can be activated in *C. elegans* after ionizing radiation (IR) to maintain genome stability (e.g. *atm-1*(hATM) and *rad-51*(hRAD51)). Various natural compounds have been shown to protect against genotoxic insults *in vitro* or, rarely investigated, in living animals, often because of their direct antioxidant capacities. Our aim is to systematically analyze the dose-response relationship between IR treatment and a subset of functional readouts in *C. elegans* including developmental timing, fertility, viability, life span and specific gene expression profiles (RT-qPCR Array). These findings will provide the basis for subsequent investigation of genoprotective effects of natural compounds with low antioxidant capacity.

By now, we have established an optimized low volume liquid culture system for easy application of natural compounds in a reproducible manner. Dose-response analyses were performed to investigate the radiosensitivity of *C. elegans* regarding fertility, viability and mean lifespan. Hereby, we confirmed that *C. elegans* is highly resistant against IR. Using this setup we were able to discover genoprotective effects of compounds with high antioxidant capacity like chlorogenic acid and myricetin. Interestingly, the marine sponge constituents Aaptamine and Agelasin D, which have only low antioxidant capacity, are even more radioprotective. Pre-treatment with these compounds leads to significantly higher viability of embryos after acute irradiation (60 or 120 Gray). Noteworthy, 24 h pre-treatment with Agelasin D prolongs the mean lifespan of adult animals in irradiated populations (60 or 120 Gray) by up to 25%. Now we aim to further develop these findings and to identify more natural compounds which distinctively influence the IR-induced gene expression profile and have beneficial effects with respect to the aforementioned functional readouts after IR. Moreover, we phenotypically characterized mutant knockout strains for specific DNA repair pathways. Using these we will test which compounds can rescue repair mutants from deleterious effects of UV radiation.

## 039

**Innate immune responses to essential virulence factors of *Pseudomonas aeruginosa*, a bacterium critical to cystic fibrosis patients****Horke, Sven**<sup>1,2</sup>; Teiber, John<sup>3</sup><sup>1</sup>Universitätsmedizin Mainz, Institut für Pharmakologie, Germany<sup>2</sup>Centrum für Thrombose und Hämostase Mainz, Germany<sup>3</sup>UT Southwestern Medical Center, Internal Medicine, Division of Epidemiology, Dallas, United States

Although many details of cystic fibrosis (CF) have been uncovered, therapeutic progress lacks behind and patients suffer from co-morbidities, especially infections by opportunistic, nosocomial pathogens. *Pseudomonas aeruginosa* (P.a.) is frequently found in CF patients, causes critical health complications and resists many antibiotics. Its virulence is regulated by a bacterial communication system termed quorum sensing (QS) and relies on distinct, secreted molecules. These also damage cells of the infected host, but many of their mechanisms are unknown. Inactivation of virulence factors is a novel, antibiotic-adjuvant strategy to combat such pathogens. The mammalian enzyme PON2 is a natural system mediating the inactivation of two critical virulence factors, the redox-active pyocyanin and the lactone 3OC12. The oxidative stress-inducing effect of pyocyanin is alleviated by PON2 due to its anti-oxidant function. Further, PON2 has a dominant role in inactivation, i.e. hydrolysis of 3OC12. Because 3OC12 is vital to P.a. virulence and lung persistence as well as to immunomodulation of host cells, there is substantial interest in identifying its receptor and the acute responses of exposed cells. Our novel data however suggest a receptor-independent pathway. We found that PON2 hydrolyzes 3OC12 to an acid, which accumulates presumably in mitochondria and causes cellular acidification. This gives rise to Ca<sup>2+</sup> liberation and p38 / eIF2α phosphorylation. Activation of other MAPK members (ERK; JNK) was PON2-independent. We thus identified a new system of how key responses in host cells are triggered by specific bacteria that threaten CF patient health. Importantly, we identified the crucial molecules relevant to CF airway epithelia along with the mechanism of action.

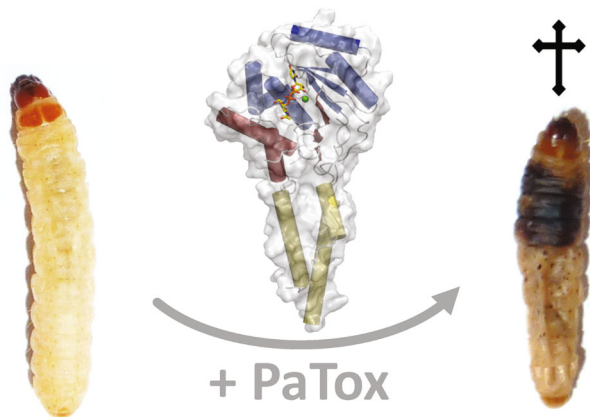
## 040

**Bacterial Toxin Kills by Tyrosine Glycosylation of Rho-GTPases****Jank, Thomas**; Steinemann, Marcus; Böhmer, Kira E.; Aktories, Klaus

Institut für Experimentelle und Klinische Pharmakologie und Toxikologie, Albert-Ludwigs-Universität Freiburg, Abt. I, Freiburg i. Br., Germany

Entomopathogenic *Photobacterium asymbiotica* is an emerging pathogen in humans. We identified a *P. asymbiotica* protein toxin (PaTox), which contains a glycosyltransferase domain and mono-O-glycosylates Y32 (or Y34) of eukaryotic Rho GTPases by using UDP-N-acetylglucosamine (UDP-GlcNAc). Tyrosine glycosylation inhibits Rho activation and prevents interaction with downstream effectors, resulting in actin disassembly, inhibition of phagocytosis and toxicity toward insects and mammalian cells. The crystal structure of the PaTox glycosyltransferase domain in complex with UDP-GlcNAc determined at 1.8-Å resolution represents a canonical GT-A fold and is the smallest glycosyltransferase toxin known. <sup>1</sup>H-NMR analysis identifies PaTox as a retaining glycosyltransferase. The modification of tyrosine residues by glycosylation expands the array of posttranslational modifications and offers a new perspective in carbohydrate, bacterial toxin and biopesticide research.

Jank, T. et al. A bacterial toxin catalyzing tyrosine glycosylation of Rho and deamidation of Gq and Gi proteins. *Nat. Struct. Mol. Biol.* 20, 1273-1280 (2013).

**Action of PaTox:**

*Photobacterium asymbiotica* PaTox kills *Galleria mellonella* insect larvae by tyrosine glycosylation of Rho

## 041

**Ang II-induced calcium signaling complexly regulates CTGF in cardiac fibroblasts****Kittana, Naim**; Albrecht, Wiebke; Jatho, Aline; Würtz, Christina; Schenk, Kerstin; Ramba, Beate; Lutz, Susanne

Universitätsmedizin Göttingen, Institut für Pharmakologie, Germany

Cardiac fibroblasts (CF) play a major role in fibrogenesis associated with heart failure as they produce ECM components and secrete important fibrosis-associated mediators, such as connective tissue growth factor (CTGF). Here we investigate the role of the angiotensin II (Ang II) type1 receptor (AT<sub>1</sub>-R)-induced, Ca<sup>2+</sup>-dependent signaling in the regulation of CTGF in neonatal rat CF. We demonstrate on one hand that the Ca<sup>2+</sup> transient in response to Ang II was diminished upon AT<sub>1</sub>-R, phospholipase-C-β and IP3 receptor inhibition by valsartan, U73122 and xestospingonin-C (XeC), respectively. On the other hand Ang II induced a strong Ca<sup>2+</sup> transient even in the absence of extracellular Ca<sup>2+</sup> and in accordance the depletion of intracellular Ca<sup>2+</sup> by thapsigargin completely inhibited the Ca<sup>2+</sup> transient similar to the chelator BAPTA-AM. Interestingly, the blockade of membranous TRPC3 channels by pyrazole 3 enhanced the Ang II-induced Ca<sup>2+</sup> transient. From this data we concluded that the most important source of calcium in CF is the ER whereas extracellular Ca<sup>2+</sup> seems to fine tune the calcium transient. In the next step we analyzed the impact of the calcium transient on the mRNA and protein level as well as on the secretion of CTGF. We found that BAPTA-AM inhibited the effect of Ang II on intracellular and secreted CTGF levels, besides it inhibited both the basal and Ang II-induced CTGF mRNA transcription. Dissection of the Ca<sup>2+</sup> pathway showed that IP3 receptor inhibition mainly reduced the Ang II-induced CTGF secretion whereas the blockade of TRPC3 channels resulted in an increase in CTGF secretion without changing its transcription. Finally, we analyzed the involvement of the Ca<sup>2+</sup>-dependent phosphatase calcineurin by using cyclosporine A as an inhibitor. This treatment had no effect on the Ang II-induced Ca<sup>2+</sup> transient, however, it induced both basal and stimulated CTGF transcription as well as CTGF secretion. The intracellular CTGF content was, however, reduced, most probably due to alterations in membrane structures as demonstrated by immunofluorescence.

In conclusion, in CF Ang II induces Ca<sup>2+</sup> transients by mobilizing Ca<sup>2+</sup> mainly from intracellular stores via the canonical G<sub>q11</sub> pathway. The contribution of extracellular Ca<sup>2+</sup> is minor and seems to tune the release of intracellular Ca<sup>2+</sup>. Ca<sup>2+</sup> coming from different sources contribute differently to the regulation of CTGF expression and secretion.

## 042

**Identification of novel mechanisms of LDL uptake into endothelium****Kraehling, Jan Robert**; Rajagopal, Chitra; Sessa, William Charles

Yale University, Pharmacology, New Haven, United States

Cardiovascular diseases are the leading cause of death in westernized countries. The majority of these patients suffer from coronary heart disease (CHD). The pathology of CHD is well understood, but the pathogenesis or the early steps of lipoprotein accumulation in the subendothelial area remains still unclear. In conditions of hypercholesterolemia, the LDL receptor (LDLR) at the surface of endothelial cells (EC) is mostly downregulated, but LDL can still pass the endothelium. We hypothesize, that there is an additional uptake route for LDL particles across the endothelium despite from the well characterized LDLR. To address this question, we developed a genome-wide siRNA high throughput screen. We used EA.hy 926 cells, a human umbilical vein endothelial cell hybridoma line with many characteristics of primary human ECs. The uptake of fluorescent labeled LDL (DiI-LDL) was visualized in 384-well plates via an automated confocal laser microscope (Opera<sup>®</sup>, Perkin Elmer). We were able to identify 53 genes, which increase the uptake of LDL particles into the endothelium. To rule out genes, which are involved in the classical clathrin-dependent endocytosis, we used fluorescent labeled transferrin and performed an identical uptake study. With this approach, we reduced the number of potential target genes to 16, only three of which are endothelial specific genes. Two of these genes are not described yet and are still named by their genome location. The third gene codes for activin A receptor-type-II-like kinase 1 (ACVRL1). It was already shown, that ACVRL1 is enriched in human coronary atherosclerotic lesions. We could show by surface plasmon resonance that LDL particles can directly bind to the receptor kinase.

Vasile E, Simionescu M, Simionescu N. Visualization of the binding, endocytosis, and transcytosis of low-density lipoprotein in the arterial endothelium in situ. *The Journal of cell biology.* 1983;96:1677-1689

Yao Y, Zebboudj AF, Torres A, Shao E, Bostrom K. Activin-like kinase receptor 1 (alk1) in atherosclerotic lesions and vascular mesenchymal cells. *Cardiovascular research.* 2007;74:279-289

Skalen K, Gustafsson M, Rydberg EK, Hultén LM, Wiklund O, Innerarity TL, Boren J. Subendothelial retention of atherogenic lipoproteins in early atherosclerosis. *Nature.* 2002;417:750-754

## 043

**Differential participation of Gβγ in the binding of GRK2 to G-protein-coupled receptors****Krasel, Cornelius**; Prokopets, Olga; Zindel, Diana; Wolters, Valerie; Bünemann, Moritz; Philipps-Universität Marburg, Institut f. Pharmakologie u. Klin. Pharmazie, Germany

G-protein-coupled receptors are generally believed to undergo homologous desensitization by the consecutive action of GRKs (which phosphorylate agonist-occupied receptors) and arrestins (which bind to phosphorylated, agonist-occupied receptors, thereby competing with heterotrimeric G-proteins). We have attempted to measure receptor desensitization by following the interaction of receptors with G $\beta\gamma$  in real time using fluorescence resonance energy transfer (FRET). GRK2 slowed down the interaction of CFP-tagged G $\beta$  with the  $\alpha_{2A}$ -adrenergic receptor but not with the A $_1$  adenosine receptor; both receptors are coupled to G $_i$ . GRK2 did not have any effect on the interaction of the G $\alpha_{i1}$  subunit with the receptor, and the GRK2(D110A) mutation, which reduces its affinity to G $\alpha_{i1}$ , did not have any effect on the GRK2-G $\beta\gamma$  interaction. The effect of GRK2 was independent of its catalytic activity but dependent on its G $\beta\gamma$ -binding activity since a GRK2 mutation that drastically reduced its affinity to G $\beta\gamma$  (R587Q) also abolished the effect of GRK2 on receptor-G $\beta\gamma$  interaction. These experiments show that GRK2 can influence the interaction between G-protein-coupled receptors and G $\beta\gamma$  in a receptor-specific manner. In an attempt to further clarify the mechanism behind this specificity, we directly investigated the interaction of mTurquoise-tagged GRK2 with YFP-tagged  $\alpha_{2A}$ -adrenergic and A $_1$  adenosine receptors using FRET. GRK2(R587Q) interacted only to a very small extent with both receptors, presumably due to its inability to translocate to the membrane. We therefore attached a CAAX motif to the C-terminus of the GRK2-mTurquoise fusion protein. CAAX-tagged GRK2 interacted very rapidly with agonist-activated receptors, showing that translocation to the membrane is time-limiting for GRK2-receptor interaction. CAAX-tagged GRK2 and GRK2(R587Q) showed virtually identical dissociation rates from the  $\alpha_{2A}$ -adrenergic receptor upon washout of agonist, but the off-rate at the A $_1$  adenosine receptor was about two-fold faster for GRK2(R587Q)-CAAX than for wild-type GRK2-CAAX. This suggests that besides its role for membrane translocation G $\beta\gamma$  has no further influence on the binding mode of GRK2 with the  $\alpha_{2A}$ -adrenergic receptor. In contrast, G $\beta\gamma$  subunits stabilize the GRK2 interaction with the A $_1$  adenosine receptor in addition to their function as a membrane anchor for GRK2.

## 044

### Efflux of cGMP dampens cGMP signals in smooth muscle cells and reduces blood vessel relaxation

Krawutschke, Christian; Koesling, Doris; Russwurm, Michael

Ruhr-Universität Bochum, Institut für Pharmakologie und Toxikologie, Germany

The second messenger cGMP plays an important role in blood vessel relaxation. cGMP is formed by NO-sensitive guanylyl cyclases and natriuretic peptide receptor guanylyl cyclases, both of which are expressed in vascular smooth muscle cells. cGMP is degraded by cyclic nucleotide phosphodiesterases; three PDE isoforms are present in smooth muscle cells, PDE1, PDE3 and PDE5.

Here, we investigated the impact of PDE3 and PDE5 on cGMP signals elicited by physiologically relevant NO concentrations and analyzed blood vessel relaxation in organ bath experiments. The use of FRET-based cGMP indicators allowed for real time measurements of cGMP signals in primary aortic smooth muscle cells. With this method, cGMP signals induced by much lower NO concentrations than those required for cGMP measurements in radioimmunoassays were detectable. The remarkable sensitivity of this approach is emphasized by the half maximally effective NO concentrations (~ 10 nM GSNO) that were comparable to those required for blood vessel relaxation in organ bath experiments.

Unexpectedly, inhibition of PDE3 did not alter the NO concentration response curve and PDE5 inhibition only caused a moderate shift of the curve (2-fold). Hence, we were wondering if efflux of cGMP across the plasma membrane contributes to the elimination of cGMP. Multi drug resistance protein 4 (MRP4), an ATP binding cassette protein, has been proposed to mediate active transport of cyclic nucleotides across the plasma membrane. At the half maximally effective NO concentration, MRP4 inhibition potentiated the cGMP signal to almost maximal levels (40% change of the FRET signal) and shifted the NO concentration response curve by a factor of 2.5. Blood vessel relaxation assessed in organ bath experiments confirmed these observations: inhibition of MRP4 enhanced GSNO-induced relaxation.

In sum, the data demonstrate that efflux of cGMP substantially contributes to its elimination and thus affects intracellular cGMP signals to an extent comparable to phosphodiesterases.

## 045

### Evaluation of risk prescriptions and physicians' feedback in a method for improving medication safety in ambulatory care

Laidig, Friederike<sup>1</sup>; May, Marcus<sup>1</sup>; Brinkmann, Julia<sup>1</sup>; Herbarth, Lutz<sup>2</sup>; Boldt, Kerstin<sup>2</sup>; Jordan, Jens<sup>1</sup>; Stichtenoth, Dirk O.<sup>1</sup>

<sup>1</sup>Medizinische Hochschule Hannover, Institut für Klinische Pharmakologie, Germany

<sup>2</sup>Kaufmännische Krankenkasse Hannover, Germany

**Abstract Objective** Medication errors in ambulatory care are frequent. Because the process of prescribing and medication therapy is more complex than in hospital settings adequate methods to avoid medication errors are difficult to implement. In our study we investigated a campaign from a health insurance company that had the aim to increase medication safety within insureds with polypharmacy and multimorbidity. **Method** An expert team consisting of clinical pharmacologists and a pharmacist analysed the medication of insureds for risk prescriptions who had an additional telephonic health coaching. Attending physicians received a report and were offered to contact the experts for counselling. Results of medication analyses of 400 insureds were categorized in

eight types of prescribing errors and feedback from the physicians was recorded. Differences in medication therapy after counselling were scanned. **Main outcome measure** The frequency of medication errors in eight categories and physicians' feedback, further changes in medications of physicians responding. **Results** Insureds were 48% female and 52% male and took an average of 13.4 drugs regularly. 16.8% of the physicians contacted replied, 13.3% had a counselling conversation. 29.2% of the physicians replying gave a positive response to the campaign, 13.8% a negative and for 56.9% a neutral feedback was given. Out of a total of n=2524 errors 26.8% occurred in the category *missing indication*, 6.8% in *PRISCUS medication*, 33.3% in *interactions*, 15.3% in *wrong dosage*, 0.9% in *contraindication*, 2.8% in *dosage adaption to renal function*, 6.9% in *double medication* and 7.2% in *gap of prescribing*. **Conclusion** A large number of medication errors appear in ambulatory care and consequently adverse drug events and hospital admissions are more likely to happen. Medication check by pharmacotherapy experts and pharmacological consulting with a high response of physicians can be a key tool to reduce these errors. Cooperation of a health insurance company and clinical pharmacologists is an effective association but needs to be optimized for better acceptance and more rapid ability to react.

## 046

### Cdk5 is implicated in breast cancer stem cell formation

Leibl, Johanna<sup>1</sup>; Zhang, Siwei<sup>1</sup>; Mandl, Melanie<sup>1</sup>; Schmoedel, Elisa<sup>2</sup>; Mayr, Doris<sup>2</sup>; Zahler, Stefan<sup>1</sup>; Vollmar, Angelika<sup>1</sup>

<sup>1</sup>LMU, Pharmazie, Pharmazeutische Biologie, München, Germany

<sup>2</sup>LMU, Pathologisches Institut, München, Germany

Breast cancer represents one of the leading causes of cancer related death of females and its incidence is growing. Despite the initial effectiveness of chemotherapy, resistance, recurrence and metastases limit therapeutic success of breast cancer treatment. The relatively high rate of relapse of aggressive breast cancer is attributed to breast cancer stem cells (CSCs). Breast CSCs are resistant to standard therapy, show high tumor-initiating potential and cause establishment of metastases. Therapeutic strategies that target breast CSCs therefore may substantially improve breast cancer treatment and patient prognosis.

Our study points to a function of Cyclin dependent kinase 5 (Cdk5) in breast CSCs. Cdk5 is a serine/threonine kinase that exerts important functions in the central nervous system. In contrast, only recently, the awareness of non-neuronal functions of Cdk5 has grown and its role in cancer is not well investigated. Recently, Cdk5 was linked to epithelial-mesenchymal transition of breast epithelial cells. Because EMT can lead to CSC formation and CSCs have mesenchymal properties, the aim of the present study was to evaluate a potential function of Cdk5 in breast CSCs. Staining of breast cancer tissues in a tissue microarray (TMA) demonstrated that Cdk5 is expressed in human breast cancer and that its expression in tumor cells is increased compared to respective healthy tissue. Furthermore, Cdk5 activity correlates with cancer cell invasiveness. Pharmacologic inhibition and genetic downregulation of Cdk5 reduces breast cancer motility and invasion. To analyze a potential function of Cdk5 in breast CSCs, we performed mammosphere assays where breast CSCs are cultivated under specific conditions that allow only specific clonal expansion of CSCs. Cdk5 inhibition, transient silencing as well as stable genetic knockdown inhibited mammosphere formation, whereas Cdk5 overexpression leads to increased number and size of mammospheres. Our results indicate Cdk5 as regulator of breast CSCs and suggest Cdk5 signalling as oncogenic pathway that drives breast cancer. Therefore, our work points to Cdk5 as potential target for addressing breast CSCs.

## 047

### Transcriptional regulation of PAR-4 thrombin receptor by sphingosine-1-phosphate enhances COX-2 expression and migration in human monocytes

Mahajan-Thakur, Shailaja<sup>1</sup>; Sostmann, Björn<sup>2</sup>; Schrör, Karsten<sup>2</sup>; Rauch, Bernhard H.<sup>1</sup>

<sup>1</sup>Universitätsmedizin Greifswald, Institut für Pharmakologie, Germany

<sup>2</sup>Universitätsklinikum Düsseldorf, Institut für Pharmakologie und Klinische Pharmakologie, Germany

The sphingolipid metabolite sphingosine-1-phosphate (S1P) regulates multiple cellular processes such as migration, proliferation and survival. In particular, S1P is a newly recognized modulator of monocyte function. Thrombin also activates inflammatory responses including monocyte migration via activation of cell surface protease-activated receptors (PARs). Therefore, we investigated the involvement of S1P and human monocyte responses to thrombin.

The cell line U937 was used as a human monocyte model. Primary monocytes were isolated from healthy volunteers using the Dynabeads® Untouched™ monocytes kit (Invitrogen). PAR expression was measured by flow cytometry, Western blotting and Taqman® real-time PCR. Cell migration was determined in a modified Boyden Chamber assay.

Incubation with S1P induced PAR-1 and PAR-4 mRNA and total protein expression in both human monocytes and U937 cells in a concentration (0.1-10  $\mu$ M) and time (1-24 h)-dependent manner. Cell surface expression of PAR-4 was markedly increased by S1P, while PAR-1 was not elevated at the surface. Incubation of human monocytes or U937 cells with S1P (1  $\mu$ M; 16 h) enhanced chemotaxis towards thrombin. This was predominantly mediated via elevated PAR-4 expression as suggested by the use of selective activating-peptides for PAR-1 and PAR-4. Accordingly, PAR-4 silencing by RNA interference attenuated the chemotactic response to thrombin or PAR-4 activation. After preincubation with S1P, thrombin or the PAR-4 activating-peptide stimulated an

enhanced phosphorylation of the kinases Akt, Erk and p38. In addition, expression of cyclooxygenase (COX)-2 was elevated by S1P and significantly amplified by thrombin or PAR-4 activation over 3 to 24 h. In comparison, expression of COX-1 was not affected. In conclusion, the bioactive lipid S1P induces an enhanced expression of the thrombin receptors PAR-1 and PAR-4 in monocytes. This results in enhanced pro-migratory and inflammatory signaling particularly via PAR-4. This mechanism may facilitate monocyte recruitment to sites of vessel injury and inflammation.

## 048

### Chemical mustards induce characteristic poly(ADP-ribosyl)ation dynamics in human keratinocytes with distinctive effects on genotoxicity

**Mangerich, Aswin**<sup>1</sup>; Debiak, Malgorzata<sup>1</sup>; Birtel, Matthias<sup>1</sup>; Ponath, Viviane<sup>1</sup>; Martello, Rita<sup>1</sup>; Lex, Kirsten<sup>1</sup>; Steinritz, Dirk<sup>1</sup>; Schmidt, Annette<sup>2</sup>; Bürkle, Alexander<sup>1</sup>  
<sup>1</sup>Universität Konstanz, Molekulare Toxikologie, Germany  
<sup>2</sup>Bundeswehr Institute of Pharmacology and Toxicology, München, Germany

Chemical mustards are potent DNA alkylating agents with mutagenic, cytotoxic, and vesicant properties. They exist as bifunctional agents, such as bis( $\beta$ -chloroethyl) sulfide (sulfur mustard, SM) or bis(2-chloroethyl)methylamine (mustine, HN2), or as monofunctional agents, such as 2-chloroethyl ethyl sulfide (half mustard, CEES). Whereas SM was previously used as a chemical warfare agent, several nitrogen mustard derivatives are being used as established chemotherapeutics.

The nucleic acid-like biopolymer poly(ADP-ribose) (PAR) is synthesized by poly(ADP-ribose) polymerases (PARPs) upon induction of genotoxic stress using NAD<sup>+</sup> as a substrate. Previously, it was shown that SM triggers cellular poly(ADP-ribose)ylation (PARylation), but a detailed characterization of this phenomenon awaits further clarification. Interestingly, due to their anti-inflammatory action, PARP inhibitors have been discussed as potential antidotes for SM exposure.

In this study, we performed a comprehensive characterization of the PARylation response in a human keratinocyte cell line (HaCaT) after treatment with SM, CEES, and HN2 on a qualitative, quantitative and functional level. In particular, we report substance-specific as well as dose- and time-dependent PARylation dynamics using independent bioanalytical methods based on single-cell immunofluorescence microscopy and isotope dilution mass spectrometry. Furthermore, we analyzed if and how PARylation contributes to mustard-induced genotoxicity. Thus, e.g., CEES-induced cell death appears to be not affected by cellular PARylation as revealed by cytotoxicity studies and the analysis of intracellular NAD<sup>+</sup> levels. On the other hand, mustard-induced poly(ADP-ribose)ylation actively participates in cellular stress response mechanisms, as it is evident from the findings that PARP inhibition impairs cellular proliferation, clonogenic survival, and genomic stability of HaCaT cells upon mustard treatment.

In conclusion, this study demonstrates that PARylation plays a functional role in mustard-induced toxicological mechanisms. To this end, PARP inhibitors exhibit therapeutic potential to treat SM-related pathologies and to sensitize cancer cells for mustard-based chemotherapy. Yet, potential long-term effects of PARP inhibition on genomic stability and therefore cancer formation should be carefully evaluated, when pursuing these developments.

## 049

### Evidence for a role of premature senescence in cardiac fibrosis

**Meyer, Kathleen**<sup>1,2</sup>; Hodwin, Bettina<sup>1</sup>; Engelhardt, Stefan<sup>1,2</sup>; Sarikas, Antonio<sup>1,2</sup>  
<sup>1</sup>Technische Universität München, Institute of Pharmacology and Toxicology, Munich, Germany  
<sup>2</sup>DZHK (German Center for Cardiovascular Research), partner site Munich Heart Alliance, Germany

**Introduction:** Premature senescence is a tumorsuppressive mechanisms leading to p16<sup>INK4a</sup> or p53-mediated cell cycle arrest upon telomere shortening or oncogenic signaling. Recent studies have demonstrated a role for premature senescence in fibrogenesis of the liver and skin fibrosis (Krizhanovsky et al., 2008; Jun and Lau, 2010).

**Aims and objectives:** The aim of this study was to investigate the pathophysiological role of premature senescence in cardiac fibrosis and to identify affected cell populations within the myocardium.

**Methods and results:** Two established murine models of cardiac fibrosis, transaortic constriction (TAC) and cardiomyocyte-specific beta1 adrenergic receptor transgenic mice (beta1-TG), were employed to study the role of premature senescence in the heart. Fibrosis was detected by Sirius Red staining and Realtime PCR (Col1a2, Col3a1). For quantification of premature senescence, the proliferation marker Ki67, cell cycle regulators p16<sup>INK4a</sup> and p21 and senescence-associated (SA)-beta-galactosidase were monitored by immunohistology, histochemistry and Realtime PCR.

In the TAC model, 3,5% Ki67 positive nuclei were detected after 2 weeks (mild fibrosis) and 0,5% after 6 weeks (severe fibrosis) when compared to 1% Ki67 positive nuclei in sham controls (n=3-7). Senescence marker p16<sup>INK4a</sup> and p21 increased 15-fold and 2-fold, respectively, six weeks after TAC when compared to sham controls (n= n=3-7; p < 0.05). SA- $\beta$ -galactosidase increased 4-fold two and six weeks after TAC, respectively, when compared to sham controls (3,5% and 4% vs. 0,5%; n=3-7; p < 0.01). In the beta1-TG model, 2% of nuclei were p16<sup>INK4a</sup> positive in five months old beta1-TG mice (mild fibrosis) and 15% at ten months of age (severe fibrosis) when compared to 0,5% in wild-type littermates (n=4-7). SA- $\beta$ -galactosidase was increased 2-fold in after 5

months and 6-fold after ten months in heart sections of TG mice when compared to WT littermates (n= 3-6; p<0.01).

Analysis of isolated primary cardiac fibroblasts and cardiomyocytes by Realtime-PCR (SA- $\beta$ -galactosidase) and co-immunostaining with the fibroblast marker vimentin identified cardiac fibroblasts as the major cell population undergoing premature senescence in cardiac fibrosis.

**Summary and conclusion:** Our results provide evidence for a critical role of premature senescence for fibrogenesis in the heart. It is tempting to speculate that pharmacological interference with senescence mechanisms might provide novel therapeutic strategies for the treatment of cardiac fibrosis.

## 050

### STRUCTURAL REQUIREMENTS FOR THE DIFFERENTIAL SIGNALING OF CCR2 CHEMOKINE RECEPTORS

**Markx, Daniel**; Koenig, Carolin; Hipp, Lisa; **Moeps, Barbara**  
 Pharmacology and Toxicology, University of Ulm, Medical Center, Germany

Chemokines and their receptors are known to regulate a wide array of leukocyte functions, including chemotaxis, adhesion, and transendothelial migration. Chemokine receptors, which are members of the G-protein-coupled receptor family, are coupled to pertussis-toxin-sensitive and, in certain cases, to pertussis-toxin-insensitive heterotrimeric G protein(s), as well as G protein-independent arrestins. Accordingly, the carboxyl-terminal portions of several GPCRs, including the CCR2 chemokine receptors, have been shown to interact with multi-protein complexes made up of heterotrimeric G protein subunits and non-G-protein-components. We have previously reported that stimulation with CCL2 of the two human CC chemokine receptors CCR2a and CCR2b transiently expressed in COS-7 or HEK293 cells resulted in enhanced serum-response-factor (SRF)-dependent transcriptional activation of a luciferase reporter gene. CCL2-dependent induction of SRF activity was specifically mediated by G $\alpha_q$  and G $\alpha_{14}$ , but not by G $\alpha_{11}$  and G $\alpha_{16}$ . Structure- function- analysis revealed that arginine<sup>313</sup> of the juxtamembrane octapeptide representing the amino-terminal-most portion of a putative 'eighth helix' of CCR2 was critically involved in G $\alpha_q$  protein activation. Thus CCL2-mediated activation of SRF was found strongly reduced in cells expressing CCR2a<sup>R313A</sup>- or CCR2a<sup>R313E</sup>- and CCR2b<sup>R313A</sup>- or CCR2b<sup>R313E</sup>-mutants. To delineate the relevance of arginine 313 to other CCL2-mediated cellular responses, (i) G $\alpha_q$ -dependent activation of extracellular regulated kinases 1/2 (ERK) and (ii) G protein-independent internalization of CCR2 receptors were analyzed in cells expressing wild-type or mutant CCR2b. The results show that arginine 313 within the putative 'eighth helix' in immediate proximity of the variable carboxyl-terminal portions of CCR2b is specifically required for the G $\alpha_q$ -mediated activation of SRF and plays a role in G protein-independent internalization, but is not involved in G $\alpha_q$ -mediated induction of ERK1/2.

## 051

### Mechanism of Tank binding kinase 1 during inflammatory nociception

**Möser, Christine**<sup>1</sup>; Stephan, Heike<sup>1</sup>; Olbrich, Katrin<sup>1</sup>; Lu, Ruirui<sup>2</sup>; Russe, Otto<sup>1</sup>; Geisslinger, Gerd<sup>1</sup>; Niederberger, Ellen<sup>1</sup>  
<sup>1</sup>pharmazentrum frankfurt/ZAFES, Institut für Klinische Pharmakologie, Frankfurt am Main, Germany  
<sup>2</sup>Universität Witten/Herdecke, Institut für Pharmakologie und Toxikologie, Germany

TANK binding Kinase 1 (TBK1) is an enzyme with high homology to the classical I- $\kappa$ B kinase subunits, IKK $\alpha$  and IKK $\beta$ . In spite of this similarity, it is mainly discussed as kinase involved in defence against viral infections by modulating type I interferons. However, in vitro studies revealed a role of TBK1 and its complex-partner inhibitor-kappaB kinase epsilon (IKK $\epsilon$ ) in the regulation of NF- $\kappa$ B activity, but the distinct mechanisms of TBK1- and IKK $\epsilon$ -mediated NF- $\kappa$ B activation are not completely understood and no in vivo data are available so far. Given the paramount role of NF- $\kappa$ B in inflammation we investigated the regulation and function of TBK1 in models of inflammatory hyperalgesia in mice.

We found that TBK1 is abundantly expressed in nociceptive neurons and astrocytes in the spinal cord. Moreover in primary cell culture of astrocytes and neurons we observed an increased expression of TBK1 mRNA and protein levels after stimulation with a cytokinmix. Beside, TBK1 mRNA and protein levels rapidly increased in the spinal cord during hind paw inflammation evoked by injection of zymosan or formalin. TNF $\alpha$ /TBK1 double-knock-out mice showed normal nociceptive responses to acute heat or mechanical stimulation. However, in inflammatory pain models TNF $\alpha$ /TBK1 deficient mice exhibited a significantly reduced nociceptive behaviour in comparison to TNF $\alpha$  knock-out control mice indicating that the kinase contributes to the development of inflammatory hyperalgesia. In TNF $\alpha$ /TBK1 double-knock-out mice, antinociceptive effects were associated with an attenuated NF- $\kappa$ B-dependent induction of cyclooxygenase-2 (COX-2). However, an altered induction of cFos, a NF- $\kappa$ B independent gene was also observed in TNF $\alpha$ /TBK1 double-knock-out mice, indicating an involvement of the MAPK-pathway. Therefore, we hypothesize that TBK1, beside IKK $\epsilon$ , is an important mediator in inflammatory pain pathways.

The work is supported by the Deutsche Forschungsgemeinschaft (NI 705/2-1), Graduate School "Biologicals" (GRK 1172) and Nachwuchsförderungsgrnt des Klinikums der Goethe Universität Frankfurt am Main.

## 052

**Real time imaging of  $G_{\alpha 13}$  signaling reveal hypersensitive LARG activation**

Müller, Anna-Lena; Bodmann, Eva-Lisa; Bünemann, Moritz

Philipps-Universität Marburg, Institut für Pharmakologie und Klinische Pharmazie, Germany

GPCR mediated G protein activation induces downstream signaling, allowing cells to exert their physiological functions. Much has been learned in the past about dynamics of classical G protein cascades, however the  $G_{12/13}$  signaling cascade has been so far difficult to investigate due to the lack of specific inhibitors and the promiscuity of their activating receptors. Here, we took a Förster resonance energy transfer (FRET)-based approach to specifically analyze thromboxane  $A_2$  receptor (TXA $_2$ )-mediated activation of heterotrimeric  $G_{13}$  proteins and their subsequent interaction with Leukemia-associated RhoGEF (LARG). Therefore, we labeled the respective proteins with cyan and yellow fluorescent proteins and verified their functional integrity by means of serum response factor (SRF)-dependent luciferase assays. Single living cells were subjected to FRET-microscopy. Thus, we found that  $G_{13}$  proteins exhibited fast (subsecond) activation upon receptor stimulation with U46619, whereas deactivation after agonist withdrawal was more than 10 times slower. These kinetics are similar to those described for  $G_{i/o}$ ,  $G_q$  and  $G_s$  proteins. Interestingly, we observed a remarkable difference in the EC $_{50}$  values between the thromboxane-mediated  $G_{13}$  activation and the thromboxane-induced  $G_{\alpha 13}$ -LARG-interaction. The  $G_{\alpha 13}$ -LARG interaction was about 25 times more sensitive to the agonist than the  $G_{13}$  activation as measured by  $\alpha_{13}$ -G $\beta_2$  interaction. This hypersensitivity of the  $G_{\alpha 13}$ -LARG interaction is accompanied by substantially slower dissociation kinetics compared to the speed of  $G_{13}$  deactivation after agonist withdrawal. These slow dissociation kinetics of G protein and effector may provide a simple mechanistic explanation for hypersensitive receptor mediated LARG activation.

## 053

**The role of  $Ca^{2+}$  in murine sinoatrial node pacemaking**

Nguyen, Huong; Stieber, Juliane; Ludwig, Andreas

Institut für Experimentelle und Klinische Pharmakologie und Toxikologie, Erlangen, Germany

Heart rhythm and rate is controlled by the spontaneous activity of pacemaker cells in the sinoatrial node (SAN), generating the diastolic depolarization. The Ryanodine receptor 2 (RyR2) releases  $Ca^{2+}$  from the sarcoplasmic reticulum (SR) and is hypothesized to facilitate the  $Na^+/Ca^{2+}$  exchanger current ( $I_{NCX}$ ), attributable for the late phase of the diastolic depolarization following the  $I_f$  current. In this work we present evidence for the vital role of SR released  $Ca^{2+}$  in sinoatrial pacemaking by electrophysiological recordings of SAN cells from RyR2 KO mice. SAN cells of KO mice showed a decelerated diastolic depolarization rate, a reduced upstroke velocity and a slightly prolonged repolarization rate. In addition to these effects, leading to an increased action potential duration and significant bradycardia, SAN cells with no visible disposition to action potential generation were found. The overall effects of the impaired SR  $Ca^{2+}$  release suggested a regulatory effect of intracellularly circulating  $Ca^{2+}$  apart from its function as a carrier. Analysis of  $I_f$  current, after modulation of intracellular  $Ca^{2+}$  content by changing the extracellular  $Ca^{2+}$  concentrations (0.2 mM, 1.8 mM, 3.6 mM), demonstrated a correlation between  $Ca^{2+}$  and the  $I_f$  current as  $Ca^{2+}$  depletion (0.2 mM) caused a deceleration of the activation kinetic. We believed the effect of  $Ca^{2+}$  on the HCN4, being the predominant isoform in SAN, was indirectly transmitted by a stimulation of  $Ca^{2+}$ /Calmodulin activated adenylate cyclase I, which we were able to detect in RT-PCR and Western Blot analysis. Taken together our data suggest, that  $Ca^{2+}$  additional to its role as a carrier inducing a depolarizing phase in the SAN cell, acts as a vital modulator in the events resulting in pacemaker activity.

## 054

**The ABCC11 variant T546M, a predictive biomarker for 5-FU induced severe leukopenia, strongly reduces ABCC11 transport activity *in vitro***Lang, Thomas<sup>1</sup>; Arlanov, Rudolf<sup>1</sup>; Ishikawa, Toshihisa<sup>2</sup>; Schwab, Matthias<sup>1,3</sup>; Nies, Anne T.<sup>1</sup><sup>1</sup>Dr. Margarete Fischer-Bosch Institute of Clinical Pharmacology, Stuttgart, Germany<sup>2</sup>RIKEN Center for Life Science Technologies, Yokohama, Japan<sup>3</sup>Institute of Experimental and Clinical Pharmacology and Toxicology, University Hospital, Department of Clinical Pharmacology, Tübingen, Germany

The multidrug resistance protein 8 (MRP8/ABCC11) mediates the active cellular efflux of several endogenous and exogenous compounds conferring resistance to antiviral agents and anticancer drugs such as 5-fluorouracil (5-FU). Missense variants of ABCC11 contribute to human disorders and interindividual variability in drug disposition and ultimately in drug response. Very recently, the ABCC11 protein variant T546M has been associated with the development of leucopenia after 5-FU monotherapy of patients. The aim of the present study was to investigate whether T546M and four common ABCC11 protein variants (R19H/A317E, V648I, H1344R) cause alterations in protein expression levels, protein targeting and ABCC11-mediated substrate transport compared to ABCC11 wild-type (WT) *in vitro*. We used the established 'Screen and Insert' technology to achieve stable and highly reproducible expression of ABCC11 (WT, variants) in human embryonic kidney (HEK293) cells. The ABCC11-mediated transport of the sulfated steroids dehydroepiandrosterone and estrone sulfate was determined in

HEK293-derived plasma membrane vesicles. For both substrates, transport activity was significantly decreased by 70-80% for T546M compared to WT, while protein targeting and total expression levels were not influenced. None of the other investigated variants had any effect on ABCC11 function. Impaired transport activity of ABCC11-T546M may contribute to an increased risk for 5-FU induced leukopenia.

## 055

***Pasteurella multocida* toxin stimulates osteoclast differentiation by activation of heterotrimeric G proteins**

Strack, Julia; Aktories, Klaus; Orth, Joachim

Institut für Pharmakologie und Toxikologie, Freiburg, Germany

*Pasteurella multocida* causes pasteurellosis in man and animals. An important virulence factor produced by serotype A and D strains is the 146-kDa protein toxin *Pasteurella multocida* toxin (PMT). PMT activates various signaling cascades by acting on the heterotrimeric G proteins  $G_{\alpha q11}$ ,  $G_{\alpha 12/13}$  and  $G_{\alpha i}$ . The molecular mechanism to stimulate heterotrimeric G proteins is a deamidation of an essential glutamine residue in the switch II region of the  $\alpha$ -subunit arresting the G protein in a permanent active state.

The toxin is the causative agent to induce atrophic rhinitis in pigs, which is characterized by rapid degradation of nose turbinate bones leading to the deformation of the snout. This effect on bone proposes an effect on cells involved in the permanent regeneration of bone, osteoblasts and osteoclasts. Recently, we provided mechanistic insights in the PMT-dependent inhibition of osteoblastogenesis. Here, we studied the effect of PMT on bone resorbing osteoclasts. As a model we used bone marrow derived osteoclast progenitor cells (CD14-positive monocytes) and RAW246.7 cells. PMT stimulated osteoclast differentiation as measured by expression of tartrate-resistant acid phosphatase and multi-nucleation. The toxin's effect was comparable to RANKL (receptor activator of nuclear factor  $\kappa$ -B ligand), the key physiological factor inducing osteoclastogenesis. Analysis of the signaling pathways elucidated that PMT induced transcriptional activity of AP-1, NF- $\kappa$ B and NFATc1, which are all essential in osteoclast differentiation. Moreover, we could show transcriptional activity and differentiation depends on transactivation of the MAP kinase cascade via  $G_{\alpha q11}$ .

The present work provides new insights, how PMT controls differentiation of osteoclasts and supports the pathophysiological understanding of bone loss during atrophic rhinitis. Finally, our results provide evidence that besides the canonical RANKL-induced pathway other signaling cascades like the ones of heterotrimeric G proteins are capable to induce or to regulate the maturation of osteoclasts.

## 056

**Pharmacological properties of L-type calcium channel blockers with potential selectivity for Cav1.3**Ortner, Nadine<sup>1</sup>; Bock, Gabriella<sup>1</sup>; Draheim, Henning<sup>2</sup>; Mauersberger, Robert<sup>3</sup>; Gust, Ronald<sup>3</sup>; Tuluc, Petronel<sup>1</sup>; Striessnig, Jörg<sup>1</sup><sup>1</sup>University of Innsbruck, Department of Pharmacology and Toxicology, Austria<sup>2</sup>Boehringer Ingelheim Pharma GmbH & Co. KG, Div. Research Germany, Ingelheim am Rhein, Germany<sup>3</sup>University of Innsbruck, Pharmaceutical Chemistry, Austria

Motor symptoms in Parkinson's disease (PD), the most common neurodegenerative movement disorder, are caused by a progressive loss of dopaminergic neurons in the substantia nigra pars compacta. Recent studies implicate Cav1.3 L-type calcium channel (LTCC)-induced dendritic calcium oscillations in the pathogenesis of PD. Available LTCC blockers cannot sufficiently distinguish between the two main brain LTCC isoforms, Cav1.2 and Cav1.3. Therefore, Cav1.3-selective antagonists could lead to neuroprotection in PD sparing Cav1.2 dependent peripheral cardiovascular side effects.

Here we investigated the pharmacological properties of two pyrimidine 2,4,6-trione derivatives with recently reported  $\approx$ 40-fold (Cp3) and  $>$ 100-fold (Cp8) selectivity for Cav1.3 vs. Cav1.2 (Kang et al., Nat. Comm. 2012). Pharmacological modulation of  $I_{Ba}$  (10 or 15mM  $Ba^{2+}$ ) or  $I_{Ca}$  (15mM  $Ca^{2+}$ ) through Cav1.3 (rat or human long splice variant, rCav1.3 $_L$ , hCav1.3 $_L$ ) and Cav1.2 (rabbit long or short C-terminus, rbCav1.2 $_L$ , rbCav1.2 $_S$ ) expressed together with b3 and a2d1 subunits in tsA-201 cells was measured using whole cell patch-clamp.

Using 100ms long depolarizations from a holding potential of -80mV (0.2Hz) or -70mV (0.05Hz) to  $V_{max}$ , both compounds reproducibly showed a slowly developing and reversible change in gating kinetics of  $I_{Ca}$ . This was characterized by a slowing of activation and inactivation kinetics, accompanied by an increase of the tail current by 4.5- (n=11, p=0.0002) or 5.5-fold (n=11, p=0.0002) for rbCav1.2 $_S$  or hCav1.3 $_L$ , respectively. This kinetic change was similar for both channel isoforms. Slowing of activation caused a decrease of initial  $I_{Ca}$  by 34% (n=11, p=0.0002) or 40% (n=12, p=0.0021) after 7ms (rbCav1.2 $_S$ ) or 4ms (hCav1.3 $_L$ ) by 50 $\mu$ M Cp8, respectively. This complex modulation was also observed for both compounds in the majority of  $I_{Ba}$  recordings. In about 30% of  $I_{Ba}$  recordings only a concentration-dependent inhibition of peak inward current was observed (2-17% or 10-27% with 10 or 50 $\mu$ M) without kinetic change. Modulation of Cav1.3 and Cav1.2 constructs was similar without evidence for selectivity.

Taken together, we could not observe potent and Cav1.3-selective activity of these compounds. Both, however, induced previously not reported changes in kinetics resembling in some aspects LTCC activators such as BAYK8644. We conclude that the reported Cav1.3 selectivity can only be observed under special experimental conditions that are difficult to reproduce.

## 057

### Identification of the host receptor for *Clostridium perfringens* TpeL toxin indicates a two-receptor model of clostridial glycosylating toxins

**Papatheodorou, Panagiotis**; Schorch, Björn; Song, Shuo; Aktories, Klaus  
Albert-Ludwigs-Universität Freiburg, Institut für Experimentelle und Klinische  
Pharmakologie und Toxikologie, Germany

Clostridial glycosylating toxins are major virulence factors of various species of pathogenic *Clostridia*. Prototypes are *Clostridium difficile* toxins A and B, which cause antibiotics-associated diarrhea and pseudomembranous colitis. The current model of the toxins' action suggests that receptor-binding is mediated by a C-terminal domain of combined repetitive oligopeptides (CROP). This model is challenged by the glycosylating *Clostridium perfringens* TpeL toxin that is devoid of the CROP domain but still intoxicates cells. Using a haploid genetic screen, we identified the host cell receptor for the TpeL toxin. Receptor-deficient cells were not intoxicated by TpeL but regained sensitivity towards the toxin after ectopic expression of the receptor. By plasmon resonance spectroscopy a  $K_D$  value of 23 nM was determined for binding of TpeL to its receptor. We further identified that the C-terminus of TpeL represents the receptor-binding domain (RBD) of the toxin. RBD-like regions are conserved in all other clostridial glycosylating toxins preceding their CROP domain. We found that CROP-deficient *C. difficile* toxin B is toxic to cells, depending on the RBD-like region but does not share the same receptor as TpeL for cell entry. Our data indicate the presence of a second, CROP-independent receptor-binding domain in clostridial glycosylating toxins and suggest a two-receptor model for the cellular uptake of clostridial glycosylating toxins. Thus, our study offers a new perspective in the understanding of the pathogenicity of this group of clinically important toxins. Identification of the cell membrane receptor and the receptor-binding domains are groundbreaking steps for the development of anti-toxin strategies.

## 058

### Oxacyclododecindione – a new promising substance in SLE treatment

**Henke, Jenny**<sup>1</sup>; Menke, Julia<sup>2</sup>; Erkel, Gerhard<sup>3</sup>; Kleinert, Hartmut<sup>1</sup>; **Pautz, Andrea**<sup>1</sup>

<sup>1</sup>Universitätsmedizin Mainz, Institut für Pharmakologie, Germany

<sup>2</sup>Universitätsmedizin Mainz, I. Med. Klinik, Germany

<sup>3</sup>Technische Universität Kaiserslautern, Molekulare Biotechnologie und Systemische Biologie, Germany

**Objective:** Oxacyclododecindione (Oxa) is a novel macrocyclic lactone isolated from the imperfect fungus *Exserohilum rostratum*. In recent studies, Oxa showed in several *in-vitro* models a high anti-inflammatory, anti-angiogenic and anti-fibrotic activity. The aim of our study was to investigate the effect of Oxa in the MRL-FAS<sup>pr</sup> mouse model. This mouse strain spontaneously develops an autoimmune disease similar to human SLE with a severe glomerulonephritis. The main cause of the disease is the production of autoantibodies, the activation of the complement system and the deposition of immune complexes. We treated female MRL-FAS lpr mice with Oxa (1mg/kg) every other day by intraperitoneally injection over a time period of five weeks. The effects of the substances were analyzed in comparison to a control group, which was treated with PBS/EtOH (10%).

**Results:** We detected on mRNA and protein level that Oxa treatment down regulates the expression of different chemokines and cytokines such as TNF $\alpha$ , INF $\gamma$ , CCL2 and RANTES in the kidney. In addition, FACS and immunohistochemical analysis revealed a significant decrease of the total number of CD20<sup>+</sup> B-cells and CD4<sup>+</sup> T-cells in the kidney. In accordance with our mRNA and protein data we detected less IL-17<sup>+</sup> and INF $\gamma$ <sup>+</sup> T-cells. Moreover, kidney function, determined by proteinuria, IgG and collagen deposition, was improved by Oxa treatment. In addition, we detected under Oxa treatment less circulating dsDNA antibodies. All data are min. \* = p < 0.05 vs. PBS/EtOH treated control group.

**Conclusion:** Our analyses provide evidence that Oxa is a new promising anti-inflammatory compound which has positive effects in the SLE model of MRL-FAS<sup>pr</sup> mice. This substance may serve as lead structure for the development of new therapeutics for the treatment of chronic inflammatory as well as fibrotic diseases. In the future, the target molecules of Oxa have to be identified to understand the molecular mechanisms of the Oxa mediated effects.

## 059

### The epigenetic mark 5hmC recruits a dynamic set of readers in the retina

**Perera, Arshan**<sup>1</sup>; Eisen, David<sup>2</sup>; Wagner, Mirko<sup>2</sup>; Laube, Silvia K<sup>2</sup>; Müller, Markus<sup>2</sup>; Biel, Martin<sup>1</sup>; Carell, Thomas<sup>3</sup>; Michalakis, Stylianos<sup>1</sup>

<sup>1</sup>Ludwig-Maximilians-Universität München, Center for Integrated Protein Science Munich CIPSM at the Department of Pharmacy – Center for Drug Research, Germany

<sup>2</sup>Ludwig-Maximilians-Universität München, Center for Integrated Protein Science at the Department of Chemistry, Germany

Hydroxylation of genomic 5-methylcytosine (5mC) by Tet enzymes has been proposed to play a key role in the formation, plasticity and function of neuronal circuits. However, the exact mechanisms controlling Tet enzyme activity and 5-hydroxymethylcytosine (5hmC) levels in neurons are not known. Here, we used the mouse retina to study the role of 5hmC during maturation of neuronal circuits. To identify specific readers of 5hmC and 5mC in retinal cells we applied a protein pull-down experiment combined with mass

spectrometry (MS) at two developmental time points: before eye opening (postnatal day (p) 11) and at a time point when retinal maturation is completed (p21). We incubated biotin coupled double-stranded DNA oligos containing 5hmC or 5mC or unmodified cytosines with nuclear protein extracts from p11 or p21 mouse retina to precipitate and purify DNA binding proteins. After tryptic digestions peptides were chemically labeled with tandem mass tags in forward and reverse experiments and subsequently analyzed using liquid chromatography coupled to MS. We identified 212 specific readers of 5hmC and 43 specific readers of 5mC in the mouse retina. The majority of readers appeared to be specific for a particular cytosine modification whereas 10 of the identified proteins were readers of both 5mC and 5hmC. There was no overlap between 5mC readers at the two developmental stages. However, eight 5hmC readers were conserved between the two ages. Gene ontology analysis revealed that biological functions related to cellular assembly and organization, DNA replication, recombination and repair or cellular morphology were significantly enriched within the set of 5hmC-specific readers whereas the set of 5mC readers was enriched in proteins involved in chromatin or histone modification or negative regulation of gene expression. In total, 23 (4 at p11 and 19 at p21) of the 5hmC readers identified in the retina are regulators of transcription. In contrast, only five 5mC readers at p11 and one at p21 could be classified as regulators of transcription. In summary, our data provide strong evidence for a role of 5hmC as epigenetic regulator in the retina.

## 060

### Aldosterone activates transcription factor Nrf2 in kidney cells both *in vitro* and *in vivo*

**Queisser, Nina**<sup>1</sup>; Oteiza, Patricia<sup>2</sup>; Link, Samuel<sup>1</sup>; Hey, Valentin<sup>1</sup>; Stopper, Helga<sup>1</sup>; Schupp, Nicole

<sup>1</sup>Universität Würzburg, Institut für Toxikologie, Germany

<sup>2</sup>University of California, Davis, Department of Nutrition and Environmental Toxicology, United States

**Aim:** Epidemiological studies found an increased risk for kidney cancer in hypertensive patients. These patients frequently exhibit hyperaldosteronism, known to contribute to kidney injury, with oxidative stress playing an important role. We investigated, *in vitro* and *in vivo*, the capacity of kidney cells to upregulate transcription factor Nrf2, key regulator of the antioxidative defense system, to prevent aldosterone-induced oxidative damage. **Results:** Aldosterone activated Nrf2 and led to the expression of enzymes involved in glutathione synthesis and detoxification. This activation was mediated by the mineralocorticoid receptor (MR) and oxidative stress. *In vitro*, aldosterone also led to the activation of Nrf2, associated with an increase of target gene levels. But while at 24 h of aldosterone exposure oxidant levels remained high, a decrease in Nrf2 activation, glutathione, and target gene levels was observed. Nrf2 induction depended on MR-triggered activation of protein kinase C, NADPH oxidase and nitric oxide synthase. Nrf2 activation could not protect cells against oxidative DNA damage, since aldosterone-induced double strand breaks and 8-oxodG lesions steadily rose. The Nrf2 activator sulforaphane enhanced the Nrf2 response *in vitro* and *in vivo* and thereby prevented aldosterone-induced DNA damage. **Conclusion:** Aldosterone-induced Nrf2 adaptive response cannot neutralize oxidative actions of chronically increased aldosterone, which therefore could be causally involved in the increased cancer incidence of hypertensive individuals. Supplements elevating the Nrf2 response might exhibit beneficial effects.

## 061

### ErbB3 in the nucleus – mechanisms of nuclear entry

**Reif, Raymond**; Adawy, Alshaimaa; Günther, Georgia

Leibniz-Institut für Arbeitsforschung an der TU Dortmund, Juniorgruppe LivTox, Germany

Members of the receptor tyrosine kinase family (RTK) are often overexpressed in tumors. In contrast to healthy tissue, RTKs are frequently located in the nuclei of tumor cells. This translocation correlates with increased tumor proliferation and poor survival in cancer. In the current study, we focus on the translocation of ErbB3, a supposedly catalytically inactive member of the RTK family. We demonstrated that ErbB3's natural ligand, HRG and stress conditions within the tumor microenvironment effectively stimulate ErbB3 nuclear translocation. This nuclear transfer is strictly dependent on functional ErbB2/ErbB3 heterodimerization and subsequent ErbB3 phosphorylation. Investigation of different endocytic pathways in T-47D and BT474 breast cancer cells provides evidence that both Arf6 and clathrin contribute to ErbB3 translocation. Moreover, ErbB3 was found to interact with importin  $\beta$ 1 which drives the internalized receptor through the nuclear pore complex into the nucleus. Once in the nucleus, ErbB3 is shown to interact with chromatin, suggesting a potential role of ErbB3 in transcriptional regulation, which remains to be elucidated.



## 062

**Quantifying ligand bias of enantiopure fenoterol derivatives in molecular and cellular  $\beta_2$ -adrenergic assay systems**

Reinartz, Michael T.<sup>1</sup>; Littmann, Timo<sup>1</sup>; Wainer, Irving William<sup>2</sup>; Ozawa, Takeaki<sup>3</sup>; Dove, Stefan<sup>4</sup>; Seifert, Roland<sup>1</sup>

<sup>1</sup>Hannover Medical School, Institute of Pharmacology, Germany

<sup>2</sup>National Institute on Aging, Laboratory of Clinical Investigation, Baltimore, United States

<sup>3</sup>The University of Tokyo, Department of Chemistry, Japan

<sup>4</sup>University of Regensburg, Department of Pharmaceutical and Medicinal Chemistry II, Germany

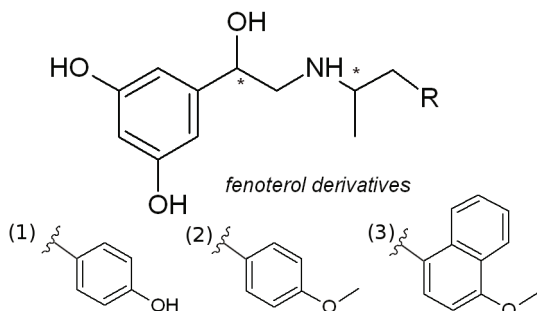
The asthma drug fenoterol (1) has two chiral centers and exists as four stereoisomers. 4'-methoxyfenoterol (2) and 4'-methoxy-1-naphthyl-fenoterol (3) were designed to increase affinity and specificity towards the  $\beta_2$ -adrenergic receptor ( $\beta_2$ AR), mainly by changing the interaction of the aminoalkyl-tail with the extended binding site [1,2]. Agonistic and antagonistic competition binding depicted these differences in affinities and binding modes. In general, the chirality-dependent order of affinities was (*R,R'*) > (*R,S'*) > (*S,R'*) > (*S,S'*). However, any minor difference in chirality and constitution can also result in distinct, ligand-specific downstream signalling qualities and strengths [3].

Here, we present a pharmacological comparison of these agonists based on combined read-outs of molecular and cellular assays to pin down indications for functional selectivity: (i) Using recombinantly expressed  $\beta_2$ AR-G $\alpha$ -fusion-proteins we measured stimulation of G $\alpha_q$  and G $\alpha_i$  GTPase activity; (ii) Using human neutrophilic granulocytes isolated from blood we characterized  $\beta_2$ AR-mediated inhibition of superoxide-production and cAMP accumulation; (iii) Using split luciferase complementation in a HEK-based cell assay we analysed  $\beta$ -arrestin2 recruitment. Complete concentration-response data enabled quantification of ligand bias between these read-outs using (*R*)-epinephrine as reference. Ligands depicted strong and some perfect bias towards G $\alpha_q$ -activation compared to G $\alpha_i$  GTPase and  $\beta$ -arrestin2 recruitment. Perfect bias of (*S,S'*)-3 towards G $\alpha_q$ -based signalling illustrated that combination of bulky derivatisation and low-affinity of a ligand can reduce its capability to activate more than the canonical pathway. We identified (*R,S'*)-3 as ligand with a unique pattern of functional selectivity, depicting the strongest bias towards G $\alpha_s$ -related signalling, against, negative bias for inhibition of O $_2^-$ -production in neutrophils and G $\alpha_q$ -activation in Sf9 membranes. With a submicromolar affinity (*R,S'*)-3 is an interesting compound to further analyse functional selectivity at the  $\beta_2$ AR. To this end, no compounds with strong bias for G $\alpha_i$  or  $\beta$ -arrestin vs. G $\alpha_q$  signalling were found. However, bias for G $\alpha_i$  compared to  $\beta$ -arrestin was observed. Our analysis of stereoisomeric ligands supports the concept of functional selectivity and enhances understanding of multiple receptor-conformations [2]. Further understanding of the mechanisms beneath could help to develop more precise drug therapies, e. g. by deactivating signalling pathways leading to adverse effects [3].

1. Jozwiak, K. et al, *Bioorg Med Chem*, 2010, 18, 728-36

2. Seifert, R. & Dove, S., *Mol Pharmacol*, 2009, 75, 13-18

3. Seifert, R., *Biochem Pharmacol*, 2013, 86, 853-61

**Chemical structures:**

Fenoterol (1), 4-methoxy-fenoterol (2), and 4-methoxy-naphthyl-fenoterol (3), stereocenters marked by asterisk.

## 063

**Correlation between *in-vivo* and *in-vitro* combination effects of triazole fungicides in the adrenal gland and H295R cells**

Rieke, Svenja; Schmidt, Flavia; Heise, Tanja; Pfeil, Rudolf; Niemann, Lars; Marx-Stoelting, Philip

Bundesinstitut für Risikobewertung, Chemikaliensicherheit, Berlin, Germany

**Background:** The current regulatory guideline regarding pesticide authorisation requires the toxicological testing of single active substances. In reality consumers are exposed to a variety of pesticide residues due to the farmers' use of different pesticides on the same plant or the intake of several pesticides via variable diet components. Consequently recent European pesticides regulation requires assessment of potential cumulative or synergistic effects. Since there are a large number of pesticides authorised within the EU, the experimental testing of all possible combinations for regulatory purposes as well as the development of mathematical predictive models are fairly impracticable in *in-vitro* experiments. In contrast, *in-vitro* models are considered being an excellent method for

the analysis of combinational effects but their meaning for the *in-vivo* situation is currently in dispute.

**Methods:** To address this question, male Wistar rats were treated with triazole fungicides individually and in combination in a broad dose range. The adrenal gland was found to be a target organ of some triazoles. For the determination of the correlation between the *in-vivo* and the *in-vitro* situation we used the cell line H295R of human adrenal cortex origin and a pathway directed transcriptomics approach. Additionally concentrations of some steroid hormones known to be altered by some azole fungicides were measured by ELISA based techniques in rat serum and cell culture supernatant.

**Results:** Significant differences but also few similarities between the *in-vivo* and the *in-vitro* situation were found. Candidates for markers identified *in-vitro* and *in-vivo* were ApoE and CYP11B2.

**Conclusion:** The applied test systems demonstrate that there is evidence for combination effects for the test substances within the selected dose range. In order to use these results for regulatory decision making further investigations are required.

## 064

**Metabolic Activation of the Antibacterial Triclocarban by Cytochrome P450 1A1 Yielding Glutathione and Protein Adducts**

Schebb, Nils Helge<sup>1</sup>; Morin, Dexter<sup>2</sup>; Buchholz, Bruce<sup>3</sup>; Buckpitt, Alan<sup>2</sup>; Hammock Bruce D<sup>2</sup>; Rice, Robert H<sup>2</sup>

<sup>1</sup>Tierärztliche Hochschule Hannover, Lebensmitteltoxikologie, Germany

<sup>2</sup>University of California, Davis, United States

<sup>3</sup>Lawrence Livermore National Laboratory, United States

Triclocarban (TCC) is a common antimicrobial preservative in personal care products, particularly in bar soaps. TCC accumulates in the aquatic environment and has biological effects on mammals. For example, it is a potent inhibitor of the soluble epoxide hydrolase, an enzyme of the arachidonic cascade thus raising the possibility of detrimental effects upon human exposure. Bathing with TCC-containing soaps results in deposition of TCC on human skin and a small portion of this amount traverses the epidermal barrier. The absorbed TCC is extensively metabolized by Cytochrome P450 monooxygenases (CYPs) to monohydroxylated derivatives. These metabolites are quickly conjugated by various glucuronosyltransferases, and the glucuronides account for the major portion of metabolites in mammalian bile. In human plasma, 2'-SO $_2$ -O-TCC is the predominant metabolite and TCC is excreted as *N*-glucuronides via the urine. Further oxidation of TCC led to quinine imines. These metabolites are highly reactive and covalently bind to glutathione and proteins *in vitro*.

In order to investigate whether the metabolic activation of TCC might occur in skin incubations with spontaneously immortalized human epidermal keratinocytes (SIK), model, were carried out with and without pre-incubation with the Ah-receptor agonist TCDD. At baseline a small but significant portion of the absorbed TCC was oxidatively metabolized by SIK while pre-incubation of SIK with 10 nM TCDD dramatically augmented metabolism of TCC. In order to test whether reactive metabolites were formed, proteins recovered from SIK incubations with <sup>14</sup>C-TCC were isolated, and the levels of bound radioactivity were measured by accelerator mass spectrometry. Up to 23  $\pm$  2 pmol/mg TCC equivalents were covalently bound to cellular protein after 24 h of incubation in cells induced with TCDD. Consistent with these findings, TCC-glutathione adduct peaks were detected in liquid chromatography (LC) analysis and scintillation counting following incubation of <sup>14</sup>C-TCC with CYP1A1, the major TCDD-inducible CYP-isoform. The main GSH-adduct was thoroughly characterized by means of liquid chromatography with high resolution mass spectrometry. These results suggest that TCC is activated via oxidative dehalogenation yielding a reactive para quinone imine. Overall, the reactive metabolites were only found in low levels which do not necessarily translate to potential adverse health effects following the use of TCC in personal care products. However, it is a surprise that reactive metabolite formation of this major ingredient in personal care products has been overlooked for more than 50 years of usage.

A. Baumann, W. Lohmann, T. Rose, K.C. Ahn, B.D. Hammock U. Karst, N.H. Schebb (2010) *Drug Metab Dispos* 38, 2130-2138.

N.H. Schebb, B. Inceoglu, K.C. Ahn, C. Morisseau, S. Gee, B.D. Hammock (2011) *Environ Sci Technol* 45 (7), 3109-15.

N.H. Schebb, B. Franze, R. Maul, A. Ranganathan, B.D. Hammock (2012) *Drug Metab Dispos* 40 (1), 25-31.

N.H. Schebb, B. Buchholz, B.D. Hammock, R.H. Rice (2012) *J Biochem Mol Toxicol* 26 (6), 230-234.

## 065

**Epac1 and Epac2 are differentially involved in inflammatory and remodeling processes induced by cigarette smoke**

Schmidt, Martina; Oldenburger, Anouk; Poppinga, Wilfred Jelco; Meurs, Herman; Maarsingh, Martina

University of Groningen, Molecular Pharmacology, Netherlands

Cigarette smoke (CS), the main risk factor for chronic obstructive pulmonary disease, induces inflammatory responses characterized by infiltration of immune cells and cytokine release. Remodeling processes, such as mucus hypersecretion and the production of extracellular matrix, proteins are also induced by CS.

We showed recently that activation of the exchange protein directly activated by cAMP (Epac), an effector of the second messenger cAMP, attenuates CS extract-induced IL-8

release from cultured airway smooth muscle cells by inhibiting NF- $\kappa$ B. We now studied the role of Epac1, Epac2 and the Epac effector phospholipase-C $\epsilon$  (PLC $\epsilon$ ) in CS-induced airway inflammation and remodeling *in vivo* in wild-type (WT), Epac1 $^{-/-}$ , Epac2 $^{-/-}$  and PLC $\epsilon$  $^{-/-}$  mice.

Mice were exposed twice a day to cigarette smoke continued for 4 days by whole body exposure. Smoke from cigarettes without a filter was transported to a 6-liter box. Control animals were treated in the same way and exposed to fresh air. On the fifth day mice were sacrificed and bronchoalveolar lavage fluid (BALF) and lung tissue was collected. Cell numbers and cytokine release was analyzed in BALF. Protein and mRNA expression was analyzed in lung homogenates.

Compared to WT mice exposed to CS, the number of total inflammatory cells, macrophages and neutrophils were lower in Epac2 $^{-/-}$  mice, whereas in PLC $\epsilon$  $^{-/-}$  mice specifically the neutrophils were lower. The secretion of interleukin-6 was also reduced in Epac2 $^{-/-}$  and PLC $\epsilon$  $^{-/-}$  mice reduced. Taken together Epac2 (in part via PLC $\epsilon$ ), but not Epac1, enhances CS-induced airway inflammation. Depletion of Epac1 in Epac1 $^{-/-}$ , however, specifically increases the level of remodeling parameters transforming growth factor- $\beta$ 1 (mRNA), collagen I (mRNA and protein) and fibronectin (mRNA and protein), suggesting that primarily Epac1 acts anti-fibrotic.

Our study shows for the first time that Epac1 and Epac2 exert different roles in inflammation and remodeling processes in mice exposed to CS. Our findings suggest that Epac1 primarily inhibits CS-induced remodeling processes, whereas Epac2 acting partly in concert with PLC $\epsilon$  increases primarily CS-induced inflammatory processes *in vivo*.

## 066

### Phospholamban monomers are more active in the presence of pentamers

Wittmann, Tanja<sup>1</sup>; Lohse, Martin J.<sup>1</sup>; **Schmitt, Joachim Paul**<sup>2,1</sup>

<sup>1</sup>Institut für Pharmakologie und Toxikologie, Universität Würzburg, Germany

<sup>2</sup>Institut für Pharmakologie und Klinische Pharmakologie, Universitätsklinikum Düsseldorf, Heinrich-Heine-Universität Düsseldorf, Germany

Phospholamban (PLN) is a key regulator of myocyte Ca<sup>2+</sup> kinetics, contraction and relaxation of the heart through its direct inhibition of the Ca<sup>2+</sup>-ATPase SERCA2A. PLN activity is attenuated upon protein kinase A (PKA)-dependent phosphorylation of PLN at Ser16. The PLN monomer is believed to be the active form of PLN. However, 80% of PLN are present as pentamers *in vivo*. The role of the PLN pentamer is yet unclear.

Using transfected HEK293 cells, we have previously shown that the PLN pentamer is a sensitive target of PKA and monomer phosphorylation occurred later than pentamer phosphorylation in analyses of time-dependent phosphorylation. To define the role of the pentamer *in vivo* we generated and characterized transgenic mice with exclusive expression of either wild type PLN (TgPLN) or a monomeric PLN mutant (TgAFA-PLN). Cardiac morphology, histology and survival of TgAFA-PLN and TgPLN mice were not different from wild type mice. Hemodynamic measurements showed no changes of left ventricular pressures and heart rate, but increased velocities of cardiac relaxation in TgAFA-PLN compared to TgPLN mice (dpd<sub>min</sub> TgAFA-PLN vs. TgPLN, -6343±247 vs. -5332±422 mmHg/s, p<0.05) and a trend towards higher contractility at baseline. Upon beta-adrenergic stimulation of hearts relaxation and contraction rates were further enhanced in all mice, but the differences in cardiac function between TgAFA-PLN and TgPLN mice were completely abolished. Western blot analyses using anti-phospho-PLN(Ser16) antibodies revealed stronger phosphorylation of PLN monomers in TgAFA-PLN than in TgPLN hearts and no difference after stimulation of PKA. Accordingly, basal enzymatic activity of SERCA2A was higher in TgAFA-PLN hearts than in TgPLN hearts and equally high after stimulation of PKA. Co-immunoprecipitation of SERCA2A and PLN as well as cross-linking of proteins indicated direct interaction of both monomeric and pentameric PLN with SERCA2A.

We showed that phosphorylation of PLN monomers is reduced in the presence of PLN pentamers leading to strong depression of SERCA2A activity. This effect of the pentamer is abolished upon stimulation of PKA. As a result, basal (but not maximal) relaxation rates are enhanced in hearts lacking PLN pentamers.

## 067

### A Force-plate actometer for the behavioral characterization of HPRT-deficient mice

Schneider, Erich H.<sup>1</sup>; Fowler, Stephen C.<sup>2</sup>; Seifert, Roland<sup>1</sup>

<sup>1</sup>Hannover Medical School, Institute for Pharmacology, Germany

<sup>2</sup>University of Kansas, Department of Pharmacology & Toxicology, Lawrence, United States

The enzyme HPRT (hypoxanthine guanine phosphoribosyl transferase) forms purine mononucleotides by transferring a ribose phosphate to a free purine base (purine nucleotide salvage pathway) and is X-chromosomally encoded. Inherited mutations of the HPRT gene may eliminate enzymatic activity and cause the Lesch-Nyhan syndrome (LND). LND leads to accumulation of hypoxanthine and uric acid, resulting in juvenile gout. Moreover, LND is associated with dopaminergic dysfunction in the striatum and compulsive self-injurious behavior. HPRT-deficient mice were generated almost three decades ago in the hope to obtain an animal model of LND [1]. In fact, the dopamine content of the striatum is reduced by more than 40 % in HPRT-deficient mice [2]. Surprisingly, however, no LND-like behavioral phenotype was found in HPRT-deficient mice. Given the alteration of dopamine content in the brain of HPRT- mice, the complete absence of any behavioral phenotype seems rather unlikely. Thus, we hypothesized that HPRT-deficient mice may show a subtly altered behavior, which differs from the

expected LND-like traits, but represents the behavioral correlate of HPRT-deficiency in mice.

To test this hypothesis, we started an unbiased behavioral characterization of HPRT-deficient C57Bl/6J mice under basal conditions. The experiments were performed with a force plate actometer [3], which is an open-field platform that continuously detects mouse movements with a resolution of up to 100 data points per second and high sensitivity. We used this method to determine the "classic" open-field parameters like locomotor activity and anxiety-like behavior. In addition, we characterized wall-rear behavior, which is difficult to quantify by standard behavioral instrumentation, but can easily be analyzed by the actometer. Specifically, we characterized number and duration of wall rears as well as offload force and time interval between wall rears. Preliminary data with mice at an age of 9-12 weeks (n=5-6 per group, littermates) suggest that offload force is reduced in HPRT- mice compared to wild-type controls. We conclude that the actometer is a promising approach to characterize the behavior of HPRT- mice that could for the first time reveal a spontaneous phenotype of HPRT- mice under homeostatic conditions.

[1] Kuehn M.R. *et al.*, *Nature* 326:295-298 (1987)

[2] Jinnah H.A. *et al.*, *J Pharm Exp Ther* 263:596-606 (1992)

[3] Fowler S.C. *et al.*, *J Neurosci Methods* 107:107-124 (2001)

## 068

### Immunomodulatory potential of azelastine

Schumacher, Stephan<sup>1</sup>; Kietzmann, Manfred<sup>1</sup>; Stark, Holger<sup>2</sup>; Bäumer, Wolfgang<sup>1,3</sup>

<sup>1</sup>University of Veterinary Medicine Hannover, Foundation, Institute of Pharmacology, Toxicology and Pharmacy, Germany

<sup>2</sup>Heinrich Heine University, Institute of Pharmaceutical and Medicinal Chemistry, Düsseldorf, Germany

<sup>3</sup>NCSCU College of Veterinary Medicine, MBS Department, Raleigh, United States

**Background:** Dendritic cells (DC) are the prototypic antigen-presenting cell type and are involved in both the sensitization and elicitation phase of allergic reactions (1). Histamine is well-known for mediating allergic symptoms like itch, edema and pain and has also been reported to modulate DC function (2). We therefore investigated the immunomodulatory potential of the histamine H1 receptor antagonist azelastine compared to that of the H1 antihistamines olopatadine, cetirizine and pyrilamine.

**Methods:** We tested H1 antihistamines in LPS-stimulated murine DC, human macrophages and in a mixed leukocyte reaction with allogeneic T cells. A receptor binding assay was performed in order to exclude possible effects on the immunomodulatory histamine H4 receptor. Finally, we evaluated the *in vivo* efficacy of the topically applied H1 receptor antagonists in a murine model of Th2-biased allergic contact dermatitis.

**Results:** Azelastine was the only compound capable of inhibiting LPS-induced TNF  $\alpha$  secretion from DCs and macrophages as well as T cell activation. These effects seemed to be mediated in part by the NF- $\kappa$ B signaling pathway, whereas we observed no affinity of azelastine to the human histamine H4 receptor. Remarkably, all H1 receptor antagonists effectively reduced hypersensitivity-induced ear swelling *in vivo*.

**Conclusion:** Azelastine was uniquely effective in modulating immune cell activation *in vitro*, but this property did not directly translate into superior *in vivo* efficacy in our particular model of allergic dermatitis. It is conceivable, however, that the exclusive effects on dendritic cell functions may be more relevant to Th1-biased allergic disorders, as it has been reported that azelastine alleviates Th1-dominated contact hypersensitivity (3).

(1) Bäumer W *et al.* *Exp Dermatol* 2006; 13: 322-9

(2) Caron G *et al.* *J Immunol* 2001; 167: 3682-6

(3) Furue M *et al.* *J Invest Dermatol* 1994; 103: 49-53.

## 069

### Effects of maternal PETN treatment of spontaneously hypertensive rats on blood pressure in the offspring

Wu, Zhixiong<sup>1</sup>; Siuda, Daniel<sup>1</sup>; Habermeier, Alice<sup>1</sup>; Li, Huige<sup>1</sup>; Closs, Ellen<sup>1</sup>; Xia, Ning<sup>1</sup>; Reifenberg, Gisela<sup>1</sup>; Daiber, Andreas<sup>2</sup>; Förstermann, Ulrich<sup>1</sup>

<sup>1</sup>Johannes Gutenberg University Medical Center, Department of Pharmacology, Mainz, Germany

<sup>2</sup>Johannes Gutenberg University Medical Center, 2nd Medical Clinic, Department of Cardiology, Mainz, Germany

Pentaerithrityl tetranitrate (PETN) is an organic nitrate used for prevention of angina pectoris in clinic. PETN has little effect on blood pressure when administered directly. The present study was designed to test the "perinatal programming" effect of PETN in spontaneously hypertensive rats, a rat model of genetic hypertension. The F0 parent SHR animals were treated with PETN (50 mg/kg/day) during pregnancy and lactation periods; the offspring received standard chow without PETN after weaning. Maternal PETN treatment had little effect on blood pressure in male offspring. In the female F1 SHR animals, however, a persistent reduction in blood pressure was observed. This long-lasting effect of maternal PETN treatment on blood pressure was accompanied by a substantial change in gene expression even evident at the age of 8 months. Maternal PETN treatment led to an upregulation of the endothelial NO synthase (eNOS), the mitochondrial superoxide dismutase (SOD2), the glutathione peroxidase 1 (GPx1) and the heme oxygenase-1 (HO-1). This was associated with epigenetic changes (enhanced

histone 3 lysine 27 acetylation and histone 3 lysine 4 trimethylation) and transcriptional activation (enhanced binding of RNA polymerase 2a to the promoter region of the abovementioned genes). In organ chamber experiment, the endothelium-dependent, NO-mediated vasodilation to acetylcholine was enhanced in aorta from female F1 SHR animal of the PETN group. This improved endothelial function, which may result from expression changes of the abovementioned genes, is likely to represent a key mechanism for the blood pressure reduction in the offspring.

## 070

### Formation of cytotoxic benzo[a]pyrene-metabolites by human skin-commensals

**Sowada, Juliane**; Lemoine, Lisa; Luch, Andreas; Tralau, Tewes

Bundesinstitut für Risikobewertung, Sicherheit von Verbrauchernahen Produkten, Berlin, Germany

The skin is our largest organ and its barrier function provides indispensable protection against everyday environmental impacts. This includes protection against exposure to polycyclic aromatic hydrocarbons (PAHs) such as benzo[a]pyrene (B[a]P). Although cytochrome P450 (CYP)-mediated activation of the latter is a model for metabolism-mediated carcinogenesis in eukaryotes, little is known about its oxidative metabolism in bacteria. At a closer look this is reason for concern because the human skin also is an extensive host-microbe interface harbouring a most diverse and dense population of microbial commensals.

In a previous study we showed that bacterial metabolism of B[a]P appears to be a universal feature of the skin's microbiome. We now report that several of the respective bacteria excrete cytotoxic metabolites. Toxic effects were seen with all cell lines tested, including HaCaT (skin) and HepG2 (liver) cells and the respective metabolites were excreted transiently (20-30 h) as well as permanently. Moreover, some metabolites were apparently toxified further as a consequence of eukaryotic phase I metabolism. Hence CYP-profiles were established to investigate the metabolites influence on human phase I metabolism. In addition we started to characterise the respective metabolites analytically as well as by means of comparative cellular assays. The data show that bacterial PAH-degradation can lead to the formation of potentially toxic metabolites on human skin. The toxification of substances by skin commensals is a new and undervalued aspect of toxicology as are the potential consequences for the human host.

## 071

### Direct monitoring of cAMP dynamics at SERCA2a reveals changes in receptor-microdomain communication in cardiac hypertrophy

**Sprenger, Julia U**; Perera, Ruwan K; Steinbrecher, Julia H.; Lehnart, Stephan E.; Nikolaev, Viacheslav

Department of Cardiology and Pneumology, Heart Research Center Göttingen, Germany

3',5'-cyclic adenosine monophosphate (cAMP) is an ubiquitous second messenger which regulates multiple physiological functions by acting in distinct subcellular microdomains. One important microdomain in cardiomyocytes is associated with sarcoplasmic/endoplasmic reticulum calcium ATPase 2a (SERCA2a) which is crucial for calcium reuptake and known to be downregulated in cardiac disease. However, real time cAMP dynamics in such microdomains and their role in cardiac disease are not well understood. Therefore, we sought to directly monitor real-time cAMP dynamics in adult cardiomyocytes within the functionally relevant microdomain associated with SERCA2a and to study how these cAMP signals are altered in cardiac hypertrophy. To achieve this goal, we generated transgenic mice expressing a novel, cardiac specific SERCA2a targeted Förster resonance energy transfer (FRET)-based sensor Epac1-PLN. To define the molecular mechanisms that confine the SERCA2a microdomain from the bulk cytosol, we compared local SERCA2a associated cAMP signals with those in the bulk cytosol (measured using the cytosolic cAMP sensor Epac1-camps). FRET experiments in freshly isolated adult ventricular myocytes revealed that local cAMP levels in the SERCA2a microdomain after  $\beta$ -adrenergic receptor ( $\beta$ -AR) stimulation were ~4-fold higher compared to the bulk cytosol. This seemed to be due to a direct phosphodiesterase (PDE)-dependent receptor-microdomain communication as this effect was abolished after global PDE inhibition. In the absence of  $\beta$ -AR stimulation, PDE3 and PDE4 were crucial for confining the SERCA2a microdomain from the cytosol. However, in cardiac hypertrophy induced by transverse aortic constriction, the local basal PDE4-mediated cAMP degradation was significantly diminished, while cAMP dynamics in the bulk cytosol were altered only after  $\beta$ -AR stimulation. Strikingly, in hypertrophy, local but not whole-cell changes in PDE activity led to a dramatic loss of receptor-microdomain communication. In summary, our approach revealed that cAMP dynamics at SERCA2a are differentially regulated compared to the bulk cytosol due to local PDE effects and direct receptor-microdomain communication. In hypertrophy, these processes are dramatically altered which might explain impaired regulation of SERCA2a activity.

## 072

### Green tea and one of its constituents, epigallocatechin-3-gallate, are potent inhibitors of human 11 $\beta$ -hydroxysteroid dehydrogenase type 1

**Stapelfeld, Claudia**; Loerz, Christine; Hintzpeter, Jan; Martin, Hans-Jörg; Maser, Edmund

Toxikologie und Pharmakologie für Naturwissenschaftler, Kiel, Germany

The microsomal enzyme 11 $\beta$ -hydroxysteroid dehydrogenase type 1 (11 $\beta$ -HSD1) catalyzes the interconversion of glucocorticoid receptor-inert cortisone to receptor-active cortisol, thereby acting as an intracellular switch for regulating the access of glucocorticoid hormones to the glucocorticoid receptor. There is strong evidence for an important aetiological role of 11 $\beta$ -HSD1 in various metabolic disorders including insulin resistance, diabetes type 2, hypertension, dyslipidemia and obesity. Hence, modulation of 11 $\beta$ -HSD1 activity with selective inhibitors is being pursued as a new therapeutic approach for the treatment of the metabolic syndrome.

It has been estimated that up to one-third of patients with diabetes mellitus consume some form of complementary and alternative medicine, involving the use of herbs, teas and other dietary supplements as alternatives to mainstream Western medical treatment. Because tea has been associated with health benefits for thousands of years, we sought to elucidate the active principle in tea with regard to diabetes type 2 prevention. Several teas and tea specific polyphenolic compounds were tested for their possible inhibition of cortisone reduction with human liver microsomes and purified human 11 $\beta$ -HSD1. Indeed, we found that tea extracts inhibited 11 $\beta$ -HSD1 mediated cortisone reduction, where green tea exhibited the highest inhibitory potency with an IC50 value of 3.749 mg dried tea leaves per millilitre.

Consequently, major polyphenolic compounds from green tea, in particular catechins were tested with the same systems. (-)-Epigallocatechin gallate (EGCG) revealed the highest inhibition of 11 $\beta$ -HSD1 activity (reduction: IC50 = 57.99  $\mu$ M; oxidation: IC50 = 131.2  $\mu$ M). Detailed kinetic studies indicate a direct competition mode of EGCG, with substrate and/or cofactor binding. Inhibition constants of EGCG on cortisone reduction were  $K_i$  = 22.68  $\mu$ M for microsomes and  $K_i$  = 18.74  $\mu$ M for purified 11 $\beta$ -HSD1. *In silico* docking studies support the view that EGCG binds directly to the active site of 11 $\beta$ -HSD1 by forming a hydrogen bond with Lys187 of the catalytic triade. Our study is the first to provide evidence that the health benefits of green tea and its polyphenolic compounds may be attributed to an inhibition of the cortisol producing enzyme 11 $\beta$ -HSD1.

## 073

### ExoY from *P. aeruginosa* is a nucleotidyl cyclase *in vivo*

**Stelzer, Tane**<sup>1</sup>; Munder, Antje<sup>2</sup>; Bähre, Heike<sup>3</sup>; Schirmer, Bastian<sup>1</sup>; Tümmler, Burkhard<sup>2</sup>; Seifert, Roland<sup>1</sup>; Hartwig, Christina<sup>1</sup>

<sup>1</sup>Hannover Medical School, Institute of Pharmacology, Germany

<sup>2</sup>Hannover Medical School, Department of Pediatric Pneumology, Allergy and Neonatology, Germany

<sup>3</sup>Hannover Medical School, Core Unit Mass Spectrometry & Metabolomics, Germany

*P. aeruginosa* is a Gram-negative bacterium and an important pathogen in nosocomial infection. The type III secretion system (T3SS) is a virulence factor which the bacteria use to inject effectors into host cells. One of these effectors is ExoY which was initially described as an adenyl cyclase (AC) with structural similarity to edema factor of *Bacillus anthracis* and CyaA of *Bordetella pertussis*<sup>1</sup>. ExoY also generates cGMP inducing gap formation and increasing endothelial permeability<sup>2</sup>. Recently, we have shown that in B103 neuroblastoma cells and HEK cells ExoY is not only a cAMP and cGMP generating enzyme, but also an uridylyl and cytidylyl cyclase<sup>3</sup>. In order to assess the pathophysiological relevance of the nucleotidyl cyclase activity *in vivo*, we examined the effect of ExoY on cyclic nucleotide (cNMP) levels in an *in vivo* lung infection model.

For the infection two mutant strains of *P. aeruginosa* (mutation of PA103 without endogenous T3SS factors) were used; one transformed with a plasmid encoding catalytically active (ExoY) and another one with inactive (K81M) ExoY. Mice were infected intratracheally either with ExoY or K81M using different doses of bacteria, dissected between 0 h – 48 h post infection, and samples were recovered. To investigate cNMP concentrations, highly sensitive and specific HPLC-MS/MS and HPLC-MS/TOF methods were used.

High concentrations of cUMP and cCMP were detected in the ExoY-infected lungs, but not in the K81M group. A guanylyl cyclase activity was also observed for ExoY. However, the concentrations of cGMP were much lower than the concentrations of cUMP and cCMP. Neither in the ExoY group nor in the K81M group changes in cAMP concentrations were detected. For all other measured cNMPs the highest concentrations were observed 8 hours post infection followed by a steady decrease. This was true for all tested bacteria doses.

In conclusion, ExoY is not only a nucleotidyl cyclase in cell culture, but also in an *in vivo* infection model. Our data indicate that cUMP and cCMP are not simply side products of a leaky nucleotidyl cyclase but rather second messenger molecules on their own right.

[1] Yahr TL, Vallis AJ, Hancock MK, Barbieri JT, Frank DW: ExoY, an adenylate cyclase secreted by the *Pseudomonas aeruginosa* type III system. *Proc Natl Acad Sci USA* 1998, 95: 13899-13904

[2] Ochoa CD, Alexeyev M, Pastukh V, Balczon R, Stevens T: *Pseudomonas aeruginosa* Exotoxin Y Is a Promiscuous Cyclase That Increases Endothelial Tau Phosphorylation and Permeability. *J Biol Chem* 2012, 287: 25407-25418

[3] Seifert R, Hartwig C, Wolter S, Reinecke D, Burhenne H, Kaever V, Munder U, Tümmler B, Schwede F, Grundmann M, Kostenis E, Frank DW, Beckert A: *Pseudomonas aeruginosa* ExoY, a cyclic GMP- and cyclic UMP-generating nucleotidyl cyclase. *BMC Pharmacology and Toxicology* 2013 14(Suppl 1): O36

### Pacemaker Current Contributions to Human Tonic and Oscillatory Autonomic Heart Rate Control

**Tank, Jens**<sup>1</sup>; Schröder, Christoph<sup>1</sup>; Heusser, Karsten<sup>1</sup>; Diedrich, André<sup>2</sup>; Mehling, Heidrun<sup>3</sup>; Luft, Friedrich C.<sup>3</sup>; Jordan, Jens<sup>3</sup>

<sup>1</sup>Medizinische Hochschule Hannover, Institut für Klinische Pharmakologie, Germany  
<sup>2</sup>Vanderbilt University School of Medicine, Department of Medicine, Division of Clinical Pharmacology, Nashville, United States  
<sup>3</sup>Medical University Charité and Max Delbrück Center for Molecular Medicine, ECRC, Berlin, Germany

**Background:** Hyperpolarization-activated and cyclic nucleotide-gated 4 (HCN4) channels producing the sinus node pacemaker current are thought to comprise the final common pathway for autonomic heart rate (HR) control. The autonomic nervous system elicits tonic and oscillatory influences on HR. Therefore, we hypothesized that selective pharmacological HCN4 inhibition with ivabradine reduces HR as well as heart rate variability (HRV) in healthy subjects. We shifted the balance between parasympathetic and sympathetic influences on heart rate gradually towards sympathetic predominance using active standing, selective norepinephrine transporter inhibition with reboxetine, or both. **Methods:** We tested 11 healthy men (21-37 years) following ingestion of placebo, ivabradine, placebo+reboxetine, ivabradine+reboxetine, and metoprolol+reboxetine at 13 and 1 hour before testing in a randomized, double-blinded, cross-over fashion. We assessed HR, HRV, and spontaneous baroreflex HR regulation supine and during active standing. **Results:** HR on placebo was 62±8 bpm in the supine position, 71±9 bpm supine with reboxetine, 95±14 bpm upright with placebo, and 123±19 bpm upright with reboxetine. Ivabradine reduced HR -4±2 bpm supine and -4±2 bpm upright with reboxetine. Ivabradine reduced HR -14±4 bpm upright and -18±5 bpm upright with reboxetine compared to placebo. Total HRV power decreased stepwise with increasing HR, both, on placebo and on ivabradine (TP-supine: placebo=2940±2203; ivabradine=2123±1307; placebo+reboxetine=2070±1800; ivabradine+reboxetine=2014±1155 ms<sup>2</sup>; TP-upright: placebo=1381±979; ivabradine=1727±1230; placebo+reboxetine=300±309; ivabradine+reboxetine=277±193 ms<sup>2</sup>). Spontaneous baroreflex sensitivity was similar with ivabradine and with placebo. In contrast, metoprolol+reboxetine reduced supine and standing HR while improving HRV and baroreflex sensitivity compared to placebo+reboxetine. **Conclusion:** HR reduction with ivabradine in healthy subjects is not associated with the expected improvement in HRV. The finding suggests that HCN4 channels contribute to tonic and oscillatory autonomic HR regulation in human subjects.

### cGMP indicator mice: Generation, characterization and first *in vivo* results.

**Thunemann, Martin**<sup>1</sup>; Wen, Lai<sup>1</sup>; Feil, Susanne<sup>1</sup>; Birk, Barbara<sup>1</sup>; Russwurm, Michael<sup>2</sup>; Shuhaibar, Leia<sup>3</sup>; Jaffe, Laurinda<sup>3</sup>; de Wit, Cor<sup>4</sup>; Han, Xiaoxing<sup>5</sup>; Fukumura, Dai<sup>5</sup>; Jain, Rakesh<sup>5</sup>; Feil, Robert<sup>1</sup>

<sup>1</sup>Universität Tübingen, Interfakultäres Institut für Biochemie, Germany  
<sup>2</sup>Ruhr-Universität Bochum, Institut für Pharmakologie und Toxikologie, Germany  
<sup>3</sup>University of Connecticut Health Center, Department of Cell Biology, Farmington, United States  
<sup>4</sup>Universität Lübeck, Institut für Physiologie, Germany  
<sup>5</sup>Massachusetts General Hospital and Harvard Medical School, Edwin L. Steele Laboratory for Tumor Biology, Department of Radiation Oncology, Boston, United States

The 2<sup>nd</sup> messenger cyclic guanosine monophosphate (cGMP) is well-known to regulate important functions of the cardiovascular and nervous system. cGMP is generated by NO-stimulated guanylyl cyclases in the cytosol or by particulate guanylyl cyclases at the plasma membrane. This subcellular compartmentalization may have important impacts on its physiological functions. However, it is not known when, where, and how much cGMP is generated in a mammalian organism *in vivo*.

Genetically-encoded cGMP indicator proteins (cGi's) allow for cGMP imaging in live cells with excellent spatial and temporal resolution. We generated mouse lines expressing the most sensitive cGi variant, cGi500 (with an EC<sub>50</sub> of ~500 nM) in the cytosol [1], or a newly-generated, membrane-targeted version of this sensor, mcGi500. In the SM22-cGi500 mouse line, the SM22 promoter drives cGi500 expression selectively in smooth muscle cells of adult mice. Other transgenic lines were generated by targeted insertion of CAG promoter-driven cGi500 or mcGi500 transgenes into the Rosa26 (R26) locus. R26-(m)cGi500-L1 lines show strong sensor expression in every cell type tested so far. R26R-(m)cGi500-L2 lines carry conditional sensor constructs, expressed only after Cre-mediated excision of a STOP cassette. Therefore, cGi500 or mcGi500 expression can be directed to any tissue of choice by mating the respective R26R-(m)cGi500-L2 line to tissue-specific Cre mice.

Initially, cGMP imaging studies were performed with cells in primary culture, or tissues freshly isolated from SM22-cGi500 and R26-(m)cGi500-L1 mice. In retina from SM22-cGi500 and aorta from R26-cGi500-L1 mice, we were able to detect cGMP transients induced with the NO-donor DEA/NO. We also visualized cGMP decreases in response to luteinizing hormone in ovarian follicles from R26-cGi500-L1 mice. Moreover, cGMP imaging was also feasible *in vivo* by intravital microscopy of live R26-cGi500-L1 mice. Using epifluorescence microscopy, we monitored DEA/NO-induced cGMP transients in resistance-type vessels of the cremaster muscle. Using multiphoton microscopy, DEA/NO-induced cGMP transients were detected in the walls of subcutaneous blood vessels accessed through a chronic skinfold chamber. Here, the cGMP transients correlated with the occurrence and extent of NO-induced vasodilation *in vivo*.

All in all, transgenic mice expressing cGi500 or mcGi500 allow cGMP imaging with high temporal and spatial resolution in intact cells, isolated tissues, and live mice. We believe that cGMP imaging *in vivo*, particularly when correlated with physiological responses, should provide deeper insights into the physiology and pathophysiology of cGMP signaling.

[1] Thunemann, M., Wen, L. et al., 2013. Transgenic Mice for cGMP Imaging. *Circulation research*, 113(4), pp.365–71.

### Ryanodine receptor calcium leak contributes to statin-induced myopathy

**Tiburcy, Matthe**<sup>1</sup>; Engel, Günther<sup>1</sup>; Sanders, Sonka-Johanna<sup>1</sup>; Sowa, Thomas<sup>2</sup>; Maier, Lars S<sup>2</sup>; Zimmermann, Wolfram H.<sup>1</sup>

<sup>1</sup>Universitätsmedizin Göttingen, Pharmakologie, Germany  
<sup>2</sup>Universitätsmedizin Göttingen, Kardiologie und Pneumologie, Germany

**Rationale:** Skeletal muscle toxicity of HMG-CoA-reductase inhibitors (statins) ranges from reversible myalgia to irreversible rhabdomyolysis. The underlying molecular mechanisms are not well defined. Tissue engineered skeletal muscle may help to gain insight into these clinically limiting side-effects and facilitate the development of strategies to minimize them. Here, we aimed to model reversible myalgia *in vitro* to decipher mechanisms contributing to statin toxicity and explore means to protect skeletal muscle.

**Methods and Results:** Engineered skeletal muscle (ESM) was generated from rat or human myoblasts, matrigel, and collagen. Isometrically suspended rat ESM developed 1.2±0.1 mN force under tetanic field stimulation (80 Hz; 200 mA; n=25). Exposure of ESM to statins (atorvastatin, simvastatin, cerivastatin, rosuvastatin, pravastatin) for 5 days resulted in a loss of force and increased fatigability in a concentration dependent manner. Cerivastatin was identified as the most potent statin with respect to muscle toxicity with a TC<sub>50</sub> (=50% force reduction) of 0.03 µmol/L (n=25/group). Cerivastatin-treated human ESM showed similar toxic damage (TC<sub>50</sub>=0.04 µmol/L, n=3-5). Importantly, ESM dysfunction was fully reversible if challenged with TC<sub>50</sub> statin concentrations (n=12-14/group). We reasoned that contractile dysfunction with increased fatigability resulted from calcium leak via the ryanodine receptor. ESM-derived myofibers treated with sub TC<sub>50</sub> cerivastatin concentrations (0.01 µmol/L) showed reduced sarcoplasmic reticulum (SR) calcium content and increased calcium spark activity which could be reversed by the RYR-stabilizing drug S107 (5 µmol/L). Co-administration of S107 (5 µmol/L) prevented statin-induced force reduction (n=16) with normalization of caspase and calpain activity (calcium-dependent proteases, n=6).

**Conclusion:** We provide evidence for a central role of ryanodine receptor leak in statin-induced myopathy by making use of a novel tissue engineered skeletal muscle model. Our data further demonstrate that RYR-stabilizing approaches can be applied to counteract statin-induced myopathy.

### Monomeric ERK2 attenuates ERK1/2-mediated pathological cardiac hypertrophy

**Tomasovic, Angela**<sup>1</sup>; Hümmert, Martin<sup>1</sup>; Ruppert, Catharina<sup>1</sup>; Lohse, Martin J.<sup>1,2</sup>; Lorenz, Kristina<sup>1,2</sup>

<sup>1</sup>University of Wuerzburg, Institute of Pharmacology, Germany  
<sup>2</sup>Comprehensive Heart Failure Center, University of Wuerzburg, Germany

The extracellular signal-regulated kinases 1 and 2 (ERK1/2) play a pivotal role in cardiac hypertrophy and cell survival. Autophosphorylation of ERK1/2 at Thr188 was shown to be a critical trigger for ERK1/2-mediated pathological cardiac hypertrophy. This autophosphorylation is induced by hypertrophic stimulation via catalytic ERK1/2 activation and dimerization. ERK dimerization facilitates Gβγ binding to ERK1/2 and subsequent ERK<sup>Thr188</sup>-phosphorylation. The aim of this study was to investigate whether the inhibition of ERK1/2 dimerization may be a therapeutic strategy to prevent cardiac hypertrophy.

To evaluate the role of monomeric ERK2 in cardiomyocyte hypertrophy and apoptosis, we used ERK2<sup>Δ174-177</sup>, an ERK2 mutant that lacks four amino acids within the ERK/ERK interface and is, thus, deficient for ERK1/2 homo- or heterodimerization. Further, co-immunoprecipitation and phosphopeptide mapping experiments revealed that ERK2<sup>Δ174-177</sup> cannot bind Gβγ subunits or be autophosphorylated at position Thr188. Overexpression of ERK2<sup>Δ174-177</sup> in neonatal rat cardiomyocytes (NRCM) resulted in a reduced hypertrophic response to phenylephrine and endothelin 1 compared to mock transfected cells or cells that overexpress wild-type ERK2. Under basal conditions, however, ERK2<sup>Δ174-177</sup> did not affect cardiomyocyte size or [<sup>3</sup>H]-isoleucine incorporation. Similarly, cardiac expression of ERK2<sup>Δ174-177</sup> in transgenic mice effectively attenuated the hypertrophic response to chronic pressure overload (i.e. heart weight, cardiomyocyte size and wall thickness) with reduced mRNA expression of collagen and the heart failure markers ANF and BNP compared to control mice. In line with these findings, monomeric ERK2 hardly localized to the nucleus in response to hypertrophic stimuli and even prevented phosphorylation of the nuclear ERK1/2 target Elk1 that is known to mediate cardiac hypertrophy. Further analyses showed that ERK2<sup>Δ174-177</sup> expression did not affect ERK1/2-mediated cell survival – neither *in vitro* nor *in vivo* – and that ERK2<sup>Δ174-177</sup> expression did not impair physiological heart growth in response to running wheel exercise.

These results show that monomeric ERK2<sup>Δ174-177</sup> effectively attenuates pressure overload induced cardiac hypertrophy without cardiac adverse effects. Inhibition of ERK1/2 dimerization might therefore be a promising strategy to interfere with ERK<sup>Thr188</sup> phosphorylation and subsequent pathological hypertrophy.

078

**Agonist evoked Ca<sup>2+</sup> elevation in mast cells depends on TRPC protein expression**  
**Tsvilovskiy, Volodymyr<sup>1</sup>**; Geminn, Julia<sup>1</sup>; Mannebach, Stefanie<sup>2</sup>; Kriebs, Ulrich<sup>1</sup>;  
 Dietrich, Alexander<sup>3</sup>; Weißgerber, Petra<sup>2</sup>; Flockerzi, Veit<sup>2</sup>; Birnbaumer, Lutz<sup>2</sup>; Freichel,  
 Marc<sup>1</sup>

<sup>1</sup>Ruprecht-Karls-Universität Heidelberg, Pharmakologisches Institut, Germany

<sup>2</sup>Universität des Saarlandes, Experimentelle und Klinische Pharmakologie und  
 Toxikologie, Homburg, Germany

<sup>3</sup>Ludwig-Maximilians-Universität München, Walther-Straub-Institut für Pharmakologie  
 und Toxikologie, Germany

<sup>4</sup>NIEHS, Laboratory of Neurobiology, NC, United States

Elevation of intracellular Ca<sup>2+</sup> concentration is essential for mast cell activation induced by different ligands including allergens leading to activation of FcεRI and phospholipase C. Such stimuli lead to formation of DAG and release of Ca<sup>2+</sup> ions from intracellular stores, and store-operated Ca<sup>2+</sup> entry is considered a major Ca<sup>2+</sup> entry pathway in mast cells, like in many other non-excitable cells. Highly Ca<sup>2+</sup>-selective currents through calcium release activated channels (CRAC) are virtually absent in the mast cells isolated from *Orai1*-deficient mice and have the great impact on FcεRI-mediated Ca<sup>2+</sup> entry and associated mast cell functions. In addition to CRAC several other agonist evoked nonselective cation channels have been described in mast cells. In peritoneal mast cells (PMC) we identified transcripts of several *Trpc* genes (*Trpc1*, *Trpc4*, *Trpc5*, *Trpc6* and *Trpc7*) that encode receptor-operated channels in many cell types. These channels conduct both Ca<sup>2+</sup> and Na<sup>+</sup> into the cell, contributing thereby either to Ca<sup>2+</sup> entry or/and depolarisation. To identify the physiological role of TRPC channel proteins for mast cell functions we used microfluorimetric measurements for the analysis of Ca<sup>2+</sup> signalling in PMC following stimulation of the FcεRI receptor and application of secretagogues known to be involved in Ca<sup>2+</sup>-dependent mast cell activation. Since specific antagonists for individual TRPC channels are still lacking and the constituents of TRPC channel complexes are unknown in mast cells like in other cells, we analysed mast cells isolated from TRPC1/C4/C5/C6 quadruple knockout mice. A significant reduction of Ca<sup>2+</sup> elevation evoked by application of various receptor agonists leading to PLC activation including antigen (DNP) and endothelin-1 was observed in PMCs isolated from TRPC1/C4/C5/C6 quadruple knockout mice. Also Ca<sup>2+</sup> elevation evoked by compound 48/80 was largely reduced in TRPC1/C4/C5/C6-deficient PMCs compared to wild type controls. The reduction in agonist evoked Ca<sup>2+</sup> elevation remained after clamping the membrane potential to 0 mV in high-potassium bath solution excluding a significant impact of indirect modulation of Ca<sup>2+</sup> entry by TRPC1/C4/C5/C6-mediated depolarisation. In our presentation, ongoing investigations of store-operated Ca<sup>2+</sup> entry in TRPC-deficient PMCs will be discussed.

079

**What can we learn about the reasons for losing OCT1 activity by exploring the worldwide genetic variability in the OCT1 gene?**

Stalman, Robert; Seitz, Tina; Brockmöller, Jürgen; **Tzvetkov, Mladen**

Institut für Klinische Pharmakologie, Göttingen, Germany

The organic cation transporter OCT1 is strongly expressed in the sinusoidal membrane of the human liver and mediates the hepatocellular uptake of a number of clinically relevant drugs like metformin, morphine, tropisetron and tramadol. In Germany 9% of the population are compound homozygous carriers of loss-of-function polymorphisms in the *OCT1* gene and therefore lack OCT1 activity. Further 40% are heterozygous carriers of these polymorphisms and have significantly reduced OCT1 activity. Less is known about the variability in other populations worldwide.

Here we report worldwide analyses of genetic variability of *OCT1*. With these analyses we aimed, first, to identify evolutionary patterns that may shed light to the reasons for the common loss of OCT1 activity and, second, to estimate the role of *OCT1* polymorphisms on drug pharmacokinetics in populations beyond Caucasians. We genotyped all 11 previously known loss-of-function *OCT1* polymorphisms in 1192 DNA samples from 54 populations worldwide. The Met420-deletion was by far the most common and the only ubiquitously observed loss-of-function polymorphism. The Arg61Cys and Gly465Arg polymorphisms were specific for Caucasians, while Ser14Phe was specific for Africans. Striking differences were observed in the frequencies of the loss of OCT1 activity in different populations. While Asians lacked any of the known loss-of-function *OCT1* polymorphisms, 70% of the native South American Indians were homozygous and the remaining 30% were heterozygous carriers of the Met420-deletion polymorphism.

In addition, we re-sequenced the promoter and the coding regions of the *OCT1* gene in all the samples using semiconductor-based massively parallel sequencing. We identified 33 novel amino acid substitutions; 4 of the substitution were predicted to cause loss of OCT1 function and were confirmed by capillary sequencing. The newly identified loss-of-function variants were predominantly found in Asian populations, but were very rare and therefore will not change our understanding for low frequency of loss of OCT1 function in Asia.

In conclusion, this study reports strong population-specific differences in the frequency of loss-of-function polymorphisms in OCT1 in different world populations. This may reflect the presence of an evolutionary selection pressure leading to the common loss of OCT1 activity.

080

**Enzyme-deficient C3-E174Q from *C. botulinum* is a modulator of cell proliferation**  
**von Elsner, Leonie**; Hagemann, Sandra; Just, Ingo; Rohrbeck, Astrid  
 MHH, Institut für Toxikologie, Hannover, Germany

The Rho-GTPases are essential regulators of various cellular processes, such as regulation of actin cytoskeleton, cell proliferation and cell apoptosis. To further investigate the cellular role of Rho-GTPases the C3-exoenzyme from *Clostridium botulinum* is often used as a cellular tool. In primary hippocampus neurons C3 mediates axon- and dendritic growth promoting effects.

Prolonged incubation (several days) of hippocampal HT22 cells with C3 resulted in growth inhibition detectable by constant cell number. Surprisingly, enzyme-deficient C3-E174Q also halted cell proliferation. Checking cell cycle regulators revealed that both, mRNA and protein level of cyclin D1 were down-regulated. Because of the lack of transferase activity of the C3-E174Q, these results strongly indicate that this anti-proliferative effect is independent of the ADP-ribosylation of cellular Rho-GTPases.

So far, the mechanism and underlying signal pathways are unknown. Exposure to significantly increased concentrations of C3 or C3-E174Q (up to 5 μM) resulted in no further enhanced proliferative effect. However, reduction of incubation time (up to 48h) resulted in reduced anti-proliferative effects. Interestingly, additional incubation with C3 plus cAMP-analogue enhanced the proliferative effect of C3. In addition, phosphorylation signal pathways were analysed with phospho-specific antibodies in Western blots. Surprisingly, an oscillatory modulation of the analysed kinases was detected.

Our results suggest that the enzymatically inactive C3-E174Q was able to work as a modulator of various pathways that are essential in the regulation of cell growth.

Rohrbeck A, Kolbe T, Hagemann S, Genth H, Just I (2012) Distinct biological activities of C3 and ADP-ribosyltransferase-deficient C3-E174Q. *FEBS J* 279:2657-71

081

**Enhanced sensitivity of phospholipase C-γ2 to Rac provides chronic lymphocytic leukaemia resistance to the Bruton's tyrosine kinase inhibitor ibrutinib *in vivo***  
**Hermkes, Elisabeth<sup>1</sup>**; Bühler, Anja<sup>1</sup>; Stilgenbauer, Stephan<sup>2</sup>; Gierschik, Peter<sup>1</sup>;  
**Walliser, Claudia<sup>1</sup>**

<sup>1</sup>Universitätsklinikum Ulm, Institut für Pharmakologie und Toxikologie, Germany

<sup>2</sup>Universitätsklinikum Ulm, Klinik für Innere Medizin III, Germany

Phospholipase C-γ2 (PLCγ2) is essential for B cell receptor (BCR) signalling and B cell development, differentiation, and function. Bruton's tyrosine kinase (Btk) is a central player in BCR signalling through its ability to phosphorylate and activate PLCγ2. Btk is essential for the survival of chronic lymphocytic leukaemia (CLL) cells and their homing to microenvironmental niches. Several small molecule Btk inhibitors were developed as a new class of targeted agents for the treatment of CLL, of which ibrutinib is the most advanced, showing impressive clinical efficacy in relapsed/refractory CLL. Ibrutinib irreversibly inhibits Btk protein kinase activity by forming a covalent bond with Cys<sup>481</sup>, resulting in decreased CLL cell proliferation, survival, and homing to and retention in tissue microenvironments [1,2]. In some cases, however, acquired resistance to ibrutinib limits its therapeutic efficacy. Chang *et al.* recently described mutations in B cell signalling components likely to confer ibrutinib resistance to five CLL patients [3]. In four cases, Cys<sup>481</sup> of Btk was replaced by Ser, in one case, Arg<sup>665</sup> of PLCγ2 was replaced by Trp. Although the PLCγ2<sup>R665W</sup> mutant was shown to cause ibrutinib-resistant enhancement and prolongation of the BCR-mediated Ca<sup>2+</sup> response in model cells, the molecular mechanisms underlying this gain-of-function remained largely unknown.

Here, we show that PLCγ2<sup>R665W</sup> displays constitutively increased basal activity upon expression in COS-7 cells, but that this increase is mainly dependent on its activation by the small GTPase Rac, a known efficacious activator of PLCγ2. The R665W mutation increases both the potency and the efficacy of various types of constitutively active Rac2 variants to activate PLCγ2. In intact cells, PLCγ2 was even sensitive to activation by wild-type Rac2, most likely through generation of low levels of activated Rac2 even in the absence of receptor stimulation. Hypersensitivity of PLCγ2<sup>R665W</sup> to Rac-mediated signalling was also evident for its activation by the upstream Rac regulator Vav1, known to play a central role in Rac activation by various B cell surface receptors.

The results not only provide direct evidence for the critical, decisive role of PLCγ2 in the maintenance of CLL, but also reveal the existence of an alternative, Rac-mediated pathway of PLCγ2 activation that is unmasked and augmented by the R665W mutation to bypass ibrutinib-mediated inhibition of Btk.

[1] Aalipour, A. and Advani, R.H. (2013) *bjh*, 1-8

[2] Byrd J.C., Furman, R.R., Coutre, S.E., Flinn, I.W., Burger, J.A., Blum, K.A., Grant, B., Sharman, J.P., Coleman, M., Wierda, W.G., Jones, J.A., Zhao, W., Heerema, N.A., Johnson, A.J., Sukbuntherng, J., Chang, B.Y., Clow, F., Hedrick, E., Buggy, J.J., James, D.F., and O'Brien S. (2013) *NEJM* 369, 32-42

[3] Chang, B.Y., Furman, R.R., Zapatka, M., Barrientos, J.C., Li, D., Steggerda, S., Eckert, K., Francesco, M., Woyach, J.A., Johnson, A.J., James, D.F., Versele, M., Byrd, J.C., Stilgenbauer, S., and Buggy, J.J. (2013) *Journal of Clinical Oncology, ASCO Annual Meeting Abstracts* 31, 7014

## 082

**RhoGEF17, a novel regulator of angiogenesis in endothelial cells****Weber, Pamina**<sup>1</sup>; Kroll, Jens<sup>2</sup>; Lutz, Susanne<sup>3</sup>; Wieland, Thomas<sup>1</sup><sup>1</sup>Medical Faculty Mannheim, Heidelberg University, Experimental Pharmacology, Germany<sup>2</sup>Medical Faculty Mannheim, Heidelberg University, Vascular Biology, Center for Biomedicine and Medical Technology, Germany<sup>3</sup>University Hospital Goettingen, Department of Pharmacology, Goettingen, Germany

Angiogenesis is characterized by an increase in endothelial permeability followed by endothelial cell (EC) activation, proliferation and migration towards the angiogenic stimulus. The actin cytoskeleton is essential for these cellular processes and monomeric GTPases of the Rho subfamily and their regulators, e.g. guanine nucleotide exchange factors (GEF), precisely coordinate these dynamics.

RhoGEF17 is a Rho-specific GEF which was found to be upregulated in EC during tumor cell-induced angiogenesis and described recently as to be bound to filamentous actin in EC. To analyze the endothelial function of RhoGEF17, we performed knockdown experiments by an adenoviral delivery of shRNA in microvascular rat fat pad EC (RFPEC). Forty eight hours after viral infection, changes in cell morphology could be detected, which included cell rounding, loss of cell-cell contacts, and dislocation of adherens junction proteins from the cell membrane into sub-membranous compartments. As a result these cells lost their capability to adhere efficiently to the substratum and to migrate in sheets in a scratch assay. However, the amount of EC displaying contact-independent single cell migration was increased. On a biochemical level, the knockdown of RhoGEF17 was paralleled by a reduced expression of cadherins, catenins and interestingly of its effector RhoA and the Rho-inactivating p190RhoGAP. Moreover, after RhoGEF17 depletion, the RFPEC exhibited an impaired proliferation capacity and the apoptosis rate of cell-cell contact-deprived EC was significantly reduced as measured by caspase activation and annexin V binding. Thus, our *in vitro* data argue for a role of RhoGEF17 in the contact-dependent regulation of EC migration and viability.

To analyze RhoGEF17 function *in vivo*, we performed a morpholino-mediated knockdown in zebrafish embryos. The RhoGEF17-depleted larvae displayed a phenotype similar to those with a VE-cadherin-knockdown featuring irregular vessel formation and increased sprouting of the subintestinal veins.

We conclude that RhoGEF17 is a required component of the multi-protein complex integrity and signalling in cell junctions and thus RhoGEF17 is apparently involved in the regulation of angiogenic processes.

## 083

**Characterisation and Identification of the protein receptor binding site in Botulinum Neurotoxin A****Weisemann, Jasmin**<sup>1</sup>; Rummel, Andreas<sup>1</sup>; Mahrhold, Stefan<sup>1</sup>; Lou, Jianlong<sup>2</sup>; Marks, James D.<sup>2</sup><sup>1</sup>Medizinische Hochschule Hannover, Institut für Toxikologie, Germany<sup>2</sup>University of California, San Francisco, Department of Anesthesia, United States

Botulinum neurotoxins (BoNTs) are the most poisonous bacterial protein toxins causing the zoonosis botulism due to blockade of acetylcholine release at the neuromuscular junction. The eight serologically different BoNT serotypes A to H are composed of three domains which play individual roles in the intoxication mechanism. The C-terminal 50 kDa H<sub>C</sub> fragment of the BoNT is responsible for neuronal binding and receptor-mediated endocytosis.

A dual receptor mechanism was proposed including initial binding to complex gangliosides and subsequent binding to a specific protein receptor. The three isoforms of the synaptic vesicle glycoprotein 2, SV2A-C, were identified as protein receptor for BoNT/A. However, information about the location of the binding site within the BoNT/A H<sub>C</sub> fragment was still lacking until recently.

Here, we characterised the SV2 protein receptor binding site of BoNT/A. We report the binding constant of BoNT/A to rat and human SV2C luminal domain 4 (454-579). Furthermore, we analysed the binding of BoNT/A to SV2C luminal domain 4 with and without C-terminal transmembrane domain and in the presence or absence of gangliosides. Binding of BoNT/A to GST-rSV2C 454-579 was inhibited in the presence of a monoclonal anti-H<sub>C</sub>A antibody with defined epitope on the backside of the unique ganglioside binding site. Employing pull down experiments, single mutations in the antibody epitope region located in H<sub>C</sub> decreased the binding of BoNT/A to rSV2C. Furthermore, the biological activity of these BoNT/A mutants was also reduced using the mouse *phrenic nerve* hemidiaphragm (MPN) assay, thereby confirming the binding data. CD-spectroscopic analysis ruled out impairment of protein folding due to mutations. In addition, key H<sub>C</sub>A mutants lost the ability to precipitate SV2A and B from rat brain synaptosome lysate.

## 084

**cCMP-induced apoptosis of S49 lymphoma cells****Wolter, Sabine**; Hartwig, Christina; Golombek, Marina; Seifert, Roland  
Hannover Medical School, Institute of Pharmacology, Germany

Apoptosis is a physiological process of cell death that plays a critical role in normal development as well as in the pathophysiology of various diseases. There is three

main pathways that lead to apoptosis: The extrinsic way begins outside the cell by activating certain receptors, the intrinsic pathway is often mediated by mitochondria leading to cytochrome c release and the third way is triggered by unfolded proteins resulting in stress of the endoplasmic reticulum, so-called ER stress. All apoptotic pathways result in activating caspases that act in a proteolytic cascade.<sup>1</sup>

Stimulation of S49 wild-type (wt) cells, derived from murine T-cell lymphoma, with cAMP increasing agents like diterpenes induce apoptosis by an intrinsic, mitochondria-dependent mechanism.<sup>2</sup> Incubation with the cell permeable acetoxy-methyl ester of the pyrimidine nucleotide cytidine-3',5'-cyclic monophosphate (cCMP-AM) causes inhibition of cell proliferation and induces caspase-dependent apoptosis in the S49 wt cells and also in cells lacking the catalytic subunit of PKA, the S49 kin<sup>-</sup> cells. Measurements of cyclic nucleotides by high specific tandem mass spectrometry show the rapid uptake of cCMP-AM but no change in the concentration of other cyclic nucleotides, indicating a lack of cross-talk. Using flow cytometry analysis and western blots we analyzed the mechanism of inducing apoptosis by cCMP. cCMP activates caspase 9 and caspase 12, leads to cytochrome c release and alters the membrane potential of the mitochondria. Some genes related to apoptosis are differentially expressed after cCMP incubation in S49 wt and S49 kin<sup>-</sup> cells, thus GADD45α is induced by cCMP. These results show that the intrinsic pathway as well as ER stress are involved in cCMP-induced apoptosis.

Apoptosis was not induced by non-membrane permeable cyclic nucleotides (cAMP; cGMP, cCMP and cUMP) or by purine and pyrimidine nucleosides. Using cCMP-agaroses we have also identified some cCMP-binding proteins, which are important in protein folding (calnexin and peptidyl-prolyl cis-trans isomerase) and some A-kinase-anchoring proteins (AKAP9 and AKAP13). Our data indicate that cCMP activates other pathways than cAMP including PKA- and PKG-independent mechanisms.

[1] Adams JM (2003) Ways of dying: multiple pathways to apoptosis. *Genes Dev*, 17: 2481-2495

[2] Yan L, Herrmann V, Hofer JK, Insel PA (2000) β-Adrenergic receptor/cAMP-mediated signalling and apoptosis of S49 lymphoma cells. *Am J Physiol*, 279: C1665-C1674

## 085

**Genetic dissection of plexin signalling in vivo.****Worzfeld, Thomas**<sup>1,2</sup>; Swiercz, Jakub<sup>2</sup>; Sentürk, Ayca<sup>3</sup>; Genz, Berit<sup>4</sup>; Korostylev, Alexander<sup>2</sup>; Deng, Suhua<sup>5</sup>; Xia, Jingjing<sup>2</sup>; Hoshino, Mikio<sup>6</sup>; Epstein, Jonathan<sup>6</sup>; Chan, Andrew<sup>6</sup>; Vollmar, Brigitte<sup>4</sup>; Acker-Palmer, Amparo<sup>3</sup>; Kuner, Rohini<sup>5</sup>; Offermanns, Stefan<sup>2</sup><sup>1</sup>Universität Marburg, Pharmakologisches Institut, Germany<sup>2</sup>Max-Planck-Institut für Herz- und Lungenforschung, Pharmakologie, Bad Nauheim, Germany<sup>3</sup>Universität Frankfurt, Institute of Cell Biology and Neuroscience and Buchmann Institute for Molecular Life Sciences, Germany<sup>4</sup>Universität Rostock, Institut für Experimentelle Chirurgie, Germany<sup>5</sup>Universität Heidelberg, Pharmakologisches Institut, Germany<sup>6</sup>Pharmakologisches Institut, Universität Marburg, Germany<sup>7</sup>National Institute of Neuroscience, NCNP, Department of Biochemistry & Cellular Biology, Tokio, Japan<sup>8</sup>University of Pennsylvania, Department of Cell and Developmental Biology, Philadelphia, United States<sup>9</sup>Mount Sinai School of Medicine, Icahn Medical Institute, New York, United States

Mammalian plexins comprise a family of transmembrane receptors for semaphorins and represent critical regulators of various processes during development of the nervous, cardiovascular, skeletal and renal system. *In vitro* studies have shown that plexins exert their effects via an intracellular R-Ras/M-Ras GTPase-activating protein (GAP) domain or by activation of RhoA through interaction with RhoGEF proteins. However, which of these signalling pathways are relevant for plexin functions *in vivo* is largely unknown. Using an allelic series of transgenic mice, we show that the GAP domain of plexins constitutes their key signalling module during development. Mice in which endogenous Plexin-B2 or Plexin-D1 is replaced by transgenic versions harbouring mutations in the GAP domain recapitulate the phenotypes of the respective null mutants in the developing nervous, vascular and skeletal system. We further provide genetic evidence that, unexpectedly, the GAP domain-mediated developmental functions of plexins are not brought about via R-Ras and M-Ras inactivation. In contrast to the GAP domain mutants, Plexin-B2 transgenic mice defective in RhoGEF binding are viable and fertile, but exhibit abnormal development of the liver vasculature. Our genetic analyses uncover the *in vivo* context-dependence and functional specificity of individual plexin-mediated signalling pathways.

## 086

**Influence of bariatric surgery on the use of some major drug classes****Yska, Jan Peter**<sup>1</sup>; van der Meer, Douwe H.<sup>1</sup>; Eilander, Willeke<sup>1</sup>; Dreijer, Albert R.<sup>1</sup>; Apers, Jan A.<sup>2</sup>; Emous, Marloes<sup>2</sup>; Totté, Erik R.e.<sup>2</sup>; Willefert, Bob<sup>3,4</sup>; van Roon, Eric N.<sup>1,3</sup><sup>1</sup>Medisch Centrum Leeuwarden, Department of Clinical Pharmacy and Clinical Pharmacology, Netherlands<sup>2</sup>Medisch Centrum Leeuwarden, Department of Surgery, Netherlands<sup>3</sup>University of Groningen, Unit of Pharmacotherapy and Pharmaceutical Care, Netherlands<sup>4</sup>University Medical Centre Groningen, Department of Hospital and Clinical Pharmacy, Netherlands

## Introduction

Patients undergoing bariatric surgery are severely obese and characterized by multidrug use for multiple comorbidities. Bariatric surgery can influence the prevalence and incidence of comorbidities, as well as the pharmacokinetics of drugs. This might lead to changes in the use of drugs.

## Aim

To study the influence of bariatric surgery on the use of medication in patients before and after surgery, focusing on type and number of medications and daily dosage.

## Methods

A retrospective and prospective observational study was carried out in Medical Centre Leeuwarden. After having obtained written informed consent drug dispensing data from pharmacies were collected from patients undergoing their first bariatric surgery between January 2008 and September 2011. Dispensing data from 6 months before until 12 months after surgery were analyzed. Drugs were classified according to the WHO-ATC classification system. Dosages of drugs were compared using defined daily dose (DDD).

## Results

450 patients were included (20.2% male). Mean age (SD) was 43.4 (10.1) yr; mean BMI (SD) was 44.9 (6.7) kg/m<sup>2</sup>. Roux-en-Y gastric bypass was performed in 74% of the patients. Mean BMI (SD) 12 months after surgery was 31.1 (5.6) kg/m<sup>2</sup>. The mean number of drugs per patient (95% CI) decreased from 3.66 (3.37-3.99) to 3.25 (3.04-3.56). The mean number of drugs per patient decreased by 71%, 36%, 27%, 47%, 24% and 33% for antidiabetics, diuretics, beta blockers, agents acting on the renin-angiotensin system, lipid modifying agents, and drugs for obstructed airway diseases respectively 12 months after surgery. From those drug classes patients used lower DDD 12 months after surgery. In contrast, a higher DDD was observed for thyroid hormone with no change in the mean number of drugs per patient.

## Conclusion

Twelve months after bariatric surgery the use of drugs decreases in terms of mean number of drugs per patient and, for some major drug classes, in dose intensity. Dispensing data from pharmacies may provide detailed information on the use of medication by patients after bariatric surgery.

## 087

### Multiwalled carbon nanotubes (MWCNT) induce DNA damage and cellular senescence in human peritoneal mesothelial LP9 cells

Reamon-Buettner, Stella Marie<sup>1</sup>; Bellmann, Bernd †<sup>1</sup>; Hackbarth, Anja<sup>1</sup>; Leonhardt, Albrecht<sup>2</sup>; Niehof, Monika<sup>1</sup>; Ziemann, Christina<sup>1</sup>

<sup>1</sup>Fraunhofer-ITEM, IVMT, Hannover, Germany

<sup>2</sup>Leibniz-Institut für Festkörper und Werkstofforschung Dresden, Germany

Multiwalled carbon nanotubes (MWCNTs) are nanomaterials with immense potential in many technological applications, such as in engineering, materials science, and medicine. Yet toxic and genotoxic effects of MWCNTs are still unclear. Notably, there is concern that certain MWCNTs may cause malignant mesothelioma, a cancer derived from mesothelial cells, particularly linked to asbestos exposure. We thus investigated the *in vitro* genotoxic activity of various tailor-made MWCNTs in primary human peritoneal mesothelial LP9 cells, under the auspices of a BMBF-funded project CarboTox (contract number: 03X0109A). LP9 cells were exposed for 24 h to 0.3-5.0 µg/cm<sup>2</sup> MWCNTs of different length, diameter, and morphology. Long amosite asbestos served as positive and milled MWCNT as material control. Using various approaches, we found that certain straight and long MWCNTs, for instance, MWCNT2 (length: 10.24 µm; diameter: 0.04 µm), MWCNT3 (length: 8.57 µm; diameter: 0.085 µm), and MWCNT3a (length: 9.3µm; diameter: 0.061 µm), exhibited marked toxic and genotoxic potential *in vitro*, as compared to the milled material control. Interestingly, these MWCNTs also induced mesothelioma in a parallel intraperitoneal *in vivo* study. Cell division was almost absent, and various types of mitotic and chromatin abnormalities occurred in the presence of the biologically active MWCNT species. In about 40% of exposed LP9 cells, DAPI staining demonstrated nuclear fragmentation, condensed chromatin, and senescence-associated heterochromatin foci (SAHF), reminiscent of apoptotic or senescent cells. Such abnormal nuclei displayed pan- or bright-staining with γH2AX, a well-known marker for DNA double-strand breaks. Consistent with cellular senescence, i.e. a state of irreversible terminal growth arrest resulting from cellular stress or DNA damage, we also observed increased expression of the gene encoding for P16INK4A, a tumor suppressor implicated in cell cycle arrest and cellular senescence. The impaired tubulin integrity noted after MWCNT exposure likely contributed also to cellular senescence induction. Altogether, our findings suggest marked genotoxic potential of long and straight MWCNTs leading to cellular senescence as a possible molecular mechanism in mesothelioma development after MWCNT exposure.

## 088

### Transgenic mice with myocardium-specific over-expression of fatty acid synthase (FASN) develop signs of cardiac hypertrophy and failure

Abd Alla, Joshua<sup>1</sup>; Graemer, Muriel<sup>1</sup>; Quitterer, Ursula

<sup>1</sup>ETH Zürich, Molekulare Pharmakologie, Switzerland

Heart failure is a major cause of death and a better understanding of pathomechanisms is urgently needed. Up-regulation of cardiac lipid metabolism genes and the major lipid-synthesizing enzyme, fatty acid synthase (*FASN*), characterizes the development of heart failure symptoms of experimental models and patients. Enhanced cardiac lipid

synthesis is often considered as a compensatory factor, which could delay the onset of cardiac insufficiency because data from mice with cardiac-specific *Fasn* deficiency indicated a cardioprotective role of *Fasn*. To further investigate the function of cardiac *FASN*, we generated mice with transgenic expression of *FASN* under control of the myocardium-specific alpha-MHC promoter. Two different transgenic lines with low and high *FASN* over-expression (2.1-fold and 6.6-fold increase over the B6 control) were generated to mimic the gradual increase of *FASN* during the transition to heart failure. Transgenic mice with low cardiac *FASN* over-expression developed cardiac hypertrophy as evidenced by an increased heart weight to body weight ratio but had preserved cardiac function. In contrast, high cardiac *FASN* expression led to signs of heart failure as documented by a significantly reduced cardiac ejection fraction, cardiac hypertrophy with dilation and enhanced cardiomyocyte death. Taken together, transgenic mice with myocardium-specific over-expression of *FASN* provide evidence for a role of *FASN* in the development of cardiac hypertrophy and signs of heart failure.

## 089

### Gastrointestinal motility: Mechanisms of action of a herbal medicinal product, STW 5

Kelber, Olaf; Okpanyi, Samuel N.; Abdel-Aziz, Heba

Steigerwald Arzneimittelwerk GmbH, Scientific Department, Darmstadt, Germany

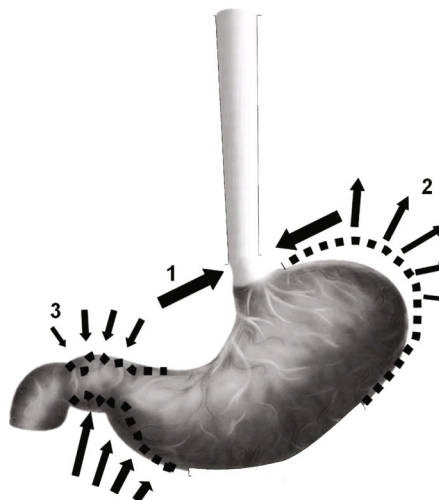
Motility-based gastrointestinal diseases are frequently treated with herbal medicinal products. A herbal medicinal product, which has been shown to be therapeutically effective in functional dyspepsia (FD) and irritable bowel syndrome (IBS) in randomized controlled clinical trials, is STW 5, a fixed combination of nine standardized herbal extracts.

A review of the clinical data on this product has been published recently [1], whereas a recent review of its motility-related mechanisms of action is missing. Therefore, a systematic database search was conducted and checked for completeness by means of hand searching and cross referencing.

There is a considerable number of publications on STW 5 [2] and on the components of the product. The first mechanistic studies on the combination [2, 3] suggested a dual mechanism of action, with a spasmolytic effect in acetylcholine induced contractions and a tonising effect in the relaxed state. This has been confirmed [4, 5] in human isolated intestinal segments [6] and in inflamed intestinal tissue *in vitro* and *in vivo* [7-9]. In the stomach, a region specific action was described *in vitro*, based on an inhibition of Ca influx via SOC channels in the gastric fundus (Fig. 1.2) and on a stimulation of Ca influx via L type Ca channels in the antrum [10] (Fig. 1.3). This region specific action has been confirmed in a human study *in vivo* [11]. In the lower esophageal sphincter (Fig. 1.1), a tonising action mediated by L type Ca channels has been shown *in vitro* [6], which has not yet been confirmed in a human study.

The *in vitro*-, *in vivo*- and human studies showed spasmolytic as well as tonising-prokinetic effects possibly relevant for the clinical effect of STW 5. Nevertheless, there are still questions open regarding details of the synergistic effects of the components of the preparation. This is typical for herbal medicinal products, as they have multiple constituents which are involved in their clinical action.

- Ottilinger et al. 2013, WMM 163:65;
- Brierley and Kelber 2011, Curr Opin Pharmacol 11: 604;
- Okpanyi et al. 1993, Acta Hort. 332:227;
- Ammon et al. 2006, Phytomed 13 SV:67;
- Heinle et al. 2006, Phytomed 13 SV:75;
- Kelm et al. 2013, ZPT 34 S1:S31;
- Schemann et al. 2008, Z Gastroenterol 46:1039;
- Michael et al. 2009, Phytomed 16:161;
- Sibaev et al. 2013, ZPT 34 S1:S31;
- Wadie et al. 2012, Int J Colorectal Dis 27:1445;
- Hohenester et al. 2004, Neurog Motil 2004, 16:765;
- Pilichiewicz et al. 2007, Am J Gastroenterol 102:1



### Motility:

Fig. 1: Mechanisms of action of STW 5 in the stomach (legend see text)

## 090

**Involvement of anti-inflammatory mechanisms in the anti-depressant effect of St John's wort**

**Kelber, Olaf**<sup>1</sup>; Müller, Jürgen<sup>1</sup>; Okpanyi, Samuel N.<sup>1</sup>; **Abdel-Aziz, Heba**<sup>1</sup>; Nieber, Karen<sup>2</sup>; Kolb, Christiane

<sup>1</sup>Steigerwald Arzneimittelwerk GmbH, Scientific Department, Darmstadt, Germany

<sup>2</sup>Institut für Pharmazie der Universität Leipzig, Germany

An increasing number of clinical and preclinical data shows that inflammatory processes may be involved in the etiology of depression [1, 2]. At least in some depressed patients inflammation markers are enhanced. An IFN- $\alpha$ -induced rise of TNF- $\alpha$  and IL-6 may induce depressive symptoms [3]. Psychic stress is not only a trigger of depressive symptoms, but also of a lower antioxidative capacity, similar to that in inflammatory diseases.

As many herbal extracts have anti-inflammatory actions, the question is, whether these are also involved into the antidepressive action of St John's wort [4]. It was addressed by a systematic data basesearch.

St Johns wort extracts and their components have been shown to have anti-inflammatory and anti-oxidative actions *in vitro* [5,6], *in vivo* [2,7] and, in dermatology, also clinically [8]. In a model of a stress induced depression, St John's wort also normalized the lowered antioxidative capacity [2] and influenced gene expression of pro-inflammatory cytokines and kinases, as e.g. Mapk8 [7].

As St John's wort extracts have anti-inflammatory properties, it is plausible that these are involved also in the therapeutic use in depression, and have possibly been underestimated up to now.

1. Dantzer R et al. 2008, Nature Reviews Neuroscience 9, 46
2. Grundmann O et al. 2010, Neuropharmacology 58, 767
3. Raison CL and Miller AH, 2011, Curr Psychiatry Rep 13, 467
4. HMPC 2009, EMA/HMPC/101304/2008
5. Birt DF et al. 2009, Pharm Biol 47, 774
6. Kraus B et al. 2010, Planta Med. 76, 1340
7. Jungke et al. 2011, Psychopharmacology 213, 757
8. Schempp CM et al. 2002, Hautarzt 53, 93

## 091

**Re-evaluation of horse chestnut seed extract as a pharmacotherapeutic approach in chronic venous insufficiency**

Müller, Jürgen<sup>1</sup>; **Kelber, Olaf**<sup>1</sup>; **Abdel-Aziz, Heba**<sup>1</sup>; Kraft, Karin<sup>2</sup>

<sup>1</sup>Steigerwald Arzneimittelwerk GmbH, Scientific Department, Darmstadt, Germany

<sup>2</sup>Chair of Natural Medicine, University of Rostock, Germany

Conservative therapy of chronic venous insufficiency (CVI) consists largely of compression treatment. However, this often causes discomfort and has been associated with poor compliance. Therefore, oral pharmacotherapy (for example oral treatment with extracts from *Aesculus hippocastanus L.*, fructus (horse chestnut seed extract, HCSE) is an attractive option.

In this overview the clinical and pharmacological evidence (studies, Cochrane review, monographs, guidelines in this indication) concerning mechanisms of action, efficacy and safety were reviewed.

The action of HCSE addresses the enhanced permeability of the venous endothelium, especially the capillaries, decreasing transfer of water from the blood to the adjacent tissue [1]. Overall, there is an improvement in CVI related signs and symptoms with HCSE compared with placebo. This is reflected in all reviews and monographs [e.g. 2, 3, 4] as well as in clinical guidelines [e.g. 5, 6]. Adverse events were usually mild and infrequent. Due to pathophysiological and methodological reasons a study duration of 12 weeks seems appropriate and sufficient to demonstrate clinical efficacy in comparison to compression treatment, as long term compliance is key factor in CVI treatment and is higher for pharmacotherapy than for compression therapy.

The evidence presented suggests that HCSE is an efficacious and safe treatment for CVI, as has been documented in studies of up to 12 weeks duration and allows, in conjunction with the good tolerability documented by pharmacovigilance data, the conclusion that the therapeutic usefulness of HCSE is well established also in long term treatment.

1. Nees S, Weiss D, Thallmeier M, Lamm P, Juchem G. Neue Aspekte zur Pathogenese und Therapie chronischer peripherer Venenleiden. Fortschr Med 2001; 24, 137
2. Commission E of BGA, Monograph *Aesculus hippocastanus*, April 15, 1994
3. EMA/HMPC, Community herbal monograph on *Aesculus hippocastanus L.*, semen, EMA/HMPC/225319/2008, 2009
4. Pittler MH, Ernst E. Horse chestnut seed extract for chronic venous insufficiency, Cochrane Database of Systematic Reviews, 2012
5. Nicolaidis AN et al. Int Angiol 2008, 27, 1
6. Ramelet AA et al. Clin Hemorheol Microcirc 2005, 30, 198

## 092

**The Arg389Gly polymorphism determines structure and activation kinetics of the human  $\beta_1$ -adrenergic receptor**

**Ahles, Andrea**<sup>1</sup>; Rochais, Francesca<sup>2</sup>; Rodewald, Fabian<sup>1</sup>; Hinz, Laura<sup>1</sup>; Bünemann, Moritz<sup>3</sup>; Engelhardt, Stefan<sup>1,4</sup>

<sup>1</sup>Technische Universität München (TUM), Institut für Pharmakologie und Toxikologie, Germany

<sup>2</sup>Universität Würzburg, Rudolf-Virchow-Zentrum für Experimentelle Biomedizin, Germany

<sup>3</sup>Philipps-Universität Marburg, Institut für Pharmakologie und Klinische Pharmazie, Germany

<sup>4</sup>DZHK (Deutsches Zentrum für Herz-Kreislauf-Forschung), Standort Munich Heart Alliance, München, Germany

Signaling properties of several G protein-coupled receptors are affected by receptor polymorphisms, which alters the response of patients to ligands at these receptors. Yet the molecular basis for the functional differences of individual receptor variants is poorly understood. Recent structural data suggest that the frequent Arg389Gly polymorphism in the proximal carboxy terminus (helix 8) of the human  $\beta_1$ -adrenergic receptor ( $\beta_1$ AR) presumably affects the stability of the receptor protein by specific interaction of arginine (but not glycine) with the intracellular part of transmembrane helix 1.

To investigate a possible impact of the Arg389Gly polymorphism on receptor conformation we developed fluorescence resonance energy transfer-based sensors for the  $\beta_1$ AR variants at position 389 and determined the activation characteristics of the receptor variants in living cells and in real time. While the Arg389- $\beta_1$ AR retained its initial speed of activation upon repeated stimulation, both the Gly389 variant and the Arg389 variant with mutation of Lys85/Thr86 in helix 1 to unpolar residues displayed a significant slowing of their activation kinetics. This indicates an important role of the helix 1 - helix 8 interface in  $\beta_1$ AR conformational changes.

In the following, we analysed the agonist-induced receptor phosphorylation as potential mechanism underlying the observed differences in  $\beta_1$ AR activation. Both determination of  $\beta_1$ AR phosphorylation of the variants and analysis of receptor activation kinetics upon mutation of putative C-terminal  $\beta_1$ AR phosphorylation sites showed that the polymorphism-specific differences in  $\beta_1$ AR activation depended on phosphorylation of the receptor through G protein-coupled receptor kinases.

We then tested whether the differences in activation kinetics would result in more effective signaling to downstream effectors. Indeed, we found agonist-induced cAMP formation to be approx. 40% more effective upon stimulation of the Arg389- $\beta_1$ AR compared to the Gly389 variant. Likewise, the interaction of the Arg389 variant with  $\beta$ -Arrestin2 was significantly enhanced.

Our findings suggest a polymorphism-specific memory of the human  $\beta_1$ AR. This is evident by faster activation of the Arg389-variant and depends on a polymorphism-specific interface of helix 8 and transmembrane helix 1. This mechanism might account for the individual drug responses observed for polymorphic variants of the  $\beta_1$ AR.

## 093

**Endothelial  $G_q/G_{11}$ -mediated signaling regulates vascular smooth muscle differentiation**

**Albarán-Juarez, Julian**<sup>1</sup>; Althoff, Till<sup>2</sup>; Wettschreck, Nina<sup>1</sup>; Offermanns, Stefan<sup>1</sup>

<sup>1</sup>Max-Planck-Institute for Heart and Lung Research, Dept. of Pharmacology, Bad Nauheim, Germany

<sup>2</sup>Charité - Center for Cardiovascular Research, Kardiologisches Forschungslabor, Berlin, Germany

Vascular smooth muscle cells (VSMCs) are plastic and can switch between a quiescent contractile state and phenotypes of increased proliferation, migration, and synthetic activity. Dysregulation of VSMCs plasticity plays a critical role in the pathogenesis of vascular diseases, including neointima formation and atherosclerosis. It is well-established that atherosclerotic lesions develop preferentially in regions of disturbed flow, suggesting that flow conditions directly or indirectly affect VSMCs differentiation. The endothelial cell layer is regarded as the primary sensory structure detecting changes in flow. However, the mechanisms underlying the regulation of VSMCs differentiation in response to changes in vascular flow are still unclear. Nevertheless, *in vitro* data suggest a role of G protein-mediated signaling pathways.

To address the role of  $G_q/G_{11}$  proteins in flow-mediated vascular function, we use mice with inducible endothelial-specific  $G_q/G_{11}$  deficiency. We have observed that endothelial-specific  $G_q/G_{11}$  deficient mice are resistant to neointima formation induced by flow cessation in the carotid artery ligation model. Furthermore, when analyzed by fluorescence microscopy 6 weeks after induction of endothelial  $G_q/G_{11}$  deficiency, the endothelial regions of aortae from  $G_q/G_{11}$  KO mice exposed to disturbed flow showed a considerably decreased expression of vascular cell adhesion molecule-1 (VCAM-1) and lower numbers of macrophage marker CD68 positive cells compared to wild-type mice aortae. In addition, we crossed endothelial specific- $G_q/G_{11}$  KO mice with atherosclerosis-prone LDL receptor KO mice. After 16 weeks of high-fat diet, compared to wild-type mice, atherosclerotic lesion formation was significantly reduced in the aortic root, aortic curvature and innominate artery of animals with endothelial  $G_q/G_{11}$  deficiency. To test whether endothelial  $G_q/G_{11}$ -mediated signaling was also involved in flow dependent responses under *in vitro* conditions, we used a flow chamber system. Exposure of human umbilical vein endothelial cells (HUVECs) to disturbed flow for 24 hours leads to up-regulation of atherogenic genes such as VCAM-1, PDGF and MCP-1 mRNAs in mock transfected HUVECs. However, transcription of these genes was significantly attenuated after siRNA-mediated knockdown of  $G_q/G_{11}$ .

Although the molecular basis of the regulation of VSMC differentiation through changes in flow is not completely understood, these results suggest that it is dependent on receptors coupled to  $G_q/G_{11}$  proteins.



094

### GHQ168, a Novel Fluoroquinolone Carboxamide: Interaction with DNA and Hepatic Oxidative Metabolism

**Albrecht, Annette Evi<sup>1</sup>**; Gareis, Marius<sup>1</sup>; Hiltensperger, Georg<sup>2</sup>; Holzgrabe, Ulrike<sup>2</sup>; Lehmann, Leane<sup>1</sup>; Esch, Harald L.<sup>1</sup>

<sup>1</sup>University of Würzburg, Section of Food Chemistry, Würzburg, Germany

<sup>2</sup>University of Würzburg, Section of Pharmaceutical Chemistry, Würzburg, Germany

GHQ168, a fluoroquinolone carboxamide, is a new potent structure against *Trypanosoma brucei*. Since the widely used fluoroquinolone Ciprofloxacin possesses a potential to intercalate into DNA and causes gene mutations, its non-covalent interaction of GHQ168 with DNA and its mutagenic potential was investigated by fluorescence contact energy transfer (FCET), viscosity of DNA and fluorescent-intercalator displacement (FID) assay and by the hypoxanthine-guanine phosphoribosyltransferase (HPRT) test in Chinese hamster V79 lung fibroblasts (V79 cells), respectively. Berenil (intercalation) and 4-nitroquinoline-N-oxide (mutagenicity) were used as positive controls. Products of the phase I metabolism could also contribute to the mutagenicity of GHQ168, since formation of a catechol seems chemically possible. Thus, oxidative metabolism was investigated using hepatic microsomes from male rats treated with Aroclor 1254 with an isocitrat-based NADPH generation system and HPLC-MS and HPLC-UV analysis.

Two of three intercalation assays were positive: a peak at 260 nm in FCET and an increase in viscosity of DNA from 1.00±0.02 to 1.07±0.02 was observed. In contrast, no effect was observed by FID. Despite its weak potential to intercalate into DNA, the mutant frequency (MF) was not affected by treatment with GHQ168 at non-cytotoxic and cytotoxic concentrations (maximum MF 10±7, control 9±3).

During the first 30 min GHQ168 (100 µM) was metabolized at a rate of 162±35 pmol/min/mg protein. However, prolongation of the incubation period up to 90 min led to a decrease in the rate of metabolism down to 47±35 pmol GHQ168/min/mg protein, indicating enzyme inhibition by GHQ168 or one of its metabolites. HPLC-MS analysis revealed the formation of at least three metabolites. The chemical structure of the metabolites was not elucidated, however, m/z ratios of the metabolites indicate that phase I metabolism includes, ring-hydroxylation, N-dearylation and β-oxidation. Since catechol formation was not observed, the resulting products are most likely devoid of structural alerts for mutagenicity.

In conclusion, GHQ168 is a weak intercalator and does not cause gene mutations in the HPRT test. Oxidative metabolism of GHQ168 leads to enzyme inhibition rather than formation of structural alerts for mutagenicity.

095

### Biomonitoring of the mycotoxin citrinin in urine samples from Bangladesh

**Ali, Nurshad<sup>1</sup>**; Blaszkewicz, Meinolf<sup>1</sup>; Hossain, Khaled<sup>2</sup>; Degen, Gisela H.<sup>1</sup>

<sup>1</sup>Leibniz-Institut für Arbeitsforschung, Chemikalienrisiken, Dortmund, Germany

<sup>2</sup>Rajshahi University, Biochemistry and Molecular Biology, Bangladesh

Citrinin (CIT) is a mycotoxin produced by several fungi of the genera *Penicillium*, *Aspergillus* and *Monascus*. CIT is nephrotoxic, and can co-occur with ochratoxin A (OTA), another nephrotoxic mycotoxin contaminant in food commodities [1]. A survey in Bangladesh documented the presence of OTA in maize [2]; but no study has been carried out on CIT contamination in foods or feed in Bangladesh. Since biological monitoring provides the best approach to assess human exposure to contaminants from various sources and by all routes, it was the aim of this study to analyze CIT and its metabolite dihydrocitrinin (HO-CIT) in urine samples collected in Bangladesh.

Urine samples were collected from inhabitants of a rural (n=32) and an urban (n=37) area in Bangladesh during May 2013. A sensitive method [3] was used for clean up of urines by immunoaffinity column and subsequent LC/MS-MS analysis of the extracts. The limits of detection (LOD) were 0.02 ng/mL and 0.05 ng/mL urine for CIT and HO-CIT.

CIT and HO-CIT were detectable in 94% and 73% of all urine samples. Urinary levels of CIT and its metabolite did not show significant correlations with age, sex and body mass index of the donors. But, excretion of CIT and its metabolite (total) was significantly higher in rural people (LOD – 7.9 ng/mL) than in urban people (LOD – 0.8 ng/mL) in Bangladesh, indicative of differences in mycotoxin exposure. Most of the people in the rural cohort of Bangladesh are farmers or farm workers involved in grain production while urban people are office workers or students. Food habits also differ between the rural and the urban cohort. It can be concluded that contaminated food commodities are major contributors for CIT exposure in humans in Bangladesh. Analysis of other mycotoxins in the two cohorts is underway and the results of biomonitoring will be compared to those in urine samples from German volunteers.

Acknowledgement: Nurshad Ali is supported by a stipend from DAAD

[1] European Food Safety Authority, EFSA (2012) Scientific Opinion on the risks for public and animal health related to the presence of citrinin in food and feed, EFSA J. 10:2605

[2] Dawlatana M, Shahida S, Rahim M, Hassan MT (2008) Investigation on the occurrence of ochratoxin A in maize in Bangladesh. Bangladesh J Sci Ind Res 43(4):495-500

[3] Blaszkewicz M, Munoz K, Degen GH (2013). Methods for analysis of citrinin in human blood and urine. Arch Toxicol 87(6):1087-1094

096

### Calmodulin-dependent regulation of the yeast TRP channel YVC1

**Amini, Mahnaz<sup>1,2</sup>**; Chang, Yiming<sup>3</sup>; Beck, Andreas<sup>1</sup>; Adam, Bertl<sup>4</sup>; Flockerzi, Veit<sup>1</sup>; Schlenstedt, Gabriel<sup>2</sup>

<sup>1</sup>Universität des Saarlandes, Experimentelle u. Klinische Pharmakologie und Toxikologie, Homburg, Germany

<sup>2</sup>Universität des Saarlandes, Institut für Biochemie und Molekularbiologie, Homburg, Germany

<sup>3</sup>ETH Zürich, Institut für Biochemie, Switzerland

<sup>4</sup>Technische Universität Darmstadt, Botanisches Institut, Germany

The yeast vacuolar conductance 1 (YVC1) is the only homolog of the group of Transient Receptor Potential (TRP) cation channel proteins present in the yeast *Saccharomyces cerevisiae*. It is located in the vacuolar membrane and it is gated by hypertonic shock, cytosolic Ca<sup>2+</sup>, stimulated by indole, and involved in osmoregulation.

We previously found calmodulin (Cmd) as a binding partner of YVC1 by using recombinant proteins. Luminometric assays using yeast cells transformed with the Ca<sup>2+</sup> sensor aequorin revealed a higher cytosolic Ca<sup>2+</sup> increase after hypertonic shock in the yeast Cmd mutant *cmd1-6*, which is unable to bind Ca<sup>2+</sup>, compared to the wild-type. Furthermore, whole-vacuolar cation currents, activated by 1 mM cytosolic Ca<sup>2+</sup>, reached higher amplitudes in the *cmd1-6* mutant than in the wild-type. On the other hand, addition of Cmd decreased the activity of the channel in the *cmd1-6* mutant as well as in wild-type cells. Yeast cells carrying YVC1 proteins with point mutations of the predicted Cmd-binding sites showed an altered activity of the channel. Further experiments were performed in HEK-293 cells transiently transfected with a YVC1-IRES-GFP plasmid. Similar to what was observed in the yeast system, hyperosmotic shock induced Ca<sup>2+</sup> signals and whole-cell currents in YVC1-expressing HEK-293 cells, measured by Fura2-AM Ca<sup>2+</sup> imaging and whole-cell patch clamp experiments, respectively. In addition HEK-293 cells overexpressing YVC1 with point mutations of the predicted Cmd-binding sites also showed an altered channel activity. In the presence of ophiobolin A, a calmodulin inhibitor, hyperosmotic shock-induced Ca<sup>2+</sup> influx was increased. This calmodulin-dependent modulation of YVC1 is in accordance with the results obtained in the yeast system. Altogether our findings suggest that calmodulin is a negative regulator of YVC1 activity.

097

### High quality in-silico models for off-target mediated toxicity developed on the basis of public in-vitro assay data – a case study for three diverse endpoints

**Anger, Lennart T.<sup>1,2</sup>**; Rohrer, Sebastian G.<sup>1</sup>; Schleifer, Klaus-Juergen<sup>1</sup>; Schrenk, Dieter<sup>2</sup>; Wolf, Antje<sup>1</sup>

<sup>1</sup>BASF SE, Computational Chemistry and Biology, Ludwigshafen, Germany

<sup>2</sup>University of Kaiserslautern, Food Chemistry and Toxicology, Germany

Chemical structure data and measured bioactivities of compounds are nowadays easily available from public and commercial databases. However, these databases contain heterogeneous data coming from different laboratories determined under different protocols and, in addition, sometimes even erroneous entries. We evaluated the use of data from bioactivity databases for the generation of high quality in-silico models for off-target mediated toxicity as a decision support in early drug discovery and crop-protection research.

The central component is a standardized and thorough quality management routine for input data from bioactivity databases. The established procedure finally enables to develop predictive QSAR models based on heterogeneous in-vitro data from multiple sources. An extended applicability domain approach was used and regression results were refined by an error estimation routine. Subsequent classification with detection and special consideration of borderline candidates led to high accuracies in external validation.

Within this study, we chose human acetylcholinesterase (hAChE) inhibition, human pregnane-X-receptor (hPXR) activation and human glucocorticoid receptor (hGR) antagonism as diverse endpoints to evaluate our (semi-) automatic workflow. Furthermore, we conducted a detailed analysis and comparison of these three data sets (data set size, in-vitro assay formats, activity distribution, structural diversity and physicochemical properties of the compounds) to evaluate potential impacts on the predictivity of the in-silico models.

We demonstrate that the standardized process is transferable to different off-targets and assay readouts. It can be used as a standard approach for generating in-silico models for off-target mediated toxicity. The developed models are well-suited as screening tools for toxic potential in pharmaceutical or crop-protection research in order to prioritize chemical classes for further development or experimental testing in early research phases.

098

### Activation of RhoA,B,C by Yersinia Cytotoxic Necrotizing Factor (CNFy) Induces Apoptosis in LNCaP Prostate Cancer Cells

**Augschach, Anke<sup>1</sup>**; List, Joachim H.<sup>1</sup>; Wolf, Philipp<sup>2</sup>; Elsässer-Beile, Ursula<sup>2</sup>; Aktories, Klaus<sup>1</sup>; Schmidt, Gudula<sup>1</sup>

<sup>1</sup>Albert-Ludwigs-Universität Freiburg, Experimentelle und Klinische Pharmakologie und Toxikologie, Freiburg i. Brsg., Germany

<sup>2</sup>Universitätsklinikum Freiburg, Klinik für Urologie, Germany

Human prostate cancer is a malignant tumor that still forms the second leading cause of cancer death in males in the U.S. The human androgen-dependent prostate cancer cell line LNCaP, which is derived from a metastatic lesion of human prostatic adenocarcinoma, is frequently used to study prostate cancer associated signaling pathways *in vitro*. Recently it was described that Rho GTPase activation in these cells leads to apoptotic responses. The Cytotoxic Necrotizing Factor 1 (CNF1, secreted by pathogenic *Escheria coli* strains) and Cytotoxic Necrotizing Factor Y (CNFY, produced by *Yersinia pseudotuberculosis*) are bacterial toxins that specifically activate Rho-GTPases by deamidation of a single glutamine.

We asked whether these Rho activators could induce apoptosis in LNCaP cells. Our results indicate that RhoA activation, induced by CNFY, does lead to intrinsic apoptosis of the cells. Analysis of the underlying signaling pathway reveals that apoptosis induction requires the activity of Rho kinase (ROCK) and myosin activation, an apoptotic pathway previously identified in cancer stem cells.

## 109

### Toxic effects of carbon nanoparticles in the respiratory tract are prevented by the compatible solute beta mannoglycerate (firoin)

**Autengruber, Andrea**<sup>1</sup>; Sydik, Ulrich<sup>1</sup>; Kröker, Matthias<sup>1</sup>; Stöckmann, Daniel<sup>1</sup>; Gotic, Marijan<sup>2</sup>; Bilstein, Andreas<sup>3</sup>; Unfried, Klaus<sup>1</sup>

<sup>1</sup>Leibniz Research Institute for Environmental Medicine, Particle cell interaction, Düsseldorf, Germany

<sup>2</sup>Ruder Bošković Institute, Division of Materials Chemistry, Zagreb, Croatia

<sup>3</sup>bitop AG, Witten, Germany

Exposure of the airways to particulate environmental air pollution leads to toxic endpoints like apoptosis, proliferation and inflammation. Our previous studies revealed that these outcomes are induced by the interaction of carbon nanoparticles (CNP) with signaling complexes located in the cell membrane. These very initial molecular events have been shown to be prevented by substances called compatible solutes. This group of compounds is known to biophysically stabilize macromolecules and membranes. Ectoine, as a model substance, has been shown to modulate CNP effects in the airways both at the level of epithelial cells and neutrophilic granulocytes.

In the current study, beta mannoglycerate (firoin) was tested for its ability to prevent toxic effects of pure carbon nanoparticles *in vitro* in lung epithelial cells (RLE-6TN), *in vivo* in the lungs of Fisher 344 rats, and *ex vivo* in peripheral human neutrophils.

The activation of MAP-kinases Erk1/2, as mediators of proliferative signaling, and Jnk1/2, which mediate CNP-specific apoptosis, were both significantly and dose dependently reduced by mM doses of firoin in RLE cells. Accordingly, proliferation and apoptosis which both occur in cultured cells after CNP exposure depending on the pre-disposition of the individual cell were significantly reduced in these experiments. Similar effects for both MAP-kinases were observed in lung epithelium of *in vivo* exposed animals. Furthermore, the application of firoin in the lungs of animals which were exposed to CNP, either together with CNP or as a preventive measure, resulted in a significant reduction of neutrophilic lung inflammation. As CNP have been described to increase the neutrophilic life span by anti-apoptotic signaling, apoptosis rates of *ex vivo* treated human neutrophils were studied in the presence of firoin. The compatible solute lead to a restoration of the natural apoptosis rate, indicating its value as strategy against chronic lung inflammation.

In summary, the data demonstrate that toxic effects of carbonaceous particles in the airways are mediated by membrane dependent signaling mechanisms and these can be attenuated *in vitro* and *in vivo* by using the compatible solute beta mannoglycerate.

## 100

### Topology and subcellular localization of TMEM2, a transmembrane protein regulating amylase secretion from acinar cells

**Bach, Aline**<sup>1</sup>; Kriebs, Ulrich<sup>1</sup>; Wissenbach, Ulrich<sup>2</sup>; Jha, Archana<sup>3</sup>; Mannebach-Götz, Stefanie<sup>2</sup>; Zimmermann, Katrin<sup>2</sup>; Vogt, Dominik<sup>1</sup>; Scholz, Anke<sup>2</sup>; Muallem, Shmuel<sup>3</sup>; Pfeifer, Alexander<sup>4</sup>; Weißgerber, Petra<sup>2</sup>; Flockerzi, Veit<sup>2</sup>; Lipp, Peter<sup>5</sup>; Tsvilovskyy, Volodymyr<sup>1</sup>; Freichel, Marc<sup>1</sup>

<sup>1</sup>Universität Heidelberg, Pharmakologisches Institut, Germany

<sup>2</sup>Universität des Saarlandes, Experimentelle und Klinische Pharmakologie und Toxikologie, Homburg, Germany

<sup>3</sup>National Institutes of Health, National Institute of Dental and Craniofacial Research, Epithelial Signaling and Transport Section, Molecular Physiology and Therapeutics Branch, Bethesda, United States

<sup>4</sup>Universität Bonn, Institut für Pharmakologie und Toxikologie, Germany

<sup>5</sup>Universität des Saarlandes, Institut für Molekulare Zellbiologie, Homburg, Germany

In a similarity search using sequence motifs conserved amongst various members of the TRP protein family we identified three non-annotated proteins termed TMEM1, TMEM2 and TMEM4. Based on hydropathy analysis, these proteins exhibit 6 to 10 membrane spanning domains. TMEM2 is expressed ubiquitously but in contrast to TRP proteins there is no evidence that TMEM2 forms ion channels in the plasma membrane following heterologous expression of its cDNA. To get insights about the cellular function of TMEM2 we performed a detailed analysis of its subcellular localization and of its topology. We generated different fusion constructs where TMEM2 is fused with its carboxy- or amino-terminus to different fluorescent proteins. In contrast to the prediction by the PSORT II algorithm TMEM2-eYFP could not be identified in the plasma membrane of several primary cells. A detailed colocalization analysis in which we

expressed marker proteins for various cellular compartments including plasma membrane (membrane targeted-tTomato), Golgi apparatus ( $\beta$ -1,4-galactosyltransferase), ER (Calreticulin-dsRed-KDEL), lysosomes (Lamp1-tagRFP-T), endosomes (mcherry-Rab4a, mcherryRab7, mcherry-Rab11) together with fluorescently labeled TMEM2 proteins in mouse embryonic fibroblasts (MEF), cardiac fibroblasts and mast cells, showed that TMEM2 is located in endosomes and lysosomes. Mutation of the two di-leucine motifs present in the amino- and carboxy-terminal amino acid sequence of TMEM2 abrogated endo-lysosomal localization indicating that these motifs are responsible for endo-lysosomal targeting of TMEM2. Deletion of TMEM2 has no influence on lysosomal  $Ca^{2+}$  release evoked by glycy-L-phenylalanine 2-naphthylamide (GPN)-mediated osmotic permeabilisation of lysosomal membranes in MEFs. Application of a fluorescence protease protection assay revealed that TMEM2 is localized in the endo-lysosomal membrane with its carboxy-terminus directed into the cytoplasm. The analysis of the topology of its amino-terminus is ongoing. Currently we analyze the localization of TMEM2-eYFP in highly polarized pancreatic acinar cells of a TMEM2-eYFP knock-add-on mouse since TMEM2-deficient acinar cells exhibited an elevated resting  $Ca^{2+}$  concentration that correlates with an increased amylase release.

## 101

### A 3'UTR polymorphism modulates mRNA stability of the oncogene and drug target Polo-like Kinase 1

**Bachmann, Hagen Sjärd**<sup>1</sup>; Akdeli, Neval<sup>1</sup>; Riemann, Kathrin<sup>1</sup>; Westphal, Jana<sup>1</sup>; Hel, Jochen<sup>1,2</sup>; Siffert, Winfried<sup>1</sup>

<sup>1</sup>Universitätsklinikum Essen, Institut für Pharmakogenetik, Germany

<sup>2</sup>Universitätsklinikum Essen, Klinik für Urologie, Germany

**Background:** The Polo-like Kinase 1 (PLK1) protein regulates cell cycle progression and is overexpressed in many malignant tissues. Overexpression is associated with poor prognosis in several cancer entities, whereby expression of PLK1 shows high inter-individual variability. Although PLK1 is extensively studied, not much is known about the genetic variability of the *PLK1* gene. Function of PLK1 and expression of the corresponding gene could be influenced by genomic variations. Hence, we investigated the gene for functional polymorphisms. Such polymorphisms could be useful to investigate whether PLK1 alters the risk for and the course of cancer and they could have an impact on the response to PLK1 inhibitors.

**Methods:** The coding region, the 5' and 3'UTRs and regulatory regions of *PLK1* were systematically sequenced. We determined the allele frequencies and genotype distributions of putatively functional SNPs in 120 Caucasians and analyzed the linkage and haplotype structure using Haploview. The functional analysis included electrophoretic mobility shift assay (EMSA) for detected variants of the silencer and promoter regions and reporter assays for a 3'UTR polymorphism.

**Results:** Four putatively functional polymorphisms were detected and further analyzed, one in the silencer region (rs57973275), one in the core promoter region (rs16972787), one in intron 3 (rs40076) and one polymorphism in the 3'untranslated region (3'UTR) of *PLK1* (rs27770). Alleles of rs27770 display different secondary mRNA structures and showed a distinct allele-dependent difference in mRNA stability with a significantly higher reporter activity of the A allele ( $p < 0.01$ ).

**Conclusion:** The present study provides evidence that at least one genomic variant of *PLK1* has functional properties and influences expression of *PLK1*. This suggests polymorphisms of the *PLK1* gene as an interesting target for further studies that might affect cancer risk, tumor progression as well as response to PLK1 inhibitors.

## 102

### Epigenetic Regulation of Cardiac Remodeling by the Lipid Droplet-Associated Protease ABHD5

Jebessa, Zegeye; **Backs, Johannes**

Universität Heidelberg, Kardiologie, Germany

Histone deacetylase 4 (HDAC4) regulates numerous gene expression programs through its signal-dependent repression of the transcription factor myocyte enhancer factor 2 (MEF2). Calcium/calmodulin-dependent protein kinase II (CaMKII) signaling promotes pathological cardiac remodeling by phosphorylating HDAC4, with consequent stimulation of MEF2 activity. We recently unmasked a mechanism whereby protein kinase A (PKA) overcomes CaMKII-mediated activation of MEF2 by regulated proteolysis of HDAC4. PKA induces the generation of an N-terminal HDAC4 cleavage product named HDAC4-NT. HDAC4-NT selectively inhibits MEF2, thereby antagonizing the pro-hypertrophic actions of CaMKII signaling. Using a number of chemical protease inhibitors, we found that the PKA-dependent HDAC4 protease belongs likely to the family of serine proteases. To further identify the individual serine protease, we screened a human serine protease siRNA library and identified abhydrolase containing domain 5 (ABHD5) to be required for PKA-induced cleavage of HDAC4 in HEK cells. ABHD5 is a lipid droplet (LD)-associated protein which dissociates from LDs in a PKA-dependent manner. In isolated rat ventricular myocytes (NRVMs), adenoviral overexpression of ABHD5 (ad-ABHD5) led to proteolysis of HDAC4 with robust production of HDAC4-NT independent of PKA activation. ABHD5 is known to activate lipolysis, but it was not previously described to act as a protease. Myocardial overexpression of ABHD5 protected mice from adverse cardiac remodeling. In contrast, inducible cardiac specific ABHD5 knockout mice developed spontaneously adverse cardiac remodeling resulting in cardiac dysfunction. Taken together, these data identify

ABHD5 as a novel player in the process of adverse cardiac remodeling and unmask a yet unknown mechanistic link between lipid metabolism and epigenetic regulation of cardiac remodeling.

103

#### HPLC-coupled mass spectrometry in cyclic nucleotide research

**Bähre, Heike**<sup>1,2</sup>; Seifert, Roland<sup>1</sup>; Kaefer, Volkhard<sup>1,2</sup>

<sup>1</sup>Hannover Medical School, Institute of Pharmacology, Germany

<sup>2</sup>Hannover Medical School, Research Core Unit Metabolomics, Germany

Endogenous low-molecular weight metabolites can be quantified by several analytical methods, such as immunoassay or high performance liquid chromatography (HPLC) with UV or fluorescence detection. However, due to its unsurpassed sensitivity and specificity tandem mass spectrometry (MS/MS) has become the "gold standard" technology in this field within the last years. HPLC-MS/MS allows the identification and quantitation of various nucleotides due to their retention times on an HPLC column and due to the intensities of their specific mass transitions and is therefore optimally suited for nucleotide analysis even in complex biological matrices such as tissues or prokaryotic and eukaryotic cell extracts [1].

The cyclic purine nucleotides cAMP and cGMP are well known second messengers playing a role in relaxation process of smooth muscle cells, in differentiation, and neurotransmission [2,3]. Furthermore, the existence of the cyclic pyrimidine nucleotides cCMP and cUMP in cell extract has been reported [4]. In bacteria, cyclic di-nucleotides were identified as important second messengers. For c-di-GMP effects on biofilm formation, motility and induction of virulence factors have been demonstrated [5], whereas c-di-AMP has a function in controlling cell size and envelope stress [6]. The cyclic dinucleotide cGAMP has only recently been described as mediator of the mammalian innate immunity [7].

Although the functions of the established cyclic nucleotide second messengers are well understood, so far only little is known about the synthesis, function and metabolism of new types of cyclic nucleotides such as cCMP, cUMP and cGAMP. Using our newly developed HPLC-MS/MS methods we analyzed various biological systems for the occurrence of established and new types of cyclic nucleotides.

[1] Beste KY, Burhenne H, Kaefer V, Stasch JP, Seifert R, Nucleotidyl cyclase activity of soluble guanylyl cyclase  $\alpha 1 \beta 1$ , *Biochemistry* 51 (2012) 194-204

[2] Rehmann H, Wittinghofer A, Bos JL, Capturing cyclic nucleotides in action: snapshots from crystallographic studies, *Nat. Rev. Mol. Cell. Biol.* 8 (2007) 63-73

[3] Hofmann F, Bernhard D, Lukowski R, et al., cGMP regulated protein kinases (cGK), *Handb. Exp. Pharmacol.* 191 (2009) 137-162

[4] Bähre H, Danker KY, Stasch JP, Kaefer V, Seifert R, Nucleotidyl cyclase activity of soluble guanylyl cyclase in intact cells, *Biochem Biophys Res Commun.* in press

[5] Römling U, Galperin MY, Gomelsky M, Cyclic di-GMP: the first 25 years of a universal bacterial second messenger, *Microbiol Mol Biol Rev.* 77 (2013) 1-52

[6] Corrigan RM, Gründling A, Cyclic di-AMP: another second messenger enters the fray, *Nat Rev Microbiol.* 11 (2013) 513-24

[7] Schaap P, Cyclic di-nucleotide signaling enters the eukaryote domain, *IUBM Life.* 65 (2013) 897-903

104

#### Evaluation of current and future therapeutics for sulfur mustard injury in immunocompetent co-culture models of human skin

**Balszuweit, Frank**<sup>1</sup>; Menacher, Georg<sup>1</sup>; Schmidt, Annette<sup>1</sup>; Blömeke, Brunhilde<sup>2</sup>; Thiermann, Horst<sup>1</sup>; Worek, Franz<sup>1</sup>; Steinritz, Dirk<sup>1</sup>

<sup>1</sup>Bundeswehr Institute of Pharmacology and Toxicology, München, Germany

<sup>2</sup>University of Trier, Department of Environmental Toxicology, Germany

Sulfur mustard (SM) is a vesicating chemical warfare agent causing skin blistering, ulceration, impaired wound healing, prolonged hospitalisation and permanent lesions.

No causative antidote is currently available, but for symptomatic therapy, anti-inflammatory compounds, including glucocorticoids and NSAID have been proposed and used in actual cases. However, due to the low number of clinical cases and a variety of pharmacological and surgical interventions used, it has been difficult to evaluate the actual benefit of anti-inflammatory therapy.

Response of immune cells, present in or migrating into skin affected by SM may have a profound effect on the subsequent clinical course and recovery. Immune cells have the potential to amplify toxicity SM by promoting extrinsic apoptosis and inflammation. They may, however, also remove cell debris and apoptotic bodies, thus mitigating toxic effects.

We adapted a co-culture model of monocyte cell line THP-1 as surrogate for dendritic cells and keratinocytes (HaCaT) to investigate SM toxicity and to evaluate current and future therapeutic strategies in this regard.

Results indicate that THP-1, exposed to SM synergistically amplify necrosis, apoptosis and inflammation. A small number of THP-1, corresponding to approx. 2% Langerhans cells in human skin, are sufficient to induce effects significantly different from those in HaCaT monocultures. Intact THP-1 however, added to severely SM-exposed HaCaT, reduced necrosis and inflammation.

A model of 2% THP-1, present at the time of SM exposure, was used to evaluate the response to anti-inflammatory treatments. Response to therapeutic compounds was far more pronounced in co-cultures, compared to HaCaT monocultures. Dexamethason reduced inflammation, but also necrosis and apoptosis. Similar results were obtained

with diclofenac. Treatment with ibuprofen, however, strongly amplified necrotic and apoptotic cell death.

In summary, co-culture models using immune cells provide more valid results than HaCaT monocultures. Findings demonstrate the need to protect immune cells against systemic SM toxicity, as intact immune cells may aid in the recovery, rather than amplifying SM toxicity. Anti-inflammatory therapy with glucocorticoids or diclofenac may not only mitigate inflammation, but help to reduce cell death. Results, however, raise serious concern against the use of ibuprofen after SM poisoning. The co-culture system is also capable to rapidly evaluate future therapies for SM injury.

105

#### Protective effect of Eleutherococcus extract on genomic damage and oxidative stress in cultured mammalian cells

**Bankoglu, Ezgi Eviülü**<sup>1</sup>; Nersesyan, Armen<sup>2</sup>; Stopper, Helga<sup>1</sup>

<sup>1</sup>Institut für Pharmakologie und Toxikologie, Toxikologie, Würzburg, Germany

<sup>2</sup>Institut für Krebsforschung, Wien, Austria

Eleutherococcus senticosus (ES) is a small woody plant which belongs to the Araliaceae family. Its natural habitats are Russia, China, Malaysia, Japan and it is used in traditional Chinese medicine. It is an adaptogen and known as "Siberian ginseng". The active components are so called eleutherosoids, which belong to the chemical classes of lignans, saponins, coumarins and other groups (Davydov et al., 2000).

The aim of the study is to investigate, whether an alcoholic extract of ES has antioxidant activity and whether it can exert protective effect against oxidative stress on mammalian cells.

The antioxidative capacity of ES was tested in a cell free assay (FRAP assay). The HL60 cell line was used to discover protective effect of ES in cells and hydrogen peroxide was chosen as positive control. The comet assay was used to detect antigenotoxic properties. Flow cytometric measurements were done to show antioxidative capacity in cells. Three different concentration of ES extract were used (0.032 %, 0.1 % and 0.32 %). In all end-points cells were pre-incubated with ES extract (30 min, at 37 °C), before treatment with hydrogen peroxide (40 µM, 30 min at 37 °C). In the FRAP assay equivalence to 25 mM of FeSO<sub>4</sub> was detected for 40 % EE. All concentrations of ES extract showed antioxidant capacity in flow cytometric measurement and antigenotoxic effect in the comet assay.

To further investigate the antigenotoxic effect (chromosome breakage and/ or whole chromosome loss) of ES extract, the cytokinesis-block micronucleus cytome assay and to further investigate the ROS scavenging activity, DHE staining will be performed. As conclusion ES clearly has a protective activity against oxidative stress and oxidative stress induced genomic damage. This protective effect is probably mediated by its antioxidant power.

106

#### A role for cutaneous CYP3A in vitamin D homeostasis?

**Baranyai, Dorothea**<sup>1</sup>; Gödtel-Armbrust, Ute<sup>1</sup>; Nestler, Sebastian<sup>2</sup>; Kleuser, Burkhard<sup>3</sup>; Wojnowski, Leszek<sup>1</sup>

<sup>1</sup>Universitätsmedizin der Johannes Gutenberg-Universität Mainz, Institut für Pharmakologie, Germany

<sup>2</sup>Universitätsmedizin der Johannes Gutenberg-Universität Mainz, Urologische Klinik und Poliklinik, Germany

<sup>3</sup>Universität Potsdam, Institut für Ernährungswissenschaft, Nuthetal, Germany

The physiological role of CYP3A expression in the skin is unknown. Our working hypothesis is that CYP3A regulates the cutaneous synthesis of vitamin D. We investigated the expression and regulation of CYP3A in skin samples, a skin-derived cell line and primary cells, and transgenic mice. The metabolic activity of CYP3A towards cutaneous vitamin D precursors was addressed by means of recombinant enzymes. CYP3A5 mRNA was the most abundant CYP3A in human skin biopsies, exceeding CYP3A4 mRNA 3- and CYP3A7 130-fold, and corresponding, respectively, to 1.3%, 0.01% and less than 0.01% of the these genes' hepatic expression levels. The expression of CYP3A43 mRNA was negligible. CYP3A5 was bi-modally expressed both on mRNA and protein level, with carriers of the expresser allele \*1 showing a 3.3-fold higher mRNA, and a 1.8-fold higher protein expression than homozygous carriers of the \*3 allele. CYP3A4/7 and CYP3A5 proteins localized mainly to the keratinocytes of the epidermis as well as to the sebaceous glands, i.e. to areas of vitamin D synthesis. The cutaneous expression of CYP3A5 was also observed in transgenic mice carrying a luciferase reporter gene under the control of a human CYP3A5 promoter. Compared to the liver, the vitamin D receptor (VDR) expression was 100-fold higher, that of CAR comparable, and that of PXR negligible. Correspondingly, CYP3A expression was increased by 1 $\alpha$ ,25-dihydroxy-vitamin D, the active vitamin D, and its precursors except of 7-dehydrocholesterol, but not by rifampicin. As revealed by two-hybrid assays, the response to 1 $\alpha$ ,25-dihydroxy-vitamin D and its precursors was mediated via VDR. Its magnitude was cell donor, cell passage and cell type-dependent. All three CYP3A isozymes metabolized vitamin D to (an) unknown metabolite(s) different from 25-hydroxy-vitamin D, the immediate precursor of the active vitamin D. Taken together, our data suggest that cutaneous CYP3A, predominantly CYP3A5, may regulate the vitamin D homeostasis via VDR-mediated induction of its metabolism. The clinical effects of the CYP3A expression status on vitamin D and bone mineral density are under investigation.

### A fluorescent NOsGC-sensor based on conjoined nitric oxide sensitive guanylyl cyclase subunits fused to FlincG

**Bartels, Joana**; Busker, Mareike; Haase, Tobias; Haase, Nadine; Behrends, Soenke  
TU Braunschweig, Institut für Pharmakologie, Toxikologie und Klinische Pharmazie, Germany

Nitric oxide sensitive guanylyl cyclase (NOsGC) converts GTP into cGMP and represents the drug target for NOsGC stimulators used in pulmonary hypertension. The catalytically active enzyme is a heterodimer consisting of a  $\beta_1$  and an  $\alpha$  subunit. We have previously shown that fusion of the  $\alpha_1$  subunit to the carboxyl-terminus of  $\beta_1$  leads to fully functional, 'conjoined' NOsGC[1]. The fluorescence intensity-based cGMP biosensor FlincG links the first 333 amino acids of the protein kinase I alpha, a cGMP binding element, to a circularly permuted GFP that serves as a fluorescence indicator[2]. The new NOsGC biosensor was derived by fusing the amino-terminus of FlincG to the carboxyl-terminus of the conjoined  $\beta_1$ - $\alpha_1$  construct. Using the spatial proximity of the cGMP-sensor FlincG and the catalytic, cGMP-producing NOsGC-domain, we developed a new tool that allows us to measure the intracellular NOsGC activity in a direct, local and quantifiable fashion.

Live cell imaging was performed using a Nikon A1 confocal microscope with a controlled light exposure module (CLEM) laser for reduced photobleaching and a microscope incubator at 37 °C and 5% CO<sub>2</sub>. The experimental setup was further complemented with a valve system and a withdraw syringe pump that allows for perfusion of cells with NO-donors or NOsGC stimulators and activators. Perfusion of HEK293 cells expressing FlincG with 8-Br-cGMP (50  $\mu$ M) led to the expected increase in fluorescence intensity. DETA/NO (100  $\mu$ M) led to a similar increase in cells expressing  $\beta_1$ - $\alpha_1$ -FlincG (Figure 1). Figure 2 shows measurement of enzyme activity using a biochemical enzyme assay in the cytosol of HEK293 cells expressing the  $\beta_1$ - $\alpha_1$ -FlincG construct.

Using the spatial proximity of the cGMP-sensor FlincG and the catalytic, cGMP-producing NOsGC-domain, we developed a new tool that allows us to visualize intracellular NOsGC activity in intact living cells. The new NOsGC-biosensor will also be used to further understand the mechanism of action and kinetics of NOsGC stimulators and activators.

[1] Haase, Nadine; Haase, Tobias; Kraehling, Jan Robert; Behrends, Soenke (2010): Direct fusion of subunits of heterodimeric nitric oxide sensitive guanylyl cyclase leads to functional enzymes with preserved biochemical properties: evidence for isoform specific activation by ciguates. In: *Biochem. Pharmacol.* 80 (11), S. 1676–1683. DOI: 10.1016/j.bcp.2010.08.007.

[2] Nausch, Lydia W. M.; Ledoux, Jonathan; Bonev, Adrian D.; Nelson, Mark T.; Dostmann, Wolfgang R. (2008): Differential patterning of cGMP in vascular smooth muscle cells revealed by single GFP-linked biosensors. In: *Proc. Natl. Acad. Sci. U.S.A.* 105 (1), S. 365–370. DOI: 10.1073/pnas.0710387105.

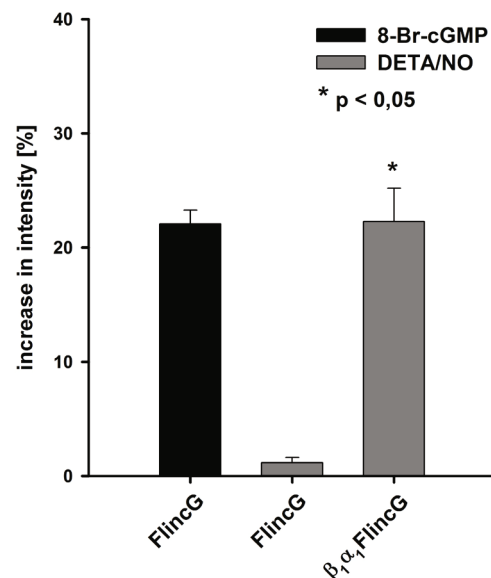


**Figure 1:** Increase in fluorescence intensity of the indicated constructs in response to 8-Br-cGMP or DETA/NO

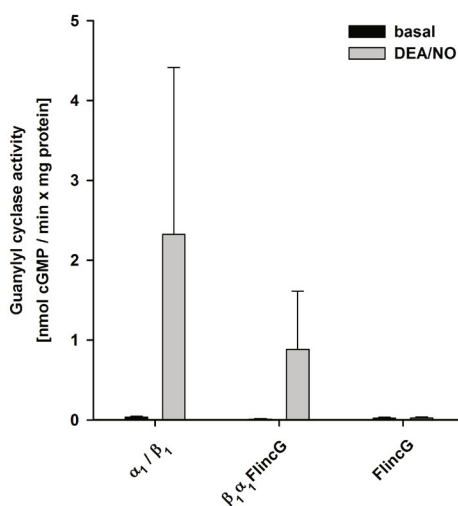


**Figure 2:** Measurement of enzyme activity using a biochemical enzyme assay in the cytosol of HEK293 cells expressing the indicated constructs

### Correlations between different endpoints in repeated dose toxicity studies: occurrence of dependent and independent effects at equal dose levels in the RepDose and the "ELINCS" database

**Batke, Monika**<sup>1</sup>; Bitsch, Annette<sup>1</sup>; Gundert-Remy, Ursula<sup>2</sup>; Gütlein, Martin<sup>3</sup>; Kramer, Stefan<sup>4</sup>; Partosch, Falko<sup>2</sup>; Seeland, Madeleine<sup>5</sup>; Stahlmann, Ralf<sup>1</sup>  
<sup>1</sup>Fraunhofer Institut für Toxikologie und Experimentelle Medizin, Chemikalienbewertung, Hannover, Germany  
<sup>2</sup>Charité - Universitätsmedizin Berlin, Institut für Klinische Pharmakologie und Toxikologie, Germany  
<sup>3</sup>Albert-Ludwigs-Universität Freiburg, Institut für PhysiK, Zentrum für Biosystemanalyse, Germany  
<sup>4</sup>Johannes Gutenberg - Universität Mainz, Institut für Informatik, Germany  
<sup>5</sup>Technische Universität München, Institut für Informatik / I12, Garching, Germany

The data basis for this analysis consists of two independent data bases containing results from repeated toxicity studies (RepDose and ELINCS). To have a consistent data set out of these both databases all data that are suitable with respect to reliability, route, species and study duration have been extracted in a so called homogenous subset.

The data set contains in total more than 2000 studies for 1046 chemicals, most of them industrial chemicals. Endpoints that do not have a clear organ attribution such as clinical chemistry have been subdivided and related to the specific organ such as clinical chemistry related to hepatotoxicity and clinical chemistry related to nephrotoxicity. The min LOEL values for each endpoint were used for further analyses.

In the present evaluation LOELs of single endpoints were analysed by Pearson correlation. The results are near to 1 for highly correlated LOELs, about 0 if no correlation of LOELs is given and <0 for inverse correlation of LOELs. With the correlation matrix effects that occur at similar dose levels are compared. Thus, the correlations are supposed to give a first input about toxicity profiling or toxicological pathways.

The matrix enables analyses for different aspects: 1) correlations of effects in different target organs, 2) correlations of different effects in one target organ (i.e. weight changes and histopathology for the male reproductive system) and 3) correlations of clinical chemistry with other effects in specific target organs.

Out of the various effects in clinical chemistry some profiles could be defined/proven as pathways for hepatotoxicity i.e. decreased cholesterol and increased ASAT/GOT as indicators of liver damages with histopathological changes (e.g.cirrhosis) or increased Bilirubin, ALAT and AP as indicators of cholestasis.

Furthermore, the analyses show that often effects may be elicited by different doses ("difference in sensitivity") indicating dose dependent disturbance of different steps in a pathway as further effects in the same target organ can be observed only at higher dose levels. Thus, it seems that the scope of examination and dose regime of a study is crucial for the outcome of possible correlations i.e. between clinical chemistry endpoints and organ toxicity.

All in all, this kind of correlation matrices on a reliable data basis can give important input in the knowledge on underlying mechanisms by elucidating relations/connections between toxic effects.

109

### Role of HA matrix in adipose tissue: Possible implications for adipose tissue expansion, inflammation and insulin resistance

**Bayer, Julia Katharina**<sup>1</sup>; Grandoch, Maria<sup>1</sup>; Fender, Anke Claudia<sup>1</sup>; Rütter, Ulrich<sup>2</sup>; Fischer, Jens Walter

<sup>1</sup>Institut für Pharmakologie und Klinische Pharmakologie, Universitätsklinikum Düsseldorf, Heinrich-Heine-Universität Düsseldorf, Germany

<sup>2</sup>Institut für Entwicklungs- und Molekularbiologie der Tiere, Heinrich-Heine Universität Düsseldorf, Germany

Obesity is one of the major risk factors for the development of insulin resistance and type II diabetes mellitus. Excessive expansion of adipose tissue leads to infiltration of immune cells contributing to adipose tissue inflammation and insulin resistance. During adipocyte differentiation extensive accumulation of the extracellular matrix component hyaluronan (HA), generally synthesized by three different HA synthase isoenzymes (HAS1-3), has been observed.

Aim of the present study was to investigate the role of HA for adipocyte function and the development of obesity and insulin resistance *in vivo* and *in vitro*.

Eight-week-old C57BL/6J mice receiving either the HA synthesis inhibitor 4-methylumbelliferone (4-MU) or placebo were fed with a diabetogenic diet (DD) for 22 weeks. Mice systemically treated with 4-MU gained significantly less weight compared to control mice (DD: 26.7 ± 1.1 g vs. DD 4-MU: 15.5 ± 1.7 g). This observation was further supported by NMR analysis revealing less total fat mass in 4-MU fed mice (DD: 0.316 ± 0.009 vs. DD 4-MU: 0.246 ± 0.009). Glucose and insulin tolerance tests showed an improved glucose and insulin tolerance in the early stages of obesity. *In vitro* studies of differentiating 3T3-L1 cells treated with 4-MU or hyaluronidase proved that adipocyte differentiation was impaired by downregulation of HA. Furthermore, monocyte adhesion assays using U937 cells demonstrated a reduction of monocyte attachment to 4-MU treated 3T3-L1 cells.

Effects on adipogenesis were not mediated by HAS3-dependant HA synthesis: No difference in weight gain or fat mass was observed in HAS3-knockout mice fed with DD. Likewise, 3T3-L1 cells transfected with siRNA against HAS3 showed no change in differentiation potential. In contrast, 3T3-L1 differentiation was inhibited by administration of HAS2 siRNA, pointing towards a HAS2-specific effect in the regulation of adipogenesis.

The results of this study indicate that the presence of HA is critical for adipose tissue expansion. Diet-induced obesity can be counteracted by inhibition of HA synthesis, suggesting positive effects on adipocyte inflammation and insulin resistance.

110

### The Cytotoxicity of Toluidine Blue

**Bekka, Elias**; Hopfer, Christine; Mückter, Harald; Gudermann, Thomas  
Walther-Straub-Institut, Toxikologie, München, Germany

**Introduction:** Phenothiazine (PZ) dyes like Toluidine Blue (TB) have a variety of diagnostic and therapeutic uses in modern medicine, e.g., in chromo diagnostics, or as antidotes against drug-induced methemoglobinemia. While their use has generally been recognized as safe, several accounts of serious arrhythmias following IV administration have been published in recent years [1]. In each case the intravenous injection of TB has been blamed, although the precise cause of the arrhythmias is unknown. We have tried to characterize the effect of TB in cultured cells in order to learn how TB exerts its cytotoxicity.

**Materials & Methods:** We exposed two different indicator cell lines to various concentrations of TB and fractionated cells using a Potter-Elvehjem homogenizer and ultracentrifugation to study the subcellular distribution of TB. Using a holographic microscope (HoloMonitor M3) we measured morphological changes of exposed cells. Cellular integrity after PZ exposure was assessed by flow cytometry. Flow cytometric assays using the fluorescent dye JC-1 were performed to monitor the mitochondrial membrane potential after PZ exposure.

**Results:** TB targets the plasma membrane and nucleus as expected from its basophilic nature [2]. We also noted that mitochondria were affected, which is consistent with reports on other PZ dyes [3] and PZ drugs [4].

Mitochondria were functionally impaired by TB, as demonstrated by the collapse of the mitochondrial membrane potential at 4 hours and 19 hours. For L929 cells, we noted that after TB exposure up to 19 hours 39 ± 5% of the cells displayed a collapsed mitochondrial membrane potential. For A549 cells the fraction was 27 ± 0.7%.

A generalized swelling of cells was observed at low concentrations of TB (5-10 µM) whereas cell volume was unaffected when cells were processed in the same way, but in absence of TB. The uptake kinetics of TB did not suggest that an active transport into the cells is involved.

**Conclusions:** TB rapidly entered the exposed cells. With regard to TB cytotoxicity, the binding of TB to the plasma membrane and the collapse of the mitochondrial membrane potential, are likely candidates for the observed cellular vulnerability [5].

[1] Zieger J et al., *Arzneimitteltherapie* (2008) 26: 461-463

[2] Kiemann JA, *Histol Histochem Methods* (2008), Pergamon Press, Oxford, pp.2-3

[3] Wondrak GT, *Free Radic Biol Med* (2007) 43: 178-190

[4] Cruz TS et al., *Biochem Pharmacol* (2010) 80: 1284-1295

[5] Brown DA, O'Rourke B, *Cardiovasc Res* (2010) 88: 241-249

111

### Deletion of the Ca<sup>2+</sup> channel β3 subunit affects agonist induced Ca<sup>2+</sup> release in fibroblasts

**Belkacemi, Anouar**; Dörr, Janka; Weißgerber, Petra; Beck, Andreas; Flockertz, Veit  
Universität des Saarlandes, Institut für Pharmakologie und Toxikologie,  
Universitätsklinikum, Homburg, Germany

β subunits of voltage-gated Ca<sup>2+</sup> channels (Ca<sub>v</sub>β) are cytoplasmic proteins and play a pivotal role in the trafficking of the pore-forming Ca<sub>v</sub>α1 subunit to the plasma membrane and in modulating the Ca<sup>2+</sup> current kinetics. We identified Ca<sub>v</sub>β3 proteins in primary mouse embryonic fibroblasts (MEFs), skin fibroblasts and cardiac fibroblasts but we did not detect any functional voltage-gated Ca<sup>2+</sup> influx in these cells. Subcellular fractionation and confocal images of HEK-293 and Cos-7 cells expressing the Ca<sub>v</sub>β3 cDNA, and of primary MEFs reveal a cytosolic localization of the β3 protein. Among the proteins potentially interacting with Ca<sub>v</sub>β3 are the inositol 1,4,5-trisphosphate receptors (IP<sub>3</sub>Rs) and the phospholipase C gamma1 (PLCγ1). We therefore co-expressed the mouse IP<sub>3</sub>R type 1, 2 and 3 and the mouse PLCγ1 cDNAs each of them with the Ca<sub>v</sub>β3 cDNA in Cos-7 cells for co-immunoprecipitation. Using a Ca<sub>v</sub>β3 antibody, the β3 protein was precipitated, and among the proteins retained by the β3 were the IP<sub>3</sub>Rs type 1, 2 and 3 and the PLCγ1 proteins, respectively, and vice versa. IP<sub>3</sub> production was increased in β3-deficient MEFs compared to wild-type MEFs under basal conditions. Lysophosphatidic acid- or bradykinin-induced IP<sub>3</sub>-dependent Ca<sup>2+</sup> release was significantly increased in MEFs isolated from β3-deficient mice compared to wild-type, whereas thapsigargin-induced Ca<sup>2+</sup> release was unaffected. Vice versa expression of Ca<sub>v</sub>β3 in Cos-7 cells, which do not express endogenous Ca<sub>v</sub>βs, decreases agonist-induced Ca<sup>2+</sup> release. Ca<sub>v</sub>β subunits contain two conserved regions, C1 and C2, of ~130 amino acids and ~150 amino acids in length, respectively. The C1 domain shares homology with Src homology domains (SH3) and C2 has minor but detectable similarity to guanylate kinase (GK) domains. Both domains are essential for the regulation of Ca<sup>2+</sup> currents through the Ca<sub>v</sub>α1 subunits. We constructed the Ca<sub>v</sub>β3 deletion mutants Ca<sub>v</sub>β3ΔSH3 and Ca<sub>v</sub>β3ΔGK to study their impact on agonist-induced Ca<sup>2+</sup> release in Cos-7 cells and co-immunoprecipitation of IP<sub>3</sub>R type 1, 2 and 3 and PLCγ1. β3ΔGK was able to interact with the IP<sub>3</sub>R type 3, whereas deletion of the SH3 domain prevents the interaction with the IP<sub>3</sub>R type 3 as well as the decrease of agonist-induced Ca<sup>2+</sup> release in Cos-7 cells. Apparently, the β3 subunit acts as a brake on IP<sub>3</sub>-dependent Ca<sup>2+</sup> release by directly interacting with the IP<sub>3</sub>R via its SH3 domain and modulates the basic levels of IP<sub>3</sub> by interacting with the PLCγ1.

112

### Evaluation of the mutagenic potential of an ethanolic extract of *Aristolochia clematitis* seeds

**Teweldeberhan, Elisabeth**; Klepper, Aaron; Krieger, Kristina; **Berg, Kerstin**; Schrenk, Dieter  
TU Kaiserslautern, Lebensmittelchemie und Toxikologie, Germany

*Aristolochia clematitis* L. (Birthwort) is a plant in the *Aristolochiaceae* family. It can be found in tropical as well as in temperate climate. Formerly, *Aristolochia* has been used in ethnomedicine, e.g. for treatment of nephropathy, rheumatism, allergy or asthma. Recently, chronic intoxication by contamination of crop with seeds from *Aristolochia* spp. or mix-up with other plants (e.g. used as food supplements) has been reported. Aristolochic acids (AA) are the main active constituents known as being nephrotoxic and carcinogenic.

In the present study an ethanolic seed extract of *Aristolochia clematitis* has been prepared. Its mutagenicity has then been analyzed using the Ames-fluctuation test with and without exogenous metabolic activation (S9-Mix) in TA97a, TA98, TA100 and TA102. A strong, concentration dependent mutagenic effect could be shown in most strains. In TA100 and TA102, which detect base-pair substitutions, the mutagenic potential decreased after addition of S9-Mix. This reduction implies that the active compounds have been detoxicated. These results agree with the AA data described in literature and indicate that aristolochic acids play a major role in the observed mutagenicity. In TA98 and TA97a metabolic activation caused an increase in mutagenic activity. There are several published studies which demonstrate that AA have no or only a weak activity in TA98 and hence other active substances must have contributed to the effect of the extract. Beside the bacterial mutation assay we used the HPRT-Assay in V79-cells to confirm mutagenicity in mammalian cells. The HPRT-Assay also showed a strong, concentration dependent increase in mutation rate. An analytical screening should give further information about the composition of the seed extract. The significant induction of mutations has to be explained by quantification of the main components. Furthermore, the identified compounds should be examined as pure substances for mutagenicity in a similar concentration range.

113

### Multidrug resistance-associated protein 4 (Mrp4) regulation by aryl hydrocarbon receptor (AhR) and nuclear factor E2-related factor-2 (Nrf2) in killifish (*Fundulus heteroclitus*) renal proximal tubules

**Bernd, Alexandra**; Mahringer, Anne; Fricker, Gert

Institut für Pharmazie und Molekulare Biotechnologie, Pharmazeutische Technologie und Biopharmazie, Heidelberg, Germany

**Background:** Polycyclic aromatic hydrocarbons, such as the dioxin 2,3,7,8-Tetrachlorodibenzodioxin (TCDD), are highly toxic, persistent environmental pollutants that accumulate in the food chain. Many of these chemicals interfere with the regulation of xenobiotic metabolism and increase the expression of drug transporters, such as Mrp4, by activating e.g. the AhR<sup>1</sup>. Mrp4 might be an important target in the development of drugs as this transport protein is both able to transport endogenous molecules as well as foreign chemicals<sup>2</sup>.

**Methods:** After killing, killifish were cut along their belly, organs were removed and tubule strands were taken out and transferred into a marine teleost saline buffer based on that of Forster and Taggart (TFB)<sup>3</sup>. Then, proximal tubules were separated and used for RNA isolation, immunostaining or transport experiments. For the latter, tubuli were transferred into foil-covered Teflon chambers containing TFB at room temperature. FluorocAMP - a fluorescent analogue of cyclic AMP - was added as specific Mrp4 substrate<sup>4</sup> in absence and presence of transporter modulators and after reaching steady state of excretion confocal fluorescent images were acquired.

**Results:** It was found *ex vivo* that Mrp4 transport activity was increased by incubation of tubules with beta-naphthoflavone (BNF) and TCDD respectively, both agonists of AhR. This effect was reversed by alpha-naphthoflavone (ANF), an AhR antagonist, and could be prevented by inhibiting both transcription and translation with actinomycin D or cycloheximide. Subsequently, it was shown that BNF also increases transport activity *in vivo*. In addition to that, we found that Mrp4 expression augments on protein and RNA level *in vivo*, too. Since phase II genes of the AhR battery are cross-linked to the Nrf2 battery<sup>5</sup>, the influence of sulforaphane (SFN), an Nrf2 ligand, was studied *ex vivo*. Here, it was found that SFN increased transport activity of Mrp4 and that SFN together with TCDD superinduced it above that was found with TCDD alone.

[1] Xu et al. Am J Physiol Gastrointest Liver Physiol 2010; 299:G126-G135

[2] Russel et al. Trends Pharmacol Sci 2008; 29: 200-207

[3] Forster RP, Taggart JV, J Cell Physiol 1950; 36(2): 251-270

[4] Reichel et al. Am J Physiol Regul Integr Comp Physiol 2007; 293: R2382-2389

[5] Köhle C, Bock KW, Biochem Pharmacol 2007; 73: 1853-1862

## 114

### Modification Of Bacterial Resistance Of *E. coli* Due To The Treatment Of Pigs With Ceftiofur

**Beyer, Anne**<sup>1</sup>; Stahl, Jessica<sup>2</sup>; Scherz, Gesine<sup>2</sup>; Rösler, Uwe<sup>3</sup>; Friese, Anika<sup>3</sup>; von Bergen, Martin<sup>4</sup>; Baumann, Sven<sup>1</sup>; Glünder, Gerhard<sup>5</sup>; Kietzmann, Manfred<sup>2</sup>; Honscha, Walther<sup>1</sup>

<sup>1</sup>University Leipzig, Faculty of Veterinary Medicine, Institute of Pharmacology, Pharmacy and Toxicology, Germany

<sup>2</sup>University of Veterinary Medicine Hannover Foundation, Institute of Pharmacology, Toxicology and Pharmacy, Germany

<sup>3</sup>Free University Berlin, Institute for Animal Hygiene and Environmental Health, Germany

<sup>4</sup>Helmholtz-Zentrum für Umweltforschung GmbH - UFZ, Department of Metabolomics, Leipzig, Germany

<sup>5</sup>University of Veterinary Medicine Hannover Foundation, Clinic for Poultry, Germany

**Introduction:** The emergence of resistant bacteria, especially to  $\beta$ -lactam-antibiotics, to extended-spectrum  $\beta$ -lactamases (ESBL)-producing *Enterobacteriaceae* has become a serious problem in both human and veterinary medicine. Several reports have been published an association between antimicrobial consumption of ceftiofur and the appearance of *E. coli* with reduced susceptibility to third-generation cephalosprins. Thus, the objective of the present study was to investigate (1) the progress of bacterial resistance in commensal *E. coli* in pigs after treatment with ceftiofur and (2) the influence on untreated animals in the same barn.

**Materials and Methods:** Twelve pigs (5-9 kg) were kept in two stalls of a stable. One group (group B) of these animals was treated with a therapeutic dosage of ceftiofur (3 mg/kg, i.m.) at three consecutive days (day 1 to 3). The other group (group A) remained untreated. After treatment, fecal samples were obtained from each pig of the two groups on several days. A qualitative examination of the susceptibility of *E. coli* was made by agardilution assay. The minimum inhibitory concentrations (MIC) of ten *E. coli* colonies per animal and day were determined by a microdilution assay. A second treatment followed with detection of MIC-values (day 29 to 31). After 45 days the control group A was treated on the same way with ceftiofur, to detect a possible influence of environmental pollution.

**Results:** Increased MIC-values were detected by the microdilution assay after the second treatment of group B. But only a small number of resistant colonies could be detected. However, after treating the control group A (day 45) a significant higher number of colonies could be determined in the trials of this group by microdilution assay. By using the method of enrichment 4 weeks after the first treatment a decreased susceptibility was detected in both groups. ESBLs were proved.

**Conclusion:** The application of third-generation cephalosporins poses the risk of developing bacterial resistance even without exposure to selective pressure. So there is a great likelihood for transfer of resistant bacteria to untreated animals where they can influence the occurrence of susceptibility of *E. coli*. A second reason could be the exposure to minimal concentrations of the active substance originating from the excretion of treated pigs.

## 115

### Cannabidiol induces heme oxygenase-1 expression in human endothelial cells

**Böckmann, Sabine;** Hinz, Burkhard

Institute of Toxicology and Pharmacology, University of Rostock, Germany

The non-psychoactive cannabinoid cannabidiol (CBD) has been associated with cardiovascular protective effects in animal and cell culture experiments. However, the underlying mechanisms are poorly understood. Using human umbilical vein endothelial cells (HUVEC) the present study investigated the impact of CBD on the expression of the vasoprotective enzyme heme oxygenase-1 (HO-1). Changes in spontaneous apoptosis of HUVEC and in the expression of intercellular adhesion molecule-1 (ICAM-1), a marker of endothelial dysfunction, were measured concomitantly. At concentrations up to 10  $\mu$ M CBD caused a concentration-dependent increase of HO-1 mRNA and protein. CBD ( $\leq 6 \mu$ M) inhibited DNA fragmentation and caspase-3 cleavage and left ICAM-1 expression virtually unaltered, whereas no anti-apoptotic action and increased ICAM-1 expression was observed with 10  $\mu$ M CBD. Transfection of HUVEC with siRNA targeting HO-1 was found to inhibit the anti-apoptotic properties of 6  $\mu$ M CBD confirming a pivotal role of HO-1 in conferring the cytoprotective action of the cannabinoid. In line with this notion, further siRNA approaches yielded the nuclear factor erythroid-2-related factor 2 as a target of CBD in mediating a HO-1-dependent anti-apoptosis. By contrast, the combination of HO-1 siRNA and 10  $\mu$ M CBD led to an overadditive increase of apoptosis and ICAM-1 expression implying HO-1 upregulation as a mechanism by which CBD may limit its own cytotoxic action at higher concentrations. Finally, experiments with receptor antagonists excluded an involvement of cannabinoid-activated receptors (CB<sub>1</sub>, CB<sub>2</sub>, transient receptor potential vanilloid 1) in the CBD effects (HO-1 induction, anti-apoptosis, ICAM-1 upregulation) reported here. Collectively, our data provide first-time proof for an induction of the HO-1 enzyme in endothelial cells as a mechanism by which CBD concentration-dependently mediates cytoprotection as well as limitation of its own toxicity.

## 116

### Atherosclerotic lesion development is attenuated by absence of the PAR-2 factor-Xa receptor in apolipoprotein E-deficient mice

**Böhm, Andreas**<sup>1,2</sup>; Flößler, Anja<sup>1</sup>; Küppers, Johannes<sup>1</sup>; Schrör, Karsten<sup>2</sup>; Rauch, Bernhard H.<sup>1,2</sup>

<sup>1</sup>Universitätsmedizin Greifswald, Institut für Pharmakologie, Germany

<sup>2</sup>Universitätsklinikum Düsseldorf, Institut für Pharmakologie und Klinische Pharmakologie, Germany

The activated coagulation factor X (FXa) is an agonist for the G-protein-coupled protease-activated receptor-2 (PAR-2). PAR-2 is expressed in vascular smooth muscle cells (SMC) and is upregulated during vascular injury and diabetes. A possible role of PAR-2 in atherosclerotic lesion development is to date unclear. In this study, we investigated the role of PAR-2 during lesion formation in atherosclerosis-prone apolipoprotein E (ApoE)-deficient mice.

PAR-2/ApoE-deficient mice were generated and fed standard chow or, beginning at 2 months age, a cholesterol-rich Western diet over 2 or 4 months in comparison with ApoE control mice (both C57/Bl6 background). Aortic plaque area was determined by Oil Red O staining, FX/FXa, the monocyte marker Mac-2, smooth muscle  $\alpha$ -actin and PAR-2 by immunostaining; apoptosis by Tunel assay. IL-6 and MCP-1 were determined by real-time PCR in aortic SMC isolated by the explant technique.

FXa and PAR-2 both were present in plaques from ApoE mice. Aortic plaque size was significantly reduced in PAR-2/ApoE compared to ApoE mice both at 2 and 4 months after cholesterol-rich diet. SMC content was decreased in ApoE mice while apoptosis was potentially increased after 4 months of cholesterol-rich chow compared to PAR-2/ApoE. Interestingly, macrophage count was markedly lower in PAR-2/ApoE mice with standard chow, but significantly increased during cholesterol feeding, while it correlated with apoptosis in the ApoE mice at 4 months, suggesting a delayed macrophage infiltration and attenuated apoptosis in the PAR-2/ApoE mice. SMC isolated from C57/Bl6 mice showed a time-dependent increase in expression of IL-6 and MCP-1 after stimulation with FXa. This was attenuated in SMC from PAR-2 mice.

In conclusion, lack of PAR-2 attenuates development of atherosclerosis in lesion-prone ApoE mice. This is associated with decreased apoptosis and delayed macrophage invasion, possibly due to reduced expression of pro-inflammatory mediators such as IL-6 and MCP-1.

## 117

### Cellular signalling pathways as targets for widening the therapeutic window of oxaliplatin

**Bormann, Stefanie;** Fritz, Gerhard

Heinrich-Heine-University, Institute of Toxicology, Düsseldorf, Germany

The platinating agent oxaliplatin is frequently used for the treatment of colorectal cancer. After entering the cell, the drug exerts its function by forming DNA monoadducts, which are subsequently processed into DNA intra- and interstrand crosslinks. Such adducts interfere with transcription and replication of the DNA which will eventually lead to cell death. However, as these cytotoxic effects are not cancer cell specific, oxaliplatin causes different adverse affects, of which neurotoxicity is the most relevant. For the purpose of improving oxaliplatin anti-cancer action and reducing neurotoxic side effects

at the same time, this work aims to modifying cellular signalling pathways in order to identify molecular targets for such improvement. As an *in vitro* model the murine colon carcinoma cell line CT26.WT and the murine neuronal cell line Neuro2a are used. Both cell lines show a dose dependent reduction in viability after treatment with oxaliplatin (IC50 6  $\mu$ M for CT26.WT and 8  $\mu$ M for Neuro2a). Preliminary experiments show a reduced cytotoxic effect of the platinum compound when Neuro2a cells are pre-treated with retinoic acid, which preserves the neuronal phenotype. Further currently ongoing experiments analyse the cytotoxic effect of oxaliplatin when the aforementioned cells are co-treated with selected protein kinase inhibitors (e.g. of the EGFR, Akt or MAPKs). Moreover, the impact of pharmacological inhibitors on oxaliplatin induced effects on gene expression, DNA damage response, and DNA repair is under investigation. Data obtained will be presented and discussed.

## 118

### Phenobarbital-mediated tumor promotion in Apc knockout mice

**Braeuning, Albert**<sup>1</sup>; Gavrilov, Alina<sup>1</sup>; Bucher, Philip<sup>1</sup>; Metzger, Ute<sup>2</sup>; Wenz, Christine<sup>1</sup>; Templin, Markus<sup>2</sup>; Schwarz, Michael<sup>1</sup>

<sup>1</sup>Universität Tübingen, Toxikologie, Germany  
<sup>2</sup>NMI, Reutlingen, Germany

In rodent liver, a single injection of N-nitrosodiethylamine (DEN) followed by chronic treatment with the antiepileptic drug phenobarbital (PB) promotes the outgrowth of hepatocellular tumors with activating mutations in *Ctnnb1*, encoding the transcription factor  $\beta$ -catenin. We now studied short- and long-term effects of PB treatment in livers of transgenic mice with hepatocyte-specific knockout (KO) of *Apc*, a negative regulator of  $\beta$ -catenin signaling.

The number of *Apc* KO hepatocytes present in the liver decreased with age, indicative of a selective disadvantage of *Apc* KO cells in the absence of PB. Treatment with PB resulted in a transient proliferative advantage of *Apc* KO hepatocytes and a long-term slowdown of *Apc* KO cell loss. Parallel analyses in a *Cx32* KO background demonstrated that the behavior of *Apc* KO hepatocytes is independent of connexin-mediated gap-junctional intercellular communication.

Following liver tumor promotion by PB in *Apc* KO mice for 10 months, tumor burden was quantified and tumors were analyzed for histological appearance, gene expression profiles, and activity of oncogenic signaling pathways. In *Apc* KO mice fed with PB, we observed an increased hepatic tumor volume fraction and tumor multiplicity, as compared to non-promoted animals. Tumors in the PB-treated *Apc* KO group were mostly eosinophilic hepatocellular adenoma with activated  $\beta$ -catenin, due to the deletion of *Apc*. These tumors exhibited striking phenotypic similarities to DEN-induced *Ctnnb1*-mutated tumors, regarding histological appearance and expression of marker proteins and mRNAs. While forming phenotypically similar tumors, the probability for *Apc* KO hepatocytes to form tumors under the conditions of PB treatment was calculated to be strikingly lower than the corresponding probability for *Ctnnb1*-mutated cells. Interestingly, a particular sub-population of tumors, *Apc* KO-driven basophilic hepatocellular carcinomas, exclusively appeared in the non-PB-treated group, but was absent from PB-promoted livers.

In conclusion, phenobarbital promotes the outgrowth of *Apc*-deficient,  $\beta$ -catenin-activated hepatocellular adenoma while simultaneously inhibiting the formation of a certain population of *Apc*-driven hepatocellular carcinoma.

## 119

### The effect of bumetanide and its lipophilic prodrug BUM 5 on the anticonvulsant potential of the GABAmimetic drug phenobarbital in the maximal electroshock seizure threshold test in epileptic mice.

**Brandt, Claudia**<sup>1,2</sup>; Töllner, Kathrin<sup>1,2</sup>; Twele, Friederike<sup>1,2</sup>; Erker, Thomas<sup>3</sup>; Brunhofer, Gerda<sup>3</sup>; Gabriel, Mario<sup>3</sup>; Löscher, Wolfgang<sup>1,2</sup>

<sup>1</sup>Stiftung Tierärztliche Hochschule, Institut für Pharmakologie, Toxikologie und Pharmazie, Hannover, Germany

<sup>2</sup>Zentrum für systemische Neurowissenschaften, Hannover, Germany

<sup>3</sup>Universität Wien, Institut für medizinische Chemie, Austria

Recent studies demonstrate a possible role of cation-chloride-co-transporters in the pathogenesis of epilepsy. Changes in the expression pattern of the  $K^+$ - $Cl^-$  co-transporter KCC2 (downregulation) and the  $Na^+$ - $K^+$ - $2Cl^-$  co-transporter NKCC1 (upregulation) lead to a GABA-shift from a hyperpolarizing to a depolarizing action caused by an accumulation of intracellular chloride. This results in a hyperexcitatory state of specific networks. In this respect the diuretic drug bumetanide has attracted growing interest. Bumetanide is an inhibitor of NKCC1 so that it is assumed that the administration of bumetanide could counteract the shift to a depolarising GABA action. Two major drawbacks of bumetanide, the diuretic potential and the low brain penetration, restrict the testing of bumetanide in experimental and clinical settings.

The aim of the study is to investigate the effect of bumetanide's prodrug BUM5 on the GABAmimetic anticonvulsant drug phenobarbital (PB) in epileptic mice. BUM5 was designed to be more lipophilic in order to penetrate into the brain and be less diuretic than bumetanide.

Drug trials were performed once a week in female NMRI mice in the maximal electroshock threshold test (MEST) beginning six weeks after a pilocarpine induced status epilepticus (SE). PB was tested alone or in combination with bumetanide or BUM5 at a dosage of 10 mg/kg i.p. with a pretreatment time of 30 min. Bumetanide (10 mg/kg i.v.) or BUM5 (13 mg/kg or 1.3 mg/kg i.v., equimolar to bumetanide) were

administered 30 min before PB injection. A group of control mice without SE underwent the same test schedule.

PB alone increased the seizure threshold by approx. 30% in both, control and epileptic mice. Bumetanide (10 mg/kg) and BUM 5 (1 mg/kg) did not effect the anticonvulsant effect of PB. However, at 10 mg/kg, BUM5 more than doubled the anticonvulsant effect of PB in epileptic mice, whereas such an effect was not seen in nonepileptic controls.

The results of this study indicate that the lipophilic prodrug of bumetanide, BUM5, could be a useful tool to study the role of NKCC1 in the pathogenesis of epilepsy and also offers a treatment option superior to the treatment with bumetanide.

## 120

### Bradykinin enhances activity of signal transducers and activators of transcription-3 via transactivation of the epidermal growth factor receptor in murine, hypothalamic cell models

**Besik, Valeria**; Gudermann, Thomas; **Breit, Andreas**

LMU, Walther Straub Institut, München, Germany

The neuropeptide bradykinin (BK) affects nociception, inflammation or blood circulation by activating bradykinin-B2-receptors (B2R) expressed in primary sensory neurons or smooth muscle cells. B2R expression has also been described in hypothalamic areas of the brain that are known to regulate food-intake and energy expenditure, but BK-induced signaling in hypothalamic cells is still poorly understood and a putative role for BK in appetite control has not been described yet. Here, we used three distinct murine cell lines (GT1-7, mHypoA-2/10 and mHypoA-2/12 cells) that originate from hypothalamic neurons. All three cell lines responded with robust calcium signals but only mHypoA-2/10 and mHypoA-2/12 cells with significant activation of extracellular-regulated kinases-1/2 (ERK-1/2) when challenged with BK. It appeared that BK-induced ERK-1/2 activation occurs via Src kinase-dependent transactivation of the epidermal growth factor receptor (EGFR). In line with these data, EGF-dependent ERK-1/2 activation was detectable in mHypoA-2/10 and mHypoA-2/12 but not in GT1-7 cells, indicating that EGFR expression is required for BK-induced ERK-1/2 activation in hypothalamic cells. Signal transducers and activators of transcription-3 (STAT-3) have been shown to play a pivotal role in food-intake reduction, when phosphorylated at tyrosine 705 by cytokines such as leptin. Here we report, that direct EGFR activation by EGF or EGFR transactivation via BK, leads to ERK-1/2-mediated phosphorylation of STAT-3 at serine 727, which is sufficient to activate STAT-3-dependent transcription in hypothalamic cells, as indicated by reporter gene assays. In conclusion, we firstly report that, BK enhances an appetite reducing pathway via EGFR transactivation in hypothalamic cell models and secondly that, ERK-1/2-mediated serine phosphorylation at position 727 is sufficient to substantially activate STAT-3 in mHypoA-2/10 or mHypoA-2/12 cells.

## 121

### Transcriptional and post-translational regulation of the transporter MRP4 (ABCC4) mediated by protein kinases

**Bröderdorf, Susanne**; Zang, Sebastian; Schaletzki, Yvonne; Ziems, Katrin; Kroemer, Heyo K.; Jedlitschky, Gabriele

University Medicine, Depart. of Pharmacology, Greifswald, Germany

**Background:** The multidrug resistance protein 4 (MRP4/ABCC4) is a member of the ATP-binding cassette transporter family and is typically known for its trans-membrane transport of nucleoside-based antiviral drugs and endogenous signaling molecules, in particular cyclic nucleotides. MRP4 has been established as an independent regulator of intracellular cyclic AMP (cAMP) levels and seems to play an important role in cell physiology in vascular smooth muscle cells (SMC) as well as in hematopoietic cells.<sup>1,2</sup> So far little is known about the regulation of MRP4. Here, we investigated the effect of cAMP on MRP4 expression and, in addition, mechanisms of post-transcriptional regulation, particularly the modulation of MRP4 plasma membrane localization.

**Methods and results:** To investigate the transcriptional regulation of MRP4, we used the megakaryoblastic leukemia M07e cells and human coronary artery SMC. To test the effect of increased intracellular cAMP levels, we treated the cells with dibutyryl cAMP and PDE inhibitor and analyzed MRP4 expression by quantitative Real-Time PCR. In both cell types a significant up-regulation of MRP4 was observed, which was not affected by addition of a protein kinase A inhibitor, however, could be reverted by addition of inhibitors of an alternative route of cAMP-signaling involving the exchange protein directly activated by cAMP (EPAC)<sup>3</sup> and MAP kinases. Furthermore, a selective EPAC activator was able to induce MRP4 transcription. This transcriptional regulation of MRP4 by cAMP was also confirmed by a luciferase reporter gene assay in HeLa cells. In addition, we investigated modulations of the plasma membrane localization of MRP4. Here, we used MRP4-transfected MDCK cells as well as SMC. MRP4 was found to be regulated by protein kinase C (PKC) activation resulting in an internalization of the transporter, as indicated by accumulation assays and immunofluorescence microscopy. The internalized MRP4 was detected in lysosomes as well as in recycling endosomes.

**Conclusions:** Enhanced cAMP levels up-regulate MRP4 expression, which will result in increased cAMP efflux. This up-regulation may be part of an auto-regulatory positive feedback loop and seems to be mediated through the EPAC signaling cascade. Furthermore, MRP4 plasma membrane localization and function was found to be modulated by PKC via an internalization of the transporter.

<sup>1</sup> Jedlitschky G, et al. (2012), *Blood*, 119:3394

<sup>2</sup> Cheepala S, et al. (2013), *Annu Rev Pharmacol Toxicol.*, 53:231

<sup>3</sup> Gloerich M, et al. (2010), *Annu Rev Pharmacol Toxicol.*, 50:355

## 122

**Opposing changes in neuronal excitability following an epileptogenic brain insult in mice and rats****Bröer, Sonia**<sup>1,2</sup>; Pilawski, Igor<sup>3</sup>; Löscher, Wolfgang<sup>1,2</sup>; Bernard, Christophe<sup>3,4</sup><sup>1</sup>Stiftung Tierärztliche Hochschule Hannover, Institut für Pharmakologie, Toxikologie und Pharmazie, Germany<sup>2</sup>Zentrum für Systemische Neurowissenschaften, Hannover, Germany<sup>3</sup>Inserm, UMR\_S 1106, Marseille, France<sup>4</sup>Aix Marseille Université, INS, France

Various brain insults, including status epilepticus (SE), can trigger epileptogenesis, a process leading to symptomatic or secondary epilepsies (the most common forms of epilepsy, which are often pharmacoresistant). In order to prevent epileptogenesis, it is important to understand the early steps of the process. These steps may vary between patients, and such variability should be taken into consideration. Using the pentetrazole (PTZ) seizure threshold as a surrogate marker for changes in neuronal excitability after an experimentally induced SE, we found different responses in rats and mice. This provides an ideal experimental situation to compare how similar brain insults lead to an identical endpoint - epilepsy - via different network reorganizations.

We induced SE in mice and rats with pilocarpine and assessed neuronal excitability during the first days after SE both *in vivo* and *in vitro*. We performed PTZ seizure thresholds prior to SE and at different time-points after the brain insult in rats and mice. Additionally, patch clamp recordings in mice hippocampal CA1 pyramidal cells were performed to measure their excitatory and inhibitory postsynaptic currents (EPSC and IPSC) and to compare their properties to those already available from a similar study of our group in rats (El-Hassar et al., J. Physiol. 2007).

Although in our model both rats and mice develop epilepsy after a latent period following SE, the PTZ seizure threshold was increased on day 1 and 2 post SE in mice, whilst the opposite was seen in rats. Thus, mice seem to be more resistant to PTZ seizures as compared to rats following SE, which was an unexpected and surprising finding.

The *in vitro* electrophysiological analysis also revealed differences between rats and mice. Whereas the frequency of GABAergic currents in CA1 pyramidal cells was decreased after SE in both species, the frequency of AMPA events was significantly enhanced in mice and decreased in rats. Furthermore, amplitude and current kinetics like rise- and decay-time were altered. These results could be a hint for a different reorganization in rats and mice after SE. As a protective mechanism, the brain can be more resistant to seizure-causing agents due to an increased inhibition; on the other hand, it is conceivable that the brain is even more susceptible towards second hits, caused by a decrease in GABA synthesis or a shift from inhibitory towards excitatory actions of GABA. The next step of the project will be to compare the reversal potential for GABA in the two species.

## 123

**Non-redundant involvement of the PI3K isoforms p110 $\gamma$  and p110 $\delta$  in the development and survival of myeloid cells****Bucher, Kirsten**<sup>1</sup>; Schmitt, Fee<sup>1</sup>; Autenrieth, Stella<sup>2</sup>; Nürnberg, Bernd<sup>1</sup>; Beer-Hammer, Sandra<sup>1</sup><sup>1</sup>Institut für Experimentelle und Klinische Pharmakologie und Toxikologie, Abteilung für Pharmakologie und Experimentelle Therapie, Tübingen, Germany<sup>2</sup>Medizinische Universitätsklinik Innere Medizin II, Abteilung Haematologie, Onkologie, Rheumatologie, Immunologie und Pulmologie, Tübingen, Germany

The class I phosphoinositide 3-kinases (PI3K) PI3K $\gamma$  and PI3K $\delta$  are heterotrimeric second messenger-generating enzymes, which are expressed in the hematopoietic system. They play important roles in function, proliferation, differentiation and survival of leukocytes. The catalytic PI3K isoform p110 $\delta$  together with its p85 adaptor is typically activated by receptor tyrosine kinases (RTKs) and/or directly by Ras proteins, whereas the catalytic isoform p110 $\gamma$  is mainly activated by GPCRs through direct interaction with G-protein  $\beta\gamma$  dimers and Ras proteins. Both PI3Ks are required for the development and function of T lymphocytes in mice. Having established a p110 $\gamma$  and p110 $\delta$  double knock-out mouse line, we previously demonstrated that the two isoforms also play specific non-redundant roles in peripheral maintenance and development of B lymphocytes. Here we used double-deficient mice to examine whether p110 $\gamma$  and p110 $\delta$  are both required for the generation and survival of various myeloid cell populations. Analysis of innate immune cell populations in p110 $\gamma\delta$  double knock-out mice revealed that, in contrast to single knock-out and WT controls, double knock-out mice exhibited drastically elevated peripheral granulocyte and monocyte counts, whereas cell numbers of peripheral dendritic cells and macrophages were significantly decreased. To analyze whether elevated granulocyte numbers in p110 $\gamma\delta$  double knock-out mice result from an altered survival, cell death was analyzed by flow cytometry. Surprisingly, cell death of granulocytes was significantly increased in double knock-out mice. At the same time, granulocytic differentiation stages were elevated in the bone marrow of double knock-out mice, which was paralleled by increased concentrations of granulocytic growth factors in the serum. Our results demonstrate a non-redundant involvement of p110 $\gamma$  and p110 $\delta$  in the development and survival of myeloid cells, influencing the homeostasis of granulocytes and other innate immune cell populations.

## 124

**Investigation of molecular effects of the hops constituents xanthohumol and isoxanthohumol in the nematode model *C. elegans*****Büchter, Christian**; Wätjen, Wim

Martin-Luther-Universität Halle-Wittenberg/ Institut für Agrar- und

Ernährungswissenschaften, Biofunktionalität sekundärer Pflanzenstoffe, Halle (Saale), Germany

The female inflorescences or cones of hops (*Humulus lupulus*) are rich sources of a variety of polyphenolic compounds. The prenylated chalcone xanthohumol (XH) can be found in hops only, where it is the main prenylflavonoid. On the contrary, the prenylated flavanone isoxanthohumol (IX) is less abundant in hops, but it is largely formed from XH during the brewing process of beer. The dietary exposure of XH and IX is therefore mostly limited to the consumption of beer. Recently, XH and IX gained attention as cancer chemo-preventive agents, displaying antioxidant, carcinogen metabolism modulating as well as anti-inflammatory properties.

However, most of these data are generated by *in vitro* studies and the knowledge of *in vivo* effects is relatively scarce. For this reason we are utilizing the well-established nematode model *Caenorhabditis elegans* for our *in vivo* studies with regard to *in vivo* anti-oxidative, stress-protective and aging modulating effects and the potential underlying molecular mechanisms.

In *C. elegans*, pro longevity effects are often associated with improved stress-resistance against various stresses e.g. heat-stress. By using a semi-automated assay system that employs the cell death probe SYTOX-Green, we were able to show that XH increased the survival at lethal heat-stress by 15.6% at the highest tested concentration (200  $\mu$ M), compared to the solvent control; however, IX was even more effective and increased the survival by 11.9% (100  $\mu$ M) and 35.7% (200  $\mu$ M), respectively. The improved heat-resistance was completely abolished in a strain containing a *daf-16* loss-of-function mutation (homolog of mammalian FOXO transcription factors). Further we tested the *in vivo* anti-oxidative potential by using the ROS indicator H<sub>2</sub>DCF-DA; XH and IX showed a slight tendency to reduce heat-induced generation of ROS at 50  $\mu$ M (XH) and from 10  $\mu$ M to 100  $\mu$ M (IX), respectively. At a concentration of 200  $\mu$ M a slight increase in ROS was detectable (XH and IX). In the *daf-16* loss-of-function mutant, an increase in ROS of up to 20% (XH 200  $\mu$ M) and 25% (IX 200  $\mu$ M) has been observed.

In conclusion, XH and IX protect *C. elegans* from heat-stress involving DAF-16 as a central factor; the results also indicate a probably hormetic mechanism of action. Currently we are investigating the effect of XH and IX on the lifespan of *C. elegans* and on the expression of cytoprotective genes (e.g. *sod-3*, *hsp-16.2*, *gst-4*) to get a better understanding of their molecular modes of action.

## 125

**Repeated-dose toxicity testing of 9 nano-particles with different surface functionalizations****Buesen, Roland**<sup>1</sup>; Wohlleben, Wendel<sup>1</sup>; Kamp, Henricke<sup>1</sup>; Strauss, Volker<sup>1</sup>; Dammann, Martina<sup>1</sup>; Treumann, Silke<sup>1</sup>; Groeters, Sibylle<sup>1</sup>; Wiench, Karin<sup>2</sup>; van Ravenzwaay, Bennard<sup>1</sup>; Landsiedel, Robert<sup>1</sup><sup>1</sup>BASF SE, Experimental Toxicology and Ecology, Ludwigshafen am Rhein, Germany<sup>2</sup>BASF SE, Product Safety, Ludwigshafen am Rhein, Germany

Oral uptake of nano-materials from food or cosmetics by consumers is likely to occur at low doses over long periods of time. To date, only few reports on *in vivo* effects of nano-materials upon subacute or subchronic oral exposure are available. The majority of these investigations address the effects of silver nanoparticles and none of these reports any non-transient toxicologically relevant effects.

Here, we present the results of two subacute oral toxicity studies in Wistar rats employing nine nano-materials with different surface functionalizations. The primary particle size was 10 nm (ZrO<sub>2</sub>), 15 nm (SiO<sub>2</sub>), 30 nm (BaSO<sub>4</sub>, OECD NM220) and 50 nm or 200 nm (Ag). The particles were coated with acid-, amino-, PEG-, acrylic- and electro-steric-functionalities.

The nano-materials were applied as suspensions via oral gavage at limit dose for 28-days. The studies were performed according to the OECD test guideline (TG) 407 including clinical observations, clinical pathology and (histo-)pathology. In addition to the basic haematological and clinical chemistry parameters, the acute phase proteins haptoglobin and alpha-2-macroglobulin as well as the protein troponin I were determined. Furthermore, mass spectrometry-based metabolite profiling was performed in serum samples making use of the MetaMap<sup>®</sup>Tox database to determine and assess metabolite patterns.

Test substance-related adverse effects were not observed with any of the nine nano-materials. Although tested at limit dose, no changes during clinical examinations, clinical pathology or pathology parameters were observed. The determination of acute phase proteins as well as troponin I did not reveal treatment-related effects. Furthermore, there were no matches with specific toxicity patterns in the MetaMap<sup>®</sup>Tox.

## 126

**Implementing the 3R methods and hurdles for their application - a perspective from the chemical industry****Buesen, Roland**; Ramirez, Tzutzuy; Schneider, Steffen; Kolle, Susanne; Mellert, Werner; Landsiedel, Robert; van Ravenzwaay, Bennard

BASF SE, Experimentelle Toxikologie und Ökologie, Ludwigshafen am Rhein, Germany



For the safety of consumer products their toxicological potential must be determined. By law, the toxicological testing often requires animal studies. According to our commitment to animal protection we apply 3R principles whenever possible, i.e. "reduce" and "replace" animal studies by new testing strategies as well as "refine" them by humane testing conditions. Herein, we report on certain hurdles that BASF SE has faced in the recent years.

Hurdles for reduction of animal numbers used for regulatory purposes exist (i) for "reproduction toxicity studies" as the basic design of the extended one-generation reproductive toxicity study is still lacking full acceptance and (ii) for "non-rodent toxicity studies" as the redundant one-year dog study is still requested by some authorities. Hurdles for application of replacement methods exist for the endpoints (iii) "eye irritation" as technical equipment is difficult to achieve for a validated and accepted assay, and (iv) "skin sensitization" as the validation process will be completed too late for registration of many substances under the European Union legislation REACH. Hurdles for refinement were encountered when (v) the propagated use of a cytotoxicity assay for the optimal selection of the starting dose in acute oral toxicity did not prove to be as useful as anticipated.

Taken together, especially in the field of *in vitro* methods, many problems can be encountered during the process of development, establishment, and their application. Some of these hurdles are technical issues, some published alternatives not fulfilling inter-laboratory reproducibility requirements, and an insufficient validation procedure. Most often, *in vitro* methods are not validated fast enough and regulatory acceptance takes too much time. Therefore, their use for regulatory purposes is often delayed and does not match legislative and political goals (e.g. Cosmetic Directive and REACH).

## 127

### Absorption and transport of 2-chloro-1,3-propanediol (2-MCPD) and its fatty acid esters by human intestinal Caco-2 cells

**Buhrke, Thorsten**<sup>1</sup>; Kuhlmann, Jan<sup>2</sup>; Lampen, Alfonso<sup>1</sup>

<sup>1</sup>Bundesinstitut für Risikobewertung, Lebensmittelsicherheit, Berlin, Germany

<sup>2</sup>SGS Germany GmbH, Hamburg, Germany

The heat-induced food contaminant 3-chloro-1,2-propanediol (3-MCPD) was recently classified as a possible human carcinogen (category 2B) by the International Agency for Research on Cancer (IARC). The carcinogenic potential of the compound was demonstrated in several animal studies with kidney and testis being the primary target organs. On the basis of these data, a TDI value of 2 µg/kg bw/day was derived.

Humans ingest 3-MCPD primarily as 3-MCPD fatty acid esters which are formed in the course of thermal treatment of fat-containing food in the presence of chloride ions. Bioavailability studies with rats have shown that these esters are nearly completely hydrolysed in the intestine thereby liberating 3-MCPD which is then readily absorbed into the body. Therefore, 3-MCPD fatty acid esters can be regarded as additional free 3-MCPD.

Recently it was shown that 3-MCPD-containing foods also contain significant amounts of the homologous compound 2-chloro-1,3-propanediol (2-MCPD) and its fatty acid esters. Whereas the toxic properties of 3-MCPD have been characterised in detail in the past few years, almost nothing is known about the toxicological potential of 2-MCPD. In particular, it is not clear so far whether 2-MCPD fatty acid esters are hydrolysed in the intestine as it was shown for 3-MCPD fatty acid esters.

Aim of the project was to examine the proposed hydrolysis of 2-MCPD fatty acid esters and the resulting release of free 2-MCPD by using differentiated Caco-2 cells, a model system for the human intestinal barrier. By using a transwell system, differentiated Caco-2 cells were incubated either with 2-MCPD or with various 2-MCPD fatty acid esters. Hydrolysis of the esters was analyzed by determining the amount of free 2-MCPD as well as the amount of the respective ester by a GC/MS method. Here we show that 2-MCPD fatty acid esters were neither absorbed by the cells nor the esters were transported via a Caco-2 monolayer. However, the esters were hydrolyzed in the presence of Caco-2 cells. Free 2-MCPD was not adsorbed by the cells, but the substance easily crossed a Caco-2 monolayer by a paracellular diffusion mechanism. From these *in vitro* studies we conclude that 2-MCPD fatty acid esters are likely to be completely hydrolysed in the human intestine, followed by a quick resorption of free 2-MCPD. The toxic properties of 2-MCPD will be examined in future studies.

## 128

### Subtype-specific voltage dependence of muscarinic receptors is determined by the ligand binding pocket

**Rinne, Andreas**<sup>1,2</sup>; Mobarec, Juan-Carlos<sup>3</sup>; Kolb, Peter<sup>3</sup>; **Bünemann, Moritz**<sup>2</sup>

<sup>1</sup>Ruhr-Universität Bochum, Institut für Physiologie, Abt. Kardiovaskuläre Physiologie, Germany

<sup>2</sup>Philipps-Universität Marburg, Pharmakologie und Klinische Pharmazie, Germany

<sup>3</sup>Philipps-Universität Marburg, Pharmazeutische Chemie, Germany

Muscarinic acetylcholine receptors (mAChR) are G protein-coupled receptors (GPCRs), which have been demonstrated to exhibit voltage-sensitivity. Based on available data that show depolarization induced activation for all Gq/11-coupled receptors and depolarization induced inhibition for all Gi/o coupled receptors that so far have been characterized to be voltage sensitive it was proposed that the G protein class affected the outcome of voltage dependence. In this study we report differential voltage sensitivity of M<sub>1</sub>R, M<sub>3</sub>R and M<sub>5</sub>R, which was not dependent on G protein coupling as determined by single cell fluorescence resonance energy transfer (FRET) photometry assays under voltage clamp conditions. Using a FRET-based biosensor that reports

conformations of M<sub>1</sub>R in HEK 293 cells we compared Carbachol (CCh)-induced receptor activation at -90 mV and at +60 mV. Depolarization caused activation of M<sub>1</sub>R, which was not affected by uncoupling of G<sub>q</sub> proteins with GTPγS. A FRET assay that senses activation of G<sub>i</sub> was used to compare the voltage dependencies of M<sub>1</sub>R, M<sub>3</sub>R and M<sub>5</sub>R. Notably, voltage dependence was subtype-specific: Depolarization caused either activation (M<sub>1</sub>R) or deactivation of the receptors (M<sub>3</sub>R or M<sub>5</sub>R). Voltage sensitivity of MR was also ligand-specific, suggesting a pivotal role of the orthosteric binding pocket: M<sub>3</sub>R displayed deactivation (CCh) or activation (Pilocarpine) induced by a depolarization to +60 mV. Computational docking studies predicted different molecular binding modes for these agonists and guided us to mutate key residues in the orthosteric binding site of muscarinic receptors. The docking of mutant M<sub>3</sub>R predicted a novel "Pilocarpine-like" binding mode for CCh which we were able to experimentally verify: the mutation of a key residue in the receptor let to switch in the direction of the voltage sensitivity of CCh activated receptors without affecting the voltage sensitivity of pilocarpine activated receptors. Together, these results demonstrate G protein independent voltage sensitivity of muscarinic receptors and suggest an important role of the orthosteric binding site in directing voltage sensitivity of GPCRs.

## 129

### Contribution of six human CYP enzymes to the metabolism of the food constituents methyleugenol, methylisoeugenol, alpha-, beta-, and gamma-asarone

**Cartus, Alexander**; Schrenk, Dieter

TU Kaiserslautern, Lebensmittelchemie und Toxikologie, Germany

Previously we investigated the phase I metabolism of different phenylpropenes (PP) present in food including the allylic methyleugenol (ME) and gamma-asarone (gA), as well as the propenyl methylisoeugenol (MIE), alpha- (αA), and beta-asarone (βA). ME, αA, and βA are carcinogenic to rodents, whereas MIE is not, and gA has not been investigated so far. Activation of ME occurs via a genotoxic mechanism by forming a side chain alcohol (1'-OH-ME) which is afterwards sulfonated. After loss of sulfate, it forms a reactive carbocation, which can react with DNA. The molecular mechanism responsible for the carcinogenicity of αA and βA is still not understood.

Here, we performed *in vitro* studies to elucidate the contribution of six prominent human cytochrome P450 enzymes (CYP) to the metabolism of the PP mentioned above. Therefore we incubated Supersomes<sup>TM</sup> (expressing human CYP1A2, 2A6, 2C19, 2D6, 2E1 or 3A4) with the test compounds at different start concentrations (50 – 800 µM) over different time spans (20 and 60 min). Main reactions were side chain hydroxylation at the 1'- and 3'-position, oxidation of those alcohols, formation of side chain epoxides and hydrolysis to the corresponding diols, demethylation, and hydroxylation of the benzene ring.

CYP1A2 was by far the most potent enzyme in all incubations with respect to turnover rates, pattern of metabolites, and catalytic efficiencies. In contrast, CYP2A6 was nearly inactive for all substrates.

In case of ME, the formation of the proximate carcinogen 1'-OH-ME, was catalyzed effectively by CYP1A2, moderately by 2C19, 2D6 and 3A4, and very weakly by 2A6 and 2E1. In contrast, CYP2E1 was most active in formation of the ME-epoxide, and the corresponding ME-diol.

CYP3A4 was the most active enzyme in formation of the side chain diols of the propenyl PP MIE, αA and βA.

Taken the different CYP activities of the used Supersomes<sup>TM</sup> and of human liver microsomes into account, CYP1A2 and 3A4 were the predominant enzymes involved in the biotransformation of the investigated PP.

## 130

### Imaging mass spectrometry of endogenous peptides in the brain

**Chatterji, Bijon**<sup>1</sup>; Dickhut, Clarissa<sup>1</sup>; Mielke, Svenja<sup>1</sup>; Krüger, Jonas<sup>1</sup>; Just, Ingo<sup>1</sup>; Glage, Silke<sup>2</sup>; Meier, Martin<sup>2</sup>; Wedekind, Dirk<sup>2</sup>; Pich, Andreas<sup>1</sup>

<sup>1</sup>Medizinische Hochschule Hannover, Institut für Toxikologie, Germany

<sup>2</sup>Medizinische Hochschule Hannover, Institut für Versuchstierkunde, Germany

In recent years, imaging mass spectrometry (IMS) has emerged as a powerful tool to study the spatial distribution of proteins, peptides, lipids and drug compounds in the brain. In this study MALDI-IMS was used to determine the distribution of endogenous peptides in a rat model of Usher's disease, which is a rare disease that is considered as leading cause of deaf-blindness in humans worldwide. Endogenous peptides are of low-molecular weight and of particular interest because they reflect the native state of the cell. They include neuropeptides and proteolytic degradation products, but very little is known about the localization of such peptides *in situ*.

*In vivo* magnetic resonance imaging (MRI) suggested morphological changes in the areas of the *colliculi superiores* and *substantia nigra* of diseased rat brains with Usher type 1-like symptoms. Therefore, we established an imaging protocol to analyze cryosections of brain tissue by MALDI-IMS to differentiate between healthy and diseased rats. Identification by MS/MS of peptides *in situ* remains challenging. Hence we found an effective way to extract endogenous peptides from brain tissue lysates to identify them by MS/MS using LC-Orbitrap and MALDI-TOF/TOF. These *m/z* values could be successfully correlated with imaging signals.

A large number of peptides were proposed for histological classification due to their specific localization in the brain, e.g. *substantia nigra*, *corpus callosum* and *hippocampus*. Indeed, several endogenous peptides showed significantly increased ion densities, particularly in the *colliculi superiores* and in the *substantia nigra* of diseased rats including peptides derived from Fsd1, dystrobrein-β and ProSAAS. Furthermore,

several proteolytic degradation products of the myelin basic protein (MBP) were identified, of which one peptide is most likely mediated by calpain-2. MBP is a major component of the myelin sheath. Hence, a decomposition of the myelin sheath correlates well with neurodegenerative effects that can be observed in Usher's disease and other neurological disorders.

Our findings contribute to the characterization of this animal model and include possible peptide markers of disease. MALDI imaging can open new perspectives, such as investigating the localization of small molecules and drug metabolites in intact tissue specimens and makes this novel technique valuable for diagnostics and addressing pharmacological questions.

Chatterji B, Pich A. MALDI imaging mass spectrometry and analysis of endogenous peptides. *Expert Rev Proteomics* 2013, 10, 381-388

Held N, Smits BM, Gockeln R, Schubert S, Nave H, Northrup E, Cuppen E, Hedrich HJ, Wedekind D. A mutation in Myo15 leads to Usher-like symptoms in LEW/Ztm-gi2 rats. *PLoS One* 2011, 6, e15669.

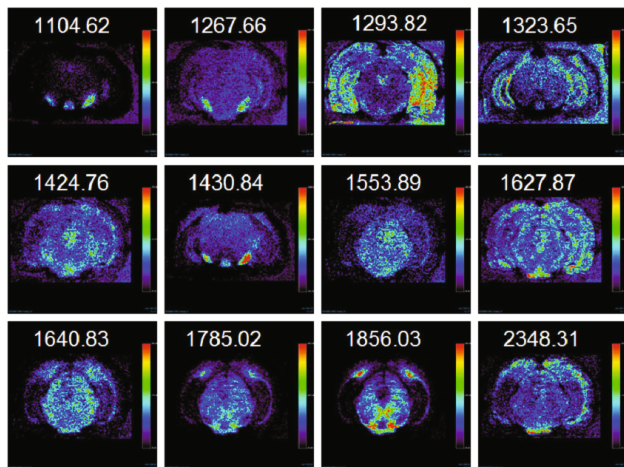


**Figure 1:** Imaging of endogenous peptides in the rat brain. The spatial distribution of selected peptides (m/z values) is shown as extracted ion images.

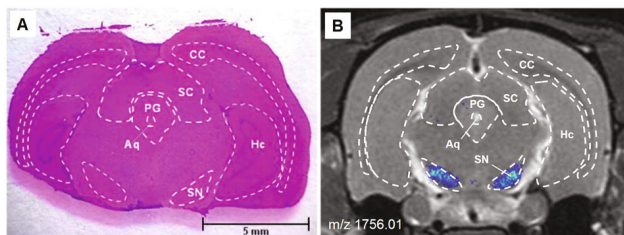


**Figure 2:** Correlation of specific ion densities with histology and MRI. M/z 1756.01 as a proteolytic fragment of the myelin basic protein was exclusively detected in the substantia nigra (blue).

## 131

### CRISPR/Cas-mediated gene knockout of the lipolysis-stimulated lipoprotein receptor (LSR) in cultured cell lines

**Czulkies, Bernd;** Hemmasi, Sarah; Aktories, Klaus; Papatheodorou, Panagiotis  
Albert-Ludwigs-Universität Freiburg, Institut für Experimentelle und Klinische Pharmakologie und Toxikologie, Germany

The lipolysis-stimulated lipoprotein receptor (LSR) is a type I single-pass transmembrane protein of the plasma membrane that is mainly expressed in the liver, but also in the intestine and in various other tissues. Previous conflicting studies suggested that LSR is involved in the cellular uptake of triglyceride-rich lipoproteins and/or in the organization of three-cellular tight junctions. In addition, we recently identified that LSR is the host cell receptor for *Clostridium difficile* binary toxin CDT (Papatheodorou *et al.*, 2011, PNAS). In order to investigate the physiological role of LSR in more detail, we generated gene knockouts in various human cell lines (e.g., CaCo-2) via the targeted CRISPR/Cas genome editing technique. The LSR knockout cells presented here are important tools for comparative loss-of-function analyses and rescue experiments that might help to unravel the precise role of the LSR protein.

## 132

### Inflammatory cytokines regulate plasma microRNA concentrations in type 2 diabetic patients with wound healing impairment

**Dangwal, Seema**<sup>1</sup>; Stratmann, Bernd<sup>2</sup>; Falk, Christine<sup>3</sup>; Tschöpe, Diethelm<sup>2</sup>; Thum, Thomas<sup>1</sup>

<sup>1</sup>Medizinische Hochschule Hannover, IMTTs, Germany

<sup>2</sup>Herz und Diabeteszentrum NRW, Diabeteszentrum, Bad Oeynhausen, Germany

<sup>3</sup>Medizinische Hochschule Hannover, IRTCT, Germany

**BACKGROUND:** MicroRNAs (miRNAs/miRs) are highly conserved small non-coding RNA molecules regulating gene expression via post-translational repression<sup>1</sup>. miRNAs, present in the body fluids in a remarkably stable form, may circulate via blood and exert paracrine effect via cellular uptake<sup>2</sup>.

**OBJECTIVES:** In present study, we investigated an influence of impaired wound healing on the plasma miRNA signature of type-2 diabetic patients.

**METHODS:** Sixty-one type-2 diabetic patients were grouped according to concomitant peripheral arterial disease (PAD) and chronic non-healing wounds (W). The study was approved by local ethical committee and all participants signed a written informed consent form. miRNA profiles of randomly pooled plasma from diabetic controls or diabetic patients with PAD+W were compared and further validated in all diabetic patients i.e. controls (n=23), patients with PAD+W (n=27) or PAD alone (n=11) vs. that of 20 healthy controls using taqman assays in qRT-PCR. Patterns of pro-inflammatory cytokine levels were screened in plasma or wound exudates. To mimic clinical findings in vitro, the release of miRNAs in culture-supernatants was measured upon cytokine stimulation of the vascular endothelial cells.

**RESULTS:** miRNA profiling revealed the circulating levels of miR-191, miR-126 and miR-200b were significantly decreased in diabetic controls vs. healthy controls (p<0.0005) but reverted in diabetes associated PAD and chronic wound condition. Higher circulating C-reactive protein and cytokine levels were observed in patients with diabetes-associated PAD and chronic wounds compared to diabetic controls (p<0.05). A significant correlation of miR-191 and miR-200b with CRP (r=0.333 and 0.329 respectively) was observed among diabetic patients. Release of miR-191 and miR-126 was increased upon cytokine stimulation of vascular endothelial cells in vitro. Overexpression of miR-200b inhibited tube formation in diabetic microvascular endothelial cells, whereas miR-191 and miR-200b overexpression decreased proliferation of high glucose treated dermal fibroblasts.

**CONCLUSIONS:** Our study reports for the first time that plasma levels of circulating miRNAs in type-2 diabetic patients presenting with chronic wounds and PAD are influenced by the underlying inflammation in these patients. Modulation of these miRNAs in dermal cells might regulate the cellular homeostasis in wound healing.

1. Dangwal S and Thum T, miRNA Therapeutics in cardiovascular disease models. *Annu Rev Pharmacol Toxicol.* 2013 Oct.2 (epub ahead of print).

2. Zampetaki A. et al., Plasma microRNA profiling reveals loss of endothelial miR-126 and other microRNAs in type 2 diabetes. 2010. *Circ Res.* 107(6):810-7

## 133

### Identification of a second receptor binding site in Botulinum Neurotoxin F

**Dehn, Christopher**<sup>1</sup>; Krez, Nadja<sup>1</sup>; Weisemann, Jasmin<sup>1</sup>; Mahrhold, Stefan<sup>1</sup>; Binz, Thomas<sup>2</sup>; Rummel, Andreas<sup>1</sup>

<sup>1</sup>MHH, Institut für Toxikologie, Hannover, Germany

<sup>2</sup>MHH, Institut für Biochemie, Hannover, Germany

The extreme toxicity of the botulinum neurotoxins (BoNT) A-H, which constitutes them as the most potent toxins known, is based on their high specificity for neuronal cells. After accumulation on the cell-surface of cholinergic neurons by utilizing gangliosides the binding to different proteins of synaptic vesicles mediates the endocytosis of the neurotoxins. BoNT/A, E and presumably BoNT/F employ the synaptic vesicle glycoprotein 2 (SV2) as protein receptor. Previously, it was shown that both the ganglioside binding pocket as well as the protein receptor binding site of those serotypes are located on the C-terminal half of the 100 kDa heavy chain (HC) of BoNT, the 50 kDa H<sub>C</sub>, which therefore is essential for uptake of the neurotoxins into cells.

The N-terminal half of H<sub>C</sub>, H<sub>N</sub>, facilitates the pH-dependent translocation of the 50 kDa light chain (LC), a Zn<sup>2+</sup>-dependent endoprotease which specifically cleaves SNARE proteins, from the endosome into cytoplasm after endocytosis of the toxin. Consequently, neural intoxication by BoNT interrupts the release of acetylcholine which leads to flaccid paralysis of muscles and inactivation of cholinergically activated glands. Aim of this study is the identification of the protein receptor binding site in the H<sub>C</sub> of BoNT/F by generation of mutations interfering with the receptor binding in a site comparable to the known SV2 binding sites in BoNT/A and E. The effect of these mutations on the SV2 binding has been determined by mouse phrenic nerve hemidiaphragm assays. Reduced neurotoxicity correlates with impaired receptor interaction. To ensure that this effect is not due to incorrect folding of the H<sub>C</sub>F mutants their secondary structure content has been verified by CD-spectroscopy. Further analysis of the mutants in SV2 binding assays and neuronal cell cultures will be conducted.

### Phospholipase C- $\epsilon$ (PLC $\epsilon$ ) induced TRPC6 activation: A common but redundant mechanism in podocytes

**Demleitner, Jana**<sup>1</sup>; Storch, Ursula<sup>1</sup>; Kalwa, Hermann<sup>1,2</sup>; Mayer, Tim<sup>1</sup>; Fiedler, Susanne<sup>1</sup>; Kannler, Martina<sup>3</sup>; Barth, Holger<sup>3</sup>; Offermanns, Stefan<sup>4</sup>; Smrcka, Alan<sup>5</sup>; Gudermann, Thomas<sup>1</sup>; Dietrich, Alexander<sup>1</sup>

<sup>1</sup>LM-Universität München, Walther-Straub-Institut für Pharmakologie, Germany

<sup>2</sup>Harvard Medical School, Brigham and Women's Hospital, Boston, United States

<sup>3</sup>Universität Ulm, Institute of Pharmacology and Toxicology University of Ulm Medical Center, Germany

<sup>4</sup>Max-Planck-Institut für Herz- und Lungenforschung, Pharmakologie, Bad Nauheim, Germany

<sup>5</sup>University of Rochester, School of Medicine and Dentistry, United States

In all eukaryotic cells, activation of phospholipase C (PLC)-coupled membrane receptors by hormones leads to an increase in the intracellular Ca<sup>2+</sup> concentration ([Ca<sup>2+</sup>]). Catalytic activity of PLCs results in the hydrolysis of phosphatidylinositol 4,5-bisphosphate to generate inositol 1,4,5-trisphosphate (IP3) and diacylglycerol (DAG) which opens DAG sensitive classical transient receptor potential channels e.g. TRPC6, initiating Ca<sup>2+</sup> influx from the extracellular space. While TRPC6 activation by PLC $\beta$ - and PLC $\gamma$ -isozymes was extensively studied, the role of PLC $\epsilon$  in TRPC activation remains elusive. Most interestingly, for both proteins mutations in patients with focal segmental glomerulosclerosis (FSGS) were identified (reviewed in 1) raising the possibility that DAG production by PLC $\epsilon$  is able to induce TRPC6 activation in podocytes *in vivo*. Along these lines, TRPC6 was co-immunoprecipitated with PLC $\epsilon$  in a heterologous overexpression system in HEK293 cells as well as in freshly isolated podocytes. Receptor-operated TRPC6 currents in HEK293 cells stably expressing TRPC6 were reduced by a specific PLC $\epsilon$  siRNA and by a PLC $\epsilon$  loss of function mutant isolated from an FSGS patient. PLC $\epsilon$  induced TRPC6 activation was also identified in murine embryonic fibroblasts (MEFs), with deleted *Gd<sub>q11</sub>* genes. Further analysis of the signal transduction pathway revealed a G<sub>12/13</sub>-mediated RhoGEF activation which induced Rho-mediated PLC $\epsilon$  stimulation. PLC $\epsilon$ <sup>2</sup> podocytes however were undistinguishable from WT podocytes in their cation influx, actin stress fibre formation and cell proliferation. These data favor a redundant role of PLC $\epsilon$ -mediated TRPC6 activation at least in MEF and podocytes where PLC $\epsilon$ -deficiency might be compensated by other PLC isoforms.

[1] Dietrich, A., Chubanov, V., Gudermann, T. (2010). Renal TRP channels. *J. of Am. Soc. Nephrol.* 21, 736-744.

### Lack of hyaluronan-synthase 3 attenuates neointimal hyperplasia after carotid artery ligation

**Dick, Lena Sophia**, Müller, Julia; Fischer, Jens Walter

Institut für Pharmakologie und Klinische Pharmakologie, Universitätsklinikum Düsseldorf, Heinrich-Heine-Universität Düsseldorf, Germany

In healthy arterial blood vessels hyaluronan (HA) expression is mainly limited to the adventitial layer and the endothelial glycocalyx. In neointimal hyperplasia HA is induced in close association with vascular smooth muscle cell (VSMC) proliferation. HA is synthesized by three HA-synthase isoforms (Has1,-2,-3) and is known to strongly affect VSMC phenotype. Lentiviral overexpression of HAS3 in human VSMC resulted in increased migration and proliferation. However, the regulation and function of HAS3 in arterial remodeling *in vivo* is unknown. Thus, the objective of the current study was to characterize the regulation of HAS3 and its functional role during neointimal hyperplasia *in vivo*.

Real time RT-PCR revealed that Has3 was the major HAS-isoenzyme in uninjured, native carotid arteries as well as in the aorta. Neointimal hyperplasia was induced by ligation of the left common carotid artery. Five days after ligation strong upregulation of Has1 and Has2 was detected whereas Has3 was surprisingly downregulated. The increase of Has2 was in line with a previous report showing that Has2 overexpression enhances neointimal hyperplasia. HAS3 has been associated with the activated phenotype of VSMC and with the generation of lower molecular weight HA. Hence, the question was addressed whether HAS3 also contributes to neointimal hyperplasia despite the lower expression level.

Next Has3-KO mice and WT mice were subjected to neointimal hyperplasia and arteries collected for histology after four weeks. Morphometric quantification (H&E-staining) revealed a significant reduction of neointimal hyperplasia in Has3-KO as indicated by reduced neointimal volume (Has3-KO,  $1.53 \times 10^4 \pm 2.29 \times 10^6 \mu\text{m}^3$  vs. WT,  $2.59 \times 10^4 \pm 3.36 \times 10^6 \mu\text{m}^3$ ,  $n = 9$ ,  $p < 0.05$ ) and reduced intima/media ratios (Has3-KO,  $0.94 \pm 0.13$  vs. WT,  $1.39 \pm 0.13$ ,  $n = 9$ ,  $p < 0.05$ ). Sections were stained for HA using HA binding protein revealing profound accumulation of HA in the neointima. However, no further decrease was detected in Has3-KO mice in line with the low expression of HAS3.

In conclusion these findings indicate that Has3-dependent HA synthesis might play a critical role for remodeling in response to vascular injury.

### The Impact of Food Deprivation on Body Weight and on Anxiety-Related and Motivated Behaviour in Rats.

**Dietze, Silke**<sup>1</sup>; Lees, Katarina<sup>2</sup>; Fink, Heidrun<sup>1</sup>; Voigt, Jörg-Peter<sup>2</sup>; Bert, Bettina<sup>1</sup>

<sup>1</sup>FU-Berlin, FB Veterinärmedizin, Institut für Pharmakologie und Toxikologie, Germany

<sup>2</sup>University of Nottingham, Sutton Bonington Campus, Loughborough, Great Britain

The guidelines set by the European Parliament (Directive 2010/63/EU) state a severity classification of procedures in laboratory animals. The severity of a food deprivation period of 24 hours is defined as 'mild' and 48 hours of food deprivation is defined as 'moderate'.

Behavioural research often requires a food deprived animal so that this animal is motivated to perform a task for which it receives a food reward.

We investigated the effects of different lengths of food deprivation periods (16, 24 and 48 hours) on body weight loss and behaviour in 5-6 months old Wistar rats with females weighing  $260 \pm 16$  g and males  $440 \pm 30$  g. Behavioural effects of food deprivation were examined in the Modified Open Field Test and Elevated Plus Maze Test. The Modified Open Field Test is based on the conflict between hunger and anxiety. Food-deprived rats were placed in a corner of the open field containing food in the centre and the number of rats beginning to eat in the first five minutes was recorded.

Males and females lost 7% of body weight after 48 hours of food deprivation, whereas 24 hours resulted in 4% body weight loss. Sixteen hours of food deprivation caused 2% body weight loss in males and 3% in females.

When exposed to the Modified Open in the last hour of food deprivation the motivation to eat in the open field under this condition increased only after 48 hours of food deprivation.

After 24 hours re-feeding, rats were exposed to the Elevated Plus Maze Test, and no behavioural effects of food deprivation were observed.

Although gender differences were seen; food deprivation up to 48 hours had only a moderate effect on body weight and an effect on emotional behaviour was observed not until 48 hours of food deprivation.

### The Cyclic Nucleotide cCMP Affects Proliferation and Apoptosis of the Human Erythroleukemia Cell Line HEL 92.1.7

**Dittmar, Fanni**<sup>1</sup>; Wolter, Sabine<sup>1</sup>; Hartwig, Christina<sup>1</sup>; Schwede, Frank<sup>2</sup>; Seifert, Roland<sup>1</sup>

<sup>1</sup>Hannover Medical School, Institute of Pharmacology, Germany

<sup>2</sup>BioLog Life Science Institute, Bremen, Germany

Adenosine 3',5'-cyclic monophosphate (cAMP) and guanosine 3',5'-cyclic monophosphate (cGMP) are well-established second messengers that regulate multiple physiological functions. The existence of additional cyclic nucleotides (cNMPs), e.g. cytidine 3',5'-cyclic monophosphate (cCMP) and uridine 3',5'-cyclic monophosphate (uCMP), was claimed many years ago.<sup>[1]</sup> Due to insufficient sensitivity and specificity of the detection methods<sup>[2]</sup>, little research was performed in this area during the past 30 years. Since a highly sensitive and specific high-performance liquid chromatography tandem mass spectrometry (HPLC-MS/MS) method has been recently established<sup>[3]</sup>, research in this field revives.<sup>[4]</sup>

The aim of our study was to examine the effect of cCMP on cell proliferation. Therefore, we used an analogue of cCMP (cCMP-AM), in which the polar phosphate is masked by an acetoxymethyl group. Thus, the molecule is highly membrane-permeant and cCMP is released inside the cell due to activity of esterases.

cCMP-AM inhibited proliferation of HEL 92.1.7 cells. This effect could be related to the initiation of apoptosis as identified via flow cytometry. Caspase 3 activation and poly (ADP-ribose) polymerase (PARP) cleavage was detected by Western Blot analysis of cell lysates, indicating the caspase-dependent mechanism of apoptosis. Using the BD™ MitoScreen Kit, the pathway could additionally be characterized as intrinsic and mitochondria-dependent. Furthermore, measurement of total content of cNMPs indicated that cCMP is not influenced by other cyclic nucleotides and is therefore solely responsible for the observed effects. The cCMP concentration was reduced after 4 hours, possibly due to the activity of phosphodiesterases or multidrug resistance-associated proteins (MRPs).

In contrast, cCMP-AM did not inhibit proliferation of K-562 cells. This may be due to very high MRP activity because cCMP concentrations were lower in K-562 cells than in HEL 92.1.7 cells. Thus, export of cNMPs is an effective mechanism of tumor resistance against cCMP-induced apoptosis.

Current studies comprise closer analyses of the apoptosis-inducing mechanism including investigations of PKA, PKG and other cNMP-AMs as well as the altered gene expression caused by cCMP using real-time PCR. Future research will focus on the changed properties of primary cells due to treatment with cCMP-AM.

[1] Newton R. et al. *Rapid Commun Mass Spectr* 2, 118–126 (1988).

[2] Gaion R. & Krishna G. *Biochem Bioph Res Commun* 86, 105–111 (1979).

[3] Beste K. et al. *PLOS ONE* 8, e70223 (2013).

[4] Beste K. & Seifert R. *Biol Chem* 394, 261–270 (2013).

## 138

**NTCP as receptor for HBV: inhibition of transport and infection**

**Döring, Barbara**<sup>1</sup>; König, Alexander<sup>2</sup>; Mohr, Christina<sup>2</sup>; Glebe, Dieter<sup>2</sup>; Geyer, Joachim<sup>1</sup>  
<sup>1</sup>Justus-Liebig-Universität Gießen, Institut für Pharmakologie und Toxikologie, Germany  
<sup>2</sup>Justus-Liebig-Universität Gießen, Institut für medizinische Virologie, Nationales Referenzzentrum für HBV und HDV, Germany

The liver-specific Na<sup>+</sup>-taurocholate cotransporting polypeptide NTCP is long known as transport protein for bile acids and some drugs, facilitating the enterohepatic circulation between liver and gut. Recently, NTCP was identified as receptor for Hepatitis B and D virus, disclosing a complete new function of this protein. Attachment of the virus occurs via the myristoylated preS1 (myr-preS1) peptide domain of the large surface protein to NTCP which represents the first step of HBV infection. Over 2 billion people have been infected with HBV and about 620,000 deaths annually are HBV-associated. Whereas an effective prophylactic vaccine is available, HBV therapy is often ineffective. The development of new therapy approaches needs a better understanding of the early steps of infection.

In our study we were interested in the relationship between NTCP function and HBV infection. Therefore, we performed HBV infection and binding assays as well as transport assays in primary hepatocytes from *Tupaia belangeri*, an established model system for HBV infection, and NTCP transfected cell lines in the presence of various bile acids and myr-preS1 peptides.

We could confirm that HBV infection is specific to NTCP transfected cells. This infection was inhibited by the myr-preS1 peptides from human (HBV) and woolly monkey (WMHBV) hepatitis B virus, but not by the myr-preS1 peptide from woodchuck (WHV) hepatitis B virus. This is consistent with the binding of the inhibiting peptides to NTCP expressing cells. Interestingly, bile acid transport function of NTCP was inhibited in the same way by HBV and WMHBV but not WHV myr-preS1 peptides. Conversely we tested, if substrates and inhibitors of NTCP have an impact on HBV infection. Indeed, bile acids like tauro- and glycocholic acid, tauro-, glyco-, and ursodeoxycholic cholic acid can dramatically reduce the susceptibility of NTCP expressing cells and PTH in a concentration-dependent manner, which was the result of decreased myr-preS1 peptide binding to the cells.

Our data show, that bile acid substrate transport and myr-preS1 virus binding at NTCP interfere with each other. This could be due to competitive interaction at the same binding domain or due to masking of the respective binding site through conformational changes in the transport protein. In future, development of drugs that block HBV binding to NTCP may open a new strategy for the management of HBV infection.

## 139

**Analysis of cell death induction by the antioxidant alpha-lipoic acid in different colorectal cancer cell lines**

**Dörsam, Bastian**; Göder, Anja; Kaina, Bernd; Fahrer, Jörg  
 Universitätsmedizin Mainz, Institut für Toxikologie, Germany

Alpha-lipoic acid (LA) is a naturally occurring dithiol compound that plays an important role in the mitochondrial energy metabolism as co-factor of multi-enzyme complexes including pyruvate dehydrogenase. Due to its antioxidative functions it is also used as dietary supplement. It has been reported previously that LA displays growth-inhibitory effects and triggers cell death in diverse tumor cell lines.

In the present study, we analyzed the mode of cell death induced by LA in colorectal cancer (CRC) cells with different p53 status (HT-29, CaCO-2 and HCT116). First, tumor cells were challenged with LA for 72 h and cell death subsequently measured with flow cytometry. In all cell lines, Annexin-V/PI staining revealed a strong induction of apoptosis. In HT-29 and CaCO-2 cells, LA induced a dose-dependent cleavage of caspase-9 associated with an increase in its activity, whereas caspase-8 cleavage was not observed. Furthermore, LA treatment resulted in the downstream activation of caspases-3/7, as demonstrated by activity assays and cleavage of their substrate PARP-1, a hallmark of apoptosis. In contrast, HCT116 cells underwent cell demise without cleavage and/or activation of caspases-3/7 and caspases-8/9 after treatment with LA (250 µM – 1000 µM) for 72 h. In line with these findings, PARP-1 cleavage was not detectable by immunoblot analysis. However, LA treatment resulted in apoptotic DNA fragmentation after 72 h as monitored by agarose DNA laddering and subG1 measurements. Additional analysis revealed a LA-induced loss of mitochondrial membrane potential (MMP) in HCT-116 cells after 72 h, which can promote the release of toxic proteins such as AIF from mitochondria. Collectively, our findings demonstrate that the antioxidant LA induces caspase-dependent and -independent cell death in CRC cells. Further experiments in HCT116 cells should address the role of AIF in LA-triggered cell death.

## 140

**The weakly membrane permeable antipsychotics amisulpride and sulpiride are substrates of the organic cation transporters from the SLC22 family**

**Dos Santos Pereira, Joao Nuno**; Tadjerpisheh, Sina; Abu Abed, Manar; Saadatmand, Ali Reza; Brockmüller, Jürgen; Tzvetkov, Mladen  
 University of Göttingen, Institute for Clinical Pharmacology, Germany

A significant fraction of psychiatric patients respond poorly to multiple drug treatments. We have hypothesized that variation in membrane transport at the blood-brain barrier

might affect drug concentration at the site of action and predetermine therapy outcome. Furthermore, membrane transporters in organs such as the gut, liver and kidney may also influence drug distribution and therapy efficacy. We have analyzed the membrane permeability of 30 psychotropic drugs with weak base properties in order to identify the ones that may depend on active transport to penetrate cell membranes. Although most of the drugs analyzed showed high membrane permeability, some drugs, including amisulpride and sulpiride, showed low membrane permeability. We have also analyzed the mRNA expression of drug transporters of the SLC22 family in primary human brain microvascular endothelial cells, and performed uptake measurements of amisulpride and sulpiride in HEK293 cells over-expressing OCT1, OCT2, OCT3, OCTN1 and OCTN2. OCTN2 was the transporter with the highest expression at the blood-brain barrier, followed by OCTN1, OCT1 and OCT3. OCT2 expression was not detectable. Amisulpride was found to be transported by all five transporters. In contrast, sulpiride was transported by OCT1 and OCT2, but not by OCT3, OCTN1 and OCTN2. OCT1 showed the highest transport ability both for amisulpride (Cl<sub>int</sub>=0.5 ml/min/mg protein) and sulpiride (Cl<sub>int</sub>=4.2 ml/min/mg protein). Common genetic polymorphisms in OCT1 reduced the uptake of both amisulpride and sulpiride. In conclusion, the weakly membrane permeable drugs amisulpride and sulpiride may use profit from organic cation transporters to penetrate the blood-brain barrier and other pharmacokinetically relevant membrane barriers.

## 141

**The anti-oxidative enzyme PON2 modulates endothelial and platelet function in blood coagulation**

**Ebert, Julia**; Wilgenbus, Petra; Horke, Sven  
 Universitätsmedizin Mainz, Institut für Pharmakologie, Germany

The blood coagulation system is a key survival mechanism that protects the organism against lethal bleeding. Excessive coagulation, however, is a common risk factor for atherothrombosis and is linked to a variety of diseases such as atherosclerosis, stroke or heart attack. Many if not all stimuli that provoke enhanced coagulation are dominantly associated with redox-triggered and inflammatory pathways. This is due to the fact that oxidative stress and inflammation dominate endogenous control of hemostasis. Here we demonstrate, for the first time, that the enzyme paraoxonase-2 (PON2) is a novel factor relevant to this concept. PON2 is a crucial anti-oxidative protein with established protective vascular functions that counteract inflammation and atherogenesis. Our studies reveal that PON2-deficiency markedly accelerates coagulation. In line with the hypothesis that PON2 triggers a redox-based modulation of coagulation, we found higher levels of reactive oxygen species in arterial vessels of PON2<sup>-/-</sup> mice. To identify the molecular link to an accelerated coagulation, we addressed endothelial effects, platelet functions and plasmatic factors. Regarding the central role of the endothelium in hemostasis, our *in vitro* studies demonstrate a distinct effect of PON2 on endothelial thrombin-signaling networks. Similarly in PON2<sup>-/-</sup> mice, gene expression analyses and surface protein profiles of isolated endothelial cells revealed a significant increase of coagulation- and inflammation-triggering factors. This implies that PON2-deficiency provokes the phenotype of an activated endothelium *in vivo*. Furthermore, PON2<sup>-/-</sup> platelets show an enhanced activity. This is due to an elevated endogenous thrombin potential and increased exposure of anionic phospholipids at the outer leaflet of the plasma membrane. In agreement, clotting times of factor depleted plasma revealed an enhanced activity of specific factors in PON2<sup>-/-</sup> plasma, mostly those of factors VIII, IX, X and XI. In conclusion, our data indicate that PON2 represents a novel modulator of coagulation, which may exert its anti-coagulant function by redox-based regulation of inflammation and hemostasis. Furthermore, PON2-knockout mice are a unique model that links redox-signaling with coagulation and atherogenesis. Consequently, these studies will advance our understanding of how redox-signaling and inflammation regulate coagulation and how this determines atherogenesis and atherothrombosis.

## 142

**ATM and ATR contribute to cellular resistance against alkylating anticancer drugs like temozolomide**

**Eich, Marcus**; Nikolova, Teodora; Roos, Wynand P.; Kaina, Bernd  
 Universitätsmedizin Mainz, Institut für Toxikologie, Germany

The PI3-kinases ATM and ATR are key proteins involved in DNA strand break recognition and their repair by homologous recombination. They also function in apoptotic and survival signalling and in cell cycle checkpoint control. In this Study, we show that human cells generated from patients with Ataxia telangiectasia and the Seckel syndrome mutated in ATM or ATR are more sensitive to the anticancer drug temozolomide (TMZ) than the corresponding wild-type cells. We extended the work to tumour models for which TMZ is applied, using a knockdown strategy based on RNA interference (RNAi). We show that human glioma and melanoma cells carrying a transient knockdown for ATM and ATR display a high level of cell death following TMZ compared to the control cells transfected with nonsense siRNA. Interestingly, the sensitization effect is greater when ATR is knocked down compared to the ATM knockdown. In the presence of MGMT, all tested cells proved to be very resistant to N-methyl-N'-nitro-N-nitrosoguanidine (MNNG) and TMZ, showing that O<sup>6</sup>-methylguanine is the main cytotoxic lesion induced by the alkylating agents. Furthermore, the ATM mutated cells harbour no defect in base excision repair (BER), which was proven by the alkaline comet assay and an *in vitro* BER assay. As shown by immunofluorescence and western blot analysis, phosphorylation of the downstream targets H2AX, CHK1 and CHK2 depends on ATR but not on ATM. Additionally, pharmacological inhibition of

CHK1 and CHK2 led to increased toxicity in glioma and melanoma cells following TMZ treatment with inactivation of CHK1 being more effective. In conclusion, the data suggest that ATM and, even better, ATR inhibition is a useful strategy in sensitizing cancer cells to TMZ and presumably also other anticancer drugs. Work is supported by DFG KA724.

143

#### A broad analysis of the estrogenic potency of phthalate diesters and their monoester metabolites

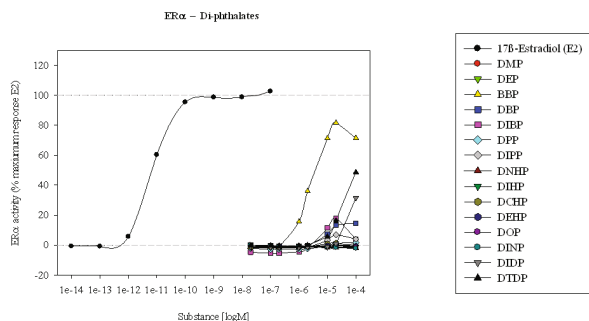
Engel, Anika; Bumke Scheer, Maja; Lampen, Alfonso

Bundesinstitut für Risikobewertung, Lebensmittelsicherheit, Berlin, Germany

For a few years, phthalates are under suspicion to act as endocrine disruptors (EDCs). EDCs are exogenous substances that have an impact on the hormonal system and hence are a potential danger to the organism. For instance EDCs can activate or inhibit hormone receptors such as the androgen or estrogen receptor. Phthalates are mainly used as softeners in plastics such as polyvinylchloride (PVC). They give flexibility and stability to the otherwise rigid synthetic material. They are used in building materials, toys, pharmaceuticals, packagings, cleaning products, medical equipment, perfumes and cosmetics. In animal studies with rats, substances such as butyl-benzyl phthalate (BBP), di-isobutyl phthalate (DIBP), di-butyl phthalate (DBP), Bis(2-ethylhexyl) phthalate (DEHP) and di-isononyl phthalate (DINP) modulate the development of the male sexual organs. Numerous epidemiologic studies suggest that phthalates have undesirable effects on the reproduction system. Such effects are for example an alteration of the semen parameters, a damage of the DNA in sperm and a reduced reproductive hormone level in male human adults. *In vitro*, certain phthalates can bind to the estrogen receptor and may have weak estrogenic activity. Due to this data six different phthalates have already been prohibited in toys by the European Union [butyl-benzyl phthalate (BBP), di-isodecyl phthalate (DIDP), di-n-butyl phthalate (DBP), bis(2-ethylhexyl) phthalate (DEHP), di-isononyl phthalate (DINP) and di-n-octyl phthalate (DnOP)].

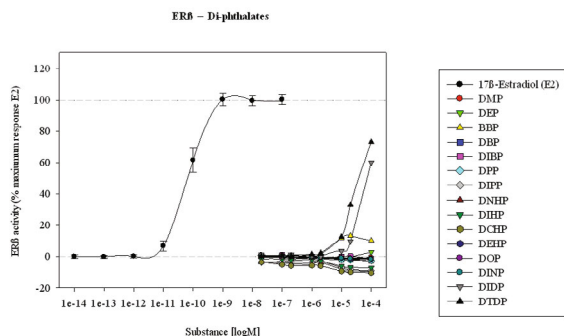
The purpose of the present study is to determine the estrogenic potency of 15 phthalate diesters and their 16 monoester metabolites in doses that are relevant in humans, using a luciferase reporter gene assay. For this purpose a cell culture system containing HEK293 cells, stably transfected with the estrogen receptor  $\alpha$  (ER $\alpha$ ) or  $\beta$  (ER $\beta$ ) was used. Six out of the 15 phthalate diesters activated the ER $\alpha$  and three activated the ER $\beta$  whereas none of the 16 phthalate metabolites caused a measurable activation of the ERs at all. Hence, it could be confirmed that the phthalate diesters studied have an activating effect on the estrogen receptor.

Furthermore, a potential phthalate inducing change in the cell viability was examined. After an incubation of the cells with the phthalates for 24 hours no change of viability could be observed in the tested concentration ranges.



#### Di-phthalates (ER $\alpha$ ):

Dose response curves of all tested di-phthalates (ER $\alpha$ )



#### Di-phthalates (ER $\beta$ ):

Dose response curves of all di-phthalates (ER $\beta$ )

144

#### TTC: A new concept for inhalation exposure

Tluczkiewicz, Inga<sup>1</sup>; Batke, Monika<sup>1</sup>; Kühne, Ralph<sup>2</sup>; Schüürmann, Gerri<sup>2</sup>; Mangelsdorf, Inge<sup>1</sup>; Escher, Sylvia<sup>1</sup>

<sup>1</sup>Fraunhofer ITEM, Chemikalienbewertung, Hannover, Germany

<sup>2</sup>The Helmholtz Centre for Environmental Research, Ecological Chemistry, Leipzig, Germany

The threshold of toxicological concern (TTC) concept allocates thresholds to structural groups of compounds below which a risk for human health is not assumed. The current TTC concept is based on in vivo data with oral exposure and may not be appropriate for toxicity after inhalation exposure e.g. because of route specific differences.

We present an integrative approach to derive threshold values for inhalation exposure. They are based on a dataset of 296 chemicals with repeated-dose toxicity studies (www.fraunhofer-rep-dose.de). Systemic and local NOEC values were discriminated. Groups of compounds with specific structural features (SF) were identified by using atom centered fragments. Few SF were explicit for local or systemic activity indicating that this mode of action is not a determining factor. The structural and toxicological boundaries of the initial SFs were further evaluated considering differences in absorption, mechanism/metabolism and sensitive targets/effects observed in the in vivo studies. 28 SF groups resulted: 9 low (L) and 19 toxic (T) groups. About 20% of the compounds are, however, not yet grouped. Compared to the Cramer classes the T and L-groups better discriminate low toxic versus toxic compounds. Two clearly distinguished TTC values are proposed. This project has been funded by the Cefic LRI ([http://www.cefic-lri.org/uploads/Project%20publications/Executive%20summary\\_update.pdf](http://www.cefic-lri.org/uploads/Project%20publications/Executive%20summary_update.pdf)).

145

#### Aryl hydrocarbon receptor polymorphism rs2066852 (A554K) is associated with Psoriasis arthropatica but not Psoriasis vulgaris in a German patient cohort

Krämer, Ursula<sup>1</sup>; Esser, Charlotte<sup>2</sup>

<sup>1</sup>IUF-Institut für Umweltmedizinische Forschung, Epidemiologie, Düsseldorf, Germany

<sup>2</sup>IUF-Institut für Umweltmedizinische Forschung, Immuntoxikologie, Düsseldorf, Germany

Psoriasis is a chronic inflammatory disease with a genetic basis. Its manifestation and severity appear influenced by environmental factors. Psoriasis presents in subtypes which affect either the skin (Psoriasis vulgaris, PsV) and/or the joints (Psoriasis arthropatica, PsA). It is of great interest to identify etiological factors which might drive these disease subsets. The aryl hydrocarbon receptor (AhR) senses a range of xenobiotic and endogenous small molecular weight chemicals, and is involved in balancing inflammatory and tolerogenic immune responses. Susceptibility to toxic AhR-ligands can depend on ligand affinities, or on genetically functional variants of AhR. In humans, the most widely studied polymorphism (rs2066853) results in an Arg554K exchange in the transactivation domain. rs2066853 leads to low AhR and CYP1B1 expression, and is linked to some cancers and to the skin pigmentation disorder vitiligo.

We determined associations of rs2066853 with PsV versus PsA. A total of 316 Psoriasis patients, 68 of them with psoriasis arthropatica, and 231 controls were studied. We used logistic regression to analyze the genetic association taking smoking into account. In agreement with literature data, smoking was a strong risk factor for non PsA forms of psoriasis (OR 3.5 (2.2-5.36)), but much less so in PsA (OR 1.86 (1.03-3.34)). The variant AhR genotype was associated with psoriasis, albeit not reaching significance. Differentiating between non PsA and PsA patients revealed, however, that the effect was mainly to the PsA patients (Odds Ratio OR 2.09 95%CI(1.09-4.00)), and not to the non PsA phenotypes (OR 1.31(0.79-2.18)). The odds-ratios hardly change (less than 10%) when adjusting for smoking, i.e. a gene-environment interaction (smoking\*rs2066853) could not be shown. In conclusion, our study identifies for the first time an AhR variant as a risk factor for psoriasis, which is specific for PsA, and stress that PsV and PsA may have different etiology. The association highlights a biochemical pathway that links chemicals with inflammatory dysregulation, such as the AhR dependent T-reg/Th17 balance, and suggests a possible exacerbating involvement of alternative AhR signaling, e.g. via NFkB, distinct for joint inflammation in PsA. Further studies are warranted, to identify differences in cytokine influences in both disease subtypes, and dissect functional transcriptional changes by rs2066853.

146

#### Iperoxo is a superpotent agonist at native presynaptic muscarinic M<sub>2</sub> and M<sub>4</sub> receptors in the mouse hippocampus and striatum

Utscheid, Justine<sup>1</sup>; Mohr, Klaus<sup>1</sup>; Schlicker, Eberhard<sup>2</sup>

<sup>1</sup>Institute of Pharmacy, Pharmacology and Toxicology Section, Bonn, Germany

<sup>2</sup>Institute of Pharmacology and Toxicology, BMZ, Bonn, Germany

Iperoxo is a particularly potent muscarinic receptor agonist (Schrage et al., 2013) which has so far been studied mainly in cells expressing human muscarinic acetylcholine receptors, classical members of the family of seven transmembrane helical receptors. The aim of the present study was to examine this drug at the preferentially G<sub>i</sub> protein-coupled M<sub>2</sub> and M<sub>4</sub> receptors in hippocampal and striatal slices, respectively, from three mouse strains.

For this purpose the inhibitory effect of iperoxo on the electrically stimulated acetylcholine release was studied in [<sup>3</sup>H]choline preincubated and superfused brain

slices. Transmitter release under control conditions was not significantly different between mouse strains (3.5-4.3% of tissue tritium for hippocampus and 3.8-4.8% for striatum). Iperoxo concentration-dependently inhibited transmitter release leading to a maximal inhibition by 70-80%. The pEC<sub>50</sub> values (means ± SEM, n=10-12) were 9.26±0.20, 8.77±0.17 and 8.77±0.09 in hippocampus and 9.41±0.27, 8.53±0.19 and 8.86±0.18 in striatum of C57BL6N, NMRI and CD1 mice, respectively. Oxotremorine, which was used for the sake of comparison, yielded pEC<sub>50</sub> values of 6.49±0.36 and 6.24±0.18 in hippocampal slices and of 6.61±0.50 and 6.68±0.32 in striatal slices from NMRI and CD1 mice (n=4), respectively.

In conclusion, iperoxo is a muscarinic receptor agonist with a potency exceeding that of oxotremorine by a factor of 250 at the native presynaptic M<sub>2</sub> autoreceptor in the mouse hippocampus and of 110 at the M<sub>4</sub> autoreceptor in the striatum. Its potency proved to be about threefold higher at the muscarinic receptors of C57BL6N when compared to NMRI and CD1 mice. Due to its outstanding potency the drug appears to be well suited for further studies aimed at a more detailed analysis of iperoxo-signaling.

Schrage, R. et al.: Br J Pharmacol. 2013 May;169(2):357-70

## 147

### The importance of soluble guanylyl cyclase in murine brown adipose tissue

**Etzrodt, Jennifer<sup>1</sup>**; Hoffmann, Linda Sarah<sup>1</sup>; Friebe, Andreas<sup>2</sup>; Pfeifer, Alexander<sup>1</sup>

<sup>1</sup>Universitätsklinikum Bonn, Institut für Pharmakologie und Toxikologie, Germany

<sup>2</sup>Universität Würzburg, Physiologisches Institut I, Germany

Brown adipose tissue (BAT) consumes energy to produce heat by thermogenesis, whereas white adipose tissue stores energy in the form of lipids. BAT contains a high amount of mitochondria which highly express the thermogenic uncoupling protein 1 (UCP1). Heat production by BAT is important for newborns to regulate their body temperature. Recent studies have shown that metabolically active BAT is present in humans. Previously we and others have shown that the cGMP/PKG pathway is crucial for the differentiation and function of BAT (Haas et al, Sci Signal, 2009; Nisoli et al. Science, 2003). cGMP is generated by soluble guanylyl cyclase (sGC) upon activation by its endogenous ligand nitric oxide. Understanding of cGMP signaling cascades in BAT is important to find new targets and strategies to fight obesity via sGC/cGMP pathway.

To investigate the role of sGC in BAT, we used sGC deficient (sGC<sup>-/-</sup>) pups and their WT littermates. BAT dependent thermogenesis in newborn mice was quantified by infrared thermography of the interscapular region. Infrared thermography revealed that the surface temperature was significantly lowered by 2°C in sGC<sup>-/-</sup> mice compared to WT mice. Interestingly, brown adipose tissue weight was 50% lower in sGC<sup>-/-</sup> mice compared to WT littermates. Gene expression analysis of the thermogenic key regulator UCP1 in BAT pads showed that mRNA levels were significantly decreased by 80% in sGC<sup>-/-</sup> mice compared to WT mice. Concomitantly, we analyzed the protein expression of UCP1 using Western blot analysis. UCP1 protein levels were significantly decreased by 20% in sGC<sup>-/-</sup> mice compared to WT mice. In addition, expression of UCP1 in sections of BAT from sGC<sup>-/-</sup> mice and their WT littermates was analyzed by immunohistochemical staining. In line, immunohistochemical analysis demonstrated that UCP1 expression was reduced in BAT from sGC<sup>-/-</sup> mice compared to their WT littermates.

In this study we showed that sGC plays an important role in the differentiation and function of brown adipose tissue in newborns. The major function of BAT is to burn energy in order to produce heat. The central role of sGC within BAT suggest that sGC could be used as a potential pharmacological target in new strategies to increase energy expenditure of BAT via sGC/cGMP-dependent mechanisms which could counteract overweight and obesity.

Haas, B., Mayer, P., Jennissen, K., Scholz, D., Berriel Diaz, M., Bloch, W., Herzig, S., Fässler, R., and Pfeifer, A. (2009). Protein kinase G controls brown fat cell differentiation and mitochondrial biogenesis. Sci Signal 2, ra78.

Nisoli, E. (2003). Mitochondrial Biogenesis in Mammals: The Role of Endogenous Nitric Oxide. Science 299, 896-899.

## 148

### The *in vivo* existing TRPV6 protein comprises a 40 amino acid extended N-terminus which is exclusively translated at a non-AUG codon

**Fecher-Trost, Claudia**; Weißgerber, Petra; Wissenbach, Ulrich; Flockerzi, Veit  
Universität des Saarlandes, Experimentelle und Klinische Pharmakologie und Toxikologie, Homburg, Germany

TRPV6 channels function as epithelial Ca<sup>2+</sup> entry pathways in the epididymis, prostate and placenta. We have shown that TRPV6 is essential for Ca<sup>2+</sup>-homeostasis in the epididymal duct and that male mice lacking functional TRPV6 channels are hypofertile making TRPV6 one of the very few channels essential for male fertility. However, the identity of the *in vivo* existing TRPV6 protein relies on predicted gene coding regions and is only known to a certain level of approximation. Using immunohistochemistry and antibody techniques, TRPV6 proteins have been identified in human placenta, mouse prostate and placenta, epididymis and the human breast cancer cell line T47D. The placental TRPV6 expression was suggested to play a role for basal Ca<sup>2+</sup> influx in placental cells and from there to the fetus. Ca<sup>2+</sup> transport from the mother to the fetus is active, because fetal Ca<sup>2+</sup> levels are higher than in the mother and the transport across the placenta increases dramatically in response to the fetus' demands for Ca<sup>2+</sup> needed for bone mineralization. With a combination of mutagenesis experiments, antibody

affinity chromatography and mass spectrometry we localized the initiation triplet and identified N-terminal protein sequences of the TRPV6 channel protein, enriched from human placenta and the breast cancer cell line T47D. Surprisingly the translation of *Trpv6* initiates at a non-AUG codon, at ACG, which is located 120 bp upstream of the annotated AUG. The annotated AUG is not used for translation initiation *in vivo*. The ACG codon, which codes for threonine is nevertheless decoded by the amino acid methionine. Not only a very rare event in eukaryotic biology the full length TRPV6 protein existing *in vivo* (TRPV6x) comprises an amino terminus extended by 40 amino acid residues compared to the annotated truncated TRPV6 protein which has been used in most studies on TRPV6 channel activity so far. The *in vitro* properties of channels formed by the extended full length TRPV6 proteins and the formerly annotated smaller TRPV6 protein are similar, but the extended N-terminus increases trafficking to the plasma membrane and represents an additional scaffold for channel assembly.

## 149

### Proliferative capacity and cytokine expression in rat bone marrow cells after *in vivo* exposure to extremely low frequency magnetic fields

**Fedrowitz, Maren**; Noack, Andreas; Römermann, Kerstin; Löscher, Wolfgang  
University of Veterinary Medicine, Dept. of Pharmacology, Toxicology, and Pharmacy, Hannover, Germany

Epidemiological data suggest an association between exposure to extremely low frequency magnetic fields (ELF-MF) and an increased risk of leukemia, particularly childhood leukemia. However, the underlying mechanisms are still unclear and need to be clarified to improve risk assessment for the public. In the present study, we used female and male Lewis and Fischer 344 (F344) rats, two inbred strains with different sensitivities towards stress, carcinogens, and ELF-MF exposure, to examine the effects on the hematopoietic system after *in vivo* ELF-MF exposure for two weeks (50 Hz, 100 µT). The proliferative capacity of bone marrow cells was determined by *ex vivo* treatment with mitogens affecting the different populations of lymphocytes. Cells were treated with three different mitogens at three concentrations: 1) Pokeweed mitogen (PWM) for stimulation of B- and T-lymphocytes; 2) Concanavalin A (ConA) for stimulation of T-cells; 3) Lipopolysaccharides (LPS) for stimulation of B-cells. After 40 h, the functionality of lymphocytes was evaluated by a BrdU proliferation assay (Roche Diagnostics GmbH), and untreated control cells were compared with mitogen-treated cells. The expression of cytokines in the culture medium was determined by an antibody membrane array for simultaneous detection of 90 rat cytokines (RayBiotech, Inc.). The *ex vivo* mitogen stimulation of primary lymphocytes from bone marrow revealed alterations in the proliferative activity after *in vivo* ELF-MF exposure. Cells from female ELF-MF-exposed rats showed decreased proliferative capacity after PWM (Lewis and F344) and ConA (F344) and were more sensitive than those from males. The expression of several cytokines differed between cells from MF-exposed females and males as well. For example, an increase in TNF-related apoptosis-inducing ligand (TRAIL) and a decrease in interleukin-1beta were observed in female cells, which differed from results in males. The most consistent ELF-MF effects on proliferative capacity were detected after PWM treatment. Therefore, the present results indicate that the interactions between B- and T-lymphocytes are affected by ELF-MF exposure, and cytokines like TRAIL and interleukin-1beta might be involved. Moreover, sex differences and the genetic background of Lewis and F344 have to be considered as important factors, which participate in ELF-MF effects.

This work is supported by the 7th Framework Program of the European Union (FP7-ENV-2011, Project ARIMMORA).

## 150

### Increased spontaneous Ca<sup>2+</sup> releases are accompanied by enhanced SERCA and NCX activities in ventricular cardiomyocytes from mice expressing CREM-IbΔC-X

**Fehrmann, Edda**; Schulte, Jan Sebastian; Seidl, Matthias Dodo; Kranick, Daniel Sebastian; Fels, Benedikt; Tekook, Marcel Alexander; Schmitz, Wilhelm; Müller, Frank Ulrich  
Westfälische Wilhelms-Universität, UKM, Institut für Pharmakologie und Toxikologie, Münster, Germany

The cAMP-dependent transcription factors CREB (cAMP response element binding protein) and CREM (cAMP response element modulator) regulate gene transcription in response to β-adrenergic stimulation and other signal transduction pathways. Transgenic mice with heart-directed expression of the inhibitory CREM isoform CREM-IbΔC-X (TG) develop a complex cardiac phenotype with spontaneous-onset atrial fibrillation and increased left ventricular performance. Here we studied in ventricular cardiomyocytes (VCs) from TG mice whether CREM is implicated in the development of arrhythmogenic alterations in intracellular Ca<sup>2+</sup> cycling.

Intracellular Ca<sup>2+</sup> transient decay (Indo-1/AM ratio) was accelerated in TG VCs (time to 50% decay in % of WT: 78±11\*). Patch clamp experiments revealed action potential (AP) prolongation in TG VCs (APD90 in ms; mean±SEM; TG, 78±10\*; WT, 33±4). Ca<sup>2+</sup> transport rates (r) of sarcoplasmic reticulum Ca<sup>2+</sup>-ATPase (SERCA) and Na<sup>+</sup>/Ca<sup>2+</sup> exchanger (NCX) determined by fitting single exponential curves to the decay of electrically and caffeine-evoked Ca<sup>2+</sup> transients showed increased SERCA and NCX activities in TG VCs (in % of WT; r<sub>SERCA</sub>: 139±6\*; r<sub>NCX</sub>: 142±5\*; TG n=30-70/6, WT n=22-53/6). These findings concur with an increased NCX current (I<sub>NCX</sub>) in TG VCs measured in patch clamp experiments and increased SERCA and NCX protein levels. Spontaneous potential arrhythmogenic Ca<sup>2+</sup> waves (CaW) and transient-like Ca<sup>2+</sup>

releases (tCaR) were investigated in unpaced Indo-1/AM loaded VCs after a prestimulation-phase (1Hz, 2Hz). The proportion of VCs with tCaR was increased while the proportion of VCs with CaW was unchanged in TG (TG vs. WT; tCaR in %; 1Hz: 15\* vs. 5; 2Hz: 14 vs. 9; TG n=66/12, WT n=67/11). Considering only VCs showing tCaR the quantity of tCaR in these VCs was unaltered. WT mice exposed to isoprenaline via osmotic minipumps indicated a 2.3-fold induction of *CREM- $\text{Ib}\Delta\text{C-X}$*  mRNA after 10h in heart homogenates. (\* $p < 0.05$  vs. WT)

Transgenic expression of *CREM- $\text{Ib}\Delta\text{C-X}$*  in mouse VCs leads to increased SERCA and NCX activities and protein levels which can explain the accelerated  $\text{Ca}^{2+}$  transient decay and AP prolongation and might contribute to increased spontaneous tCaR. Since short *CREM* isoforms like *CREM- $\text{Ib}\Delta\text{C-X}$*  and *ICER*/small *ICER* isoforms<sup>1</sup> are inducible by  $\beta$ -adrenergic stimulation in the mouse heart the transient inhibition of the *CRE*-dependent gene transcription by induced *CREM* isoforms may contribute to arrhythmogenesis in chronic heart disease.

<sup>1</sup>Seidl MD, Nunes F, Fels B, Hildebrandt I, Schmitz W, Schulze-Osthoff K, et al. A novel intronic promoter of the *Crem* gene induces small *ICER* (*smICER*) isoforms. *FASEB J*. 2013.

## 151

### Dabigatran increases M2/M1-macrophage ratio in visceral adipose tissue of LDL receptor knockout mice

**Feldmann, Kathrin**<sup>1</sup>; Grandoch, Maria<sup>1</sup>; Lehr, Stefan<sup>2</sup>; Fischer, Jens Walter<sup>1</sup>

<sup>1</sup>Institut für Pharmakologie und Klinische Pharmakologie, Universitätsklinikum Düsseldorf, Heinrich-Heine-Universität Düsseldorf, Germany

<sup>2</sup>Institut für Klinische Biochemie und Pathobiochemie, Deutsches Diabetes Zentrum, Düsseldorf, Germany

Obesity is associated with chronic low-grade inflammation, promoting the development of insulin resistance (IR) and diabetes mellitus type 2 (T2DM). Patients with T2DM have increased concentrations of circulating tissue factor and thrombin-antithrombin complexes leading to increased risk of thrombotic events (Boden *et al.* 2007). Thrombin is also involved in inflammatory processes, implicating a possible role for thrombin in obesity-related inflammation and T2DM. Indeed, argatroban, a direct thrombin inhibitor, ameliorated IR in a genetic model of obesity and T2DM (male *db/db* mice, Mihara *et al.* 2010).

The aim of this study was to investigate whether the oral thrombin inhibitor dabigatran etexilate (dabigatran) might have effects on adipose tissue function and inflammation in a mouse model of diet-induced obesity.

For this purpose female, 10 weeks old low-density lipoprotein receptor-deficient (*LDLR*<sup>-/-</sup>) mice received a Western-type diet containing 5 mg/g dabigatran or matching placebo for 20 weeks.

Body-mass-index, weight gain and whole body fat content, determined by NMR measurement, were the same in both groups. However, immunohistochemistry of visceral adipose tissue showed a significant increase in adipocyte size (dabigatran  $1.868 \pm 0.2279$  fold of placebo,  $n=15,14$ ) and macrophage content as determined by mac-2 staining (number of crown-like structures/100 adipocytes: dabigatran  $3.714 \pm 0.9106$  fold of placebo,  $n=10$ ). Fasting plasma glucose levels, glucose-tolerance and IR were impaired on the Western-type diet; but no differences between dabigatran- and placebo-treated animals were detected. Flow cytometric analysis of the stromal vascular fraction indicated that the increase in macrophage ( $\text{CD11b}^+\text{F4/80}^+$ ) content is driven by an accumulation of  $\text{CD11c}^+$ -macrophages, known to be associated with an anti-inflammatory phenotype. The number of pro-inflammatory  $\text{CD11c}^+$ -macrophages was reduced by dabigatran. In addition multiplex analysis of plasmatic cytokines revealed an increase of eotaxin (dabigatran  $2.118 \pm 0.4846$  fold of placebo,  $n=4,5$ ), a chemoattractant for eosinophils, which promote the M2-like polarization of macrophages in adipose tissue (Wu *et al.* 2011).

These results indicate that (i) thrombin inhibition by dabigatran was metabolically neutral in a model of T2D despite adipocyte hypertrophy and (ii) increases eotaxin and M2 macrophage accumulation in visceral adipose tissue of female *LDLR*<sup>-/-</sup> mice.

This work was funded in part by Boehringer Ingelheim.

## 152

### Does aging influence the tolerance development after chronic $\Delta^9$ -tetrahydrocannabinol treatment in mice?

**Feliszek, Monika**<sup>1</sup>; Bilkei-Gorzo, Andras<sup>2</sup>; Schlicker, Eberhard<sup>1</sup>

<sup>1</sup>Universität Bonn, Institut für Pharmakologie und Toxikologie, Germany

<sup>2</sup>Universität Bonn, Institut für Molekulare Psychiatrie, Germany

The main psychoactive ingredient of marijuana,  $\Delta^9$ -tetrahydrocannabinol ( $\Delta^9$ -THC) produces behavioral effects like hypomotility e.g. in rodents. These effects are mediated by the cannabinoid  $\text{CB}_1$  receptor which is highly expressed in the central nervous system. Long-term treatment with  $\Delta^9$ -THC produces tolerance in mice already after few days of administration. The development of tolerance in rodents may vary depending on age.

We determined the behavioral effects of the chronic and acute treatment with  $\Delta^9$ -THC in young adult (8 weeks) and aged (12 months) of C57Bl/6J mice. The motor activity of mice was measured in an open-field apparatus after acute and chronic  $\Delta^9$ -THC treatment and compared to the activity of age-matched control (vehicle treated) animals. Following behavioral analysis the effect of the cannabinoid agonist CP 55,940 on

[<sup>35</sup>S]GTP $\gamma$ S binding on hippocampal membranes isolated from these mice was determined.

The analysis of  $\Delta^9$ -THC 3 mg/kg treated animals showed slight and mostly insignificant differences between the corresponding age groups both with respect to the behavioral studies and [<sup>35</sup>S]GTP $\gamma$ S binding experiments and therefore we increased the dose to 10 mg/kg  $\Delta^9$ -THC.

Although the biochemical analysis has not yet been completed for 10 mg/kg  $\Delta^9$ -THC treated cohorts, the motility tests revealed the following results. The acutely treated animals showed hypomotility in rearing behavior and distance travelled compared to the controls in both age groups. The young adult animals tended to develop tolerance to  $\Delta^9$ -THC after chronic treatment in the distance travelled whereas the aged mice did not. With respect to rearing behavior chronic  $\Delta^9$ -THC treatment led to the development of tolerance in both age groups.

In conclusion, aging decreases tolerance development after chronic treatment with  $\Delta^9$ -THC in distance travelled but not in rearing.

## 153

### Sick sinus syndrome in HCN1-deficient mice

**Fenske, Stefanie**<sup>1</sup>; Marks, Vanessa<sup>1</sup>; Königsbauer, Stefanie<sup>1</sup>; Hassan, Sami I.<sup>1</sup>; Becirovic, Elvir<sup>1</sup>; Hammelmann, Verena<sup>1</sup>; Kupatt, Christian<sup>2,3</sup>; Biel, Martin<sup>1,3,4</sup>; Wahl-Schott, Christian<sup>1,3,4</sup>

<sup>1</sup>Pharmakologie für Naturwissenschaften, Department Pharmazie, Ludwig-Maximilians-Universität München, Germany

<sup>2</sup>Medizinische Klinik und Poliklinik I, Klinikum Großhadern, Ludwig Maximilians University, München, Germany

<sup>3</sup>DZHK (German Center for Cardiovascular Research), partner site Munich Heart Alliance, München, Germany

<sup>4</sup>Center for Integrated Protein Science CIPS-M, München, Germany

Sinus node dysfunction (SND) is a major clinically relevant disease that is associated with sudden cardiac death and is responsible for >50% of surgical implantations of permanent pacemakers per year worldwide. Frequently, SND occurs in heart failure and hypertension, conditions that lead to electric instability of the heart. Although the pathologies of acquired SND have been studied in detail, little is known about the molecular and cellular mechanisms that cause congenital SND.

Here, we show that the HCN1 protein is highly expressed in the sinoatrial node and is colocalized with HCN4, the main sinoatrial pacemaker channel isoform. The cardiac phenotype of HCN1-deficient mice was characterized by a detailed functional characterization of pacemaker mechanisms in single isolated sinoatrial node cells, explanted beating sinoatrial node preparation, telemetric in vivo electrocardiography, echocardiography, and in vivo electrophysiology. On the basis of these experiments we demonstrate for the first time that mice lacking the pacemaker channel HCN1 display congenital SND characterized by bradycardia, sinus dysrhythmia, prolonged sinoatrial node recovery time, increased sinoatrial conduction time, and recurrent sinus pauses. As a consequence of SND, HCN1-deficient mice display a severely reduced cardiac output. In conclusion, we propose that HCN1 stabilizes the leading pacemaker region within the sinoatrial node and hence is crucial for stable heart rate and regular beat-to-beat variation. Furthermore, we suggest that HCN1-deficient mice may be a valuable genetic disease model for human SND.

## 154

### Refinement of Acute Inhalation Toxicity Studies: The Isolated Perfused Rat Lung as a Screening Tool for Surface-Active Substances

**Fischer, Monika**<sup>1</sup>; Dasenbrock, Clemens<sup>1</sup>; Windt, Horst<sup>2</sup>; Koch, Wolfgang<sup>2</sup>

<sup>1</sup>Fraunhofer Institut für Toxikologie und Experimentelle Medizin, Toxikologie und Umwelthygiene, Hannover, Germany

<sup>2</sup>Fraunhofer Institut für Toxikologie und Experimentelle Medizin, Aerosolforschung u. Chemische Analytik, Hannover, Germany

New surface-active agents in waterproofing sprays are often tested for acute inhalation toxicity in vivo on the basis of OECD Test Guideline 403. A screening test using the isolated perfused rat lung (IPRL) is proposed in order to reduce the number of acute inhalation tests and to refine these. The test comprises exposure of IPRLs to aerosolised formulations of the water proofing agents and on-line monitoring of respiratory parameters.

Substances revealing harmful effects on the IPRL, such as impaired lung compliance and atelectasis formation, did also show changes in respiratory parameters up to mortality in in vivo tests with rats. Thus, pre-testing in the IPRL allows the identification of surface-active substances causing acute inhalation toxicity.

To assess the potential lung toxicity of seven formulations, each tested in two male and two female IPRLs, we evaluated changes in the respiratory parameters tidal volume, compliance, and resistance, edema and atelectasis formation, taking into account the inhaled doses. These IPRL results were compared with available in vivo results and a good or excellent correlation in six out of seven cases was revealed.

In conclusion, the use of the IPRL is well suited for screening substances showing acute "physical" inhalation toxicity. Therefore, for future assessment of surface active substances, it is suggested to use this test prior to in vivo inhalation tests. Formulations with no acute harmful effects on the IPRL need to be further investigated in vivo for

complete risk assessment. However, substances showing strong reactions in the IPRL will most likely cause lung damage in vivo. This is why testing in live animals is not recommended in order to avoid possible pain, suffering or distress.

## 155

### Cannabinoid-1 receptor in cardiac fibrosis

**Foinquinos, Ariana;** Fiedler, Jan; Zimmer, Karina; Remke, Janet; **Batkai, Sandor;** Thum, Thomas  
MHH, IMTTS, Hannover, Germany

The endocannabinoid system is an emerging target in cardiac diseases owing to its role in fibrosis, inflammation and cell death. The deregulation of this system has been implicated in myocardial infarction and consequent heart failure. We have shown previously the cardioprotective effects of chronic CB1 blockade in cardiac injury models such as diabetes and doxorubicin toxicity. A recent study suggests that CB1 antagonist improves cardiac function and reduces adverse remodeling after myocardial infarction, but the exact mechanism of these beneficial effects is still unknown. The aim of the present study was to identify the signaling pathways and investigate their involvement in the chronic effect of CB1 inhibition in cardiac fibrosis and left ventricular remodeling. In a mouse model of cardiac fibrosis, angiotensin II (All, 3 mg/kg/day) was administered by osmotic minipumps for 14 days. CB1 receptor antagonist rimonabant, or vehicle was given every second day during the All administration period. At the end, hemodynamic parameters were measured by non-invasive echocardiography, cardiac pressure volume catheter was used to evaluate global functional parameters and cardiac tissue was collected for histologic and biochemical evaluation. Two weeks of All infusion significantly increased systolic pressure in all groups, irrespective of treatment. Although no difference in systolic parameters was found between the groups, cardiac dysfunction was shown by altered myocardial performance index, which was prevented by CB1 antagonist treatment. Fibrosis, assessed by collagen deposition, was significantly reduced in the CB1 antagonist group. This was confirmed by downregulation of pro-fibrotic genes e.g. CTGF and Col1a1 in the same group. In vitro studies using activated 3T3 cells suggest that CTGF is downregulated after rimonabant treatment. Fibrogenic activation of primary fibroblast isolated from mice hearts induced extracellular matrix genes expression e.g. Col1a1, CTGF and fibrillin, which was sensitive to CB1 antagonist treatment.

In conclusions, we found that chronic CB1 antagonist treatment in All-induced mice preserved LV function and cardiac fibrosis was reduced with concomitant downregulation of fibrogenic genes. The study helps to better understand the anti-fibrotic action of chronic CB1 treatment. Novel generation of CB1 inhibitors, devoid of neuropsychiatric side-effects, may be therapeutically explored in chronic heart failure.

## 156

### Biomonitoring of mycotoxins in urine: Pilot study in mill workers

**Föllmann, Wolfram;** Ali, Nurshad; Blaszkewicz, Meinolf; Degen, Gisela H.  
Leibniz-Institut für Arbeitsforschung, Dortmund, Germany

Contamination of grains with mycotoxins results in a dietary background exposure of the general population. In occupational settings, e.g. during processing of raw materials, an additional mycotoxin exposure by inhalation is possible (Degen 2011, World Mycotoxin Journal 4:315-327). Biomonitoring is an integrative approach to assess human exposure from various sources and by all routes. A pilot study was conducted to compare the levels of urinary biomarkers in mill workers to those in a control group with dietary intake alone to investigate a possible workplace exposure to mycotoxins.

Workers (n=18) from 3 grain mills in North Rhine Westphalia, Germany, provided spot urines during shift, and volunteers (n=13) from IfADo with matched age structure served as control group. The mycotoxins selected for biomarker analysis were deoxynivalenol (DON), zearalenone (ZEN) and ochratoxin A (OTA). Urine sample clean-up was performed by immunoaffinity columns (DON, ZEN) or liquid-liquid-extraction (OTA) for sensitive analysis by LC-MS or HPLC. Also mycotoxin metabolites were analyzed: DOM-1, OT $\alpha$ ,  $\alpha$ - and  $\beta$ -ZEL, and enzymatic hydrolysis with  $\beta$ -glucuronidase/arylsulfatase was performed to include phase-II metabolites which are formed in the organism.

DON, OTA and ZEN were detected in all urine samples from mill workers and controls. DOM-1, OT $\alpha$ ,  $\alpha$ - and  $\beta$ -ZEL were detected less frequently in the urines, which may be due to differences in mycotoxin metabolism between individuals. In both cohorts, DON was detected in the highest concentrations (mean 6  $\mu$ g/g creatinine); OTA (mean 0.1  $\mu$ g/g creatinine) and in particular ZEN (mean 0.03  $\mu$ g/g creatinine) and its metabolites appeared in urine at lower concentrations. DON biomarker levels in the two cohorts were not significantly different. For OTA and ZEN slightly higher concentrations were found in the mill worker urines, but the difference was not significant. The urinary levels for DON and OTA measured in this study are similar to values reported in other studies performed in Europe. For ZEN and its metabolites no comparable studies are available up to now. From the results we can conclude that the levels of the mycotoxins measured in all urine samples reflect mainly dietary exposure of the people. An additional occupational exposure of mill workers if any is apparently very low at the investigated workplaces.

**Acknowledgement:** This study was supported by EU Ziel 2-Programm NRW 2007-2013 (EFRE)

## 157

### Mechanosensitivity of podocytes: Role of purinergic P<sub>2</sub>X channels

**Forst, Anna-Lena;** Olteanu, Vlad Sorin; Gudermann, Thomas; Mederos Y Schnitzler, Michael; Storch, Ursula  
Walther Straub Institut für Pharmakologie und Toxikologie, München, Germany

Podocytes are specialized highly differentiated visceral epithelial cells of the kidney glomerulus. Hypertension and the resulting increase in mechanical load to podocytes are believed to result in podocyte damage. The molecular identity of proteins sensing the mechanical force however is poorly understood. Because the classical transient receptor channel type 6 (TRPC6) interacts with the MEC-2 homologue podocin, it was suggested that TRPC6 could form a mechanosensitive ion channel in podocytes. We could confirm that podocytes respond to mechanical stimuli with increased inward cation currents. However, these currents were not mediated by TRPC6 since TRPC6 knock-out podocytes responded in a similar way as control podocytes. To analyze the role of mechanosensitive G<sub>q/11</sub>-protein coupled receptors as mechanosensors in podocytes we used 2 mM of the G-protein inhibitor GDP- $\beta$ S. GDP- $\beta$ S did not reduce the increase in inward currents and neither did 50  $\mu$ M suramin, which blocks all purinergic P<sub>2</sub>Y receptor and P<sub>2</sub>X<sub>1/2/3/5</sub> channels at this concentration. Instead, the observed currents were significantly decreased by the specific P<sub>2</sub>X<sub>4</sub> blocker 5-BDBD (10  $\mu$ M) indicating a participation of P<sub>2</sub>X<sub>4</sub> channels on mechanically induced currents. Quantitative RT-PCR confirms the expression of several P<sub>2</sub>X channels with P<sub>2</sub>X<sub>2</sub> and P<sub>2</sub>X<sub>4</sub> showing the highest mRNA expression levels. Interestingly, extracellularly perfused ATP induced similar inward currents as observed with hypotonic stimulation. Furthermore, our findings indicate that podocytes are mechanosensitive by releasing ATP upon hyposmotically induced membrane stretch thereby activating P<sub>2</sub>X channels.

## 158

### Berufsbegleitendes Postgradualstudium "Toxikologie und Umweltschutz"

**Franke, Heike;** Graefe, Adelgunde  
Universität Leipzig, PGS Toxikologie, Germany

Toxikologie, die „Lehre von den schädlichen Wirkungen chemischer Stoffe auf lebende Organismen“, ist heute zu einem bedeutenden interdisziplinären Fachgebiet heran gewachsen, welches einer ständigen Zunahme an Kenntnissen und Regulatorien unterliegt.

„Toxikologie und Umweltschutz“ – nennt sich unser Postgradualstudienprogramm an der Universität Leipzig, das Naturwissenschaftlern die Möglichkeit bietet, eine Qualifikation im Fach „Toxikologie und Umweltschutz“ zu erlangen. Akademikerinnen und Akademiker aus verschiedenen Arbeitsgebieten und mit unterschiedlicher Berufspraxis haben die Möglichkeit, ihr Wissen auf toxikologierelevanten Gebieten der Biologie, Chemie, Pharmazie, Ökologie, Umwelt und Agrarwissenschaften zu vertiefen und darüber hinaus für die Toxikologie und den Umweltschutz unerlässliche medizinische, analytische, tierversuchskundliche und juristische Kenntnisse zu erwerben. Das seit 1987 einzige universitäre Aufbaustudium dieses Fachgebietes in Deutschland ist berufsbegleitend konzipiert und bietet 12 Module (Intensiv-Wochenlehrgänge; kleine praxisrelevante Demonstrationsveranstaltungen) zur Auswahl. Blended-Learning-Angebote unterstützen die in den Modulen angebotenen Themenkomplexe. Jeweils im September eines geraden Jahres beginnt die neue Matrikel an der Medizinischen Fakultät der Universität Leipzig. Nach etwa 2,5 Jahren kann man den Abschluss zum „Fachwissenschaftler (Bezeichnung des Grundstudiums) für Toxikologie“ erwerben, der an die Teilnahme von 10 Präsenzmodulen, die Einarbeitung in ein spezielles Thema der Toxikologie durch Anfertigung einer Abschlussarbeit sowie die bestandene Abschlussprüfung gebunden ist. Einzelne Module können auch separat absolviert werden.

Die Ziele dieser Spezialisierung in allgemeiner und spezieller Toxikologie, sowie umweltrelevanter Themen sind u.a. die Vermittlung von Wissen und Fähigkeiten zur rascheren Einarbeitung und Beurteilung toxikologischer Fragestellungen, die Vermittlung von Kenntnissen zur Entwicklung und Anwendung toxikologischer Prüf- und Analysenverfahren in Übereinstimmung mit den international und national gültigen Richtlinien einschließlich der Qualitätskontrolle sowie für die Mitwirkung bei der Erarbeitung von Gutachten und Zertifikaten auf der Grundlage geltender Rechtsvorschriften sowie Bewertungen von Gesundheits- und Umweltrisiken bei der Entwicklung und Herstellung von Produkten.

Informationen über das Postgradualstudium „Toxikologie und Umweltschutz“:  
[www.uni-leipzig.de/toxikologie](http://www.uni-leipzig.de/toxikologie)

## 159

### Effects of the D<sub>2</sub> receptor partial agonist 2-bromoterguride on body weight and body fat composition after chronic administration in rats

**Franke, Robert T.;** Pertz, Heinz H.<sup>2</sup>; Fink, Heidrun<sup>1</sup>; Brosda, Jan<sup>1</sup>

<sup>1</sup>Freie Universität Berlin, Fachbereich Veterinärmedizin - Institut für Pharmakologie und Toxikologie, Germany

<sup>2</sup>Freie Universität Berlin, Institut für Pharmazie, Germany



**Objectives:** Schizophrenia is a chronic mental illness. Current antipsychotic therapy is limited in efficacy and associated with severe adverse effects such as extrapyramidal side effects, weight gain and changes in body fat composition. Dopamine D<sub>2</sub> receptor partial agonists represent a sophisticated option to gain an effective antipsychotic treatment with a lower risk of adverse effects. *In vitro* and *in vivo* data revealed that the terguride derivative 2-bromoterguride is a partial agonist at dopamine D<sub>2</sub> receptors with promising antipsychotic characteristics [1].

**Methods:** In this study, we aimed at investigating with the same doses as used before [1] the chronic effects of 2-bromoterguride (0.1 and 0.3 mg/kg for 21 days; twice daily) on food and water intake, body weight and fat tissues (gonadal, retroperitoneal, inguinal and interscapular) in female Sprague-Dawley rats. Additionally, the influence of chronic 2-bromoterguride administration on spontaneous behaviour in the open field box and cataleptic behaviour in the bar and grid test were examined. The atypical antipsychotic olanzapine (2 mg/kg) was used as a positive control.

**Results:** In contrast to olanzapine, chronic 2-bromoterguride administration did not induce changes in food and water intake, body weight and body fat composition when compared to the vehicle group. 2-Bromoterguride caused no cataleptic behaviour but decreased spontaneous locomotion.

**Conclusions:** 2-Bromoterguride shows no liability for weight gain and does not change body fat composition after chronic administration. To sum up, both doses of 2-bromoterguride cause a mild sedation but do not induce the above mentioned adverse effects. The present study confirms our previous observations [1] that the D<sub>2</sub> receptor partial agonist 2-bromoterguride may be a promising candidate for the treatment of schizophrenia with negligible adverse effects.

[1] F. Jantschak, J. Brosda, R.T. Franke, H. Fink, D. Möller, H. Hübner, P. Gmeiner, H.H. Pertz (2013). Pharmacological profile of 2-bromoterguride at human dopamine D<sub>2</sub>, porcine serotonin 5-hydroxytryptamine 2A, and α<sub>2</sub>C-adrenergic receptors, and its antipsychotic-like effects in rats. *J Pharmacol Exp Ther.* 347:57-68.

## 160

### Hyaluronan-synthesis regulates angiogenesis

Freudenberger, Till<sup>1</sup>; Driesen, Tobias<sup>1</sup>; Schuler, Dominik<sup>2</sup>; Weyrauther, Beate<sup>1</sup>; Heiss, Christian<sup>2</sup>; Kelm, Malte<sup>2</sup>; Fischer, Jens Walter<sup>1</sup>

<sup>1</sup>Institut für Pharmakologie und Klinische Pharmakologie, Universitätsklinikum

Düsseldorf, Heinrich-Heine-Universität Düsseldorf, Germany

<sup>2</sup>Klinik für Kardiologie, Pneumologie und Angiologie, Universitätsklinikum Düsseldorf, Germany

**Background** Angiogenesis is defined as formation of new vessels from pre-existing ones. Upon endothelial cell sprouting, developing sprouts elongate and endothelial tubes then become stabilized by recruitment of 'periendothelial' cells (PC). In this context, extracellular matrix (ECM) plays a role in neo-vessel stabilization and exogenous hyaluronan (HA) has been described to influence angiogenesis. However, it is unknown which role endogenous HA-synthesis by HA-synthases (HAS) 1-3 plays in angiogenesis. **Methods** Tube formation of human coronary artery endothelial cells (HCAEC) on matrigel was analysed using 4-methylumbelliferone (4-MU), a HA-synthesis-inhibitor, for 24 hours. To investigate a potential role of HA in the interactions of HCAEC with PC, HCAEC and murine aortic cells (mAC) were co-cultured for 7 days, immunocytochemically stained and mRNA-expression of genes related to the HA-system was analysed. To assess angiogenesis *in vivo*, recovery of limb perfusion in male Has3 KO- as well as wild-type (WT)-mice was analysed after induction of unilateral hind limb ischemia applying laser-doppler-perfusion-imaging. Capillary-density in calf muscles 35 days post-OP was analysed after CD31-staining. **Results** 4-MU compromised the structural integrity of endothelial tubes but enhanced their formation as evidenced by an increased number of branching points and closed meshes per high power field. Interestingly, also co-culture of HCAEC and mAC led to formation of tube-like endothelial structures and these phenotypic changes were accompanied by changes in mRNA-expression of genes related to the HA-matrix. Specifically, mRNA-expression of Has1 was reduced in mAC in co-culture while mRNA-expression of the HA receptor CD44 was reduced in HCAEC in co-culture. After surgical induction of unilateral hind limb ischemia, Has3 KO-mice showed a strong trend towards impaired perfusion of ischemic hind limbs (determined as % perfusion of the non-ischemic hind limb) in later stages of recovery. Impaired perfusion was accompanied by a reduced number of capillaries/high power field in sections of ischemic calf muscles in Has3 KO- vs. WT-mice. **Conclusion** These data suggest that HA-synthesis by Has3 is important for angiogenesis *in vivo*. Although the underlying mechanisms are not known yet, results support the hypothesis that endogenous HA-synthesis plays a role in establishment of cell-cell contacts during tube formation and in the interactions of endothelial cells with PC.

## 161

### *Haemanthus coccineus* extract and its main alkaloid narciclasine display anti-inflammatory activity *in vitro* and *in vivo*

Fuchs, Simone<sup>1,2</sup>; Saarberg, Werner<sup>3</sup>; Bondarenko, Alexander I.<sup>4</sup>; Erdelmeier, Clemens A. J.<sup>3</sup>; Koch, Egon<sup>3</sup>; Fürst, Robert<sup>1</sup>

<sup>1</sup>Goethe-Universität/Biozentrum, Pharmazeutische Biologie, Frankfurt am Main, Germany

<sup>2</sup>LMU München/Department Pharmazie, Pharmazeutische Biologie, Germany

<sup>3</sup>Dr. Willmar Schwabe GmbH & Co.KG, Präklinische Forschung, Karlsruhe, Germany

<sup>4</sup>Medizinische Universität Graz, Institut für Molekularbiologie und Biochemie, Austria

*Haemanthus coccineus* (Amaryllidaceae) extracts (HCEs) have been used in traditional African medicine against febrile colds and asthma. Interestingly, main ingredient of the extract, the non-basic alkaloid narciclasine, was recently reported to induce apoptosis in different tumor cell lines [1]. Beyond this anti-cancer action, we hypothesized that HCE and narciclasine could exhibit an anti-inflammatory potential.

Dried bulbs of *H. coccineus* were extracted using 60 % (w/w) ethanol. The ethanol was largely removed and the remaining solution was partitioned with ethyl acetate. The organic phase was separated and dried (DER 50:1). The resulting HCE contained 2.2% narciclasine. In an ear edema model in mice induced by croton oil or arachidonic acid (AA), HCE was found to clearly reduce edema formation upon oral application (450 mg/kg). *In vitro*, HCE (3 ng/ml to 10 µg/ml) concentration-dependently inhibited the proliferation of lymphocytes and the synthesis of pro-inflammatory cytokines (TNF-α, IL-6, IL-1 β) in murine macrophages without inducing cell cytotoxicity. Moreover, HCE decreased the TNF-α-induced adhesion of leukocytes to human endothelial cells (ECs) and the surface expression of EC adhesion molecules (ICAM-1, VCAM-1, E-selectin) without affecting EC viability. Extract fractions containing basic alkaloids did not display any activity, whereas the main (non-basic) alkaloid narciclasine (1 nM to 10 µM) clearly reduced adhesion molecule expression. We could reveal that HCE as well as narciclasine attenuated TNF-α-triggered NF-κB-dependent gene expression (reporter gene assay) without influencing NF-κB DNA-binding activity (gel shift assay), IκB-α degradation (Western blot), or p65 nuclear translocation (microscopy). Moreover, first results indicate that narciclasine could induce hyperpolarization in ECs (patch clamp). These interesting phenomena are currently under further investigation. In conclusion, our study highlights that the use of HCE/narciclasine could represent a novel interesting anti-inflammatory approach.

1. Ingrassia, L. et al.: *J. Transl Oncol.* 2008, 1(1): 1-13.

## 162

### Left ventricular function after DOCA treatment is preserved in mice lacking endothelial mineralocorticoid receptors

Fürst, David<sup>1</sup>; Lother, Achim<sup>1,2</sup>; Berger, Stefan<sup>3</sup>; Bode, Christoph<sup>2</sup>; Moser, Martin<sup>2</sup>; Hein, Lutz<sup>1</sup>

<sup>1</sup>Institute of Experimental and Clinical Pharmacology and Toxicology, University of Freiburg, Germany

<sup>2</sup>Heart Center, University of Freiburg, Department of Cardiology and Angiology I, Germany

<sup>3</sup>German Cancer Research Center, Heidelberg, Germany

### Introduction

Antagonists of the mineralocorticoid receptor (MR) are well established in heart failure therapy. Anyhow, their use is subject to some notable restrictions like impaired kidney function or hyperkalemia. Thus, novel therapeutic approaches are needed which combine both, efficacy and safety. Previous studies suggest distinct roles for MR in different cell types in the heart such as cardiac myocytes or macrophages. The presented study was designed to determine the cell type-specific function of MR in endothelial cells during cardiac disease.

### Methods and results

We created a mouse model with endothelial-specific MR gene deletion (MR<sup>Cdh5Cre</sup>) using the Cre/loxP system under control of the cadherin 5 promoter. MR mRNA expression was decreased by more than 90% in endothelial cells isolated from MR<sup>Cdh5Cre</sup> hearts (P<0.001, n=4 per group). MR<sup>Cdh5Cre</sup> and control mice underwent unilateral nephrectomy and received desoxycorticosterone (DOCA, 2.5 mg/d s.c.) and NaCl (1% with drinking water) for 6 weeks.

MR deletion from endothelial cells prevented left ventricular dysfunction after DOCA treatment as determined by echocardiography (ejection fraction, DOCA 50.17 ± 2.21% vs. sham 64.9 ± 2.01%; MR<sup>Cdh5Cre</sup> DOCA 63.1 ± 2.21% vs. sham 65.6 ± 2.01%, P<0.001, n=6-10 per group) or left ventricular catheterization. Of note, MR deletion in endothelial cells did not affect arterial blood pressure.

*In vitro* aldosterone inhibited capillary sprouting in isolated aortic rings segments from control (8.8 ± 1.4 vs. untreated 16.5 ± 1.3 capillary sprouts per ring, P<0.01) but not from MR<sup>Cdh5Cre</sup> mice (24.8 ± 1.8 vs. untreated 22.8 ± 2.0 capillary sprouts per ring, n=5-6 aortic rings per group). This finding was confirmed *in vivo* when aldosterone inhibited vascularization of subcutaneous tubes containing matrigel, growth factors and 100 nM aldosterone or vehicle in control but not in MR<sup>Cdh5Cre</sup> mice.

Expression analysis of isolated cardiac endothelial cells from untreated MR<sup>Cdh5Cre</sup> mice revealed a downregulation of genes involved in reactive oxygen species production (*Nox2*, *Nox4*) or leucocyte adhesion (*Icam1*, *Vcam1*) as compared to control mice.

### Conclusion

Mice lacking the mineralocorticoid receptor in endothelial cells were protected from left ventricular functional deterioration after DOCA treatment. Endothelial cell MR deletion prevented the anti-angiogenic effects of aldosterone *in vitro* and *in vivo*.

## 163

**Factors contributing to 17 $\beta$ -estradiol and estrone levels in the mammary gland of healthy women: a pilot study**

**Futh, Susanne**<sup>1</sup>; Schmalbach, Katja<sup>1</sup>; Esch, Harald L.<sup>1</sup>; Waldhofen, Ulrike<sup>2</sup>; Eckert, Peter<sup>3</sup>; Lehmann, Leane<sup>1</sup>

<sup>1</sup>University of Würzburg, Section of Food Chemistry, Würzburg, Germany

<sup>2</sup>Praxis für Plastische & Ästhetische Chirurgie, Bad Kissingen, Germany

<sup>3</sup>Praxis Prof. Dr. med. Peter Eckert Facharzt für plastische Chirurgie, Würzburg, Germany

Exposure of the female mammary gland (MG) to the endogenous estrogen 17 $\beta$ -estradiol (E2) increases the risk to develop tumors. The lack of correlation between E2 levels in plasma and MG, led to the hypothesis that the amount of E2 available for estrogen receptor (ER) activation in the MG is determined by (i) aromatization of adrenal precursors by cytochrome P450-dependent monooxygenase (CYP) 19A1, (ii) interconversion of the weak estrogen estrone (E1) and E2 by 17 $\beta$ -hydroxysteroid dehydrogenases (HSD) 1 and 2, and (iii) hydrolysis of E2- and E1-sulfate, by steroid sulfatase (STS). However, up to now, levels of E1 and E2 in the MG of healthy women have not been analyzed in conjunction with transcript levels of the respective enzymes.

To overcome the limitations of immunoassays used in most studies reporting E2 and E1 levels in the female MG, a GC-MS/MS method using deuterated E2 and E1 for quantitation was developed and applied to MG tissues obtained from cosmetic reduction surgery. Information on age, body-mass-index (BMI), number of pregnancies and hormone supplementation were provided. Menopausal status of women with previous pregnancies was determined by histological lobule-typing. HSD1, HSD2, STS, and the proliferation marker Ki67, sensitive to ER activation, were determined by quantitative Taqman probe-based real time PCR. Eventually, statistical correlation analysis between E2, E1, E2+E1, E2/E1 ratio and menopausal status, hormone supplementation, BMI, and transcript levels as well as, where appropriate, comparison of means were performed.

A total of 29 tissues from 20 premenopausal, 7 postmenopausal and 2 women of undetermined menopausal status were analyzed. 4 samples were below the limit of determination for both E2 and E1 (0.5 and 0.2 pmol/g tissue, respectively). In 22 tissues, E1 levels were higher than that of E2, and a positive correlation was observed between E2 and E1 levels. Also, a weak positive correlation was observed between E2 levels and BMI, both in all, pre- and postmenopausal women. Furthermore, E2/E1 ratios rather than E2 or E2+E1 levels correlated positively with Ki67 transcript levels in premenopausal women without hormone supplementation. Interestingly, neither mean E2, nor E1 levels were affected by menopausal status or hormone supplementation. Over all tissues, no correlations of E2 and/or E1 were observed with Ki67, CYP19A1, STS and HSDs. Likewise, HSD1/HSD2 ratios did not correlate with E2/E1 ratios.

In conclusion, despite the low number of tissues analyzed so far, impact of BMI on MG E2 levels and correlation between E2/E1 ratio and premenopausal MG proliferation becomes apparent.

Supported by DFG Le1329/10-1

## 164

**Inhibition of macrophage migration by C. botulinum exoenzyme C3**

**Rohrbeck, Astrid**; **Genth, Harald**; Rotsch, Jacqueline; May, Martin; May, Michaela; Hagemann, Sandra; Huelsenbeck, Stefanie C.; Just, Ingo  
Hannover Medical School, Toxicology, Germany

C3-like exoenzymes are produced by various microorganism including *Clostridium botulinum* (C3bot), *Bacillus cereus*, and *Staphylococcus aureus*. C3bot is the prototype of C3-like exoenzymes, that specifically ADP-ribosylates and thereby inactivates Rho(A/B/C). C3-like exoenzymes are not yet regarded as virulence factors, as the lack of cell entry domains results in a poor accessibility of the C3-like exoenzymes to cells. In this study, the sensitivity of various cell lines to C3bot has been re-investigated. Primary monocytes as well as cultured macrophage-like cells including J774A.1 cells and RAW macrophages exhibit a ten-fold higher sensitivity to C3bot than fibroblasts and epithelial cells. RhoA ADP-ribosylation by C3bot resulted in the transient formation of pronounced bipolar protrusions based on defective tail retraction. The formation of bipolar protrusion resulted in inhibited macrophage migration. These findings suggested that macrophages appear to be target cells of C3bot. The migration of macrophage ensures their recruitment to the site of pathogen invasion or tissue damage. Inhibition of macrophage migration likely preserves the survival of C3-producing microorganisms. The observations of this study re-enforce the paradigm of a role of C3-like exoenzymes as virulence factors.

## 165

**Safety of acute and chronic administration of cyclosporine A in a seizure and an epilepsy model**

Handreck, Annelie<sup>1,2</sup>; Mall, Eva Maria<sup>1</sup>; Elger, Deborah Annina<sup>3</sup>; Gey, Laura<sup>1,2</sup>; **Gernert, Manuela**<sup>1,2</sup>

<sup>1</sup>Institut für Pharmakologie, Toxikologie und Pharmazie, Tierärztliche Hochschule, Hannover, Germany

<sup>2</sup>Zentrum für Systemische Neurowissenschaften, Hannover, Germany

<sup>3</sup>Leibniz Universität, Hannover, Germany

In about 30% of patients suffering from epilepsy, seizures still occur despite appropriate treatment with antiepileptic drugs. Neural transplantation of inhibitory cells into seizure initiating or propagating brain regions is one promising approach to overcome this problem of pharmacoresistance. Depending on the grafted cell type (e.g. xenotransplantation), an immunosuppression is necessary to prevent host tissue reactions or graft rejection. However, conflicting data indicate that a treatment with the commonly used immunosuppressive drug cyclosporine A (CsA) might itself act pro- or anticonvulsant in different seizure and epilepsy models.

In the present study, we comprehensively investigated the effect of daily treatment (15 days) with different doses (5 mg/kg vs. 10 mg/kg), application routes (i.p. vs. s.c.), and preparations of CsA (pure substance, Sigma-Aldrich, solved in Cremophor EL, vs. a dilution of the ready-to-use-drug Sandimmun®, Novartis, containing Cremophor EL and ethanol) on seizure thresholds in rats. We used two different rat models, an acute seizure threshold test and a chronic epilepsy model. The individual seizure thresholds of the rats were determined at different time points: 7 days prior to the beginning of immunosuppression (control threshold), 2 hours after the first application (acute), at day 8 and 15 of treatment (chronic), and again 7 days after the end of immunosuppression (day 22, washout). Additionally, behavioral tests were conducted to detect putative adverse effects of the immunosuppression. Finally, blood samples were taken 150 minutes after drug administration for analysis of CsA whole blood levels.

Independent of the dose, the application route, and the drug preparation, CsA did not cause acute changes of seizure thresholds in the two rat models used. Chronic injection of pure CsA or Sandimmun® also did not cause robust changes of seizure thresholds. The resorption of intraperitoneally applied CsA from Sandimmun® significantly exceeded the resorption from the pure CsA preparation. Observed adverse effects included transient gastrointestinal problems such as diarrhea. Our data indicate that immunosuppression with 10 mg/kg Sandimmun® i.p. rather than pure CsA is a safe and feasible option for use in neural transplantation experiments in epilepsy models.

Supported by the DFG (FOR 1103, GE1103/7). A. Handreck is supported by the Prof. Dr. Peter and Jytte Wolf Foundation for Epilepsy.

## 166

**Chronic focal delivery of the antiepileptic drug vigabatrin into the subthalamic nucleus (STN) for epilepsy treatment**

**Gey, Laura**<sup>1,2</sup>; Gernert, Manuela<sup>1,2</sup>; Löscher, Wolfgang<sup>1,2</sup>

<sup>1</sup>Institut für Pharmakologie, Toxikologie und Pharmazie, Stiftung Tierärztliche Hochschule Hannover, Germany

<sup>2</sup>Zentrum für Systemische Neurowissenschaften Hannover, ZSN, Germany

A major limiting factor in treating patients with intractable epilepsy is the occurrence of unacceptable adverse effects after systemic administration of antiepileptic drugs in high doses. One promising strategy to overcome this problem is the focal delivery of antiepileptic drugs directly into brain regions involved in seizure modulation. In a previous study in rats we could demonstrate strong anticonvulsant effects without severe adverse effects in response to acute bilateral microinjection (MI) of vigabatrin (VGB), an irreversible inhibitor of the GABA-degrading enzyme GABA-aminotransferase (GABA-T), into the STN. The STN is a key basal ganglia structure involved in remote control of seizures emanating from the limbic system.

This study investigates, if chronic MI of VGB into the STN of rats using implantable microinfusion pumps leads to long-lasting anticonvulsant effects in the pentylenetetrazole (PTZ) seizure threshold test, an acute seizure model. In order to assess the dose for chronic MI, acute bilateral MI of 10  $\mu$ g VGB into the STN was performed followed by neurochemistry in post mortem tissue 4 and 24 hours later. VGB was detectable in high concentrations within the STN and adjacent brain tissues. GABA-T was completely inhibited. Accordingly, compared to control animals, GABA levels were significantly elevated, without influencing the activity of the GABA-synthesizing enzyme glutamic acid decarboxylase (GAD). In a next step, chronic MI over a period of 3 weeks bilaterally into the STN was therefore conducted using infusion of 10  $\mu$ g VGB per day. Preliminary data show a significant increase in PTZ seizure thresholds up to 2 weeks, in individual rats even up to 3 weeks. The loss of anticonvulsant efficacy after 3 weeks in most rats could be the consequence of a tolerance development due to feedback GAD inhibition in response to the high GABA levels. Indeed, the GAD activity was reduced in the STN in those rats after chronic MI of 10  $\mu$ g VGB daily. GABA-T was completely inhibited. No adverse effects were observed.

We currently investigate, if chronic MI of 5  $\mu$ g VGB daily into the STN exerts anticonvulsant effects without inducing GAD inhibition. In further studies, chronic MI of VGB into the STN will be investigated in a chronic epilepsy model.

VGB was provided free of charge by Sanofi-Aventis Deutschland GmbH. Supported by a grant (FOR 1103 / GE1103/7-2) from the German Research Foundation (Bonn, Germany). L. Gey is supported by the Konrad-Adenauer-Stiftung e.V.

## 167

**Biased ligands for  $\alpha_{2A}$ -adrenoceptors**

**Gilsbach, Ralf**<sup>1</sup>; Barg, Margareta<sup>1</sup>; Ozawa, Takeaki<sup>2</sup>; Hein, Lutz<sup>1</sup>

<sup>1</sup>Institute of Experimental and Clinical Pharmacology and Toxicology, Freiburg, Germany

<sup>2</sup>School of Science, 2Department of Chemistry, Tokyo, Japan

$\alpha_{2A}$ -adrenoceptors mediate diverse physiological functions of the sympathetic system and are targets for pharmacological therapy. However the therapeutic potential of these receptors is limited by diverse side effects. Knowledge about the contribution of the

three  $\alpha_2$ -adrenoceptor subtypes to pharmacological and physiological actions was derived from gene-targeting in mice. These studies indicate that most pharmacologically relevant functions rely on  $\alpha_{2A}$ -adrenoceptors. This subtype is known to inhibit exocytosis of norepinephrine from central and peripheral adrenergic neurons. In addition  $\alpha_{2A}$ -adrenoceptors have been identified in several neuronal and non-neuronal cell-types. Recent studies indicate that  $\beta$ -arrestin signaling is involved in  $\alpha_2$ -adrenoceptor mediated responses. To characterize  $\beta$ -arrestin recruitment properties of  $\alpha_{2A}$ -adrenoceptor ligands a split click beetle luciferase complementation assay was established. Data of this cell culture assay were accompanied by G-protein signaling studies. The derived results provide first evidence for biased signaling properties of  $\alpha_{2A}$ -adrenoceptor ligands. Remarkably, the enantiomers dexmedetomidine and levomedetomidine showed characteristic differences. In case of dexmedetomidine  $EC_{50}$ -values and maximal evoked responses did not show major differences between G-protein activation ( $pEC_{50} = 8.56 \pm 0.04$ ; max.  $96.3\% \pm 0.9\%$ ) and  $\beta$ -arrestin 2 recruitment ( $pEC_{50} = 8.98 \pm 0.09$ ; max.  $102.4\% \pm 1.9\%$ ). In contrast levomedetomidine recruited  $\beta$ -arrestin 2 to  $\alpha_{2A}$ -adrenoceptors with lower  $EC_{50}$ -values and higher maximal responses ( $pEC_{50} = 5.82 \pm 0.28$ ; max.  $22.4\% \pm 0.8\%$ ) as compared to G-Protein activation ( $pEC_{50} 7.38 \pm 0.1$ ; max.  $8.32\% \pm 1.04\%$ ). Thus, levomedetomidine is a biased ligand of the  $\alpha_{2A}$ -adrenoceptor. This knowledge will help to clarify the relevance of  $\beta$ -arrestin signaling for  $\alpha_{2A}$ -adrenoceptors pharmacology and is expected to provide new avenues for future drug development.

## 168

### Evidence for dynamic association of GPCRs, ligands and G-proteins at the trans-Golgi network of thyroid cells.

**Godbole, Amod**<sup>1,2</sup>; Lohse, Martin J.<sup>1,2</sup>; Calebiro, Davide<sup>1,2</sup>

<sup>1</sup>Inst fuer Pharmakologie und Toxikologie, AG Calebiro, Wuerzburg, Germany  
<sup>2</sup>Rudolf Virchow Centre, AG Calebiro, Wuerzburg, Germany

Whereas G-protein coupled receptors (GPCRs) have been long believed to signal through cyclic AMP only at cell surface, our group has previously shown that GPCRs not only signal at the cell surface but can also continue doing so once internalized together with their ligands, leading to persistent cAMP production (1). This phenomenon, which we originally described for the thyroid stimulating hormone receptor (TSHR) in thyroid cells, has been observed also for other GPCRs (2-4). However, the intracellular compartment responsible for such persistent signaling was insufficiently characterized. The aim of this study was to follow by live-cell imaging the internalization and trafficking of TSHR, TSH and effector proteins in thyroid cells. Mouse primary thyroid cells were transfected with fluorescently tagged receptors, G-proteins and/or subcellular markers by electroporation, stimulated with fluorescently labeled TSH and visualized using a combination of total internal reflection fluorescence (TIRF) and highly inclined thin illumination (HILO) microscopy. The results suggest that TSH is internalized in complex with its receptor and both remain colocalized in/on intracellular vesicles for at least 20 minutes after stimulation. The internalized TSH, and presumably also TSHR, shows a partial colocalisation with  $G_{\alpha_s}$  on vesicles located near the nucleus. Because of these findings and previous reports that G-proteins are localized at the trans-Golgi network (TGN), we used a red-fluorescent TGN marker, sialyltransferase(ST)-RFP, to visualize this compartment. Our preliminary results indicate the presence of TSH-TSHR complexes in vesicles/tubules belonging to the TGN. These findings suggest the coexistence of receptor, ligand and G-protein at the trans-Golgi network, which may represent the compartment responsible for persistent cAMP signaling after TSH-TSHR internalization.

- [1] Calebiro D, Nikolaev VO, Gagliani MC, de Filippis T, Dees C, Tacchetti C, Persani L, Lohse MJ. (2009) Persistent cAMP-signals triggered by internalized G-protein-coupled receptors. *PLoS Biol.* 7:e1000172.  
[2] Calebiro D, Nikolaev VO, Persani L, Lohse MJ. (2010) Signaling by internalized G-protein-coupled receptors. *Trends Pharmacol. Sci.* 31:221-8.  
[3] Irannejad R, Tomshine JC, Tomshine JR, Chevalier M, Mahoney JP, Steyaert J, Rasmussen SG, Sunahara RK, El-Samad H, Huang B, von Zastrow M. (2013) Conformational biosensors reveal GPCR signalling from endosomes. *Nature.* 495:534-8.  
[4] Lohse MJ, Calebiro D. (2013) Cell biology: Receptor signals come in waves. *Nature.* 495:457-8.

## 169

### *Toxoplasma gondii* and memory in aging

**Gajewski, Patrick D.**; Falkenstein, Michael; Hengstler, Jan G.; **Golka, Klaus**

Leibniz Research Centre for Working Environment and Human Factors, Dortmund, Germany

Almost 30% of humans present a *Toxoplasma gondii* positive antibody status and its prevalence increases with age. The central nervous system is the main target. However, little is known about the influence of asymptomatic i.e. latent Toxoplasmosis on cognitive functions in humans. To investigate neurocognitive dysfunctions in asymptomatic older adults with *Toxoplasma gondii* positive antibody status a double-blinded neuropsychological study was conducted. The participants were classified from a population-based sample (N=131) of healthy participants with an age of 65 years and older into two groups with 42 individuals each: Toxoplasmosis positive (T-pos; IgG>50 IU/ml) and Toxoplasmosis negative (T-neg; IgG=0 IU/ml). The outcome measures were a computer-based working-memory test (2-back) and several standardized psychometric tests of memory and executive cognitive functions. T-pos

seniors showed an impairment of different aspects of memory. The rate of correctly detected target symbols in a 2-back task was decreased by nearly 9% (P=0.020), corresponding to a performance reduction of about 35% in working memory relative to the T-neg group. Moreover, T-pos seniors had a lower performance in a verbal memory test, both regarding immediate recall (10% reduction; P=0.022), delayed recognition (6%; P=0.037) and recall from long-term memory assessed by the word fluency tests (12%; P=0.029). In contrast, executive functions were not affected. The effects remained mostly unchanged after controlling for medication. The impairment of memory functions in T-pos seniors was accompanied by a decreased self-reported quality of life. Because of the high prevalence of asymptomatic Toxoplasmosis and an increasing population of older adults this finding is of high relevance.

## 170

### N-Acetyltransferase 2 phenotypes, enzyme activity and urinary bladder cancer risk

**Selinski, Silvia**<sup>1</sup>; Blaszkewicz, Meinolf<sup>1</sup>; Ickstadt, Katja<sup>2</sup>; Hengstler, Jan G.<sup>1</sup>; **Golka, Klaus**<sup>1</sup>

<sup>1</sup>Leibniz Research Centre for Working Environment and Human Factors, Dortmund, Germany

<sup>2</sup>Faculty of Statistics, TU Dortmund University, Germany

Polymorphisms of N-acetyltransferase 2 (NAT2) are well known to modify urinary bladder cancer risk as well as efficacy and toxicity of pharmaceuticals via reduction in the enzyme's acetylation capacity. Nevertheless, the discussion about optimal NAT2 phenotype prediction, particularly differentiation between different degrees of slow acetylation, is still controversial. Therefore, we investigated the impact of single nucleotide polymorphisms and their haplotypes on slow acetylation in vivo and on bladder cancer risk. For this purpose, we used a study cohort of 1,712 bladder cancer cases and 2,020 controls genotyped for NAT2 by RFLP-PCR and for the tagSNP rs1495741 by TaqMan® assay. A subgroup of 344 individuals was phenotyped by the caffeine test in vivo. We identified an 'ultra-slow' acetylator phenotype based on combined \*6A/\*6A, \*6A/\*7B and \*7B/\*7B genotypes containing the homozygous minor alleles of C282T (rs1041983, \*6A, \*7B) and G590A (rs1799930, \*6A). 'Ultra-slow' acetylators have significantly about 32 and 46 % lower activities of caffeine metabolism compared with other slow acetylators and with the \*5B/\*5B genotypes, respectively (P < 0.01, both). The 'ultra-slow' genotype showed an association with bladder cancer risk in the univariate analysis (OR = 1.31, P = 0.012) and a trend adjusted for age, gender and smoking habits (OR = 1.22, P = 0.082). In contrast, slow acetylators in general were not associated with bladder cancer risk, neither in the univariate (OR = 1.02, P = 0.78) nor in the adjusted (OR = 0.98, P = 0.77) analysis. In conclusion, this study suggests that NAT2 phenotype prediction should be refined by consideration of an 'ultra-slow' acetylation genotype.

## 171

### $\beta_2$ -Adrenoceptor Signaling and Regulation of NADPH Oxidase Activity in Human Neutrophils

**Göttle, Martin**; Brunskole Hummel, Irena; Seifert, Roland  
Medizinische Hochschule Hannover, Pharmakologie, Germany

Human neutrophils are essential for host defense against infectious agents such as bacteria or viruses and play major roles in autoimmune diseases including bronchial asthma. The neutrophil respiratory burst includes NADPH oxidase-mediated  $O_2^{\cdot-}$  formation, which is regulated by cAMP-based signaling cascades. Agonists at the  $\beta_2$ -adrenoceptor ( $\beta_2AR$ ) are generally assumed to elevate cAMP levels by  $G_s$  proteins, triggering reduced  $O_2^{\cdot-}$  production. However, it is known that the  $\beta_2AR$  can also couple to  $G_i$  proteins,  $G_q$  proteins and  $\beta$ -arrestins, triggering responses distinct from  $G_s$  protein effects [1]. Moreover, ligand-specific receptor conformations and functional selectivity or biased signaling have been described, mostly in recombinant systems [2].

The aim of our project is to characterize the role of  $\beta_2AR$  signaling in the regulation of  $O_2^{\cdot-}$  production in human neutrophils with a series of ligands and to probe the concept of ligand-specific signaling.  $\beta_2AR$  downstream events are investigated by determining G protein activation in the GTPase assay, by measuring intracellular cAMP-levels, and by monitoring  $\beta_2AR$ -mediated effects on  $O_2^{\cdot-}$  production.

Correlations of efficacy and potency data obtained from the different assay formats were rather poor [3]. Specifically, potencies of isoprenaline, adrenaline and salbutamol were higher in the  $O_2^{\cdot-}$  assay than in the cAMP assay. Epinephrine and dichlorisoproterenol were lacking agonistic activity in the cAMP assay, whereas inhibitory effects of both ligands were readily observed in the  $O_2^{\cdot-}$  assay. The efficacy of salbutamol was significantly higher in the  $O_2^{\cdot-}$  assay as compared to the cAMP assay. Moreover, PKA inhibitors did not reverse isoprenaline-induced inhibition of fMLP-mediated  $O_2^{\cdot-}$  production.

Taken together, these discrepancies – in addition to the traditional pathway via  $G_s$  – point to more complex signaling events being involved in  $\beta_2AR$ -mediated regulation of NADPH oxidase activity. We will apply further pharmacological tools in order to elucidate the interplay of various signaling pathways involved in  $\beta_2AR$ -dependent neutrophil regulation.

[1] Wenzel-Seifert et al. (2000) *Mol. Pharmacol.* 58(5):954-66.

[2] Seifert (2013) *Biochem. Pharmacol.* 86(7):853-61

[3] Brunskole Hummel et al. (2013) *PLoS One* 8(5):e64556

172

### Human neutrophils are activated by Clostridium difficile Toxin B via formyl peptide receptor

Gov, Sebastian<sup>1</sup>; Olling, Alexandra<sup>1</sup>; Just, Ingo<sup>1</sup>; Neumann, Detlef<sup>2</sup>; Gerhard, Ralf<sup>1</sup>

<sup>1</sup>Medizinische Hochschule Hannover, Toxikologie, Germany

<sup>2</sup>Medizinische Hochschule Hannover, Pharmakologie, Germany

*Clostridium difficile* is known to be the most common cause of antibiotic associated diarrhea and pseudomembranous colitis for decades. Two large toxins (TcdA/TcdB) produced by this bacterium are the main pathogenicity factors. They are known to act as glucosyltransferases, functionally inactivating their substrate proteins of the Rho GTPase-family.

*C. difficile*-induced pseudomembranous colitis is associated with tremendous infiltration of neutrophils into the affected intestine. We investigated the effect of TcdA and TcdB on freshly isolated human peripheral granulocytes. Therefore, neutrophils were stimulated with native toxin A and B and various recombinant toxin fragments (rTcdA/rTcdB). Activation of neutrophils in terms of rise in intracellular free Ca<sup>2+</sup> concentration was measured by Fura-2 assay. Recombinant TcdA had no effect on neutrophil activation. Recombinant TcdB however induced a marked influx of calcium into cells and an increase in intracellular free calcium within seconds. By applying different toxin fragments the N-terminal glucosyltransferase domain (GTD) of TcdB was determined to be sufficient to stimulate neutrophils while TcdBAGTD was unable to do so. Beside calcium influx ROS generation and neutrophil degranulation were also shown to be potentially triggered by rTcdB.

In contrast to rTcdB native TcdB exhibited almost no neutrophil activating properties. However, incubation of native TcdB at 37°C for 4 hours or limited proteolytic digestion using trypsin uncovered epitopes that were sufficient for neutrophil activation.

Our results pointed towards a formyl peptide-like effect of TcdB. Transfection experiments with HEK-293 cells proved the formyl peptide receptor activating ability of the glucosyltransferase domain of TcdB.

Taken together, the glucosyltransferase domain of TcdB is sufficient to activate neutrophils in a fMLP-like manner. This effect is of particular interest since it shows that pro-inflammatory effects can be triggered by TcdB fragments that are generally considered as inactive. These results underline the importance of TcdB which is able to trigger pro-inflammatory signalling independently of its cytotoxic glucosyltransferase activity.

173

### Effective and safe drug prescribing – Implementation of a novel teaching concept for undergraduate medical students

Grabowski, Katja<sup>1</sup>; Sostmann, Kai<sup>2</sup>; Plener, Joachim<sup>2</sup>; Avila, Javier<sup>2</sup>; Harms, Tina<sup>2</sup>; Buron, Sandra<sup>2</sup>; Douros, Antonios<sup>1</sup>; Kreuz, Reinhold<sup>1</sup>; Peters, Harm<sup>2</sup>; Bolbrinker, Juliane<sup>1</sup>

<sup>1</sup>Charité-Universitätsmedizin Berlin, Institut für Klinische Pharmakologie und Toxikologie, Germany

<sup>2</sup>Charité – Universitätsmedizin Berlin, Dieter Scheffner Fachzentrum für medizinische Hochschullehre und evidenzbasierte Ausbildungsforschung, Germany

#### Introduction

Drug prescribing is an essential therapeutic intervention in clinical practice but often medical students and junior doctors feel poorly prepared for this professional skill. Thus, appropriate teaching concepts for safe and effective prescribing need to be implemented in the undergraduate medical curriculum. Here we present the design, implementation, and evaluation of a web-based practical training tool for pharmacological database search and collaborative knowledge management using a Wikisystem in a Clinical Pharmacology and Therapeutics teaching course.

#### Methods

The course - based on a Blended Learning-concept - was designed as a regular course for third-year medical students at the Charité - Universitätsmedizin Berlin. An initial facultative eLearning part provided an introduction to databases and websites relevant for drug therapy focusing on content and navigation. In the following mandatory course students were able to focus their practical skills training on solving problems related to drug prescribing as presented in a case vignette.

#### Results

In summer term 2013 174 students attended the mandatory course. Of these 78% accessed the online-course prior to the mandatory training. 80% of the students (n=85) who evaluated the overall course - including facultative online-course and mandatory course - rated this teaching concept as "excellent" or "very good". 82% stated that the two parts of the course represented a very reasonable complementary teaching approach.

#### Discussion

Compared to traditional teaching and eLearning approaches the adherence of 78% of the students to the online modul shows the need to implement eLearning into a Blended Learning scenario. We successfully implemented a curricular teaching course in Clinical Pharmacology and Therapeutics focusing on searching and handling of reliable pharmacological databases and websites. Web-based training provides an opportunity to enhance the students' ability to initiate, monitor, and modify pharmacotherapy in an appropriate and state-of-the-art fashion for a specific patient. The Blended Learning-design offers the advantage of concentrating on practical skills training under teacher guidance during the time of the mandatory course.

174

### Elastase controls atherosclerotic plaque stability by activation of the unfolded protein response

Grechowa, Irina<sup>1</sup>; Wallrath, Anja<sup>2</sup>; Wilgenbus, Petra<sup>1</sup>; Dorweiler, Bernhard<sup>2</sup>; Horke, Sven<sup>1</sup>

<sup>1</sup>Universitätsmedizin Mainz, Institut für Pharmakologie, Germany

<sup>2</sup>Universitätsmedizin Mainz, Klinik und Poliklinik für Herz-, Thorax- und Gefäßchirurgie, Germany

Atherosclerosis is the primary process that leads to cardiovascular diseases, the major cause of death in industrialized societies. During atherosclerosis, activation of the endoplasmic reticulum (ER) stress pathway known as the unfolded protein response (UPR) is observed. This pathway critically determines plaque stability. Moreover, the serine protease elastase plays an important role as it induces death of endothelial cells (ECs) and smooth muscle cells (SMCs), but also breaks down the fibrous cap of atherosclerotic plaques. Rupture and erosion of plaques are the most abundant causes for atherothrombosis, myocardial infarction, unstable angina and stroke. Increased concentrations of elastase were found in patients with symptomatic stenosis. It has been proposed that elastase signals via the protease-activated receptor-1 (PAR-1) and mounts a Ca<sup>2+</sup>-increase. Both events may induce the UPR pathway and cell death, but this has not been demonstrated. Therefore, a detailed understanding of underlying elastase/PAR-1 signaling pathways may have the potential to develop novel therapeutic anti-atherogenic options, a regimen currently tested in clinical trials. In this work we present immunohistochemical analyses of formalin-fixed and paraffin-embedded tissue sections of A. carotis intima plaques of patients with symptomatic stenosis. These were stained with markers for cellular inflammation (macrophages, granulocytes) and UPR activation / cell death (TUNEL, KDEL, CHAC1, cleaved Caspase3, ATF3, CHOP). Indeed we found an increased infiltration of pro-inflammatory cells and a highly significant induction of UPR markers. Furthermore, double-staining co-localization analyses demonstrated active UPR in ECs, macrophages and SMCs. Further, elastase-treated endothelial cells underwent an apoptotic cell death, while necrosis, necroptosis or autophagy played only minor roles. This process appeared to be dependent on PAR-1 and it involved the UPR, as we found GRP78, p-eIF2 $\alpha$ , sXBP1 and CHOP signaling. Thus, our data suggest that elastase plays a significant role in plaque stability and EC survival via activation of the ER stress pathway that leads to subsequent EC death. This likely represents the molecular link between elastase/PAR-1 and atherosclerosis.

175

### The methyleugenol metabolite 3'-oxomethylisoeugenol acts as catalytic topoisomerase I inhibitor in human colon carcinoma cells

Groh, Isabel Anna Maria<sup>1</sup>; Schröter, Anika<sup>2</sup>; Marko, Doris<sup>2</sup>; Esselen, Melanie<sup>1</sup>

<sup>1</sup>Technische Universität Kaiserslautern, Fachbereich Chemie Fachrichtung Lebensmittelchemie und Toxikologie, Germany

<sup>2</sup>Universität Wien, Institut für Lebensmittelchemie und Toxikologie, Austria

Methyleugenol is a natural alkenylbenzene which is found in several herbs and spices. As essential oil extracts methyleugenol is used as a flavouring food agent and as a fragrance in cosmetics [Gardner *et al.*, 1997]. We have previously reported that methyleugenol and selected oxidative metabolites exhibited a genotoxic potential *in vitro* [Groh *et al.*, 2012]. In the present study, we addressed the question whether topoisomerase inhibition contribute to the observed DNA-damaging properties of the respective test compounds. Methyleugenol and 1'-hydroxymethyleugenol did not affect topoisomerase I (relaxation assay) and topoisomerase II (decatenation assay) activity, respectively. Methyleugenol-2',3'-epoxide decreased topoisomerase I activity at the highest tested concentration of 200  $\mu$ M. The catalytic activity of topoisomerase I was completely suppressed by 3'-oxomethylisoeugenol (3'-OXO-MiE) at concentrations  $\geq$  0.1  $\mu$ M. Furthermore, we showed that both metabolites exhibited topoisomerase inhibiting properties in the cell-free system and they did not stabilize the DNA-topoisomerase I intermediate in the human colon carcinoma cell line HT29. In the comet assay a significant decrease of the DNA-strand breaking effects of the topoisomerase I poison camptothecin (100  $\mu$ M) by pre- and co-incubation with 3'-OXO-MiE ( $>$  10  $\mu$ M) for 1.5 h was observed. After a prolonged incubation time of 24 h DNA-damaging properties of 3'-OXO-MiE itself gained increasing importance. However, pre- and co-incubation with 3'-OXO-MiE (100  $\mu$ M) significantly suppressed the camptothecin-induced DNA / topoisomerase I complex formation in HT29 cells. In conclusion, a selected methyleugenol metabolite was found to act as catalytic topoisomerase I inhibitor *in vitro*, inhibiting DNA-strand breaks and suppressing the cleavable complex formation induced by the classical topoisomerase poison camptothecin.

I. Gardner, H. Wakazono, P. Bergin, I. de Waziers, P. Beaune, J.G. Kenna and J.Caldwell "Cytochrome P450 mediated bioactivation of methyleugenol to 1'-hydroxymethyleugenol in Fischer 344 rat and human liver microsomes", *Carcinogenesis*, 1997, Vol. 18, 1775-1783

IAM Groh, A.T. Cartus, S. Vallicotti, J. Kajzar, K.H. Merz, D. Schrenk, M.Esselen, "Genotoxic potential of methyleugenol and selected methyleugenol metabolites in cultured Chinese hamster V79 cells", *Food and Function*, 2012

176

### Regulation of *Cyp2e1* transcription by beta-catenin and hepatocyte nuclear factor 1 alpha

Groll, Nicola<sup>1</sup>; Petrikat, Tamara<sup>2</sup>; Colnot, Sabine<sup>3</sup>; Rothbauer, Ulrich<sup>1</sup>; Göpfert, Jens<sup>1</sup>; Braeuning, Albert<sup>2</sup>

<sup>1</sup>NMI, Reutlingen, Germany

<sup>2</sup>Universität Tübingen, Toxikologie, Germany

<sup>3</sup>Institut Cochin, Paris, France

The liver is the main organ for xenobiotic metabolism. Under normal conditions, hepatocytes near the efferent central veins of the liver lobules express the highest levels of most drug-metabolizing enzymes. In contrast to many other drug-metabolizing enzymes, which can be transcriptionally activated by different ligand-activated transcription factors, cytochrome P450 (CYP) 2E1 is mainly regulated by post-transcriptional stabilization upon substrate binding. Less is known about the transcription of the *Cyp2e1* gene, which is thought to be rather constitutive and involves hepatocyte nuclear factor (HNF) 1 alpha.

We show that the expression of *Cyp2e1* is up-regulated in mouse liver tumors with activated beta-catenin and in hepatocytes with transgenic expression of mutant, constitutively active beta-catenin<sup>S33Y</sup>, whereas it is absent from beta-catenin knockout hepatocytes. Activation of beta-catenin in primary hepatocytes induces *Cyp2e1* mRNA expression *in vitro*.

Analysis of the murine *Cyp2e1* promoter via chromatin immunoprecipitation reveals a highly conserved beta-catenin/T-cell factor (TCF) binding site in the upstream promoter region, close to the known conserved HNF1a binding motif. Different *Cyp2e1* promoter-driven luciferase reporter vectors were generated and employed to test the functionality of the TCF site and its interaction with HNF1a *in vitro*. Site-directed mutagenesis experiments show that the HNF1a binding site is involved in the regulation of *Cyp2e1* by beta-catenin. Additional experiments were conducted to analyze possible protein-protein interactions of beta-catenin and HNF1a.

In conclusion, we show that *Cyp2e1* is a direct target of the Wnt/beta-catenin signaling pathway and is coordinately regulated by beta-catenin and HNF1a.

177

### Dermal absorption studies *in vitro* and their influencing parameters

Fabian, Eric; Guth, Katharina; Wölk, Samuel; van Ravenzwaay, Bernard; Landsiedel, Robert

BASF SE, Experimental Toxicology and Ecology, Ludwigshafen, Germany

Skin absorption is an *in vitro* method described in OECD guideline 428 and the technical guidance GD 28. Since the study design and experimental parameters can be varied, we performed systematic investigations under defined experimental conditions to understand influencing parameters and develop an optimized testing protocol for dermal absorption studies *in vitro*.

Investigations of dermal absorption were performed with skin preparations of rats, pigs and humans in Franz like diffusion cells. Investigated integrity tests of these preparations were trans-epidermal electrical impedance (TEER), trans-epidermal water loss (TEWL), trans-epidermal tritiated water flux (<sup>3</sup>H<sub>2</sub>O) and absorption and flux of a <sup>3</sup>H-labeled internal standard (ISTD). Experiments were performed to address the following parameters: *ex vivo* skin preparations (gender, age, localization, preparation), reconstructed skin models, storage and freezing-cycles, static versus flow through, concentration of test compounds, donor vehicle and receptor fluids. We used different model compounds, e.g. testosterone or caffeine which could be analyzed by liquid scintillation counting, HPLC or photometry. Absorbed doses (%), absorption rates and permeability constants (Kp) were calculated.

Although TEER, TEWL and <sup>3</sup>H<sub>2</sub>O allowed the identification of invalid skin preparations in principle, ISTD was the only continuously differentiable integrity parameter correlated to the absorptions of test compounds. Variations in skin preparation and testing in static or in flow-through systems had minor influence on Kp. Main impacts on Kp were observed for thickness of SC, donor vehicle and receptor fluid, test substance concentrations as well as *ex vivo* vs. reconstructed skin preparations. In our experiments the barrier function of reconstructed skin was inappropriate for absorption testing. Since the test substance, its concentration and donor vehicle are reflected by the applied formulated product these parameters have to parallel the real exposure scenario and will intentionally predetermine the study results.

178

### Multi-Label-Classification to predict repeated dose toxicity in the context of REACH

Batke, Monika<sup>1</sup>; Bitsch, Annette<sup>1</sup>; Gundert-Remy, Ursula<sup>2</sup>; Gütlein, Martin<sup>3</sup>; Helma, Christoph<sup>4</sup>; Kramer, Stefan<sup>5</sup>; Maunz, Andreas<sup>6</sup>; Partosch, Falko<sup>2</sup>; Seeland, Madeleine<sup>7</sup>; Stahlmann, Ralf<sup>8</sup>

<sup>1</sup>Fraunhofer Institut für Toxikologie und Experimentelle Medizin, Chemikalienbewertung, Hannover, Germany

<sup>2</sup>Charité - Universitätsmedizin Berlin, Institut für Klinische Pharmakologie und Toxikologie, Germany

<sup>3</sup>Albert-Ludwigs-Universität Freiburg, Institut für Physik, Zentrum für Biosystemanalyse, Germany

<sup>4</sup>in silico toxicology gmbh, Basel, Switzerland

<sup>5</sup>Johannes Gutenberg - Universität Mainz, Institut für Informatik, Germany

<sup>6</sup>Oncotest GmbH, Freiburg, Germany

<sup>7</sup>Technische Universität München, Institut für Informatik, Garching, Germany

Repeated dose toxicity is a very complex toxicological endpoint and several attempts have been made to get an acceptable prediction of this endpoint to fill data gaps in the REACH dossiers without using too many animal studies. In the present project, we do apply Multi-Label-Classification (MLC) to simultaneously predict multiple toxic effects of chemical compounds. The final, validated MLC models are well documented and published as freely accessible prediction web service.

The predicted target values are based on toxicity endpoints from over 2000 repeated dose toxicity studies in rats with sub-acute or sub-chronic duration and oral or inhalation application. The data basis was joined from publicly available repeated dose toxicity data of industrial chemicals (RepDose data base), and confidential toxicity data of the European List of Notified Chemical Substances (ELINCS) data base. Although this data set with 1022 compounds and 28 endpoints is very comprehensive and detailed from a toxicological point of view it is extremely sparse for statistical analysis: 82% of the experimentally derived endpoint values are missing as the endpoint was either not considered in the particular study, or there was no measurable effect in all investigated dose groups.

We have discretized the numeric endpoint values to the binary class values 'active' and 'inactive'. Thus, the LOEL values have been clustered, while taking the study duration into account.

We calculated physico-chemical descriptors and structural fragments as input features for the prediction models. The structural fragments have been computed by matching the dataset compounds with established, pre-defined lists of SMARTS (SMiles ARbitrary Target Specification) patterns.

We evaluated various MLC algorithms with a 10-times repeated 10-fold cross-validation. The selected MLC technique 'Ensemble of Classifier Chains' (ECC) exploits correlations between endpoints by repeatedly building chains of multiple classifiers in randomized orders. The overall predictive performance of this method is 68% Area-under-ROC (AUC) (63% sensitivity, 61% selectivity). We compared the ECC approach with 'Predictive Clustering Trees' (PCT) which is an alternative MLC method; PCT which is slightly less predictive, but is applied within this project to create categories. This project is part of a BMBF project 'Strategies to develop chemical categories in the context of REACH'.

179

### How do "digital natives" learn pharmacology? A mixed-methods study on the use of learning media by undergraduate medical students.

Gutmann, Joanna<sup>1</sup>; Kühbeck, Felizian<sup>2</sup>; Berberat, Pascal<sup>2</sup>; Fischer, Martin<sup>3</sup>; Engelhardt, Stefan<sup>1</sup>; Sarikas, Antonio<sup>1</sup>

<sup>1</sup>Technische Universität München, Institute of Pharmacology and Toxicology, Munich, Germany

<sup>2</sup>Technische Universität München, Medizinisches Zentrum für Ausbildungsforschung und Lehre, Germany

<sup>3</sup>Ludwig-Maximilians-Universität, Lehrstuhl für Didaktik und Ausbildungsforschung in der Medizin, München, Germany

**Background:** The current generation of undergraduate medical students has grown up in an environment in which the internet and computer-based technologies are an integral part of life ("Digital Natives", Prensky, 2001). While it is widely acknowledged that this generation is more technologically savvy than their predecessors, it remains to be investigated if their use of learning media is fundamentally different.

**Objectives:** To analyze the use and acceptance of learning media by undergraduate medical students in pharmacology.

**Methods:** A mixed-methods study consisting of quantitative (online surveys) and qualitative (semi-structured interviews) methods was conducted during a 5 week pharmacology course (26 days of lectures and seminars, followed by 10 days of self-study) with undergraduate medical students at Technische Universität München. Daily online surveys were conducted to solicit the 3 most frequently used learning media of the previous day from a list of 10 different items (textbooks > 300 pages, textbooks < 300 pages, lecture slides, smartphone apps, internet search, e-learning cases, podcasts, e-books, written notes, exam questions).

**Results:** 258 of 372 students (69%) participated in the online survey with a daily average of 73 (SD: 26). The most used learning media were lecture slides (27%), smartphone apps (22%) followed by written notes (15%), textbooks > 300 pages (10%), e-learning cases (8%) and internet search (8%). The numbers indicate the proportion of each learning medium in percent in relation to all learning media on the list. The use of digital media was markedly higher than printed media (77% vs. 23%). Media use throughout the course did not vary significantly, with exception of textbooks (> 300 p) that were predominately used in the teaching period ( $p=0,034$ ,  $\phi=0,26$ ; Wilcoxon/Bonferroni test). Interviews revealed that textbooks were preferred for primary learning due to their systematic and comprehensive presentation of data, while digital media (in particular smartphone apps) were valued for easy accessibility, spatial and temporal flexibility and stringent presentation of data.

**Summary and Conclusions:** This study is the first "real-time" longitudinal analysis on the use and acceptance of learning media by undergraduate students in pharmacology. Both quantitative and qualitative data revealed a high acceptance and use of digital learning media, in particular smartphone apps.

### BrdU screening – Short-time test for reliable prediction of carcinogenicity for MWCNT

**Hackbarth, Ania**<sup>1</sup>; Schaudien, Dirk<sup>2</sup>; Bellmann, Bernd †<sup>1</sup>; Ernst, Heinrich<sup>2</sup>; Leonhardt, Albrecht<sup>3</sup>; Steinberg, Pablo<sup>4</sup>; Rittinghausen, Susanne<sup>2</sup>

<sup>1</sup>Fraunhofer, ITEM, Inhalationstoxikologie, Hannover, Germany

<sup>2</sup>Fraunhofer, ITEM, Pathologie, Hannover, Germany

<sup>3</sup>Leibniz-Institut für Festkörper und Werkstofforschung, Institut für Festkörperchemie, Dresden, Germany

<sup>4</sup>Tierärztliche Hochschule, Lebensmitteltoxikologie, Hannover, Germany

Since the discovery of the excellent features of MWCNT, there is an increase of their potential application. Despite that, they are discussed to have a toxic potential depending on their length and fiber-like shape. For this reason, potential adverse biological effects of MWCNT are investigated in vivo (rat) in a project funded by the German BMBF (contract No. 03X0109A).

Tailor-made MWCNT with different lengths and diameters were produced and suspended in artificial lung medium using ultrasonic treatment. The MWCNT were injected once intraperitoneally (i.p.) in rats in two dose groups (low: 1 x 10<sup>9</sup> WHO fibers; high: 5 x 10<sup>9</sup> WHO fibers) in a BrdU screening test (MWCNT 1, 2, 3) and a carcinogenicity study (MWCNT 1, 2, 3, 3a). Long amosite asbestos (0.1 x 10<sup>9</sup> WHO fibers) served as positive control, ground MWCNT and Printex 90 (5 mg/rat) as negative controls. Suspension and length / diameter distribution were measured in SEM.

Proliferation of cells in the diaphragmatic peritoneum was investigated in a short-time screening test 3, 6 and 12 months after i.p. injection of fibers in rats, using the BrdU method and measurement of peritoneal thickness. Furthermore, in a carcinogenicity study, animal mortality and tumor development were monitored over two years.

The BrdU screening test exhibited a time-independent significant increase in cell proliferation after injection of MWCNT 1<sub>(high)</sub> (L = 7.9 µm; D = 0.037 µm), MWCNT 2<sub>(low/high)</sub> (L = 10.24 µm; D = 0.04 µm), and MWCNT 3<sub>(low/high)</sub> (L = 8.57 µm; D = 0.085 µm) as well as after the exposure to long amosite asbestos (L = 13.95 µm; D = 0.39 µm). MWCNT 2<sub>(high)</sub> and 3<sub>(low/high)</sub> induce significant dose-dependent thickening of the peritoneum after i.p. injection, independent of time (3 and 6 months). The screening test after 12 months could not be statistically evaluated because of high mortality (sacrificed moribund) in MWCNT treated groups.

The carcinogenicity study shows a high dose independent mortality in MWCNT 3 treated groups after 8 months. MWCNT 2 and 3a show a high dose dependent mortality. By evaluating the tumor development, MWCNT 2, 3 and 3a (L = 9.3 µm; D = 0.062 µm) exhibit a higher mesothelioma incidence than MWCNT 1.

In conclusion, some MWCNT (MWCNT 2, 3) mediate enhanced proliferation of peritoneal cells in the diaphragm in rats which correlates well with the result in mesothelioma development.

### Neuronal stem cell factor SOX11 is a target of the tandem miRNAs miR-212 and miR-132. Results from a genome-wide miRNA screen in focal and non-focal brain tissue of therapy-resistant epilepsy patients.

**Haensch, Sierk**<sup>1,2</sup>; Zhao, Yi<sup>3</sup>; Chhibber, Aparna<sup>2</sup>; Cascorbi, Ingolf<sup>1</sup>; Kroetz, Deanna L.<sup>2</sup>

<sup>1</sup>University Hospital Schleswig-Holstein, Campus Kiel, Institute of Experimental and Clinical Pharmacology, Germany

<sup>2</sup>University of California, San Francisco, USA, School of Pharmacy, Department of Bioengineering and Therapeutic Sciences, San Francisco, CA, United States

<sup>3</sup>University Hospital Schleswig-Holstein, Campus Kiel, Department of Nuclear Medicine, Molecular Image, Diagnostics and Therapy, Germany

**Introduction:** Epilepsy is a common chronic neurological disorder characterized by spontaneous recurrent seizures. Seizure-induced neural reorganization and molecular alterations may lead to neuronal networks with increased excitability. There is increasing evidence that expression of microRNAs (miRNAs) is deregulated in neuronal disorders. We hypothesize that an altered miRNA-mediated regulation of target genes predisposes to generate recurrent epileptic seizures.

**Patients and Methods:** Hippocampal focal and cortical non-focal brain tissue samples from 13 patients diagnosed with MTS (mesial temporal sclerosis) who underwent neurosurgery have been screened for miRNA expression using TaqMan<sup>®</sup> arrays. To compare miRNA expression between brain regions a Mann-Whitney-U test was performed using R. In silico approaches were used to filter for potential phenotype-relevant target genes. After cloning 3'-UTR sequences containing predicted miRNA binding sites into psiCHECK2 or pmirGLO vectors and performing site-directed mutagenesis reporter gene assays were conducted to confirm RNA interference of selected candidate miRNAs with their respective target genes. For further functional elucidation target gene and candidate miRNA expression was time-dependently monitored in differentiating cortical neurons obtained from neonatal rats under cell culture conditions and after transfection of antagonists.

**Results:** Out of 754 miRNAs, 201 were detected in both tissue types. Among other miRNA miR-212-3p was differently expressed in the hippocampus relative to the cortex (3.8-fold lower, p=0.0001, q=0.01). Interestingly, miR-212-3p shares the same primary transcript and the same seed sequence with miR-132-3p (1.4-fold lower, p=n.s.) (tandem miRNAs). Bioinformatic analysis and filtering for target genes identified five genes important for neuronal regulation, signal transmission and drug efflux. Reporter gene experiments confirmed four target genes post-transcriptionally regulated by miR-212-3p (ABCG2, SOX11, ADCY1 and MECP2). Additionally, in differentiating cortical neurons an inverse time-dependent expression of Sox11 and miR-212-3p/miR-132-3p could be shown. Reporter gene assays with mutated SOX11-3'-UTR vector constructs revealed two binding sites for miR-212-3p and miR-132-3p. Moreover, in order to disrupt the miRNA-controlled Sox11 expression both miRNAs had to be antagonized.

**Conclusion:** Differential miRNA regulation could contribute to an altered function of several genes resulting in impaired neural differentiation, imbalanced neuronal excitability and accelerated drug export. This work was supported by a fellowship from DFG (Ha 6112/1-1) and NIH grant GM61390.

### Induction of ABCG2 secretory activity in the mammary gland of dairy animals by arylhydrocarbon receptor (AhR)-activating dioxins and pesticides

**Halwachs, Sandra**; Waßermann, Louise; Honscha, Walther

Universität Leipzig, Institute of Pharmacology, Pharmacy and Toxicology, Germany

Our recent studies showed that dioxin and the pesticide prochloraz induced ABCG2 activity in primary bovine mammary epithelial cells. The efflux transporter ABCG2 represents the main route for active secretion of drugs and toxins into human and dairy milk. Thus, ABCG2 regulation by AhR-activating environmental contaminants is of great toxicological relevance. However, there is so far no detailed information on AhR-dependent ABCG2 regulation in dairy animals. We therefore investigated the effect of various pollutants on ABCG2 efflux activity in MDCKII cells stably expressing mammary ABCG2 from dairy cows (bABCG2) or goats (cABCG2). Generally, cells were incubated with selected environmental contaminants for 12, 24, 48, 72 or 96 h. AhR activity in MDCKII cells was assessed using the 7-ethoxyresorufin-O-deethylase (EROD) assay. We determined functional ABCG2 efflux activity in MDCKII-bABCG2 and -cABCG2 cells by the H33342 accumulation assays or transepithelial flux studies using 2-Amino-1-methyl-6-phenylimidazo[4,5-b]pyridine (PhIP). Chosen chemical concentrations corresponded to the 1- or 10-fold maximum residue levels in edible ruminant tissues. Mammary ABCG2 mRNA levels were detected by quantitative RT-PCR and bABCG2 promoter activity was determined by reporter assays.

The AhR-activating contaminants TCDD, Aroclor 1254, prochloraz (PZ) or iprodione caused a dose- and time-dependent induction of AhR in MDCKII-bABCG2 and -cABCG2 cells. Moreover, TCDD and PZ significantly induced ABCG2 activity. Specificity of ABCG2 activity was shown by the ABCG2 inhibitor Ko143. Furthermore, the AhR antagonists salicylamide and CH 223191 blocked TCDD- or PZ-induced ABCG2 activity. Further mechanistic studies indicated that stimulation of ABCG2 activity by both contaminants is due to binding of the activated AhR to DRE motifs in the 5'-untranslated region of bABCG2 and cABCG2. This finally resulted in a dose- and time-dependent up-regulation of bABCG2 and cABCG2 gene expression. The non-AhR inducers PCB 101 and pesticide tolclofos-methyl caused no alteration in AhR or ABCG2 activity and transporter mRNA levels. Altogether, our results showed AhR-dependent transcriptional up-regulation of bovine and caprine mammary ABCG2 secretory activity by AhR-activating dioxins and pesticides. Thus, our results suggested that animal exposure with these environmental contaminants may increase the risk of potential harmful residues of ABCG2 substrates in dairy milk.

### Role of binucleated hepatocytes in hepatotoxicity and liver regeneration

**Hamad, Seddik**<sup>1,2</sup>; Friebe, Adrian<sup>3</sup>; Begher-Tibbe, Brigitte<sup>1</sup>; Othman, Amnah<sup>1</sup>; Vartak, Amruta<sup>1</sup>; Hoehme, Stefan<sup>3</sup>; Edlund, Karolina<sup>1</sup>; Vonrecklinghausen, Inis<sup>1</sup>; Drasdo, Dirk<sup>3,4</sup>; Hengstler, Jan G.<sup>1</sup>

<sup>1</sup>Leibniz Research Centre for Working Environment and Human Factors (IfADo) at Dortmund TU, Systems Toxicology, Germany

<sup>2</sup>Faculty of Veterinary Medicine, South Valley University-Qena, Department of Forensic Medicine and Veterinary Toxicology, Egypt

<sup>3</sup>Interdisciplinary Centre for Bioinformatics (IZBI), University of Leipzig, Multicellular Systems Biology, Germany

<sup>4</sup>Institut National de Recherche en Informatique et en Automatique (INRIA), Rocquencourt/Paris, France

The adult liver consists of mono- and binucleated hepatocytes. Binucleated hepatocytes are formed postnatally by nuclear division without subsequent cytokinesis. The role of binucleated hepatocytes in hepatotoxicity and liver regeneration is still not fully understood. To bridge this gap we studied their role in mice after intoxication with hepatotoxic compounds and in cultivated hepatocytes. Liver toxicity and regeneration were induced in adult male C57BL6/N or J mice by a single injection or repetitive intraperitoneal injections of carbon tetrachloride, respectively. Then livers were harvested 60 minutes after BrdU administration at 2 and 16 days after intoxication. Vibratome liver slices (100 µm thick) were co-stained with antibodies to visualize bile canalicular and sinusoidal networks, the pericentral hepatocytes as well as cell nuclei. Both semi-manual (IMARIS) and fully-automated (CellSys7) techniques were used to quantify the liver micro-architecture and hepatocyte nuclei in 3D slices. Quantification of binucleated hepatocytes revealed that approximately 40 % of the hepatocytes are binucleated. The remaining fractions were distributed between mononucleated (60%), trinucleated (5%) and tetranucleated (less than 1%) hepatocytes. However, during and after intoxication and regeneration this profile was completely shifted towards more mononucleated hepatocytes. The quantification of hepatocytes in S-phase (revealed by BrdU incorporation and Ki67 immunostaining) indicated that more binucleated hepatocytes entered the cell cycle during acute and chronic liver damage. Moreover, time-lapse microscopy analysis of cultivated mouse hepatocytes revealed that preferentially binucleated hepatocytes divide after stimulation with hepatocyte growth factor. Eighty percent of all analyzed dividing hepatocytes were binucleated. All binucleated hepatocytes formed two mononucleated cells after division. Interestingly, binucleated hepatocytes represented the preferentially dividing cells also after further

types of liver damage, such as partial hepatectomy, CCl<sub>4</sub>-induced fibrosis and MDR2 knockout fibrosis. In conclusion, binucleated hepatocytes represent the major dividing cell type in the regenerating liver.

Godoy P, Hewitt NJ, Albrecht U et al., (2013) Recent advances in 2D and 3D *in vitro* systems using primary hepatocytes, alternative hepatocyte sources and non-parenchymal liver cells and their use in investigating mechanisms of hepatotoxicity, cell signaling and ADME. *Arch Toxicol* 87:1315-1530.

Hoehme S, Brulport M, Bauer A, Bedawy E, Schormann W, Hermes M, Puppe V, Gebhardt R, Zellmer S, Schwarz M, Bockamp E, Timmel T, Hengstler JG, Drasdo D. Prediction and validation of cell alignment along microvessels as order principle to restore tissue architecture in liver regeneration. *Proc Natl Acad Sci USA*. 2010 Jun 8;107(23):10371-10376.

Zellmer S, Schmidt-Heck W, Godoy P, Weng H, Meyer C, Lehmann T, Sparna T, Schormann W, Hammad S, Kreuz C, Timmer J, von Weizsäcker F, Thürmann PA, Merfort I, Guthke R, Dooley S, Hengstler JG, Gebhardt R. Transcription factors ETF, E2F, and SP-1 are involved in cytokine-independent proliferation of murine hepatocytes. *Hepatology*. 2010 Dec;52(6):2127-2136.

Hammad S. (2012). Modelling of the bile canalicular network during liver regeneration and fibrosis after carbon tetrachloride intoxication. Doctoral thesis. Giessen University, Giessen – Germany.

Braeuning A, Singh Y, Rignall B, Buchmann A, Hammad S, Othman A, von Recklinghausen I, Godoy P, Hoehme S, Drasdo D, Hengstler JG, Schwarz M. Phenotype and growth behavior of residual  $\beta$ -catenin-positive hepatocytes in livers of  $\beta$ -catenin-deficient mice. *Histochem Cell Biol*. 2010 Nov;134(5):469-481.

## 184

### Quantification of transporters in the liver via Ms- based immunoassays

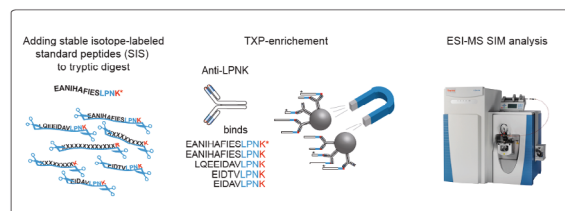
**Hammer, Helen S.**; van Den Berg, Bart H. J.; Weiß, Frederik; Planatscher, Hannes; Joos, Thomas O.; Pötz, Oliver  
Naturwissenschaftliches und medizinisches Institut an der Universität Tübingen, Biochemie, Reutlingen, Germany

Liver transporters are an important component of the xenobiotics metabolism. They transport endo- and exogene substances from blood into hepatocytes and vice versa. The substances are activated by phase I enzymes and conjugated to hydrophilic molecules by phase II enzymes. Subsequently conjugates are exported either into bile canaliculi or back into the blood by additional transporters (phase III) to be secreted via bile or urine. Transporter expression levels and activity influence the velocity of the metabolism and the efficiency of the first pass effect. These transporters are also essential to maintain barriers in several organs (blood-brain-barriers, placenta-barrier...). Additionally, overexpression of export transporters leads to multiple drug resistance in tumors. Therefore, transporters activity and expression levels are relevant for many pharmacological and toxicological questions. However, transporters cannot be detected by conventional bioanalytical methods such as sandwich immunoassays because they are hydrophobic multi-transmembrane proteins. For this reason, we develop a test system to quantify the expression level of transporters via mass spectrometry-based immunoassays.

Hydrophobic proteins are measurable by this method because denatured samples are digested with trypsin and analyzed on peptide level. From each protein, one peptide which can be assigned unambiguously, is identified via tandem MS and quantified by means of an isotope labeled reference. Prior to MS-read-out the peptides are enriched by antibodies which recognize a very short c-terminal epitope. These epitopes are selected in such way that they are common in peptides derived from several transporters and therefore allow the analysis of transporter groups with few antibodies. Currently, we have generated 29 antibodies covering 23 ABC and SLC transporters in eight different species - in total 108 proteins.

The established assay is used to analyze *in vitro* induction studies. These results will be correlated with pharmacokinetic studies of transporters in different cell lines such as CaCo2 and HepaRG. The major advantage of this method is that samples from different model organisms can be analyzed with the same assay which enhances the comparability of experiments. The established assays are tested in mice and rats first. Therefore, the transporter concentrations in different tissues are determined and compared to literature.

- Eisen D, Planatscher H, Hardie DB, Kraushaar U, Pynn CJ, Stoll D, Borchers C, Joos TO, and Poetz O. 2013. G protein-coupled receptor quantification using peptide group-specific enrichment combined with internal peptide standard reporter calibration. *Journal of proteomics*.
- Gottesman MM, Fojo T, and Bates SE. 2002. Multidrug resistance in cancer: role of ATP-dependent transporters. *Nature reviews. Cancer* 2(1):48–58.
- Hoeppe S, Schreiber TD, Planatscher H, Zell A, Templin MF, Stoll D, Joos TO, and Poetz O. 2011. Targeting peptide termini, a novel immunoaffinity approach to reduce complexity in mass spectrometric protein identification. *Molecular & cellular proteomics : MCP* 10(2):M110.002857.



### Triple X Proteomics (TXP):

Explanation of the TXP work flow using the example of MDR1

## 185

### Role of A-kinase anchoring proteins in airway smooth muscle phenotype modulation

**Han, Bing**; Poppinga, Wilfred Jelco; Driessen, Saskia; Maarsingh, Harm; Schmidt, Martina

University of Groningen, Department of Molecular Pharmacology, Netherlands

Airway remodeling is a main feature of asthma and is characterized by increased airway smooth muscle (ASM) mass, the latter known to contribute to airway hyperresponsiveness and lung function decrease. The platelet-derived growth factor (PDGF) is believed to enhance ASM proliferation and thereby airway remodeling. We reported earlier that cAMP inhibits PDGF-induced ASM phenotype modulation through its effectors exchange protein directly activated by cAMP (Epac) and protein kinase A (PKA). Interestingly, A-kinase anchoring proteins (AKAPs) coordinate the communication between cAMP and its effectors via compartmentalization. Here we studied the role of AKAP-PKA interactions in PDGF-induced ASM phenotype modulation using the AKAP-PKA complex inhibitor peptide st-Ht31. Treatment with st-Ht31 increased basal DNA synthesis measured by [<sup>3</sup>H]-thymidine incorporation, but did not further enhance PDGF-induced DNA synthesis. St-Ht31 also increased the expression of the cell cycle regulator cyclinD1 and the phosphorylation of retinoblastoma protein under basal conditions but not under the PDGF conditions. In accordance, st-Ht31 lowered  $\alpha$ -SMA gene expression under basal conditions, again leaving PDGF-induced  $\alpha$ -SMA gene expression unchanged. Cell cycle studies using FACS analysis showed that st-Ht31 stimulated G1-G2 progression of ASM cells. In conclusion, AKAP-PKA interactions play an important role in regulation of ASM proliferation by compartmentalizing cAMP signaling.

## 186

### Role of bicarbonate and soluble adenylyl cyclase in the regulation of nucleoside 3',5'-cyclic monophosphates

**Hasan, Alan**; Wolter, Sabine; Seifert, Roland

Medizinische Hochschule Hannover, Institut für Pharmakologie, Germany

The cyclic purine nucleotides adenosine 3',5'-cyclic monophosphate (cAMP) and guanosine 3',5'-cyclic monophosphate (cGMP) are established second messengers, involved in the regulation of many physiological processes. They are generated by nucleotidyl cyclases and degraded by phosphodiesterases. For cAMP generation, nine membrane adenylyl cyclases (mAC 1-9) and a soluble adenylyl cyclase (sAC) have been described.<sup>1,2</sup> sAC plays a very important role in male fertility, secretory processes and mitochondrial function. sAC is expressed, amongst others, in brain and kidney and has also been detected in HEK293 cells and other cell lines.<sup>2,3</sup> The main aim of this project was to analyze the substrate specificity of sAC specifically with regard to cytidine 3',5'-cyclic monophosphate (cCMP) and uridine 3',5'-cyclic monophosphate (cUMP) formation. The influence of bicarbonate, a known sAC stimulator and KH7, a selective inhibitor of sAC,<sup>4</sup> on basal nucleoside 3',5'-cyclic monophosphate (cNMP) concentrations in HEK293 and rat neuroblastoma cells (B103) were analyzed. A recombinant sAC (-His tagged) was investigated *in vitro*. Concentrations of the cNMPs were measured by a highly sensitive and specific HPLC-MS/MS technique. cNMPs were found basally in HEK293 and B103 cells cultured in DMEM medium in the order cAMP > cUMP > cCMP > cGMP. cNMP concentrations decreased under "resting medium" (MCDB 153 Medium, Sigma; main difference compared to DMEM is the lower bicarbonate concentration), for cUMP, cCMP and cGMP even below the detection limit. Bicarbonate (40 mM) increased the concentration of cNMPs under resting medium in HEK293 cells; cAMP 7-fold compared to the level under resting medium; cCMP, cUMP, cGMP from no detection to concentrations even higher than the basal concentrations under DMEM. A similar picture was seen in B103 cells. The increased cNMP concentrations induced by bicarbonate in HEK293 cells were concentration-dependently inhibited by KH7. In B103 cells the mAC activator forskolin had no influence on cNMP concentrations except on cAMP. These findings lead us to conclude that sAC but not mACs possesses a broader substrate specificity than assumed. If future studies reveal a specific function of cUMP and cCMP, we will have here a possible pharmacological intervention spot.

[1] Sunahara R.K., Taussig R., *Mol. Interv.* 2: 168 – 84, 2002.

[2] Tresguerres M. et al., *Kidney Int.* 79: 1277 – 1288, 2011.

[3] Geng W. et al., *Am J Physiol.* 288: C1305 – C1316, 2005.

[4] Bitterman J.L. et al., *J Pharmacol Exp Ther.* 347: 589 – 98, 2013.

## 187

### Effects of Sulfonylureas on Adipocytes

**Hass, Moritz**; Frieling, Constanze; Mayer, Peter; Haas, Bodo  
BfArM, Bonn, Germany

Glitazones or insulin sensitizers are anti-diabetic drugs mediating their effects via activation of the transcription factor peroxisome proliferator-activated receptor  $\gamma$  (PPAR $\gamma$ ), which plays a key role in adipocyte differentiation. The anti-diabetic effects of glitazones appear in part to be mediated by inhibition of cyclin-dependent kinase 5 (CDK5)-mediated phosphorylation of PPAR $\gamma$  at Ser273<sup>1,3</sup> in adipocytes resulting in a positive anti-diabetic expression profile. Cytokines (adipokines) such as tumor necrosis

factor  $\alpha$  (TNF $\alpha$ ) have been shown to induce PPAR $\gamma$  Ser273 phosphorylation, thereby increasing the expression of pro-diabetic adipokines like monocyte chemoattractant protein-1 (MCP-1). We have previously demonstrated that sulfonylureas (SU) like glibenclamide and glimepiride, which are thought to mediate their anti-diabetic effects via glucose-independent insulin liberation from pancreatic  $\beta$ -cells, have an influence on PPAR $\gamma$  and the expression of adipokines in primary human adipocytes<sup>2</sup>, however, the exact mechanism underlying these effects are not known. Therefore, we investigated whether SU alter the phosphorylation of PPAR $\gamma$  at Ser273 in an *in vitro* phosphorylation assay, in adipocytes *in vitro* and in adipose tissue in mice. In addition, the effects of SU on adipocyte differentiation and the change in the anti-diabetic expression profile were examined by Real-time PCR. Currently, no antibody directed against phospho-Ser273 of PPAR $\gamma$  is commercially available. Therefore, we produced this antibody by immunizing rabbits with a phospho-Ser273 peptide derived from the PPAR $\gamma$  sequence. The affinity purified antibody detected phosphorylated PPAR $\gamma$  specifically at Ser273 upon stimulation with TNF $\alpha$  in Western blot experiments. TNF $\alpha$  induced PPAR $\gamma$  Ser273 phosphorylation in a time- and concentration-dependent manner in primary human adipocytes, in murine 3T3-L1 adipocytes and in adipose tissue of TNF $\alpha$  injected mice. Treatment of cells and mice with SU or Rosiglitazone prior to TNF $\alpha$  challenge resulted in a reduction of PPAR $\gamma$  Ser273 phosphorylation *in vitro* and *in vivo*. Furthermore, SU were able to block CDK5-mediated PPAR $\gamma$  phosphorylation in an *in vitro* phosphorylation assay. The alteration of the PPAR $\gamma$  phosphorylation state upon SU treatment was correlated with the reduced expression of pro-diabetic adipokines (e.g. MCP-1). Taken together, our data indicate that SU have anti-diabetic glitazone-like actions on human adipocytes *in vitro* and *in vivo* in mice by reducing PPAR $\gamma$  Ser273 phosphorylation resulting in a positive anti-diabetic expression profile.

<sup>1</sup>Anti-diabetic drugs inhibit obesity-linked phosphorylation of PPAR $\gamma$  by Cdk5. Choi et al; Nature; Vol 466|22 July 2010| doi:10.1038/nature09291

<sup>2</sup>Glitazone-like action of glimepiride and glibenclamide in primary human adipocytes. P. Mayer et al; Diabetes, Obesity and Metabolism 13: 791–799, 2011.

<sup>3</sup>Antidiabetic actions of a non-agonist PPAR $\gamma$  ligand blocking Cdk5-mediated phosphorylation. Choi et al; Nature, Letter; Vol 477 | 22 September 2011 | doi:10.1038/nature1038

## 188

### A hydrophobic residue in position 15 of the rP2X3 receptor slows desensitization and allows for robust calcium imaging responses

**Hausmann, Ralf;** Kuhlmann, Daniel; Schumacher, Michaela; Schmalzing, Günther  
RWTH Aachen, Molekulare Pharmakologie, Germany

P2X receptors are trimeric ATP-gated cation channels involved in fast signal transduction in many cell types. The homotrimeric P2X3 receptor plays a role in sensory neurotransmission and nociception. To overcome the bias that results from fast desensitization of the P2X3 receptor in dose-response analyses, a non-desensitizing P2X2-X3 receptor chimera has been used as a surrogate for the P2X3 receptor in functional assays. In the present study, we show that only three P2X2-specific amino acid residues, <sup>19</sup>P<sup>21</sup>V<sup>22</sup>I, are needed to confer a slowly desensitizing phenotype to the P2X3 receptor. The strongest delay in desensitization of the P2X3 receptor by a single residue was observed when <sup>15</sup>Ser was replaced by Val or another hydrophobic residue. We suggest that the mechanism of desensitization of the P2X3 receptor may involve the movement of an N-terminal inactivation domain, in analogy to the "hinged-lid" or "ball and chain" mechanisms of voltage-gated Na<sup>+</sup> and K<sup>+</sup> channels, respectively. Pharmacologically, the S<sup>15</sup>V-rP2X3 mutant was indistinguishable from the wt-P2X3 receptor. Analysis of the S<sup>15</sup>V-rP2X3 receptor in 1321N1 astrocytoma cells by a common calcium-imaging-based assay showed 10-fold higher calcium transients relative to those of the wt-P2X3 receptor. The S<sup>15</sup>V-rP2X3 cell line enabled reliable calcium-imaging analysis of antagonistic potencies and correctly reported the mechanism of action of the P2X3 receptor antagonists A-317491 and TNP-ATP. Together, these data suggest that the S<sup>15</sup>V-rP2X3 mutant may be suitable not only for automated fluorescence-based screening of molecule libraries for identification of lead compounds but also for facilitated pharmacological characterization of specific P2X3 receptor ligands.

## 189

### Involvement of adipose tissue in the interplay between chronic inflammatory bowel disease and atherosclerosis

**Heinisch, Nina;** Fischer, Jens Walter; Grandoch, Maria  
Institut für Pharmakologie und Klinische Pharmakologie, Universitätsklinikum Düsseldorf, Heinrich-Heine-Universität Düsseldorf, Germany

Inflammatory bowel disease (IBD), a state of chronic intestinal inflammation, is characterized by infiltration of inflammatory cell subsets mainly involving lymphocytes such as CD4<sup>+</sup> T cells and the destruction of the mucosal architecture. In several clinical trials an increased risk of atherosclerosis and cardiovascular events in patients with IBD could be demonstrated, but the underlying mechanisms still remain unknown. Besides systemic action of the chronic intestinal inflammation on the arterial wall, other compartments such as adipose tissue might also be involved. According to their size, adipocytes show different gene expression patterns and secrete soluble factors like adipokines and chemokines, which in turn modulate the development of atherosclerosis. Therefore, aim of the present study was to analyze the possible interrelationships between colitis, atherosclerosis and adipose tissue.

For this purpose male, ApoE-deficient mice received 5 repeating cycles of dextran sodium sulfate (DSS) applied in the drinking water to induce chronic colitis (DSS group) or drinking water without DSS alone (control group) each followed by a 2 week recovery phase without DSS. DSS treatment led to a reduction in weight gain compared to the control group. Determination of the extent of atherosclerosis in the aorta revealed an increased plaque score in particular in the abdominal aorta of the DSS-treated animals compared to the control group. Additionally, the plaque volume in the innominate artery was elevated in DSS-treated animals. Analysis of visceral adipose tissue revealed an enhanced infiltration of macrophages in animals treated with DSS as determined by immunohistochemistry (F4/80 staining). Furthermore, adipocyte size was decreased in the DSS-colitis group in the visceral as well as periaortic adipose tissue.

The results of the present study show that experimental chronic colitis in ApoE-deficient mice resembles the pro-atherosclerotic phenotype described in patients with IBD. Besides systemic effects, changes in adipose tissue morphology could possibly modulate the inflammatory response leading to accelerated atherosclerosis.

## 190

### A coculture model for the *in vitro* prediction of sensitizing chemicals

**Hennen, Jennifer;** Blömeke, Brunhilde  
Universität Trier, Umwelttoxikologie, Germany

Many chemicals can induce skin sensitization following dermal exposure. While some of these can directly induce an immune response (haptens), others depend on activation via air oxidation or enzymatic conversion (pre-/prohaptens). Keratinocytes can impact on chemical-induced activation of dendritic cells (DC) not only by secretion of danger signals and inflammatory mediators, but also by generation of reactive metabolites. For improving the identification of sensitizing chemicals, we combined the metabolic competent keratinocyte cell line HaCaT and the monocytic cell line THP-1, as model for DC activation, in a direct coculture setup. Technically, we exposed the THP-1/HaCaT coculture to various chemicals for 24h and then analyzed expression of cell surface molecules CD86 and CD54 as activation markers on THP-1 cells via flow cytometry (1). In this study we tested the functionality of our coculture model using 26 chemicals, comprising 16 sensitizers (ranging from extreme to weak sensitizers) and 10 non-sensitizers. Among the sensitizers, 5 are classified as haptens and 11 as putative pre-/prohaptens. Comparing the chemical-induced upregulation of cell surface markers on THP-1 in the absence and presence of keratinocytes revealed that HaCaT keratinocytes can clearly modulate response of THP-1 cells, demonstrating active participation of keratinocytes in danger signaling in our coculture model. This could be confirmed in a coculture model with primary keratinocytes instead of HaCaT cells. In conclusion, the active cross talk between keratinocytes and THP-1 cells in our model can refine the *in vitro* detection of sensitizing chemicals.

Funding:

This work was partly supported by the Federal Office of Public Health (FOPH, Switzerland, 11.004203) and the Professorinnen-Programm des Bundes und der Länder (Germany).

(1) Hennen J, Aeby P, Goebel C, Schettgen T, Oberli A, Kalmes M, et al. Cross Talk between Keratinocytes and Dendritic Cells: Impact on the Prediction of Sensitization. Toxicol Sci. 2011;123(2):501-10.

## 191

### Differentiation of mouse embryonic stem cells into cells of the cardiovascular system as model for cardiotoxicity

**Hennicke, Tatiana;** Fritz, Gerhard  
Universitätsklinikum Düsseldorf, Institut für Toxikologie, Germany

For four decades anthracyclines have played an important role in the treatment of a variety of types of cancer because of their efficiency. However, their use is associated with significant harms, of which cardiotoxicity is the most important. The essential components of the cardiovascular system are the heart, blood, and blood vessels. Endothelial cells and smooth muscle cells line the entire of blood vessels, thereby acting as a semi-selective barrier between the vessel lumen and the surrounding tissue. Due to their barrier function endothelial cells and also smooth muscle cells are exposed to high concentrations of cyto- and genotoxins, which can induce stress responses and cell death. Mechanisms of anthracycline-induced cardiotoxicity and the mainly affected cell type are still unclear.

To find out, if there are differences between the main cell types of the cardiovascular system regarding their DNA damage response, we established a differentiation system of mouse embryonic stem cells (mESC), which uses several growth factors and small molecules for a directed differentiation. Analysis of the mRNA and protein expression of endothelial and smooth muscle specific markers was performed by RT-PCR and immunocytochemistry, respectively. In addition prototypical functions of the differentiated cell types were monitored. Thereby the cells could be characterized as endothelial-like (EC) and smooth muscle-like cells (SMC). RT-PCR-based mRNA expression analysis of genes involved in DNA damage response and repair showed, that several of these genes (for example Rad51, MSH2, Brca2) are upregulated in mESCs compared to thereof derived ECs and SMCs. To analyze if there are differences in the repair capacity of these cells, the level of S139 phosphorylated H2AX ( $\gamma$ H2AX) was analyzed by immunocytochemistry and Western blot. After ionizing irradiation there were more  $\gamma$ H2AX-foci in the differentiated SMCs compared to differentiated ECs and mESCs, whereas the basal level of  $\gamma$ H2AX was the highest in mESCs. Preliminary data indicate



that the endothelial differentiated cells have the best repair capacity. Currently, repair status and DNA damage response of these cells following doxorubicin treatment are under investigation.

Summarizing, our data show, that the applied differentiation protocol results in different, functionally competent, cell types of the cardiovascular system which are useful for toxicological analyses.

192

#### Modulation of Rho-regulated pathways for the prevention of doxorubicin induced cardiotoxicity

**Henninger, Christian**<sup>1</sup>; Ohlig, Jan<sup>2</sup>; Merx, Marc<sup>2</sup>; Fritz, Gerhard<sup>1</sup>

<sup>1</sup>Düsseldorf University Hospital, Institute of Toxicology, Germany

<sup>2</sup>Düsseldorf University Hospital, Department of Cardiology, Pneumology and Angiology, Germany

Inhibition of the signalling of small Rho (Ras homologous) GTPases with the HMG-CoA reductase inhibitor lovastatin (LOV) has been shown to reduce DNA damage formation and cell death after treatment with topoisomerase II poisons like doxorubicin (DOX) or etoposide in HUVEC and H9c2 cells. Further experiments pointed to the inhibition of the small GTPase Rac1 to be majorly responsible for the protective effects of LOV against topoisomerase II poisoning *in vitro*. Since cardiotoxicity is the most severe dose limiting side effect of chemotherapy with DOX, we aimed to comparatively investigate the cytoprotective effect of the pan-Rho GTPase inhibitor LOV and the Rac1 GTPase specific inhibitor NSC23766 in an *in vivo* mouse model for DOX-induced cardiotoxicity.

To this end, we treated male C57BL/6 mice three times a week with LOV (10 mg/kg b.w., p.o.) or with NSC23766 (5 mg/kg b.w., i.p.). DOX was administered two times a week in week one, two and three of the experiment (2x3 mg/kg b.w. per week, i.p.). Echocardiography was performed before the first DOX injection, 24 h after the third DOX injection and one week after the last DOX injection. DNA double strand break formation, apoptotic cell death and changes in RNA levels of a subset of genes known to be early markers for cardiotoxicity were analysed in heart tissue one week after the last DOX injection.

DOX treatment did not influence systolic heart functions but lead to diastolic dysfunction which was prevented by treatment with the statin or Rac1 inhibitor. In line with this, we found significant more DOX-induced DNA double-strand breaks and apoptotic cells in heart sections of mice which were not co-treated with the Rho modulators. The DOX-induced increase in RNA levels of ANP, CTGF and Mfn2 (established markers for cardiotoxicity, pro-fibrotic changes and mitochondrial fusion, respectively) were lowered in the co-treated groups. Altogether, Rac1 inhibition mimicked a major part of the protective effects caused by the statin. Nonetheless, treatment with LOV was still more potent in protecting mouse hearts from DOX-induced DNA double-strand break formation, apoptotic cell death and raise of RNA levels of cardiotoxicity markers pointing to additional effects of statins beyond the inhibition of Rac1.

Based on the data we suggest that including statins into DOX-based therapeutic regimen will be beneficial by lowering cardiotoxicity.

193

#### The antiplatelet drugs ticlopidine and clopidogrel release 5-HT from enterochromaffin-like QGP-1 cells through activation of TRPA1

**Schulze, Anja**; Hartung, Philipp; Urban, Nicole; Schaefer, Michael; **Hill, Kerstin**

Universität Leipzig, Rudolf-Boehm-Institut für Pharmakologie und Toxikologie, Germany

Thienopyridine drugs such as ticlopidine, clopidogrel and prasugrel are widely used to prevent platelet aggregation *in vivo* by inhibiting the binding of ADP to the P2Y<sub>12</sub> receptor. Side effects that arise during therapy include severe emesis and nausea, which frequently occurs under treatment with ticlopidine and clopidogrel, but are less common with prasugrel.

Utilising calcium imaging and electrophysiological measurements, we here present that antiplatelet drugs also act on transient receptor potential A1 channel (TRPA1). In general, TRPA1 is believed to function as an irritant sensor in the skin and the lung, but recent studies also suggest a role of TRPA1 in the regulation of gastrointestinal function via the release of 5-HT and other transmitters. We here present that heterologously expressed human TRPA1 is activated by ticlopidine (EC<sub>50</sub> = 7.2 ± 0.6 μM), clopidogrel (EC<sub>50</sub> = 5.4 ± 1.0 μM) and, to a lesser extent, by prasugrel (EC<sub>50</sub> = 16.6 ± 1.2 μM). Electrophysiological experiments demonstrated the activation of typical TRPA1 currents by these compounds. Also the enterochromaffin model cell line QGP-1, which endogenously expresses TRPA1, revealed TRPA1-mediated strong calcium signals and whole cell currents upon stimulation with ticlopidine and clopidogrel, whereas responses to prasugrel were only weak. Moreover, application of ticlopidine and clopidogrel, but not of prasugrel, induced a secretion of 5-HT from QGP-1 cells, which could be prevented by HC-030031, a TRPA1-specific blocker.

Taken together, we demonstrate that besides their well characterised effects on P2Y<sub>12</sub> receptors, thienopyridine antiplatelet drugs also act on human TRPA1 channels, suggesting that TRPA1 activation might contribute to adverse effects, such as vomiting and nausea, which can occur during treatment with the 1<sup>st</sup> and 2<sup>nd</sup> generation thienopyridines ticlopidine and clopidogrel.

194

#### Human carbonyl reductase 1 as a novel target of the natural phenolic compound curcumin

**Hintzpetter, Jan**; Hornung, Jan; Martin, Hans-Jörg; Maser, Edmund

Institute of Toxicology and Pharmacology for Natural Scientists, Kiel, Germany

Human carbonyl reductase 1 (CBR1), among other reductases, is the most effective human reductase in converting the antitumor drug and anthracycline daunorubicin (DAUN) to daunorubicinol (DAUNOL). DAUN is one of the most highly effective antineoplastic agents ever developed and is widely used to treat a variety of cancers. However, its alcohol metabolite DAUNOL has significantly reduced antitumor activity and shows increased cardiotoxicity, thereby limiting the clinical use of DAUN. Thus, inhibition of CBR1 may increase the efficacy and decrease the toxicity of DAUN. Indeed, in various cell culture models it has been demonstrated that inhibition of CBR1 by known inhibitors (e.g. 4-amino-1-*tert*-butyl-3-(2-hydroxyphenyl)pyrazolo[3,4-*d*]pyrimidine (hydroxy-PP)) enhanced the effectiveness and decreased the cardiotoxicity of the anticancer drug DAUN by preventing its reduction to DAUNOL.

Here, we report that the natural phenol curcumin found in *Curcuma longa* is a new and promising potent inhibitor of CBR1. Curcumin directly interacts with CBR1 and acts as a uncompetitive inhibitor with respect to the substrate 2,3-hexandione and as a competitive inhibitor with respect to NADPH. Molecular modelling supports the finding that curcumin occupies the cofactor binding site of CBR1. Intensive inhibition kinetic studies revealed an IC<sub>50</sub> value of 386 nM and an inhibition constant K<sub>i</sub> of 160 nM. Additionally, previous studies with curcumin and daunorubicin co-treated rats already showed that curcumin at least effectively prevented heart tissue damage. Our results suggest that curcumin can strongly inhibit CBR1 activity and therefore may even enhance the therapeutic effectiveness of the antineoplastic drug DAUN. In summary, we provide evidence that a combination of curcumin and DAUN might represent a novel approach for a successful cancer therapy and/or chemoprevention.

195

#### Response to various treatments in hematopoietic stem cells and HL-60 cells

**Hintzsche, Henning**; Taichrib, Katharina; Stopper, Helga

Universität Würzburg, Institut für Pharmakologie und Toxikologie, Germany

The hematopoietic system consists of various different cell types. All of these cells originate from one type of progenitor cells: hematopoietic stem cells. Understanding the response towards different biological stimuli in cells of the hematopoietic system is important for a variety of disease, such as immune deficiency, cancer etc. Not much is known about the difference between hematopoietic stem cells and differentiated cells or cell lines regarding DNA damage, apoptosis, DNA repair and other endpoints.

The aim of this study was to investigate several important biological endpoints in HL-60 and hematopoietic stem cells and to compare the results. As a marker for cell function, oxidative stress was quantified after treatment with hydrogen peroxide. DNA repair was measured with a modified repair comet assay after exposure to UV radiation and subsequent treatment with aphidicoline. Cell cycle alterations as one central control mechanism of cells were measured after nocodazole arrest. As genotoxicity endpoint, DNA strand breaks were measured in the comet assay after treatment with methyl methanesulfonate. Epigenetic changes were assessed as histone deacetylation after incubation with phorbol ester. Upon treatment with sodium arsenite, apoptosis was measured by annexin V staining.

In HL-60 cells, all endpoints were significantly altered after treatment. Preliminary results of experiments with the hematopoietic stem cells and the comparison with the HL-60 cells are presented and discussed.

196

#### Immune- and miRNA-response to recombinant interferon beta - a biomarker evaluation study to guide development of type I Interferon- based therapies: rationale, design and methodology

**Hinze, Annette Viktoria**<sup>1</sup>; Coenen, Martin<sup>1</sup>; Wolber, Uta<sup>1</sup>; Hartmann, Gunther<sup>1</sup>; Holdenrieder, Stefan<sup>1</sup>; Müller, Markus<sup>2</sup>; Coch, Christoph<sup>1</sup>

<sup>1</sup>Institut für Klinische Chemie und Klinische Pharmakologie, Studienzentrale des Studienzentrums Bonn, Germany

<sup>2</sup>Universitätsklinikum Bonn, Neurologie, Germany

#### Introduction:

Multiple Sclerosis is a chronic inflammatory disorder of the central nervous system. However the pathogenesis of relapsing-remitting multiple sclerosis (RRMS) is still poorly understood and with limited therapeutic options. As not all patients benefit from treatment with the established therapeutic regimen there is a need for new options to improve the efficacy of current MS treatment. Inducing type I Interferon as well as suppressing a Th17 response by targeting the innate immune receptor RIG-I is a promising new approach. A specific ligand for RIG-I is in preclinical testing. Therefore, the Res1 study was designed to analyze the immune response to standard treatment with recombinant IFN-β to establish biomarkers for the safety and efficacy of the RIG-I ligand.

#### Methods/design:

Res1 is a single center, prospective, open label, non-randomized phase I trial. Three different cohorts (20 healthy volunteers, 20 patients with relapsing-remitting multiple sclerosis and ongoing Interferon-beta treatment and 10 patients with relapsing-remitting

multiple sclerosis starting on Interferon-beta treatment) will receive standard Interferon-beta-1a therapy for nine days. The study will be conducted according to the principles of ICH-GCP and the Declaration of Helsinki on the phase I unit of the Institute of Clinical Chemistry and Clinical Pharmacology and in the Department of Neurology, both University Hospital Bonn. Interferon-beta-induced cytokine levels, surface marker on immune cells, mRNA- and miRNA-expression as well as psychometric response will be investigated as target variables.

#### Discussion:

The Rest study will assess biomarkers to safely guide the dose steps within the first in man study with a RIG-I ligand. The data can additionally be used for the development of other therapies based on type I Interferon such as TLR ligands. Moreover, it will help to understand the Interferon-beta induced immune response and attending emotional changes in a controlled in vivo setting.

## 197

### Maturation of Engineered Heart Tissue (EHT) by Permanent Electrical Stimulation

**Hirt, Marc N.**<sup>1,2</sup>; Boedinghaus, Jasper<sup>1</sup>; Schaaf, Sebastian<sup>1,2</sup>; Mitchell, Alice<sup>3</sup>; Eder, Alexandra<sup>1,2</sup>; Luther, Pradeep K.<sup>3</sup>; Börmchen, Christian<sup>4</sup>; Stenzig, Justus<sup>1,2</sup>; Hansen, Arne<sup>1,2</sup>; Eschenhagen, Thomas<sup>1,2</sup>

<sup>1</sup>University Medical Center Hamburg-Eppendorf, Department of Experimental Pharmacology and Toxicology, Germany

<sup>2</sup>DZHK (German Centre for Cardiovascular Research), partner site Hamburg/Kiel/Lübeck, Germany

<sup>3</sup>Imperial College, Faculty of Medicine, National Heart & Lung Institute, London, Great Britain

<sup>4</sup>University Medical Center Hamburg-Eppendorf, Dermatology and Venereology Department and Clinic, Germany

#### Background

Cardiac tissue engineering aims at replacing or supporting necrotic myocardium by transplantation, at generating a screening platform for cardiotoxic drug effects or at modeling cardiac diseases *in vitro*. It is desirable for all these applications to generate an artificial construct that displays a similar maturation state as native cardiac tissue. In the present study we investigated the effect of long-term electrical stimulation on maturation of engineered heart tissue (EHT).

#### Methods

EHTs were generated from neonatal rat heart cells (rEHTs) and differentiated human induced pluripotent stem cells (hEHTs). Electrical stimulation with carbon-steel electrodes was performed from day 4 on; rEHTs were paced with 0.5 Hz for 18 days, hEHTs with 1.5–2 Hz for 10 days. Contractile parameters of EHTs were assessed three times a week. EHTs were subjected to calcium- and isoprenaline concentration response curves, histology, immunohistochemistry, electron-, confocal-, and multi-photon-microscopy. Gene expression was analyzed by microarray analysis.

#### Results

Compared to control EHTs, electrically stimulated rEHTs almost tripled in force normalized to cross-sectional area (0.29 mN/mm<sup>2</sup> vs. 0.10 mN/mm<sup>2</sup>) whilst spontaneous beating activity decreased in paced rEHTs. Forces of stimulated hEHTs were 48% higher than their respective controls. Additionally, contraction (rEHTs, n = 8–11 each: +104%; hEHTs, n = 7 each: +53%) and relaxation velocity (rEHTs, n = 8–11 each: +99%; hEHTs, n = 7 each: +45%) increased. The inotropic effect of isoprenaline on rEHTs was more pronounced (n = 4 each: +51%) and the calcium response shifted to more physiological calcium concentrations resulting in a higher EC<sub>50</sub>. More compact and longitudinally orientated cardiomyocytes, clearer definition of sarcomeres and stronger connexin-43 labeling indicated advanced maturation of paced EHTs. 2-Photon-Microscopy revealed a higher density of cardiomyocytes and more myocytes in deep regions of rEHTs. Electron microscopy showed improved cardiomyocyte ultrastructure in terms of myofibril composition, mitochondrial abundance and arrangement in stimulated rEHTs.

#### Conclusion

These data suggest that continuous electrical stimulation of EHTs from rat and human origin improves functional properties and ameliorates maturation in both rat and human EHTs. This will increase the informative value of *in vitro* EHT applications and might pave the way for its future clinical application.

## 198

### Farnesyl pyrophosphate acts as an antagonist at the human platelet P2Y<sub>12</sub>-receptor

**Hoffmann, Kristina**; von Kügelgen, Ivar

Universität Bonn, Institut für Pharmakologie und Toxikologie, Germany

The nucleotide P2Y<sub>12</sub>-receptor plays a prominent role in ADP-induced platelet aggregation. It is the pharmacological target of the active metabolites of the thienopyridines clopidogrel and prasugrel and of the newly licensed compound ticagrelor, which is the first perorally active and reversible inhibitor of platelet aggregation. Högberg et al. (*Thromb Haemost* 2012; 108:119-32) described an antagonistic action of farnesylpyrophosphate (FPP), an intermediate product in the HMG-CoA reductase pathway, at the platelet P2Y<sub>12</sub>-receptor. In the present study we analyzed the interaction of FPP with recombinant wild type and mutant human P2Y<sub>12</sub>-receptors, stably expressed in CHO Flp-In cells. Receptor function was assessed by quantification of cellular cAMP with a [<sup>3</sup>H]cAMP-radioaffinity assay. Cellular cAMP production was accelerated by the use of forskolin [10 μM]. The synthetic ADP-analogue

2-methylthio-ADP (2-MeSADP) inhibited forskolin-induced cAMP accumulation in a concentration-dependent manner at all P2Y<sub>12</sub>-receptor constructs tested. The addition of FPP [30 μM] led to a rightward shift of the concentration-response-curve of the agonist in a surmountable manner at the wild type receptor with an apparent pK<sub>B</sub> value of 5.2. Similar results were obtained at R256A-mutant P2Y<sub>12</sub>-receptors and receptors fused at the c-terminus to enhanced cyan fluorescent protein (ECFP). At C194A-mutant receptors, the antagonistic potency of FPP was significantly increased with an apparent pK<sub>B</sub> value of 6.3. In contrast, at K280A-mutant P2Y<sub>12</sub>-receptors fused to ECFP, a smaller rightward shift of the concentration-response-curve of 2-MeSADP by FPP was observed, whereas the maximal effect of the agonist was decreased in the presence of FPP. Thus the present data show FPP to be an antagonist at the P2Y<sub>12</sub>-receptor, suggesting a possible interaction of the HMG-CoA reductase pathway with platelet P2Y<sub>12</sub>-receptor function. The amino acid residues C194 and K280 may be involved in the interaction of FPP with the receptor protein.

## 199

### Dissecting the role of TRPC6-channels in bleomycin-induced pulmonary fibrosis

**Hofmann, Katharina**<sup>1</sup>; Aumiller, Verena<sup>2</sup>; Yildirim, Önder<sup>3</sup>; Gudermann, Thomas<sup>1</sup>; Königshoff, Melanie<sup>2</sup>; Dietrich, Alexander<sup>1</sup>

<sup>1</sup>LM-Universität München, Walther-Straub-Institut für Pharmakologie, Germany

<sup>2</sup>Comprehensive Pulmonary Center, Lung Repair and Regeneration, München, Germany

<sup>3</sup>Comprehensive Pulmonary Center, Immunopathology of COPD, Neuherberg, Germany

Pulmonary fibrosis (PF) is a progressive lung disease of unknown cause ultimately leading to death. Current evidence indicates that the fibrotic response is driven by abnormally activated alveolar epithelial cells (AECs) caused by epithelial injury e.g. cigarette smoke, mechanical stress or by drugs like bleomycin. AEC produce profibrotic mediators (e.g transforming growth factor β and angiotensin II) which initiate aberrant epithelial-fibroblast crosstalk and induce the formation of fibroblast and myofibroblast foci through the proliferation of resident mesenchymal cells. Moreover, fibrocytes from the peripheral blood are attracted and migrate to the injured areas facilitated by an increased vascular permeability. Classical Transient Receptor Potential channel 6 (TRPC6) is an unselective cation channel highly expressed in different lung tissues. TRPC6 might contribute to pulmonary fibrosis since it is known that the channel plays an important role in myofibroblast transdifferentiation and wound healing in cardiac and dermal fibroblasts (1). Moreover, TRPC6 is responsible for increased vascular permeability in lungs (2) which might help circulating fibrocytes to migrate to the injured areas. To study a potential role of TRPC6 in PF we analyze function, histology, gene and protein expression in WT and *Trpc6*<sup>-/-</sup> lungs after bleomycin-instillation. Initial results indicate that TRPC6-deficient lungs expose a less severe pulmonary fibrosis than WT lungs. In the future we will investigate primary alveolar epithelial cells and primary murine fibroblasts from bleomycin-treated and untreated WT and *Trpc6*<sup>-/-</sup> animals to understand molecular differences in cell functions induced by cation influx through TRPC6. Defining TRPC6 function in these cells will help to identify pharmacological targets for new therapeutic options in PF.

[1] Davis, J., Burr, A. R., Davis, G. F., Birnbaumer, L., and Molkenin, J. D. (2012) A TRPC6-dependent pathway for myofibroblast transdifferentiation and wound healing *in vivo*. *Dev. Cell* 23, 705-715.

[2] Weissmann, N., Sydykov, A., Kalwa, H., Storch, U., Fuchs, B., Mederos y Schnitzler, M., Brandes, R. P., Grimminger, F., Meissner, M., Freichel, M., Offermanns, S., Veit, F., Pak, O., Krause, K. H., Schermuly, R. T., Brewer, A. C., Schmidt, H. H., Seeger, W., Shah, A. M., Gudermann, T., Ghofrani, H. A., and Dietrich, A. (2012) Activation of TRPC6 channels is essential for lung ischaemia-reperfusion induced oedema in mice. *Nat. Commun.* 3, 649.

## 200

### A spatial pattern of radical formation regulates endothelial sprouting angiogenesis and is controlled by PON2

**Horke, Sven**<sup>1,2</sup>; Wilgenbus, Petra<sup>1</sup>

<sup>1</sup>Universitätsmedizin Mainz, Institut für Pharmakologie, Germany

<sup>2</sup>Centrum für Thrombose und Hämostase Mainz, Germany

The modulation of blood vessel formation by activation or inhibition of angiogenesis is of outstanding interest. On the one hand, this is true for e.g. myocardial infarction or stroke, because induction of angiogenesis may reduce ischemia / reperfusion damage and tissue loss. On the other hand, cancer therapy often employs angiogenesis inhibitors to starve tumor cells. Clinical inhibitors interfere with receptor signaling, but offer only limited benefit. Therefore, we investigated other, receptor-independent mechanisms and explored redox signaling. It is known that reactive oxygen species (ROS) are involved in sprouting of endothelial cells (ECs) and have the capacity to both activate and impede angiogenesis. However, there is limited knowledge about the precise radical species, its spatial arrangement or dominant effector molecules. *Ex vivo* aortic ring angiogenesis assays with wildtype mice showed a precise spatial pattern of radical formation in EC outgrowths. Normally, high radical levels focused on tip and branch areas, while low levels were seen in intermittent sections. As superoxide appeared to be the dominant radical, we analyzed the role of O<sub>2</sub>-producing systems. Further, to verify the importance of organized spatial ROS production, we also employed mice deficient for PON2, a mitochondrial anti-oxidant enzyme. In sprouting ECs, PON2<sup>-/-</sup> lead to higher ROS production in a disorganized fashion with disturbed spatial pattern. This severely

diminished angiogenic response in aortic ring assays, slowed retina vascularization in PON2<sup>-/-</sup> mice and also blocked tube formation in human ECs. Although several antioxidants efficiently diminished ROS in PON2<sup>-/-</sup> vessels, only specific superoxide scavengers rescued EC sprouting. Finally, expression profiling studies from isolated ECs revealed several genes altered by PON2<sup>-/-</sup>-induced ROS formation, potentially pointing at further underlying signaling circuits. Collectively, the precise arrangement of radicals in a distinct spatial pattern is needed to establish appropriate angiogenic responses, a process regulated by PON2.

## 201

### Visualisation of silver nanoparticle-protein interactions with autometallographic staining

**Horzowski, Sabine**; Bober, Hannah; Lichtenstein, Dajana; Niemann, Birgit; Lampen, Alfonso

Federal Institute for Risk Assessment, Department of Food Safety, Berlin, Germany

The application of silver nanoparticles in food contact materials and dietary supplements results in a potential increased oral uptake. Several studies show the uptake of silver nanoparticles by intestinal cells and other cell types, but for a comprehensive risk assessment the mode of action of the resorbed nanoparticles has to be investigated as well.

Inside the body, nanoparticles are exposed to different biological environments, where proteins bind to the surface of nanoparticles to form a coating known as protein corona. The protein corona can critically affect the interaction of the nanoparticles with the cellular structures. Therefore, the analysis of the specific protein corona should give first indications for the mode of action of resorbed nanoparticles inside the tissues of the body. To identify nanoparticle-protein interactions different isolated proteins and a whole cell lysate of human intestinal cells have been incubated with characterized silver nanoparticles which were separated via gel electrophoresis. The gels were stained by adapting an autometallographic histological method to identify the silver particles in the gels combined with different protein staining methods, to analyse the nanoparticle-protein interactions.

Autometallographic staining (AMG) of unbound and protein-bound silver nanoparticles was successfully applied on protein-bound silver after separation of the incubated proteins in agarose gels as well as polyacrylamid gels (PAGE). The best co-staining of proteins could be achieved by combining the autometallography with coomassie-blue staining compared to silver staining of proteins and the fluorescent protein staining SYPRO Ruby.

In summary, the agarose gels show intact protein-nanoparticle interactions whereas the SDS-PAGE only shows silver nanoparticles, silver ions and the proteins separately due to the tight pores and the stringent string reducing conditions in the polyacrylamid gels. Additionally, the AMG is suitable to differentiate between silver nanoparticles and silver ions. For the tested silver nanoparticles glutathione-S-transferase, glutathione and BSA could be identified as possible interaction partners via autometallographic staining.

## 202

### OATP1A2 is expressed in erythrocytes and involved in the transport of antimalarial drugs

**Hubeny, Andrea**<sup>1</sup>; Keiser, Markus<sup>2</sup>; Siegmund, Werner<sup>2</sup>; Grube, Markus<sup>1</sup>

<sup>1</sup>Institut für Pharmakologie, Allgemeine Pharmakologie, Greifswald, Germany

<sup>2</sup>Institut für Pharmakologie, Klinische Pharmakologie, Greifswald, Germany

**Background:** The expression and function of organic anion transporting polypeptides (OATPs) in pharmacokinetic important organs like liver or intestine has been addressed in numerous studies. However, little is known about their expression and function in specific compartments such as blood cells like erythrocytes (RBCs). Since these cells represent target structures for drugs like antimalarial compounds, transport processes may also be of pharmacological relevance. Therefore, we examined the interaction of antimalarial compounds with human OATPs and studied their expression in erythrocytes.

**Methods:** Functional studies were carried out by using human erythrocytes and transporter (OATP1A2, OATP2B1 and OATP1B1) overexpressing MDCKII cells. Using these cells, competition assays between standard transporter substrates (estrone-3-sulfate for OATP1A2/ OATP2B1 and bromosulphthaleine for OATP1B1) and antimalarial drugs (quinine, chloroquine, mefloquine, primaquine, pyrimethamine, artesinin and artesunate) were performed. In addition, direct transporter-mediated uptake was studied for quinine.

Transporter expression in RBCs was studied on mRNA level by real-time PCR using K562 cells, an established *in vitro* model for RBCs. In addition, western blot and immunofluorescence analysis were performed using human RBCs.

**Results:** On functional level, we were able to show a significant inhibition of OATP1A2 and OATP1B1 by several antimalarial drugs. This interaction was most prominent for OATP1A2 with half maximal inhibition constants (IC<sub>50</sub>-values) of 0.8 ± 1.4 µmol/l for quinine, 1.1 ± 1.7 µmol/l for chloroquine, 6.1 ± 1.5 µmol/l for mefloquine and 5.6 ± 2.3 µmol/l for primaquine. Focusing on the most potent inhibitor quinine, subsequent uptake studies revealed an OATP1A2-mediated transport of this compound, which was sensitive to the OATP1A2 inhibitor naringin.

With regard to OATP expression, OATP1A2 and OATP2B1 were found to be expressed in K562 cells and RBCs, while OATP1B1 could not be detected. Immunofluorescence analysis indicated for both transporters a localization in the plasma membrane of RBCs.

**Conclusion:** While several OATPs interact with antimalarial compounds like quinine, chloroquine, mefloquine and primaquine *in vitro*, only OATP1A2 and OATP2B1 were found to be expressed in erythrocytes. Here, OATP1A2-mediated quinine uptake may influence intracellular drug concentrations and action.

## 203

### Candesartan attenuates disease progression in two mouse models of dilated cardiomyopathy

**Hummel, Regina**; Ludwig, Andreas; Stieber, Juliane

Friedrich-Alexander-Universität Erlangen-Nürnberg, Institute of Experimental and Clinical Pharmacology and Toxicology, Germany

**Background:** Dilated cardiomyopathy (DCM) is a myocardial disease characterized by varying degrees of ventricular dysfunction and dilatation with a poor long-term prognosis. Treatment options are limited and mainly targeted at relieving symptoms of heart failure. Effective prevention of structural changes of the myocardium would be desirable. ACE-inhibitors are usually used, but recent studies suggest that angiotensin receptor 1 (AT<sub>1</sub>) blockers including candesartan may be more effective. Besides blood pressure lowering, targeting AT<sub>1</sub> receptors may positively influence cardiac remodeling due to inverse agonism of candesartan or other unknown mechanisms.

**Objectives:** We investigated characteristic properties and the effectiveness of the AT<sub>1</sub> receptor inhibitor candesartan in the treatment of DCM.

**Methods:** Time-specific deletion of the cardiac ryanodine receptor RyR2 (model 1) or the L-type calcium channel Ca<sub>v</sub>1.2 (model 2) in mice induces a condition resembling human DCM. Model 1 and 2 mimic slow and rapid progression of the disease, respectively. Mice were treated orally with candesartan (2.5 mg/kg per day). Cardiac arrhythmias were assessed by telemetric ECG recordings as well as action potential recordings of isolated ventricular myocytes.

**Results:** Treatment with candesartan significantly prolonged survival especially of model 2 animals. Candesartan treated animals showed less cardiomyocyte degeneration and cardiac fibrosis. ECG-recordings of model 2 animals demonstrated markedly less arrhythmias in the candesartan group compared to controls. In addition the action potential duration (APD) of isolated wildtype left ventricular cardiomyocytes treated with candesartan (1 µM) was significantly shorter than the APD of untreated cells.

**Discussion:** This study demonstrates that treatment with candesartan improves survival and cardiac fibrosis in mouse models of DCM and suggests a potential antiarrhythmic effect of the drug. These properties may contribute to the therapeutic effect of candesartan also in other cardiovascular diseases.

## 204

### Dermal, oral and inhalation exposure of children to fragrance allergens in scented toys: A comparative study

**Hutzler, Christoph**; Masuck, Ines; Luch, Andreas

Bundesinstitut für Risikobewertung, Sicherheit verbrauchernaher Produkte, Berlin, Germany

According to the revised European Toys Safety Directive 2009/48/EC toys intended for children should not contain fragrance ingredients which could cause contact allergy. Fragrances are among the most common causes for contact allergy in children. According to the Directive, 55 allergenic fragrances are banned and another 11 require declaration on the package when exceeding the limit value of 100 mg/kg. Toys like dolls or puzzles are scented to highlight the product, or to displace unpleasant odors. Scented toys have yet been placed on the European market, and therefore may present a possible route for children for getting exposed to allergenic fragrances via skin penetration, inhalation or mouthing. Therefore, the aim of our study was to compare these exposure routes of children to fragrance allergens present in scented toys.

To estimate the inhalation exposure of children to fragrance allergens in scented toys, information about the emission of these compounds is mandatory. For this purpose four scented toys purchased from online toy stores were tested in a 1 m<sup>3</sup> test chamber at consumer conditions for seven days to characterize individual emission profiles of fragrances.

To estimate the dermal and oral exposure discs punched out from each of seven toy samples purchased from online toy stores were incubated in water at room temperature. The incubation in water simulated the migration of fragrances from toys to saliva and sweat during dermal contact and mouthing.

Finally, the exposure levels of children to fragrance allergens in scented toys were calculated. During dermal and oral contact with scented toys children could be exposed to levels of fragrances in the range of microgram per kg body weight and day. In contrast, fragrance levels that might be inhaled by children were in the range of nanogram per kg body weight and day.

## 205

### In mice the histamine H<sub>4</sub>-receptor is expressed on non-hematopoietic cells and plays a role in experimental colitis.

**Isaev, Rukijat**; Schirmer, Bastian; Seifert, Roland; Neumann, Detlef

Institut für Pharmakologie, Zentrum Pharmakologie und Toxikologie, Hannover, Germany

#### Background

The histamine H<sub>4</sub> receptor (H<sub>4</sub>R) belongs to the family of G-protein coupled receptors. It is expressed on hematopoietic cells, in which upon ligation with histamine it induces the production of proinflammatory factors. In previous studies we have shown that the H<sub>4</sub>R plays a role in the pathogenesis of DSS-induced colitis in mice, a model of inflammatory bowel disease (IBD). Increasing evidence now indicates that the H<sub>4</sub>R may be present also on non-hematopoietic cells. However, there is still no definitive proof of its functional expression on non-hematopoietic cells. To investigate this hypothesis, in the present study we generated bone marrow chimera of wild type and H<sub>4</sub>R-deficient mice and submitted them to DSS-induced colitis.

#### Methods

For the generation of bone marrow chimera bone marrow cells from H<sub>4</sub>R-deficient BALB/c mice as well as from wild type mice were harvested. These cells were transplanted into H<sub>4</sub>R-deficient and wild type mice, which were previously irradiated to eliminate the endogenous hematopoietic system. Recipient mice of each strain were separated into two groups: one receiving the H<sub>4</sub>R-deficient bone marrow and the second the wild type bone marrow. Thus, following experimental and control groups were generated: (1) H<sub>4</sub>R-deficient bone marrow into wild type mice (H<sub>4</sub>R<sup>-/-</sup> → WT), (2) WT → H<sub>4</sub>R<sup>-/-</sup>, (3) WT → WT and (4) H<sub>4</sub>R<sup>-/-</sup> → H<sub>4</sub>R<sup>-/-</sup>. Six weeks after bone marrow transplantation, all four groups were fed with 3% DSS in drinking water for seven days to induce colitis. Body weight and Disease Activity Index (DAI) were recorded daily. Finally, the colon of each mouse was evaluated histologically.

#### Results

During the treatment with DSS, a distinct loss of body weight was observed for the group WT → WT, which was absent in the group H<sub>4</sub>R<sup>-/-</sup> → H<sub>4</sub>R<sup>-/-</sup>. Clinical signs of colitis were observed in the group WT → WT, but not in the group H<sub>4</sub>R<sup>-/-</sup> → H<sub>4</sub>R<sup>-/-</sup>. In the group H<sub>4</sub>R<sup>-/-</sup> → WT the loss of body weight was similar to that observed in WT → WT mice. In contrast, in WT → H<sub>4</sub>R<sup>-/-</sup> mice the loss of body weight was reduced, similar to H<sub>4</sub>R<sup>-/-</sup> → H<sub>4</sub>R<sup>-/-</sup> mice. DAI and histological signs of inflammation were highest in the groups WT → WT and H<sub>4</sub>R<sup>-/-</sup> → WT as compared to WT → H<sub>4</sub>R<sup>-/-</sup> and H<sub>4</sub>R<sup>-/-</sup> → H<sub>4</sub>R<sup>-/-</sup>.

#### Discussion

These results indicate that the H<sub>4</sub>R is expressed functionally on non-hematopoietic cells and that its deficiency on non-hematopoietic, but not on hematopoietic cells plays a protective role in experimental colitis in mice. In future studies, we want to investigate and define the non-hematopoietic cell types, which express the H<sub>4</sub>R.

## 206

### Tissue-specific expression of estrogen metabolizing enzymes in livers and mammary glands of ovariectomized female Wistar rats

**Jäger, Sabrina**<sup>1</sup>; Schmalbach, Katja<sup>1</sup>; Blei, Tina<sup>2</sup>; Soukup, Sebastian<sup>3</sup>; Diel, Patrick<sup>2</sup>; Kulling, Sabine<sup>3</sup>; Lehmann, Leane<sup>1</sup>

<sup>1</sup>University of Würzburg, Section of Food Chemistry, Würzburg, Germany

<sup>2</sup>German Sport University, Institute of Cardiovascular Research and Sports Medicine, Department of Molecular and Cellular Sports Medicine, Cologne, Germany

<sup>3</sup>Max Rubner Institute (MRI), Department of Safety and Quality of Fruit and Vegetables, Karlsruhe, Germany

The ovariectomized (ovx) female Wistar rat exposed to the hormone 17β-estradiol (E2) represents a common test animal for the investigation of the influence of phytoestrogens, such as the extensively investigated isoflavones (IF), on the sensitivity of the mammary gland (MG) towards E2. Although tissue-specific biotransformation affects the action of both E2 and IF, and the isozymes involved in the biotransformation of E2 and IF are known, a comprehensive quantitative overview of the tissue-specific expression of the respective isozymes has been lacking.

To close this gap, 12 female ovx Wistar rats were fed a diet containing 518±27 ppm total IF aglycones and were exposed to either 4 µg E2/kg bw/day or to vehicle for 3 days by s.c. injection. In liver (HEP) and MG, transcript levels of 6 cytochrome P450-dependent monooxygenases (CYPs), 5 UDP-glucuronosyltransferases (Ugts), 3 sulfotransferases (Sults), 7 glutathione-S-transferases (Gsts), catechol-O-methyltransferase (Comt), and NAD(P)H dehydrogenase (Nqo) 1, known to metabolize E2 and/or IF and metabolites thereof, were determined by quantitative Taqman® probe-based realtime PCR and were expressed as fold (\*) Hprt (housekeeping gene).

Most important for IF metabolism, UGT transcript levels were generally high in HEP (Ugt2b2, 60\*Hprt>1a1>1a5>2b1>1a8, 0.06\*Hprt); whereas in MG, even the main Ugt1a8, only amounted to 0.03\*Hprt>2b1>2b2>1a5>1a1, 0.002\*Hprt. In contrast, although the profile of Sults was different between HEP and MG (SULT1b1, 4.3\*Hprt>1a1>1e1, 0.003\*Hprt and 1a1, 1.3\*Hprt>1e1>1b1, 0.01\*Hprt, respectively), total transcript levels were comparable.

Transcripts of all tested CYPs (predominately involved in E2 activation) were detected in HEP (1a2, 19\*Hprt>2b2>1a1>2b1>3a2>1b1, 0.004\*Hprt). In contrast, in MG, CYP1b1 was the main CYP (0.27\*Hprt), followed by 2b1>1a1>2b1>2b2>1a2, 0.004\*Hprt. Particularly important for deactivation of E2 metabolites, both Comt (HEP 44\*Hprt; MG 1.0\*Hprt), Nqo1 (HEP 1.2\*Hprt; MG 0.2\*Hprt) and all Gsts analyzed were detected in both tissues, and Gsts exhibited tissue-specific isozyme profiles (HEP: a3, 38\*Hprt<m1<m2<a2<a4<t2 treatment with E2 did not change the qualitative picture in both tissues, but significantly decreased relative mRNA levels of Ugt1a5 and Comt in HEP and Gst1 in MG (t-test, p<0.05).

Thus for the first time, HEP and MG of the widely-used female ovx Wistar rat were characterized regarding quantitative transcript levels of IF and E2 metabolizing enzymes.

Supported by the DFG (Le1329/10-1 IsoCross).</m1<m2<a2<a4<t2

## 207

### LPS treatment of mice overexpressing protein phosphatase 5 in the heart

**Jahn, Tina**; Gergs, Ulrich; Neumann, Joachim

Institut für Pharmakologie und Toxikologie, Med. Fakultät, Martin-Luther-Universität Halle-Wittenberg, Halle/Saale, Germany

We previously described a mouse model with cardiac specific overexpression of protein phosphatase 5 (PP5), a serine threonine protein phosphatase, under control of the alpha myosin heavy chain promoter. Transgenic mice (TG) were compared to wild type (WT) littermates (Gergs et al. Int J Cardiol 154:116[2012]). From functional studies we hypothesized that TG would be better able to cope with septic shock. To this end, mice were treated with 25 mg lipopolysaccharide (LPS) per kg body weight or isotonic sodium chloride (NaCl) as a control, intraperitoneally. Three and seven hours thereafter, echocardiography was performed in order to assess the decline in cardiac function. RNA was isolated from the heart, converted to cDNA and quantitative PCR was performed. In WT and TG hearts, treated with NaCl, no change in ejection fractions (EF) was noted. Before LPS treatment, the EF was smaller in TG than in WT (50.2 ± 2.8% vs. 64.5 ± 3.0%, p<0.05, n=6) and declined with LPS treatment (p<0.05) to a greater extent in TG compared to WT (20.6 ± 2.8% vs. 29.1 ± 2.5%, p<0.05, n=6). ANP expression was similar and low in TG and WT and did not change in TG and WT after LPS treatment. CD14 expression was elevated after LPS only in WT but not in TG. MD2 Expression declined after LPS in WT and to greater extent in TG. IL1b expression was stimulated by LPS treatment in a similar way in WT and TG. In contrast, IL6 was increased by LPS from low basal levels in WT and declined from a high basal level in TG. TNFα expressions were stimulated less in TG than in WT by LPS. In conclusion, under our experimental conditions, cardiac function declined more in PP5 mice than in WT, possibly due to different gene regulation. Hence PP5 overexpression may compromise resilience to stress like sepsis in patients (supported by DFG).

## 208

### Simultaneous determination of cellular uptake of superparamagnetic iron oxide nanoparticles (SPION) and their cytotoxicity employing multiparameter flow cytometry

**Janko, Christina**; Zaloga, Jan; Dürr, Stephan; Tietze, Rainer; Friedrich, Ralf P.; Cicha, Iwona; Lyer, Stefan; Alexiou, Christoph

HNO-Klinik, Kopf- und Halschirurgie, Sektion für experimentelle Onkologie und Nanomedizin (SEON), Erlangen, Germany

Superparamagnetic iron oxide nanoparticles (SPION) have shown great potential in biomedical applications. Although SPION have been successfully tested as carriers in magnetic drug targeting approaches or as contrast agents in magnetic resonance imaging previously, further investigations of SPION uptake into cells and their biological consequences on cell viability are of special interest. Since classical methods to estimate cellular SPION content as Prussian Blue staining and transmission microscopy are time consuming and are not appropriate for high throughput analyses of additional parameters, we developed a flow cytometry based method to determine the cellular SPION uptake in combination with the analysis of three cell viability markers reflecting the tier model of nanotoxicity.

Cells taking up nanoparticles increase their side scatter in a dose and time dependent manner which can be easily determined by flow cytometry. Calibrating cellular side scatter changes against the results from the established spectrophotometric iron determinations of cell lysates (370 nm absorption) initially enabled us to calculate absolute SPION contents per cell reproducibly. Consequently, in the subsequent measurements the quantification of the intracellular iron oxide content was possible exclusively from the cellular side scatter changes. In parallel, staining of the cells with the fluorescent markers DiIC(1.5), AnnexinV-Fitc, and propidium iodide further provided information about mitochondrial membrane potential, phosphatidylserine exposure and plasma membrane integrity, thus drawing a comprehensive picture of the cellular viability. Additionally, the record of the cell count indicated the proliferative capacity of the cells.

Taken together, our established multiparameter flow cytometry based approach is easy, fast, and most importantly, links the amount of engulfed iron oxide nanoparticles to the elicited cellular effects, thus allowing us to perform reliable dose-dependent risk assessments of iron oxide nanoparticles for medical applications.

209

**RhoA controls myofibroblast characteristics in cardiac fibroblasts**

**Jatho, Aline**; Kittana, Naim; Schenk, Kerstin; Ramba, Beate; Lutz, Susanne  
Herzzentrum Universitätsmedizin Göttingen, Pharmakologie, Germany

RhoA is known to play a role in the context of heart diseases. Nevertheless, its function in cardiac fibroblasts, especially during the development of myocardial fibrosis, is still unknown. Due to the fact that RhoA is a strong regulator of the cytoskeleton and found to be involved in secretory processes, we investigated the effect of its lentivirus-induced knockdown in cardiac fibroblasts.

Downregulation of RhoA in neonatal rat cardiac fibroblasts (NRCF) by about 80%, changes the cell morphology towards an epithelial-like phenotype. This was accompanied by a disorganization of higher order actin structures including stress fibers and geodesic domes. In addition, focal adhesion sites were significantly smaller and more randomly distributed than in the respective control cells. Functionally, the knockdown of RhoA increased the adhesion velocity on plastic and collagen surfaces, especially within the first hour. On a molecular level, all actin cytoskeleton-associated proteins investigated were unchanged besides the myofibroblast marker smooth-muscle actin. By migration experiments it could also be shown that knockdown cells migrate significantly slower on a plane surface but interestingly faster through a porous membrane.

Moreover, in RhoA-depleted NRCF the fraction of acetylated tubulin, which is known to be involved in intracellular vesicle-dependent transport processes, was found elevated. In addition the Golgi network was smaller and more compact in knockdown cells. This data led to further investigation of secretory processes with focus on the profibrotic factor CTGF whose secretion was increased under basal conditions in RhoA knockdown cells. Since acetylated tubulin is a specific substrate of HDAC6, treatment of RhoA-depleted cells with the specific inhibitor Tubastatin A did not only increase the fraction of acetylated tubulin and rescue the Golgi structure but in accordance to our hypothesis also the quantity of secreted CTGF. Interestingly this could not be seen in control cells. Treatment of cardiac fibroblasts with Tubastatin A also significantly decreases proliferation rate.

Therefore we hypothesize that RhoA controls myofibroblast characteristics in cardiac fibroblast via remodeling and posttranslational modification of the cytoskeleton.

210

**Uptake of G protein activating *Pasteurella multocida* toxin into host cells**

**Jehle, Doris**; Aktories, Klaus; Orth, Joachim  
Universität Freiburg, Institut für Experimentelle Pharmakologie und Toxikologie, 1, Germany

*Pasteurella multocida* is a facultative pathogenic bacterium in the respiratory tract of animals. It produces the protein toxin PMT (*P. multocida* toxin), which is a major virulence factor of the organism. In pigs PMT induces the so called atrophic rhinitis characterized by rapid degradation of nasal turbinate bones. PMT is a 146 kDa AB-type toxin with the receptor binding and translocation domain at the N-terminus and the catalytic domain at the C-terminus of the protein. PMT leads to permanent activation of heterotrimeric G proteins of the  $G_{\alpha}$ ,  $G_{\alpha_{11}}$  and  $G_{\alpha_{2/13}}$  family by deamidation of a glutamine residue in the switch II region of the  $\alpha$ -subunit.

The knowledge concerning the uptake of PMT is not comprehensive. The toxin enters the cells via receptor-mediated endocytosis. Recently, it was reported that PMT interacts with phospholipids, e.g. sphingomyelin or phosphatidylcholine, on the membrane of eukaryotic cells (Brothers MC et al. 2011). However, no protein receptor was identified so far. Therefore, we performed pull-down experiments with PMT and identified a cell surface protein interacting specifically with the N-terminal part of PMT. This is in concordance with the AB-type domain model of PMT.

For a number of bacterial protein toxins a processing/cleavage during uptake was described to release the biological active portion into the cytosol. This cleavage depends on inherent protease domains of the toxin or cytosolic proteases. Incubating CaCo2 cells with  $^{125}$ I-labeled PMT revealed two toxin fragments with approximately 55 and 90 kDa. Using sortase-mediated site specific fluorescence labeling we identified the processed N- and C-terminal fragments of PMT and a potential cleavage region.

Our studies support the understanding of the uptake and translocation of PMT into host cell. Moreover, identification of the toxin's receptor may provide new therapeutic approaches.

211

**Detoxification of PAH dihydrodiolepoxides by glutathione conjugate formation in human small intestinal cells**

**John, Andrea**<sup>1</sup>; Hessel, Stefanie<sup>2</sup>; Lampen, Alfonso<sup>2</sup>; Seidel, Albrecht<sup>1</sup>

<sup>1</sup>Biochemisches Institut für Umweltcarcinogene, Prof. Dr. Gernot Grimmer Stiftung, Grosshansdorf, Germany

<sup>2</sup>Bundesinstitut für Risikobewertung, Lebensmittelsicherheit, Berlin, Germany

The continuous low level uptake of polycyclic aromatic hydrocarbons (PAH) in the general non-smoking population occurs mainly by contaminated food like grilled meat and smoked fish. PAH including the carcinogens benzo[a]pyrene (BP) and dibenzo[a,h]pyrene (DBP) are resorbed in the gastrointestinal tract and can be activated to the genotoxic metabolites BP-7,8-dihydrodiolepoxide (BPDE) and DBP-11,12-

dihydrodiolepoxide (DBPDE) which may be detoxified subsequently by glutathione (GSH) conjugation catalysed by various glutathione S-transferases.

Differentiated human intestinal Caco-2 cells were applied as a model system to further investigate the intestinal detoxification of the ultimate carcinogens BPDE and DBPDE. While in previous experiments cells were exposed to racemic PAH dihydrodiolepoxides (DH), in the present study racemic *anti*-BPDE or *anti*-DBPDE were used to avoid the stereoselective formation of the *R,S,S,R*-dihydrodiolepoxide (DE) enantiomer by CYP450 as precursor for GSH conjugation. Application of the Transwell™ system enabled to investigate the efflux direction of GSH conjugates which were subsequently measured in cell culture supernatants by LC-MS/MS.

While DH treatments had previously shown increasing GSH conjugate formation up to 48 hours, the maximum of GSH conjugate excretion after DE incubations was observed around 8 hours. However, for both sets of incubated metabolites (DH and DE) the ratio of the formed GSH conjugate diastereomers is very similar for both PAH. Differences in the direction of the transport of GSH conjugates formed from bay region BPDE and fjord region DBPDE were observed: BPDE conjugates were preferentially excreted into apical direction (in vivo the intestinal lumen side), whereas for DBPDE conjugates the basolateral efflux dominated (in vivo the blood stream side).

In conclusion, the ultimate carcinogens BPDE and DBPDE are detoxified in Caco-2 cells by glutathione S-transferases to form GSH conjugates which undergo subsequently an active transport out of the cells. The comparison of the results of DH with those of DE point to a high degree of stereoselectivity involved in the conjugation reaction and/or transport process. Interestingly not only the absolute stereochemistry of the GSH conjugate but also the parent PAH structure determines the particular excretion pathway of the formed GSH conjugates.

212

**Human butyrylcholinesterase isolated from plasma for analytical method development**

**John, Harald**<sup>1</sup>; Breyer, Felicitas<sup>2</sup>; Mizaikoff, Boris<sup>2</sup>; Schmidt, Christian<sup>1</sup>; Worek, Franz<sup>1</sup>; Thiermann, Horst<sup>1</sup>

<sup>1</sup>Bundeswehr Institute of Pharmacology and Toxicology, Munich, Germany

<sup>2</sup>University of Ulm, Institute of Analytical and Bioanalytical Chemistry, Germany

Organophosphorus compounds (OP) like nerve agents or pesticides covalently bind to butyrylcholinesterase (hBChE, EC 3.1.1.8) thus inhibiting this hydrolyzing enzyme. Consequently, hBChE is thought to become an effective scavenger useful for therapeutic treatment of OP poisoning and its corresponding OP adducts are valuable biomarkers for analytical verification purposes [1].

Therefore, related research requires the pure endogenous human enzyme that unfortunately is not commercially available from respective suppliers in an appropriate quality. Accordingly, a modified procedure primarily based on the findings of Lockridge et al. [2] and Saxena et al. [3] was developed to purify the enzyme from human citrate plasma as natural source.

Human hBChE was isolated from plasma by four consecutive chromatographic steps. Protein elution was monitored on-line by UV-detection (280 nm) and eluates of each purification step were fractionated continuously for off-line analysis of i) hBChE enzyme activity by Ellman assay, ii) protein purity by gel electrophoresis, and iii) protein identity by matrix-assisted laser desorption/ionization (MALDI) mass spectrometry and electronic MASCOT database search. Fractions of highest enzymatic activity were subjected to the next chromatographic step, respectively. A number of separated protein impurities were identified exhibiting chromatographic properties similar to hBChE. Finally, the enzyme was obtained in supreme purity thus enabling characterization of glycosylation and enzyme activity.

This material was used for *in vitro* incubation with diverse OP to establish a  $\mu$ -liquid chromatography-electrospray ionization tandem mass spectrometric method ( $\mu$ LC-ESI MS/MS) for detection of hBChE adducts. After reaction with OP, the protein was enzymatically cleaved by pepsin, ultrafiltered and subsequently chromatographed [4]. This bioanalytical method is a prerequisite for verification of poisoning in exposure scenarios.

[1] John et al., In: "Handbook of toxicology of Chemical Warfare Agents" (R. Gupta, ed.), Academic Press/Elsevier, Amsterdam (2009) 755-790

[2] Lockridge et al., *J. Med. Chem. Biol. Radiol. Def.* 3 (2005) 1-20

[3] Saxena et al., *Protein Express. Purif.* 61 (2008) 191-196

[4] Fiddler et al. *Chem. Res. Toxicol.* 15 (2002) 582-590

213

**Lysine residues essential for biological activity are phosphorylated by nerve agents: a mass spectrometric study on ubiquitin adducts**

**John, Harald**<sup>1</sup>; Schmidt, Christian<sup>1</sup>; Blum, Marc-Michael<sup>2</sup>; Breyer, Felicitas<sup>3</sup>; Worek, Franz<sup>1</sup>; Thiermann, Horst<sup>1</sup>

<sup>1</sup>Bundeswehr Institute of Pharmacology and Toxicology, Munich, Germany

<sup>2</sup>Organisation for the Prohibition of Chemical Weapons (OPCW), OPCW Laboratory, Rijswijk, Netherlands

<sup>3</sup>University of Ulm, Faculty of Natural Sciences, Germany

Organophosphorus compounds (OP) like pesticides and nerve agents are known to form protein adducts by phosphorylation of amino acid side chains *in vitro* and *in vivo*. Binding to the serine residue of the active site in acetyl- and butyrylcholinesterase is well defined for causing and monitoring of acute toxicity [1]. Modifications of tyrosine and serine

residues in albumin do not provoke toxicological effects but are valuable for post-exposure analysis [2]. OP adducts to ubiquitin (Ub), that is ubiquitously present in the extra- and intracellular space, were not described so far. We incubated Ub with V-type nerve agents (Chinese VX, Russian VX, VX) *in vitro* for analysis and identification of reaction products by matrix-assisted laser desorption/ionization mass spectrometry (MALDI MS) and  $\mu$ -liquid chromatography coupled to electrospray ionization ( $\mu$ LC-ESI MS) [3].

Mono-, di-, and triphosphorylated Ub molecules were detected indicating different reactive centres. Based on tryptic peptide mass fingerprint (PMF) as well as MALDI and ESI MS/MS analyses Ub was found to be modified at one tyrosine but surprisingly with much higher selectivity at lysine residues (K) that are essential for important regulatory processes (polyubiquitylation). At least 6 out of 7 K reacted with the nerve agents by nucleophilic substitution connecting the  $\epsilon$ -amino with the phosphoryl moiety of the OP. In addition, we also found that lysine phosphorylation induced consecutive intramolecular cyclization by formation of an isopeptide bond between the former modified  $\epsilon$ -amino group and the carboxylic side chain of an adjacent glutamic acid residue (E).

These results demonstrate that Ub in principle represents a possible target for nerve agent binding. This finding might be of relevance for either pathophysiological effects or biomonitoring of OP exposure. In fact, data on chemical reactivity with respect to amino acid selectivity as well as to consecutive reactions provide novel data enabling better understanding of the interaction between these poisons and endogenous proteins.

[1] John et al., In: "Handbook of toxicology of Chemical Warfare Agents" (R. Gupta, ed.), Academic Press/Elsevier, Amsterdam (2009) 755-790

[2] John et al. *Anal. Bioanal. Chem.* 398 (2010) 2677-2691

[3] Schmidt et al. *Anal. Bioanal. Chem.* (submitted)

## 214

### Determination of toxic tropane alkaloids in different biological matrices by MALDI-TOF MS(MS)

Schmidt, Christian<sup>1</sup>; Rychlik Michael<sup>2</sup>; Thiermann, Horst<sup>1</sup>; Worek, Franz<sup>1</sup>; **John, Harald<sup>1</sup>**  
<sup>1</sup>Bundeswehr Institute of Pharmacology and Toxicology, Munich, Germany  
<sup>2</sup>Technical University Munich, Analytical Food Chemistry, Germany

Herbal tea infusions and hot water extracts of leaves from jimson weed (*Datura stramonium*), of leaves and fruits from deadly nightshade (*Atropa belladonna*) as well as herbal tea infusions fortified with atropine and scopolamine often cause light to severe poisoning after accidental or intentional ingestion [1]. Therefore, selective analytical methods with toxicological and forensic relevance are required to prove the presence of these tropane alkaloids.

Matrix assisted laser desorption/ionization time-of-flight (MALDI-TOF) mass spectrometric methods are typically used for analysis of high molecular weight biomolecules e.g. proteins and peptides [2-4]. For the latter MS/MS methods are used to obtain sequence information. Intense MALDI-matrix signal background (e.g. of  $\alpha$ -cyanohydroxycinnamic acid, CHC) below  $m/z$  500 was seen as limiting factor for the determination of low molecular weight compounds (LMWC). Nevertheless, optimization of MALDI-matrix concentration as well as of spotting and ionization processes could unravel most challenges for determination of LMWC [5,6].

We used common CHC (1 mg/ml, ACN/0.1% TFA 80:20 v/v) as MALDI-matrix for MS(MS) determination of natural and synthetic tropane alkaloids (atropine, cocaine, homatropine, ipratropium, N-butylscopolamine, scopolamine) as it enables homogenous crystallization and consequently better reproducibility and access to automated measurements. To obtain optimum mass accuracy, spectra were calibrated by internal MALDI-matrix signals. For unambiguous determination of LMWC in different matrices (e.g. plant material, tea, mammalian plasma, beverages, etc.) MS/MS measurements were carried out allowing exact identification and comparison to fragment spectra libraries.

Due to ion suppression effects and in source decay, quantification by an external calibration curve even in the presence of an internal standard appeared inappropriate with respect to precision. To minimize effects of sample matrix we chose the standard addition method with d3-atropine as internal standard and an initial dilution step prior to sample preparation. Inter-experimental reproducibility (e.g. point-to-point and shot-to-shot signal) were highly improved when calculating the intensity ratio of analytes and internal standard.

We present detection limits of tropane alkaloids in different matrices and application of that MALDI method for semi-quantitative determination of tropane alkaloids in plants and herbal tea infusions in toxicologically relevant concentrations.

[1] John In: "LC-MS in drug bioanalysis" (QA. Xu, TL. Madden, eds.), Springer, NY, USA (2012) 287-348

[2] Machetjevass et al. *J. Chromatogr. B.* 803 (2004) 121-130

[3] John et al. *Anal. Biochem.* 362 (2007) 117-125

[4] John et al. *Anal. Bioanal. Chem.* 398 (2010) 2677-2691

[5] Persike, Karas *Rapid Commun. Mass Spectrom.* 23 (2009) 3555-3562

[6] Wang et al. *J. Chromatogr. A* 1216 (2009) 2169-2178

## 215

### High-resolution LC-MS Analysis of target cells treated with *Clostridium difficile* Toxins.

**Junemann, Johannes**

Institut für Toxikologie, Hannover, Germany

The anaerobic bacterium *Clostridium difficile* is one of the most common nosocomial pathogens and triggers antibiotic-associated gastrointestinal infections ranging from mild diarrhea to life-threatening pseudomembranous colitis. Toxins TcdA and TcdB are the

two major virulence factors of *C. difficile* that specifically glucosylate and inactivate small GTPases. The consequences are reorganization of the cytoskeleton, loss of cell-cell contacts, and finally cell death.

A comprehensive proteome analysis was conducted using Caco-2 cells that were treated for different time periods with wild type TcdA or mutant TcdA. Short (5 h) and long term (24 h) effects on the colonic proteome were analyzed using labelling with heavy stable isotopes. Proteins were fractionated by SDS-PAGE, and after tryptic digestion peptides were analyzed and quantified by LC-MS. Results were verified by western blot and MRM analysis. The activity of clostridial glucosylating toxins was evaluated *in vivo* by identification of their target GTPases and determination of their glucosylation rate.

Wild type TcdA induced considerable changes in the protein profile of colon cells. More than 800 proteins of the over 6000 identified proteins were altered in their abundance. Higher abundant proteins were involved in regulation, metabolic processes, respiratory chain complexes, endocytosis, and organelle function. Less abundant proteins participate in cell-cycle, translation, cytoskeleton organisation, and RNA binding. Glucosyltransferase deficient TcdA induces only changes after short incubation periods. Regulation of several proteins was confirmed by western blot and MRM analysis. Besides the known targets RhoA, RhoC, and RhoG of TcdA, glucosylation was also identified in Rap1(A/B), Rap2(A/B/C), Ral(A/B), and (H/K/N)Ras which had not been considered as TcdA targets before. This proteome analysis demonstrates that TcdA affects several cellular processes that have not been considered before to be affected by clostridial glucosylating toxins.

Based on the SILAC method we developed a technique to quantify the glucosylation extend of modified small GTPases using an internal standard of proteins labeled by heavy stable isotopes. Kinetic and dose response correlations will be determined to analyze glucosylation in detail in colonic cells.

## 216

### Elevated oxygen tension enhances the toxicity of diquat and paraquat in A549 human lung adenocarcinoma cells and L929 mouse fibroblasts

**Juretschke, Christian**; Hopfer, Christine; Mückter, Harald; Gudermann, Thomas  
 Walther-Straub-Institut, Toxikologie, München, Germany

**Introduction:** Diquat (DQ) and paraquat (PQ) are potent rsin-fast herbicides, which are being used worldwide. Both are bipyridyl molecules, but in spite of their structural similarities their toxicity *in vivo* and *in vitro* is different. At present, there is no antidote available. A proposed mechanism of PQ and DQ toxicity is the production of reactive oxygen species (ROS), which may eventually lead to cell death. We have studied the effect of different oxygen levels on the toxicity in cultured cells.

**Materials & Methods:** The toxicity of both herbicides was assessed in two different cell lines by measuring cell viability, metabolic activity and glutathione levels. We exposed human lung adenocarcinoma cells (A549) and mouse fibroblasts (L929) to various concentrations of DQ and PQ. Cellular glutathione (GSX – measured with the Tietze assay) and formazan formation (measured with the XTT assay) were used to assess the metabolic activity of the cells. Cell viability was determined with trypan blue (a marker of membrane integrity). For the exposure to oxygen we employed an *in-vitro* exposure apparatus described previously [1].

**Results:** In both cell lines, DQ was more toxic than PQ. The half-maximal effective concentrations (EC<sub>50</sub>) are shown in Table 1. After exposure for 24 h the herbicides were removed and fresh Dulbecco's Modified Eagle Medium (DMEM) added to study the recovery of cells. At >1.8 mM (DQ) and >5.9 mM (PQ) in A549 cells there was no recovery. L929 cells reacted in a same way, the critical concentrations being >0.2 mM for DQ and >1.3 mM for PQ.

At 95% oxygen for 16 h, the DQ/PQ-exposed cells had lower GSX levels as compared to cells cultured in ambient air (Table 2). Cell viability was also lower in the exposed cells, especially for DQ. Both cell lines reacted similarly. The XTT assay supported the previous described results.

**Conclusions:** The enhanced toxicity of both DQ and PQ at elevated oxygen tension appears to be a general feature of viologen poisoning, which may affect pulmonary and non-pulmonary cells in a similar way. Breathing pure oxygen – the often applied remedy in respiratory distress situations – may be a poor choice for victims of DQ and PQ poisoning.

[1] Mückter H et al. (1998) *J Pharmacol Toxicol Meth*, 40: 63-69

	toxicant	ambient	high	ambient	high
		oxygen level	oxygen level	oxygen level	oxygen level
		A549	A549	L929	L929
EC <sub>50</sub>	DQ	2.4 mM ± 1.2		0.5 mM ± 0.4	
EC <sub>50</sub>	PQ	6.3 mM ± 4.0		2.4 mM ± 1.7	

**Table 1:**  
Cytotoxicity of DQ and PQ at different oxygen tension (XTT method)

	toxicant	ambient	high	ambient	high
		oxygen level	oxygen level	oxygen level	oxygen level
		A549	A549	L929	L929
GSX	DQ	27.4±9.8	13.3±2.3	15.4±2.6	13.2±1.3
GSX	PQ	44.6±7.4	36.8±5.6	23.4±0.4	20.1±3.7

**Table 2:**  
Cellular glutathione after exposure to DQ or PQ

217

### Oxidant-induced activation of cGMP-dependent protein kinase Ia contributes to neuropathic pain processing after nerve injury

**Kallenborn-Gerhardt, Wiebke**<sup>1</sup>; Lorenz, Jana Elena<sup>1</sup>; Lu, Ruirui<sup>1,2</sup>; Eaton, Philip<sup>3</sup>; Geisslinger, Gerd<sup>1,4</sup>; Schmidtke, Achim<sup>1,2</sup>

<sup>1</sup>Institut für Klinische Pharmakologie, Klinikum der Johann Wolfgang Goethe-Universität, Frankfurt, Germany

<sup>2</sup>Institut für Pharmakologie und Toxikologie, Universität Witten/Herdecke, Germany

<sup>3</sup>Cardiovascular Division, King's College London, Great Britain

<sup>4</sup>Fraunhofer Institute for Molecular Biology and Applied Ecology, Project Group Translational Medicine and Pharmacology (IME-TMP), Frankfurt, Germany

Lesions or damage to the peripheral or central nervous system induce changes in the nociceptive system that are often accompanied with neuropathic pain. Treatment of neuropathic pain can be difficult with only 40-60% of patients achieving potential pain relief. Several signaling pathways have been identified that are involved in the processing of pain. Recent data indicate that oxidants such as hydrogen peroxide exert specific signaling functions during the processing of neuropathic pain. However, the mechanisms by which oxidants regulate pain processing *in vivo* remain poorly understood. Here, we show that cGMP-dependent protein kinase Ia (cGKIa), which can be activated by oxidants independently of cGMP, serves as a primary redox target in sensory neurons. After peripheral nerve injury, oxidant-induced cGKIa activation is increased in dorsal root ganglia of mice. cGKIa knock-in mice, in which the oxidant mediated activation of cGKIa is blocked, demonstrated reduced neuropathic pain behavior after injury to peripheral nerves, while acute nociceptive, inflammatory, and cGMP-induced pain behaviors were not impaired in these mice. Our results suggest that oxidant-induced activation of cGKIa specifically contributes to neuropathic pain processing *in vivo*. Prevention of cGKIa redox activation could be a potential novel strategy to manage neuropathic pain.

**Acknowledgements:** This work was supported by the Deutsche Forschungsgemeinschaft (SFB815-A14) and in part by LOEWE-Schwerpunkt "Anwendungsorientierte Arzneimittelforschung".

218

### ADP receptor-mediated cellular responses in vascular endothelium, signal transduction via endogenous hydrogen peroxide.

**Kalwa, Hermann**; Sartoretto, Juliano; Romero, Natalia; Michel, Thomas

Brigham and Women's Hospital, Cardiovascular Medicine Division, Boston, United States

ADP activates a family of cell surface receptors that modulate signaling pathways in a broad range of cells. ADP receptor antagonists are widely used to treat cardiovascular disease states. Here we identify a novel role for the stable reactive oxygen species hydrogen peroxide (H<sub>2</sub>O<sub>2</sub>) in mediating cellular responses activated by the G protein-coupled P2Y1 receptor for ADP. We found that ADP-dependent phosphorylation of key endothelial signaling proteins— including endothelial nitric oxide synthase, AMP-activated protein kinase and the actin-binding MARCKS protein— was blocked by pre-incubation with PEG-catalase, which degrades H<sub>2</sub>O<sub>2</sub>. ADP treatment promoted the H<sub>2</sub>O<sub>2</sub>-dependent phosphorylation of c-Abl, a non-receptor tyrosine kinase that modulates the actin cytoskeleton. Cellular imaging experiments using fluorescence resonance energy transfer-based biosensors revealed that ADP-stimulated activation of the cytoskeleton-associated small GTPase Rac1 was independent of H<sub>2</sub>O<sub>2</sub>. However, Rac1-dependent activation of AMPK, the signaling phospholipid PIP<sub>2</sub>, and the c-Abl-interacting protein Crkl are mediated by H<sub>2</sub>O<sub>2</sub>. We transfected endothelial cells with differentially-targeted HyPer2 H<sub>2</sub>O<sub>2</sub> biosensors, and found that ADP promoted a marked increase in H<sub>2</sub>O<sub>2</sub> levels in the cytosol and caveolae, and a smaller increase in mitochondria. We performed a screen for P2Y1 receptor-mediated receptor tyrosine kinase transactivation, and discovered that ADP transactivates Flt-3, a receptor tyrosine kinase expressed in these cells. Our observation that P2Y1 receptor-mediated responses involve Flt-3 transactivation may identify a new mechanism whereby cancer chemotherapy with receptor tyrosine kinase inhibitors promotes vascular dysfunction. Taken together, these findings establish a critical role for endogenous H<sub>2</sub>O<sub>2</sub> in control of ADP-mediated signaling responses in the vascular wall.

219

### Comparison of three different growth media for *C. elegans* with respect to their suitability for toxicity tests with Copper and Cadmium.

**Kamalakkannan, Shyam Sundar**; Sacher, Beate; Glahn, Felix; Foth, Heidi  
Martin-Luther-Universität, Institut für Umwelttoxikologie, Halle / Saale, Germany

*C. elegans* is the first multicellular organism to have its Genome completely sequenced. It is a transparent nematode, about 1 mm in length that lives in temperate soil environments. It is comparatively easy to grow, to maintain and to handle these worms in laboratory. The Average Lifespan of these worms is about 2 – 3 Weeks and thus shorter than that of commonly used animals in toxicological analysis, which adds to its advantages. The Effects can also be monitored easily in it when compared with other animal Toxicity experiments.

Cadmium (Cd) is known as wide spread environmental contaminant. Copper (Cu), despite being a vital trace metal, can also induce toxic effects through induction of

oxidative stress at higher concentrations. Cd and Cu were used as model compounds to optimize commonly used protocols for toxicity tests on *C. elegans*. Our aim was to find sensitive but robust endpoints for toxicity tests.

We compared three different growth media for *C. elegans*, Nematode Growth Medium (NGM), S – Medium and K – Medium, in order to find the medium most suitable for toxicity tests with heavy metals. In all three media the effects of Cd and Cu on the viability of *C. elegans* were analyzed and compared.

From our study we could identify that K-Medium is most suitable for toxicity tests on *C. elegans* with heavy metals. NGM does not seem to be appropriate as it shows formation of precipitates upon addition of heavy metals.

The worms were exposed to various concentrations of Cd and Cu in K-Medium as acute and sub-chronic exposures for 24 - 96 h. After 24 h of exposure to 356 µM of Cd, the viability of the worms was reduced to 98 %. Whereas, after the same time of exposure to 1007 µM of Cu, the viability of the worms was reduced to 94 %. This data shows that the acute exposure to Cd and Cu does not have a strong effect on the viability of the worms. After 96 h of exposure to 285 µM of Cd, the viability of the worms was reduced to 52 %. Whereas, after the same time of exposure to 63 µM of Cu, the viability of the worms was reduced to 42 %. So apparently Cu has a higher sub-chronic toxicity in *C. elegans* than Cd.

220

### Do presynaptic cannabinoid CB<sub>1</sub> receptors play a role in the inhibition of the neurogenic vasopressor response induced by transverse aortic constriction in pithed rats?

**Karabowicz, Piotr**<sup>1</sup>; Schlicker, Eberhard<sup>2</sup>; Toczek, Marek<sup>1</sup>; Malinowska, Barbara<sup>1</sup>

<sup>1</sup>Medical University of Białystok, Department of Experimental Physiology and Pathophysiology, Poland

<sup>2</sup>University of Bonn, Institute of Pharmacology and Toxicology, Germany

During acute heart failure, sympathetic activation accompanied by noradrenaline release is a prominent cause of arrhythmias and cardiac dysfunction. The aim of our study was to examine the influence of acute heart failure on the neurogenic vasopressor response.

Experiments were performed on pithed and vagotomized rats. Increases in systolic blood pressure (SBP) were induced 4 times (S<sub>1</sub>-S<sub>4</sub>) by electrical stimulation (0.75 Hz, 1 ms, 50 mV, 5 impulses) of preganglionic sympathetic nerve fibers innervating resistance vessels or by intravenous injection of phenylephrine (10 nmol/kg). Acute heart failure was elicited by transverse aortic constriction (TAC) immediately after S<sub>1</sub>. Basal SBP before S<sub>1</sub> was 68.2±1.5 mmHg (n=28). It was increased (S<sub>1</sub>) by 43.1±2.2 (n=16) and 47.5±4.4 mmHg (n=12) by electrical and chemical stimulation, respectively. TAC or vasopressin infusion (in sham operated rats) elevated basal SBP to 185.4±4.5 mmHg (n=16) and 174.7±4.1 (n=12), respectively. The electrically-stimulated increases in SBP (S<sub>2</sub>-S<sub>4</sub> applied 15 min after TAC in 10 min intervals) were reduced by about 60% in TAC but not in sham operated rats. The phenylephrine-induced vasopressor responses during S<sub>2</sub>-S<sub>4</sub> were changed neither in TAC nor in sham operated rats. In subsequent experiments the cannabinoid receptor CB<sub>1</sub> antagonist AM251 (0.3 and 3 µmol/kg) or the cannabinoid receptor agonist CP55940 (1 µmol/kg), the antagonist of α<sub>2</sub>-adrenergic receptors, rauwolfscine (0.1 µmol/kg) and the inhibitor of the norepinephrine transporter, desipramine (0.1 µmol/kg) were administered 5 minute before S<sub>1</sub>. None of the above compounds modified the inhibitory effect of TAC on the neurogenic vasopressor response.

In conclusion acute heart failure induced by transverse aortic constriction inhibits vasopressor responses via presynaptic mechanism(s), however, presynaptic cannabinoid CB<sub>1</sub> and α<sub>2</sub>-adrenergic receptors and the norepinephrine transporter are not involved. Thus, the precise mechanism(s) remain(s) to be established.

221

### Characterization of uptake and efflux transporters in fresh isolated and cryopreserved primary hepatocytes of different species by using radiolabeled substrates

**Keiser, Markus**<sup>1</sup>; Ullrich, Anett<sup>2</sup>; Jia, Jia<sup>1,2</sup>; Patrzyk, Maciej<sup>3</sup>; Busemann, Alexandra<sup>3</sup>; Heidecke, Claus-Dieter<sup>2</sup>; Siegmund, Werner<sup>1</sup>; Runge, Dieter<sup>2</sup>

<sup>1</sup>University Medicine of Greifswald, Department of Clinical Pharmacology, Germany

<sup>2</sup>PRIMACYT Cell Culture Technology GmbH, Schwerin, Germany

<sup>3</sup>University Medicine of Greifswald, Department of Surgery, Germany

Primary mammalian hepatocytes are used for several *in vitro* applications like testing of drug metabolism, toxicity and transporter assays. However, little is known about species-specific differences in the activity of uptake and efflux transporter or the effect of cryopreservation on transport kinetics. Therefore, we characterized the uptake and the efflux transport of different substrates in fresh isolated or cryopreserved hepatocyte cultures of different species.

Human, rat, dog and monkey hepatocytes were incubated in serum free media. Two days after cell isolation or after thawing (only monkey and dog) a concentration dependent uptake of [<sup>3</sup>H]- estrone-3-sulfate (E<sub>3</sub>S) was measured in presence or absence of bromosulfophthaleine (BSP) using liquid scintillation counting. To measure the efflux activity of P-glycoprotein (P-gp) and multidrug resistance protein (MRP) 2 mediated in human, dog and monkey hepatocytes cells were incubated shortly with [<sup>3</sup>H]-talinalolol (Tal) or [<sup>3</sup>H]-estradiol-17β-glucononide (E17β-Gln), respectively. Intracellular concentration of Tal and E17β-Gln were measured after 5 – 120 minutes in presence or absence of the P-gp inhibitor PSC833 or the MRP2 inhibitor MK571.

E<sub>1</sub>S revealed high affinity to human ( $K_m = 14.6 \mu\text{mol/l}$ ;  $V_{\text{max}} = 913 \text{ pmol/mg} \times \text{min}$ ), monkey ( $K_m = 6.2 \mu\text{mol/l}$ ;  $V_{\text{max}} = 220 \text{ pmol/mg} \times \text{min}$ ), dog ( $K_m = 75.6 \mu\text{mol/l}$ ;  $V_{\text{max}} = 2.847 \text{ pmol/mg} \times \text{min}$ ) and rat hepatocytes ( $K_m = 14.2 \mu\text{mol/l}$ ;  $V_{\text{max}} = 124 \text{ pmol/mg} \times \text{min}$ ) and was inhibited in the presence of BSP. Cryopreserved cells showed significant differences in  $V_{\text{max}}$ -values of E<sub>1</sub>S uptake in monkey hepatocytes.

In human hepatocytes, Tal efflux was decelerated in cells incubated with PSC833 while MK571 had no effect on MRP2 mediated efflux of E17 $\beta$ -Gln. While monkey hepatocytes showed a decelerated efflux of Tal and E17 $\beta$ -Gln in the presence of PSC833 and MK571, dog hepatocytes showed only a decelerated efflux of E17 $\beta$ -Gln in cells incubated with MK571 while PSC833 had no effect on P-gp mediated efflux of Tal. When compared with fresh hepatocytes, cryopreserved cells showed no differences on efflux transport in monkey and dog hepatocytes.

E<sub>1</sub>S is a suitable substrate to verify the functionality of uptake transporters in freshly primary hepatocytes of humanoids, rats and dogs. P-gp mediated transport can be verified with Tal in human and monkey hepatocytes and MRP2 efflux can be verified in dog hepatocytes using E17 $\beta$ -Gln as a substrate. Moreover, cryopreservation had almost no effect on transport kinetics in monkey and dog hepatocytes.

This work was supported by the Ministry of Economy, Labor and Tourism of Mecklenburg-Vorpommern (Grant V630-F-108-2011/040 and V630-S-108-2011/039).

## 222

### Comparative BAL analysis and histopathology of the lower respiratory tract after inhalation exposure to nano CeO<sub>2</sub> in a 5-day and 28-day rat study

Keller, Jana<sup>1</sup>; Groeters, Sibylle<sup>1</sup>; Küttler, Karin<sup>1</sup>; Ma-Hock, Lan<sup>1</sup>; Volker, Straus<sup>1</sup>; Wiench, Karin<sup>2</sup>; van Ravenzwaay, Bennard<sup>1</sup>; Landsiedel, Robert<sup>1</sup>

<sup>1</sup>BASF SE, Experimentelle Toxikologie und Ökologie, Ludwigshafen am Rhein, Germany  
<sup>2</sup>BASF SE, Produktsicherheit, Ludwigshafen am Rhein, Germany

CeO<sub>2</sub> nanoparticles are widely used for biomedical, commercial and industrial applications. To assess hazard potential of air-born CeO<sub>2</sub> nanoparticles, CeO<sub>2</sub> (NM212), an OECD depository material, is tested in a combined chronic and carcinogenicity long-term inhalation study (OECD TG 453) in rats within the framework of the EU-project NanoREG.

As a preparation work for the long-term inhalation study, 5-day and 28-day studies were performed in female rats. The rats were whole-body exposed to 0.5, 5 and 25 mg/m<sup>3</sup> CeO<sub>2</sub> for 6 h/d, 5 d/week for 1 and 4 weeks in the 5- and 28-day studies, respectively. A variety of biological endpoints were examined including broncho-alveolar lavage (BAL) and histopathology immediately after exposure and after an exposure free period of three or four weeks.

In the 5-day and the 28-day studies, a concentration-related increase of biochemical and cytological parameters (e.g. polymorph nuclear neutrophils, PMN) were observed in BAL fluid. These findings indicate a moderate inflammation in the lung after inhalation exposure. Consistent to the BALF results, increased absolute and relative lung weights and concentration-related histological changes in the lungs and lung-associated lymph nodes were observed. The histological effects were alveolar histiocytosis, granulomatous inflammation in the lung, and macrophage aggregates with particles in bronchial-associated lymphoid tissue and lung associated lymph nodes. The 5-day study resulted in consistent findings with lower severity and incidences. The outcomes of the 5-day study contribute to the EU-project NanoMILE. The no observed adverse effect levels (NOAEL) for CeO<sub>2</sub> is 0.5 mg/m<sup>3</sup> in both 5- and 28-day studies.

## 223

### Reduction of survival and development of cardiac hypertrophy by G<sub>12</sub> deficiency in $\beta_1$ -adrenoceptor overexpressing mice

Keller, Kirsten<sup>1</sup>; Maaß, Martina<sup>2</sup>; Dizayee, Sara<sup>1</sup>; Müller-Ehmsen, Jochen<sup>2</sup>; Birnbaumer, Lutz<sup>2</sup>; Engelhardt, Stefan<sup>1</sup>; Herzig, Stefan<sup>1</sup>; Matthes, Jan<sup>1</sup>

<sup>1</sup>Universität zu Köln, Institut für Pharmakologie, Germany

<sup>2</sup>Uniklinik Köln, Klinik III für Innere Medizin, Germany

<sup>3</sup>NIH, Transmembrane Signaling Group, North Carolina, United States

<sup>4</sup>Technische Universität München, Institut für Pharmakologie und Toxikologie, Germany

**Background:**  $\beta$ -blockers are an essential part of heart failure therapy, e.g. aiming at prevention of detrimental cardiac overstimulation due to increased catecholamine levels. While  $\beta_1$ -adrenoceptors exclusively couple to stimulatory G<sub>s</sub> proteins,  $\beta_2$ -adrenoceptors have been shown to couple to inhibitory G<sub>i</sub> proteins, too. In a mouse model of  $\beta_2$ -adrenergic overexpression additional G<sub>12</sub>-knockout led to severely impaired survival times indicating a protective role for G<sub>12</sub> (Förster et al., Proc Natl Acad Sci 2003;100:14475-80). In the current study we investigate the role of G<sub>12</sub> in mice overexpressing the human  $\beta_1$ -adrenoceptor, i.e. a heart failure model not directly affecting the G<sub>s</sub>-signaling cascade.

**Methods:** Crossbreeding of mice with cardiac overexpression of the human  $\beta_1$ -adrenoceptor ( $\beta_1$ -tg) with mice deficient for G<sub>12</sub> (G<sub>12</sub>-k.o.) generated the desired genotype ( $\beta_1$ -tg/G<sub>12</sub>-k.o.). Mean survival time was calculated by Kaplan-Meier estimation and compared to wildtype mice (wt) and littermates with either  $\beta_1$ -adrenoceptor overexpression ( $\beta_1$ -tg) or G<sub>12</sub>-deficiency (G<sub>12</sub>-k.o.), respectively. At an age of 307 $\pm$ 13 days mice were examined by echocardiography and subsequently killed. Ventricle/body weight ratio was compared by ANOVA followed by LSD-analysis. Ventricular tissue was immediately frozen and stored for qPCR analysis.

**Results:** Log-rank test revealed a significantly decreased survival of double-transgenic mice compared to all other genotypes (in days (mean $\pm$ sd):  $\beta_1$ -tg/G<sub>12</sub>-k.o. 356 $\pm$ 42, n=37;

wt 668 $\pm$ 60, n=201;  $\beta_1$ -tg 561 $\pm$ 39, n=196; G<sub>12</sub>-k.o. 511 $\pm$ 66, n=45; p<0.05). Furthermore,  $\beta_1$ -tg/G<sub>12</sub>-k.o. showed a significantly increased ventricle/body weight ratio, indicating ventricular hypertrophy (in % (mean $\pm$ sd):  $\beta_1$ -tg/G<sub>12</sub>-k.o. 0.7 $\pm$ 0.1, n=7; wt 0.47 $\pm$ 0.08, n=10;  $\beta_1$ -tg 0.44 $\pm$ 0.04, n=14; G<sub>12</sub>-k.o. 0.50 $\pm$ 0.03, n=13; p<0.05). Preliminary analysis of echocardiographic recordings confirms cardiac hypertrophy and dysfunction.

**Summary:** Despite there is no direct coupling of  $\beta_1$ -adrenoceptors to G<sub>i</sub> proteins lack of G<sub>12</sub> caused a significant reduction of survival time and a significant ventricular hypertrophy in  $\beta_1$ -transgenic mice ( $\beta_1$ -tg/G<sub>12</sub>-k.o.) compared to mice with either G<sub>12</sub> deficiency or cardiac  $\beta_1$ -adrenoceptor overexpression. This confirms earlier findings indicating a (cardio-) protective role for G<sub>12</sub> even in a context of a G<sub>s</sub>-independent hypertrophic stimulus. Our data promote the idea that G<sub>12</sub> upregulation as observed in human heart failure might be adaptive and beneficial.

## 224

### The herbal preparation, STW 5, protects against radiation-induced intestinal mucositis.

Khayyal, Mohamed T.<sup>1</sup>; Abdel-Aziz, Heba<sup>2</sup>; El-Ghazaly, Mona A.<sup>3</sup>; Abdel-Naby, Doaa H.<sup>3</sup>; El-Hazek, Rania<sup>3</sup>

<sup>1</sup>Faculty of Pharmacy, Cairo University, Department of Pharmacology, Kairo, Egypt

<sup>2</sup>Steigerwald Arzneimittelwerk GmbH, Wissenschaftliche Abteilung, Darmstadt, Germany

<sup>3</sup>National Centre for Radiation Research & Technology, Department of Pharmacology, Cairo, Egypt

Intestinal mucositis is a common side-effect in patients undergoing radiotherapy<sup>1</sup>. The search for agents that prevent radiation-induced mucositis may offer new therapeutic strategies for maintaining intestinal mucosal integrity in such patients. Pathogenesis of mucositis involves production of pro-inflammatory cytokines and reactive oxygen metabolites<sup>2,3</sup> and increased apoptosis in intestinal epithelium. STW 5 is an herbal multi-component preparation with potent anti-oxidant and anti-inflammatory properties in intestinal inflammatory disorders<sup>4,5</sup>, making it an attractive candidate to study its potential usefulness in mucositis. Intestinal mucositis was induced experimentally in rats by exposing them to whole body irradiation from a Caesium <sup>137</sup> source at a radiation dose of 6 Gray. Three days later, rats developed intestinal mucositis, judged by histological examination of the small intestine and derangement of associated parameters in intestinal homogenates and serum. STW5 was given orally for 5 days to rats in graded doses of 2 – 10 ml/kg before exposing them to radiation and continued for 3 days after exposure. Pretreatment with STW 5 led to dose-dependent reduction in histological changes. Histologically, irradiation caused shortening and fusion of villi, activation of mucus secreting glands, inflammatory cell infiltration of lamina propria and mucosal atrophy. Inflammation markers: tumor necrosis factor and myeloperoxidase activity in homogenates were also raised. The changes were associated with a rise in thiobarbituric acid reactive substances, reduction in glutathione and in protein content of intestinal homogenates. Biomarkers of intestinal tissue injury: plasma diamineoxidase was raised while citrulline<sup>6</sup> was significantly reduced. Apoptosis was evidenced by a rise in cytosolic calcium, depletion of mitochondrial cytochrome c and B-cell lymphoma 2. Most histological changes and associated derangement in the parameters tested were largely prevented by STW 5. The findings pave the way to a new therapeutic approach in management of radiation induced mucositis.

<sup>1</sup>Costa G and Donaldson SS (1979) N Engl J Med 300, 1471–1474, <sup>2</sup>MacNaughton WK (2000) Aliment Pharmacol Ther. 14, 523-528, <sup>3</sup>Linard C et al (2003) Am J Physiol Gastrointest Liver Physiol. 285, 556-565, <sup>4</sup>Khayyal MT et al (2006) Phytomedicine. 13 Suppl 5, 56-66, <sup>5</sup>Schempp H et al (2006) Phytomedicine. 2006;13 Suppl 5, 36-44 <sup>6</sup>Lutgens L and Lambin P (2007) World J. Gastroenterol., 13, 3033 – 3042

## 225

### AMP-activated kinase (AMPK) and its role in (inflammatory) pain

King, Tanya Sarah<sup>1</sup>; Russe, Otto; Möser, Christine; Geisslinger, Gerd; Niederberger, Ellen

Institut für Klinische Pharmakologie, Universitätsklinikum Frankfurt am Main, Germany

The AMP-activated kinase (AMPK) is a cellular energy sensor which is activated by an increase in the intracellular AMP-concentration occurring after ATP-consuming processes. When activated, AMPK regulates a number of cellular functions including metabolism of glucose and lipids and resolution of inflammation. Our previous work as well as recent publications showed that activation of AMPK also leads to anti-nociceptive effects which are at least partially based on modulation of signal transduction mechanisms in the spinal cord. Recently, it has been shown that salicylic acid is able to modulate AMPK activity. In our contemporary project we intend to investigate if AMPK is generally affected by NSAIDs and contributing to their anti-inflammatory and anti-nociceptive activity.

So far, effects of AMPK were mostly investigated after pharmacological activation. However, activation of AMPK has also been described in response to modulation of certain life conditions, e.g. increase of exercise/training or reduction of food-uptake. Furthermore, AMPK activity can be influenced by age or gender. We are investigating the effects of physiological AMPK modulation on inflammatory nociception. We have established models for exercise and calorie reduction and could already show modulation of AMPK activation and the nociceptive behavior in young vs old mice and mice that had access to food ad libitum vs mice that were on a diet.



Russe OQ, et al. Activation of the AMP-activated protein kinase reduces inflammatory nociception. *J Pain*. 14(11):1440-40, 2013  
 Hawley SA, et al. The ancient drug salicylate directly activates AMP-activated protein kinase. *Science*. 336(6083):918-22, 2012

226

#### A generic system for increased expression and stabilization of G protein-coupled receptors by directed evolution

**Klenk, Christoph**; Ehrenmann, Janosch; Plückthun, Andreas  
 Universität Zürich, Biochemisches Institut, Switzerland

Most G protein-coupled receptors (GPCRs) are difficult to express and exhibit low protein stability after solubilization. Thus, GPCRs remain one of the most challenging class of proteins to conduct structural and biophysical studies. To overcome these limitations, we have recently developed a directed evolution method for high functional GPCR expression and simultaneous thermo-stabilization based on periplasmic expression of randomized receptors in *E. coli* and subsequent selection of highly expressing variants using fluorescent ligands and flow cytometry. With this evolutionary approach key residues within the receptor sequence can be rapidly identified which are responsible for improved biophysical properties without greatly affecting the pharmacological features of the receptor. However, so far this technology was limited by the availability of small and specific fluorescent ligands for a specific receptor. Here we present a novel system to evolve GPCRs for improved expression and stability without the need for specific fluorescent ligands. We have engineered a fluorescence-activating module based on Designed Ankyrin Repeat Proteins (DARPs) which specifically bind and activate a small fluorogen. When fused to the N-terminal domain of a GPCR these modules are targeted to the periplasmic space after correct insertion of the receptor into the membrane, thus allowing direct measurements of functional receptor expression in *E. coli*. Combining this technology with our directed evolution approach we were able to evolve GPCRs from highly diverse libraries without any specific ligand for each receptor. With this generic approach receptors with poor expression properties for which no or only ligands with poor pharmacokinetic properties are available can now easily be evolved for increased expression and protein stability.

Sarkar CA, Dodevski I, Kenig M, Dudli S, Mohr A, Hermans E, Plückthun A. Directed evolution of a G protein-coupled receptor for expression, stability, and binding selectivity. *Proc Natl Acad Sci U S A*. 2008  
 Schlinkmann KM, Hillenbrand M, Rittner A, Künz M, Strohn R, Plückthun A. Maximizing detergent stability and functional expression of a GPCR by exhaustive recombination and evolution. *J Mol Biol*. 2012

227

#### Differential Regulation of PP1-Mediated Somatostatin Receptor Dephosphorylation by $\beta$ -Arrestin1 and 2

**Kliwer, Andrea**; Petrich, Aline; Pöll, Florian; Schulz, Stefan  
 Jena University Hospital - Friedrich Schiller University Jena, Department of Pharmacology and Toxicology, Germany

**Background:** Desensitization of G protein-coupled receptors (GPCRs) signaling is essential for the maintenance of cellular homeostasis. For many GPCRs, agonist-dependent regulation involves the coordinated phosphorylation of a series of serine and threonine residues within the carboxyl-terminal tail of the receptor. This phosphorylation facilitates binding of  $\beta$ -arrestins, which in turn mediate desensitization of G protein-dependent signaling. In addition,  $\beta$ -arrestins serve as a scaffold to facilitate receptor internalization and to initiate a second wave of signaling. Although the mechanisms of agonist-induced phosphorylation have been deciphered for many GPCRs, the regulation of their dephosphorylation remains poorly understood.

**Methods:** Here, we have used a combination of phosphosite-specific antibodies, chemical protein phosphatase inhibitors and siRNA knock down screening to identify catalytic and regulatory subunits of protein phosphatase 1 (PP1) as GPCR phosphatase that catalyzes dephosphorylation of the  $ss_2$  and  $ss_5$  somatostatin receptors.

**Results:** We have identified protein phosphatase 1 $\beta$  (PP1 $\beta$ ) as GPCR phosphatase for rapid dephosphorylation of the  $ss_2$  and PP1 $\gamma$  for the  $ss_5$  receptor. Dephosphorylation is initiated directly after receptor activation at or near the plasma membrane. We also show that  $ss_2$  and  $ss_5$  receptors differ substantially in the temporal dynamics of their dephosphorylation and trafficking patterns. As a functional consequence of diminished PP1 $\beta$  activity, we have found that somatostatin-induced ERK activation was aberrantly enhanced and prolonged. In addition, we show that PP1 $\beta$  and  $\beta$ -arrestin1 exist as constitutive complex that mediates rapid dephosphorylation of  $ss_2$  receptor at or near the plasma membrane. By contrast,  $\beta$ -arrestin2 is not essential for rapid  $ss_2$  receptor dephosphorylation.

**Conclusion:** This different phosphatase specificity has in turn profound consequences for the dephosphorylation dynamics and trafficking patterns of GPCRs. We demonstrate a novel mechanism for fine tuning unconventional  $\beta$ -arrestin-dependent GPCR signaling in that recruitment of PP1 $\beta$  to activated GPCRs facilitates dephosphorylation and, hence, leads to disruption of the  $\beta$ -arrestin-GPCR complex. Furthermore, our findings reveal a novel scaffolding function of  $\beta$ -arrestin1 that facilitates efficient targeting of PP1 $\beta$  to phosphorylated GPCRs.

**Significance:** Rapid dephosphorylation by the  $\beta$ -arrestin1/PP1 $\beta$  complex or PP1 $\gamma$  is required for receptor resensitization and termination of  $\beta$ -arrestin signaling.

Pöll, F., Doll, C., and Schulz, S. (2011) *J Biol Chem* 286(38), 32931-32936.  
 Petrich, A., Mann, A., Kliwer, A., Nagel, F., Strigli, A., Märten, J. C., Pöll, F., and Schulz, S. (2013) *Mol Endocrinol* 27(4), 671-682.  
 Kliwer, A., and Schulz, S. (2013) *Naunyn-Schmiedeberg's Arch Pharmacol* (accepted).

228

#### Hepatotoxic combination effects of triazole fungicides in-vivo and in HepG2 cells

**Knebel, Constanze**; Heise, Tanja; Schmidt, Flavia; Rieke, Svenja; Pfeil, Rudolf; Niemann, Lars; Marx-Stoelling, Philip  
 Bundesinstitut für Risikobewertung, Chemikaliensicherheit, Berlin, Germany

**Background:** The authorization of pesticides requires extensive toxicological testing. Risk assessment is performed for single substances. However, consumers are exposed to multiple residues of pesticides via the diet. Therefore experimental investigations of potential combination effects are necessary. The aim of this project was to investigate hepatotoxic combination effects of a widely used group of fungicides – the triazoles – and additionally identify potential markers for the analysis of combination effects *in-vitro*. **Methods:** Within the framework of a 28-day-feeding-study in rats, we analyse combination effects of triazoles in a broad dose range. In this subproject, activity of liver enzymes of treated and untreated rats was measured in *in-vivo* experiments. In addition, investigations of gene expression in a human hepatocellular carcinoma (HepG2) cell line after treatment with triazoles were performed and the results were compared to *in-vivo* experiments which were carried out previously.

**Results:** The results of the *in-vivo* enzyme activity measurements indicate combination effects of the tested substances. The experiments revealed a significant induction of enzyme activity of CYP2B1 and CYP3A4 with cyproconazole and epoxiconazole separately and combined. The Imidazole prochloraz revealed furthermore a significant induction of enzyme activity of CYP1A1 and CYP1A2. The combination of all three substances leads to a significant induction of enzyme activities of CYP1A1, 1A2, 2B1 and 3A4. However, further modelling is needed to conclude whether or not the combination effects adhere to the model of dose additivity. The experiments in HepG2 cells identified two potential marker genes for the analysis of combination effects in this cell line (CYP1A1 and CYP19A1).

**Conclusion:** The test systems used show that there is evidence for combination effects of the test substances within the selected dose range. In order to use these results for regulatory decision making further testing is needed.

229

#### Studying the role of STIM proteins and Orai Ca<sup>2+</sup> channels in precapillary pulmonary arterial smooth muscle cells (PASMC)

**Koch, Diana**<sup>1</sup>; Braun, Attila<sup>2</sup>; Gudermann, Thomas<sup>1</sup>; Dietrich, Alexander<sup>1</sup>  
<sup>1</sup>LM-Universität München, Walther-Straub-Institut für Pharmakologie, Germany  
<sup>2</sup>Universität Würzburg, University Hospital and Rudolf Virchow Center for Experimental Biomedicine, Germany

Although Ca<sup>2+</sup> influx is an essential component for hypoxic pulmonary hypertension (HPH) and vascular remodeling, the role of novel Ca<sup>2+</sup> influx channels of the STIM/Orai families is still elusive. Stromal interaction molecule (STIM) proteins acting as sensors for Ca<sup>2+</sup> in intracellular stores and activating store-operated Ca<sup>2+</sup>-permeable Orai channels at the plasma membrane were originally identified in T-cells (1), but are also expressed in many other different tissues. Store-operated Ca<sup>2+</sup> entry (SOCE) after emptying the internal Ca<sup>2+</sup> stores by thapsigargin or cyclopiazonic acid (CPA) has already been investigated in quiescent vascular smooth muscle cells (2), but not in precapillary pulmonary arterial smooth muscle cells (PASMC) which are responsible for HPH. We hypothesize that down-regulation of STIM1 and Orai1 proteins may reduce Ca<sup>2+</sup> influx after CPA-induced Ca<sup>2+</sup> release from internal stores in PASMC. Thus, we established a double heterozygote (*Stim1*<sup>+/+</sup>/*Orai1*<sup>+/+</sup>) C57BL/6 mouse line by using two independent *Stim1*<sup>+/+</sup> and *Orai1*<sup>+/+</sup> mouse lines created by the 'gene trap' technology, because *Stim1*<sup>-/-</sup>/*Orai1*<sup>-/-</sup> mice are embryonic lethal. After identification of *Stim1*<sup>+/+</sup>/*Orai1*<sup>+/+</sup> mice by genotyping using primer binding in the  $\beta$ -geo cassette and in the adjacent genomic DNA, down-regulation of STIM1 and Orai1 mRNA was confirmed by quantitative reverse-transcription (RT)-PCR. PASMC were isolated from lungs of these mice and grown on glass cover slips (3). After depletion of internal Ca<sup>2+</sup> stores by 10 $\mu$ M CPA in Ca<sup>2+</sup>-free HEPES solution containing 2mM EGTA extracellular Ca<sup>2+</sup> solution was added to quantify store-operated calcium influx. Most interestingly, *Stim1*<sup>+/+</sup>/*Orai1*<sup>+/+</sup> PASMC showed a reduced CPA-induced SOCE after restoring Ca<sup>2+</sup> compared to PASMC isolated from wild-type (WT) mice. Next, we will evaluate STIM/Orai function for PASMC proliferation and will analyze hypoxic pulmonary hypertension *in vivo* by using smooth-muscle cell specific STIM-deficient mouse models.

[1] Feske S. (2007). Calcium signalling in lymphocyte activation and disease. *Nat. Rev. Immunol.* 7, 690-702.

[2] Potier M. et al. (2009). Evidence for STIM1- and Orai1-dependent store-operated calcium influx through ICRAc in vascular smooth muscle cells: role in proliferation and migration. *FASEB J.* 23, 2425-2437.

[3] Weissmann N. et al. (2006). Classical transient receptor potential channel 6 (TRPC6) is essential for hypoxic pulmonary vasoconstriction and alveolar gas exchange. *Proc. Natl. Acad. Sci. U.S.A.* 103, 19093-19098.

## 230

**INHIBITION OF CYCLOPHOSPHAMIDE-INDUCED URINARY BLADDER PAIN IN RATS BY AN ETHANOLIC CAPSICUM EXTRACT**Palea, Stefano<sup>1</sup>; Saarberg, Werner<sup>2</sup>; Erdelmeier, Clemens A. J.<sup>2</sup>; Koch, Egon<sup>2</sup><sup>1</sup>UROSphere, Faculté des Sciences Pharmaceutiques, Toulouse cedex 04, France<sup>2</sup>Dr. Willmar Schwabe Pharmaceuticals, Preclinical Research, Karlsruhe, Germany

Fruits of chili pepper (*Capsicum* spp.) are not only consumed as a pungent spice but are also employed for medicinal purposes. Thus, use of *Capsicum* extracts has a long tradition in folk medicine as rubefaciant and topical analgesic for the treatment of various neuropathic and musculoskeletal pain conditions. Recently, a patch with a high concentration of capsaicin, the main active component of chili pepper, has been approved in the EU and USA for treatment of painful peripheral neuropathies. In addition, intravesical instillation of capsaicin has been demonstrated to be a useful therapeutic alternative for the management of persistent bladder pain and overactive bladder. The analgesic effect of capsaicin is due to blockade of nociceptive sensory nerves which selectively express TRPV1 receptors. Capsaicin is a potent agonist on this non-selective cation channels and initially causes a stimulation which is followed by receptor desensitization. Because of this mode of action topical administration of capsaicin has a rather inconvenient side-effect as the patient initially experiences a unpleasant burning sensation. Thus, it was the aim of the present study to evaluate the efficacy of an orally applied ethanolic (70% w/w) extract from *C. annuum* fruits on different pain conditions with a focus on urinary tract related pelvic pain.

For this purpose, cyclophosphamide-induced cystitis in rats was used as a relevant model to test therapeutic approaches for the treatment of interstitial cystitis/painful bladder syndrome (IC/PBS). IC/PBS is a chronic inflammatory disease characterized by visceral pain and urinary symptoms. It was observed that subacute (4 days) oral administration (1, 3, 10 and 75 mg/kg) of the extract reversed, in a dose dependent manner, the induced visceral allodynia and hyperalgesia. The analgesic effect of *Capsicum* extract appears to be mediated by interference with pain transmission and not anti-inflammatory action because analysis of croton oil-induced ear-edema in mice and bladder weight in the cystitis model revealed no antiphlogistic activity.

The obtained data indicate that *Capsicum* extracts may be an interesting oral treatment option for complex pain conditions, such as urologic chronic pelvic pain syndromes (UCPPS) as an example of a common syndrome with ambiguous pain perceptions and a strong psychological component for which no standard therapy is yet available.

## 231

**Molecular effects of lignans in *C. elegans***Koch, Karoline; Wätjen, Wim; Havermann, Susannah; Büchter, Christian  
Martin-Luther-Universität Halle-Wittenberg, Halle (Saale), Germany

A diet rich in vegetables, fruits and grains is associated with protective effects against various age-related diseases. Bioactive substances like fiber and secondary plant compounds seem to contribute to these health effects. While the biological mechanism of fiber has been extensively studied the mode of action of secondary plant compounds is mostly unknown due to their structural variety.

In this study we investigated representative compounds out of the class of lignans: pinoresinol (PINO), matairesinol (MAT), secoisolariciresinol (SECO), sesamin (SES) and schisanrin B (SB) which are oligomers of phenylpropanoids and occur mostly in flax seed and grains. *In vitro* antioxidative capacity was measured with the TEAC assay: The flax seed lignans PINO, MAT and SECO showed a comparable radical scavenging activity as trolox while SES and SB were not effective. In order to study *in vivo* effects of the plant compounds we utilized the nematode *C. elegans*. Because of its ease in handling, its short lifespan and the availability of genetically modified strains the nematode is a well-established model to study age-associated markers and signaling pathways. Since cellular stress is associated with various age-associated diseases we analyzed survival rates and intracellular levels of reactive oxygen species (ROS) in thermally stressed nematodes after incubation with lignans. Intracellular levels of ROS were analyzed by measuring the fluorescence intensity of DCF and survival rates were determined by using the nucleic acid stain SYTOX green. Further on we measured the autofluorescence of the age marker lipofuscin and analyzed the expression of the FoxO homologue DAF-16 in a transgenic *C. elegans* strain to investigate if the antioxidative effect of the lignans was mediated by the modulation of this insulin-like signaling pathway. We were able to show that *C. elegans* is an appropriate model to study the effects of secondary plant compounds like lignans.

## 232

**Comparative cardiac gene expression in PP5 and PP2A overexpressing mice**

Köhler, Carolin; Bollmann, Paula; Gergs, Ulrich; Neumann, Joachim

Institut für Pharmakologie und Toxikologie, Med. Fakultät, Martin-Luther-Universität Halle-Wittenberg, Halle/Saale, Germany

Cardiac overexpression of the catalytic subunit of PP2A in hearts of transgenic mice (PP2A-OE) leads to profound cardiac hypertrophy and attenuated  $\beta$ -adrenergic contractile effects. In contrast, overexpression of the protein phosphatase 5 (PP5) only led to mild cardiac hypertrophy in previous series of experiments (Gergs et al. Int J

Cardiol 154:116[2012]). Using gene chip analysis and Western blotting, we identified some target genes in PP2A-OE hearts (Gergs et al. Naunyn Schmiedebergs Arch Pharmacol 383(Suppl 1):60[2011]). Here, we wanted to study the very same targets in PP5 overexpressing mice (PP5-OE). To this end, 100  $\mu$ g of cardiac homogenates, which lie within the linear range of the system, were transferred to membranes and incubated with commercially available primary antibodies and thereafter with appropriate secondary antibodies. Resulting fluorescence was quantified using a Typhoon<sup>TM</sup> imager. Relative cardiac weights amounted to 4.47  $\pm$  0.13 mg/g in wild type (WT) and 4.84  $\pm$  0.76 mg/g in PP5-OE but to 4.3  $\pm$  0.1 and 6.6  $\pm$  0.1 mg/g in WT and PP2A-OE, respectively. Under these experimental conditions, in cardiac samples of PP5-OE the expression of calmodulin-dependent kinase II, heat shock protein (HSP) 90, the catalytic subunit of PP2A, thrombin and fibrinogen remained unchanged, whereas the expression of superoxide dismutase (SOD) and HSP 25 were increased to 126 % and 277 %, respectively (n=6-8, p<0.05). For comparison, the expression of HSP 25 was more increased in PP5-OE than in PP2A-OE, whereas SOD remained unchanged in PP2A-OE. Interestingly, the protein expression of PP5 itself was increased in PP2A-OE. These data are partially contrary with regard to the gene chips experiments. The present data firstly underscore the bias in gene chip data and secondly may indicate that different signal transduction pathways lead to hypertrophy in PP2A-OE compared to PP5-OE.

## 233

**Pre-clinical publication patterns of newly launched drugs**Köster, Ursula<sup>1</sup>; Nolte, Ingo<sup>1</sup>; Michel, Martin<sup>2,3</sup><sup>1</sup>Tierärztliche Hochschule Hannover, Klinik für Kleintiere, Germany<sup>2</sup>Johannes Gutenberg Universität, Institut für Pharmakologie, Mainz, Germany<sup>3</sup>Boehringer Ingelheim Pharma GmbH & Co KG, Dept. Regional Medicine & Scientific Affairs, Germany

While clinical data define the efficacy and safety of drugs, preclinical data are important for their mechanistic understanding, particularly for newly launched drugs. As there are no formal guidelines which preclinical data need to be communicated at which time to the scientific community, the publication pattern of such data apparently differs considerably between drugs, but specific data are not available. Therefore, we have systematically explored how much, what and when such data were published for newly approved drugs for human use. For selected years between 1991-2011 all drugs newly approved within that year were identified on the FDA website. For each identified drug a systematic Medline search was performed including all aliases for original full papers reporting preclinical data and published up to one year after approval. The following analyses were performed: a) number of publications per compound; b) time between publication and approval; c) journal type (pharmacology vs. other science vs. clinical); d) question types (mechanisms of action, potency, selectivity, efficacy etc.); e) model system (molecular, cellular, isolated tissue, in vivo and native vs. genetically modified); f) species being studied; g) physiology vs. pathophysiology study; h) affiliation of author (academic vs. industry). In total our analysis covered >120 drugs from 6 approval years and identified >1400 published original articles reporting non-clinical findings. This confirmed the expected heterogeneity in publication pattern. E.g. the number of published articles per compound ranged between 0 and 90 and did not exhibit a clear trend over time (mean/median per approval year: 1991: 19/13, 1996: 14/9, 2001: 9/3, 2006: 9/5, 2007: 8/2, 2011: 8/5). In most cases publications clustered between the year prior to and immediately after approval. Most data were published in clinical and non-pharmacological basic science journals. While rats and mice were used most often, a broad range of species was investigated. The use of genetically modified organisms became increasingly important in recent years.

## 234

**The influence of Statins on bone tissue in ovariectomized rats.**Seferos, Nikolaos<sup>1</sup>; Kotsiou, Antonia<sup>1</sup>; Petrokokkinos, Luke<sup>2</sup>; Tesseromatis, Christine<sup>1</sup><sup>1</sup>Medizinische Schule Uni-Athen, Pharmakologie, Greece<sup>2</sup>Medizinische Schule Uni-Athen, Physik, Greece

Osteoporosis a silent, progressive, systemic skeletal disease characterized by impaired bone architecture with decreased bone mass density affecting women in menopausal and after menopausal stage and men in the third age, mainly in the ratio 6:1.

Periodontitis a chronic inflammatory, multifactorian disease has been associated with general osteoporosis.

Statins, inhibitor of HMG-CoA-reductase, seems to interfere in bone formation exerting anabolic and antiresorptive effect.

The study investigates the bone density in mandible and femur in an ovariectomized (OVX) rat model of osteoporosis in order to test the effect of simvastatin on bone size parameters.

50 Wistar female rats aged 4-6 weeks, weighting 200-300g were randomized in five groups.

Animals in Group 1,2 and 3 (n=10) were ovariectomized and group 4 and 5 serve as controls. Group 2,3 and 5 were treated with simvastatin 0,5 mg/kg/daily p.o. for 3 months. Sizes parameters of the isolated femur, mandible and uterus were measured, BMD(bone mass density) via dual energy X-Ray absorptiometry (DEXA) and laboratory serum findings were estimated.

Ovariectomy leads to experimental menopause with decreased uterus weight and reduction of all parameters in femur and mandible (weight, specific weight, bone weight/body weight) that have been restored under the influence of statins. DEXA results

showed significant decrease of BMD in ovariectomy group / controls while statins treatment decrease the severity of BMD lose. The serum IL-13 as osteogenesis index seems to be positive influenced by statins treatment.

Bone parameters	Group 1	Group 2	Group 3	Group 4	Group 5
Body weight g	291.11±65.28	303.57±51.37	276.67±47.08	256.67±25.03	247.85±23.2
Femur weight g	2.7578±0.5368*	2.9943±0.5545	3.325±0.39	3.79±0.7785	3.85±0.8
Mandible weight g	2.2835 ±0.2537	2.32±0.02	2.38±0.0735*	2.4±0.18	2.4±0.16
Femur volume cm <sup>3</sup>	2.4344±0.5865*	2.0329±0.6122*	2.33±0.3194*	3.15±0.6232	3.2±0.7
Mandible volume cm <sup>3</sup>	1.408 ±0.33	1.34±0.11*	1.4±0.1*	1.72±0.2	1.79±0.3
Femur specific weight g/cm <sup>3</sup>	1.1467±0.1190	1.5386±0.3079*	1.4283±0.1061*	1.2050±0.0841	1.38±0.05
Mandible specific weight g/cm <sup>3</sup>	1.62±0.27	1.7±0.057*	1.77±0.12*	1.41±0.15	1.45±0.21
Femur weight / Body weight g/g	0.0097±0.0022*	0.0102±0.0028*	0.0124±0.0028*	0.01467±0.002	0.0147±0.2
Mandible weight / Body weight g/g	0.0079±0.0016	0.0077±0.0014	0.0091±0.0016*	0.009±0.0006	0.009±0.002
Uterus weight g	2.855±0.8174*	2.7714±1.245	2.8083±1.054	3.2189±0.6634	3.17±0.002
Uterus weight / Body weight g/g	0.0112±0.0037	0.0096±0.0051	0.0101±0.0048	0.0107±0.0044	0.127±0.004
BMD femur g/cm <sup>2</sup>	0.158±0.010	0.181±0.006	0.179±0.003	0.188±0.012	0.189±0.09
BMD mandible g/cm <sup>2</sup>	0.198±0.011	0.215±0.008	0.211±0.009	0.208±0.010	0.21±0.09

(statistik t-test \* p<0,05)

## 235

**Tissue engineered muscle to investigate skeletal muscle regeneration in vitro**  
**Krämer, Lena Katharina; Tiburcy, Malte;** Markov, Aleksej; Zimmermann, Wolfram H.  
 Universitätsmedizin Göttingen, Pharmakologie, Germany

**Introduction:** Skeletal muscle regeneration is driven by the extensive regenerative capacity of satellite cells which may be reduced in disease states. Analysis of satellite cell function in vitro is limited as they quickly differentiate and lose their phenotype. We hypothesized that (1) skeletal muscle (ESM) with functional satellite cell niches can be engineered in vitro and (2) exploited to study skeletal muscle regeneration.

**Methods and Results:** We generated engineered skeletal muscle (ESM) from rat myoblasts, matrigel, and collagen (1.25x10<sup>6</sup> cells/ESM). In contrast to conventional 2D culture, ESMs exhibited Pax7-positive cells in satellite cell-characteristic niches: m-cadherin+, caveolin+ cells adjacent to muscle fiber and underneath collagen-4+ basal membrane. Immune staining indicated that the majority of Pax7 positive satellite cells were quiescent (Ki67-, MyoD-). We next tested if satellite cells would entail regenerative capacity using a cardiotoxin injury model. Treatment with 25 µg/ml cardiotoxin caused muscle cell destruction and contractile failure after 48 hrs. However, Pax-7 positive satellite cells were spared and entered the cell cycle to proliferate and differentiate into regenerating muscle fibres (eMHC-positive). After 7 days of recovery

we found a partial regeneration of contractile force (33±4% of control, n=6-11/group). This regenerative response was inhibited if the muscle was irradiated (30 Gy) before injury confirming the essential role of proliferating and differentiating satellite cells for regeneration in vitro. We then tested if regeneration may be influenced by inhibition of Notch signaling which has been shown to positively regulate satellite cell activation and proliferation. Treatment with a gamma secretase inhibitor (1 µM) after injury inhibited the regenerative response with ~50% lower regenerated contractile force compared to vehicle treated ESM (n=3).

**Conclusion:** We established a model of skeletal muscle regeneration in vitro and provide proof of concept evidence for its utility to screen for wanted or unwanted drug effects on regeneration.

## 236

### Induction of CREM-isoforms in the heart after beta adrenergic stimulation

**Kranick, Daniel Sebastian;** Seidl, Matthias Dodo; Fels, Benedikt; Schmitz, Wilhelm; Müller, Frank Ulrich  
 Westfälische Wilhelms-Universität, Institute of Pharmacology and Toxicology, Münster, Germany

Beta adrenergic stimulation and subsequent activation of the cAMP signaling cascade plays an important role in the progression of heart failure. In response to cAMP elevation transcription factors like CREM (cAMP responsive element modulator) regulate the transcriptional response of their target genes. The multiexonic Crem-gene encodes a multitude of isoforms, and exhibits 6 different intronic promoters (P1-6). Its structure can be described by the following pattern (in which hyphens stand for introns and bold letters for exons):

P1 - A0 - P5 - A - B - Ψ - P3 - θ1 - P4 - θ2 - C - E - F - G - P2 - X - P6 - γ - H - la - lb  
 Although much effort was put in elucidating the existing Crem-isoforms and their role in different tissues, less is known about the cardiac expression-pattern of CREM isoforms. Here we investigate the expression of Crem-isoforms in human heart tissue (HHT) and mouse cardiomyocytes (MCM) and study the induction of Crem-transcripts after beta adrenergic stimulation.

Performing PCR with subsequent cloning we were able to identify 8 (HHT) and 6 (MCM) isoforms transcribed by the P1 or P5 promoter, 2 (HHT) and 3 (MCM) isoforms derived from the P2 promoter (inducible cAMP early repressor (Icer)), none isoform transcribed by the P3, 1 isoform (MCM) transcribed from the P4 promoter and 4 (MCM) and 2 (HHT) isoforms transcribed by the recently identified P6 promoter (small Icer (smIcer); Seidl, M. D. et al. 2013, FASEB journal). Almost all isoforms lacked the glutamine-rich regions (C and G) and semiquantitative RT-PCR revealed Icer-isoforms (X-H-la and X-H-lb) as most abundant in the human myocardium. Beta adrenergic stimulation of murine hearts for 10 h by osmotic minipumps induced P1/P5 (B-H-la 1.9-fold; B-H-lb 1.7-fold; B-E-F-H-la 2.2-fold; B-E-F-H-lb 5.5-fold), P2-Icer (X-H-la 21.6-fold; X-H-lb, 33.4-fold) and P6-smIcer-derived (γ-H-la 3.5-fold; γ-H-lb 3.6-fold) mRNA transcription compared to basal levels.

In conclusion, we identified a multitude of Crem-isoforms in the heart. Their predominantly short structure and the lack of the glutamine-rich regions involved in transactivation, implicating an inhibitory function of these isoforms. The strong induction of short CREM splice variants notably Icer mRNAs by beta adrenergic stimulation, suggests an important function of these isoforms in the myocardium, particularly under pathophysiological conditions like heart failure. (Supported by the DFG)

Seidl, M. D. et al. (2013) A novel intronic promoter of the Crem gene induces small ICER (smICER) isoforms. FASEB journal, Epub ahead of print

## 237

### Combined EGF receptor tyrosine kinase inhibition and inhibition of hyaluronan synthesis attenuates growth of esophageal squamous cell carcinoma cells in vitro

**Kretschmer, Inga;** Freudenberger, Till; Twarock, Sören; Fischer, Jens Walter  
 Institut für Pharmakologie und Klinische Pharmakologie, Universitätsklinikum Düsseldorf, Heinrich-Heine-Universität Düsseldorf, Germany

Hyaluronan (HA), a carbohydrate component of the extracellular matrix can be found in the stroma and parenchyma of tumours. It stimulates cell survival, proliferation and migration via its receptors such as CD44 and activation of downstream signalling such as PI3K/AKT and MAPK pathways. These pathways are also stimulated by the epidermal growth factor (EGF). Erlotinib, an EGF receptor tyrosine kinase inhibitor, was shown to be effective in the treatment of esophageal squamous cell carcinoma (ESCC). The aim of the study was to determine if synergistic effects can be achieved by concurrent erlotinib treatment and inhibition of HA synthesis using 4-methylumbelliferone (4-MU). First, co-cultures of murine skin fibroblasts (SF) and ESCC cells were used. In direct co-culture of SF and ESCC cells combined erlotinib and 4-MU treatment led to increased overall PARP cleavage as compared to erlotinib alone. In direct co-culture mRNA expression of Has2 and Has3 was increased in SF. In order to study the role of increased Has2 mRNA expression for erlotinib sensitivity, ESCC cells were cultured with Has2 knockdown SF and control SF. There was no significant difference in overall apoptosis in both groups, suggesting that increased Has2 expression in SF was not critical to counteract apoptosis after erlotinib treatment. In ESCC cell monoculture, even low dose erlotinib (1µM) resulted in a decreased number of cells per well compared to control. Importantly, cell-count was significantly lower after treatment with 4-MU plus erlotinib as compared to single agents and the combination index calculated by the Chou-Talalay method was <1, suggesting synergism. Interfering with HA-signalling by

siCD44 also reduced the number of cells. The reduction was more pronounced when siCD44 was combined with erlotinib treatment. In a 3D culture of ESCC cells, erlotinib (1µM) and its combination with 4-MU attenuated the growth of multicellular tumour spheroids. Both 4-MU and erlotinib alone and in combination decreased ERK phosphorylation after 24 hours. However, only the combination of erlotinib and 4-MU showed a sustained reduction in ERK phosphorylation after 10 days of treatment. In conclusion, simultaneous inhibition of both EGFR signalling and HA-signalling resulted in synergistic inhibition of ESCC growth.

## 238

### Characterisation of OrfX-Proteins produced by *Clostridium botulinum* Type E Beluga

**Kroh, Amelie**<sup>1</sup>; Lübke, Johanna<sup>1</sup>; Kruel, Anna Magdalena<sup>1</sup>; Krüger, Maren<sup>2</sup>; Dörner, Brigitte G.<sup>2</sup>; Rummel, Andreas<sup>1</sup>

<sup>1</sup>MHH, Institut für Toxikologie, Hannover, Germany

<sup>2</sup>Robert Koch-Institut, Zentrum für Biologische Gefahren und Spezielle Pathogene - Biologische Toxine (ZBS3), Berlin, Germany

Food-borne botulism is caused by one of the most potent toxins in the world, botulinum neurotoxin (BoNT), and there is a high interest to decipher the molecular mechanism of intoxication, beginning from oral ingestion to final blockade of acetylcholine release in neuronal cells. The naturally occurring BoNTs that have seven major serotypes (termed A–G) are secreted together with non-toxic neurotoxin-associated proteins (NAPs) in the form of progenitor toxin complexes (PTC). Remarkably, the PTC exhibits ~360–16,000-fold greater oral toxicity in comparison to the free toxin, although the mechanism is unknown. Naturally, BoNT/A, B, C, D and G are produced together with four NAPs, which include non-toxic non-hemagglutinin (NTNHA) and three hemagglutinins (HAs: HA70, HA33 and HA17). On the other hand, some clostridial genomes encoding BoNT/E and F lack *ha* genes, but contain three genes of unknown function termed *orfX1-3* in addition to *ntnha*. The function of these OrfX proteins is largely unknown. We have previously shown that BoNT and NTNHA of serotype A assemble into a minimally functional PTC (M-PTC/A) in which NTNHA forms a tight complex with BoNT and protects it from host gastrointestinal destruction<sup>1</sup>. A similar complex is formed by BoNT/E<sup>2</sup>. The large PTC (L-PTC) of BoNT/A and B display a significantly increased oral toxicity due to association of M-PTC with three HAs which assemble into a 3-fold symmetric hetero-dodecameric complex, the HA complex, containing nine glycan-binding sites that help to accumulate the L-PTC on the intestinal lumen through host carbohydrate receptors<sup>3</sup>. However, an analogous L-PTC of serotype E is unknown. The function of the proteins OrfX-1, -2, -3 and p47 of the strain *Clostridium botulinum* type E beluga has not been investigated. We expressed OrfX1-3 recombinantly and generated specific rabbit antisera. We could demonstrate that OrfX1-3 are secreted by *C. botulinum* type E beluga parallel to BoNT/E-NTNHA-E by ammonium sulphate precipitation and Western blotting. In contrast to HA complex, the secreted OrfX proteins did not disrupt the tight junctions of the human intestinal carcinoma cell line Caco-2. Currently, the glycan binding characteristics and a putative association of OrfX1-3 with M-PTC/E are analysed. Furthermore, the formation of a putative OrfX complex analogous to the HA complex is investigated.

<sup>1</sup> Botulinum neurotoxin is shielded by NTNHA in an interlocked complex. Gu S, Rumpel S, Zhou J, Strotmeier J, Bigalke H, Perry K, Shoemaker CB, Rummel A, Jin R. *Science*. 2012 Feb 24;335(6071):977-81.

<sup>2</sup> Molecular assembly of progenitor complex of botulinum neurotoxin serotype E. Eswaramoorthy S, Sun J, Cai S, Li H, Singh BR, Swaminathan S. 50th Annual Interagency Botulism Research Coordinating Committee (IBRCC) Meeting, October 20-23, 2013, Annapolis, MD

<sup>3</sup> Structure of a bimodular botulinum neurotoxin complex provides insights into its oral toxicity. Lee K, Gu S, Jin L, Le TT, Cheng LW, Strotmeier J, Kruel AM, Yao G, Perry K, Rummel A, Jin R. *PLoS Pathog*. 2013;9(10):e1003690.

## 239

### An ergothioneine transporter knock-out zebrafish to investigate the physiological function of ergothioneine

**Krüger, Johanna**; Pfeiffer, Carolin; Tuschy, Thorsten; Gründemann, Dirk  
Uniklinik Köln, Institut für Pharmakologie, Germany

Polymorphisms within the human ergothioneine transporter (ETT) gene (human gene symbol *SLC22A4*) are associated with chronic inflammatory diseases like rheumatoid arthritis, ulcerative colitis, Crohn's disease, and cataract. Based on histidine betaine, ergothioneine (ET) is a derivative of 2-thio-imidazole. Mammals are unable to synthesize ET and thus depend on dietary ET. Because of the double-bonded sulfur, ET is expected to provide antioxidative protection. However, the precise physiological function of ergothioneine (ET) is still unresolved.

Here we have procured, based on retroviral insertion, an ETT knock-out zebrafish (*Danio rerio*) (ETT<sup>-/-</sup>). In whole-fish lysates of homozygous knock-out animals, ET content (0.06 ± 0.01 ng/g wet mass; n=3) was reduced more than 1000-fold compared to wild-type (138 ± 61 ng/g wet mass; n = 3). Similarly, all examined organs contained virtually no ET.

The expression profile of ETT in wild-type zebrafish was analyzed by RT-PCR and real-time RT-PCR and validated by measuring ET tissue content. Strong signals were obtained with kidney, intestine, skin, brain and eye. Using the LC-MS difference shading method we scanned comprehensively for molecular differences between unstressed

wild-type and knock-out fishes. Carnitine and acetyl carnitine were reduced across all examined tissues of knock-out fish by a factor of 2.0 ± 0.2, and 1.7 ± 0.1, respectively. Also, 4-hydroxyquinoline was significantly reduced in ETT<sup>-/-</sup> fish. Peroxide stress by incubation in 50 µmol/l *tert-butyl* hydroperoxide yielded no further LC-MS/MS difference shading signals.

Incubation in sublethal concentrations of Pb<sup>2+</sup> and Cu<sup>2+</sup> led to an increase of the lipid peroxidation markers 4-hydroxy-2,3-trans-nonenal (HNE) and malondialdehyde (MDA) in knock-out versus wild-type zebrafish.

The ergothioneine transporter knock-out zebrafish represents a new model to analyze the consequences of a total lack of ET and thus opens an opportunity to at last understand the benefit of accumulating ET in certain tissues.

1. Fork C, Bauer T, Golz S, Geerts A, Weiland J, Del Turco D, Schömig E, Gründemann D. (2011). OAT2 catalyses efflux of glutamate and uptake of orotic acid. *Biochemical Journal* 436:305-12

2. Gründemann D, Harfinger S, Golz S, Geerts A, Lazar A, Berkels R, Jung N, Rubbert A, Schömig E. (2005). Discovery of the ergothioneine transporter. *Proc. Natl. Acad. Sci. U.S.A.* 102:5256-61

3. Golling G, Amsterdam A, Sun Z, Antonelli M, Maldonado E, Chen W, Burgess S, Haldi M, Artzt K, Farrington S, Lin SY, Nissen RM, Hopkins N. (2002). Insertional mutagenesis in zebrafish rapidly identifies genes essential for early vertebrate development. *Nat Genet* 31:135-40

4. Amsterdam A, Burgess S, Golling G, Chen W, Sun Z, Townsend K, Farrington S, Haldi M, Hopkins N. (1999). A large-scale insertional mutagenesis screen in zebrafish. *Genes Dev* 13:2713-24

## 240

### Normal rat kidney cells differ in their sensitivity towards various platinum compounds

**Krüger, Katharina**; Fritze, Gerhard

Universitätsklinikum Düsseldorf, Institut für Toxikologie, Germany

**Background:** Platinating agents are frequently used for the treatment of various types of cancer. Cisplatin and carboplatin are extensively used in the therapy of urogenital cancers, whereas oxaliplatin is mainly used in colorectal cancer treatment. After entering the cell platinating agents form DNA monoadducts which are processed into intra- and interstrand crosslinks. These adducts may impair DNA replication, transcription and trigger cell death. The clinically most relevant adverse effect associated with cisplatin treatment is nephrotoxicity. Here, we addressed the question whether rat renal proximal tubular cells (NRK-52E) and glomerular endothelial cells (RGE) differ in their response following treatment with various platinum compounds.

**Methods:** To characterize the toxic effects of the aforementioned platinum compounds, cell viability was determined using the MTT assay. A subset of signal transduction pathways involved in platinum-induced cytotoxicity as well as the level of S139 phosphorylated H2AX (γH2AX) were analyzed by Western blot. Western blot analysis together with the ApoOne assay were used to monitor activation of caspases. In addition, the amount of Pt-GpG-intrastrand crosslinks was determined via Southwestern blot analysis.

**Results:** Cisplatin reduced the viability of both types of kidney cells more efficiently than oxaliplatin, which again was more cytotoxic than carboplatin. RGE cells were more sensitive towards the platinum compounds than NRK-52E cells. Cisplatin stabilized p53 in both cell lines more efficiently than carboplatin. p38 kinase was not phosphorylated following 8 h of platinum treatment. Cisplatin treatment resulted in the highest level of γH2AX. Moreover, carboplatin required longer exposure times to increase the amount of γH2AX protein. Furthermore, cisplatin induced higher levels of Pt-GpG-intrastrand crosslinks than carboplatin, which required a prolonged incubation period to form these adducts. RGE cells repaired Pt-GpG-intrastrand crosslinks more efficiently than NRK-52E cells and showed less caspase activation.

**Conclusion:** Out of the various platinum compounds tested, cisplatin shows the highest toxicity in renal proximal tubular cells as well as in glomerular endothelial cells. The latter are particularly sensitive to the cytotoxic effects of the above-named platinum compounds, although they reveal reduced activation of caspases and higher repair capacity of intrastrand crosslinks than NRK-52E cells.

## 241

### Correlation of toxicity and material properties: oral and inhalation exposure of 16 surface-functionalized nanomaterials

**Buesen, Roland**<sup>1</sup>; Ma-Hock, Lan<sup>1</sup>; Wohlleben, Wendel<sup>1</sup>; Groeters, Sibylle<sup>1</sup>; Geiger, Dominik<sup>2</sup>; van Ravenzwaay, Bennard<sup>1</sup>; Landsiedel, Robert<sup>1</sup>

<sup>1</sup>BASF SE, Experimental Toxicology and Ecology, Ludwigshafen am Rhein, Germany

<sup>2</sup>BASF SE, Product Safety, Ludwigshafen am Rhein, Germany

16 nanomaterials were tested by short-term inhalation studies (R. Landsiedel, et al. *Advanced Materials* 22.24 (2010): 2601-2627) and oral gavage (28-day OECD TG407). The results were correlated to the complete physical-chemical properties (according to the REACH R7.1 nano-specific guidance) and to the in-situ corona structures (in lung surfactant, pure lipids, serum-containing media)

The surface of suspended nanoparticles with sizes of 10 nm (ZrO<sub>2</sub>), 15nm (SiO<sub>2</sub>) and 50 nm or 200 nm (Ag) received -acid, -amino, -PEG, and -steric functionalities. The organic molecules were bound to the surface of the particles to improve properties such

as processability, solubility or stability of the products. All results were benchmarked against OECD reference materials (TiO<sub>2</sub>, ZnO, BaSO<sub>4</sub>). None of the materials elicited an adverse effect in oral testing (see separate poster). For inhalation at up to 50 mg/m<sup>3</sup>, inflammations of the lung were observed with most of the nanomaterials. In general, functionalizations reduced the acute inflammatory response, especially for negative charges and for sterically stabilized materials. The correlation of inflammatory potency (e.g. monitored by PMN) to in-situ corona parameters is vanishing. A weak correlation was found between the particle's affinity to phospholipids and the deposition rate, but not further correlated to clearance. In contrast, correlations are strong with the chemical composition of the core particle, suggesting grouping and prioritization for in-vivo testing by surface charge and by core substances. The project NanoGEM (Nanostructured materials – Health, Exposure and Material Properties, 2010 – 2013) involved 19 research institutions and companies, supported by the Federal Ministry of Education and Research (BMBF).

## 242

### Effect of Rho GTPase overexpression in a 3D breast epithelial system

**Lang, Sarah**<sup>1</sup>; Brummer, Tilman<sup>2</sup>; Aktories, Klaus<sup>1</sup>; Schmidt, Gudula<sup>1</sup>

<sup>1</sup>Institut für Experimentelle und Klinische Pharmakologie und Toxikologie, Albert-Ludwigs-Universität Freiburg, I, Germany

<sup>2</sup>Institut für Molekulare Medizin und Zellforschung, Albert-Ludwigs-Universität Freiburg, Germany

Rho GTPase family members are regulatory key players in numerous cellular functions [1]. Their deregulation was shown to substantially contribute to tumor progression by affecting adhesive and motile properties of cells [2]. In particular, an essential role in the process of metastasis was assigned to RhoC [3] whereas RhoA has been reported to provoke either anti- or prometastatic behaviour depending on the cellular context and the type of study [4].

In order to obtain deeper insights into the effect of transient Rho GTPase overexpression on benign epithelial cells, we generated a doxycycline-inducible mammary epithelial cell line that overexpresses either wildtype RhoA or C simultaneously with GFP.

Interestingly, in this model system RhoA and RhoC inhibit each other by reduced expression levels and activity status. Epithelial cells such as MCF10A cultured in 3D recapitulate numerous features of the glandular epithelium in vivo and form three-dimensional hollow acini. This phenotype changes dramatically upon doxycycline induction, as RhoA and RhoC overexpressing cells disrupt the normal acinus architecture. Our current investigation indicates that this represents an invasive process. Hence, our model system will serve as a valuable tool to test bacterial Rho-targeting toxins in a pharmacological context.

1. Jaffe, A. B., and Hall, A., Rho GTPases: Biochemistry and Biology. Annual Review of Cell and Developmental Biology, 2005, 21:247-269

2. Ellenbroek, S. I., and Collard, J. G., Rho GTPases: functions and association with cancer. Clin Exp Metastasis 2007, 24:657-672

3. Hakem, A., et al., RhoC is dispensable for embryogenesis and tumor initiation but essential for metastasis. Genes and Development, 2005, 19:1974-1979

4. Bellovin, D.L., et al., Reciprocal regulation of RhoA and RhoC characterizes the EMT and identifies RhoC as a prognostic marker of colon carcinoma. Oncogene, 2006, 25: 6959-6967

## 243

### Transgenic mice show functional heterodimerization between vascular angiotensin II AT1 receptor and bradykinin B2 receptor

**Quitterer, Ursula**; **Langer, Andreas**; Graemer, Muriel; Abdalla, Said  
ETH Zürich, Molekulare Pharmakologie, Switzerland

Heterodimerization of the B2 receptor (B2R) for the vasodepressor bradykinin with the AT1 receptor (AT1R) for the vasopressor angiotensin II sensitizes AT1R-stimulated signalling of transfected and native smooth muscle cells. The AT1R–B2R heterodimer is also of pathophysiological relevance and contributes to the angiotensin II hyperresponsiveness of patients with preeclampsia hypertension. To further investigate the physiological function of the AT1R–B2R heterodimer, we established transgenic animal models with and without B2 receptor expression. To obtain mice with the same genetic background, the B2 receptor was reconstituted in B2R-deficient mice by a B2R transgene under control of the CMV promoter, which directs ubiquitous expression of a transgene. Confocal FRET imaging with FITC-labelled B2R-specific antibodies as donor and TRITC-labelled AT1R-specific antibodies as acceptor revealed the interaction of AT1R–B2R in the aortic media of Tg-B2R+ mice at a distance of less than 9 nm while the AT1R–B2R heterodimer was absent in the aorta of Tg-B2-/- mice. Concomitant with the absence of the AT1R–B2R heterodimer, the angiotensin II-stimulated vasopressor response of Tg-B2-/- mice was significantly reduced compared to Tg-B2R+ mice with efficient AT1R–B2R heterodimerization. Taken together, our data provide strong evidence that the B2R for the vasodepressor bradykinin sensitizes the angiotensin II AT1R-stimulated vasopressor response by heterodimerization.

## 244

### Tarbp2 binding to TRPC4 promotes changes of cytosolic Ca<sup>2+</sup> and thereby leads to a dynamic regulation of Dicer activity

**Latta, Lorenz**; Zimmermann, Jasmin; Beck, Andreas; Wissenbach, Ulrich; Flockerzie, Veit

Universität des Saarlandes, Experimentelle und Klinische Pharmakologie und Toxikologie, Homburg, Germany

The mammalian TRPC4 protein is a member of the transient receptor potential canonical subfamily of TRP proteins. TRPC4 proteins form non-selective Ca<sup>2+</sup>-conducting cation channels which are activated upon stimulation of receptors coupling to G<sub>α<sub>i</sub>/G<sub>α<sub>o</sub></sub>- and G<sub>α<sub>q</sub>/G<sub>α<sub>11</sub></sub>-dependent signaling pathways [1] or receptor tyrosine kinases. Several proteins have been implicated to interact and modulate TRPC4 function although the way of modulation / regulation is not known in detail. By using the TRPC4 cytosolic C-terminus as a prey in a modified yeast two-hybrid system we identified Tarbp2, a double-stranded RNA binding protein (dsRBP) which in mammals is part of the RNA-induced silencing complex including Argonaute and Dicer [2]. Tarbp2 increases carbachol induced Ca<sup>2+</sup> entry via TRPC4 channels in HEK293 cells stably expressing TRPC4 and the muscarinic receptor type 2. In addition, Dicer activity is shown to be increased in the presence of Ca<sup>2+</sup>. A ~130 kD Dicer fragment in addition to the full length ~220 kD Dicer protein is detectable in the presence but not in the absence of Ca<sup>2+</sup> indicating that the increase in [Ca<sup>2+</sup>] promotes proteolysis of the Dicer protein. Proteolysis is already apparent at 10 mM [Ca<sup>2+</sup>] and after 1 minute. Using N- and C-terminal Flag-tagged Dicer proteins, anti-Flag and two anti-Dicer antibodies which recognize different epitopes of Dicer, the Ca<sup>2+</sup>-dependent cleavage site within Dicer was mapped to a region C-terminal of alanine<sub>1133</sub> apparently near position 1150 (serine<sub>1150</sub>). The N-terminal Dicer fragment contains the ATPase/hel, DUF283 and PAZ domains and the other contains the two tandem RNase III domains and the C-terminal dsRBD. A very similar proteolytic processing of the endogenous Dicer protein has been identified in *C.elegans* [3] with cleavage near position 1200 which corresponds to position 1155 in the human enzyme. In addition very similar ~130 and ~90 kD fragments were obtained by proteolysis of full length recombinant human Dicer by endoproteinase Glu-C [4]. The C-terminal fragment lacking regulatory domains (helicase, DUF, and PAZ) was shown to be catalytically active [3, 4], although miRNA specific [3]. These results are conceivable with a model that Tarbp2 upon binding to TRPC4 modulates Ca<sup>2+</sup> entry which then promotes proteolytic activation of Dicer, most probably by Ca<sup>2+</sup>-dependent calpain proteases, leading to Dicer-dependent formation of noncoding RNAs.</sub></sub>

[1] Tsvilovskyy, V.V., et al., *Deletion of TRPC4 and TRPC6 in mice impairs smooth muscle contraction and intestinal motility in vivo*. Gastroenterology, 2009, 137(4): p. 1415-24.

[2] Rossi, J.J., *Mammalian Dicer finds a partner*. EMBO reports, 2005, 6(10): p. 927-9.

[3] Sawh, A.N. and T.F. Duchaine, *A truncated form of dicer tilts the balance of RNA interference pathways*. Cell reports, 2013, 4(3): p. 454-63.

[4] Ma, E., et al., *Coordinated activities of human dicer domains in regulatory RNA processing*. Journal of molecular biology, 2012, 422(4): p. 466-76.

## 245

### Pancreatic β-cell Gα<sub>i2</sub> stimulates insulin secretion

**Leiss, Veronika**<sup>1</sup>; Flockerzie, Katarina<sup>1</sup>; Birnbaumer, Lutz<sup>2</sup>; Schürmann, Annette<sup>3</sup>; Nürnberg, Bernd<sup>1</sup>

<sup>1</sup>Institut für Pharmakologie, Tübingen, Germany

<sup>2</sup>The National Institute of Environmental Health Sciences, North Carolina, United States

<sup>3</sup>Deutsches Institut für Ernährungsforschung, Nuthetal, Germany

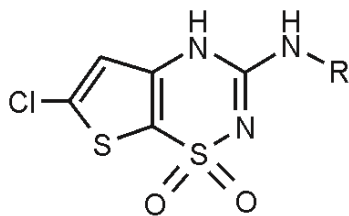
Insulin, a peptide hormone secreted from the β-cells of the endocrine pancreas, is an important regulator of blood glucose homeostasis. The pan-Gα<sub>i0</sub> inhibitor *Bordetella pertussis toxin* (PTx), also known as islet-activating protein (IAP), stimulates insulin release via direct effects on islets. Genetic ablation of Gα<sub>i</sub> in mice resulted in a similar phenotype, whereas the specific role of the major Gα<sub>i</sub> isoform, Gα<sub>i2</sub>, in regulating insulin secretion remains unclear. To analyze the functional role of Gα<sub>i2</sub> in β-cells, we generated β-cell-specific Gα<sub>i2</sub>-deficient mice (Gα<sub>i2</sub><sup>βCKO</sup>). *In vivo* analysis of glucose homeostasis in Gα<sub>i2</sub><sup>βCKO</sup> revealed normal blood glucose levels but significantly decreased plasma insulin levels as compared to littermate controls. Analyzing isolated islets of the Gα<sub>i2</sub>-targeted mouse line we examined various modulators of insulin secretion. We found that L-arginine- (10 mM) and L-ornithine- (10 mM) induced insulin secretion was significantly reduced in islets lacking β-cell Gα<sub>i2</sub>. In the same set of experiments no differences were detected when insulin release was stimulated by high glucose concentrations. As insulin release is triggered by an increase of the intracellular calcium concentration [Ca<sup>2+</sup>], we tested the involvement of Gα<sub>i2</sub> in the regulation of [Ca<sup>2+</sup>], by performing Ca<sup>2+</sup> measurements in dispersed islets. The Gα<sub>i2</sub>-deficient β-cells showed an increase in [Ca<sup>2+</sup>] at 16 mM glucose compared to control β-cells. In contrast, the increase of [Ca<sup>2+</sup>] was significantly reduced upon L-arginine treatment in Gα<sub>i2</sub><sup>βCKO</sup> dispersed β-cells. These findings were further supported by the reduced responses of Ca<sup>2+</sup>-increases following activation of insulin secretion by co-treatment with glucose (16 mM) and L-arginine (10 mM) in Gα<sub>i2</sub><sup>βCKO</sup> β-cells. In conclusion, our data show that Gα<sub>i2</sub> co-stimulates the release of insulin at physiological glucose concentrations in the presence of a calcium dependent manner by increasing the intracellular calcium mobilization.

### Thieno-thiadiazine derivatives displace [<sup>3</sup>H]-glibenclamide-binding to SUR1-type K<sub>ATP</sub> channels by an allosteric mechanism

**Lemoine, Horst**; Sachs, Alexander; Abdullah, Sarah; Küper, Joachim; Grüttner, Dagmar; Rauhaus, Karsten; Schmidt, Claas

Universität Düsseldorf, Inst. f. Lasermedizin (MWF), Duesseldorf, Germany

New potassium channel openers (KCO) of the thieno-thiadiazine (TTD)-type initially developed as agonists for SUR1-type K<sub>ATP</sub> channels (Nielsen et al., J Med Chem 45: 4171, 2002) were characterized in SUR2B-type K<sub>ATP</sub> channels as agonists (e.g. R=methylcyclobutyl = NNC462) and antagonists (e.g. R=methylcyclopropyl = NNC414) (Teschner et al., this journal 379, R56, 2009) which allosterically interact with [<sup>3</sup>H]-P1075 for SUR2B-binding (Lemoine et al., this journal 383, R39, 2011). To clarify their mode of action on SUR1, the compounds were tested in CHO-cells stably transfected with SUR1/Kir6.2. Using DiBAC<sub>4</sub>(3) for testing membrane potential effects by fluorescence (505/525 nm) NNC462 and NNC414 were characterized as agonists by hyperpolarisation with pEC<sub>50</sub>-values of 7.98±0.02 and 6.54±0.02 (-log M), respectively. To test the mode of interaction of compounds with sulphonylureas on SUR1-receptors we designed radioligand binding experiments with [<sup>3</sup>H]-glibenclamide (G). Saturation binding experiments performed with [<sup>3</sup>H]-G in CHO receptor membranes in the absence and presence of 2 mM ATP/Mg<sup>2+</sup> revealed a homogeneous class of binding sites characterized by pK<sub>D</sub>-values of 9.28±0.02 and 9.15±0.03 (-log M) and B<sub>max</sub>-values of 2.59±0.05 and 2.02±0.04 pmol/mg protein, respectively. Competition binding with [<sup>3</sup>H]-G in CHO receptor membranes revealed biphasic curves with high- (& 2 mM ATP/Mg<sup>2+</sup>) and low-affinity- (without ATP) components (pK<sub>D</sub>, -log M): 8.00±0.06 / 3.99±0.07 for NNC462 and 7.21±0.013 / 3.97±0.04 for NNC414. High affinity binding correlated with agonistic effects on K<sub>ATP</sub> channels. To examine if TTD-agonists interact competitively with sulphonylurea antagonists on SUR1-receptors, additional competition binding curves with the TTD-agonists were performed in intact cells using increasing [<sup>3</sup>H]-G concentrations (0.1, 0.6, 1.0, 6.0 nM). Competition curves with NNC462, however, did not reveal any dependence of pIC<sub>50</sub> for inhibition on [<sup>3</sup>H]-G concentration, thus contradicting a competitive interaction of TTD-agonists and G, but showed invariant pIC<sub>50</sub>-values between 6.7 and 6.9 (-log M). Thus, independent, non-overlapping binding sites on SUR1-receptors have to be assumed for high-affinity TTD-agonists and sulphonylurea blockers.



**Thieno-thiadiazine:**  
Chemical structure

### The M<sub>2</sub> muscarinic acetylcholine receptor-induced RhoA activation in cardiac myocytes requires intact caveolae and a complex formation of p190RhoGAP with RGS3, caveolin-3 and eNOS.

**Levay, Magdolna**; Abt, Christian; Wieland, Thomas

Institut für Experimentelle und Klinische Pharmakologie und Toxikologie, Mannheim, Germany

Regulator of G protein signaling (RGS) proteins are GTPase activating proteins (GAPs) for heterotrimeric G protein α subunits and therefore important negative regulators of G protein coupled receptor (GPCR) signals. RGS3 is one of the RGS proteins known to be upregulated in human heart failure. RGS3 acts as GAP for the α-subunits of G<sub>12</sub> and G<sub>13</sub> proteins and it exists in several splice variants. Besides its GAP activity, the RGS3L isoform has an additional function. It switches the activation of monomeric G protein Rac1 to the activation of RhoA after M<sub>2</sub> muscarinic acetylcholine receptor (M<sub>2</sub>AChR) stimulation. This switch requires a Gβγ mediated activation of PI3Ks, but the mechanism is still not understood. p190RhoGAP is one of the most important RhoGAPs, which is able to change the Rac1-RhoA balance in the cell. The activation of p190RhoGAP is likely dependent of tyrosine-nitration by endothelial nitric oxide synthase (eNOS) localized in the caveolae. Therefore the aim of the study was to investigate the possible role of the caveolae, p190RhoGAP and eNOS in the RGS3L-mediated RhoA activation in cardiac myocytes.

The carbachol-induced RhoA activation in the presence of RGS3L was attenuated when the cells were treated with methyl-β-cyclodextrin disrupting caveolae by cholesterol depletion. Similarly, the eNOS inhibitor L-NAME also suppressed the carbachol-induced RhoA activation. By reciprocal co-immunoprecipitations in NRCM we detected an interaction of p190RhoGAP with eNOS as well as an interaction of p190RhoGAP with Caveolin3 and RGS3L. Interestingly, stimulation of NRCM with carbachol increased the interaction of these proteins. The complexes could be also visualized by a proximity ligation assay.

We conclude that the complex formation of p190RhoGAP with RGS3L, eNOS and caveolin-3, the activation of eNOS which occurs most likely in caveolae, is important for the appearance of a carbachol-induced RhoA activation in cardiac myocytes which could mediate the described M<sub>2</sub>AChR-induced increase in cardiac contractility.

### Development of an *in silico* pre-screen for reproductive toxicity within the EU project ChemScreen

**Lewin, Geertje**<sup>1</sup>; van der Burg, Bart<sup>2</sup>; Batke, Monika<sup>1</sup>; Escher, Sylvia<sup>1</sup>; Mangelsdorf, Inge

<sup>1</sup>Fraunhofer Institute for Toxicology and Experimental Medicine (ITEM), Chemical Risk Assessment, Hannover, Germany

<sup>2</sup>BioDetection Systems b.v., XH Amsterdam, Netherlands

Assessment of reproductive toxicity is still the most animal requiring process in toxicity testing. Besides that, it is time- and cost-consuming. Compared to other fields in toxicology, alternative methods are rare and none have reached regulatory acceptance yet. Until this goal is reached, it is of outstanding importance to develop new testing strategies while using existing toxicological data to the best extent. Within the EU project ChemScreen (Chemical substance *in vitro/in silico* screening system to predict human and ecotoxicological effects), the Fraunhofer ITEM QSAR team analyzed whether existing *in vivo* data or structural properties can be used for identifying substances with reproductive toxicity.

The predictivity of repeated dose toxicity (RDT) studies for reproductive toxicity was analysed by comparing chemicals, where both endpoints were investigated. By comparing data in the Fraunhofer Databases on reproductive toxicity FeDTeX and repeated dose toxicity RepDose it could be shown that RDT studies can provide initial information on reproductive toxicity. Predictions could be enhanced, if RDT would be improved by minor methodological adaptations, by including functional parameters such as oestrus cyclicity data or sperm parameters. These improvements would not require additional animals within the study design.

Structural alerts for adult reproductive and immature developmental toxicity for studies in FeDTeX were identified by use of the OECD Toolbox and correlated to toxicological pathways analysed in *in vitro* studies by partners within ChemScreen. A first list of 32 structural alert entities was provided. Hereby, a distinction was made, on effect level, for gender affected, target affected and developmental stage. A further sub-analysis was performed for compounds causing structural anomalies in the offspring. A vice-versa test with known endocrine disruptors and developmental toxicants substantiated the identified structural alerts.

In conclusion, a relevant number of potential reproductive and developmental toxicants could be identified ahead of *in vivo* studies by using existing data, *in vitro* tests or structural alerts thus supporting prioritizations of animal testing.

### Obesity-induced dysfunction of endothelial nitric oxide synthase in perivascular adipose tissue

**Xia, Ning**<sup>1</sup>; Horke, Sven<sup>1</sup>; Habermeier, Alice<sup>1</sup>; Closs, Ellen<sup>1</sup>; Reifenberg, Gisela<sup>1</sup>; Wu, Zhixiong<sup>1</sup>; Siuda, Daniel<sup>1</sup>; Förstermann, Ulrich<sup>1</sup>; Mikhed, Yuliya<sup>2</sup>; Daiber, Andreas<sup>2</sup>; Li, Huige<sup>1</sup>

<sup>1</sup>Johannes Gutenberg University Medical Center, Department of Pharmacology, Mainz, Germany

<sup>2</sup>Johannes Gutenberg University Medical Center, 2nd Medical Clinic, Department of Cardiology, Mainz, Germany

Perivascular adipose tissue (PVAT) has recently been recognized as a novel modulator of vascular function. In agreement with this concept, the present study demonstrates an important role of PVAT in obesity-induced vascular dysfunction. In PVAT-free aortas from mice fed a high-fat diet (HFD) for 20 weeks, the endothelium-dependent, NO-mediated vasodilator response to acetylcholine remained normal. In contrast, a clear reduction in the vasodilator response to acetylcholine was observed in aortas from obese mice when the PVAT was left in place. In immunohistochemistry analysis, staining of endothelial NO synthase (eNOS) could be clearly seen in the aortic PVAT as well as in the aortic endothelium. Acetylcholine-induced vasodilation in the mouse aorta (either with or without PVAT) was completely blocked by the NOS inhibitor L-NAME, indicating that this response is NO-dependent. Thus, the reduced vasomotor function in the aorta of obese mice was likely to result from a dysfunction of eNOS in PVAT, but not in the endothelium. Indeed, PVAT NO production was significantly reduced in obese mice compared to lean control mice, as detected by 4,5-diaminofluorescein diacetate (DAF2-DA) staining with a Zeiss Laser Scanning Microscope (LSM). HFD had no effect on the expression of eNOS at mRNA or protein levels, neither in PVAT nor in endothelium. However, obesity led to a reduction of eNOS phosphorylation at serine 1177 (and thus in eNOS activity) in aortic PVAT, but not in the aorta itself. Acetylcholine enhanced the serine 1177 phosphorylation of PVAT eNOS in control mice, but not in obese mice. A number of kinases are known to phosphorylate eNOS at serine 1177, with Akt and AMPK being the most important ones. The reduced PVAT eNOS serine 1177 phosphorylation in obesity was associated with a reduced Akt phosphorylation at serine 473 (and thus reduced activity), whereas the activity of AMPK remained unchanged. Therefore, the reduced eNOS activity was likely to be due to an inhibition of Akt. Another potential mechanism underlying the reduced NO production in PVAT seemed to be a deficiency of L-arginine due to an induction of arginases. In conclusion, a reduction of PVAT NO production is likely to be implicated in the obesity-induced vascular dysfunction.

250

#### Human medicinal products: environmental risk assessment for volatile anaesthetics

**Krome, Kristin**; Hahn, Stefan; Schwonbeck, Susanne; Könnecker, Gustav; **Licht, Oliver**  
Fraunhofer ITEM, Chemikalienbewertung, Hannover, Germany

The environmental risk assessment of medicinal products for human use requires the calculation of a worst case Predicted Environmental Concentration (PEC) in surface water. This calculation is based on the assumption that the parent active ingredient is released to the wastewater after excretion from the human body. However, commonly used volatile inhalational anaesthetics are introduced into the atmosphere as the main target compartment and only minor amounts ( $\leq 5\%$ ) are excreted via urine. For three inhalational anaesthetics modelling tools were used to determine the PECs for the environmental compartments air, water and soil after administration to humans and excretion directly into the atmosphere. In addition, for those amounts of the parent compounds as well as for its metabolites, which are expected to reach the water compartments via urinary excretion, the conventional method of exposure estimation according to European Guideline EMEA/CHMP/SWP/4447/00 (2006) was used. PEC values of the parent substances in water and soil as well as PEC values of the metabolites were compared to the Predicted No Effect Concentrations (PNEC) retrieved from literature data to calculate a reliable risk towards aquatic and terrestrial organisms. Until now, no guidelines for the estimation of environmental risks arising from atmospheric contamination have been developed in Europe. Thus, ozone depletion potential, potential contribution to global warming and long distance transport were assessed using literature data. The described procedure enables, in our view, a more appropriate way of assessing risks of volatile anaesthetics towards air, water and soil.

251

#### Uptake of iron oxide nanoparticles as a function of their coating in human intestinal model

**Lichtenstein, Dajana**<sup>1</sup>; Bertin, Annabelle<sup>2</sup>; Fiedler, Doreen<sup>1</sup>; Horzowski, Sabine<sup>1</sup>; Palavinskas, Richard<sup>3</sup>; Niemann, Birgit<sup>1</sup>; Thünnemann, Andreas<sup>2</sup>; Lampen, Alfonso<sup>1</sup>

<sup>1</sup>BfR Bundesinstitut für Risikobewertung, Lebensmittelsicherheit, Berlin, Germany  
<sup>2</sup>BAM Bundesanstalt für Materialforschung und -prüfung, Polymere in Life Science und Nanotechnologie, Berlin, Germany

<sup>3</sup>BfR Bundesinstitut für Risikobewertung, Sicherheit in der Nahrungskette, Berlin, Germany

Products containing engineered nanoparticles (ENPs) are already manufactured and begin to have an impact on food-associated industries. Here, nanotechnology tools are used in the entire food chain, for example, during cultivation (agriculture), industrial processing, and food packaging, as well as in dietary supplements. Up to now, nanotoxicology inhalation has been extensively studied, but for a comprehensive risk assessment studies for oral exposure scenarios are imperative as well. Here, the uptake and transport of ENPs across the intestinal barrier is one important aspect and especially the coating of ENPs plays a crucial role.

Three differently coated iron oxide nanoparticles were characterised and toxicologically analysed to examine the influence of the ENP coating on the uptake of these particles in human intestinal epithelial (Caco-2) cells. The coating materials are quercetin, polyacrylic acid and glucose. The physicochemical characterisation was evaluated by A4F in combination with DLS, SAXS and Zetaziser. For transport studies the Transwell<sup>®</sup> system, high pressure chemical digestion and AAS were used, as well as CTB and MTT assay for toxicological testing. Additionally, particle uptake was visualized by TEM.

All investigated particles are similar in core size but differ in their zeta potential. No reduced viability of Caco-2 cells was observed for all particles up to 200  $\mu\text{g/ml}$  iron. Uptake and transport appear to be a function of shell charge. A negatively charged shell (high zeta potential) leads to a higher uptake and transport level, which is shown here by quercetin coated nanoparticles. For positively charged nanoparticles only a slight uptake could be observed.

Here, we could show a coating dependent uptake and transport of iron oxide nanoparticles in human intestinal Caco-2 cells. According to the coating material of the nanoparticles a correlation between an increasing negative zeta potential and transport rate or uptake was observed. Therefore, the zeta potential could be a potential indicator for iron oxide nanoparticle uptake in human intestine. Furthermore, TEM pictures indicate an endocytotic pathway as well as diffusion as uptake mechanism.

252

#### Differential recruitment of $\beta$ -arrestin by stereoisomers of $\beta_2$ -adrenoceptor agonists

**Littmann, Timo**<sup>1</sup>; Wainer, Irving William<sup>2</sup>; Ozawa, Takeaki<sup>3</sup>; Göttle, Martin<sup>1</sup>; Seifert, Roland<sup>1</sup>

<sup>1</sup>Hannover Medical School, Institute of Pharmacology, Germany

<sup>2</sup>National Institutes of Health, National Institute on Aging, Bethesda, United States

<sup>3</sup>The University of Tokyo, Department of Chemistry, Japan

The concept of functional selectivity has become the basic principle for interpreting G-protein-coupled receptor (GPCR)-signalling over the past few years. Receptors form ligand-specific conformations, which are capable of activating different signalling pathways. From this follows that GPCRs do not just couple to their originally attributed

types of G-proteins (canonic signalling) but also signal via  $\beta$ -arrestins, other types of G-proteins and various types of MAP-kinases. The result is a new understanding of GPCRs where the receptor can no longer be described as a simple on/off-switch, but rather as a dynamic element that turns on different signalling pathways in different intensities depending on the bound ligand. This, in turn, means that every ligand can have its own specific signalling profile, which is referred to as biased signalling [1]. Some stereoisomers of e.g.  $\beta_2$ -sympathomimetics, which are not separated from their racemic mixtures, show paradoxical pro-inflammatory effects. These effects could be traced back to specific biasing of those stereoisomers towards pro-inflammatory cellular responses [2].

In this study, we investigated the influence of stereoisomerism of a set of  $\beta$ -adrenergic ligands and their derivatives on  $\beta$ -arrestin1 and -2 recruitment to the  $\beta_2$ -adrenoceptor ( $\beta_2\text{AR}$ ).

HEK293 cells expressing  $\beta_2\text{AR}$  and  $\beta$ -arrestin1 or -2 were incubated with various stereoisomers of  $\beta$ -adrenergic drugs and ligand-induced  $\beta$ -arrestin recruitment was quantified using a split-luciferase assay [3].

The analysis of  $\beta$ -arrestin2-recruitment yielded a distinct order in potency and efficacy depending on stereochemistry. Ligands possessing one stereocenter - e.g. norepinephrine, salbutamol - are consistently more potent and efficacious in the (*R*)- than in the (*S*)-configuration. On the other hand, ligands like fenoterol - or derivatives such as methoxyfenoterol, methoxydesmethoxyfenoterol - containing two stereocenters showed the order of potency and efficacy (*R,R'*) > (*R,S'*) > (*S,R'*) > (*S,S'*). Interestingly, the stereoisomers of methoxynaphthylfenoterol do not fit into this order. Here the (*S,R'*)-configuration shows a significantly higher efficacy than the (*R,S'*)-configuration.

Our study shows stereospecific  $\beta$ -arrestin recruitment of clinically used  $\beta$ -adrenergic receptor ligands.

[1] Seifert R (2013) *Biochem Pharmacol* 86:853-861

[2] Takakura H, et al. (2012) *ACS Chem Biol* 7:901-910

[3] Volcheck GW, et al. (2005) *Clin Exp Allergy* 35:1341-1346

253

#### Artesunate, a semi-synthetic plant extract, sensitizes glioblastoma cells to the anticancer drug temozolomide

**Lokan, Stefanie**; Kniznik, Anna; Steinmetz, Vanessa; Kaina, Bernd

Universitätsmedizin Mainz, Toxikologie, Germany

Glioblastoma are the most common malignant brain tumors in adults. Since they are highly resistant to radio- and chemotherapy, standard treatments offer only a palliative survival advantage. Hence, finding effective alternative treatments is of great importance. We have investigated the impact of artesunate on glioma cells. Artesunate has been utilised in traditional Chinese medicine for hundreds of years, where it is used for fever treatment. Today, artesunate is used as first-line therapy for malaria. Artesunate is a powerful inducer of reactive oxygen species. We have shown that artesunate has genotoxic and cytotoxic potential and induces oxidative DNA damage including DNA double-strand breaks. Further, our results show that artesunate increases the formation of autophagosomes. The accumulation of autophagosomes might lead to cell death, which is executed by apoptosis and necrosis. Despite increasing interest in therapeutic application of artesunate, the effect of artesunate combination with radio- and chemotherapy of gliomas is not well understood. We provide evidence that artesunate sensitizes glioblastoma cells to the first-line drug temozolomide with autophagy being centrally involved. The data suggest a potential advantage of combining artesunate and temozolomide as a novel strategy in the therapy of glioblastoma. Work is supported by Deutsche Krebshilfe (Nr.1100085).

254

#### The novel antiepileptic drug imepitoin compares favourably to other GABA-mimetic drugs in a seizure threshold model in mice and dogs

**Löscher, Wolfgang**; Hoffmann, Katrin; Twele, Friederike; Töllner, Kathrin

Tierärztliche Hochschule Hannover, Institut für Pharmakologie, Germany

Recently, the imidazolinone derivative imepitoin (Pexion<sup>®</sup>, Boehringer Ingelheim Vetmedica/Germany) has been approved for treatment of canine epilepsy. Imepitoin acts as a low-affinity partial agonist at the benzodiazepine (BZD) site of the GABA<sub>A</sub> receptor and is the first compound with such mechanism that has been developed as an antiepileptic drug (AED). This mechanism offers several advantages compared to full agonists, including less severe adverse effects and a lack of tolerance and dependence liability, which has been demonstrated in rodents, dogs, and non-human primates. In clinical trials in epileptic dogs, imepitoin was shown to be an effective and safe AED. Recently, seizures in dogs have been proposed as a translational platform for human therapeutic trials on new epilepsy treatments.

In the present study, we compared the anticonvulsant efficacy of imepitoin, phenobarbital and the high-affinity partial BZD agonist abecarnil in the timed i.v. pentylenetetrazole (PTZ) seizure threshold test in dogs and, for comparison, in mice. Furthermore, adverse effects of treatments were compared in both species.

All drugs dose-dependently increased the PTZ threshold in both species, but anticonvulsant efficacy was higher in dogs than mice. At the doses selected for this study, imepitoin was slightly less potent than phenobarbital in increasing seizure threshold, but markedly more tolerable in both species. Effective doses of imepitoin in

the PTZ seizure model were in the same range as those suppressing spontaneous recurrent seizures in epileptic dogs, demonstrating that the PTZ test correctly predicts the anticonvulsant potency of such a drug in a clinical trial. The study demonstrates that low-affinity partial agonists at the benzodiazepine site of the GABA<sub>A</sub> receptor, such as imepitoin, offer advantages as a new category of AEDs. Hopefully, the favourable profile of imepitoin for treatment of epilepsy in dogs will reactivate the interest in partial BZD site agonists as novel treatments for human epilepsy, too.

## 255

### Doxorubicin-induced left ventricular dysfunction is prevented by ablation of cardiac myocyte mineralocorticoid receptors in mice

**Lothar, Achim**<sup>1,2</sup>; Gilsbach, Ralf<sup>1</sup>; Moser, Martin<sup>2</sup>; Bode, Christoph<sup>2</sup>; Berger, Stefan<sup>3</sup>; Hein, Lutz<sup>1</sup>

<sup>1</sup>Institute of Experimental and Clinical Pharmacology and Toxicology, University of Freiburg, Germany

<sup>2</sup>Heart Center, University of Freiburg, Department of Cardiology and Angiology I, Germany

<sup>3</sup>German Cancer Research Center, Heidelberg, Germany

#### Introduction

Doxorubicin is a cytostatic agent still widely used in the therapy of various tumors. However, its benefit is severely limited by doxorubicin-induced cardiotoxicity that occurs in up to 10 % of patients treated with doxorubicin. Antagonists of the mineralocorticoid receptor (MR) are well established in chronic heart failure therapy. Thus, this study was designed to evaluate the significance of MR in cardiac myocytes for doxorubicin cardiotoxicity.

#### Methods and Results

Cardiac myocyte-specific deletion of the MR gene (MR<sup>MLCCre</sup>) in mice was achieved using the Cre/loxP system. MR<sup>MLCCre</sup> mice and Cre-negative littermates (wild-type) were treated with 15 mg doxorubicin / mg body weight i.p. in order to induce acute doxorubicin cardiotoxicity. 12 days after doxorubicin treatment left ventricular function as assessed by echocardiography (ejection fraction MR<sup>MLCCre</sup> 88.1 ± 3.2% vs. wild-type 71.9 ± 4.6, P<0.05) or left ventricular catheterization (dp/dt<sub>max</sub> MR<sup>MLCCre</sup> 5681 ± 337 mmHg/s vs. wild-type 4461 ± 261 mmHg/s, P<0.01) were improved in MR<sup>MLCCre</sup> mice as compared to wild-type mice. Cardiac fibrosis was increased after doxorubicin treatment without differences between the genotypes. The anti-apoptotic *Bcl-2* (B-cell lymphoma 2) gene was upregulated in hearts from MR<sup>MLCCre</sup> mice after doxorubicin treatment as assessed by qRT-PCR (1.60 ± 0.13-fold vs. wild-type, P<0.01). Among 588 genes regulated in myocytes isolated from untreated MR<sup>MLCCre</sup> vs. wild-type mice as determined by cDNA micro-array experiments (n=3, >1.5-fold, P<0.05) we found a significant enrichment of genes assigned to gene ontology terms "regulation of apoptosis" or "regulation of cell death", including *Bcl-2/212* (1.91-fold upregulated vs. control, P<0.05). Bioinformatical analysis further revealed an overrepresentation (4.6-fold vs. whole genome, P=0.019) of genes belonging to the mTOR (mammalian target of rapamycin) pathway among the differentially expressed genes. Increased mTOR activity has previously been associated with preserved cardiac function after doxorubicin treatment.

#### Conclusion

Mice lacking the mineralocorticoid receptor in cardiac myocytes were protected from doxorubicin induced left ventricular dysfunction. This might be associated with an activation of anti-apoptotic gene programmes and enhanced mTOR signaling in MR-deficient mice. The findings from this study might provide the rationale for the use of MR antagonists in patients treated with doxorubicin.

## 256

### Phosphodiesterase 2A localized in the spinal cord regulates pain processing

**Lu, Rui**<sup>1,2</sup>; Kallenborn-Gerhardt, Wiebke<sup>2</sup>; Bothe, Aaron<sup>2</sup>; Thomas, Dominique<sup>2</sup>; Schlaudraff, Jessica<sup>3</sup>; Real, Catherine Isabell<sup>1</sup>; Ferreirós Bouzas, Nerea<sup>2</sup>; Geisslinger, Gerd<sup>2</sup>; Del Turco, Domenico<sup>3</sup>; Schmidtko, Achim<sup>1,2</sup>

<sup>1</sup>Institut für Pharmakologie und Toxikologie, Universität Witten/Herdecke, ZBAF, Germany

<sup>2</sup>Pharmazentrum Frankfurt/ZAFES, Institut für Klinische Pharmakologie, Goethe-Universität, Frankfurt am Main, Germany

<sup>3</sup>Institut für Klinische Neuroanatomie, Neuroscience Center, Goethe-Universität, Frankfurt am Main, Germany

Phosphodiesterase 2A (PDE2A) is an evolutionarily conserved enzyme that catalyzes the degradation of the cyclic nucleotides cAMP and/or cGMP. Recent studies reported the expression of PDE2A in the spinal cord, pointing to a potential contribution to the processing of pain. However, the functions of PDE2A in spinal pain processing *in vivo* remained elusive. We here demonstrate that PDE2A is distinctly expressed in the superficial dorsal horn of the spinal cord, and that its expression is up-regulated in response to hindpaw inflammation. Administration of the selective PDE2A inhibitor BAY 60-7550 increased the nociceptive behavior of mice in animal models of inflammatory pain. Moreover, BAY 60-7550 increased the pain hypersensitivity induced by cAMP analogs, and it increased the cAMP levels in spinal cord tissues. Our findings indicate that PDE2A contributes to the processing of pain in the spinal cord.

## 257

### Resistance of *Bacillus anthracis* edema factor activation against calmodulin oxidation

**Lübker, Carolin**<sup>1</sup>; Tang, Wei-Jen<sup>2</sup>; Urbauer, Jeffrey<sup>3</sup>; Urbauer, Ramona<sup>3</sup>; Seifert, Roland

<sup>1</sup>Hannover Medical School, Institute of Pharmacology, Germany

<sup>2</sup>The University of Chicago, Ben May Department for Cancer Research, United States

<sup>3</sup>The University of Georgia, Department of Chemistry, Athens, United States

Calmodulin (CaM)-activated adenyl cyclase (AC) toxin edema factor (EF) from *Bacillus anthracis* plays an important role in anthrax disease [1]. The NADPH-oxidase in neutrophils produces superoxide anions for host defense against bacteria. CaM-activated EF corrupts host defence by generation of high concentrations of cAMP, which inhibits the NADPH-oxidase [2]. Superoxide and superoxide-derived radicals can also oxidize methionine residues in CaM. It is important to better understand the interaction of EF and oxidized CaM as a possible target for the development of new drugs against anthrax disease because there is a lack of effective and selective EF inhibitors [3].

We used CaM-wildtype (wt) with nine methionine (Met) residues and CaM-mutants, where one or more Met are substituted against non-oxidizable leucine (Leu) residues, for in-vitro oxidation by H<sub>2</sub>O<sub>2</sub> and radiometric analysis of the AC activity of EF.

The efficacy of the AC activity stimulated by CaM-wt oxidized with 0.05-5 mM H<sub>2</sub>O<sub>2</sub> for 24 h was almost like unoxidized CaM-wt, but the potency was decreased for oxidized CaM-wt with 5 mM H<sub>2</sub>O<sub>2</sub>. Oxidized CaM-wt with 50 mM H<sub>2</sub>O<sub>2</sub> for 24 h did not activate EF anymore. The oxidation of distinct Met residues in CaM-mutants did not alter the efficacy, but the potencies were decreased. Only the CaM-mutant with two Met to Leu substitutions and consequently seven oxidized Met residues was not able to fully stimulate EF.

Taken together, our results show that EF is resistant against oxidation of Met in CaM in contrast to other CaM-targets like the membranous adenyl cyclase 1, which is more sensitive against CaM oxidation [4]. This feature allows the toxin to generate high rates of cAMP although the NADPH-oxidase produces superoxide anions for host defense.

[1] Hicks CW, Sweeney DA, Cui X, Li Y, Eichacker PQ (2012) An overview of anthrax infection including the recently identified form of disease in injection drug users. *Intensive Care Med* 38:1092-1104

[2] Wright GG, Mandell GL (1986) Anthrax toxin blocks priming of neutrophils by lipopolysaccharide and by muramyl dipeptide. *J Exp Med* 164:1700-1709

[3] Seifert R, Dove S (2013) Inhibitors of *Bacillus anthracis* edema factor. *Pharmacol Ther* 140:200-212

[4] Lübker C, Moskovitz J, Urbauer J, Bieber Urbauer R, Seifert R (2013) Regulation of adenyl cyclase 1 by oxidized calmodulin and calmodulin mutants. *Naunyn-Schmiedeberg's Arch Pharmacol* 386 (Abstracts of the 79<sup>th</sup> Annual Meeting of the German Society for Experimental and Clinical Pharmacology and Toxicology, March 5-7, 2013, Halle, Germany) Suppl 1: S49/198

## 258

### Hepatotoxic pyrrolizidine alkaloids – Structure-dependent interaction with nuclear receptors

**Luckert, Claudia**<sup>1</sup>; Hessel, Stefanie<sup>1</sup>; Lenze, Dido<sup>2</sup>; Lampen, Alfonso<sup>1</sup>

<sup>1</sup>Bundesinstitut für Risikobewertung, Lebensmittelsicherheit, Berlin, Germany

<sup>2</sup>Charité-Universitätsmedizin Berlin, Institut für Pathologie, Germany

1,2-unsaturated pyrrolizidine alkaloids (PA) belong to the most toxic compounds. These substances are found in several plants such as *Asteraceae* and *Boraginaceae* families. Acute PA poisoning by food contamination causes severe damage to liver; long-term, sub-lethal doses may cause cumulative damage or cancer.

A previous whole genome  $\mu$ -array analysis of PA in primary human hepatocytes revealed potential interactions of PA with certain nuclear receptors acting or working as transcription factors. Employing reporter gene assays it was analyzed whether PA can activate or inhibit the nuclear receptors RAR $\alpha$ , RXR $\alpha$ , LXR $\alpha$ , FXR, PPAR $\alpha$ , PPAR $\delta$ , PXR, ER $\alpha$  and ER $\beta$ . As PXR mediates CYP3A4 promoter activity a potential induction or inhibition of CYP3A4 promoter activity was additionally investigated. To cover the most frequently occurring PA structures (retroecine, heliotridine and otonecine type as well as monoester, diester and cyclic diester) the four PA senecionine, heliotrine, echimidine and senkirkine were selected as representative PA. Heliotrine was found to inhibit the transactivation of LXR $\alpha$ , RXR $\alpha$ , PPAR $\alpha$ , PPAR $\gamma$ , PPAR $\delta$  and PXR. Senecionine activated ER $\alpha$  and  $\beta$ . Echimidine was the only PA that activated PXR. Consequently, it also exclusively induced CYP3A4 promoter activity. Neither interactions nor transactivation could be observed for senkirkine.

In conclusion, the prediction from the  $\mu$ -array data suggesting an interaction of PA with different nuclear receptors could be confirmed. However, the interactions were found to be heterogeneous between the structurally different PA. This suggests a specific structure-activity relationship of PA concerning their interaction with nuclear receptors.

## 259

### Influence of silybin hemisuccinate on lipopolysaccharide (LPS) induced systemic inflammation and consecutive liver dysfunction in mice

**Werner, Markus**; Löser, Konstantin; Lenhardt, Isabell; **Lupp, Amelie**

Universitätsklinikum Jena, Institut für Pharmakologie und Toxikologie, Germany



Despite recent advances in critical care, sepsis, septic shock and subsequent multi-organ failure remain an important cause of morbidity and mortality in intensive care units. With about 20-25% of patients displaying a severe inflammatory reaction with associated organ failure impaired liver function can be observed, which has been shown to be of major consequence for overall patient outcome. However, although extensive research efforts have been made, no specific therapy exists so far for the treatment of sepsis and of liver failure in sepsis.

Thus, the aim of the present study was to evaluate if silybin hemisuccinate, which is used e.g. as a hepatoprotectant in emergency cases after death cap poisoning or after intoxication with hepatotoxic drugs is able to ameliorate the LPS-induced systemic inflammation and consecutive liver dysfunction in mice and thus can possibly serve as a new treatment option in sepsis.

For this purpose, male 60-day-old mice were assigned to four treatment groups: (1) controls, (2) LPS treatment, (3) treatment with silybin hemisuccinate, (4) treatment with LPS plus silybin hemisuccinate. LPS was administered once at a dosage of 5 mg/kg body weight, silybin hemisuccinate twice daily (starting one hour before LPS treatment) either at a dosage of 200 mg/kg body weight (in the 24h-short-term experiment) or of 50 mg/kg body weight (in the 72h-long-term experiment). 24 or 72 hours after LPS administration animals were sacrificed and organ weights and different physiological parameters (body temperature, blood glucose levels) as well as various parameters representing liver damage or liver function or indicating oxidative stress in liver but also in different other tissues were assessed.

LPS caused a distinct decrease in body temperature and blood glucose levels as well as in liver glycogen content and biotransformation capacity together with an increase in oxidative stress in different organs. Whereas in the 24h-short-term experiment on the whole no significant influence of silybin hemisuccinate was observed, in the 72-long-term experiment a distinct protective effect was seen on many of the parameters tested not only in liver, but also in other organs such as brain and kidney.

Altogether, these results point to a protective effect of silybin hemisuccinate in the long term in systemic inflammation which was not restricted to liver tissue only, thus suggesting that silybin hemisuccinate may possibly serve as a new treatment option in sepsis.

## 260

### A second wave of protein kinase A signalling after internalization of the thyroid stimulating hormone receptor

Lyga, Sandra<sup>1,2</sup>; Calebiro, Davide<sup>1,2</sup>

<sup>1</sup>Institut für Pharmakologie und Toxikologie, Würzburg, Germany

<sup>2</sup>Rudolf Virchow Zentrum, Würzburg, Germany

The thyroid stimulating hormone (TSH), a prototypical large protein hormone, regulates the function of thyroid cells by binding to a G-protein-coupled receptor (GPCR), which activates the cAMP/PKA-pathway. Although GPCRs have been thought to signal only from the cell surface, our recent findings suggest that internalized TSH receptors (TSHR) continue signalling via G<sub>αs</sub> and cAMP from an intracellular compartment, where they are found together with their ligand. This causes a persistent cAMP increase and possibly specific effects (1). Whereas there is increasing evidence that endosomal signalling might be shared by different GPCRs (2-4), the consequences downstream of cAMP are largely unknown. In this study, we have further investigated this phenomenon in primary mouse thyroid cells at the level of the cAMP-dependent protein kinase (PKA), by analysing the subcellular localization and kinetics of PKA activation in the presence or absence of endocytosis inhibitors. PKA activity was measured by fluorescence resonance energy transfer (FRET) in living primary mouse thyroid cells transfected with the AKAR2 sensor. The results indicate that the activation of PKA in response to TSH in the whole cell is biphasic (τ first phase: ~ 1.6 min; τ second phase: ~ 1.1 min; delay: ~ 1.4 min). The second (late) phase was virtually absent in cells pretreated with dynasore, a small-molecule dynamin inhibitor. Moreover, we found that the PKA R11b subunit is located on membranes of the Golgi/trans-Golgi network, where the internalized TSH/TSHR complex, Gas and adenylyl cyclase are also apparently located. Our data suggest that TSHR internalization and signalling from this intracellular compartment might be required for the late phase of PKA activation in thyroid cells. These findings strengthen the hypothesis that the Golgi/trans-Golgi network might serve as a specialized intracellular platform for GPCR signalling.

[1] Calebiro D, Nikolaev VO, Gagliani MC, de Filippis T, Dees C, Tacchetti C, Persani L, Lohse MJ. (2009) Persistent cAMP-signals triggered by internalized G-protein-coupled receptors. *PLoS Biol.* 7:e1000172.

[2] Calebiro D, Nikolaev VO, Persani L, Lohse MJ. (2010) Signaling by internalized G-protein-coupled receptors. *Trends Pharmacol. Sci.* 31:221-8.

[3] Irannejad R, Tomshine JC, Tomshine JR, Chevalier M, Mahoney JP, Steyaert J, Rasmussen SG, Sunahara RK, El-Samad H, Huang B, von Zastrow M. (2013) Conformational biosensors reveal GPCR signalling from endosomes. *Nature.* 495:534-8.

[4] Lohse MJ, Calebiro D. (2013) Cell biology: Receptor signals come in waves. *Nature.* 495:457-8.

## 261

### The vasodilatory APJ receptor agonistic peptide apelin attenuates human platelet aggregation

Wirtz, Christopher<sup>1</sup>; Mahajan-Thakur, Shailaja<sup>1</sup>; Böhm, Andreas<sup>1</sup>; Strohbach, Anne<sup>2</sup>; Felix, Stephan<sup>2</sup>; Busch, Ralf<sup>2</sup>; Rauch, Bernhard H.<sup>1</sup>

<sup>1</sup>Universitätsmedizin Greifswald, Institut für Pharmakologie, Germany

<sup>2</sup>Universitätsmedizin Greifswald, Klinik und Poliklinik für Innere Medizin B, Germany

Apelin is an endogenous ligand for the G-protein-coupled angiotensin receptor-like-1 (APJ) receptor. Produced as preproapelin, it is cleaved into several bioactive peptides such as apelin-12, -13 and -17. Apelin and APJ are expressed in several tissues such as the vessel wall, the heart and several tumors. However, the presence or a presumable function of the apelin/APJ system in platelets has not been reported to date. Therefore, we investigated APJ expression and the functional effects of different apelin isoforms in human platelets.

Human platelet-rich plasma (PRP) was utilized for the detection of apelin and the APJ receptor by immunofluorescence studies, Western blotting and flow cytometry, respectively. Functional effects of the apelin-12, -13 and -17 on platelet aggregation were determined by light transmission aggregometry.

Expression of the APJ receptor was observed predominantly in the outer membrane of resting platelets in comparison with granule markers. In addition, cell surface expression of the receptor was confirmed by flow cytometry. Compared to untreated controls, protein signals for APJ appeared to be decreased within platelet lysates upon activation with thrombin receptor-activating peptide (AP1). Platelet aggregation was induced by ADP or AP1 (10 - 30 μM, respectively). Preincubation of human platelets with the different apelin forms for 30 sec to 5 min attenuated platelet aggregation by up to 20%. In particular, apelin-17 significantly inhibited aggregation induced by ADP or AP1 compared to controls, while apelin-12 and -13 were less effective. This inhibitory effect of apelin was prevented after preincubation with the eNOS inhibitor L-NAME (300 μM), pointing to an NO-dependent underlying mechanism.

Taken together, these data suggest that APJ is expressed at the surface of resting human platelets. The APJ ligand apelin may function as an endogenous inhibitor of aggregation or possibly platelet hyperactivity via stimulation of platelet NO-release.

## 262

### New 3D-co-culture model and microbio-reactor for lung exposure experiments

Mai, Patrick<sup>1</sup>; Fernekorn, Uta<sup>2</sup>; Hampl, Jörg<sup>2</sup>; Schober, Andreas<sup>2</sup>; Foth, Heidi<sup>1</sup>

<sup>1</sup>Martin-Luther-University Halle-Wittenberg, Institute of Environmental Toxicology, Halle (Saale), Germany

<sup>2</sup>Ilmenau University of Technology, Department of Nano-Biosystem Technology, Germany

Lung diseases like cancer, infection or chronic obstructive pulmonary disease (COPD) belong to the ten leading causes of deaths in high- and low-income countries. To develop new and potent drugs or to describe the pathological processes in the lung, there is a need for valid lung models which can be used for basic or pharmaceutical research. Additionally, an interest in reducing animal testing corresponding to the 3R-Principle is given.

The Martin-Luther-University Halle-Wittenberg and the Ilmenau University of Technology are establishing a new 3D-co-culture model of epithelial and endothelial cells and an exposure system to validate this physiological alveolar model. MatriGrids consisting of 187 cavities serve as a 3-dimensional cell support structure to culture epithelial lung cells on the apical site and endothelial cells on the basal side of the structure under air-liquid-interface (ALI) conditions. With the 3-dimensional characteristics of the cell support structure and the double-sided ALI-culture, cells will be cultured in an in vitro environment which is much more representative of the in vivo lung environment. First experiments show that vitality and metabolic activity of an alveolar epithelial cell line (A549) are not influenced in an ALI-culture compared to a liquid-liquid-interface (LLI)-culture. In the cavities of the MatriGrid the cell line forms a monolayer with expression of cell-adhesion molecules (ZO-1, E-Cadherin).

In addition, ALI-cultures make a direct exposure of cells possible with no negative time or dose dependent medium effects. This is necessary for significant and repeatable exposures with xenobiotics. The new exposure system based on normal 24-well microtiter plates (MTP) whose cover is equipped with tubing for the delivery and extraction of xenobiotics. A special tip on each tube brings xenobiotics into close proximity with the cells so that well defined exposures are possible. The final advantage is the option to work sterily and simultaneously compare exposed and unexposed samples on the same MTP.

In future work, this new 3D-co-culture alveolar model and the innovative exposure system will be used for measurements of epithelial and endothelial cell reactions to clearly define exposure of xenobiotics. Qualified methods like ELISA, FACS or immunohistochemical staining are used after exposure to analyse changes in cytokine levels or the expression of cell-adhesion molecules caused by the exposure of xenobiotics.

## 263

### 8-hydroxoguanosine as a marker for RNA oxidation in cells and urine

Mandel, Philipp; Schupp, Nicole

Universität Würzburg, Toxikologie, Germany

The oxidation of RNA via reactive oxygen species (ROS) is intensively studied in this decade, because elevated RNA damage was found in many degenerative diseases, like in Parkinson and Alzheimer. A dysfunction of mRNA leads to a reduction in protein synthesis or to the production of truncated and therefore possibly inoperable proteins. In addition, the function of non-coding RNAs, increased for example in cancer and diabetes, is essentially unknown, but they also can be damaged by ROS.

The aim of this study was to detect oxidative damage to RNA *in vitro* and *in vivo* via the biomarker 8-hydroxoguanosine (8-oxoG). 8-oxoG was quantified with HPLC-MS/MS methods either directly in cells and also in urine of hypertensive animals, in which we have recently found markers of oxidatively damaged DNA.

First results with hydrogen peroxide as the oxidizing agent show a dose- and time-dependent increase of 8-oxoG in cultivated kidney cells. As further oxidizing agents the

blood pressure-regulating hormones aldosterone and angiotensin II will be tested *in vitro*. Treatment of animals with these two compounds led to an elevated excretion rate of 8-oxoG in comparison to the respective control groups.

In summary, 8-oxoG is easy to measure in cells as well as in urine compared to cellular markers of DNA oxidation. Hydrogen peroxide, as well as the ROS-inducing aldosterone and angiotensin II increased the amount of the RNA damage marker.

## 264

### Heterologous Regulation of Agonist-Independent $\mu$ -Opioid Receptor Phosphorylation by Protein Kinase C

**Mann, Anika**; Illing, Susann; Schulz, Stefan

Institut für Pharmakologie und Toxikologie, Jena, Germany

#### BACKGROUND AND PURPOSE:

Homologous agonist-induced phosphorylation of the  $\mu$ -opioid receptor is initiated at carboxyl-terminal S375 followed by phosphorylation of T370, T376 and T379. In HEK293 cells, this sequential and hierarchical multi-site phosphorylation is specifically mediated by G protein-coupled receptor kinases 2 and 3. In the present study, we provide evidence for a selective and dose-dependent phosphorylation of T370 after activation of PKC by phorbol esters.

#### EXPERIMENTAL APPROACH:

Here, we identify kinases that mediate agonist-independent phosphorylation of the  $\mu$ -opioid receptor using a combination of phosphosite-specific antibodies, kinase inhibitors and siRNA knock-down screening in HEK293 cells. In addition, we show with phosphosite-specific antibodies that S363 is constitutively phosphorylated in mouse brain *in vivo*.

#### KEY RESULTS:

We show that activation of protein kinase C (PKC) by phorbol esters or heterologous activation of substance P receptors co-expressed with  $\mu$ -opioid receptors in the same cell leads to a selective and dose-dependent phosphorylation of T370 that specifically requires the PKC $\alpha$  isoform. Inhibition of PKC activity did not compromise homologous agonist-driven T370 phosphorylation. In addition, we show that S363 is constitutively phosphorylated in both HEK293 cells and mouse brain *in vivo*. Constitutive S363 phosphorylation requires ongoing PKC activity. When basal PKC activity is diminished, S363 can also be substrate for homologous agonist-stimulated phosphorylation.

#### CONCLUSIONS & IMPLICATIONS:

The present results unravel novel mechanisms of heterologous regulation of MOR phosphorylation by PKC. These findings represent a useful starting point for definitive experiments elucidating the exact contribution of PKC-driven MOR phosphorylation to diminished MOR responsiveness in morphine tolerance and pathological pain.

## 265

### A 18 kDa membrane protein affects cytosolic Ca in the presence of the inhibitor of endocytosis, dynasore

**Mannebach, Stefanie**; Frohnweiler, Katja; Dörr, Janka; Flockerzi, Veit

Universität des Saarlandes, Experimentelle und Klinische Pharmakologie und Toxikologie, Homburg, Germany

Recently, a novel membrane protein in *Drosophila melanogaster* was shown to be localized in presynaptic vesicles. It appears to mediate a Ca influx after vesicle fusion with the plasma membrane. Disruption of the corresponding gene leads to endocytotic defects in *drosophila* (Yao et al., Cell 2009). Apparently, this protein plays a role in exo- and endocytosis and could serve as a Ca channel supplying Ca required for endocytosis. In addition and alternatively it may determine clonal selection by forcing cells to undergo apoptosis.

We have identified a 171 amino acid (aa) protein (18 kDa) in mouse which shares 26.3% aa sequence identity with the fly protein and which we call mouse Flower-like or mFl. The mFl protein is encoded by a unique gene on chromosome 2. After expression of a His-SUMO-mFl-fusion protein in *E.coli*, the purified recombinant protein was used for immunization of rabbits. The affinity purified anti-mFl antibody recognizes mFl proteins in brain, pancreas, thymus, lung, colon and kidney.

Using RT-PCR the "full length" mFl transcript could be identified in brain, pancreas, liver, thymus, heart, spleen, mast cells and kidney. Furthermore we have amplified, cloned and sequenced a novel Flower orthologue transcript in *Cos-7* kidney cells from *african green monkeys* which is 172 aa in length and 90% identical to the mouse and 77% to the human protein. The mFl antibody detects Flower signals in vesicular-like structures and apparently not in the plasma membrane of *Cos-7* cells. After treatment with Dynasore, an inhibitor of endocytosis (Kirchhausen et al., Cell 2006), the proteins recognized by the antibody move towards the plasma membrane, indicating that Flower proteins localized in vesicles may reach the plasma membrane after exocytosis, as has been proposed for *Drosophila* Flower. After heterologous expression of the mFl cDNA in *Cos-7* cells we observed a slow increase in cytosolic calcium in the presence of the inhibitor of endocytosis, Dynasore.

To analyze mFl function *in vivo* we have generated mFl deficient mouse lines using gene targeting. Very recently first knock out animals were available. No 18kDa mFl proteins were detected in lysates from brain, kidney and thymus from mice homozygous for the knock-out allele using the anti-mFl antibody, thereby independently confirming mFl gene-deficiency and the specificity of the antibody. Using these mice we now are able to analyze the function of mFl proteins in the whole organism.

## 266

### Deletion of the TRPM4 channel in mice leads to augmented cardiac inotropic response to $\beta$ -adrenergic stimulation.

**Mathar, Ilka**<sup>1</sup>; Uhl, Sebastian<sup>1</sup>; Kecskes, Miklos<sup>2</sup>; van der Mieren, Gerry<sup>3</sup>; Jacobs, Griet<sup>2</sup>; Londoño, Juan E.C.<sup>1</sup>; Flockerzi, Veit<sup>4</sup>; Voets, Thomas<sup>2</sup>; Nilius, Bernd<sup>2</sup>; Herjigers, Paul<sup>3</sup>; Freichel, Marc<sup>1</sup>; Vennekens, Rudi<sup>1</sup>

<sup>1</sup>Universitätsklinikum Heidelberg, Pharmakologisches Institut, Germany

<sup>2</sup>KU Leuven, Laboratory of Ion Channel Research, Belgium

<sup>3</sup>KU Leuven, Research Unit of Experimental Cardiac Surgery, Belgium

<sup>4</sup>Universität des Saarlandes, Experimentelle & klinische Pharmakologie, Homburg, Germany

TRPM4 proteins constitute Ca<sup>2+</sup> activated, but Ca<sup>2+</sup> impermeable, non-selective cation channels and are expressed both in atrial and ventricular cardiomyocytes. The physiological function of TRPM4 in the heart remains however incompletely understood. To investigate the functional role of the TRPM4 channel in cardiac myocytes and cardiac contractility we used TRPM4 knockout mice and performed live cell Ca<sup>2+</sup> imaging, patch clamp electrophysiology, contractility recordings of isolated ventricular papillary muscle as well as *in vivo* measurements of ECG and pressure-volume loops since TRPM4-specific agonists/antagonists are not available. In *Trpm4*<sup>-/-</sup> mice, cardiac muscle displays an increased  $\beta$ -adrenergic inotropic response and measurements of ventricular action potential duration show a significantly decreased time for 50% and 90% repolarization. We provide evidence that this change in action potential shape leads to an increased driving force for L-type Ca<sup>2+</sup> current during the action potential. Furthermore, we investigated the contribution of various steps of the  $\beta$ -adrenergic signaling cascade to the augmented positive inotropic response in the absence of TRPM4, and whether the closely related TRPM5 additively contributes to this process using *Trpm4/Trpm5*<sup>-/-</sup> mice. The increased positive inotropic response in *Trpm4*<sup>-/-</sup> papillary muscles, is not observed after inhibition of cAMP breakdown using IBMX without active enhancement of ATP hydrolysis. Additionally, the contractility of *Trpm4*<sup>-/-</sup> papillary muscles was also increased during ischemia simulation.

We conclude that TRPM4 (i) is activated by the rise in intracellular calcium during a ventricular action potential, (ii) acts as a brake on AP repolarization, and (iii) thereby reduces the driving force for Ca<sup>2+</sup> influx through L-type Ca<sup>2+</sup> channels and thus contractile force. This contribution of TRPM4 is specifically important during  $\beta$ -adrenergic stimulation, when the Ca<sup>2+</sup> current and the Ca<sup>2+</sup> transient are strongly enlarged. Considering the  $\beta$ -adrenergic signaling pathway in detail, we show evidence that TRPM4 activity becomes prominent for cardiac contractility especially under ATP consuming conditions. Our results show that functional TRPM4 proteins are novel determinants of the inotropic effect of  $\beta$ -adrenergic stimulation on the ventricular heart muscle and could be novel pharmacological targets to achieve increased  $\beta$ -adrenergic inotropy.

## 267

### Toxicity classifications of cargoes enhance occupational health for international crews on bulk cargo ships

**Mazurek, Nicole**; Höfer, Thomas

Bundesinstitut für Risikobewertung, Wissenschaftliche Querschnittsaufgaben, Berlin, Germany

**Introduction:** Occupational health standards for seafarers on ships, in particular those under flags of convenience, are often at low level. In general, internationally binding maritime regulations by the International Maritime Organisation (IMO) are focusing on safer maritime shipment only. Basically, there is a lack of easy-to-understand cargo information for crews on board. The International Maritime Solid Bulk Cargoes (IMSBC) Code became mandatory in January 2011. In respect to health risks, potential lethal poisoning and skin corrosion were the only aspects covered by the regulation. For an amendment additional health aspects were introduced based on the United Nations' Globally Harmonized System of Classification and Labelling (GHS). Although these criteria were deduced from exposure scenarios, the impact on safety information on all 152 cargo types transported on bulk carriers was unknown. **Approach:** We evaluated and classified the health hazards based on GHS rules. The 152 categories of solid bulk cargoes listed in the code cover all solid raw materials shipped for the world's economy. Although requested by IMO, safety information from industry did not become available. Therefore, the evaluations could be based on publicly available toxicological data only.

**Results:** More than 50% of all materials are potentially hazardous to health according to the criteria taken. However, for many cargoes compositions do vary so much that worst-case classifications had to be generated. In most cases, the GHS classification is triggered by non-CMR long-term health hazards and the skin/eye irritation potential. A number of the cargoes listed in the code could not be classified as they represent questionable chemical categories with insufficiently specified composition. **Conclusion:** The United Nations approved GHS system offered the chance to introduce already internationally harmonized health hazard classification into a lowly developed regulative area without long and controversial debates. Without the GHS the amendment of a global maritime code for better health protection standards would have taken many years. The GHS classifications will open the way to general label health warnings to be understood by all kinds of nationalities on board vessels.

## 268

**Effects of dimaprit in histamine H<sub>2</sub>-receptor overexpressing mice****Meister, Julia**; Gergs, Ulrich; Neumann, Joachim

Institut für Pharmakologie und Toxikologie, Med. Fakultät, Martin-Luther-Universität Halle-Wittenberg, Halle/Saale, Germany

In mouse cardiac preparations, histamine is ineffective, presumably because of lack of receptor protein expression. Hence, we have generated transgenic mice (TG) that overexpress the human H<sub>2</sub> receptor in the heart. In these TG hearts, histamine exerts positive chronotropic (PCE) and positive inotropic (PIE) effects. To further characterize the functionality of the overexpressed receptor, we have studied the effects of dimaprit, a compound that mainly acts agonistic at H<sub>2</sub> receptors. In isolated electrically stimulated left atrial preparations, dimaprit exerted a concentration dependent PIE, starting at 10 nM and reaching plateau at 3 μM with an -logEC<sub>50</sub> value of 6.39 ± 0.17 (n=9) compared to 6.73 ± 0.16 (n=5; p>0.05) for histamine. The EC<sub>20</sub> values were comparable irrespective whether histamine and after washout dimaprit was applied or vice versa. Furthermore, 10 μM cimetidine shifted the -logEC<sub>50</sub> value of dimaprit to 4.73 ± 0.18 (p<0.05; n=9). In isolated spontaneously beating right atria, dimaprit elicited a PCE with an -logEC<sub>50</sub> value of 6.92 ± 0.47 (n=6) that was shifted to 5.41 ± 0.24 (p<0.05; n=7) by cimetidine. The -logEC<sub>50</sub> value of dimaprit in left atrial preparations was not different from the -logEC<sub>50</sub> value of right atrial preparations (p>0.05). In right atrial preparations of TG (n=15), more often spontaneous arrhythmias were noticed compared to WT (n=10) (p<0.05). In isoflurane-anaesthetized mice, dimaprit (100 μl; 10<sup>-2</sup> M) increased heart rate from 493 ± 8 bpm to 542 ± 15 bpm (p<0.05; n=5) and ejection fraction from 60 ± 2.1 % to 79 ± 3.1 % (p<0.05; n=5) in TG but not in WT, using echocardiography with a Vevo 2100 system. These PIE and PCE were blocked by 100 μl cimetidine (50 mM). The present data indicate that in our transgenic model dimaprit acts as H<sub>2</sub> receptor agonist and confirms that we have successfully overexpressed a functional H<sub>2</sub> receptor with the expected agonist and antagonist sensitivity in the heart *in vitro* and *in vivo* (supported by DFG).

## 269

**Different Implementations of Multiple Choice Questions in Pharmacological Examination: Effects on Performance and Acceptance among Examinees****Meizer, Andreas**<sup>1</sup>; Gergs, Ulrich<sup>2</sup>; Neumann, Joachim<sup>2</sup>; Lukas, Josef<sup>1</sup><sup>1</sup>Institut für Psychologie, Martin-Luther-Universität Halle-Wittenberg, Halle/Saale, Germany<sup>2</sup>Institut für Pharmakologie und Toxikologie, Martin-Luther-Universität Halle-Wittenberg, Halle/Saale, Germany

Multiple choice questionnaires are widely used for assessment in educational scenarios. In its simplest form examinees choose the (one and only) correct answer from a set of *n* alternatives (single choice; SC), which is the predominantly used form in medical education and examination with *n* = 5. However, this procedure involves some methodological problems, most serious of which: If examinees choose the correct alternative, it is inferred, they would have also known, that all other four are incorrect; a conclusion, which cannot be sustained upon critical contemplation.

To circumvent this problem, we propose to use true multiple choice questions (MC), where the examinees choose all *k* correct alternatives from a set of *n* alternatives (0 ≤ *k* ≤ *n*) and each *k* for a specific question is unknown to the examinees. The aim of our study was to test three different implementations of this new type of questions: (1) a modified traditional format looking essentially the same as its SC counterpart with a box in front of each alternative, where true alternatives need to be checked and false alternatives need to be left blank, (2) a true/false format with two boxes behind each alternative, where examinees indicate, whether an alternative is true or false and (3) a rating scale format with four boxes behind each alternative, where examinees rate an alternative on a 4-point-scale ranging from "1: definitely false" to "4: definitely true".

In an empirical study first-year clinical students in medicine (*N* = 211) took part in an obligatory exam in pharmacology. Following the exam students were asked to answer ten additional questions from the pool of questions for the current curriculum, which were appropriately adapted to the MC format. The different implementations were randomly distributed among the students. Different scoring methods were applied and signal detection parameters estimated.

Results show about equal performance in all three implementations with slight advantages for the rating scale format when performance in the exam proper is controlled, *F*(2,158) = 4.605, *p* = .011. Even though, when asked to provide feedback about their experiences with the different implementations, this format was consistently judged more demanding than the other two, *F*(2,156) = 9.798, *p* < .001. This might be due to the rating scale format appearing to be "more different" from students prior experience with examination formats and might even have compromised actual performance.

## 270

**DPP10 is involved in PKC modulation of the transient outward current I<sub>to</sub>****Metzner, Katharina**; Schaefer, Michael; Kämmerer, Susanne

Rudolf-Boehm Institut für Pharmakologie und Toxikologie, Leipzig, Germany

Protein Kinase C (PKC) regulates the activity of a number of cardiac ion channels, including voltage-gated potassium channels. The transient outward current (I<sub>to</sub>), which

plays an important role in determining the action potential duration, has also been described to be modulated by PKC. It has been shown that PKC activation decreases Kv4.3 currents in expression systems as well as in native rat cardiomyocytes. The pore-forming α-subunit Kv4.3 contains several consensus PKC phosphorylation sites. Two splice variants of Kv4.3 are present in the human ventricle; the longer splice variant (Kv4.3-L) contains a 19-amino acid insert at the C-terminus with a PKC phosphorylation consensus site. During heart failure, I<sub>to</sub> is reduced due to the down-regulation of the short Kv4.3 isoform whereas the expression of the Kv4.3-L is increased. Kv4.3 proteins interact with different β-subunits (KChIP2, dipeptidyl peptidases DPPs). It is not known whether these β-subunits are involved in the I<sub>to</sub> regulation by PKC. Using the web-based program NetPhos potential phosphorylation sites have been predicted in DPP6-S and DPP10.

Therefore, we have studied the effect of PKC activation on the channel complex including DPPs in CHO cells. CHO cells stably expressing Kv4.3-L/KChIP2 were transiently transfected with DPP6-S or DPP10a. Cells were pre-incubated for 30 minutes with the PKC activator PMA (100 nM) or with the PKC inhibitor BIM (5 μM). K<sup>+</sup> currents were measured at 23°C using the whole-cell voltage-clamp technique.

After PKC activation by PMA, I<sub>to</sub> of control cells expressing Kv4.3/KChIP2 was reduced by 24% due to the phosphorylation of Kv4.3-L. The same effect was observed with co-expression of DPP6-S, indicating that I<sub>to</sub> was not affected by a PKC dependent DPP6-S phosphorylation. In contrast, expression of DPP10 led to a reduction of I<sub>to</sub> by 78%, suggesting an additional functionally relevant phosphorylation of the β-subunit by PKC. Furthermore, PKC inhibition by BIM increased I<sub>to</sub> of the CHO expression system co-transfected with DPPs. Pre-incubation of the transfected cells with BIM prevented the PMA-induced decrease in I<sub>to</sub>.

In summary, the β-subunit DPP10a may serve as an additional target for I<sub>to</sub> modulation by PKC. Since DPP10 is up-regulated in heart failure, the phosphorylation of the β-subunit by PKC could contribute to the dramatic decrease in I<sub>to</sub> in these patients.

## 271

**Effects of high ozone concentrations (>500ppm) in A549 human lung adenocarcinoma cells and L929 mouse fibroblasts****Meyer, Johannes**; Hopfer, Christine; Mückter, Harald; Gudermann, Thomas

Walther-Straub-Institut, Toxikologie, München, Germany

**Introduction:** Ozone is considered an airborne environmental toxicant, but may also pose an occupational risk in industrial workplaces. Low-conc (≤500ppb) ozone exposure typically leads to apoptosis in affected tissues with a release of nucleotides, cytokines, etc. However, with technical processes much higher ozone concentrations are common, e.g. >500ppm. At higher concentrations ozone does not only act as a respiratory irritant, but inflicts severe damage to the lungs (edema, fibrosis).

We challenged two different cell lines with oxygen/ozone mixtures to study the effects of high ozone (up to 10,000ppm).

**Materials & Methods:** Human lung adenocarcinoma cells (A549) and mouse fibroblasts (L929) were exposed to ozone in a steady-flow in-vitro apparatus as described previously [1] to observe cellular damage and responses.

We performed FACS analyses to screen single cells for signs of apoptosis like caspase 3, 8, and 9. The tumor suppressor p53 was tested with a sandwich ELISA. Oxidative stress caused by ozone and the effects of DMSO as a cytoprotectant were determined with FACS analysis using JC-1 (a marker of mitochondrial membrane potential).

**Results:** In the range of 10<sup>2</sup> – 10<sup>5</sup> ppm ozone for 1h both cell lines showed almost identical concentration-effect relationships and EC<sub>50</sub> values for caspase 3, 8, and 9. FACS analysis of JC-1 fluorescence showed similar EC<sub>50</sub> values, suggesting the breakdown of mitochondrial membrane potential and the activation of caspases were interrelated. In both cell lines, p53 was elevated at the end of the exposure period and increased even further over the next 4 hours. The incubation with DMSO (1% v/v) decreased the amount of JC-1 positive cells (A549: 37±4% vs 53±6%; L929: 37±4% vs 49±12%) as compared to the absence of DMSO.

**Conclusions:** The direct exposure of cells to high ozone concentrations for >1h results in severe damage of cellular membranes and initiates signals of apoptosis. In the presence of DMSO cells showed an enhanced tolerance to ozone, but its usefulness may be limited by the self-toxicity of DMSO.

[1] Mückter H et al. (1998) J Pharmacol Toxicol Meth, 40: 63-69

## 272

**Development of molecular imaging tools to investigate protein phosphatase type-1 and type-2A localisation and dynamics in living cells****Meyer-Roxlau, Stefanie**; Dewenter, Matthias; Vettel, Christiane; El-Armouche, Ali

Universitätsmedizin Göttingen, Institut für Pharmakologie, Germany

**Background:** The compartment-dependent dysregulation of the β-adrenoceptor (AR) cAMP/protein kinase A (PKA) signalling pathway is a characteristic feature of the diseased cardiomyocyte. Over the last years it became evident that PKA-dependent phosphorylation is subject to complex regulatory mechanisms, including antagonizing Ser/Thr phosphatases PP-1, PP-2A and the distal amplifier of PKA signalling PP-1-inhibitor-1 (I-1). The aim of this study was to monitor the localisation, putative β-AR/cAMP/PKA dependent dynamics and protein-protein interactions in living cardiomyocytes.

**Methods and Results:** To this end we generated the fusion proteins PP-1-CFP, PP-2A-CFP and I-1-YFP, which allow subcellular localisation studies and more importantly, real time changes e.g. after pharmacologic stimulation. We tested these constructs in HEK293 cells, where all three proteins showed cytosolic as well as nuclear distribution. Interestingly, while I-1 appeared to be diffusely expressed in both compartments, the

phosphatases additionally formed dense spots within the nucleus. I-1 is a regulatory subunit of PP-1 and dephosphorylated by PP-2A at its PKA-phosphorylation site. To monitor PP-1/I-1 and PP-2A/I-1 interaction and dynamics, we co-transfected HEK293 cells and measured fluorescence resonance energy transfer (FRET) under basal conditions and after  $\beta$ -AR stimulation. In this setting, PP-1 and I-1 appeared to already form a complex under basal conditions in which the proximity of the fluorophores was prominently altered after  $\beta$ -AR stimulation. This alteration was reversed by PKA-inhibitor H89 indicating that the loss of proximity is caused by PKA-dependent phosphorylation of I-1 and the consequently conformational changes. PP-2A/I-1 FRET on the other hand remained unaltered, reflecting the more fluctuant interaction between these proteins. We currently generate corresponding adenoviral constructs to transduce healthy and diseased cardiomyocytes to visualize interactions and dynamics in particular within respective microdomains e.g. the sarcoplasmic reticulum.

**Conclusion:** These novel tools will help to define the spatiotemporal dynamics of phosphatases within their endogenous microdomains in living cardiomyocytes and moreover to decipher the molecular links between altered signal transduction in healthy versus diseased cardiomyocytes.

## 273

### Efficiency of the skin barrier function: On the penetration of additives and contaminants from consumer products

**Mielke, Nastasia;** Hutzler, Christoph; Kappenstein, Oliver; Vieth, Bärbel; Luch, Andreas  
Federal Institute for Risk Assessment, Safety of Consumer Products, Berlin, Germany

Additives for plastics (e.g. PVC), elastomers and thermoplastic elastomers (TPE), among them softeners, stabilizers, colorants and vulcanization accelerators, are used in a variety of commodities. Some of them may cause adverse effects in humans. Beside additives with a defined function, contaminants can be part of the material, e.g. polycyclic aromatic hydrocarbons (PAH), primary aromatic amines (pAA) or a group of Non-Intentionally Added Substances (NIAS) including reaction products, impurities and decomposition products.

Most of these components are not covalently bound to the polymer and are therefore able to continuously leach or gas out of the polymer. Even under normal conditions as well as due to a continual use in combination with a mechanical load of the material and intensive skin contact, consumer products containing the above mentioned additives can contribute to the body burden.

We investigated consumer products to create a specific additive profile of selected plastics. Those highly contaminated or that contained critical substances were analyzed in diffusion tests using Franz-cells to determine their potential to pass the skin barrier. In these Franz-cell studies different skin models including artificial skin, porcine skin and a synthetic membrane were compared with regard to their potential to imitate human skin properties in limiting diffusion and migration of plastic additives and impurities. In comparison to these Franz-cells studies different mixtures of ethanol/water have been used for simulating the release and exposure during dermal contact. The screening analysis for additive profiles as well as the quantification of identified compounds were performed using GC-MS/MS. Components found in commodities like handles of hammers or wheels of a children's handcart are, for example, the lead compound of PAH benzo[a]pyrene and aromatic amines such as *N*-isopropyl-*N*-phenyl-*p*-phenylenediamine (Vulkanox 4010), the latter being used as antioxidant/antiozonant in rubber. Additionally, the permeation pathway of PAH through the skin has been visualized in cryosections using fluorescence microscopy. The results demonstrate that dermal uptake of some components like PAH is far from negligible and thus contribute to the internal exposure and the health risks that may be associated to this.

## 274

### In-vitro-Release and antibacterial effect of enrofloxacin-containing bone cement

**Mielke, Stefanie;** Stahl, Jessica; Kietzmann, Manfred  
University of Veterinary Medicine Hannover Foundation, Department of Pharmacology, Toxicology and Pharmacy, Germany

**Introduction:** The combination of polymethylmethacrylate (PMMA) with antibiotics like vancomycin or gentamicin is used as an efficient method to protect from infections after orthopedic implantations. Thus, the aim of this study was to investigate the release and antibacterial effect of enrofloxacin from bone cement. Furthermore, the influence of bone cement on two murine cell lines (keratinocytes (MSC) and fibroblasts (L929)) regarding to proliferation-rate and viability was examined.

**Material and Methods:** Enrofloxacin-loaded bone cement cylinders (25 mg/g or 50 mg/g PMMA) were incubated in 10 millilitres phosphate buffered solution (PBS) up to 40 weeks. Elution kinetics was analyzed by measuring the antibiotic concentration in PBS (incubation medium) at different time points by high-performance liquid chromatography. Antibacterial activity was investigated by a brilliant-black reduction test with *Geobacillus stearothermophilus* var. *calidolactis* C95. For antimicrobial testing elution probes were taken after 3 and 24 hours as well as 20 weeks. Furthermore, bio-activity was tested against *Escherichia coli* ATCC 25922 (*E. coli*). To analyze the biocompatibility, MSC and L929 were used to determine the proliferation-rate and viability by BrdU- and MTS-assay.

**Results:** In the first hours, PMMA releases the highest amount of enrofloxacin. Afterwards, the enrofloxacin-concentration decreases. The brilliant-black reduction test shows that the incubation media have an antimicrobial activity against *Geobacillus stearothermophilus* var. *calidolactis* C95, but this activity decreases with increasing time

points. Furthermore, the incubation media are antibacterial against *E. coli*, but the activity declines during time. PMMA shows no influence on proliferation and viability of MSC or L929.

**Conclusion:** During the first hours, the enrofloxacin-concentration is high enough to operate antibacterial. Afterwards, the concentration and thus the antimicrobial activity decrease. This implies that low enrofloxacin-concentration could result in resistance development. The development of antibacterial resistance has to be studied in further investigations.

The study was supported by the „Graduate College – Collaborative Research Centre DFG 599 Biomedical Engineering“.

## 275

### Simultaneous Quantification of Multiple DNA Adducts by UPLC-MS/MS in Human Tissue Samples

**Monien, Bernhard;** Schumacher, Fabian; Glatt, Hansruedi; Sachse, Benjamin; Herrmann, Kristin

Deutsches Institut für Ernährungsforschung, Gentoxische Nahrungsmittelkontaminanten, Nuthetal, Germany

The applicability of LC-MS/MS methods for the quantification of individual DNA adducts in human biomatrices has been demonstrated. However, the exposure to environmental carcinogens is not confined to single compounds and the utility of particular DNA adducts as human biomarkers is debatable. Alternatively, monitoring of an array of DNA adducts provides a survey of the inner exposure to reactive metabolites that may be a tool for the molecular epidemiology of cancer. An analytical technique is in need for the joint quantification of many DNA adducts without losing too much sensitivity compared to the analysis of individual ones, also because amounts of human DNA are usually small. We collected a library of 16 stable isotope-labeled internal reference substances of DNA adducts derived from environmental carcinogens, e. g. benzo[a]pyrene, and food carcinogens, e. g. methyleugenol and furfuryl alcohol. The molecular structures of the adducts as well as reported techniques for their work-up and LC-MS/MS quantification differ significantly. The performance of DNA adduct analytical techniques depends on two critical steps: enrichment of the analytes following enzymatic hydrolysis of the DNA sample and the chromatographic separation preceding mass spectrometric quantification. In this work, the adduct enrichment of four different techniques was compared using all available reference substances of DNA adducts. The solid-phase extraction with Oasis columns (Waters GmbH, Eschborn) generated the best results for most of the analytes. Further, we tested different UPLC-columns and solvent systems for the chromatographic fractionation. The resulting optimal method allows for a satisfactory quantification of about 80 % of the DNA adducts. It is currently applied to adduct analyses in DNA samples of human liver, lung, kidney and colon. Initial results indicate that particularly the adducts of methyleugenol, *N*<sup>2</sup>-(*trans*-methylisoeugenol-3'-yl)-2'-deoxyadenosine and *N*<sup>2</sup>-(*trans*-methylisoeugenol-3'-yl)-2'-deoxyguanosine are frequent in human DNA of lung and colon.

## 276

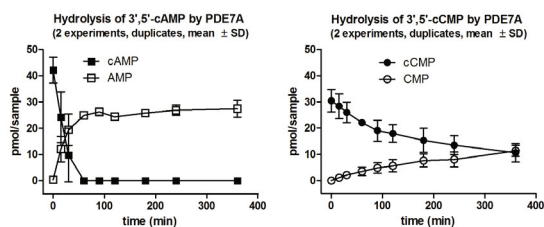
### Enzymatic characterization of PDE7A1, a phosphodiesterase that hydrolyzes the potential second messenger 3',5'-cCMP

**Monzel, Maike;** Kuhn, Maike; Bähre, Heike; Seifert, Roland; Schneider, Erich H.  
Hannover Medical School, Institute for Pharmacology, Germany

The cyclic purine nucleotides 3',5'-cAMP and 3',5'-cGMP are well-known second messengers. Their formation by nucleotidyl cyclases and degradation by phosphodiesterases (PDEs) is targeted by several pharmacologic interventions. The physiological role and intracellular metabolism of the cyclic pyrimidine nucleotides 3',5'-cCMP and 3',5'-cUMP has still to be elucidated. In an effort to identify 3',5'-cCMP-hydrolysing PDEs, we had investigated 3',5'-cNMP specificity of eight recombinant enzymes (PDE1B, 2A, 3A, 3B, 4B, 5A, 8A,9A) by fluorescence-based [1] and highly-sensitive HPLC-MS/MS detection methods [2]. In our present study, an HPLC-MS/MS-based characterization of the substrate specificity of five additional PDEs (PDE1A, 6AB, 7A1, 10A1, 11A1) was performed. The experiments revealed that PDE7A1 is the only enzyme that hydrolyzes significant amounts of 3',5'-cCMP in addition to the main substrate 3',5'-cAMP. Subsequently, we studied enzyme kinetics of purified GST-tagged truncated PDE7A (consensus sequence of PDE7A1 and PDE7A2). Our HPLC-MS/MS method allows us to quantify both the substrates (3',5'-cAMP or 3',5'-cCMP) and the hydrolysis products (5'-cAMP or 5'-cCMP) with high accuracy. Accordingly, we can follow the course of the enzymatic reaction by using two parameters (cf. figure below). The initial velocity of 3',5'-cCMP degradation at a substrate level of 3  $\mu$ M and at 30 °C amounted to ~24 % of the 3',5'-cAMP hydrolysis rate. Our data indicate that PDE7A regulates intracellular 3',5'-cCMP concentrations. The relatively low hydrolysis rate of 3',5'-cCMP compared to 3',5'-cAMP suggests that 3',5'-cCMP could also regulate PDE7A-mediated 3',5'-cAMP hydrolysis as a kind of naturally occurring inhibitor. In future experiments we will address the effects of PDE7A-activity, PDE7A inhibitors and 3',5'-cCMP in intact cells.

[1] Reinecke, D., et al., *PLoS One*, 2013. 8(1): p. e54158.

[2] Reinecke, D., et al., *FEBS Lett*, 2011. 585(20): p. 3259-62.

**PDE7A1 activity:**

PDE7A-mediated hydrolysis of 3',5'-cAMP and 3',5'-cGMP and formation of reaction products

**277****CRTC1 deficient mice show cardiac hypertrophy and decreased protein levels of RGS2**

**Morhenn, Karoline**<sup>1</sup>; Schröder, Sabine<sup>1</sup>; Pahl, Anja<sup>1</sup>; Schlossarek, Saskia<sup>2</sup>; Carrier, Lucie<sup>3</sup>; Eschenhagen, Thomas<sup>4</sup>; Cardinaux, Jean-René<sup>5</sup>; Lutz, Susanne<sup>4</sup>; Guo, Zhenheng<sup>5</sup>; Oetjen, Elke<sup>1</sup>

<sup>1</sup>Institut für Klinische Pharmakologie und Toxikologie, Universitätsklinikum Hamburg-Eppendorf, Pharmakologie für Pharmazeuten, Germany

<sup>2</sup>Institut für Experimentelle Pharmakologie und Toxikologie, Universitätsklinikum Hamburg-Eppendorf, Germany

<sup>3</sup>Center for Psychiatric Neuroscience, Prilly-Lausanne, Switzerland

<sup>4</sup>Universitätsklinikum Göttingen, Pharmakologie, Germany

<sup>5</sup>University of Kentucky School of Medicine, Department of Physiology, Lexington, United States

Maladaptive cardiac hypertrophy leads to heart failure, one of the common causes for hospitalization. Chronic beta-adrenergic signaling contributes to the pathogenesis of cardiac hypertrophy, as evidenced by the therapeutic success of beta-adrenoceptor antagonists. Our previous data showed that the protein content of the CREB transcriptional coactivator CRTC1 (cAMP Regulated Transcriptional Coactivator 1) is elevated in hearts of mice and humans under conditions of maladaptive hypertrophy and CRTC1 becomes activated through beta-adrenergic signaling. In the present study we investigated the role of CRTC1 in the pathogenesis of cardiac hypertrophy.

Mice deficient of CRTC1 were studied. As an indicator for hypertrophy, the ratio of heart weight to tibia length was analyzed. CRTC1 deficient mice showed a significant increase compared to their wildtype siblings. As measured by immunoblot, no significant differences concerning SERCA and phospholamban protein contents were observed.

It is known that the Regulator of G-Protein Signaling 2 (RGS2) reduces hypertrophy via reduction of G<sub>αq</sub>-protein induced signaling and that RGS2 gene transcription is induced by CREB (1;2). In heart tissue from 10 to 13 week old CRTC1 deficient mice we found a 60% decrease in RGS2 protein levels compared to the wildtype siblings by immunoblotting [n = 8 (WT), n = 7 (KO)]. To further show the regulation of RGS2 by CRTC1, HEK cells were transiently transfected with a luciferase reporter gene under control of the murine RGS2 promoter (-867 bp to +1 bp) or its mutant lacking the CREB binding-site. Overexpression of CRTC1 increased the transcriptional activity of the RGS2 wildtype promoter which was further slightly enhanced after stimulation with the beta-adrenoceptor agonist isoprenalin.

Our data show that CRTC1 stimulates RGS2 gene expression, suggesting that under hypertrophy inducing conditions CRTC1 protects against or retards the development of maladaptive hypertrophy by regulating RGS2 expression, thereby presumably decreasing G<sub>αq</sub>-mediated hypertrophic signaling. Thus, CRTC1 might provide a novel target for the treatment of cardiac hypertrophy and furthermore heart failure.

[1] Xie Z, Liu D, Liu S, Calderon L, Zhao G, Turk J, Guo Z (2011) Identification of a cAMP-response element in the regulator of G-protein signaling-2 (RGS2) promoter as a key cis-regulatory element for RGS2 transcriptional regulation by angiotensin II in cultured vascular smooth muscles. *J Biol Chem.* 286:44646-44658

[2] Zhang P, Mende U (2013) Functional role, mechanisms of regulation, and therapeutic potential of regulator of G protein signaling 2 in the heart. *Trends Cardiovasc Med.* doi: 10.1016/j.tcm.2013.07.002.

**278****Filamin A interacts with Megakaryoblastic Leukemia 1 (MKL1) to regulate transcriptional activity of the Serum Response Factor (SRF) cofactor**

Kircher, Philipp<sup>1</sup>; Nossek, Maximilian<sup>1</sup>; Drexler, Maria<sup>1</sup>; Grosse, Robert<sup>2</sup>; Gudermann, Thomas<sup>1</sup>; **Muehlich, Susanne**

<sup>1</sup>Ludwig-Maximilians-Universität Muenchen, Walther-Straub-Institut fuer Pharmakologie und Toxikologie, Germany

<sup>2</sup>Philipps-Universität Marburg, Pharmakologisches Institut, Germany

Megakaryoblastic Leukemia 1 (MKL1) is a transcriptional coactivator of Serum Response Factor (SRF), which regulates fundamental biological processes like cell migration, organization of the cytoskeleton and cell proliferation. MKL1 conveys

stimulatory signals from RhoA to SRF at least partially via MKL1 translocation into the nucleus.

Here, we identify the actin binding protein Filamin A (FLNa) as a novel MKL1 binding partner. We demonstrate that the interaction between MKL1 and FLNa is required for MKL1/SRF transcriptional activation and for the expression of MKL1 target genes. This is based on the ability of FLNa (i) to impair MKL1 phosphorylation, thereby maintaining MKL1 in the nucleus and (ii) to mediate an association between F-actin and MKL1 that facilitates MKL1 transcriptional activation. An MKL1 deletion mutant unable to bind to FLNa profoundly reduced cell motility and invasion. Thus, MKL1 nuclear localization and actin/MKL1-dependent gene expression and cell migration appear to require the interaction with FLNa. Our results identify FLNa as a novel cellular transducer linking actin polymerization with MKL1/SRF activity.

**279****Hierarchical Organization of Multi-Site Phosphorylation at the CXCR4 C Terminus and association with the WHIM syndrome**

**Mueller, Wiebke**; Schütz, Dagmar; Nagel, Falko; Schulz, Stefan; Stumm, Ralf

Universitätsklinikum Jena - Friedrich-Schiller-Universität, Institut für Pharmakologie und Toxikologie, Germany

The CXCL12-chemokine receptor CXCR4 regulates cell migration during ontogenesis and disease states including cancer and inflammation. It is well established that CXCL12-stimulated CXCR4 receptors activate Gi protein-dependent signal transduction pathways and undergo C-terminal phosphorylation and internalization. Mutations in the CXCR4 gene affecting C-terminal phosphorylation sites are a hallmark of WHIM syndrome, a genetic disorder characterized by a gain-of-CXCR4-function. To better understand how multi-site phosphorylation of CXCR4 is organized and how perturbed phosphorylation might affect CXCR4 function, we developed novel phosphosite-specific CXCR4 antibodies and studied the differential regulation and interaction of C-terminal phosphorylation sites in human embryonic kidney cells (HEK293). CXCL12 promoted a robust and fast phosphorylation at S346/347 by GRK2/3 which preceded phosphorylation at S324/325 and S338/339. WHIM syndrome-associated CXCR4 truncation mutants which lost the S346/347 site displayed strongly impaired phosphorylation at the remaining Serines as well as reduced CXCL12-induced receptor internalization. Also a S346-348A mutant showed strongly impaired CXCL12-promoted phosphorylation at the other Serines, defective internalization, gain of calcium mobilization, and reduced desensitization. Thus, the triple serine motif S346-S348 contains a major initial CXCR4 phosphorylation site and is required for efficient subsequent multi-site phosphorylation and receptor regulation. Hierarchical organization of CXCR4 phosphorylation explains why small deletions at the extreme CXCR4 C terminus typically associated with WHIM syndrome severely alter CXCR4 function.

**280****Interleukin-6 increases hyaluronan synthesis in cardiac fibroblasts which leads to an immunomodulatory myofibroblast phenotype**

**Müller, Julia**<sup>1</sup>; Grandoch, Maria<sup>1</sup>; Gorresen, Simone<sup>2</sup>; Garbers, Christoph<sup>3</sup>; Ding, Zhaoqing<sup>3</sup>; Scheller, Jürgen<sup>2</sup>; Schrader, Jürgen<sup>1</sup>; Fischer, Jens Walter<sup>1</sup>

<sup>1</sup>Universitätsklinikum der Heinrich-Heine-Universität Düsseldorf, Institut für Pharmakologie und Klinische Pharmakologie, Germany

<sup>2</sup>Universitätsklinikum der Heinrich-Heine-Universität Düsseldorf, Klinik für Kardiologie, Pneumologie und Angiologie, Germany

<sup>3</sup>Universitätsklinikum der Heinrich-Heine-Universität Düsseldorf, Institut für Biochemie und Molekularbiologie II, Germany

<sup>4</sup>Universitätsklinikum der Heinrich-Heine-Universität Düsseldorf, Institut für Molekulare Kardiologie, Germany

Interleukin-6 (IL-6) is known to be an important part of the inflammatory response to acute myocardial infarction (AMI). We reported previously that IL-6 induces expression of the hyaluronan (HA) synthases (Has) 1 and -2 in the early phase post AMI and establishment of an HA-rich microenvironment in the infarcted heart of C57BL/6J mice. The causal role of IL-6 for HA induction was confirmed by use of an IL-6-blocking antibody.

The role of HA in the acute phase after AMI is so far unknown. Therefore we attempted to unravel the effects of increased HA synthesis in cardiac fibroblasts (CF).

CF isolated from male C57BL/6J mice were treated with IL-6 and the soluble IL-6 receptor (sIL-6R) eliciting IL-6 trans-signaling. Stimulation for 48 h led to synthesis of a pericellular HA coat and the development of a myofibroblast phenotype as evidenced by increased HA synthesis and expression of  $\alpha$  smooth muscle actin ( $\alpha$ SMA, Acta2), shown by immunofluorescence staining and induction of Acta2 mRNA ( $2.40 \pm 0.54$  fold of control, n=6, p<0.05). This increase was in part inhibited when CF were treated with 4-methylumbelliferone (4-MU), a HAS inhibitor. Next it was considered that the HA matrix may modulate the secretory functions of myofibroblastic CF in response to IL-6. Multiplex analysis of supernatants of IL-6-stimulated CF (24 h) revealed elevated concentrations of MCP1 ( $2.09 \pm 0.22$  fold of control, n=3, p<0.05), CXCL1 ( $7.72 \pm 1.36$  fold of control, n=3, p<0.05) and CSF3 ( $4.61 \pm 0.96$  fold of control, n=3, p<0.05). Additionally, TNF $\alpha$ , CCL5, CSF2, IL-13 und IL-11 showed trends towards induction. Subsequently increased mRNA expression in response to IL-6 trans-signaling was detected of Mcp1 ( $2.09 \pm 0.40$  fold of control, n=5, p<0.05), Cxcl1 ( $5.39 \pm 0.92$  fold of control, n=6, p<0.05), Csf3 ( $4.29 \pm 1.21$  fold of control, n=7, p<0.05), Tnfa ( $4.77 \pm 0.89$  fold of control, n=6, p<0.05) and Csf2 ( $8.11 \pm 1.26$  fold of control, n=5, p<0.05). To investigate whether this induction is dependent on upregulation of HA-synthesis by Has1

and Has2 CF were isolated from mice lacking CD44, a key receptor for HA-mediated signaling. Indeed, the IL-6 mediated upregulation of Csf3 (WT  $5.07 \pm 0.95$  vs. CD44<sup>-/-</sup>  $1.48 \pm 0.21$ , n=5-9) and Tnfa (WT  $3.74 \pm 0.36$  vs. CD44<sup>-/-</sup>  $2.44 \pm 0.25$ , n=5-8) was reduced in CD44<sup>-/-</sup> CF. The present data suggest that IL-6-induced HA synthesis and subsequent CD44-signaling augments the immune modulating properties of the secretory myofibroblast phenotype in CF.

## 281

### Gq/11 proteins in tanyocyte signaling

**Müller-Fielitz, Helge:** Krajka, Victor; Wenzel, Jan; Benzin, Anika; Schwaninger, Markus  
Universität zu Lübeck, Institut für Experimentelle und Klinische Pharmakologie und Toxikologie, Germany

The hypothalamic network plays an important role in the regulation of different endocrine and physiological functions. Largely unknown players in this network are the so-called tanyocytes. The cell bodies of these specialized ependymal glial cells contact to the cerebrospinal fluid in the wall of the 3rd ventricle and send processes into the hypothalamic nuclei and the median eminence. Recent findings indicated that tanyocytes are chemosensors responding to a number of signals such as glucose, ATP and histamine with intracellular calcium waves and suggested an important role in regulating hypothalamic functions (1). However, the intracellular signaling in tanyocytes remain largely unknown.

To investigate the role of Gq/G11-coupled signalling pathways in tanyocytes we systematically studied different stimuli (carbachol, thyrotropin-releasing hormone (TRH) and ATP) by measuring intracellular calcium in living brain slices of mice lacking the alpha subunits of Gq and G11 specifically in ependymal or GLAST-positive cells. Here we show that the Gq/11-mediated signalling pathway plays an essential role in the calcium response of the different stimuli. Three to four weeks after deletion of the Gq subunit tanyocytes showed severely reduced calcium responses.

Furthermore, we were able to differentiate for the first time different subtypes of tanyocytes with pharmacological tools. After application to the medium ATP stimulated calcium waves all over the tanyocytic layer. However, carbachol and TRH activated only subpopulations of tanyocytes. The so-called alpha-1 and alpha-2 tanyocytes, which are close to the arcuate and ventromedial hypothalamic nuclei, were stimulated by carbachol. TRH stimulated only the tanyocytes in the media eminence, termed beta-2 tanyocytes.

In summary, tanyocytes are active signalling cells within the brain that can respond to a number of transmitters and metabolites and may therefore be involved in various feedback mechanisms.

(1) Frayling, C., Britton, R., and Dale, N. (2011). ATP-mediated glucosensing by hypothalamic tanyocytes. *J.Physiol.* 589, 2275-2286.

## 282

### Analysis of nitric oxide sensitive guanylate cyclase activation based on measurement of direct Mant-GTP fluorescence

**Neidhardt, Inga:** Busker, Mareike; Behrends, Soenke  
TU Braunschweig, Institut für Pharmakologie, Toxikologie und Klinische Pharmazie, Germany

NO sensitive guanylate cyclase (NOsGC) is a drug target for classic nitrovasodilators, NOsGC stimulators (e.g. riociguat or BAY 41-8543) and activators (e.g. cinaciguat). We have recently used a fluorescent substrate analogue, 2'-Mant-3'-dGTP, as an acceptor for tryptophan fluorescence in resonance energy transfer to study NO induced conformational changes leading to activation of the enzyme[1]. We found that NO binding to the amino-terminal heme binding domain is transmitted to the carboxyl-terminal catalytic domain by direct interaction between the heme binding and catalytic domain and through the coiled coil helix.

In the current study we concentrate on drug induced changes of 2'-Mant-3'-dGTP fluorescence at 445 nm after direct excitation at 350 nm. We found that an increase in fluorescence correlates with enzyme activation: Figure 1 shows significant increases in 2'-Mant-3'-dGTP fluorescence of the purified NOsGC enzyme in response to the NO donor DEA/NO and the activator cinaciguat. Consistent with the NO-insensitivity of the NOsGC mutant  $\alpha_1 / \beta_1$ , H105A in enzyme activity determinations, no increase in 2'-Mant-3'-dGTP fluorescence was detectable for DEA/NO. The same mutant shows increased enzyme activity in response to cinaciguat which corresponds with the significant increase in fluorescence shown in Figure 1. Figure 2 shows experiments with the analogue of riociguat, BAY 41-8543, and a mutant enzyme ( $\alpha_1$  W466F /  $\beta_1$ ) that shows decreased responsiveness to NO, but wild-type like enzyme activity in the presence of NO and BAY 41-8543. Again fluorescence data mimic enzyme activity data: the  $\alpha_1$  W466F /  $\beta_1$  mutant shows no increase in fluorescence in the presence of DEA/NO, but a significant increase in the combined presence of DEA/NO and BAY 41-8543.

Fluorescence of 2'-Mant-3'-dGTP increases with the lipophilicity of the solvent. The positive correlation between enzyme activity and direct fluorescence of the Mant-labeled substrate analogue indicates that the hydrophobicity in the binding pocket of the substrate increases on activation. Based on the crystal structure of the human NOsGC in the inactive state[2] and comparison with the structure of the adenylate cyclase in the active state[3], Allerston et al. proposed the concept that the substrate binding site of

guanylate cyclase changes to a more closed conformation on activation. Considering the localization of the Mant-GTP complex in adenylate cyclase[4], our data support the concept that NOsGC changes to a more closed conformation when activated by NOsGC stimulators, activators or NO.

[1] Busker M, Neidhardt I, Behrends S. Nitric Oxide Activation of Guanylate Cyclase Pushes the  $\alpha_1$  Signaling Helix and the  $\beta_1$  Heme Binding Domain closer to the Substrate Binding Site. *2014 J Biol Chem* 289: 476-484

[2] Allerston CK, von Delft F, Gileadi O. Crystal structures of the catalytic domain of human soluble guanylate cyclase. *PLoS One.* 2013;8(3):e57644

[3] Tesmer JJ, Sunahara RK, Gilman AG, Sprang SR. Crystal structure of the catalytic domains of adenylate cyclase in a complex with G $\alpha$ . *Science.* 1997 Dec 12;278(5345):1907-16

[4] Mou TC, Gille A, Fancy DA, Seifert R, Sprang SR. Structural basis for the inhibition of mammalian membrane adenylate cyclase by 2'-(3'-O-(N-Methylanthraniloyl)-guanosine 5'-triphosphate. *J Biol Chem.* 2005 Feb 25;280(8):7253-61

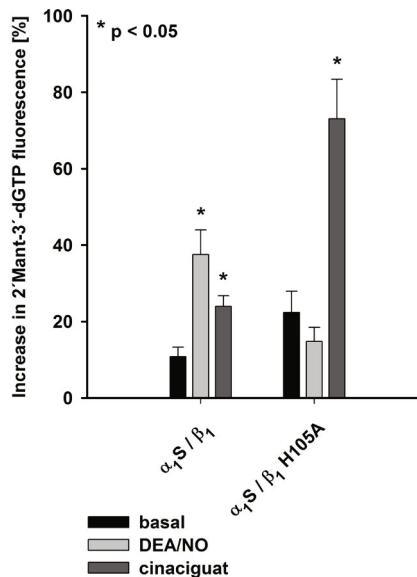


**Figure 1:** Increase in 2'-Mant-3'-dGTP fluorescence of the purified NOsGC enzyme in response to DEA/NO and cinaciguat

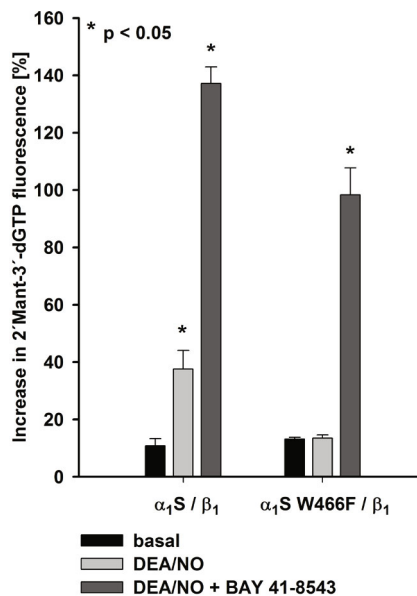


**Figure 2:** Increase in 2'-Mant-3'-dGTP fluorescence of the purified NOsGC enzyme in response to DEA/NO and BAY 41-8543

283

### Identifying of cUMP-binding proteins

**Neumann, Martin**<sup>1</sup>; Schwede, Frank<sup>2</sup>; Pich, Andreas<sup>3</sup>; Wolter, Sabine<sup>1</sup>; Seifert, Roland<sup>1</sup>

<sup>1</sup>Medizinische Hochschule Hannover, Institut für Pharmakologie, Germany

<sup>2</sup>Biology Life Science Institute, Forschungslabor und Biochemia Vertrieb, Bremen, Germany

<sup>3</sup>Medizinische Hochschule Hannover, Institut für Toxikologie, Germany

The cyclic purine nucleotides adenosine 3' 5'-cyclic monophosphate (cAMP) and guanosine 3' 5'-cyclic monophosphate (cGMP) are known second messengers. They are synthesized by nucleotidyl cyclases (NCs) and cleaved by phosphodiesterases (PDEs). Important target proteins of cAMP and cGMP are the cAMP-dependent protein kinase (PKA) and the cGMP-dependent protein kinase (PKG), playing key roles in the regulation of cellular functions. Recently, cytosine 3' 5'-cyclic monophosphate (cCMP) has been shown to bind to the regulatory subunit of PKA and a regulatory role for this cyclic nucleotide was suggested [1]. Basal levels of pyrimidine nucleotides, cCMP and uridine 3' 5'-cyclic monophosphate (cUMP), were detected in different cell lines by liquid chromatography-mass spectrometry analysis (LC-MS). NCs and PDEs may have a much broader substrate specificity than supposed and PDE3A effectively cleaves cUMP [2]. Moreover, bacterial toxins have an uridylyl cyclase function [3]. These data suggest that cCMP and cUMP may have characteristics of a second messenger [4].

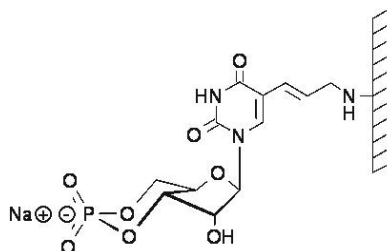
To uncover a putative biological function of cUMP, we started to identify cUMP binding proteins. Extracts of HeLa-cells, A549-cells and mouse lung tissue were prepared and incubated with cUMP that was attached by different linkers to an agarose matrix. Proteins binding to cUMP were identified by LC-MS. Initial experiments showed that cUMP binds to the regulatory subunit of PKA and, therefore, could participate in regulation of processes related to PKA. Several proteins like calnexin (chaperones), AKAP9 (A-kinase anchoring protein) and myomegalin (phosphodiesterase-interacting protein) bound to cUMP agarose. In conclusion, affinity chromatography coupled to LC-MS constitutes a feasible approach to identify cUMP-binding proteins.

[1] Hammerschmidt A et al. (2012) *PLoS One* 7: e39848

[2] Reinecke et al. (2011). *FEBS Lett.* 585, 3259 – 3262

[3] Göttle M et al. (2012) *Toxins (Basel)*. 7: 505-35

[4] Beste KY et al. (2013) *Biol. Chem.* 394: 261-70



### 5-Aminoallyl-cUMP-Agarose:

One of the agarose matrices used for affinity chromatography. The pyrimidine ring is linked to the matrix via its C5-atom.

284

### Establishment of pathway-specific gene expression analysis using the example of the paraquat action on human lung epithelial cells

**Niehof, Monika**; Augustin, Christian; Hansen, Tanja

Fraunhofer ITEM, In Vitro and Mechanistic Toxicology (IVMT), Hannover, Germany

The aim of the present study was the establishment of "Pathway Arrays" (RT<sup>2</sup> Profiler PCR Arrays, SABiosciences) with which the expression of a variety of genes can be assessed simultaneously. These arrays combine real-time PCR performance and the ability of microarrays to detect the expression of many genes simultaneously. Paraquat, an herbicide, was used as test substance. It evolves its toxic effects by forming reactive oxygen species (ROS). ROS can lead to the activation of transcription factors, which regulate the transcription of genes relevant for inflammatory response, cell growth, differentiation or apoptosis. Paraquat is preferably accumulated in alveolar epithelial cells type II. Therefore, the human alveolar epithelial cell line A549 was used in this study. Due to the effect of Paraquat on inflammatory response an array for the NFκB-Signaling-Pathway was used for establishment (84 genes). About 40% of the tested genes were significantly regulated. A classification of the genes into functions showed that, as expected, a great number of cytokines, being involved in inflammatory response, were regulated (e.g. IL8, IL1A, IL1R1, TNF, TLR4, CSF2). Furthermore, it could be shown that Paraquat regulate different transcription factors (e.g. EGR1, STAT1, JUN, FOS), which could take part in the regulation of cytokine expression. To validate the array results 15% of the genes (13 genes, "up", "down" and "unregulated") were chosen. The expression of these genes was completely confirmed via real-time RTqPCR with the Lightcycler™ (Roche). The results of this study show that the establishment of these arrays was successful and that they yield a high precision and quality. The "Pathway-Arrays" take much less time compared to the analysis of individual genes and represent a fast knowledge-based alternative to genome-wide gene expression analysis in toxicogenomic studies.

285

### The gH2AX assay for genotoxicity testing

**Nikolova, Teodora**; Dvorak, Mirek; Jung, Fabian; Adam, Isabell; Krämer, Elizabeth;

Kaina, Bernd

Universitätsmedizin, Institut für Toxikologie, Mainz, Germany

DNA damage leads to activation of the cellular DNA damage response (DDR). This signalling network results in activation of various DNA repair proteins and chromatin structure modulators. A frequent manifestation of DDR is the phosphorylation of histone 2AX (gH2AX), which can be visualised as gH2AX foci by immunocytochemistry. In the present study, we analysed whether gH2AX is a reliable biomarker for DNA damage-inducing agents. We selected 14 well-characterised genotoxic compounds and compared them with 10 non-genotoxic chemicals in the well-characterised CHO cell system. We measured quantitatively γH2AX by manual and automatic scoring of γH2AX foci, and by flow cytometry counting of γH2AX positive cells. In parallel, we determined the cytotoxicity dose-response using the MTT cell proliferation/viability assay. We show that a) all genotoxic agents were able to induce dose-dependently γH2AX in the cytotoxic range whereas no induction was observed after treatment with non-genotoxicants; b) manual scoring of γH2AX foci and automated scoring gave similar results, with the automated scoring being faster and more reproducible; c) data obtained by foci counting and FACS analysis of γH2AX positive cells showed a significant correlation, suggesting that the γH2AX flow cytometric assay gives reproducible results and additional data on the cell cycle distribution of γH2AX positive cells. However, because of qualitative assessment of nuclear foci, the microscopic evaluation may be more useful; d) γH2AX foci were co-localised with 53BP1 and Rad51, supporting the notion that the foci represent true DNA double-strand breaks. The automated analysis of γH2AX foci allows a rapid and reliable determination of genetic damage in mammalian cells and appears to be useful for genotoxicity testing.

286

### Drug-induced trafficking of P-glycoprotein in human brain capillary endothelial cells

**Noack, Andreas**<sup>1</sup>; Noack, Sandra<sup>2</sup>; Hoffmann, Andrea<sup>2</sup>; Maalouf, Katia<sup>3</sup>; Büttner, Manuela<sup>4</sup>; Couraud, Pierre-Olivier<sup>5,6,7</sup>; Romero, Ignacio A.<sup>8</sup>; Weksler, Babette<sup>9</sup>; Alms, Dana<sup>9</sup>; Römermann, Kerstin<sup>1</sup>; Naim, Hassan Y.<sup>3</sup>; Löscher, Wolfgang<sup>1,10</sup>

<sup>1</sup>University of Veterinary Medicine Hannover, Department of Pharmacology, Toxicology, and Pharmacy, Germany

<sup>2</sup>Hannover Medical School, Department of Trauma Surgery, Germany

<sup>3</sup>University of Veterinary Medicine Hannover, Department of Physiological Chemistry, Germany

<sup>4</sup>Hannover Medical School, Institute of Functional and Applied Anatomy, Germany

<sup>5</sup>INSERM, U1016, Institut Cochin, Paris, France

<sup>6</sup>INSERM, UMR8104, Centre National de la Recherche Scientifique (CNRS), Paris, France

<sup>7</sup>Université René Descartes, Paris, France

<sup>8</sup>The Open University, Milton Keynes, Department of Biological Sciences, Great Britain

<sup>9</sup>Weill Medical College of Cornell University, Division of Hematology and Medical Oncology, New York, United States

<sup>10</sup>Center for Systems Neuroscience, Hannover, Germany

Pharmacotherapy of epilepsy is affected by the blood-brain barrier (BBB). Since drug resistance at the BBB may be caused by overexpression and increased activity of the drug transporter P-glycoprotein (P-gp), manipulation of Pgp is a promising strategy to prevent multidrug resistance. The aim of this project is to better understand the regulation and function of P-gp in endothelial cells of the BBB. P-gp membrane trafficking from subcellular stores to the cell surface is a regulatory mechanism that has not yet been studied in brain endothelial cells. Through this mechanism the cells can rapidly increase their P-gp activity. To investigate P-gp trafficking at the BBB, a doxycycline-inducible MDR1-EGFP gene cassette was integrated into the genome of human brain capillary endothelial cells (hCMEC/D3) by lentiviral transduction. hCMEC/D3-MDR1-EGFP cells were isolated and enriched by using a cell sorter. In the presence of doxycycline, these cells exhibited a 15-fold increase in Pgp-EGFP fusion protein expression compared to doxycycline-off conditions, which was associated with an increased efflux of the Pgp substrate rhodamine 123 (Rho123). The chemotherapeutic agent mitomycin C (MMC) was used to study drug-induced trafficking of Pgp. Confocal fluorescence microscopy of single hCMEC/D3-MDR1-EGFP cells revealed that Pgp redistribution from intracellular pools to the cell surface occurred within 2 h of MMC exposure. Pgp-EGFP exhibited a punctuate pattern at the cell surface compatible with concentrated regions of the fusion protein in membrane microdomains, i.e., lipid rafts, which was confirmed by Western blot analysis of biotinylated cell surface proteins in Lubrol-resistant membranes. MMC exposure also increased the functionality of Pgp as assessed by Rho123 uptake. However, this increase occurred with some delay after the increased Pgp expression and coincided with the release of Pgp from the Lubrol-resistant membrane complexes. Disrupting rafts by depleting the membrane of cholesterol increased the functionality of Pgp. Our data present the first direct evidence of drug-induced Pgp trafficking at the human BBB and indicate that Pgp has to be released from lipid rafts to gain its full functionality.

## 287

**Deletion of G $\alpha_1$  proteins in white adipose tissue protects from weight gain**

**Novakovic, Ana**<sup>1</sup>; Leiss, Veronika<sup>1</sup>; Sartorius, Tina<sup>2</sup>; Machann, Jürgen<sup>3</sup>; Häring, Hans-Ulrich<sup>2</sup>; Nürnberg, Bernd<sup>1</sup>

<sup>1</sup>Institut für experimentelle und klinische Pharmakologie und Toxikologie, Abteilung für Pharmakologie und Experimentelle Therapie, Tübingen, Germany

<sup>2</sup>Universitätsklinikum Tübingen, Innere Medizin IV, Germany

<sup>3</sup>Radiologische Universitätsklinik Tübingen, Diagnostische und Interventionelle Radiologie, Germany

Obesity is a condition in which there is an over-accumulation of lipids and fatty acids in subcutaneous and/or visceral adipose tissue. The breakdown or storage of fatty acids is regulated by hormones signalling *via* G-protein coupled receptors (GPCRs) among others. Hormone binding results in the activation of the respective GPCR leading to the dissociation of heterotrimeric G-proteins into G $\alpha$  subunits and G $\beta\gamma$  dimers. The G $\alpha_{10}$  protein family constitutes one of four G $\alpha$  superfamilies showing a sequence identity of up to 95% within the G $\alpha$  subgroup (G $\alpha_1$ , G $\alpha_2$ , G $\alpha_3$ ). Due to this high homology it has been suggested that G $\alpha$  proteins have redundant functions, i.e. they are activated by a similar set of GPCRs and signal to an overlapping array of effectors. G $\alpha_2$  and G $\alpha_3$  are both expressed in white adipose tissue. Interestingly, both G $\alpha_2$ - and G $\alpha_3$ -deficient mice show a lean phenotype compared to their respective littermates, but time occurrence of the weight difference is detectable in a genotype-dependent manner. G $\alpha_2$ -deficient mice are lean already at birth, whereas G $\alpha_3$ -deficient mice stop gaining more weight at 36-weeks of age. Magnetic resonance imaging (MRI) revealed that 18-week-old G $\alpha_2$ -deficient mice had reduced lean mass and significantly lower amounts of subcutaneous and visceral adipose tissue. In contrast, G $\alpha_3$ -deficient mice showed significantly low body weights first at 36-weeks of age. The reduced fat mass determined by MRI reached statistical significance at 56-weeks of age. To analyse adipocyte-differentiation, we isolated pre-adipocytes, and induced their differentiation. Significantly less Oil-red-O-positive G $\alpha_2$ -deficient adipocytes were detectable, whereas G $\alpha_3$ -deficient pre-adipocyte-differentiation was similar to wild-type cells. Our data suggest a specific and independent role of both isoforms in adipocyte-differentiation as well as regulation of adipose tissue mass. We conclude that deletion of G $\alpha_2$  and G $\alpha_3$  protects from weight gain in an age-dependent manner and results in a lean phenotype.

## 288

**Precision cut lung slices: a novel *in vitro* model to demonstrate that bronchoconstriction is a key player in airway remodelling**

**Oenema, Tiitske**<sup>1,2</sup>; Maarsingh, Harm<sup>1,2</sup>; Bos, Sophie<sup>1,2</sup>; Smit, Marieke<sup>1,2</sup>; Groothuis, Geny<sup>3</sup>; Meurs, Herman<sup>1,2</sup>; Gosens, Reinoud<sup>1,2</sup>

<sup>1</sup>University of Groningen, Molecular Pharmacology, Netherlands

<sup>2</sup>Groningen Research Institute for Asthma and COPD (GRIAC), Netherlands

<sup>3</sup>University of Groningen, Pharmacokinetics, Toxicology and Targeting, Groningen Research Institute of Pharmacy, Netherlands

Bronchoconstriction has been proposed to underlie airway remodelling. However, the mechanisms involved are still poorly understood. An important contributor to airway remodelling, in particular airway smooth muscle remodelling is the multifunctional cytokine TGF- $\beta$ , which can facilitate airway smooth muscle maturation by inducing the expression of contractile proteins. The aim of this study was to develop an *in vitro* model which allows investigation of mechanisms involved in the bronchoconstriction-induced airway remodelling. To this aim, precision cut lung slices of guinea pigs were used. Lung slices were viable for at least 2 days. Stimulation with either methacholine or TGF- $\beta_1$  augmented the expression of contractile proteins makers including sm-myosin, sm- $\alpha$ -actin and calponin after 2 days. The expression of sm-myosin was particularly enhanced in the peripheral airways (<100  $\mu$ m), and to a slightly smaller extent in the central airways (> 400  $\mu$ m). Inhibition of actin polymerization by Latrunculin A or of TGF- $\beta$  receptor kinase by SB431542 prevented the methacholine effects and the effects of other bronchoconstricting agents including histamine and KCl on contractile protein expression. This indicates the release of biologically active TGF- $\beta$  in response to bronchoconstriction, ensuing contractile protein expression and thus airway smooth muscle remodelling. The anticholinergic tiotropium bromide inhibited the methacholine-induced contractile protein expression in a concentration-dependent manner. Collectively, bronchoconstriction induces the release of biologically active TGF- $\beta$  and promotes remodelling. Muscarinic receptor induced remodelling can be counteracted by the use of the anticholinergic tiotropium bromide. Precision cut lung slices are a valid *in vitro* model to study mechanisms involved in airway remodelling induced for example, by bronchoconstriction.

Funding: Chiesi Pharmaceuticals

## 289

**Determination of the penicillin antibiotics amoxicillin, penicillin V, and piperacillin in diverse sewage samples**

**Oertel, Reinhard**; Schlobach da Costa, Caroline; Schubert, Sara; Kirch, Wilhelm TU-Dresden, Inst. für Klinische Pharmakologie, Germany

The use of pharmaceuticals and therefore their input into the aquatic environment after passing the sewer system and sewage treatment plants (STPs) is of increasing concern. In a research project on risk management in water sixteen antibiotics and three antifungals were determined in influent and effluent of a STP in Dresden for the duration

of one year. An analytical method including the sample concentration and purification with solid phase extraction, the chromatographic separation by reversed phase and hydrophilic interaction chromatography (HILIC) technique and the detection by a tandem mass spectrometer with the multiple reaction monitoring mode was developed and optimized. The concentration of drugs depends on the sewage quantity. The water volume of the total influent of the STP was monitored. The volume of the final effluent of the STP is nearly the same with a time shift and calculably. In this study the three  $\beta$ -lactam antibiotics and their stability were examined more detailed. The low limit of quantification ranged from 20 to 100 ng/L. The stability of amoxicillin, penicillin V, and piperacillin in waste water is limited. Amoxicillin and penicillin V were detected only in fresh samples of the influent. A decrease of the piperacillin concentration in influent samples was observed. But in the final effluent after the denitrification process in the STP piperacillin was more stable.

## 290

**Targeting inflammatory T lymphocytes with conditional chemokine receptor antagonist expression for a tissue-specific therapy of chronic inflammatory disorders**

**Ogrissek, Nadine**; Radeke, Heinfried H.; Pfeilschifter, Josef M.

Uniklinikum Frankfurt am Main, Allgemeine Pharmakologie und Toxikologie, Germany

During an immune response certain chemokines are especially important for extravasation of T cells into inflamed tissue. An exaggerated chemokine receptor signaling is known to be involved in the pathogenesis of autoimmunity and therefore these receptors are promising targets for the treatment of chronic inflammatory disorders like type-1-diabetes or psoriasis.

In previous experiments our group already confirmed the efficacy of promising chemokine receptor antagonists. CXCL11(4-79) has antagonistic function for CXCR3 and CXCL12(P2G2) inhibits CXCR4. Their expression and secretion could be shown in *Pichia pastoris* and antagonistic function has been proven by a reduction of T cell migration *in vitro* and *in vivo*.

Now we want to develop a cell-based therapy for chronic inflammation with a treatment that is based on the combined effect of CXCL11(4-79) and CXCL12(P2G2). By targeting of stable transduced T cells these antagonists should be conditional expressed and secreted directly in the centre of inflammation, resulting in inhibition of further T cell accumulation.

To realize this project we cloned lentiviral constructs, optimized transduction of T cells and confirmed antagonist expression and secretion. At the moment we are measuring the inhibition efficiency of these antagonists *in vitro* with cell migration assays. In parallel we are testing a TCR-inducible vector system to ensure a well regulated antagonist expression. Finally we would like to test this cell therapy *in vivo* in a relevant mouse model of type-1-diabetes.

Supported by the DFG graduate school GRK1172 and Merck KGA

## 291

**p63RhoGEF accelerates the onset of cardiac contractile dysfunction induced by increased afterload**

**Ongherth, Anita**; Pasch, Sebastian; Ramba, Beate; Zafar, Sarah; Zoremba, Marcel; Blume, Roland; Würtz, Christina; Lutz, Susanne  
Universitätsmedizin Göttingen, Pharmakologie, Germany

**Background:** p63RhoGEF, identified as a specific mediator of G $\beta_{11}$ -dependent RhoA activation, is mainly expressed on mRNA level in cardiovascular and brain tissue. However, its role in the heart is so far not clear. Recently we found that in the adult rodent heart the strongest p63RhoGEF expression takes place in interstitial and vascular cells and to a lesser extent in cardiomyocytes.

**Methods:** To identify the functional role of this guanine nucleotide exchange factor *in vivo*, we generated a global knockout mouse model and studied its outcome under basal conditions and after transverse aortic constriction (TAC) in young animals. For investigations on a cellular level, cardiac fibroblasts (CF) from adult knockout (ko) and wild type (wt) mice were isolated and cell morphology as well as the expression of fibroblast-specific factors were studied.

**Results:** Under basal conditions p63RhoGEF-ko mice showed no significant changes in heart geometry and contractile function compared to wt littermates. One week after TAC the p63RhoGEF-ko animals displayed a clear worsening of contractile parameters, including ejection fraction and fractional area shorting which was not observed in the respective wt and sham operated animals. However, over time the contractile dysfunction decreased in TAC-operated wt animals to the same extent as in p63RhoGEF ko animals. In contrast, the progression of cardiac hypertrophy was not different between both genotypes. To further investigate differences between ko and wt animals, we analyzed changes in heart tissue morphology and gene expression and could show that p63RhoGEF ko animals displayed a slightly higher degree of cardiac fibrosis.

On a cellular level, our data revealed that in ko-CF displaying a change in cell geometry the transcription of collagen 1a and of the myofibroblast marker smooth muscle actin was higher than in the wt-CF and the transcription of the fibrosis-associated factors CTGF and TGF- $\beta$  1, which became induced by Ang II, were unchanged.

**Conclusion:** In summary, our data points to a role of p63RhoGEF in the onset of contractile dysfunction in an afterload model most probably by propagating fibrotic processes.



## 292

**Investigation of *N*-Glucuronidation of the Carbanilide Triclocarban****Ostermann, Annika**; Willenberg, Ina; Schebb, Nils Helge

Stiftung Tierärztliche Hochschule Hannover, Institut für Lebensmitteltoxikologie und Chemische Analytik, Germany

Triclocarban (TCC, 3,4,4'-Trichlorocarbanilide) is an antibacterial commonly used in soaps and other personal care products (PCP). This application has been declared as safe in an evaluation by the European Union in 2005. However a small but significant portion of TCC is dermally absorbed during the use of PCP. Recent studies show that TCC is a nanomolar inhibitor of the soluble epoxide hydrolase, an enzyme of the arachidonic acid cascade that plays a central role in the regulation of inflammation and pain.

For a comprehensive evaluation of the impact of TCC on human health it is crucial to characterize human exposure to this antibacterial. Urine sampling is best suited for these biomonitoring studies because samples can be collected frequently and in a non-invasive manner.

In humans TCC is renally excreted following direct phase II metabolism as *N*- and *N'*-glucuronides. Upon exposure these glucuronides can be found in human urine at concentrations up to 1 µM which makes them ideal biomarkers. However, these metabolites are not commercially available and attempts to synthesize them chemically failed. Furthermore, incubation experiments with microsomes from liver or kidney cells yielded only trace amounts of TCC-*N*-glucuronides.

The aim of this project was to find and characterize a cell culture based system which is suitable to generate TCC-*N*-glucuronides in relevant amounts and to optimize an extraction protocol for the isolation of these metabolites in preparative scale.

*N*-glucuronidation of TCC in humans is catalyzed by UDP-glucuronosyltransferases (UGT) most likely by UGT1A9 which is expressed in the kidney. Therefore three different kidney cell lines, CACI-2, MDCK as well HEK 293, were screened for their UGT activity. The cells were incubated with 4-(Trifluoromethyl)umbelliferone (TFMU), a standard substrate for UGT, and the formation of TFMU-glucuronides was quantified by means of liquid chromatography with fluorescence detection (LC-FD). In these experiments, a significant UGT activity could only be shown for CACI-2 cells.

Incubations of CACI-2 cells with TCC led to the formation of both *N*-glucuronides in the cell culture medium. With a conversion rate of 10% within 24 h a considerable amount of the TCC was conjugated. Utilizing an optimized two step liquid/liquid extraction procedure significant amounts of both TCC-*N*-glucuronides could be extracted as crude mixture. The approach is currently scaled up and combined with further purification steps to allow isolating both metabolites for NMR-analysis and to use them as analytical standards.

## 293

**Insulin and diabetes from a toxicological point of view****Othman, Eman Maher**; Stopper, Helga

Pharmakologie und Toxikologie institut, Würzburg Universität, Germany

Diabetes mellitus (DM), a disease with almost 350 million people affected, worldwide will be the 7<sup>th</sup> leading cause of death in 2030. Diabetic patients develop different types of complications, among them, an increased rate of malignancies such as colon and kidney cancers. Hyperinsulinemia, the high insulin blood level characteristic for early diabetes type II, was identified as a risk factor for cancer development. In our studies we showed that an elevated insulin level can induce oxidative stress, resulting in DNA damage in colon cells in vitro, and in kidney cells in vitro and in vivo (in Zucker diabetic fatty rats, ZDF) where we found that insulin also induced genomic damage in kidneys from healthy, lean ZDF rats, which were infused with insulin to yield normal or high blood insulin levels, while keeping blood glucose levels constant, the amounts of ROS and the tumor protein (p53) were elevated in the high-insulin group compared with the control level group. ROS and p53 were also elevated in diabetic obese ZDF rats. Further; we elucidated the signaling pathway of insulin-mediated genotoxicity which is effective through oxidative stress induction in colon and kidney. The signaling mechanism is started by phosphorylation of the insulin (IR) and insulin-like growth factor (IGF-1R) receptors, followed by activation of PI3K which in turn activates AKT. Subsequently, mitochondria and NADPH oxidase isoforms (Nox1 or Nox4 in colon and kidney, respectively) are activated for reactive oxygen species (ROS) production, and the resulting excess ROS can attack the DNA causing DNA oxidation. We conclude that hyperinsulinemia represents an important risk factor for cancer initiation or progression as well as a target for cancer prevention in diabetic patients.

## 294

**Impact of cell culture and particle parameters on the toxicity of zinc oxide nano-micro structures in vitro to fibroblasts****Papavlassopoulos, Heike**<sup>1</sup>; Mishra, Yogendra K.<sup>2</sup>; Kaps, Sören<sup>2</sup>; Paulowicz, Ingo<sup>2</sup>; Abdelaziz, Ramzy<sup>3</sup>; Elbahr, Mady<sup>3,4</sup>; Maser, Edmund<sup>1</sup>; Adelung, Rainer<sup>2</sup>; Röhl, Claudia<sup>5</sup><sup>1</sup>Christiana Albertina University Kiel, Institute of Toxicology and Pharmacology for Natural Scientists, Germany<sup>2</sup>Christiana Albertina University Kiel, Functional Nanomaterials, Institute for Materials Science, Germany<sup>3</sup>Christiana Albertina University Kiel, Nanochemistry and Nanoengineering, Institute for Materials Science, Germany<sup>4</sup>Helmholtz-Zentrum Geesthacht, Institute of Polymer Research, Nanochemistry and Nanoengineering, Germany<sup>5</sup>ZEBET - Alternative Methods to Animal Experiments, Federal Institute for Risk Assessment, Berlin, Germany

The increased use of nano-structured zinc oxide in biomedical and consumer products requires a better understanding of their adverse biological effects and cytotoxic behaviour.

To address this question we have focussed on two aspects in the present study: First, we have investigated the influence of material properties of nano-microscale ZnO tetrapods (ZnO-T) on cytotoxicity. Second, the impact of cell culture conditions of normal human dermal fibroblasts (NHDF) on their sensitivity towards ZnO-T was examined.

Therefore, we have treated NHDF for 24h with different concentrations of a) ZnO-T with different particle ages, b) ZnO-T with different surface charges induced by UV illumination and O<sub>2</sub> treatment and c) ZnO-T with different morphologies. Furthermore, the sensitivity of NHDF towards ZnO-T was examined depending on cell density and number of preceding cell passages. After 24h treatment the cytotoxicity was determined by the MTT-test.

Concerning material properties, our results show that aging and surface charge of ZnO-T have almost no effect on cytotoxicity in our in vitro system, whereas morphology associated with changes in surface properties influenced the cytotoxic potential of ZnO nanostructures significantly insofar as an increased surface area was associated with enhanced cytotoxicity. Considering the impact of cell culture conditions, cell density as well as the number of preceding cell passages strongly affect the sensitivity of NHDF towards ZnO-T. We have observed that a high cell density decreases the sensitivity of NHDF with passage numbers < P16 compared to a lower cell density. Vice versa, a high cell density increases the sensitivity of older NHDF (passage numbers > P21) compared to a lower cell density.

The results demonstrate that cell culture conditions as well as material properties can significantly influence the toxic potency of zinc oxide nano-micro structures in fibroblast cultures.

## 295

**Development of chemical categories by optimized clustering strategies**Batke, Monika<sup>1</sup>; Bitsch, Annette<sup>1</sup>; Gundert-Remy, Ursula<sup>2</sup>; Gütlein, Martin<sup>3</sup>; Helma, Christoph<sup>1</sup>; Kramer, Stefan<sup>5</sup>; Maunz, Andreas<sup>3</sup>; Partosch, Falko<sup>2</sup>; Seeland, Madeleine<sup>6</sup>; Stahlmann, Ralf<sup>1</sup><sup>1</sup>Fraunhofer Institut für Toxikologie und Experimentelle Medizin, Chemikalienbewertung, Hannover, Germany<sup>2</sup>Charité- Universitätsmedizin Berlin, Institut für Klinische Pharmakologie und Toxikologie, Germany<sup>3</sup>Albert-Ludwigs-Universität Freiburg, Institut für Physik, Zentrum für Biosystemanalyse, Germany<sup>4</sup>in silico toxicology gmbh, Basel, Switzerland<sup>5</sup>Johannes Gutenberg - Universität Mainz, Institut für Informatik, Germany<sup>6</sup>Technische Universität München, Institut für Informatik / 112, Garching, Germany

According to the OECD definition a chemical category is a group of chemicals whose physicochemical and human health and/or ecotoxicological properties and/or environmental fate properties are likely to be similar or follow a regular pattern. The building of categories has often been tried on the basis of conventional structure based approaches where similarities are based on functional groups, common constituents and physicochemical properties only.

In the present project we developed an approach by which toxicological and structural properties likewise contribute to the building of chemical categories for (sub)chronic toxicity. As data basis we used two databases on repeated-dose toxicity (RepDose and the "ELINCS" data base). The toxicological data are organized into organ toxicity in parts splitted into subgroups according to similarities at the phenotypic and at the mechanistic level. For the definition of a category, the following characteristics were considered: organ investigated, not investigated, no findings, findings; potency in terms of no observed adverse effect level (NOAEL), organ specificity.

Several clustering methods have been tested in the project and in the final version a multi-label clustering by using predictive clustering trees (PCT) was established.

Several critical decisions had to be considered carefully during development and refinement of the method; they concerned the structural features and chemicals properties on the one hand and the toxicological data set on the other. Decision had to be taken on:

- the selection of the appropriate features and their SMARTS description
- the non-inclusion of PC parameters
- the use of imputation methods to handle missing values
- the level of detail for a consistent representation of toxicological data versus the density of data in the matrix.

During method development all resulting categories (clusters) were visualized by using CheS-Mapper (1) and were checked by expert judgment for their plausibility. One important decision about a stopping criterion for clustering was the use of toxicological variance data in combination with a statistical significance test.

In the process of developing this new approach we needed many incremental improvements; the final approach produces a set of useful and representative clusters now.

This project is supported by BMBF in the funding focus "Ersatzmethoden zum Tierversuch"

(1) <http://opentox.informatik.uni-freiburg.de/ches-mapper/>

## 296

**Caffeine concentrations in breastfed babies and unborn children – physiological based modelling as a decision aid****Partosch, Falko**<sup>1</sup>; Mielke, Hans<sup>2</sup>; Gundert-Remy, Ursula<sup>1,2</sup><sup>1</sup>Charité Universitätsmedizin Berlin, Institut für Klinische Pharmakologie und Toxikologie, Germany<sup>2</sup>Bundesinstitut für Risikobewertung, Chemikaliensicherheit, Berlin, Germany

There are concerns in relation to the risk of adverse health effects as a result of the intake of caffeine in the general population and in specific target groups (e.g. pregnant and breast feeding women) at recommended doses of (300 mg/day Scientific Committee on Food (SCF) 1999; 400 mg FDA, USA; 2002; 200 mg for women in the childbearing age, Belgium, 2008).

In this controversy, some data on the internal exposure of the unborn child and of the nursed infant can inform for decision making. We established a physiologically based kinetic model and simulated the concentration of caffeine in a breast fed neonate after the nursing mother had consumed caffeine at levels between 150 mg and 600 mg. We also simulated the concentration in utero/fetal compartment during pregnancy assuming caffeine consumption of the pregnant woman at the same levels as the nursing mother. Physiological data for pregnant women, nursing mothers, and newborns were taken from published data sources as were data describing metabolic elimination. Partitioning into tissues was calculated after Schmitt (2008). For evaluation of the model predictions we used published experimental data of the concentration in blood of nursing mothers after 150 mg caffeine (Hildebrandt and Gundert-Remy, 1983). As the pharmacological/toxicological effect is related to the concentration we calculated the peak concentrations. Simulations with 150 mg caffeine dose were in good accordance with experimental data. Peak maternal caffeine concentration in the blood was 2.65 mg/l after 150 mg of caffeine, 3.5 mg/l after 200 mg, 5.4 mg/l after 300 mg, 7.2 mg/l after 400 mg and 10.9 mg/l after 600 mg caffeine. Peak concentration was 0.2, 0.3, 0.4, 0.6 and 0.9 mg/l in the newborn's blood and 1.6, 2.1, 3.2, 4.3 and 6.6 mg/l in the utero/fetal compartment.

Whereas for nursed infants adverse effects would not be expected after a single dose of even 600 mg the simulated concentrations in the utero/fetal compartment indicate that even 150 mg can have adverse effect on the fetus.

Hildebrandt R, Gundert-Remy U (1983) Lack of pharmacological active saliva levels of caffeine in breast fed infants. *Pediatric Pharmacology* 2, 233-244.

Schmitt W (2008) General approach for the calculation of tissue to plasma partition coefficient. *Toxicology In Vitro* 22, 457-467.

## 297

**Additives in tobacco products: On their role in addictiveness and attractiveness****Paschke, Meike**; Hutzler, Christoph; Henkler, Frank; Luch, Andreas

German Federal Institute for Risk Assessment (BfR), Department of Product Safety, Berlin, Germany

The addictiveness and attractiveness of tobacco products is likely to be enhanced by additives and certain constituents of tobacco smoke. For cigarettes, some 600 agents are being used in manufacturing processes. Menthol and other flavors might mask the unpleasant taste of nicotine and, thus, are suspected to increase the depth of inhalation as well as nicotine up-take. Addictiveness might also be affected by certain pyrolysis products of endogenous or supplemented carbohydrates.

We used pyrolysis—gas chromatography/mass spectrometry (Py-GC/MS) to identify the follow-up products of 20 different tobacco additives like raw cane sugar, molasses or cocoa during thermal decomposition. To simulate the smoking process of a cigarette, the individual additives were pyrolyzed at 350°C, 700°C or 1000°C. At these conditions we observed the generation of aldehydes, different heterocyclic compounds, polycyclic aromatic hydrocarbons (PAHs), as well as compounds from other chemical classes. For instance pyrolysis of raw cane sugar mainly leads to the formation of furanes. In addition, ketones, esters, pyranones, pyrrolidines and naphthalene could be also found in the pyrograms. Furthermore different flavoring agents, used to create a characteristic taste of tobacco products, were also pyrolyzed. However, these compounds were found rather being stable under these conditions.

Attractiveness can be enhanced by flavors that might appeal to certain consumer groups. According to the new European legislation, characteristic flavors, such as strawberry, candy, vanillin or chocolate will be prohibited. Product surveillance will therefore require analytical means to define selected characteristic flavors. A comprehensive headspace-solid phase microextraction (HS-SPME)—GC/MS method was developed to screen different strawberry tobacco products for their volatile additives. The results were compared to non-flavored, blend characteristic flavored and other fruity flavored cigarettes as well as fresh and dried strawberries. With this method the following five compounds of strawberry flavor were predominantly identified: methyl hexanoate, ethyl hexanoate, linalool,  $\gamma$ -decalactone and methyl cinnamate. All of these compounds could be detected in cigarettes and fine cut tobacco, which were advertised to have a strawberry taste. However, in strawberry flavored shisha tobacco, liquids for e-cigarettes, snus or snuff these compounds were only occasionally detected.

## 298

**Thrombin receptor PAR-4 deficiency protects against exaggerated intimal thickening in diabetes mellitus****Pavic, Goran**<sup>1</sup>; Rauch, Bernhard H.<sup>2</sup>; Fischer, Jens Walter<sup>1</sup>; Schrör, Karsten<sup>1</sup>; Fender, Anke<sup>1</sup>Institut für Pharmakologie und Klinische Pharmakologie, Universitätsklinikum der Heinrich-Heine Universität, Düsseldorf, Germany<sup>2</sup>Ernst-Moritz-Arndt-Universität Greifswald, Institut für Pharmakologie, Germany

**Aim:** Diabetes is a vascular disease associated with increased thrombin generation and accelerated vascular remodeling. Thrombin promotes vascular smooth muscle cell (SMC) proliferation and migration via protease-activated receptors (PAR-1, PAR-3 and PAR-4). We recently reported upregulation of PAR-4 in human vascular smooth muscle cells (SMC) exposed to high glucose. PAR-4 may therefore play a unique role in the vascular complications of diabetes. The aim of the present study was to examine PAR-4 as a potential novel mediator linking hyperglycemia, hypercoagulation and vascular remodeling in diabetes.

**Methods & Results:** PAR-4 immunofluorescence was increased in coronary arteries and saphenous veins obtained from diabetic vs. non-diabetic patients, and in aorta and carotid arteries obtained from streptozotocin-induced diabetic vs. non-diabetic C57BL/6 mice. Vascular PAR-4 but not PAR-1 mRNA expression was also increased in male C57BL/6 mice with streptozotocin-induced type 1 diabetes (blood glucose >500 mg/dL) compared to non-diabetic controls (blood glucose <280 mg/dL). Three weeks after induction of diabetes, the increase in vascular PAR-4 mRNA expression was approximately 10 to 15-fold. The left carotid artery was ligated at this time-point to induce neointima formation. Four weeks after carotid artery ligation, mice were sacrificed and arteries collected for morphometric quantification (H&E-staining). Neointima formation was comparable in non-diabetic wild-type and PAR-4<sup>-/-</sup> mice, suggesting minimal involvement of PAR-4 in vascular remodeling under normoglycemic conditions. In diabetic wild-type mice, neointimal hyperplasia was markedly augmented, but this increase was absent in diabetic mice lacking PAR-4.

**Conclusion:** These findings demonstrate for the first time that (i) vascular PAR-4 is upregulated in diabetic patients and in mice with streptozotocin-induced diabetes, and (ii) PAR-4 deficiency protects against the enhanced vascular remodeling response to carotid artery ligation in these mice. Collectively these data suggest a critical role of PAR-4 in the vascular complications of diabetes, and that a development of PAR-4 inhibitors might serve to limit proliferative and inflammatory processes in restenosis-prone diabetic patients, particularly those patients in whom severe bleeding due to selective PAR-1 blockade or complete thrombin inhibition must be avoided or who not require anticoagulation.

## 299

**Basic leucine zipper and W2 domain is a novel Wnt component with a potential role in cardiogenesis and cardiac remodeling****Pavlova, Elena**; Noack, Claudia; Zafriou, Maria-Patapia; Zimmermann, Wolfram H.; Zelaryan, Laura

Institute of Pharmacology, University Medical Center Göttingen, Goettingen, Germany

Understanding the mechanisms causing progressive damage and halting repair will be the basis of new therapeutic concepts for preventing heart failure progression. In line with the notion that pathways involved in embryonic cardiogenesis may help to activate repair mechanisms in the injured heart, our previous data suggest that regulation of canonical Wnt signaling may be instrumental in cardiac remodeling.

We previously identified the Krüppel-like factor (KLF) 15 as novel cardiac Wnt-inhibitor playing a role in heart homeostasis. We aim to characterize the molecular components of the cardiac specific Wnt regulation in cardiac cells. The analysis of *Klf15* knockout (KO) mice showed enhanced Wnt transcriptional activation exclusively in the heart although KLF15 deletion was global, suggesting a cardiac specific complex regulating the Wnt cascade in these mice. By means of an Y2H screen we identified the interaction of BZW2 with KLF15 and beta-catenin and validated it *in vitro* and *in vivo*. A reporter assay showed BZW2 to significantly repress beta-catenin/Tcf-dependent transcription. BZW2 expression was detected in the early embryonic developing heart and almost exclusively in the adult heart in comparison to kidney, liver, lung, spleen, and brain. Similar to the observed Wnt activation in *Klf15* KO mice, BZW2 expression was increased in cardiac tissue whereas no regulation was observed in other organs. Important is that *Klf15* KO mice showed cardiac dysfunction and were susceptible to stress. BZW2 was also found upregulated in Angiotensin II-induced hypertrophy in murine and in human failing hearts.

Our data suggest that BZW2 may form part of a specific cardiac complex participating in the Wnt cascade and a novel potential role of BZW2 in cardiac cell biology of the embryonic and adult heart upon remodeling.

## 300

**Betulin - a plant-derived cytostatic drug - enhances antitumor immune response****Pfarr, Kathrin**<sup>1</sup>; Danciu, Corina<sup>2</sup>; Dehelean, Cristina<sup>2</sup>; Pfeilschifter, Josef M.<sup>1</sup>; Radeke, Heinfried H.<sup>1</sup><sup>1</sup>Immune Pharmacology, pharmazentrum, Clinic of the Goethe University, Frankfurt/Main, Germany<sup>2</sup>University of Medicine and Pharmacy „Victor Babes”, Timisoara, Romania

Conventional cytostatic cancer treatments rarely result in a curative success. New therapeutic strategies are more promising by targeting the tumor microenvironment, inhibiting angiogenesis and antagonizing the immunosuppressive activity of established tumors. Following up this, plants provide a broad spectrum of potential drugs for cancer therapy, such as betulin, a pentacyclic triterpene of the birch tree representing the reduced congener of betulinic acid. Triterpene acids are known for their antiangiogenic and differentiation inducing effects. The anticancer activity of betulinic acid has been linked to its ability to directly trigger mitochondrial membrane permeabilization, a central event in the apoptotic process. In contrast to the potent cytostatic action towards different tumor cell lines, non-neoplastic cells and normal tissue remain relatively resistant.

This study aimed to investigate the antitumor activity on melanoma cells and the immune modulating effect on dendritic cells and T cells of phytochemicals, especially betulin. By means of MTT and CFSE proliferation assay as well as nuclear DAPI staining we could confirm that betulin decreased the proliferation rate of the highly metastatic B16F10 and the low metastatic B164A5 melanoma cell line. In addition, Annexin V/7-AAD staining showed that betulin induced a higher rate of apoptosis in melanoma cells as compared to primary bone marrow derived dendritic cells (BMDCs) of C57BL/6 mice. Furthermore, evaluated by co-incubation assays and ELISA read-out, we found that betulin elevated significantly the TLR4 stimulated IL-12p70 production of murine BMDCs. We could further show, that this increased secretion of IL-12p70 protein is due to an increased IL-12p35 mRNA expression while IL-12p40 mRNA level remained unchanged. Interestingly, these results are in contrast to data of genistein, another plant metabolite with antitumor properties, which caused a down regulation of IL-12p70 production of mBMDCs. Subsequent ex vivo experiments utilizing OT I spleen cells revealed that the betulin-elevated activation of dendritic cells loaded with ovalbumin results in enhanced T cell stimulation, assessed by betulin dependent increase in IL-2 and IFN- $\gamma$  production of T cells.

In summary, cytostatic agents like betulin that simultaneously exhibit immune stimulatory activity hold a great promise as a novel approach for an integrated cancer therapy.

### 301

#### Isolation and Characterisation of Human Non-Parenchymal Liver Cells for a Potential Use in Functional Co-Culture Liver Models

**Pfeiffer, Elisa**<sup>1</sup>; Kegel, Victoria<sup>1</sup>; Burkhardt, Britta<sup>2</sup>; Seehofer, Daniel<sup>1</sup>; Nüssler, Andreas<sup>2</sup>; Damm, Georg<sup>1</sup>

<sup>1</sup>Charité Universitätsmedizin Berlin, Campus Virchow Klinikum, Klinik für Allgemein-, Visceral- und Transplantationschirurgie, Germany

<sup>2</sup>Eberhard Karls Universität Tübingen, Berufsgenossenschaftliche Unfallklinik Tübingen, Klinik für Unfall- und Wiederherstellungschirurgie, Germany

Primary Human Hepatocytes (PHH) are considered to be the "gold standard" for *in vitro* testing of xenobiotic metabolism and hepatotoxicity. PHH cultivation in 2D monocultures leads to dedifferentiation and loss of functions. Reconstruction of the *in vivo* tissue architecture by 3D- and co-cultures is a promising approach to solve some of these problems. It is well known that hepatic Non-Parenchymal Cells (NPC) like, Kupffer Cells (KC), Liver Endothelial Cells (LEC) and Hepatic Stellate Cells (HSC), play a central role in many pathophysiological of the liver. Aim of the present study was the establishment of a protocol for the simultaneous isolation of human PHH and NPC as well as testing their suitability for a potential use in functional co-culture liver models.

Human liver cells were isolated from healthy liver tissue after surgical liver resections by a two-step EDTA/collagenase perfusion technique. PHH and NPC were separated by an initial centrifugation at 50 x g. The obtained cell fractions were purified by Percoll density gradient centrifugation. NPC were separated using specific adherence properties and magnetic activated cell sorting. Cells were identified and characterised by specific immunofluorescence staining. Furthermore viability and activation level of isolated NPC were analyzed by the determination of mitochondrial activity, synthesis of extra cellular matrix proteins as well as the detection of inflammatory signals.

Beside PHH we isolated and separated KC, LEC and HSC in a good quality and quantity. NPC were clearly identified by IF staining for specific cell markers and cell properties, like phagocytosis (KC) or specific autofluorescence (HSC). Characterisation of KC revealed a donor- and tissue quality dependent activation measured by intracellular ROS formation. Similarly, HSC demonstrated a time- and cultivation dependent activation observed by transformation into myofibroblasts linked to an increased expression of  $\alpha$  Smooth Muscle Actin.

We established a protocol for the simultaneous isolation of human PHH and NPC with a high purity and quality. Activation level of mono-cultured NPC depends on donor anamnesis, liver tissue quality and cell culture conditions. Therefore a stringent donor selection for the creation of functional co-culture models is indispensable. Further investigations are in progress for the establishment and characterisation of PHH and NPC co-cultures.

### 302

#### Formation of depurinating adducts of the food contaminant patulin with and without involvement of glutathione

**Pfenning, Carolin**; Esch, Harald L.; Lehmann, Leane

University of Würzburg, Section of Food Chemistry, Würzburg, Germany

The mycotoxin patulin (PAT), a frequent contaminant in fruits and products thereof, has mutagenic potential at submicromolar concentrations in the *hprt* locus of Chinese hamster V79 cells, most sensitive to base substitutions caused by e.g. DNA adducts. In

contrast, small electrophiles such as PAT are assumed to be inactivated by intracellular glutathione (GSH). Thus, in the present study, the reactivity of PAT towards DNA bases was investigated by incubation of PAT with nucleobases (NuB) in the presence or absence of GSH under cell-free conditions followed by subsequent LC-MS/MS analysis. Since the mutagenic potential of a DNA adduct depends, among others, on its chemical structure, main reaction products of PAT were characterized concerning their stability, i.e. their potential to form apurinic sites, by carrying out the same reactions with nucleosides (NuS) and monitoring the occurrence of both NuS adducts and the respective NuB adducts (a) without thermolysis, (b) after specific cleavage of the destabilized glycosidic bond of labile adducts by neutral thermolysis (100°C, 10 min), and (c) after cleavage of glycosidic bonds of all adducts by acidic thermolysis (88% formic acid, 70°C, 15 min).

In this way, two different structures of DNA adducts were identified: i) DNA adducts substituted with one or two molecules of NuB, even occurring in the presence of GSH, and ii) DNA adducts with one molecule of NuB and GSH each, revealing mixed GSH-PAT-DNA adducts which have neither been described for PAT nor for any other  $\alpha,\beta$ -unsaturated carbonyl compound before. LC-MS/MS analysis revealed a product pattern containing i) for adenine 5 NuB monoadducts and 7 NuB diadducts, as well as 7 mixed adducts, ii) for guanine 6 NuB monoadducts and 6 mixed adducts, iii) for thymine 2 NuB monoadducts and 3 NuB diadducts, as well as 4 mixed adducts, and iv) for cytosine 3 NuB monoadducts and 3 NuB diadducts, as well as 6 mixed adducts. Furthermore, 3 main adducts with adenine, among them 2 mixed GSH-PAT-adenine adducts, were classified to be putatively depurinating adducts.

Depurination of labile adducts leading to the generation of apurinic sites and subsequently to gene mutations could contribute to the PAT-induced mutations observed in the *hprt* gene.

### 303

#### Functional proteome analysis of *Clostridium botulinum* C3 exoenzyme treated hippocampal cells

Schroeder, Anke; Rohrbeck, Astrid; Just, Ingo; **Pich, Andreas**

Hannover Medical School, Institute of Toxicology, Germany

C3 exoenzyme of *Clostridium botulinum* (C3botWT) ADP-ribosylates small GTPases Rho A/B/C which leads to their functional inactivation. Treatment with C3botWT has a promoting effect on neuronal development in primary hippocampal neurons which leads to reorganization of the cytoskeleton and strong morphological changes.

We started a comprehensive proteome analysis to study primary and subsidiary effects in the proteome of neuronal cells after treatment with C3botWT and the transferase-deficient mutant C3botE174Q. Hippocampal HT22 cells were treated with C3botWT or C3botE174Q for 24 h to 144 h and protein abundance was calculated using a SILAC triple labeling. Peptides were analyzed using nanoLC and Orbitrap MS (Thermo Fisher Scientific) and MaxQuant software was used for identification and quantification of proteins. The proteome dataset was analyzed using the interaction database STRING. For visualization the resulting protein network was combined with the proteome data using the software Cytoscape.

C3botWT already induced morphological changes after 24 h and possess a moderate alteration of the proteome of HT22 cells. More than 4000 proteins were identified and the strongest effect with over 789 significant regulated proteins revealed after 144 h C3botWT treatment. Consistent with already known results an antiproliferative effect and a dysregulation of cytoskeletal proteins was detected. Moreover, upregulation of mitochondrial and lysosomal proteins, cell adhesion proteins and proteins of the carbohydrate and glucose metabolism could be assigned to C3botWT treatment. Upregulated as well as downregulated proteins belong to signal transduction and cytoskeleton organization. Lower abundance was detected for nucleic proteins of ribosome biogenesis or transcription. However, treatment of cells with the catalytic inactive mutant C3botE174Q exhibits no alteration of the proteome.

Kinetic and dose response correlations of ADP ribosylated Rho GTPases were determined using an internal standard of heavy stable isotopes labeled proteins.

### 304

#### Rats with low brain angiotensinogen levels are protected against development of diet-induced obesity

**Piehl, Martina**<sup>1</sup>; Schuchard, Johanna<sup>1</sup>; Stötting, Ines<sup>1</sup>; Bader, Michael<sup>2,3</sup>; **Raasch, Walter**<sup>1,4</sup>

<sup>1</sup>Universität Lübeck, Institut für Experimentelle und Klinische Pharmakologie und Toxikologie, Germany

<sup>2</sup>Max Delbrück Centrum für Molekulare Medizin, Molekularbiologie von Hormonen im Herz-Kreislaufsystem, Berlin, Germany

<sup>3</sup>DZHK (German Centre for Cardiovascular Research), partner site Berlin, Germany

<sup>4</sup>DZHK (German Centre for Cardiovascular Research), partner site Hamburg/Kiel/Lübeck, Lübeck, Germany, Germany

AT1-receptor blockers (ARB) are established for treatment of hypertension. In recent studies we demonstrated that ARB diminished food intake, weight gain and fat mass in rats, while energy expenditure was enhanced. Moreover, ARB induced alterations in hypothalamic mRNA levels of (an)orexigenic peptides and restored leptin sensitivity suggesting a central mechanism in regulating food behavior. The aim of this study was to verify whether central Renin-Angiotensin-System has impact on weight regulation and food behavior.

Studies were performed by using transgenic rats [TgR(ASrAogen)L680] (TGR) with a brain specific deficiency of angiotensinogen. Age matched Sprague Dawley (SD) rats were used as wild type controls. Both strains were fed with high calorie cafeteria diet (CD) or standard chow for 3 months. Weight gain, food intake, fat mass energy expenditure, plasma leptin, hypothalamic RNA levels of (an-)orexigenic peptides and glucose utilization were monitored.

In comparison to SD, TGR 1.), show a significant lower body weight while chow feeding; 2.), do not develop obesity during CD-feeding, since BMI, girth and fat mass remained unchanged; 3.), have normal baseline leptin plasma concentration independent on feeding regime, whereas plasma leptin of SD rat was markedly increased due to CD; 4.), show a clearly reduced energy intake; 5.), have a higher, strain-dependent energy expenditure which is additionally enhanced during CD-feeding; 6.), have enhanced mRNA POMC levels, whereas mRNA NPY levels are diminished in both strains during CD-feeding; 7.), show improved glucose utilization since HOMA index and insulin response in oral glucose tolerance test of SD rats was increased compared to TGR in particular after CD-feeding.

In conclusion, the central RAS has an impact on body weight regulation, feeding behavior and also metabolic disorders. When angiotensinogen and also AngII levels are low in brain, rats seem to be protected against development of diet induced obesity. Thus, we speculate that the antiobese effects of ARB are at least partially mediated by a brain-related mechanism.

### 305

#### Subcellular calcium handling during transition from hypertrophy to heart failure in ventricular myocytes of spontaneously hypertensive rats

Plackic, Jelena; Pluteanu, Florentina; Nikonova, Yulia; Preisenberger, Judit; Kockskämper, Jens

Philipps-Universität Marburg, Institut für Pharmakologie und Klinische Pharmazie, Germany

#### Question

Little is known about the onset and trigger for transition from compensated hypertrophy to heart failure (HF). We hypothesized that maladaptive remodeling of cardiomyocyte structure and subcellular Ca signaling would contribute to transition from compensated hypertrophy to HF. To test this we studied cyto- and nucleoplasmic Ca transients (CaTs) and morphological alterations of ventricular myocytes (VM) from old spontaneously hypertensive rats (SHR).

#### Methods

VM were isolated from 15-20 months old SHR. The presence of pulmonary edema was used to define SHR with HF. Two groups of SHR were studied: HF SHR (lung weight/tibia length (LW/TL) >50mg/mm) and pre-HF SHR (LW/TL <50mg/mm). Age-matched, normotensive Wistar-Kyoto rats (WKY) were used as controls. VM were electrically stimulated (1Hz, RT) and subcellular Ca transients (CaTs) were recorded by confocal imaging (8µM Fluo-4/AM). Ca stores were imaged with Mag-Fluo-4/AM (10µM). SR and perinuclear Ca loads were evaluated using rapid application of caffeine (10mM).

#### Results

Left ventricle, VM and nuclei were significantly enlarged to the same extent in both pre-HF and HF SHR as compared to WKY. The density of nuclear tubules was increased in nuclei of HF SHR compared to both pre-HF SHR and WKY nuclei. Pre-HF (n=78) and HF SHR VM (n=61) had higher cyto- and nucleoplasmic CaT amplitudes than WKY (n=99), but there were no differences between pre-HF and HF SHR VM. Nucleo-to-cytoplasmic ratio of CaT amplitude and of diastolic Ca was also equally increased in both pre-HF and HF SHR VM as compared to WKY. There was a positive correlation between systolic cytoplasmic and nucleoplasmic Ca levels in all three groups. The correlation was steeper in pre-HF SHR compared to both HF SHR and WKY myocytes. Calcium propagation from the subnucleolemmal to the central nuclear region was faster in HF SHR than in WKY or pre-HF SHR nuclei. SR and perinuclear Ca load and fractional Ca release was increased in pre-HF and HF SHR VM, but again there were no differences between pre-HF and HF.

#### Conclusions

Cyto- and nucleoplasmic Ca handling of pre-HF and HF SHR VM is augmented. There are, however, no major differences in either cyto- or nucleoplasmic Ca handling between pre-HF and HF SHR VM suggesting that the development of HF in this animal model of hypertensive heart disease does not involve Ca-dependent alterations as a key mechanism.

### 306

#### A-kinase anchoring proteins coordinate cigarette smoke extract-induced IL-8 release by airway smooth muscle cells

Poppinga, Wilfred Jelco<sup>1,2</sup>; Oldenburger, Anouk<sup>1,2</sup>; Klusmann, Enno<sup>3</sup>; Timens, Wim<sup>4,2</sup>; Heijink, Irene H.<sup>4,2</sup>; Maarsingh, Harm<sup>5</sup>; Schmidt, Martina<sup>1,2</sup>

<sup>1</sup>University of Groningen, Molecular Pharmacology, Netherlands

<sup>2</sup>University of Groningen, University Medical Center Groningen, Groningen Research Institute of Asthma and COPD (GRIAC), Netherlands

<sup>3</sup>Max-Delbrück-Centrum für Molekulare Medizin, Anchored Signalling, Berlin, Germany

<sup>4</sup>University of Groningen, University Medical Center Groningen, Pathology & Medical Biology, Netherlands

<sup>5</sup>Palm Beach Atlantic University, Pharmaceutical Sciences, West Palm Beach, United States

Chronic obstructive pulmonary disease (COPD) is a chronic inflammatory disorder mainly caused by cigarette smoke. Current pharmacotherapy involves  $\beta_2$ -agonists and phosphodiesterase inhibitors. Both drugs elevate cyclic AMP (cAMP), but relieve a distinct subset of COPD symptoms. A distinction potentially mediated by A-kinase anchoring proteins (AKAPs), which are known to compartmentalize cAMP signaling by binding the main cAMP effector protein kinase A (PKA). Currently, the functional implications of AKAPs in ASM functioning is not known and reports on alterations in their expression in lung diseases is lacking. In the current study we investigated the role of AKAPs in inhibition of cigarette smoke extract (CSE)-induced IL-8 release from immortalized human airway smooth muscle (ASM) cells by the  $\beta_2$ -agonist fenoterol. Disruption of PKA-AKAP complexes with st-Ht31 caused a significant increase of IL-8 release at the basal level. Treatment with st-Ht31 prevented reduction of CSE-induced IL-8 release by fenoterol. St-Ht31 increased basal ERK1/2 phosphorylation and prevented the reduction of CSE-induced ERK1/2 phosphorylation by fenoterol. Using an RII-overlay with radioactively labelled PKA-RII subunits and immunoblotting, we identified AKAP5, AKAP12, AKAP8, AKAP9 and Ezrin in ASM lysates. Cell exposure to CSE showed a decreased AKAP5, AKAP12 and AKAP9 expression level. AKAP5 and AKAP12 are known to interact with the  $\beta_2$ -adrenoceptor, and could therefore affect the receptor sensitivity perfectly matching the effect of st-Ht31 on the IL-8 release. We continued looking at these AKAPs in COPD patients. In lung tissue homogenates of COPD patients in both GOLD stages II and IV, the mRNA expression of AKAP5 and AKAP12 was decreased compared to control subjects. No significant difference was seen between the two different GOLD stages. A comparison of control and COPD subjects showed no clear difference in protein expression on immunohistochemistry. In conclusion, CSE alters the expression pattern of  $\beta_2$ -adrenoceptor-associated AKAP5 and AKAP12 in ASM cells. The suppressive effect of the  $\beta_2$ -agonist fenoterol on CSE-induced IL-8 release is coordinated by AKAPs. Therefore, a decrease of AKAP5 and AKAP12 as observed in COPD patients may affect pharmacotherapy. Supported by the Dutch Lung Foundation (NAF 3.2.11.015).

### 307

#### CpG-methylation characterizes cardiomyocytes in development and disease

Preißl, Sebastian<sup>1</sup>; Gilsbach, Ralf<sup>1</sup>; Grüning, Björn<sup>2</sup>; Köbele, Claudia<sup>1</sup>; Schnick, Tilman<sup>1</sup>; Hein, Lutz<sup>1</sup>

<sup>1</sup>Institut für Experimentelle und Klinische Pharmakologie und Toxikologie, Abteilung 2, Freiburg, Germany

<sup>2</sup>Bioinformatik, Institut für Informatik, Freiburg, Germany

#### Background:

Cardiac gene expression is changed during development, maturation and in disease. The epigenetic mechanisms controlling these alterations in cardiomyocytes are only partially known. DNA methylation and histone modifications are important epigenetic modulators. To elucidate whether these marks are altered during development and disease, whole genome DNA methylation profiles and histone modifications including H3K27ac, H3K27me3, H3K4me3 and H3K4me1 were determined in pure cardiomyocyte nuclei.

#### Methods and Results:

Murine cardiomyocyte nuclei were isolated and purified from different developmental stages and after induction of cardiac pressure overload by transverse aortic constriction (TAC) in adult mice. We analysed bisulfite converted DNA and immunoprecipitated histone marks by massive parallel sequencing with high depth. The obtained data sets were compared to public data of ES-cells (Creighton, M. P. et al. PNAS (2010), Stadler, M. B. et al. Nature (2011)).

Bioinformatic analysis identified 79,655 differentially methylated regions (DMRs) with an average size of 840 base pairs (bp, median 584 bp, maximum 150 kbp) in adult cardiomyocyte nuclei as compared with ES-cells. Transcription factor binding site prediction revealed strong enrichment ( $p < 10^{-50}$ ) of binding motifs for Gata1-4, Nkx2.5, Tbx5, Tbx20 and Mef2c in demethylated regions of cardiomyocyte nuclei. These transcription factors are known to be crucial for the cardiac lineage. Binding sites of factors known to be important for pluripotency were highly methylated in cardiomyocytes as compared with ES-cells. Demethylation was accompanied by H3K27ac and H3K4me1 enrichment indicating enhancers. DMRs acquired during pressure overload were mostly located in intergenic regions, too. Remarkably, a distinct fraction of disease DMRs overlapped with developmental DMRs. Methylation levels of these DMRs partially resembled the newborn DNA methylation pattern. They were adjacent to genes involved in cardiac muscle cell development, cardiac morphogenesis and in energy metabolism.

#### Conclusions:

The study established high resolution maps of CpG methylation and histone modifications in pure cardiomyocyte nuclei. These data enable identification of distal cis-regulatory action of transcription factors in cardiomyocytes. In hypertrophic cardiomyocytes, part of the differentially methylated genomic regions resembled a developmental DNA methylation pattern.

### 308

#### Cannabinoids inhibit angiogenic properties of endothelial cells via increasing TIMP-1 release from lung cancer cells

Ramer, Robert; Fischer, Sascha; Hausteiner, Maria; Hinz, Burkhard  
Institute of Toxicology and Pharmacology, University of Rostock, Germany

Cannabinoids exert antiangiogenic properties as part of their antitumorigenic action. In this context cannabinoids have been suggested to act directly on endothelial cells via

decreasing viability and migration or indirectly via modulation of angiogenesis-related factors released from cancer cells. However, comprehensive studies on a probable tumor-endothelial interaction are currently missing. Using Boyden chamber and tube formation assays the present study revealed a decreased migration and tube formation of human umbilical vein endothelial cells (HUVEC) suspended in conditioned media from A549 lung cancer cells that were treated with cannabidiol (CBD),  $\Delta^9$ -tetrahydrocannabinol (THC), R(+)-methanandamide (MA) or the selective CB<sub>2</sub> agonist JWH-133. By contrast, comparable antiangiogenic effects were not observed when cannabinoids were added to HUVEC directly. The antimigratory effect of CBD, THC and MA was reversed when A549 cells were pretreated with antagonists to cannabinoid receptors (CB<sub>1/2</sub>) or to transient receptor potential vanilloid 1 (TRPV1). Migration and tube formation were also diminished when HUVEC were incubated with recombinant tissue inhibitor of matrix metalloproteinases-1 (TIMP-1) that has recently been demonstrated to be upregulated by cannabinoids in cancer cells. Knockdown of cannabinoid-induced TIMP-1 expression in A549 cells by siRNA targeting TIMP-1 or intercellular adhesion molecule-1 (ICAM-1), an upstream trigger of TIMP-1 expression (Ramer et al., FASEB J 2012;26:1535-48), led to a reversal of the cannabinoid-mediated decrease of HUVEC migration. Inhibition of HUVEC migration by conditioned media of cannabinoid-treated cells was confirmed by use of two other lung cancer cell lines (H460, H358). Collectively, these results suggest a pivotal role of TIMP-1 and its upstream trigger ICAM-1 in conferring anti-angiogenic effects of cannabinoids via an intercellular tumor-endothelial cell communication.

### 309

#### Validation of the Yeast Androgen Screen for identification of Endocrine Active Substances that interact with the androgen receptor

**Ramirez-Hernandez, Tzutzyu<sup>1</sup>**; Woitkowiak, Claudia<sup>1</sup>; Huener, Hans-Albrecht<sup>1</sup>; Schönlaue, Christine<sup>2</sup>; Hollert, Henner<sup>2</sup>; Brosch, Susanne<sup>3</sup>; Zierau, Oliver<sup>3</sup>; Vollmer, Guenter<sup>3</sup>; Jaeger, Martina<sup>4</sup>; Poth, Albrecht<sup>4</sup>; Higley, Eric<sup>5</sup>; Hecker, Markus<sup>5</sup>; Landsiedel, Robert<sup>1</sup>; van Ravenzwaay, Bennard<sup>1</sup>

<sup>1</sup>BASF SE, Experimental Toxicology and Ecology, Ludwigshafen am Rhein, Germany

<sup>2</sup>RWTH, University of Aachen, Germany

<sup>3</sup>Technical University Dresden, Germany

<sup>4</sup>Harlan Cytotest Cell Research GmbH, Roßdorf, Germany

<sup>5</sup>University of Saskatchewan, Saskatoon, Canada

Endocrine disruptor compounds (EDCs) are a group of natural or synthetic compounds that have the capacity to interact with the endocrine system of living organisms and consequently causes adverse health effects in an intact organism, its progeny, or (sub)populations. Due to the potential impact on human health, there is increasing interest in assessing the risk of the exposure to EDCs. Currently, several *in vitro* and *in vivo* assays have been developed and few of them validated and regulatory accepted. Herein, we report on the inter-laboratory validation of a yeast androgen screen assay (YAS), which is a non-animal alternative that identifies potential EDCs that interact with the androgen receptor (AR). The validation exercise was performed in 5 laboratories from Canada and Germany. It demonstrates that the method can be performed with a high intralaboratory reproducibility (>90%) and also among the laboratories (between reproducibility >85%). The analysis of the predictivity was performed using 15 reference blinded compounds, the data demonstrates a very low rate of false predictions, resulting in a specificity above 95% and a sensitivity >85%. Remarkably, the accuracy to identify agonistic compounds was >90% and >87% for the antagonistic effects. In conclusion, the validation exercise demonstrates that the method is suitable to be used as a robust *in vitro* alternative to identify EDCs that interact with the AR.

### 310

#### In search of new reliable diagnostic biomarkers for systemic sclerosis: IL-33/ST2 and sphingolipids

**Ranglack, Annika<sup>1</sup>**; Köhm, Michaela<sup>2</sup>; Pfeilschifter, Josef M.<sup>3</sup>; Burkhardt, Harald<sup>2</sup>; Radeke, Heinfried H.<sup>1</sup>

<sup>1</sup>pharmazentrum frankfurt/Institut für allgemeine Pharmakologie und Toxikologie, Immunpharmakologie, Frankfurt am Main, Germany

<sup>2</sup>Universitätsklinikum Frankfurt, CIRI/Rheumatologie, Frankfurt am Main, Germany

<sup>3</sup>pharmazentrum frankfurt/Institut für allgemeine Pharmakologie und Toxikologie, Frankfurt am Main, Germany

Systemic Sclerosis (SSc) is an orphan and clinically heterogeneous disease with an unclear etiology. It is characterized by impaired angiogenesis, underlying autoimmunity and multi-organ fibrosis. Currently there is no established biomarker for the diagnosis of early SSc and no effective therapy.

In a cohort of 28 SSc patients we could confirm that S1P is elevated in serum compared to an age matched control group (Tokumura, 2009). In addition results from these sphingolipid measurements reveal elevated dihydro-S1P (dhS1P) levels in the serum of SSc patients. However, there was no difference in the IL-33 serum concentration as it has been shown by Yanaba (2009) comparing SSc patients with healthy individuals. Only 2 out of 28 patients showed increased IL-33 levels. Neither S1P nor IL-33 levels were correlated with C-reactive protein, complement factor C3, C4 concentrations or anti-nuclear antibodies in the blood profile. Interestingly, we could show significantly increased concentration of soluble ST2 (sST2) in the serum of SSc patients. sST2 is the soluble form of the IL-33 receptor. The regulation of sST2 seems to be independent of IL-33 because there is no correlation between sST2 and IL-33 serum levels. Furthermore we could show effects of an established symptomatic treatment

(*i.v.* infusions with the vasodilatory drug iloprost) on the analysed serum parameters before and after therapy. SSc patients receiving 5 days *i.v.* iloprost infusions show significantly reduced concentrations of S1P, dhS1P and sST2. These results suggest a connection between S1P or dhS1P and vascular events in SSc. Considering the elevated S1P and dhS1P levels in SSc patients the question arises if the increase in these sphingolipids serum levels plays a beneficial role in the progression of SSc. Moreover our results indicate that sST2 may be linked to the pathogenesis or at least could be promising prognostic marker of SSc.

Tokumura, Akira; Carbone, Laura D.; Yoshioka, Yasuko; Morishige, Junichi; Kikuchi, Masaki; Postlethwaite, Arnold; Watsky, Mitchell A. (2009): Elevated serum levels of arachidonoyl-lysophosphatidic acid and sphingosine 1-phosphate in systemic sclerosis. In: *Int J Med Sci* 6 (4), S. 168–176

Yanaba, Koichi; Yoshizaki, Ayumi; Asano, Yoshihide; Kadono, Takafumi; Sato, Shinichi (2011): Serum IL-33 levels are raised in patients with systemic sclerosis: association with extent of skin sclerosis and severity of pulmonary fibrosis. In: *Clin Rheumatol* 30 (6), S. 825–830.

### 311

#### Influence of cellular localization of survivin and DNA double-strand break repair on the resistance of glioblastoma cells against alkylating and topoisomerase I inhibiting anticancer drugs

**Reich, Thomas<sup>1</sup>**; Diesler, Kathrin; Aasland, Dorth; Kaina, Bernd; Christmann, Markus; Tomcic, Maja

Universitätsmedizin Mainz, Institut für Toxikologie, Germany

Despite a constant progress in medical care the brain tumors WHO grade III and IV (*Glioblastoma multiforme*) have a worse prognosis and remain incurable. Therefore the identification of novel predictive/prognostic markers is important for the diagnostics and the choice of therapy. In the last decade inhibitors of apoptosis proteins (IAP), particularly survivin and XIAP (X-linked inhibitor of apoptosis protein), were shown to be promising targets, as they are selectively expressed in tumors and their expression correlates with the grade of malignancy and therapy response. Apart from being an anti-apoptotic factor, survivin plays a role during chromosome segregation in mitosis. It passively penetrates into the nucleus but is actively exported out of the nucleus through its C-terminal nuclear export sequence (NES). Until now a nuclear accumulation of survivin was observed upon exposure to ionizing radiation, where survivin seems to support DNA double-strand break repair; it is unclear whether DNA lesions introduced by alkylating compounds or TOP1 inhibitors have an impact on survivin localization and how this affects cellular survival. To answer this question, we generated glioblastoma cell clones stably expressing either a GFP-survivin or a NES-mutated GFP-survivin fusion protein (GFP-NESmut-survivin). In colony-forming assays, we observed that the cell clones with strong GFP-survivin expression were mostly protected against TMZ and TPT, whereas the cell clones expressing GFP-NESmut-survivin were most sensitive. Using immune fluorescence, we could observe that GFP-survivin was efficiently exported out of the nucleus, whereas the mutated GFP-survivin retained in the nucleus and even accumulated during the time course of TMZ exposure. The same effect was observed when GFP-survivin expressing glioblastoma cells were incubated with leptomycin B, an inhibitor of the nuclear export. Neither GFP-survivin nor GFP-NESmut-survivin co-localized with  $\gamma$ H2AX foci, but interestingly, cells expressing GFP-NESmut-survivin showed significantly more TMZ-induced  $\gamma$ H2AX foci as compared to the GFP-survivin expressing cells. This correlates with the observed overall survival after exposure to the drugs. Our preliminary data show that only survivin localized in the nucleus renders glioblastoma cells hypersensitive to TMZ and TPT, which stresses nuclear survivin to be a beneficial prognostic marker and supports the use of nuclear export inhibitors as adjuvant drugs.

### 312

#### Structure modeling – comparing spheroids with *in vivo* situation

**Reif, Raymond<sup>1</sup>**; Günther, Georgia<sup>1</sup>; Ghallab, Ahmed<sup>2</sup>

<sup>1</sup>Leibniz-Institut für Arbeitsforschung an der TU Dortmund, Juniorguppe LivTox, Germany

<sup>2</sup>Leibniz-Institut für Arbeitsforschung an der TU Dortmund, Germany

There is a great demand on animal replacing test systems. Currently liver spheroids are an intensively investigated cultivation system for *in vitro* toxicological studies. A beneficial feature of spheroids is the establishment of a high differentiation state of the hepatocytes, compared to conventional cultures. Here we show the formation of bile canalicular structures of spheroids, which shows a high similarity to the *in vivo* situation. In a functional assay, the uptake of bile acids into the hepatocytes could be shown and these bile acids were also secreted in bile canalicular structures. Moreover, we managed to study compound uptake into spheroids using time lapse microscopy. In resulting movies the uptake can be quantified and kinetic parameters determined. Two-photon microscopy enables us to study the uptake of these compounds also *in vivo*. Comparison of the kinetic parameters determined for in spheroids and *in vivo* helps to extrapolate to the *in vivo* situation.

## 313

**TNF and IP-10 cause progression from salutary inflammation to organ-damaging hyperinflammation in the pre-injured lung****Reiss, Lucy Kathleen;** Uhlig, Stefan

Universitätsklinikum der RWTH Aachen, Institut für Pharmakologie und Toxikologie, Germany

**Rationale:** Due to its huge external surface, the lung is permanently subjected to inflammatory stimuli entering via the airways. Additionally, the lung can be challenged by systemic inflammation. In most cases inflammation is only mild and results in removal of the pathogen or clearance of the wound. In some cases, inflammation exacerbates to uncontrolled hyperinflammation and causes organ damage instead of healing. We suggest that salutary inflammation and destructive hyperinflammation are two distinct modules, which become activated depending on the severity of injury. This study was designed to investigate whether the pro-inflammatory mediators IL-6 and CXCL10 on the one hand or TNF and IP-10 (CXCL10) on the other hand can cause a switch to hyperinflammation.

**Methods:** Anaesthetised C57/BL6 mice were instilled with 50µL HCl pH=2 or saline and then ventilated for 1 hour, before either TNF+IP-10 or IL-6+CXCL10 (5µg of each mediator) were aerosolized in 50µL PBS into the lungs. Control groups received 50µL PBS. Ventilation was continued for further 6 hours. Lung mechanics, oxygenation and cardiovascular parameters were monitored during ventilation. Pro-inflammatory mediators, leukocyte recruitment, microvascular permeability and histology were examined in the lungs.

**Results:** Neither instillation of PBS nor of HCl pH=2.0 caused pulmonary dysfunction as demonstrated by unimpaired lung mechanics and arterial oxygenation. In acid pre-treated lungs, pro-inflammatory mediators, neutrophil counts and microvascular permeability were slightly increased. Administration of IL-6+KC did not augment pulmonary inflammation. In contrast, application of TNF+IP-10 exacerbated the inflammation and caused pulmonary failure in lungs pre-injured with HCl pH=2, but not in healthy control lungs.

**Conclusion:** We suggest that IL-6 and CXCL10 are mediators of the basic salutary inflammation module, whereas TNF and IP-10 belong to a set of mediators that drive inflammation into hyperinflammation.

## 314

**Characterisation of a polyunsaturated fatty acid activation site in TRPL****Riehle, Marc;** Harteneck, Christian

Experimental and Clinical Pharmacology and Toxicology, Eberhard Karls University Hospitals and Clinics, University of Tübingen, Pharmacology and Experimental Therapy, Germany

Arachidonic acid (AA), a C20 polyunsaturated fatty acid (PUFA), and its miscellaneous metabolic products (like thromboxane, leukotriens etc.) play an important role in living cells. They modulate cellular signalling pathways and thereby are involved in many physiologic processes. PUFAs are ligands for a variety of integral plasma membrane proteins, such as G protein-coupled receptors or ion channels, initiating intracellular signalling cascades or modulating ion homeostasis, respectively. PUFAs and derivatives have been described to activate ion channels of the TRP family, i.e. TRP<sup>1</sup>, TRPV<sup>1</sup>, TRPV<sup>2</sup>, TRPV<sup>3</sup> as well as modulate TRPM<sup>2</sup>, TRPV<sup>3</sup> or inhibit TRPM<sup>8</sup>. PUFAs are released from membrane lipids in a receptor-induced, phospholipase C-dependent manner subsequent to the generation of diacylglycerols (DAG) from phosphatidylinositol-4,5-bisphosphat. Whereas mammalian TRPC channels (TRPC3, TRPC6, TRPC7) mediate calcium entry by DAG-dependent activation, two of the Drosophila counterparts TRPL and TRPY are stimulated by PUFAs. In contrast, the third member of this family, TRP, is insensitive to both, DAG and PUFA. Sequence alignment of TRP, TRPL and TRPY provides the unique possibility to identify the PUFA activation site through site-directed mutagenesis of positions that are conserved in TRPL and TRPY, but are different from TRP. These amino acids in TRPL were each replaced by the respective amino acids of TRP. Mutant channels were analyzed in transiently transfected HEK293 cells using 5,8,11,14-eicosatetraynoic acid (ETYA), a non-metabolizable AA analogue, as a pharmacological tool, which inhibits a variety of AA metabolising enzymes, and mimics a PUFA-dependent activation of TRPL and TRPY. Among the 43 mutations studied, we identified 18 amino acid positions in TRPL that are necessary for its PUFA-mediated activation. These amino acids are localized in the transmembrane domains of TRPL, as well as in a domain of the cytosolic C-terminus close to the plasma membrane. *Vice versa*, we obtained PUFA-sensitive gain-of-function TRP mutants by transferring the corresponding amino acids of TRPL to TRP. Our data suggest a cooperative participation of amino acids in the transmembrane domains and in the C-terminus in the activation by PUFAs as a unique feature of TRP channels.

1 Jörs et al., J. Biol. Chem. 2006; 281 29693-702

2 Hwang et al., Proc. Natl. Acad. Sci. U S A. 2000 97 6155-60.

3 Nilius et al., Proc. Natl. Acad. Sci. U S A. 2004; 101 96-401.

4 Hara et al., Mol. Cell 2004; 9 163-173

5 Hu et al., J. Cell Physiol. 2006; 208 201-12.

6 Andersson et al., J. Neurosci. 2007; 27 3347-55.

## 315

**Biological effects of inhalable substances – development of a concept to standardize in vitro studies using aerosols****Ritter, Detlef<sup>1</sup>;** Arndt, Hendrik<sup>2</sup>; Knebel, Jan<sup>1</sup><sup>1</sup>Fraunhofer Institut ITEM, In-Vitro and Mechanistic Toxicology, Hannover, Germany<sup>2</sup>Hochschule Emden/Leer, EUTEC Institut, Germany

The state-of-the-art method for lung related research in vitro is the air-liquid-interface culture (ALI) technique involving biological models (cell lines, primary cells, etc.) on microporous membranes. Techniques to use such ALI- models in inhalation related in vitro approaches have improved fundamentally and at the same time led to varying exposure setups. Concerning investigations on pure gases the reproducibility and relevance of these strategies could recently be shown in a prevalidation study comprising round-robin testing of several chemical gases, resulting in a prediction model [1]. However, in case of aerosols the comparability of results of individual labs is still lacking and has to be clearly improved to create relevant results.

Therefore, as a first step, defined model setups together with model aerosols are needed to characterize different exposure procedures in individual labs and thus generate comparable and relevant data.

To establish a test system which can easily be applied in different exposure setups, an entire concept was developed involving aerosols generated by nebulization and drying of salt solutions including toxic and non-toxic substances of different particle sizes. The aerosols were applied in an ALI exposure setup (P.R.I.T. @ ALI ExpoCube) on A549 cells and toxic effects were investigated based on viability measurements (WST-1).

A first group consisting of one positive and one negative substance (SDS and NaCl) including different particle sizes was investigated in the aerosol exposure and resulted in reproducible dose- and substance dependent toxic effects with a higher toxicity using positive control (SDS) than the negative aerosol (NaCl).

Thus, the proposed concept was successfully tested as a first step to set up a panel of positive and negative substances which can be used to generate aerosols for the characterisation of aerosol inhalation investigation procedures in vitro. By including simple methods for aerosol generation and quantification, a relevant cell line and fast and easy read-out methods, this concept can be applied easily to different exposure applications in vitro. Therefore, it can clearly improve the relevance of data generated using such methods by a concept of standardisation and normalization in the future.

[1] G. Linsel, M. Bauer, E. Berger-Preiß, C. Gräbsch, H. Kock, M. Liebsch, R. Pirow, D. Ritter, L. Smirnova, J. Knebel (2011) Prevalidation study for testing toxic effects of inhalable substances (gases).

1. edition. Dortmund: Bundesanstalt für Arbeitsschutz und Arbeitsmedizin 2011. ISBN: 978-3-88261-131-1, 43 pages

## 316

**Role of biglycan in the age-associated malignancy of melanomas****Röck, Katharina;** Wladarz, Jessica Romy; Fischer, Jens Walter

Institut für Pharmakologie und Klinische Pharmakologie, Düsseldorf, Germany

For the malignant melanoma age has been shown to be an independent adverse prognostic indicator of overall survival. Both, the incidence of cutaneous melanomas as well as the malignancy of the tumor, increase drastically with age. Furthermore, melanomas in young patients grow faster and planar, whereas melanomas in older patients reveal a slow growing however invasive and metastatic phenotype. One possible regulator of this phenomenon is the extracellular matrix of the tumor stroma. Biglycan (BGN), a small leucine rich proteoglycan is a collagen binding constituent of the extracellular matrix. By activation of signaling cascades through e.g. toll like receptors BGN is a known regulator of cellular phenotypes thereby possibly influencing tumor progression and immune responses.

*Ex vivo* BGN mRNA expression was found to be increased (4.22±0.88 fold of young patients) in fibroblasts derived from old patients (>60 years) compared to young patients (<40 years) as well as *in vivo* in young (10 weeks) versus old mice (1.5 years). The growth of subcutaneously injected B16F10 melanoma cells in young and old mice was significantly reduced in old mice (0.32±0.13 fold of young mice) resembling the slower progression in old patients as detailed above. *In vitro* B16F10 melanoma cells were co-cultured with pre-senescent and senescent fibroblasts. Higher expression level of BGN in senescent fibroblasts was correlated with an induction of p21 (3.70±1.28 fold of control) and reduction of proliferation (0.58±0.076 fold of control) in B16F10 cells. Importantly, an increase in AKT2 (1.81±0.28 fold of control), which is associated with increased invasiveness of tumor cells, was found. These effects could be mimicked by treatment of the B16F10 cells with BGN core protein. In addition BGN stimulation induced markers for the epidermal-mesenchymal transition (EMT). EMT has been described as the predominant step in cancer invasiveness and metastasis. Indeed, BGN treatment of B16F10 cells increased the ability for anchorage independent cell growth (2.19±0.54 fold of control) as shown by soft agar assay and invasiveness (2.56± 0.188 fold of control) as detected by wound healing assay.

Taken together BGN seemingly modifies the tumor behavior by reducing the growth rate however leading to a more invasive and metastatic phenotype with increasing age.

317

### ***Clostridium botulinum* C3 exoenzyme and a 26<sup>mer</sup> C3-peptide induce changes in gene expression in primary Schwann cells**

**Rohrbeck, Astrid**<sup>1</sup>; Stahl, Frank<sup>2</sup>; Hagemann, Sandra<sup>1</sup>; Just, Ingo<sup>1</sup>; Haastert-Talini, Kirsten<sup>3</sup>

<sup>1</sup>Hannover Medical School, Institute of Toxicology, Germany

<sup>2</sup>Leibniz University of Hannover, Institute for Technical Chemistry, Germany

<sup>3</sup>Hannover Medical School, Institute for Neuroanatomy, Germany

Schwann cells play a crucial role in endogenous repair of peripheral nerves due to their ability to dedifferentiate from the myelinating phenotype and to migrate, proliferate and express regeneration promoting factors. In animal models of spinal cord injury (SCI), grafting Schwann cells into the lesion site has been shown to promote axonal regeneration and myelination. We have shown that *Clostridium botulinum* C3 exoenzyme, its enzymatically inactive form C3-E174Q and a 26<sup>mer</sup> C-terminal peptide fragment covering amino acid 156-181 (C3<sup>156-181</sup>) of C3 enhanced dendritic as well as axonal growth in organotypic cultures *in vitro*. Furthermore, we demonstrated that C3<sup>156-181</sup> administration at the lesion site accelerates motor recovery of rat sciatic nerves after crush injury or nerve autotransplantation *in vivo*. The mechanism underlying the specific support of axonal regeneration by C3<sup>156-181</sup> is still in debate.

To further elucidate the effect of C3 and 26<sup>mer</sup> C3-peptide in peripheral nervous system, we compared gene expression profiles of untreated rat neonatal Schwann cells with those treated with C3 or C3<sup>156-181</sup> for 72 h. For expression analysis, microarrays covering 400 neuronal genes were used. Array data were normalized and analyzed for significant differences using standard two-state pooled-variance *t*-test (1% and 5% probability of error).

Using *t*-test to compare treated (C3 and C3<sup>156-181</sup>) with untreated cells, we identified 27 transcripts (12 down-regulated and 6 up-regulated genes) and 25 transcripts (21 down-regulated and 2 up-regulated genes), respectively, which were at least 1.8-fold differentially expressed. When the C3 versus untreated gene expression profile was compared to the C3<sup>156-181</sup> versus untreated, 5 genes were found to be commonly altered in Schwann cells.

Based on differentially expressed genes, we identified genes significantly down-regulated, which are involved in glutamate uptake and inhibition of apoptotic genes. Our microarray-based expression profiling revealed novel C3-regulated genes in Schwann cells possibly involved in the axonotrophic effects of C3 and the C3-peptide.

318

### **Binding of *Clostridium botulinum* C3 exoenzyme to intact cells.**

**Rohrbeck, Astrid**; von Elsner, Leonie; Hagemann, Sandra; Just, Ingo  
Hannover Medical School, Institute of Toxicology, Germany

C3 from *Clostridium botulinum* (C3) specifically modifies Rho GTPases RhoA, RhoB, and RhoC by ADP-ribosylation. The confined substrate profile of C3 is the basis for its use as pharmacological tool in cell biology to study cellular functions of Rho GTPases. Although C3 exoenzyme does not possess a cell-binding/translocation domain, C3 is able to efficiently enter intact cells, including neuronal and macrophage-like cells. The mechanism of uptake is not yet understood.

In the present work, binding of C3 to the hippocampus-derived HT22 cell line and macrophage-like cell line J774A.1 was characterized by means of binding assays. C3 bound in a concentration-dependent but in a non-saturable manner to HT22 and J774A.1 cells. Pronase-pretreatment of intact cells significantly reduced C3 binding and inhibited C3 cell entry. To elucidate whether glycosylation is important for the C3-protein binding, intact cells were incubated with glycosidase F prior to incubation with C3. Surprisingly, removal of sugar residues resulted in an increased binding of C3 but reduced cell entry. To explore the involvement of phosphorylation in the binding process of C3, intact HT22 and J774A.1 cells were pretreated with vanadate prior to incubation with C3. Inhibition of de-phosphorylation by vanadate resulted in an increased binding of C3. Thus, interactions between C3 and cell proteins might require phosphorylation. To differentiate between intra- and extracellular phosphorylation, intact cells were treated with CIP (calf intestine phosphatase) to removed extracellular phosphates. The removal of phosphate residues by CIP results in strong reduction of the C3-protein interaction. In sum, C3 binding assays revealed that the C3 protein interaction partner is proteinaceous and that glycosylation and phosphorylation are critical for efficient binding of C3 to intact cells.

319

### **The antiepileptic drug lamotrigine is a substrate of breast cancer resistance protein**

**Römermann, Kerstin**<sup>1</sup>; Fedrowitz, Maren<sup>1</sup>; Löscher, Wolfgang<sup>1,2</sup>

<sup>1</sup>University of Veterinary Medicine Hannover, Department of Pharmacology, Toxicology and Pharmacy, Germany

<sup>2</sup>Center for Systems Neuroscience, Hannover, Germany

The multidrug transporter hypothesis is one current hypothesis for pharmacoresistant epilepsy, which proposes active extrusion of antiepileptic drugs (AEDs) by multidrug transporters like P-glycoprotein (Pgp; MDR1) or breast cancer resistance protein (BCRP) at the blood-brain barrier. An overexpression of those multidrug transporters may impede AEDs to reach their intended site of action. Recently, we have shown, that

several AEDs can be identified as substrates for Pgp when using a highly sensitive concentration equilibrium transport assay (CETA), which allows evaluating active transport almost independently of the passive permeability component (Luna-Tórtos et al., Neuropharmacology 2008). Previous *in vitro* studies using conventional bi-directional transcellular transport assays failed to identify AEDs as substrates of human BCRP, whereas *in vivo* studies with Bcrp1-knockout mice gave hints for Bcrp1-mediated transport of AEDs. Therefore the aim of this study was to examine the Bcrp-mediated transport of AEDs by using CETA. MDCKII-cells as wildtype or overexpressing human BCRP or murine Bcrp1 were seeded on microporous insert-membranes, dividing the chamber in an apical and a basolateral compartment. For CETA, the tested AEDs were given to each compartment in equal concentrations and samples were taken from both chambers at different time points. By performing CETA, we could show for the first time *in vitro*, that the AED lamotrigine is a substrate of murine Bcrp1 and human BCRP in different therapeutic relevant concentrations. This transport could be inhibited by using the specific Bcrp-inhibitor Ko143. The other tested AEDs phenytoin, phenobarbital, valproate, carbamazepine, topiramate and levetiracetam could not be identified as Bcrp substrates by using CETA. The present study indicates that at least for the AED lamotrigine Bcrp could play a role for pharmacoresistant epilepsy, which is in line with the multidrug transporter hypothesis.

Luna-Tórtos, C., Fedrowitz, M. and W. Löscher: Several major antiepileptic drugs are substrates for human P-glycoprotein. Neuropharmacology, 55(8):1364-75, 2008.

320

### **The transcription factor ER81 affects $\beta$ -adrenergic signaling in the heart**

**Rommel, Carolin**<sup>1</sup>; Rösner, Stephan<sup>1</sup>; Mayer, Sandra<sup>1</sup>; Gilsbach, Ralf<sup>1</sup>; Nikolaev, Viacheslav<sup>2</sup>; Hein, Lutz<sup>1</sup>

<sup>1</sup>Institut für Exp. und Klin. Pharmakologie und Toxikologie Universität Freiburg, Germany

<sup>2</sup>European Heart Research Institute Göttingen Universität Göttingen, Kardiologie und Pneumologie, Germany

**Background:** The transcription factor ER81 (*ETS related 81*) belongs to the large family of ETS-transcription factors. These factors play an important role in diverse developmental processes and cancer formation. Cardiac *ER81* mRNA expression is increased in failing human hearts. However mechanical unloading by a left ventricular assist device leads to normalization of ER81 expression. Thus, the aim of the present study was to investigate the physiological and pathophysiological role of ER81 in the heart.

**Methods and Results:** We generated transgenic mice overexpressing ER81 under control of the cardiomyocyte-specific  $\alpha$ -myosin heavy chain gene ( $\alpha$ MHC) promoter. Ventricular phenotyping revealed no evidence for morphological changes, hypertrophy or fibrosis in ER81 transgenic mice (ER81 <sup>$\alpha$ MHC</sup>) compared to wild-type (WT) mice. Interestingly, the functional inotropic response to intravenous dobutamine infusion was severely blunted in ER81 transgenic mice. To identify potential aberrations in contractility, isometric contractile force measurements on isolated left atria were performed in organ baths. Left atria of wild-type mice responded to increasing concentrations of isoprenaline and NKH477 (water-soluble analog of forskolin) with an increase in contractility, whereas the maximal positive inotropic responses to these substances were significantly reduced in ER81 <sup>$\alpha$ MHC</sup> atria. To gain further insight into 3',5'-cyclic adenosine monophosphate (cAMP) dynamics in cardiomyocytes, fluorescence resonance energy transfer (FRET) based cAMP measurements were performed in isolated adult mouse ventricular cardiomyocytes which were transfected with recombinant adenovirus encoding the cAMP sensor Epac1-camps for 48 h. Stimulation with 100 nM isoprenaline induced an increase in cytosolic cAMP concentrations in wild-type and ER81 <sup>$\alpha$ MHC</sup> cardiomyocytes. Maximal isoprenaline induced responses and kinetics were similar in both genotypes. Interestingly, ER81 <sup>$\alpha$ MHC</sup> cardiomyocytes showed faster kinetics of subsequent cAMP degradation than wild-type cardiomyocytes which indicates possible differences in phosphodiesterase expression and activity. Potential cardiac ER81 target genes which may contribute to the observed phenotypes were identified by whole genome expression analysis.

**Conclusion:** The ETS-transcription factor ER81 influences cardiac  $\beta$ -adrenergic signaling. Thus, ER81 may play an important role in the pathogenesis of chronic heart failure possibly via changes in cAMP signaling.

321

### **Extracellular UTP and ATP induce transient p38 and ERK1/2 MAPK phosphorylation in cardiac myocytes**

**Rothkirch, Daniel**<sup>1</sup>; Gergs, Ulrich<sup>1</sup>; Dhein, Stefan<sup>2</sup>; Neumann, Joachim<sup>1</sup>

<sup>1</sup>Institut für Pharmakologie und Toxikologie, Med. Fakultät, Martin-Luther-Universität Halle-Wittenberg, Halle/Saale, Germany

<sup>2</sup>Klinik für Herzchirurgie, Herzzentrum Leipzig, Germany

Extracellular UTP and ATP can be released from the mammalian heart during pathological conditions such as ischemia, hypoxia or reperfusion. In humans, UTP and ATP levels are increased during myocardial infarction. ATP and UTP can act via P2 purinoceptors which are further divided in P2X<sub>1-7</sub> and P2Y<sub>1-14</sub> receptors. As previously shown, ATP and UTP can induce inotropic effects in cardiac preparations of mice and man. The aim of the present work was to study the signal transduction pathway involved. Therefore, we studied the effects of UTP and ATP on MAPK phosphorylation in isolated adult mice cardiac myocytes, in neonatal rat cardiac myocytes and in human atrial tissue using phosphorylation-specific antibodies. UTP and ATP increased time and

concentration-dependently MAPK phosphorylation up to 300 % for ERK1/2 and p38 with a maximum effect at 5 to 10 minutes after application of UTP or ATP in cardiac myocytes (n=3 preparations each). The UTP-induced phosphorylations were blocked by the P2 purinoceptor antagonist PPADS (Pyridoxalphosphate-6-azophenyl-2',4'-disulfonic acid) but not by the adenosine receptor antagonist DPCPX (8-Cyclopentyl-1,3-dipropylxanthine), the P2 purinoceptor antagonist reactive blue, or the adenylyl cyclase inhibitor SQ22536 (9-(Tetrahydro-2-furanyl)-9H-purin-6-amine). Moreover, 100  $\mu$ M ATP or UTP increased ERK1/2 and p38 MAPK-phosphorylation in isolated human atrial tissue obtained by bypass surgery. In summary, not only in animal cardiac myocytes but also in human cardiac tissue, ATP and UTP induced a transient phosphorylation of MAP kinases with different time maxima and receptor antagonist patterns, suggesting a comparable signal transduction cascade. Interestingly, the inotropic effects lasted much longer than MAPK phosphorylation. This indicates that further downstream phosphorylations are involved in the sustained positive inotropic effect. Additional studies are necessary to elucidate the subsequent signaling pathway.

### 322

#### Selectivity profiling of novel harmine derivatives as potent and selective DYRK1 inhibitors

**Rüben, Katharina**<sup>1</sup>; Wurzbauer, Anne<sup>2</sup>; Sippl, Wolfgang<sup>3</sup>; Bracher, Franz<sup>2</sup>; Becker, Walter<sup>1</sup>

<sup>1</sup>Uniklinik RWTH Aachen, Institute of pharmacology and toxicology, Germany

<sup>2</sup>LMU München, Department of pharmacy - center for drug research, Germany

<sup>3</sup>MLU Halle-Wittenberg, Institute of pharmacy, Halle (Saale), Germany

Protein kinases play essential roles in almost all cellular processes and consequently have become one of the most intensively investigated classes of drug targets. Although there is a growing interest in developing chemical probes for the functional characterization of kinases, just a small fraction of the human kinome can be effectively targeted with selective small-molecule inhibitors to date. One kinase that has attracted increasing interest as a potential drug target due to its role in the pathology of Down syndrome is the dual specificity tyrosine-phosphorylation-regulated kinase 1A (DYRK1A). The over-activity of DYRK1A, which results from the increased dosage of the DYRK1A gene located on the human chromosome 21, is thought to contribute to the neurological abnormalities associated with Down syndrome.

The  $\beta$ -carboline alkaloid harmine is one of the most potent and selective DYRK1A inhibitors presently available but has the disadvantage of inhibiting monoamine oxidase A (MAO-A) with a high affinity. Based on the already favorable properties of harmine as a DYRK1A inhibitor, we aimed to develop harmine analogues that lack MAO-A inhibition. We identified AnnH75 as a new compound that inhibited DYRK1A with an  $IC_{50}$  value of 184 nM in radioactive assays but had no effect on MAO-A at 1  $\mu$ M. AnnH75 reduced the phosphorylation of the known DYRK1A substrates SF3B1 and Septin 4 in cultured cells ( $IC_{50}$  = 363 nM) and showed minimal toxicity for HeLa and PC12 cells up to concentrations of 10  $\mu$ M. Kinome profiling against a panel of 300 kinases at a concentration of 1  $\mu$ M revealed that only 4 off-target kinases were inhibited by more than 90% by AnnH75 (DYRK1B, CLK1, CLK4, Haspin). In summary, the new  $\beta$ -carboline compound AnnH75 is a potent, selective and cell permeable DYRK1A inhibitor that can be used as a valuable chemical probe for revealing the role of DYRK1A in cellular processes.

### 323

#### Insulinotropic Effect of High Potassium Concentration beyond Plasma Membrane Depolarization

**Rustenbeck, Ingo**; Belz, Michael; Willenborg, Michael; Görgler, Nele; Schumacher, Kirstin

Technische Universität Braunschweig, Institut für Pharmakologie und Toxikologie, Germany

Currently, the first phase of the glucose-induced insulin secretion is attributed to the existence of a limited pool of readily releasable granules, the exocytosis of which is triggered by the depolarization-induced  $Ca^{2+}$  influx via voltage-dependent  $Ca^{2+}$  channels. In experiments designed to dissect the signalling pathways of nutrient secretagogues, the depolarizing effect of glucose metabolism is often replaced by a strong  $K^+$  depolarization, typically evoked by raising the extracellular  $K^+$  concentration to 40 mM. The question as to whether  $K^+$  depolarization is an appropriate experimental substitute for the physiological nutrient-induced depolarization of the beta cell plasma membrane was investigated using primary mouse beta cells and islets. At basal glucose 40 mM  $K^+$  induced a massive monophasic response, whereas 15 mM  $K^+$  had only a minimal insulinotropic effect, even though the increase in the cytosolic  $Ca^{2+}$  concentration ( $[Ca^{2+}]_i$ ) was not inferior to that by 20 mM glucose. In voltage-clamp experiments  $Ca^{2+}$  influx appeared as nifedipine-inhibitable inward action currents in the presence of sulphonylurea plus TEA to block compensatory outward  $K^+$  currents. Under these conditions 15 mM  $K^+$  induced prolonged action currents and 40 mM  $K^+$  transformed the action current pattern into a continuous inward current. Correspondingly, 15 mM  $K^+$  led to an oscillatory increase, 40 mM  $K^+$  to a plateau of  $[Ca^{2+}]_i$  superimposed on the  $[Ca^{2+}]_i$  elevated by sulfonylurea plus TEA. Raising  $K^+$  to 15 or 40 mM in the presence of sulfonylurea (+/- TEA) led to a fast further increase of insulin secretion. This was reduced to basal levels by nifedipine or  $CoCl_2$ . The effects of 15 mM  $K^+$  on depolarization, action currents and insulin secretion were mimicked by adding 35 mM  $Cs^+$ , those of 40 mM  $K^+$  by adding 35 mM  $Rb^+$ , in parallel with their ability to substitute for  $K^+$  as permeant cation. In conclusion, the alkali metals,  $K^+$ ,  $Rb^+$  or  $Cs^+$  do not simply trigger the activity of voltage-dependent  $Ca^{2+}$  channels, but concentration-dependently

transform the pattern of  $Ca^{2+}$  influx into the pancreatic beta cell and may thus generate stimuli of supraphysiological strength for insulin secretion.

### 324

#### PKA and CaMKII-mediated phosphorylation of Histone H3S28 during pathological $\beta$ -adrenergic stimulation

**Saadatmand, Ali Reza**<sup>1</sup>; Dewenter, Matthias<sup>1</sup>; Meyer-Roxlau, Stefanie<sup>1</sup>; Vettel, Christiane<sup>1</sup>; Lehmann, Lorenz<sup>2</sup>; Backs, Johannes<sup>2</sup>; El-Armouche, Ali<sup>1</sup>

<sup>1</sup>Universitätsmedizin Göttingen, Department of Pharmacology, Germany

<sup>2</sup>University of Heidelberg, Department of Cardiology, Angiology and Pulmology, Germany

**Background:** There is growing evidence that abnormal epigenetic modifications are linked to arrhythmias and maladaptive cardiac remodeling, eventually leading to heart failure and sudden cardiac death. Histone phosphorylation may modify chromatin structure and/or provide a "code" for the recruitment of specific proteins to chromatin regulating gene transcription. Evolutionarily conserved phosphorylation residues on the amino-terminal tail of H3 are Ser 10, Thr 11 and Ser 28 (P-H3S10, P-H3T11, P-H3S28). Myocardial CaMKII, PKA, protein phosphatase 1 (PP-1) and PP-2A have emerged as transducers of cardiac stress responses. Here, we hypothesized that dysregulations in H3 phosphorylation, is linked to cardiac pathology by modifying chromatin dynamics and gene transcription and analyzed the specific contribution of CaMKII, PKA, PP-1 and PP-2A.

**Methods and Results:** In a canine model of rapid pacing induced HF, immunoblotting revealed that P-H3S28 was markedly enhanced in failing myocardium whereas P-H3S10 and P-H3T11 were not affected (n=6, p<0.05). Accordingly, pathological  $\beta$ -adrenergic stimulation with isoproterenol of isolated rat cardiomyocytes induced selective H3S28 hyper-phosphorylation. Time-dependent analysis by immunocytochemistry and immunoblotting revealed that P-H3S28 was detectable as early as 3 min and further increased beyond 24 hours of isoproterenol treatment. To determine whether this phosphorylation is mediated by PKA or CaMKII, we used specific inhibitors i.e. PKI and KN93, respectively. Our results indicate that both kinases mediate phosphorylation of H3S28 but whereas PKA mediated the acute phosphorylation events, the onset of CaMKII-dependent phosphorylation was clearly delayed. Accordingly, in mice with myocardial CaMKII $\delta$  overexpression, which show severe cardiomyopathy and premature death, H3S28 phosphorylation increased significantly. Conversely, by using the PP-inhibitors okadaic acid and PP-1-inhibitor-1 we show that PP-1 but not PP-2A antagonizes both PKA and CaMKII mediated H3S28 phosphorylation.

**Conclusion:** We show selective hyper-phosphorylation of H3S28 after pathological  $\beta$ -adrenergic stimulation with dual signaling pathways mediated by PKA in short-term and by CaMKII in long-term. It appears likely that chronic increases in sympathetic tone, as occur in HF, activate predominantly CaMKII to stimulate H3S28 phosphorylation, which is insufficiently antagonized by PP-1. Whether and how this alteration induces a CaMKII specific pathological gene program is currently under investigation. Identifying the functional significance of specific epigenetic marks may represent a promising future therapeutic tool.

### 325

#### Tissue distribution of DNA adducts of furfuryl alcohol in different mouse models: Impact of sulfotransferase status, sex, dose and DNA repair

**Sachse, Benjamin**<sup>1</sup>; Meinel, Walter<sup>2</sup>; Glatt, Hansruedi<sup>2</sup>; Monien, Bernhard<sup>1</sup>

<sup>1</sup>German Institute of Human Nutrition (DIfE), Genotoxic Food Contaminants, Nuthetal, Germany

<sup>2</sup>German Institute of Human Nutrition (DIfE), Nutritional Toxicology, Nuthetal, Germany

Furfuryl alcohol (FFA), a furan derivative, occurs in many heat-processed foodstuffs as it is formed via thermal dehydration of pentoses. It is also a precursor for the production of furan resins. Therefore, inhalation is besides oral intake a second route of exposure for industry workers. FFA induced renal tubule neoplasms in male B6C3F1 mice and nasal neoplasms in male F344/N rats in a 2-year inhalational study of the National Toxicology Program and was classified as a moderately potent rodent carcinogen. However, results of standard mutagenicity tests were at best weakly positive. We showed that FFA was mutagenic in *Salmonella typhimurium* TA100 expressing human (h) sulfotransferase (SULT)1A1 but not in the SULT-deficient parental strain. Furthermore, 2-methylfuran adducts,  $N^2$ -((furan-2-yl)methyl)-2'-deoxyguanosine ( $N^2$ -MF-dG) and  $N^2$ -((furan-2-yl)methyl)-2'-deoxyadenosine ( $N^2$ -MF-dA), were formed as a specific consequence for the exposure of FFA and have been detected in DNA samples from TA100-hSULT1A1 and from liver, kidney and lung of FVB/N-mice taking up furfuryl alcohol with the drinking water over 28 days. However, the impact of SULTs on the adduct formation *in vivo* remained unclear. We conducted an animal experiment using four mouse lines with varying human and murine (m) SULT status (wild-type, ko mSult1a1, ko mSult1d1 and hSULT1A1/1A2 x ko mSult1a1 x ko mSult1d1). DNA adduct formation was examined using UPLC-ESI-MS/MS operating in the multiple reaction monitoring mode. The main DNA adduct of FFA,  $N^2$ -MF-dG, was detected in all investigated tissues (liver, kidney, lung, colon and small intestine) of male and female wild-type mice. Highest adduct levels were observed in the liver. The other tissues showed approximately 3- to 8-fold lower levels. In all four mouse lines adduct formation was higher in female mice than in male mice. The absence of mSult1d1 did not affect DNA adduct formation in most tissues. Instead, knock out of mSult1a1 caused a decrease of  $N^2$ -MF-dG in all investigated tissues except the small intestine. Mice expressing hSULT1A1/1A2 but lacking the two murine Sult forms had higher adduct levels in liver, kidney, lung and small intestine compared to wild-type mice. Altogether, it was demonstrated that sulfo conjugation,



particularly mediated by hSULT1A1/1A2 and mSult1a1, plays an important role in the bioactivation of FFA to a genotoxic agent *in vivo*.

## 326

### Leukotriene B<sub>4</sub>/BLT1 act as gatekeeper of neutrophil recruitment into the skin in autoantibody-induced skin inflammation

Sezin, Tanya; Ludwig, Ralf; Zillikens, Detlef; Sadik, Christian

UKSH, Klinik für Dermatologie, Lübeck, Germany

Recruitment of neutrophils into the skin is a hallmark of skin inflammation, but the molecular mechanisms mediating early neutrophil recruitment into the skin are still poorly understood.

We set out to elucidate the mechanisms of early neutrophil recruitment into the skin in organ-specific, autoantibody-induced skin inflammation (EBA) in the mouse. Inflammation in this model is driven predominantly by neutrophils infiltrating the dermis.

We found that in this model early neutrophil recruitment into the skin absolutely depends on the lipid mediator leukotriene B<sub>4</sub> (LTB<sub>4</sub>) and its receptor BLT1. Thus, deficiency in 5-lipoxygenase, a key enzyme in the biosynthesis of leukotrienes, or in BLT1, the high-affinity receptor for LTB<sub>4</sub>, conferred dramatic resistance to disease.

While wild-type mice developed severe clinical signs of EBA, including skin blistering, erythema, erosions, and crusts all over their body, and histopathologically displayed massive dermal infiltration predominantly with neutrophils, 5-lipoxygenase- (*Alox5*<sup>-/-</sup>) and BLT1-deficient (*Ltb4r1*<sup>-/-</sup>) mice did not develop signs of disease, neither clinically, nor histopathologically. Although anti-Col7 antibodies expectedly bound to basal membrane in these knockout mice, the skin, remarkably, remained devoid of neutrophils, suggesting a severe defect in the recruitment of neutrophils into the skin in *Alox5*<sup>-/-</sup> and *Ltb4r1*<sup>-/-</sup> mice.

Intradermal injection of exogenous LTB<sub>4</sub> into *Alox5*<sup>-/-</sup> mice restored disease, indicating that LTB<sub>4</sub> is the only leukotriene essential for autoantibody-induced skin inflammation. Similarly, adoptive transfer of either wild-type or *Ltb4r1*<sup>-/-</sup> neutrophils into the dermis of *Ltb4r1*<sup>-/-</sup> mice restored disease, albeit the latter did so to a lesser extent. These findings suggest that LTB<sub>4</sub> is required to recruit neutrophils into the skin, but that LTB<sub>4</sub> is dispensable for the activation of neutrophils within the skin.

We also examined the role of LTB<sub>4</sub>/BLT1 in imiquimod-induced psoriasis-like dermatitis, another model of sterile skin inflammation. In this model, skin inflammation is induced by epicutaneous application of imiquimod, a TLR7/8 agonist. In contrast to autoantibody-induced skin inflammation, deficiency in 5-lipoxygenase or BLT1 did not significantly modulate the course of TLR7/8 activation triggered skin inflammation, revealing that dependency of skin inflammation on LTB<sub>4</sub>/BLT1 is apparently stimulus-specific.

Altogether, our results hint at a role of LTB<sub>4</sub>/BLT1 as critical gatekeeper of neutrophil egress into the skin in organ-specific, autoantibody-induced inflammation. LTB<sub>4</sub>/BLT1 are hence promising pharmacological targets for the treatment of autoimmune blistering skin diseases.

## 327

### Accuracy and completeness of drug information in Wikipedia: a comparison with standard textbooks of pharmacology

Kräenbring, Jona; Monzon Penza, Tika; Engelhardt, Stefan; Sarikas, Antonio

Technische Universität München, Institute of Pharmacology and Toxicology, Munich, Germany

**Background:** The online resource Wikipedia is increasingly used by undergraduate medical students for knowledge acquisition and learning (1). However, the lack of a formal editorial review and the heterogeneous expertise of contributors often results in skepticism by lecturers if Wikipedia should be recommended to students as an information source.

**Objective:** The aim of this study was to systematically analyze the accuracy and completeness of drug information in Wikipedia in comparison to standard textbooks of pharmacology.

**Methods:** Drug specific information of 100 randomly selected curricular drugs was extracted from two German standard textbooks of pharmacology (2,3). Five different categories (indication, mechanism of action, pharmacokinetics, adverse effects, contraindications) were analyzed. The data overlap of the textbooks was compared to the German version of Wikipedia (<http://de.wikipedia.org>) and accuracy and completeness of each category evaluated. Missing information in Wikipedia was re-evaluated for didactic relevance.

**Results:** The overall score of the drug information in Wikipedia was 84% (SD 15%) with regard to completeness and 99.7% (SD 2%) with regard to accuracy when compared to standard textbooks (the textbook data overlap was set to 100%). Table 1 depicts the results of Wikipedia in each category. Of drug information missing in Wikipedia, 62.5% was rated as not didactical relevant for undergraduate pharmacology teaching. The resulting corrected completeness score was 93.5% (SD 15%).

	Completeness (SD)	Accuracy (SD)
Indication	0.91 (0.19)	1.00 (0.03)
Mechanism of action	0.88 (0.21)	1.00 (0.03)
Pharmacokinetics	0.68 (0.38)	1.00 (0.03)
Adverse effects	0.84 (0.27)	1.00 (0.04)
Contraindications	0.68 (0.40)	1.00 (0.00)
<b>Overall</b>	<b>0.84 (0.15)</b>	<b>1.00 (0.02)</b>
<b>Corrected</b>	<b>0.94 (0.15)</b>	<b>1.00 (0.02)</b>

**Summary and Conclusions:** Our results suggest that Wikipedia is an accurate and informative source of drug information for undergraduate medical students, in particular if used in combination with other learning materials.

- Judd T, Kennedy G. 2010. Expediency-based practice? Medical students' reliance on Google and Wikipedia for biomedical inquiries. *Br J Educ Technol.* 42(2): 351-360.
- Aktorius K, Förstermann U, Hofmann FB, Starke K., editors. *Allgemeine und spezielle Pharmakologie und Toxikologie.* München: Urban & Fischer; 2011.
- Lüllmann H, Mohr K, Hein L., editors. *Pharmakologie und Toxikologie.* Stuttgart: Thieme; 2010.

## 328

### Proteomic investigations into mechanisms of hepatocellular toxicity induced by 3-MCPD and its dipalmitate in rat liver

Sawada, Stefanie; Oberemm, Axel; Meckert, Christine; Potkura, Jana; Rozycki, Christel; Lampen, Alfonso

Bundesinstitut für Risikobewertung, Lebensmittelsicherheit, Berlin, Germany

Thermal treatment of fat-containing foodstuff in the presence of salt leads to formation of 3-monochloropropane-1,2-diol (3-MCPD) and its fatty acid esters. Upon hydrolytic cleavage, these substances are metabolized to 3-MCPD. Results from rat carcinogenicity studies indicate a carcinogenic potential of 3-MCPD. Similar, but reduced effects were observed for 3-MCPD palmitic esters in a rat 90-days feeding study. In order to obtain deeper insights into toxicity mechanisms of 3-MCPD and one of its esters, a comparative proteomic approach was initiated, which was based on a 28-days repeated-dose feeding study with male Wistar rats. Animals received equimolar doses of 3-MCPD (10 mg/kg body weight) and 3-MCPD-dipalmitate (53 mg/kg body weight). Additionally, a low dose of 13.3 mg/kg body weight of dipalmitate was applied. Liver samples were snap-frozen and analyzed using two-dimensional gel electrophoresis-mass spectrometry. Ingenuity Pathways Analysis was used for data mining. In all treatment groups several toxicologically relevant processes and pathways were enhanced, including fatty acid metabolism and oxidative stress response. Generally, effects were more pronounced in the 3-MCPD dipalmitate treatment groups. Downregulation in the expression of several isoforms of glutathione-S-transferases as well as a reduction of peroxisome proliferator-activated receptor  $\alpha$  was observed in the livers of animals treated with 3-MCPD dipalmitate only. General results indicate a similar toxicity of 3-MCPD and its dipalmitate with regard to the induction of oxidative stress. However, the esters could potentially induce specific mechanisms of liver toxicity, which may contribute to different long-term effects compared to 3-MCPD.

## 329

### Nuclear translocation of heme oxygenase during hypoxia: analysis with deletion mutants and chimeric constructs

Schäfer, Bianca; Linnenbaum, Monika; Behrends, Soenke

TU Braunschweig, Institut für Pharmakologie, Toxikologie und Klinische Pharmazie, Germany

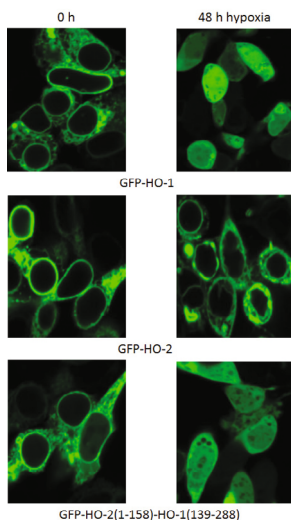
Heme oxygenase (HO) degrades heme to biliverdin, iron and carbon monoxide. There are two relevant isoforms, inducible HO-1 (33 kDa) and constitutive HO-2 (36 kDa). Both contain short carboxy-terminal hydrophobic sequences that act as anchors to the endoplasmic reticulum (ER). Under hypoxia, the hydrophobic anchor of HO-1 is cleaved by an as yet unknown protease leading to translocation to the cytosol and the nucleus. Under the same conditions HO-2 remains at the outer ER-membrane[1]. Nuclear HO-1 is thought to play a role in resistance to effective treatment of chronic myeloid leukemia with the tyrosine kinase inhibitor imatinib[2]. The goal of the current study was to localize the sequence in HO-1 which is important for nuclear translocation.

Overexpression of amino-terminal fusions of HO-1 with GFP (GFP-HO-1) in HEK293 cells and subsequent analysis by confocal laser scanning microscopy showed localization at the ER and translocation to the cytosol and nucleus in response to hypoxia (48 h, 1 % O<sub>2</sub>). Deletion of the carboxy-terminal anchor (GFP-HO-1-ΔC266) led to nuclear and cytosolic localization under both conditions[1]. Amino-terminal deletion mutants GFP-AN181-HO-1 and GFP-AN262-HO-1 showed the expected ER localization, but led to inconsistent results after exposure to hypoxia. We concluded that the extensive deletions may change the overall protein fold of HO that seems to be necessary for the translocation process. As a consequence we tested chimeras between HO-1, which translocates in response to hypoxia, and HO-2, which is resistant to translocation. The first characterized chimera GFP-HO-2(1-158)-HO-1(139-288) localized to the ER and translocated like the GFP-HO-1 control. This indicates that the determinants for translocation lie within amino acids 139-288 of HO-1. The following sequence motifs with potential relevance for translocation of HO-1 are present in this region: a leucine-rich region or nuclear export sequence (position 207-221), a PEST-domain or calpain recognition site[3] (position 239-254).

[1] Linnenbaum et al. 2012, Heme Oxygenase Isoforms Differ in Their Subcellular Trafficking during Hypoxia and Are Differentially Modulated by Cytochrome P450 Reductase

[2] Tibullo et al. 2013, Nuclear Translocation of Heme Oxygenase-1 Confers Resistance to Imatinib in Chronic Myeloid Leukemia Cells

[3] Lin et al. 2007, Heme Oxygenase-1 Protein Localizes to the Nucleus and Activates Transcription Factors Important in Oxidative Stress



#### Translocation of HOs :

In response to hypoxia GFP-HO-1 and the chimera GFP-HO-2(1-158)-HO-1(139-288) translocate from the ER to the cytosol and the nucleus, whereas GFP-HO-2 stays at the ER-membrane under both conditions.

### 330

#### Identification of protein partners interacting with the transporter MRP4/ABCC4 in platelets

**Schaletzki, Yvonne**; Bröderdorf, Susanne; Kromrey, Marie-Luise; Kroemer, Heyo K.; Jedlitschky, Gabriele

University Medicine, Depart. of Pharmacology, Greifswald, Germany

**Background:** The multidrug resistance protein 4 (MRP4/ABCC4) mediates the cellular export of several drugs as well as endogenous signaling molecules. MRP4 is expressed in several tissues as well as in blood cells including platelets. Here it may be involved in the storage and release of mediators including ADP.<sup>1</sup> The subcellular localization of MRP4 is dependent on the cell type. In polarized cells MRP4 may localize either to apical or basolateral plasma membranes or to intracellular storage compartments as the delta-granules of platelets.<sup>1</sup> In patients with delta-storage pool deficiencies, which lead to impaired function of platelets, a disturbance of the correct localization of MRP4 was observed.<sup>2</sup> It has been recognized that protein-protein interactions are important for transporter localization and their function. We therefore investigated protein interactions of MRP4 especially in platelets.

**Methods and results:** We screened for possible adaptor proteins binding to the C-terminus of MRP4 containing a PDZ interaction motif in platelets. The approach included a pull-down system with a glutathione S-transferase/MRP4 fusion protein and with a synthetic peptide consisting of the C-terminal MRP4 sequence coupled to a sepharose matrix. In addition, co-staining of MRP4 with possible interacting proteins in immunofluorescence microscopy as well as coimmunoprecipitation studies were performed. Candidates identified as possible interaction partners of MRP4 in platelets comprises a heat shock protein and several PDZ domain-containing adaptor proteins, including NHERF-1/EBP50 and proteins which were so far mainly described in neurons. To investigate the role of these proteins for the localization of MRP4 we performed siRNA knock-down experiments for the identified protein partners.

**Conclusions:** MRP4 interacts with several proteins mainly via its C-terminal PDZ domain. These interactions may be fundamental for the correct localization and function of MRP4.

<sup>1</sup>Jedlitschky, G, et al., (2012), Blood, 119:3394

<sup>2</sup>Jedlitschky, G, et al., (2010), Am. J. Pathol., 176: 1097

### 331

#### Sphingosine-1-phosphate inhibits the cytokine production of IL-12 and IL-23 in activated dendritic cells

**Schaper, Katrin**<sup>1</sup>; Kietzmann, Manfred<sup>1</sup>; Bäumer, Wolfgang<sup>2</sup>

<sup>1</sup>Stiftung Tierärztliche Hochschule Hannover, Institut für Pharmakologie, Toxikologie und Pharmazie, Germany

<sup>2</sup>NCSU College of Veterinary Medicine, MBS Department, Raleigh, United States

Sphingosine-1-phosphate (S1P) is involved in the modulation of many cell functions such as lymphocyte trafficking and signaling as well as keratinocyte proliferation, whereby S1P acts via 5 G-protein coupled receptors. Less is known about the effects of S1P on cytokine production, particularly on the interaction between dendritic cells (DCs) and keratinocytes, both cell types which are crucial for the initiation and maintenance of chronic inflammatory skin diseases like atopic dermatitis or psoriasis. Particularly cytokines of the IL-12 family play a dominant role in many inflammatory diseases as they have a significant impact on T-helper cell function. In the present study we show that S1P decreased the production of the pro-inflammatory cytokines IL-12 and IL-23 in LPS-stimulated bone marrow derived DCs as well as in the crosstalk with activated keratinocytes in a dose dependent manner. Thereby we identified an important role for the common subunit p40. By using specific S1P receptor agonists and antagonist we

showed that S1P modulates the cytokine profile mainly via S1P receptor 1. While decreasing IL-12 and IL-23 secretion, S1P partially enhanced IL-27 production in DCs. To elucidate the mechanism of the different mode of action on the IL-12 family cytokine production, we investigated the mitogen-activated protein kinase (MAPK) and phosphatidylinositol 3-kinase (PI3K) pathways. By using specific MAPK-inhibitors we showed that extracellular signal-regulated kinase (ERK), p38 and c-Jun N-terminal kinase (JNK) differently regulate each pathway of each cytokine. In summary, these data implicate, that S1P has an anti-inflammatory impact on the production of IL-12 family cytokines, indicating therapeutic potential for S1P treatment of several inflammatory diseases like psoriasis and atopic dermatitis.

Figure 1

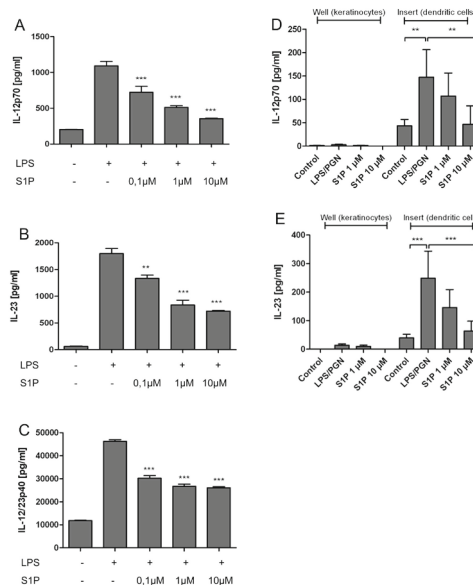


Figure 1: The impact of Sphingosine-1-phosphate on cytokine production of dendritic cells

### 332

#### Glucosylation of Ras-GTPases catalyzed by *Clostridium difficile* Toxin A

**Schelle, Ilona**<sup>1</sup>; Lücke, Arlen-Celina<sup>1</sup>; Popoff, Michel<sup>2</sup>; Just, Ingo<sup>1</sup>; Genth, Harald<sup>1</sup>

<sup>1</sup>Hannover Medical School, Toxicology, Germany

<sup>2</sup>Institut Pasteur, Unité des Bactéries anaérobies et Toxines, Paris, France

Toxin A (TcdA) and Toxin B (TcdB) from *Clostridium difficile* are the major pathogenicity factor of *C. difficile*-associated diarrhoea (CDAD) and its severe form the pseudomembranous colitis (PMC). Treatment of cultured cell lines with TcdA or TcdB results in actin depolymerization and a loss of cell-cell-interaction and cell-matrix adhesion, resulting in cell rounding ("cytopathic effects"). TcdA and TcdB-further induced cytotoxicity, including inhibited cell cycle progression and cell death ("cytotoxic effect"). TcdA and TcdB enter their mammalian target cells by receptor-mediated endocytosis and escape from the early endosome. Subsequently, the N-terminally located glucosyltransferase domain is auto-proteolytically cleaved off and released into the cytosol. TcdA and TcdB are regarded as acceptor-selective glucosyltransferase, which mono-O-glucosylate and thereby inactivate small GTPases.

Within the last years, several glucosylation-sensitive antibodies have been identified allowing the detection of glucosylated small GTPases in toxin-treated cells, including Rac1(Mab102) and Ras(Mab27H5), in terms the loss of immunoblot detection of the respective GTPases. In this study, these antibodies are exploited to analyze the glucosylation of Rac and Ras in African green monkey epithelial (Vero) cells. Rac and Ras are shown to be time- and concentration-dependently glucosylated in TcdA-treated Vero cells. Thereby, Rac is more efficaciously glucosylated than Ras. In contrast, TcdB selectively glucosylates Rac but not Ras. Ras from TcdA-treated cells is further shown to inactive, as analyzed in terms of missing precipitation of cellular Ras to the Ras binding domain of the Ras effector Raf kinase. These observations are apparently inconsistent with former observations from *in vitro* studies exploiting recombinant GTPases and purified holo-TcdA, showing that TcdA selectively glucosylates Rho but not Ras family GTPases. Re-analysis of the acceptor GTPase spectrum of TcdA *in vitro* was next performed exploiting the recombinantly prepared glucosyltransferase domain (TcdA-542). TcdA-542 preferably glucosylated RhoGTPases but also glucosylated RasGTPases to some extent. In sum, TcdA-542 exhibits a broader acceptor GTPase spectrum as holo-TcdA purified from *Clostridium difficile*. *In vitro* analysis exploiting recombinant TcdA-542, which corresponds to the auto-proteolytically cleaved domains in the cytosol of target cells, more precisely predicts the acceptor GTPase spectrum of *in vivo* substrates than full-length TcdA.

333

### Effects of carryover of subtherapeutic antimicrobial dosages on the susceptibility of commensal *E. coli*

Scherz, Gesine<sup>1</sup>; Stahl, Jessica<sup>1</sup>; Glünder, Gerhard<sup>2</sup>; Kietzmann, Manfred<sup>1</sup>

<sup>1</sup>Stiftung Tierärztliche Hochschule Hannover, Institut für Pharmakologie, Toxikologie und Pharmazie, Germany

<sup>2</sup>Stiftung Tierärztliche Hochschule Hannover, Klinik für Geflügel, Germany

Several studies demonstrate that an antibiotic treatment of livestock can cause the accumulation of antibiotics and their metabolites in the direct environment of animals. This can lead to a resumption of the antimicrobials and their metabolites. Thus, the aim of this study was to determine the influence of carryover of enrofloxacin as a representative of the fluoroquinolones on the development of bacterial resistance of *E. coli* in the intestinal flora of poultry. Enrofloxacin becomes metabolized to the active metabolite ciprofloxacin, which is used as a broad spectrum antibiotic in human medicine.

To measure the effects of carryover of enrofloxacin on the commensal intestinal flora of poultry minimal inhibitory concentrations (MIC) of *E. coli* were determined in four different treatment groups of enrofloxacin applied via drinking water (n = 6 chickens):

Group A acted as untreated control, B received the recommended dosage (10 mg/kg) for five days, the groups C and D were treated with subtherapeutic dosages to simulate a carry-over situation scenario (C: 0.3 mg/kg, D: 1.0 mg/kg) via 21 days followed by the recommended dosage over five days. Additionally, the distribution of enrofloxacin and its metabolite ciprofloxacin under the recommended treatment of the animals were measured by analyzing sedimented dust and air filters. Both compounds could be detected in the analyzed elements.

To evaluate the development of antibacterial resistance the epidemiological cut-off ( $\leq 0.125 \mu\text{g/mL}$ ) and the clinical breakpoint ( $\geq 2.0 \mu\text{g/mL}$ ) were used.

Chicken treated with the recommended dosage (B) developed low-level-resistances with MIC-values between the epidemiological cut-off and the clinical breakpoint. These isolates are categorized as non-wildtypes.

Group C, which received the subtherapeutic dosages of 0.3 mg/kg conducted similarly, after the successional recommended treatment, low-level resistances remained.

Under the treatment with 1.0 mg/kg enrofloxacin (D) low-level- and high-level or rather clinical resistances (MIC-values  $\geq 32 \mu\text{g/mL}$ ) developed. The latter ones were preselected by the following therapeutic treatment and have been detectable even after a waiting period of 20 weeks.

In conclusion, during animal treatment antibiotic contaminations occur in the direct environment. In this study each exposition of the commensal *E. coli* to enrofloxacin caused at least *E. coli*-isolates, which can be categorized as non-wildtypes. The uptake of carryover-dosages of 1.0 mg/kg generated clinical resistances. It has to be investigated whether carryover level of that size occur in commercial fattening farms.

334

### Genetic ablation of Cullin-RING ubiquitin ligase 7 results in cardiomyocyte hypertrophy and increased fractional shortening

Scheufele, Florian<sup>1,2</sup>; Engelhardt, Stefan<sup>1,2</sup>; Sarikas, Antonio<sup>1,2</sup>

<sup>1</sup>Technische Universität München, Institute of Pharmacology and Toxicology, Munich, Germany

<sup>2</sup>DZHK (German Center for Cardiovascular Research), partner site Munich Heart Alliance, Germany

**Introduction:** The Ubiquitin-Proteasome System (UPS) is a selective protein degradation pathway that is critically involved in the pathogenesis of several cardiac disorders (Schlossarek and Carrier, 2011). The Cullin-RING ubiquitin ligase 7 (CRL7) consists of the Cullin 7 (CUL7) scaffold protein, the SKP1 adaptor, the ROC1 RING finger protein and the substrate receptor FBXW8. We previously identified insulin receptor substrate 1 (IRS-1), a critical mediator of PI3K/Akt and Erk MAPK signaling as CRL7 substrate (Xu et al., 2008).

**Objective:** To investigate the pathophysiological role of CRL7 in the heart and its contribution to cardiac hypertrophy.

**Methods:** Tamoxifen-inducible cardiomyocyte (CM)-specific Cul7 knockout mice were generated by crossing Cul7<sup>lox/lox</sup> and Myh6-Mer-Cre-Mer<sup>Tg(1/0)</sup> mice. Knockdown of CUL7 upon Tamoxifen administration was validated by immunoblot and qPCR analyses. Cardiac function was monitored by echocardiographic measurement of fractional shortening (FS) and assessment of heart weight-to-tibia length (HW/TL) and lung weight-to-tibia length (LW/TL) ratios. CM hypertrophy was analyzed by WGA staining and quantification of CM cross sectional area (CSA) by automated microscopy. Signaling pathways were investigated by immunoblot analyses of Akt<sup>P-Ser473</sup> and Erk<sup>Thr202/Tyr204</sup>.

**Results:** CUL7 knockdown in isolated CM of Cul7<sup>lox/lox</sup>, Myh6-Mer-Cre-Mer<sup>Tg(1/0)</sup> (designated Cul7<sup>-/-</sup> mice) upon Tamoxifen application was approx. 90% when compared to Cul7<sup>+/+</sup>; Myh6-Mer-Cre-Mer<sup>Tg(1/0)</sup> (designated Cul7 wild-type mice) animals (n=4; p<0.05). We observed a significant increase of FS in Cul7<sup>-/-</sup> mice 6 weeks upon Cul7 ablation when compared to Cul7 wild-type animals (26.3 % vs. 20.3 %; n=8-9; p<0.05). In addition, CSA was markedly increased in left ventricular CMs of Cul7<sup>-/-</sup> mice (610  $\mu\text{m}^2$  vs. 483  $\mu\text{m}^2$ ; n=7; p<0.05). No significant changes in HW/TL (9.6 mg/mm vs. 9.6 mg/mm; n=7) or LW/TL (8.9 mg/mm vs. 8.8 mg/mm; n=7) were observed in Cul7<sup>-/-</sup> mice when compared to wild-type controls. Immunoblot analysis of isolated CM revealed a 50% increase in Akt activation (as evidenced by Akt S473 phosphorylation) in Cul7<sup>-/-</sup> mice when compared to Cul7 wild-type animals (n=7, p<0.05), while P-Erk remained unchanged.

**Summary and Conclusion:** Genetic ablation of Cul7 in cardiomyocytes resulted in improved cardiac function, increased CM hypertrophy and was associated with hyperactivation of the PI3K / AKT signaling pathway. It is tempting to speculate that CRL7 may constitute a novel regulator of cardiac hypertrophy via modulation of the PI3K / AKT signaling pathway in the heart.

335

### Histamine H<sub>4</sub> receptor antagonist JNJ777120 ameliorates DSS-induced colitis in BALB/c mice

Schirmer, Bastian<sup>1</sup>; Isaev, Rukijat; Rezniczek, Thomas; Seifert, Roland; Neumann, Detlef

Hannover Medical School, Institute of Pharmacology, Germany

#### Background

Inflammatory bowel disease (IBD) is an idiopathic, chronic-recurring disease of the gut severely affecting the quality of patients' live and possibly limiting their life expectancy. Since there is currently no effective and specific therapeutic target in the treatment of IBD, it is of extraordinary economical and scientific interest to discover new specifically acting agents. Blockade of histamine H<sub>4</sub> receptor (H<sub>4</sub>R) has been shown to ameliorate several inflammatory diseases (e.g. asthma in mice, colitis in rats). Thus, selective H<sub>4</sub>R antagonist JNJ777120 is a promising agent for elucidating the role H<sub>4</sub>R plays in IBD. To address the question if JNJ777120 is capable of modifying this severe chronic disease the pharmacon can be used in a well established murine IBD model in which oral administration of dextrane sodium sulfate (DSS) leads to damage of intestinal epithelium and consequent bowel inflammation.

#### Materials / methods

In consideration of the biological half-life of JNJ777120 (two hours) we used osmotic pumps for continuous subcutaneous delivery of the agent (360 nmol/day) for a one-week period. Mice were watered with either pure or DSS-charged water and were treated with JNJ777120 or the solvent alone (50 % DMSO/PBS) as control. Body weight and disease score were measured daily. On day eight after first DSS application we euthanized the animals, collected the sera and performed histological, immunohistochemical and cellular analyses of the colons.

#### Results

H<sub>4</sub>R blockade results in reduced weight loss, lower histological disease score and a reduction of mouse mast cell protease (mMCP)-6 concentrations in tissue slices and tissue lysates of DSS-treated animals compared to control animals without H<sub>4</sub>R blockade.

#### Discussion

Because there is currently no specific therapeutic option for IBD the salutary effect of JNJ777120 in the murine DSS-induced colitis is very intriguing. In further studies we want to confirm our current findings and to address the role the H<sub>4</sub>R plays on different cell types and how it can be linked to a better pathophysiological understanding of IBD. Last not least H<sub>4</sub>R blockade as an alternative to the unspecific and/or expensive immunosuppressive treatment would be of high economic interest.

336

### The effector protein ExoY secreted by *Pseudomonas aeruginosa* augments the inflammatory reaction in the respiratory tract of mice

Hartwig, Christina<sup>1</sup>; Schirmer, Bastian<sup>1</sup>; Stelzer, Tane<sup>1</sup>; Munder, Antje<sup>2</sup>; Tümmler, Burkhard<sup>2</sup>; Seifert, Roland<sup>1</sup>

<sup>1</sup>Hannover Medical School, Institute of Pharmacology, Germany

<sup>2</sup>Hannover Medical School, Department of Pediatrics, Clinical Research Group "Pseudomonas genomics", Germany

*P. aeruginosa* is an important opportunistic pathogen. Infection with the gram-negative bacterium causes serious pulmonary, urogenital and systemic inflammation in immunodeficient patients. Most prominently, *P. aeruginosa* is the key organism responsible for pneumonia in cystic fibrosis patients, defining the course of the disease as well as its prognosis<sup>1</sup>. *P. aeruginosa* produces a wide variety of effector proteins and injects them into host cells via the type III secretion system<sup>2</sup>. One of the effectors, injected by this needle-like structure is ExoY, which can be found in 90% of clinical isolates from *P. aeruginosa*. Despite of the highly frequent ExoY occurrence, its function is still unknown. The identification and understanding of the bacterial mechanism to damage infected cells or suppress an adequate immune reaction are fundamental for the development of new therapeutic strategies. While previous publications described ExoY to be apathogenic, our recent *in vivo* studies demonstrated a distinct role of ExoY as a pathogenic factor of *P. aeruginosa*.

Our murine infection model allows the interpretation of a broad spectrum of parameters. Shortly, B6 mice were infected with *P. aeruginosa*, either with a strain expressing functional ExoY (ExoY) or a catalytically inactive ExoY mutant (K81M)<sup>3</sup> by intratracheal instillation with  $1 \times 10^{10}$  colony forming units (cfu) or PBS in the control group. Mice were sacrificed at different time points (0-48 h) after infection and bacterial infection was characterized by analyzing the migration of neutrophils into the lung and production of inflammatory cytokines in the respiratory tract using multiplex measurements.

Infection doses of  $10^8$  cfu/mouse lead to ExoY-dependent, severe pathological changes in lung tissue and to increased mortality. Even more distinct effects were seen at concentrations of  $10^5$  cfu/mouse. Within 4 to 8 hours after infection animals started to develop severe signs of infection and lung inflammation. Progressively, animals became lethargic and even succumbed to death after 24 - 48 hours. Inflammatory lung reaction was characterized by interstitial edema, hemorrhagic infiltration and formation of necrotic/apoptotic areas in the tissue. This could be caused by a significantly increased secretion of proinflammatory factors such as IL-6, IL-1, MCP-1 and KC in the ExoY infected group.

In conclusion, ExoY is - in contrast to previously held opinions - a pathogenic factor of *P. aeruginosa* and hence, a new drug target.

1.) Hurley MN, Camara M, Smyth AR. Novel approaches to the treatment of *Pseudomonas aeruginosa* infections in cystic fibrosis. Eur Respir J 2012 40: 1014-1023.

2.) Hauser AR. The type III secretion system of *Pseudomonas aeruginosa*: infection by injection. Nat Rev Microbiol 2009 7: 654-665

3.) Yahr TL, Vallis AJ, Hancock MK, Barbieri JT and Frank DW. *ExoY, an adenylate cyclase secreted by the Pseudomonas aeruginosa type III system*. Proc. Natl. Acad. Sci. 1998. 95:13899-13904

### 337

#### The combination of tiotropium and olodaterol is highly effective to inhibit carbachol-induced bronchoconstriction in human precision-cut lung slices

Schleppütz, Marco<sup>1</sup>; Maihöfer, Nina<sup>1</sup>; Rieg, Annette Dorothea<sup>1</sup>; Westphal, Saskia<sup>2</sup>; Perez-Bouza, Alberto<sup>3</sup>; Braunschweig, Till<sup>4</sup>; Schröder, Thomas<sup>4</sup>; Spillner, Jan<sup>5</sup>; Autschbach, Rüdiger<sup>5</sup>; Pieper, Michael Paul<sup>6</sup>; Uhlig, Stefan<sup>1</sup>; Martin, Christian<sup>1</sup>

<sup>1</sup>Uniklinik RWTH Aachen, Institute of Pharmacology and Toxicology, Germany

<sup>2</sup>Uniklinik RWTH Aachen, Institute of Pathology, Germany

<sup>3</sup>UKB Universitätsklinikum Bonn, Institute of Pathology, Germany

<sup>4</sup>Luisenhospital Aachen, Department of Surgery, Germany

<sup>5</sup>Uniklinik RWTH Aachen, Department of Cardiothoracic and Vascular Surgery, Germany

<sup>6</sup>Boehringer Ingelheim Pharma GmbH & Co. KG, Div. Research Germany, Biberach an der Riß, Germany

**Rationale:** In COPD patients, pharmacological monotherapy is often not sufficient to improve health status and the frequency of exacerbations. Therefore combination therapies with long acting bronchodilators and inhaled corticosteroids are recommended. Precision-cut lung slices (PCLS) are well suited to study the impact of drugs on bronchoconstriction (BC) *in vitro*. Thus, the aim of the present study was to evaluate the combination of tiotropium and the novel long acting  $\beta$ -agonist olodaterol on BC in human PCLS.

**Methods:** Human lung lobes were received from cancer patients undergoing lobectomy. After pathological inspection, lobes were filled with agarose and PCLS were prepared from tumor free tissue. BC in PCLS was followed by videomicroscopy. In the first set, concentration-response curves with carbachol ( $10^{-8}$  –  $10^{-3}$  M) were performed in the presence and absence of tiotropium ( $10^{-11}$  –  $10^{-8}$  M) or olodaterol ( $10^{-10}$  –  $10^{-8}$  M). In the second set, to test the combined effect of tiotropium and olodaterol, concentration-response curves with carbachol were conducted at tiotropium ( $10^{-9.5}$  M) or olodaterol ( $10^{-9}$  M) alone, their combination or without any antagonist.

**Results:** Tiotropium inhibited carbachol-induced BC in PCLS concentration-dependently and  $10^{-9.5}$  M tiotropium was determined as a suitable inhibitory concentration for the combination study. Olodaterol also inhibited BC in PCLS, and  $10^{-9}$  M olodaterol were considered appropriate as inhibitory concentration for the combination study. In the final combination study the logEC<sub>50</sub>-values for carbachol-induced BC were determined to -6.0±0.2 under control conditions, -5.6±0.1 for  $10^{-9.5}$  M tiotropium, -5.4±0.2 for  $10^{-9}$  M olodaterol and -4.2±0.2 for the combination of tiotropium and olodaterol.

**Conclusion:** *In vitro* the combination of tiotropium ( $10^{-9.5}$  M) and olodaterol ( $10^{-9}$  M) inhibited carbachol-induced BC more effectively than each bronchodilator alone. As the study was performed on human lung tissue, correlation to the *in vivo* situation is likely. Therefore, the combination of tiotropium and olodaterol is conceivable beneficial in the treatment of human patients.

### 338

#### Determination of Sulfamethoxazole, Azithromycin and Ketoconazole in serum, urine and waste water – method validation and comparison of matrices

Schlobach da Costa, Caroline

Institut für Klinische Pharmakologie TU Dresden, Germany

**Abstract for the conference: "80. DGPT Jahrestagung 2014"**

Poster presentation

**Abstract title:** Determination of sulfamethoxazole, azithromycin and ketoconazole in serum, urine and waste water – method validation and comparison of matrices

**Authors:** Caroline Schlobach da Costa<sup>1</sup>, Dipl. Chem. Robert Gurke<sup>1</sup>, Dipl.-Ing. Chem. Julia Rossmann<sup>1</sup>, Prof. Dr. med. Dr. med. dent. Wilhelm Kirch<sup>1</sup>, Dr. rer. nat. Reinhard Oertel<sup>1</sup>

**Affiliations:**

<sup>1</sup>Institute of Clinical Pharmacology, Faculty of Medicine Carl Gustav Carus, Technische Universität Dresden, Germany

**Keywords:** antibiotics, waste water, urine, serum, SPE, LC-MS/MS, validation

**Abstract:**

In a previous research project on risk management in water sixteen antibiotics and three antifungals were determined in different sewage samples. Three of these drugs should be examined more detailed. The aim is a comparison of the matrices: human serum, urine and waste water, in order to find a good method to detect the two antibiotics sulfamethoxazole and azithromycin and moreover the antimycotic ketoconazole. This study contains the optimization and validation of a method that determines three pharmaceuticals simultaneously using solid phase extraction (SPE) and liquid chromatography-triple quadrupole tandem mass spectrometry (LC-MS/MS). The analytes were separated using a gradient separation and a reversed phase C<sub>18</sub> column. For quantitation and calibration an internal standard of trimethoprim D9, voriconazole and sulfamethoxazole C13 was used. The validation of the method and a final runtime of 7 minutes made it possible to advance the determination and to analyze a huge number of volume limited samples in a day. The recoveries, matrix effects, method variability, detection limit and limit of quantification, the precision (relative standard deviation R.S.D.) and accuracy were determined and compared.

Barrett, B., Borek-Dohalský, V., Fejt, P., Vaingátová, S., Huclová, J., Nemeč, B., & Jelínek, I. (2005). Validated HPLC-MS-MS method for determination of azithromycin in human plasma. *Analytical and bioanalytical chemistry*, 383(2), 210–7. doi:10.1007/s00216-005-0018-5

Feng, J., Wang, L., Dai, I., Harmon, T., & Bernert, J. T. (2007). Simultaneous determination of multiple drugs of abuse and relevant metabolites in urine by LC-MS-MS. *Journal of analytical toxicology*, 31(7), 359–68. Retrieved from http://www.ncbi.nlm.nih.gov/pubmed/17725883

Gros, M., Petrović, M., & Barceló, D. (2006). Development of a multi-residue analytical methodology based on liquid chromatography-tandem mass spectrometry (LC-MS/MS) for screening and trace level determination of pharmaceuticals in surface and wastewaters. *Talanta*, 70(4), 678–90. doi:10.1016/j.talanta.2006.05.024

### 339

#### MicroRNA-106b: Potential noncoding RNA associated with anti-proliferative activity of butyrate

Schlörmann, Wiebke; Renner, Caroline; Naumann, Stefanie; Gleis, Michael

Institut für Ernährungswissenschaften, Lehrstuhl für Ernährungstoxikologie, Jena, Germany

Colorectal cancer is one of the most common cancers worldwide. A hallmark of cancer is a dysregulated cell-cycle and enhanced cell proliferation. The expression of cell cycle regulators can be influenced by miRNAs, whereas their activity can be regulated by histone deacetylase (HDAC) inhibitors. Butyrate, which is produced during bacterial fermentation of fiber in the colon, is a potent HDAC inhibitor, which is able to suppress the growth of colon cancer cells.

The aim of this study was to investigate whether the anti-proliferative effects of butyrate are mediated by miRNAs.

Therefore, HT29 colon adenocarcinoma cells were incubated with 2, 4 and 10 mM butyrate and Trichostatin A (TSA, 3.3  $\mu$ M) as positive control. The expression of miRNA-106b and the mRNA and protein expression of the cell cycle regulator p21 as one of the targets were measured after 24 and 48 h using RT-qPCR and Western-Blot. The effect of butyrate on HT29 cell growth was determined after 24 and 48 h via DAPI assay. The same experiments were carried out in miRNA-106b mimic transfected HT29 cells.

Butyrate and TSA significantly reduced miRNA-106b expression in HT29 cells (~0.5-fold). miRNA-106b mimic transfected HT29 cells showed elevated levels of miRNA-106b expression, which could not be reduced upon butyrate or TSA incubation. Butyrate and TSA significantly increased mRNA expression of p21 with significantly higher levels in transfected HT29 cells (14.6-fold, 4 mM, 48 h) compared to non-transfected cells (3.9-fold). Protein expression of p21 was significantly increased upon butyrate treatment in non-transfected (e.g. 43.0-fold, 10 mM, 24 h) and to a lesser extend in transfected HT29 cells (31.0-fold) in a dose dependent manner. Butyrate was able to significantly reduce HT29 cell growth (~0.5 fold) but without significant differences compared to transfected HT29 cells.

The results indicate a potential role for miRNA-106b in butyrate mediated induction of p21 mRNA and protein expression as well as HT29 cell growth inhibition.

### 340

#### Do frequently used opioids exhibit biased signaling at the $\mu$ opioid receptor?

Schmid, Benedikt<sup>1,2,3</sup>; Mayer, Stefanie<sup>2,3</sup>; Brede, Marc<sup>4</sup>; Hoffmann, Carsten<sup>2,3</sup>

<sup>1</sup>Universitätsklinik Würzburg, Interdisziplinäres Zentrum für Klinische Forschung, Germany

<sup>2</sup>Universität Würzburg, Biomedizinisches Zentrum, Rudolf-Virchow-Zentrum, Germany

<sup>3</sup>Universität Würzburg, Institut für Pharmakologie und Toxikologie, Lehrstuhl für Pharmakologie, Germany

<sup>4</sup>Universitätsklinik Würzburg, Klinik und Poliklinik für Anästhesiologie, Germany

Opioids currently represent the gold standard in the treatment of severe acute and chronic pain. Despite the opioids' huge clinical importance, little data are available regarding the downstream signaling properties of each of those substances used in countless patients every day. The desired anesthetic effect of opioid drugs is mainly ascribed to the  $\mu$  subtype of opioid receptors (OPRM). The first wave of signaling triggers the activation of an inhibitory G-protein heterotrimer. A second signal wave manifests in the phosphorylation dependent recruitment of  $\beta$ -arrestin2 to the receptor and is often followed by receptor internalization. To study the signaling properties of opioid based drugs, we assessed both ligand-induced G<sub>i</sub>-activation and subsequent  $\beta$ -arrestin2 recruitment to the receptor in living transfected HEK293 cells. We tested a total of 13 clinically relevant opioid agonists, two antagonists, two physiologically occurring metabolites, and utilized the synthetic full agonist DAMGO as reference compound. G<sub>i</sub> activation was quantitatively assessed using a previously published fluorescence resonance energy transfer (FRET) assay for which G<sub>o</sub> and G<sub>i</sub> subunits were tagged with yellow (YFP) or cyan fluorescent protein (CFP), respectively. Upon receptor activation, the G<sub>i</sub> complex undergoes conformational changes which lead to a change in the FRET ratio. Full concentration-response curves are given for all substances. This assay allowed to clearly differentiate between full and partial agonists (e.g. fentanyl, sufentanil and tramadol), or antagonists (e.g. naloxone).  $\beta$ -arrestin2 recruitment was assessed by dynamic confocal microscopy of CFP-tagged OPRM and  $\beta$ -arrestin2-YFP. Maximum  $\beta$ -arrestin2 recruitment was quantitatively determined as the percentage of YFP-tagged  $\beta$ -arrestin2 translocating to the membrane 10 min after application of saturating opioid ligand concentrations. Since the OPRM was fluorescently

tagged, we were able to measure receptor internalization subsequent to  $\beta$ -arrestin2 recruitment. We confirmed that receptor internalization for the OPRM was a dynamin-dependent process, since pre-incubating cells with 80  $\mu$ M dynasore (a specific dynamin inhibitor) strongly diminished OPRM internalization. Taken together, our data provide evidence that some clinically used opioids exhibit preference for one signaling pathway or the other. Therefore, our data hint towards biased agonism of some opioids for either G<sub>i</sub> activation or  $\beta$ -arrestin2 recruitment.

### 341

#### The Raf kinase inhibitor protein (RKIP) is mainly phosphorylated at serine 153 and bound to GRK2 under physiological conditions in the heart

**Schmid, Evelyn**<sup>1</sup>; Deiss, Katharina<sup>1</sup>; Denzinger, Sabrina<sup>1</sup>; Weidendorfer, Markus<sup>1</sup>; Schmitt, Joachim<sup>2</sup>; Lohse, Martin J.<sup>1</sup>; Lorenz, Kristina<sup>1</sup>

<sup>1</sup>Universität Würzburg, Institut für Pharmakologie, Germany

<sup>2</sup>Universitätsklinikum Düsseldorf, Institut für Pharmakologie und klinische Pharmakologie, Germany

RKIP is a modulator of several protein kinases. Via direct interaction with the kinases Raf1 or G protein-coupled receptor kinase 2 (GRK2), RKIP either attenuates pathological growth or ameliorates G protein-coupled receptors (GPCRs) signaling. PKC mediated RKIP phosphorylation at Ser153 and dimerization are modifications of RKIP that coordinate its regulatory functions.

The aim of this study was to investigate the physiological role of RKIP in cardiomyocytes and to evaluate the impact of RKIP phosphorylation at Ser153 on its cellular function.

In order to determine the basal modifications of endogenous RKIP in mouse hearts, we analyzed RKIP phosphorylation by dephosphorylation experiments in heart lysates and after application of a PKC inhibitor (GF109203x) via Langendorff perfusion of the heart. We found that cardiac RKIP is highly phosphorylated under basal conditions. Cross-linking experiments also showed that RKIP is preferentially bound to GRK2 under these conditions. In line with these findings, cardiac overexpression of wild-type RKIP (RKIP-tg) resulted in significant inhibition of GRK2. However, GRK2 activity was not affected by overexpression of the RKIP mutant that is deficient for phosphorylation at Ser153 (RKIP<sup>S153A</sup>). Evaluation of the effects of RKIP on cardiac function by measurements of left ventricular speeds of contraction and relaxation and fractional shortening revealed a positive inotropic and lusitropic phenotype of RKIP-tg, which was absent in RKIP<sup>S153A</sup> transgenic mice. The hypercontractile phenotype in combination with GRK2 inhibition strongly suggests that the increase in contractility is induced by enhanced GPCR signaling. A primary effect of wild-type RKIP on cardiomyocyte's contractile function was further substantiated by accelerated calcium transients in adult cardiomyocytes isolated from RKIP-tg mice as well as in adenovirally transduced neonatal rat cardiomyocytes. While wild-type RKIP did not affect the activation of extracellular signal-regulated kinases 1/2 (ERK1/2), phosphorylation-deficient RKIP<sup>S153A</sup> inhibited ERK1/2, which are the effector kinases of Raf1, with subsequent induction of cardiomyocyte apoptosis and attenuated growth of the heart.

Taken together, the cellular role of RKIP is strongly dependent on its phosphorylation state. Under physiological conditions in the heart, RKIP is mainly phosphorylated and, therefore, enhances cardiac contractility via binding to GRK2.

### 342

#### The mobility of mesenchymal stem cells is dramatically reduced after contact with alkylating agents

**Schmidt, Annette**; Thiermann, Horst; Steinritz, Dirk

Institut für Pharmakologie und Toxikologie der Bundeswehr, München, Germany

The chemical warfare agent sulfur mustard (SM), also known as mustard gas, was first used in World War I. Although prohibited by the OPCW, significant amounts of SM still exist and have still to be regarded as a threat for military personnel and civilians. The effect of sulfur mustard (SM) towards the direct injured tissues of the skin, eyes and airways is well investigated. Little is known on the effect of SM to mesenchymal stem cells (MSC). However, this is an interesting aspect as here wound healing is dramatically impaired and it is known today that MSC play an important role e.g. in chronic impaired wound healing. Therefore we wanted to get deeper understanding on the interaction between SM and MSC and if such findings might become useful to improve mustard gas induced wound healing. We used mesenchymal stem cells, isolated from femoral heads from healthy donors and treated them with a wide range of SM to ascertain the dose-response-curve. Using the determined inhibitory concentrations IC1 (1  $\mu$ M), IC5 (10  $\mu$ M), IC10 (20  $\mu$ M) and IC25 (40  $\mu$ M) we analyzed the migratory ability and the differentiation capacity under influence of SM. It turned out that already very low concentrations of SM showed a strong effect to the migratory activity whereas the differentiation capacity seemed not to be affected. Thus, it can be concluded that a link between MSC and the impaired wound healing after SM exposure exists. Comparable to patients with chronic impaired wound healing MSC exposed to SM have shown a reduced migratory activity. The fact that MSC are able to tolerate very high concentrations of SM and still do not lose their differentiation capacity may reveal new ways of treating wounds caused by sulfur mustard.

### 343

#### Cumulative hepatotoxic effects of (triazole fungicides at mRNA level examined *in vivo* (rat) and in HepaRG cells

**Schmidt, Flavia**<sup>1</sup>; Rieke, Svenja<sup>1</sup>; Niemann, Lars<sup>1</sup>; Pfeil, Rudolf<sup>1</sup>; Steinberg, Pablo<sup>2</sup>; Marx-Stoelling, Philip<sup>1</sup>; Heise, Tanja

<sup>1</sup>Bundesinstitut für Risikobewertung, Chemikaliensicherheit, Berlin, Germany

<sup>2</sup>Tierärztliche Hochschule, Inst. f. Lebensmitteltoxikologie und Chemische Analytik, Hannover, Germany

**Background:** Risk assessment of pesticide residues in or on food and food products is an important field of regulatory toxicology. In general, the toxicological evaluation of pesticides is based on the evaluation of single substances, although in fact consumers are exposed to multiple residues via the diet. Consequently, it has to be considered whether mixture effects could appear after exposure to human-relevant dose levels.

**Methods:** To investigate experimentally potential substance interactions and combination effects, we selected two triazole fungicides, cyproconazole and epoxiconazole, as well as the imidazole prochloraz as test compounds. Our study approach is based on gene expression analyses of liver samples from a 28-day feeding study with male Wistar rats and of a human cell line (HepaRG) by using pathway-focused PCR arrays. The aim of this study is to compare *in vivo* and *in vitro* data with regard to gene expression alterations after single and combined (triazole) exposure, in order to collect evidence for potential species differences between rats and humans. Furthermore, it should be evaluated if this liver cell model is appropriate to explore mixture effects.

**Results:** The gene expression analyses of the *in vivo* and *in vitro* samples reveals clear combination effects. In addition to alterations in gene expression of xenobiotic metabolizing enzymes we could also identify dysregulated genes that are related to various liver diseases like phospholipidosis, steatosis or cholestasis. Moreover, we observed modifications in the expression of immunotoxicity-associated genes. While the potency of all three test compounds is approximately similar in liver samples from rats, it could be observed that the imidazole prochloraz has the greatest potency in HepaRG cells.

**Conclusion:** The test systems used show that there is evidence for combination effects of the test substances within the selected dose range. In order to use these results for regulatory decision making further testing is needed.

### 344

#### A-kinase anchoring proteins contribute to loss of E-cadherin and bronchial epithelial barrier by cigarette smoke

**Schmidt, Martina**; Poppinga, Wilfred Jelco; Oldenburger, Anouk; Meurs, Herman; Maarsingh, Harm

University of Groningen, Molecular Pharmacology, Netherlands

Airway epithelium forms the first barrier towards environmental insults which is disturbed by cigarette smoking, a major risk factor for developing COPD. We aimed to unravel the underlying mechanisms in order to search for strategies to restore the barrier. A-kinase anchoring proteins (AKAP) maintain endothelial barrier function and coordinate the subcellular localization of protein kinase A. However, the role in epithelial barrier function is unknown. Here we studied the role of AKAPs in regulating human bronchial epithelial barrier.

Human bronchial epithelial cells (16HBE14o-) were pretreated with 30  $\mu$ M st-Ht31, an inhibitor of the AKAP-PKA interaction, 30 min prior to stimulation with 1% cigarette smoke extract (CSE). CSE was prepared by combusting 2 research cigarettes without a filter through 25 ml of medium, the obtained solution is 100%. Expression of AKAPs and E-cadherin was measured by western blot and RT-PCR. Interaction between AKAP9 and E-cadherin was analyzed by immunoprecipitation and immunofluorescence. Loss-of-function studies were performed using AKAP9 siRNA, non-targeting siRNA served as control. Epithelial barrier function was measured using electric cell substrate impedance sensing (ECIS). Lung tissue was stained for AKAP9 and E-cadherin using immunohistochemistry.

CSE reduced barrier function in HBE cells and the expression of the adhesion molecule E-cadherin specifically at the cell membrane. In addition, CSE reduced the protein expression of the AKAP family member AKAP9 at the cell membrane. The expression of AKAP5 and AKAP12 was unaffected by CSE. AKAP9 interacted with E-cadherin, presumably indicating that the reduction of both proteins is related. Interestingly, disruption of AKAP-PKA interactions by st-Ht31 prevented the CSE-induced reduction of E-cadherin and AKAP9 protein expression, promoting their membrane localization, and subsequent loss of barrier function.

Silencing of AKAP9 prevented the ability of st-Ht31 to restore CSE-induced loss of E-cadherin. E-cadherin, but not AKAP9, protein expression was reduced in lung tissue from COPD patients compared to controls. However, AKAP9 mRNA expression was decreased in primary bronchial epithelial cells from current smokers compared to non-/ex-smokers.

In conclusion, AKAP proteins importantly regulate the maintenance of the bronchial epithelial barrier by regulating the E-cadherin expression at the cell membrane.

### Role of host cell chaperones/PPIases during uptake of diphtheria toxin in human cells

**Schnell, Leonie**; Schuster, Manuel; Mohr, Katharina; Birkhofer, Carina; Langer, Simon; Barth, Holger  
Universitätsklinikum Ulm, Institut für Pharmakologie und Toxikologie, Germany

Diphtheria toxin (DT) is the causative agent of diphtheria and belongs to the group of single-chain AB-type protein toxins. DT is composed of an A-fragment (DTA) which corresponds to the catalytic (C) domain and a B-fragment which comprises the receptor-binding (R) and transmembrane (T) domains. Receptor-binding is followed by receptor-mediated endocytosis and internalization into early endosomal vesicles. Acidification of the endosomal lumen induces membrane insertion of the T domain and pore formation as well as partial unfolding of the C domain necessary for translocation of DTA into the cytosol. Here, DTA catalyzes ADP-ribosylation of elongation factor 2 resulting in disruption of protein synthesis and finally cell death by apoptosis [1]. Our group demonstrated for other ADP-ribosylating toxins such as C2 toxin, iota toxin and CDT that the host cell chaperone Hsp90 and peptidyl-prolyl *cis/trans* isomerases (PPIases) including cyclophilin A (CypA) and FK506-binding protein (FKBP)51 facilitate translocation of their enzyme subunits across endosomal membranes [2,3]. Moreover, by using recombinant fusion toxins, we and others found that membrane translocation of DTA was facilitated by the same cytosolic factors and the essential role of Hsp90 for DT entry is already confirmed [4,5]. Prompted by these findings, we investigated the role of Hsp90 and PPIases for translocation of DTA when native DT was applied to human cells. We demonstrated by analyzing cell morphology and cell viability that specific pharmacological inhibition of Hsp90, cyclophilins and FKBP51 protected HeLa cells from intoxication with DT. Moreover, less EF-2 was ADP-ribosylated in DT-treated cells in the presence of the inhibitors, indicating an essential role of Hsp90, Cyps and FKBP51 in the uptake of DTA into the host cell cytosol. The inhibitors had no effect on enzyme activity of DTA, proteolytic activation or receptor-binding of DT but inhibited the pH-dependent translocation of DTA across the cytoplasmic membranes of living cells, implicating that Hsp90 and the PPIases facilitate membrane translocation of DTA. *In vitro*, purified DTA specifically bound to immobilized recombinant Hsp90, CypA, Cyp40 and FKBP51 indicating their involvement in the membrane transport of DTA. The data not only provide new knowledge about the molecular mechanisms of DT uptake into cells but also might lead to development of novel therapeutic strategies to prevent cellular uptake of DT and thereby diphtheria.

- [1] Murphy (2011) *Toxins* 3, 294-308.  
[2] Barth (2011) *Naunyn-Schmied Arch Pharmacol* 383, 237-245.  
[3] Kaiser et al. (2012) *Cell. Microbiol.* 14, 1193-1205.  
[4] Dmochewicz et al. (2011) *Cell. Microbiol.* 13, 359-373.  
[5] Ratts et al. (2003) *J Cell Biol* 160, 1139-1150.

### Valproic acid treatment increased histone H4 acetylation in the atria of CREM-IbΔC-X transgenic mice

**Scholz, Beatrix**<sup>1</sup>; Stein, Juliana<sup>1</sup>; Himmler, Kirsten<sup>2</sup>; Schulte, Jan Sebastian<sup>1</sup>; Heinick, Alexander<sup>1</sup>; Schmitz, Wilhelm<sup>1</sup>; Müller, Frank Ulrich<sup>1</sup>

<sup>1</sup>Westfälische Wilhelms-Universität Münster, Institut für Pharmakologie und Toxikologie, Germany

<sup>2</sup>Medizinische Hochschule Hannover, Institut für Zell- und Molekularpathologie, Germany

**Rational:** The transcription factors CREB and CREM (cAMP-response element binding protein and modulator) regulate gene transcription, inter alia, in response to cAMP. Phosphorylation of CREB by protein kinase A (PKA) enables recruitment of the transcriptional co-factor CREB binding protein (CBP). CBP has an intrinsic histone acetyltransferase activity, which makes chromatin accessible to the transcription-activating machinery resulting in gene expression. Mice with heart-directed expression of the human cardiac splice variant CREM-IbΔC-X (TG) show atrial dilatation and different morphological and physiological alterations in atria preceding spontaneous-onset atrial fibrillation (AF). Here, we tested the hypothesis that a gain in histone acetylation by treatment with histone deacetylase inhibitors (HDACs) attenuates the atrial phenotype of TG mice.

**Methods and results:** In weeks 5-12 or 5-30 of life TG and wild-type (WT) mice were treated with the HDACs valproic acid (VPA, HDAC, specific for class I-II; 0.71% wt/vol, dissolved in water), vorinostat (SAHA, HDAC, specific for class I-II; solubilized in 5 molar equivalents of HOP-β-CD in water) or vehicle (Veh).

In week 12 the atrial weight/body weight ratio in Veh-treated TG mice (n=34) was 1.7-fold\* higher, however in VPA-treated TG mice (n=30) only 1.2-fold\* (n.s. vs. Veh-treated WT) higher as compared to Veh-treated WT mice (n=32). Hence, VPA reduced the atrial enlargement in TG mice. In contrast to VPA, SAHA treatment increased the atrial weight/body weight ratio of TG mice (n=11) 2.1-fold\* as compared to Veh-treated TG mice (n=30). Atrial cardiomyocyte length was not different between TG groups after both HDAC<sub>s</sub> treatments. ECG recordings showed that long-term treatment of TG mice with VPA (n=26) (up to week 30) deferred the development of AF by two weeks. SAHA treatment had no effect on the development of AF in TG mice. Western Blot analysis of Veh-treated TG atria (n=9) revealed, that VPA treatment significantly increased histone H4 acetylation by 20%\* (n=10). The acetylation of histone H3 in TG atria was not affected by VPA. (\*p<0.05 vs. Veh-treated WT, #p<0.05 vs. Veh-treated TG)

**Conclusions:** It is possible to attenuate the atrial phenotype of TG mice by treatment with the class I specific HDAC, VPA in line with an increased histone H4 acetylation. Since on the other hand the class II specific HDAC, SAHA worsened atrial alterations in TG mice, the effect may depend on the HDAC specificity of HDAC<sub>s</sub>.

### Analyzing dermal absorption data of chemicals

**Scholz, Roland**; Hahn, Stefan; Bitsch, Annette  
Fraunhofer Institut für Toxikologie und Experimentelle Medizin, Chemikalienbewertung, Hannover, Germany

Knowledge about the exposure to chemical substances forms an inevitable part of risk assessments and is as such required for many regulatory authorization processes. In the past, the focus was on inhalation and oral uptake; the dermal route was often disregarded. This might have been guided by the general assumption that skin provides a robust barrier to the external environment.

However, the skin forms a large surface for chemical exposure and thus, dermal absorption could be a crucial dimension that contributes to internal exposure. Penetration through skin is a complex process depending on very different factors such as 1) physicochemical properties of the test compound, 2) solvent/vehicle, 3) skin condition, 4) interactions between chemical and skin or metabolism in skin 5) test conditions (dose, area, duration, etc.). Thus, a general prediction on the basis of one single test might be misleading. In addition, measured endpoints differ with the used test system (in-vitro: steady-state flux and permeability coefficient, in-vivo: absorption rate in % of applied dose). Theoretical equations and models have been developed to describe transport of chemicals through the skin but so far they have limited acceptance. Within the new EU legislations (e.g. BPD/BPR, PPP) the dermal exposure got enhanced attention and dermal exposure including absorption data has to be considered. If there is a lack of absorption data for biocides a skin absorption rate of 100% has to be used as default. This prediction assumes complete absorption of the total amount of the substance getting in contact to the skin surface independent of the load and duration which seems to be rather implausible.

Therefore, we gathered publicly available information e.g. from the EDETOX Database (1) and the eChemPortal (2) and built-up a separate database. This database should allow to match chemicals to certain absorption ranges and to identify common structural features which might trigger higher skin absorption. In addition information about concentration effects and other influencing factors can be extracted from this data pool. As dermal absorption depends not only on substance inherent property, but also on the exposure situation, a reasonable prediction of dermal absorption requires consistent and comparable data from various exposure situations and can consequently be achieved by a comprehensive database.

- [1] <http://edetox.ncl.ac.uk>, 01.08.2013  
[2] [www.echemportal.org](http://www.echemportal.org), 01.08.2013

### Effects of small molecules inhibitors on AKAP-Lbc-mediated RhoA activation - implications for cardiac hypertrophy and cancer

**Schrade, Katharina**<sup>1</sup>; Eldahshan, Adeb<sup>1,2</sup>; Zühlke, Kerstin<sup>1</sup>; Fernandes, Joao<sup>1</sup>; Wieland, Thomas<sup>1</sup>; Rosenthal, Walter<sup>1</sup>; Klussmann, Enno<sup>1</sup>

<sup>1</sup>Max-Delbrück-Centrum für Molekulare Medizin (MDC) Berlin-Buch, Germany

<sup>2</sup>Leibniz-Institut für Molekulare Pharmakologie im Forschungsverbund Berlin e.V. (FMP), Germany

<sup>3</sup>Institut für Experimentelle und Klinische Pharmakologie und Toxikologie Maybachstr. 14, Mannheim, Germany

A-kinase anchoring proteins (AKAPs) comprise a family of around 50 scaffolding proteins, which coordinate different intracellular signaling pathways through interactions with signaling proteins such protein kinases, protein phosphatases and/or phosphodiesterase.

AKAP-Lbc binds protein kinase A (PKA) and additionally functions as a guanine nucleotide exchange factor (GEF). Upon stimulation, the GEF domain of AKAP-Lbc catalyzes the activation of the small GTP-binding protein RhoA. RhoA controls many fundamental cellular processes such as cellular growth, gene expression and actin remodeling. Pathological changes of RhoA signaling are often in response to chronic stress signals that may lead to diverse symptoms and diseases such as cardiomyocyte hypertrophy, heart failure or cancer.

To analyze the relevance of the AKAP-Lbc-RhoA signaling complex in such pathogenic states, small molecule inhibitors have been identified during a screening of a library of about 18,000 small molecules. We are currently defining the structure-activity relationship of an identified hit, Scaff10 and its derivatives, to optimize the compound with regard to specificity and affinity. The small molecules inhibit the AKAP-Lbc-RhoA interaction *in vitro*, the AKAP-Lbc-mediated activation of RhoA in response to LPA in HEK293 cells and in response to α1-adrenoceptor stimulation in cardiac myocytes. The project may pave the way to a new concept for the treatment of cardiac hypertrophy and/or cancer where AKAP-Lbc-mediated RhoA activation is involved in the control of proliferation.

- [1] P. Skrobin, S. Grossmann, G. Schäfer, W. Rosenthal, und E. Klussmann, „Chapter Five - Mechanisms of Protein Kinase A Anchoring“, in *International Review of Cell and Molecular Biology*, Bd. Volume 283, Kwang Jeon, Hrsg. Academic Press, 2010, S. 235–330.  
[2] D. Diviani, J. Soderling, und J. D. Scott, „AKAP-Lbc Anchors Protein Kinase A and Nucleates Gα12-selective Rho-mediated Stress Fiber Formation“, *J. Biol. Chem.*, Bd. 276, Nr. 47, S. 44247–44257, Nov. 2001.  
[3] A. Hall, „Rho GTPases and the Actin Cytoskeleton“, *Science*, Bd. 279, Nr. 5350, S. 509–514, Jan. 1998.  
[4] S. Etienne-Manneville und A. Hall, „Rho GTPases in cell biology“, *Nature*, Bd. 420, Nr. 6916, S. 629–635, Dez. 2002.  
[5] G. K. Carnegie, J. Soughayer, F. D. Smith, B. S. Pedroja, F. Zhang, D. Diviani, M. R. Bristow, M. T. Kunkel, A. C. Newton, L. K. Langeberg, und J. D. Scott, „AKAP-Lbc

- Mobilizes a Cardiac Hypertrophy Signaling Pathway", *Mol. Cell*, Bd. 32, Nr. 2, S. 169–179, Okt. 2008.
- [6] A. Appert-Collin, S. Cotecchia, M. Nenniger-Tosato, T. Pedrazzini, und D. Diviani, „The A-kinase anchoring protein (AKAP)-Lbc-signaling complex mediates  $\alpha 1$  adrenergic receptor-induced cardiomyocyte hypertrophy", *Proc. Natl. Acad. Sci.*, Bd. 104, Nr. 24, S. 10140–10145, Dez. 2007.
- [7] J. Heineke und J. D. Molkenin, „Regulation of cardiac hypertrophy by intracellular signalling pathways", *Nat. Rev. Mol. Cell Biol.*, Bd. 7, Nr. 8, S. 589–600, Aug. 2006.
- [8] J. A. Towbin und N. E. Bowles, „The failing heart", *Nature*, Bd. 415, Nr. 6868, S. 227–233, Jan. 2002.
- [9] L. V. Aelst und C. D'Souza-Schorey, „Rho GTPases and signaling networks", *Genes Dev.*, Bd. 11, Nr. 18, S. 2295–2322, Sep. 1997.
- [10] D. Toksoz und D. A. Williams, „Novel human oncogene lbc detected by transfection with distinct homology regions to signal transduction products", *Oncogene*, Bd. 9, Nr. 2, S. 621–628, Feb. 1994.
- [11] Y. Zheng, M. F. Olson, A. Hall, R. A. Cerione, und D. Toksoz, „Direct involvement of the small GTP-binding protein Rho in lbc oncogene function", *J. Biol. Chem.*, Bd. 270, Nr. 16, S. 9031–9034, Apr. 1995.
- [12] D. Diviani, L. Abuin, S. Cotecchia, und L. Pansier, „Anchoring of both PKA and 14-3-3 inhibits the Rho-GEF activity of the AKAP-Lbc signaling complex", *EMBO J.*, Bd. 23, Nr. 14, S. 2811–2820, Juli 2004.
- [13] J. P. Demaret, S. Brunie, J. P. Ballini, und P. Vigny, „Geometry of intercalation of psoralens in DNA approached by molecular mechanics", *Photochem. Photobiol.*, Bd. 50, Nr. 1, S. 7–21, Juli 1989.

### 349

#### Crataegus special extract WS<sup>®</sup> 1442 improves heart rate variability in conscious guinea pigs

**Schramm, Enrico**; Melcher, Silas; Koch, Egon

Dr. Willmar Schwabe GmbH & Co. KG, Präklinische Forschung, Karlsruhe, Germany

Functional syndromes are disorders for which no mechanistic cause can be demonstrated, but rather organism-inherent procedures that are prone to nervous, sensory or psychological factors are assumed as underlying pathomechanisms.

This often concerns the cardiovascular system and the percentage of afflicted patients in general practice is about 10-15%. Potential triggering causes for these syndromes are stress, excessive work load, weather changes or other distressing situations. Treatment is particularly needed when fluctuations in blood pressure, palpitations, tachycardia, cardiac arrhythmias, vertigo and fainting limit the quality of life. The main treatment options are psychotherapeutic assistance and in more severe cases drugs like beta-blockers, antidepressants or anxiolytics (1).

For studies on the physiology of the cardiovascular system and in clinical cardiology the measurement of the heart rate variability (HRV) is often used as a tool to determine the influence of the autonomic nervous system on cardiovascular dynamics. A reduced HRV has a high predictive value for cardiovascular diseases and occurs frequently in people suffering from acute emotional stress as well as in patients with anxiety, depression, or post-traumatic stress disorder.

WS<sup>®</sup> 1442, a special dry extract from hawthorn (*Crataegus* spp.) leaves with flowers, is an approved drug for the treatment of reduced cardiac performance according to NYHA stage II. Previous studies have shown that WS<sup>®</sup> 1442 exerts positive inotropic, vasodilatory, antithrombotic, anti-inflammatory, antioxidant and antiarrhythmic effects (2). It was the aim of this study to evaluate if WS<sup>®</sup> 1442 also improves heart rate variability in mildly stressed male guinea pigs.

For the experiments, gently restraint animals were prepared for recording of a standard ECG (lead III) and baseline data were obtained over a period of 30 min. Subsequently, the guinea pigs were orally treated with WS<sup>®</sup> 1442 (30, 100 or 300 mg/kg) and ECG recording was continued for 4 hours. Time-based HRV parameters (e.g., SD, RMSSD, NN50, and Pointcare Plot) were calculated using a software program. WS<sup>®</sup> 1442 caused a significant and dose-dependent increase in HRV which was most clearly pronounced 3 h after administration. These pharmacological effects indicate that WS<sup>®</sup> 1442 can ameliorate stress-induced cardiovascular symptoms.

(1) Herrmann, C. & Rüger, U. (1999). Dts. Ärzteblatt 96, A-131-A-136.

(2) Koch, E. & Malek, F. A. (2011). *Planta medica*, 77(11), 1123-1128.

### 350

#### IDENTIFICATION OF PIGMENTS AND TATTOO INK INGREDIENTS BY PYROLYSIS-GAS CHROMATOGRAPHY/MASS SPECTROMETRY (Py-GC/MS)

**Schreiber, Ines**<sup>1</sup>; Laux, Peter<sup>1</sup>; Hutzler, Christoph<sup>1</sup>; Luch, Andreas<sup>1,2</sup>

<sup>1</sup>Bundesinstitut für Risikobewertung, Sicherheit von Verbrauchernahen Produkten, Berlin, Germany

<sup>2</sup>Freie Universität Berlin, Institut für Pharmazie, Germany

To enable risk assessment, tattoo inks used on the market need to be monitored for the presence of prohibited compounds. Since most pigments and polymeric ingredients of tattoo inks are insoluble and involatile finding the appropriate analytical means reveals challenging. In the literature, identification of soluble pigments is mainly carried out using liquid chromatography (LC) coupled to ultraviolet (UV) absorption spectroscopy. With insoluble pigments, the use of matrix-assisted laser desorption/ionization (MALDI) time-of-flight (ToF) mass spectrometry as well as Fourier transform infrared (FT-IR) spectroscopy has been reported. Common disadvantages of all of these methods are

either the need for high purity reference pigments, insufficient transfer of analytes into solution, or the lack of suitable spectra libraries.

Alternatively, Py-GC/MS provides a quick and reliable method for pigment decomposition and product identification via comparison to pure pigments or tattoo ink formulations. Here, we pyrolyzed pigments or tattoo inks at 800°C followed by gas chromatographic separation and electron impact ionization (EI) mass spectrometry. Using this method the chemical structures of unknown parental compounds could be assigned based on the decomposition patterns compiled in the mass spectra library provided by the United States National Institute of Standards and Technology (NIST). For instance, the release of the potentially carcinogenic aromatic amine 2-methoxyaniline from the azo pigment Yellow74 has been observed. Additionally, polymers used for pigment dispersion like polyvinyl pyrrolidones and polysiloxanes were identified simultaneously.

Our goal is to establish a pyrogram library of commonly used pigments and other ingredients in tattoo inks applicable in substance screening. Based on this, false declaration of tattoo pigments, suspicious additives and carcinogenic cleavage products can be easily identified. It remains to be investigated whether the fragments identified by Py-GC/MS will be also generated through sunlight exposure or laser removal. If so, this method might be suited to predict exposure of the tattooed consumer towards toxic substances like aromatic amines during sun bathing or laser treatment.

### 351

#### Migration of differentiated HL-60 cells can be induced by NR8383 rat macrophages following challenge with TiO<sub>2</sub>, SiO<sub>2</sub> or soot

**Schremmer, Isabell**; Rosenkranz, Nina; Brüning, Thomas; Bünger, Jürgen; Westphal, Götz

Ruhr-Universität Bochum, Institut für Prävention und Arbeitsmedizin der Deutschen Gesetzlichen Unfallversicherung Institut der Ruhr-Universität Bochum (IPA), Germany

Accumulation of neutrophils in the lung is a hallmark of inflammatory reactions towards particulate matter. This study investigated if the migration of neutrophils to sites where macrophages try to cope with particles can be reconstructed *in vitro*.

Methods: We challenged NR8383 rat macrophages with up to 300 µg/mL coarse and fine silica (SiO<sub>2</sub>  $\Delta$  5 µm and 10 - 20 nm), titanium dioxide (TiO<sub>2</sub>: coarse anatase and rutile  $\Delta$  5 µm, fine rutile  $\Delta$  100 nm and anatase  $\Delta$  < 25 nm), and fine soot ( $\Delta$  200 nm) for 16 hours. The cells and the particles were removed and the supernatants were used to induce cell migration of differentiated HL-60 cells (dHL-60 cells).

Results: challenge of NR8383 rat macrophages with 100 and up to 300 µg/mL PM resulted in cell supernatants which were able to induce dose dependent cell migration of dHL-60 cells. Initially FCS was used as positive control. However due to its strong inductive potency we used SiO<sub>2</sub> as positive control in the successive experiments. The test shows up to be very robust and reproducible. The induction potency was as follows: coarse > fine silica > coarse rutile > fine rutile » fine soot > coarse = fine anatase.

Conclusion: challenge with SiO<sub>2</sub>, TiO<sub>2</sub> or soot near cytotoxic concentrations caused NR8383 cells to secrete compounds which are able to induce migration of dHL-60 cells. This test system might be useful to yield a deeper insight in PM induced inflammatory processes.

### 352

#### Toxicological databases: modern tools to reduce, refine and replace animal testing

**Schröder, Katrin**; Simetska, Nelly; Escher, Sylvia; Mangelsdorf, Inge

Fraunhofer Institute for Toxicology and Experimental Medicine - ITEM, Chemical Risk Assessment, Hannover, Germany

Implementation of the 3R principles (Reduction, Refinement and Replacement of animal testing) in hazard and risk assessment is a prior goal in several regulations, e.g. REACH. Read across, applying QSAR models, integrated test strategies or grouping approaches are very valuable tools to achieve this goal. All these tools demand systematic and structured analyses of available data which can easily be performed with high quality relational databases containing all relevant parameters for analyzing: structural data, data on study design, and toxicological endpoints. Current major concerns are complex toxicological studies such as long term repeated dose studies or studies on reproductive toxicity and toxicological studies on nanomaterials that are time and costs intensive and require the testing of numerous animals. For efficiently analyzing the available data, Fraunhofer ITEM developed three relational databases each with special focus on repeated dose toxicity (RepDose), fertility and developmental toxicity (FeDTex), both sponsored by CEFIC LRI and particle and fiber toxicity (PaFtoX). RepDose contains currently about 3000 studies with 800 chemicals in rodents, FeDTex 535 studies with 269 chemicals in rodents and rabbits and PaFtoX 131 studies in rodents with 17 different materials (65 different (nano)materials based on primary size or 87 different materials based on primary and secondary size). These databases can be used as stand-alone or in combination linked by the Fraunhofer Toxtool (FTT), an overarching database. The databases have been or are currently used to address the following issues:

- 1) Development of an integrated testing strategy (ITS) for repeated dose toxicity. This ITS evaluates under which conditions high quality old studies can still be used for regulatory risk assessment. (OSIRIS).
- 2) Derivation of reliable factors used for time extrapolations or route to route extrapolations (ERASM).

- 3) Use of existing animal data to develop integrated test strategies by identifying critical targets and by validation of alternative methods covering diverse adverse outcome pathways ((OSIRIS, ChemScreen, AImT2, Detective, Exitox).
- 4) Evaluation of the predictive power of RepDose studies for reproductive toxicity (ChemScreen).
- 5) Grouping approaches for nanomaterials (ongoing research)
- 6) Identification of structural alerts for endocrine properties of chemicals (ChemScreen)

### 353

#### Impact of oxidative metabolism on the topoisomerase inhibitory potential of genistein

**Schroeter, Anika**; Marko, Doris

Universität Wien, Institut für Lebensmittelchemie und Toxikologie, Austria

One of the major isoflavones found in soy and soy based products is genistein, which has been associated with a broad range of beneficial health effects. However, beside of potential beneficial effects also undesired genotoxic properties have been reported [1]. After consumption of genistein-containing products the isoflavone may undergo phase I oxidative metabolism, which leads to the formation of mainly C-6, C-8, C-3' hydroxylated metabolites. Little is known so far about the biological activity profile of these metabolites [2]. In the present study we therefore investigated if the oxidative metabolites of genistein might contribute to the genotoxic effect of the parent compound with special emphasis on the impact on human topoisomerases and DNA integrity.

The inhibitory potential on topoisomerases was investigated in the cell-free decatenation assay and in the human colon cancer cell line HT29 by conducting the 'isolating *in vivo* complexes of enzyme assay' (ICE assay). Potential DNA strand breaks were detected via comet assay after 1 h and 24 h of incubation.

Under cell-free conditions 3'-OH-genistein exhibited topoisomerase inhibitory properties comparable to genistein and showed only slightly weaker effects than genistein in HT29 cells in the ICE Assay. In contrast, hydroxylation in 6-position was found to diminish the topoisomerase inhibitory properties, inhibiting topoisomerase II in the cell-free assay only in the highest tested concentration of 250 µM. Furthermore, 6-OH-genistein exhibited no topoisomerase poisoning effects within cells. After 1 h of incubation no significant increase in the rate of DNA strand breaks was detectable in the comet assay for all three substances. However, after 24 h of incubation 3'-OH-genistein exceeded the effects of the parent compound significantly at concentrations  $\geq 200$  µM. After additional treatment with formamidopyrimidine DNA glycosylase (fpg) 3'-OH-genistein showed higher DNA damaging potential than genistein. In contrast, 6-OH-genistein exhibited only weak DNA strand breaking potential up to 250 µM with and without additional fpg treatment.

The results indicate that depending on the position of hydroxylation the genotoxic potential of genistein is modulated. Hydroxylation on 6-position seems to decrease the genotoxic potential whereas hydroxylation at the B ring might cause an increase. Further experiments are needed to elucidate the underlying mechanism for the enhanced genotoxicity of 3'-OH-genistein, which cannot be solely explained by the potential to inhibit topoisomerase II.

[1] Mortensen, A., Kulling, S. E., Schwartz, H., Rowland, I., *et al.*, Analytical and compositional aspects of isoflavones in food and their biological effects. *Molecular Nutrition & Food Research* 2009, 53, S266- S309.

[2] Kulling, S. E., Honig, D. M., Metzler, M., Oxidative metabolism of the soy isoflavones daidzein and genistein in humans *in vitro* and *in vivo*. *J Agric Food Chem* 2001, 49, 3024-3033.

### 354

#### The Progress Test Medizin as a valuable source to evaluate knowledge acquisition and retention in pharmacology

**Schubert, Sebastian**<sup>1</sup>; Bolbrinker, Juliane<sup>2</sup>

<sup>1</sup>Charité - Universitätsmedizin Berlin, Dieter Scheffner Fachzentrum für medizinische Hochschullehre und evidenzbasierte Ausbildungsforschung, Germany

<sup>2</sup>Charité - Universitätsmedizin Berlin, Institut für Klinische Pharmakologie und Toxikologie, Germany

The Progress Test Medizin (PTM) is a longitudinal assessment of medical students' knowledge acquisition and retention over the course of the curriculum established in 1999 at the Charité – Universitätsmedizin Berlin. The PTM is conducted twice a year at the beginning of each semester and consists of 200 multiple-choice-questions (MCQs) designed to reflect graduation level knowledge. For each test, a different set of MCQs is randomly selected from a database containing more than 5000 MCQs with approximately the same number of questions per medical subject in each test. Importantly, there is no pass/fail decision made by the test results. By now, 17 medical faculties (14 in Germany, 3 in Austria) implemented the PTM and more than 12,000 students took part in the 29th PTM at the beginning of winter semester 2013/2014.

For pharmacology, an average of 10 MCQs is placed in each PTM. In addition, 10 MCQs per test that are assigned to other medical subjects, e.g. internal medicine, cover also pharmacological topics. The PTM does not differentiate between the subjects Pharmacology/Toxicology and Clinical Pharmacology. To illustrate the potential value of the PTM to evaluate knowledge acquisition and retention in pharmacology, we analyzed data of the PTM performed at the Charité from 2002-2013. The increase of knowledge in pharmacology over the course of the traditional curriculum at the Charité

(Regelstudiengang) is represented both by the results of a single MCQ and the combined mean results in pharmacology over time. The latter are compared with knowledge acquisition in internal medicine, the mean results of students from our reformed novel curriculum (Modellstudiengang Medizin Charité) as well as all other cooperating medical faculties. One representative MCQ serves as an example for a teaching content that demonstrates a lack of sustained knowledge retention over time. In summary, analyzing data of the PTM bears the potential to evaluate the success of knowledge transfer in pharmacology and to identify knowledge gaps. The latter might serve as a basis to specifically modify the curriculum and teaching strategy in pharmacology.

Nouns, Z. M., & Georg, W. (2010). Progress testing in German speaking countries. *Medical Teacher*, 32, 467-470.

### 355

#### Antibese effects of Angiotensin(1-7)

**Schuchard, Johanna**<sup>1</sup>; Piehl, Martina<sup>1</sup>; Stötting, Ines<sup>1</sup>; Bader, Michael<sup>2,3</sup>; Raasch, Walter<sup>1,4</sup>

<sup>1</sup>Universität Lübeck, Institut für Experimentelle und Klinische Pharmakologie und Toxikologie, Germany

<sup>2</sup>Max Delbrück Centrum für Molekulare Medizin, Molekularbiologie von Hormonen im Herz-Kreislaufsystem, Berlin, Germany

<sup>3</sup>DZHK (German Centre for Cardiovascular Research), partner site Berlin, Germany

<sup>4</sup>DZHK (German Centre for Cardiovascular Research), partner site Hamburg/Kiel/Lübeck, Lübeck, Germany, Germany

Angiotensin(1-7) [Ang(1-7)] is a metabolite of AngII and AngI. As an agonist at the MAS receptor, Ang(1-7) reveals cardiovascular effects. Ang(1-7) was also described in some reports to improve insulin sensitivity and to regulate body weight. In this view, body weight was tendentially lessened after Ang(1-7) treatment. Accordingly, fat mass was shown to be reduced in transgenic rats with higher Ang(1-7) levels but to be increased in MAS receptor deficient mice. The aim of this study was to investigate the antibese effect of Ang(1-7) in the transgenic rat model TGR(A1-7)3292 overexpressing Ang(1-7). Sprague Dawley (SD) rats served as wild type controls.

Rats received either high calorie cafeteria diet (CD) or standard chow diet for 3 months. Gain in body weight and food intake was weekly monitored. In addition, daytime-dependent food intake was continuously measured when energy expenditure was determined in parallel by indirect calorimetry. Leptin sensitivity was examined by monitoring food intake and body weight after repetitive leptin injections within 3 days. Insulin sensitivity was assessed by measuring the glucose utilization after insulin injections. Blood pressure and heart rate was determined by plethysmography.

In contrast to SD rats, TGR(A1-7)3292 have 1.), a diminished body weight when they were regularly fed with chow; 2.), TGR(A1-7)3292 are protected against developing obesity although they were fed with CD; 3.), TGR(A1-7)3292 have normal baseline leptin plasma concentration independent on feeding regime; 4.), TGR(A1-7)3292 show a clearly reduced energy intake which is mainly related to a lower CD-intake; 5.) TGR(A1-7)3292 remain leptin sensitive despite chronic CD-feeding; 6.), TGR(A1-7)3292 have a higher, strain-dependent energy expenditure; 7.), TGR(A1-7)3292 but not SD rats remain insulin sensitive after the 3-months lasting CD-feeding period; 8.), TGR(A1-7)3292 did not develop a mild hypertension after CD-feeding which was clearly observed in SD rats; and 9.), TGR(A1-7)3292 reveal a strain-dependent decrease in heart rate and left ventricular weight independent on feeding regime.

We conclude, that Ang(1-7) has a biological impact beside its potency on cardiovascular parameters for regulating food behaviour and body weight. The latter effects may participate in the observed loss of body weight after chronic AT<sub>1</sub>-receptor blockade and may induce the development of Ang(1-7) like agonists as a pharmacological tool to prevent or to cure obesity.

### 356

#### Arrhythmogenic consequences of chronic $\beta$ -adrenoceptor stimulation investigated in mouse ventricular cardiomyocytes.

**Schulte, Jan Sebastian**; Tekook, Marcel Alexander; Fehrmann, Edda; Seidl, Matthias Dodo; Heinick, Alexander; Scholz, Beatrix; Schmitz, Wilhelm; Müller, Frank Ulrich

Westfälische Wilhelmsuniversität, UKM, Institut für Pharmakologie und Toxikologie, Münster, Germany

Studies on mice investigating effects of chronic  $\beta$ -adrenoceptor stimulation in the heart were mostly focused on the development of detrimental structural remodeling and systolic dysfunction seen in heart failure. The arrhythmogenic consequences of an electrical and structural remodeling in the heart induced by chronic isoprenaline treatment in mice to our best knowledge have so far not been systematically examined.

We therefore treated wild-type mice by the use of osmotic minipumps with isoprenaline (ISO, 30mg/kg/d) or sodium chloride as controls (NaCl) for 14 days and subsequently investigated the occurrence of arrhythmogenic events in ventricular cardiomyocytes (VCs) using the patch clamp technique and calcium imaging.

VCs from ISO mice were enlarged (in % of NaCl, Area:  $115 \pm 4^*$ ; Length:  $104 \pm 3$ ; Diameter:  $111 \pm 2^*$ ,  $n=700-900/7-9$ ), and action potentials (APs) were prolonged in ISO VCs (NaCl vs. ISO, in ms, APD50:  $5.1 \pm 0.6$  vs.  $11.7 \pm 1.9^*$ ; APD90:  $46 \pm 4.6$  vs.  $88.35 \pm 11.8^*$ ;  $n=27/8$  vs.  $34/10$ ). At the same time early afterdepolarisations (EADs) were detected in VCs from ISO but not NaCl treated mice (VCs with stable EADs, NaCl vs. ISO:  $0/27$  vs.  $11/45^*$ ). Parameters of Ca<sup>2+</sup> homeostasis (diastolic Ca<sup>2+</sup>, Ca<sup>2+</sup> transient



amplitude, time to peak) investigated in field stimulated Indo-1/AM loaded VCs were not altered between groups except an accelerated  $Ca^{2+}$  transient decay (time to baseline [TTB] in % of NaCl, TTB50%:  $80 \pm 4^*$ ; TTB90%:  $81 \pm 5^*$ ;  $n=44/7$  vs.  $64/9$ ). The occurrence of spontaneous APs (sAP) and spontaneous  $Ca^{2+}$  releases (sCaR) as a potential source for delayed afterdepolarizations and sAPs was detected using stimulation-rest protocols. The number of VCs displaying sAPs was increased in the ISO group (VCs with sAP in %, NaCl vs. ISO:  $9$  vs.  $27^*$ ;  $n=23/8$  vs.  $37/9$ ). The rate of sCaRs in event positive VCs was increased in ISO (NaCl vs. ISO:  $1.8 \pm 0.3$  vs.  $7.1 \pm 2.5^*$ ;  $n=9-11/7$ ) whereas the proportion of VCs showing sCaRs was not different between groups ( $n=44-47/7$ ). [values=mean $\pm$ SEM;  $n$ =VCs/animal; \* $p$ <0.05 vs. NaCl]

Besides the well documented structural remodeling and systolic dysfunction induced by chronic  $\beta$ -adrenoceptor stimulation, chronic isoprenaline administration in mice leads to an increase in arrhythmic events in VCs. Thus, this mouse model may also serve to investigate the mechanisms and time course of an arrhythmic remodeling induced by chronic  $\beta$ -adrenoceptor stimulation which plays an important role in the development of heart failure. (supported by IZKF Münster)

### 357

#### Analysing reproductive toxicity studies using the FeDTeX Database – Does an F2-generation provide an additional benefit?

**Schulz, Florian**; Lewin, Geertje; Magelsdorf, Inge; Batke, Monika; Escher, Sylvia  
Fraunhofer Institute for Toxicology and Experimental Medicine ITEM, Chemical Risk Assessment, Hannover, Germany

Numerous animal studies are required under the EU program on Registration, Evaluation, Authorisation and Restriction of Chemicals (REACH). Developmental and reproductive toxicity studies are expected to be the major cost factor and the major consumer of animals. Thus, there is great necessity to develop new alternative testing strategies. One opportunity may be the replacement of the conventional two-generation reproduction toxicity study (OECD 416) by the recently implemented extended one-generation reproduction toxicity study (EOGRTS, OECD guideline 443). Existing animal data can be integrated in the process of development by validation of alternative methods.

The Fraunhofer Fertility and Developmental Toxicity in experimental animals database (FeDTeX DB) currently covers 269 chemicals with 535 developmental and reproduction toxicity studies conducted in rodents and rabbits during the last three decades. Comparing the generation NOELs of multi-generation reproduction studies, the F1 generation was identified as most responsive. In contrast, the NOEL of the F2 generation was lower than the F1 NOEL only in 10% of the studies. The detailed analysis of the underlying effects in these studies left only 3 studies, where the LOEL of F2 was lower than in F1 or F0. Additionally, the observed F1-effects would clearly have triggered mating of F1 in an EOGRTS design. Thus, the impact of the F2 generation on the study NOEL is low and critical effects would not have been missed following the EOGRTS protocol. Furthermore, an impaired F1-fertility was only observed in 5 studies at the study LOEL. In all these studies, effects on reproductive organs or an impaired fertility were already adequately detected in F0.

In conclusion, studies following the EOGRTS protocol may serve as an alternative in toxicity testing strategies.

### 358

#### The Inhibitory Effect of Diazoxide on Insulin Secretion – a Re-Investigation

**Schumacher, Kirstin**; Willenborg, Michael; Rustenbeck, Ingo  
Technische Universität Braunschweig, Institut für Pharmakologie und Toxikologie, Germany

Background and aims: Glucose-induced insulin secretion is mediated by a bifurcating pathway generating "triggering" and "amplifying" signals. The standard protocol to demonstrate the amplifying effect of glucose is to provide the triggering signal by  $K^+$  depolarization while the KATP channels are clamped open by diazoxide to ensure that glucose metabolism is uncoupled from membrane potential regulation. Any further increase in secretion which is caused by the addition of glucose is then believed to be mediated by the amplifying pathway which is known to involve the cataplerosis of mitochondrial metabolites but has otherwise remained enigmatic. Since diazoxide has been reported to affect mitochondrial metabolism at experimentally relevant concentrations (1), the suitability of diazoxide as a pharmacological tool was re-investigated using mouse pancreatic islets and beta cells. Results: 15 mM  $K^+$  mimicked the extent of the slow-wave depolarization by glucose (19–20 mV) and raised  $[Ca^{2+}]_i$  levels as produced by 20 mM glucose. However, this  $K^+$  concentration produced only a modest transient increase of insulin secretion. When glucose was raised from a substimulatory (5 mM) to a moderate stimulatory concentration (10 mM) in the continuing presence of 15 mM  $KCl$ , a marked increase of insulin secretion with a biphasic pattern resulted. The addition of 250  $\mu M$  diazoxide abolished the stimulated secretion. This was unexpected since the beta cell plasma membrane was still depolarized by  $K^+$  and since the presence of 10 mM glucose ought to produce sufficient amplifying signals. Compared with the presence of 10 mM glucose plus 15 mM  $KCl$  the addition of diazoxide led to a moderate decrease of the ATP/ADP ratio and an equally moderate increase of the ATP/AMP ratio. However, these changes do not sufficiently explain the cessation of secretion. Using TIRF microscopy of insulin-secreting cells labelled with insulin-EGFP and Rhodamine 123 showed that mitochondria co-exist with insulin granules in the immediate submembrane space. Conclusions: Diazoxide may inhibit insulin secretion by mechanisms in addition to the opening of KATP channels. In

view of the reports that diazoxide affects mitochondrial metabolism (1) and that mitochondria form microcompartments with ion channels in excised patches from beta cells (2), it is conceivable that mitochondrial signals locally required to prime insulin granules for fusion competence are abolished by diazoxide.

[1] Grimmshann T, Rustenbeck I. Direct effects of diazoxide on mitochondria in pancreatic B-cells and on isolated liver mitochondria. *Br J Pharmacol*. 1998; 123:781-8.

[2] Rustenbeck I, Dickel C, Herrmann C, Grimmshann T. Mitochondria present in excised patches from pancreatic B-cells may form microcompartments with ATP-dependent potassium channels. *Biosci Rep*. 1999;19:89-98.

### 359

#### Effect of diet-induced obesity on murine models of contact hypersensitivity

**Schumacher, Stephan**<sup>1</sup>; Bäumer, Wolfgang<sup>1,2</sup>  
<sup>1</sup>University of Veterinary Medicine Hannover, Foundation, Institute of Pharmacology, Toxicology and Pharmacy, Germany  
<sup>2</sup>NCSU College of Veterinary Medicine, MBS Department, Raleigh, United States

**Background:** Obesity has emerged into a worldwide epidemic that is associated with cardiovascular disease, insulin resistance and type 2 diabetes (1). It is now increasingly recognized as a chronic low-grade inflammatory condition with a predominance of classically activated macrophages and Th1 cells (2). Here we investigated whether diet-induced obesity would selectively influence the severity of Th1-biased allergic contact dermatitis.

**Methods:** Male and female C57BL/6 mice were fed a high fat diet (HFD) or matched control diet for 16 weeks. Starting after 9 weeks of HFD animals were sensitized against 2,4-dinitrofluorobenzene (DNFB; Th1-dominated) or 2,4 toluene 2,4-diisocyanate (TDI; Th2-dominated) and allergic ear swelling was challenged after 9, 12 and 16 weeks.

**Results:** Male mice gained much more weight on HFD and became severely insulin-resistant after 16 weeks, which was not the case for female mice. After 12 weeks of HFD we observed significantly reduced ear swelling after TDI challenge in male mice. However, this difference could not be confirmed after 16 weeks. We found no effects of diet-induced obesity in female mice or on DNFB-induced hypersensitivity, respectively.

**Conclusion:** Although obesity has been reported to result in chronic low-grade inflammation, this does not seem to aggravate a Th1-dominated allergic skin reaction.

(1) Ouchi N et al. *Nat Rev Immunol* 2011; 11: 85-97

(2) Lumeng CN and Saltiel AR *J Clin Invest* 2011; 121: 2111-7.

### 360

#### Mini organ cultures of human lung and bronchial tissue as 3D models for lung toxicity testing.

**Schumacher, Berit**<sup>1</sup>; Wiese, Jan<sup>1</sup>; Schön, Ilona<sup>2</sup>; Sandner, Annett<sup>2</sup>; Glahn, Felix<sup>1</sup>; Foth, Heidi<sup>1</sup>  
<sup>1</sup>Martin-Luther-Universität, Institut für Umwelttoxikologie, Halle / Saale, Germany  
<sup>2</sup>Martin-Luther-Universität, Universitätsklinik und Poliklinik für Hals-, Nasen-, Ohrenheilkunde, Kopf- und Halschirurgie, Halle / Saale, Germany

In this study we want to demonstrate that mini organ cultures of human lung (L-MOC) and bronchial tissue (B-MOC) can be a useful 3D *in-vitro* tool in inhalation toxicology. Cell cultures of different complexity have become commonly used as model systems. A major advantage of a 3D mini organ cultures is that they are more realistic and closer to the conditions in the human body than cell lines or primary cells (2D models).

To describe and monitor the cultivation of the MOCs we determined the viability, intracellular GSH-level, gene expression profiles and, as a marker for tissue disruption, the enzymatic activity of matrix-metallo-proteinase 2 (MMP2).

The MOCs are healthy tissue which is derived from lung tumour resections of lung cancer patients and are cultivated on plates covered with 1.5% agar. They can be cultivated for a long period (up to 74 days) without losing their viability. For characterization single specimens were fixed and stained with H&E and subjected to histological examination afterwards. As a marker of oxidative stress the level of intracellular glutathione (GSH) was determined by HPLC. In both culture models (L- and B-MOC) the GSH-level was increased slightly over time during normal cultivation. The GSH-level was approximately 1.4 to 1.5 fold higher after 14 days in culture with a maximum of 2 fold after 18 days. This might be explained by a progressive epithelialization of the mini organ cultures. In further experiments we modulated the intracellular GSH content. Therefore we used 50  $\mu M$  BSO (buthionine sulfoximine) to decrease GSH level to 20 % compared to untreated control. The enzymatic activity of MMP-2 was up regulated slightly in B-MOC during the cultivation starting on the 10<sup>th</sup> day and increased with ongoing cultivation time. MMP2 was stably secreted during the cultivation time in L-MOC. The BSO addition stimulated the MMP2 activity demonstrated by gelatin zymography. Western blots confirmed the zymographic data.

In gene expression analyses on day 14 of culture high expression of manganese superoxide dismutase (SOD-2) and interleukin-8 (IL-8) were found in both L- and B-MOC. Moreover the ATP dependent transporters MRP1 and 3 could be detected. In further experiments the expression of oxidative stress related genes (HIF-1 $\alpha$ , Nrf-2, HO-1) over time was examined.

According to our study MOC of bronchus and lung represent versatile lung models still capable to react to oxidative stress and useful for a broad array of analytical tests.

## 361

**Induction of DNA repair processes by angiotensin II****Schupp, Nicole**; Brand, Susanne

Universität Würzburg, Institut für Toxikologie, Germany

Angiotensin II (AngII), the reactive peptide of the blood pressure-regulating renin-angiotensin-system, leads to the formation of reactive oxygen species and DNA damage in vitro and vivo. Reactive oxygen species cause numerous DNA lesions including single-strand breaks, double strand breaks and oxidative DNA base modifications. To investigate the influence of AngII on DNA repair, we examined different repair processes including PARP and ATM activity and base excision repair.

To analyze the effect of AngII-induced repair activity, pig kidney cells (LLC-PK1) were incubated with AngII concentrations between 50 and 400 nM. Immunocytochemistry analysis revealed a dose-dependent induction of phosphorylation of the DNA damage sensor protein ATM, which could be prevented by the ATM inhibitor KU-55933. Coincubation with KU-55933 also prevented phosphorylation of the downstream target H2AX. Furthermore, AngII-induced DNA damage measured by comet assay was repaired after a repair time of 30 min, whereas the presence of KU-55933 inhibited the DNA repair. Use of the PARP inhibitor 3-aminobenzamide had the same effect in the comet assay.

Repair of oxidative DNA base lesions occurs primarily via the DNA base excision repair pathway, initiated by two classes of glycosylases, OGG1 and NEIL1. Western blot analysis of both glycosylases revealed an AngII-induced upregulation of the expression of OGG1 and NEIL1.

In summary, we could show that ATM-phosphorylation and subsequent activation of different downstream targets like H2AX and also PARP are necessary for repair after AngII treatment. In addition, NEIL1- and OGG1-expression is induced after AngII treatment in order to manage an increased level of oxidative base damage.

## 362

**Radiation mediated cell death of esophageal squamous cell carcinoma cells is enhanced by down-regulation of stromal hyaluronan synthase 2****Schütze, Alexandra**<sup>1</sup>; Röck, Katharina<sup>1</sup>; Sack, Maren<sup>2</sup>; Brenneisen, Peter<sup>2</sup>; Jendrossek, Verena<sup>3</sup>; Fischer, Jens Walter<sup>1</sup><sup>1</sup>Universitätsklinikum Düsseldorf, Institut für Pharmakologie und Klinische Pharmakologie, Germany<sup>2</sup>Universitätsklinikum Düsseldorf, Institut für Biochemie und Molekularbiologie I, Germany<sup>3</sup>Universitätsklinikum Essen, Institut für Zellbiologie, Germany

Radiotherapy is commonly used in the management of esophageal carcinomas. Hyaluronan (HA), a major carbohydrate constituent of the extracellular matrix, is synthesized by three hyaluronan synthases (HAS1-3). Through interaction with its receptors e.g. CD44 and RHAMM HA is known to mediate complex cellular responses thereby regulating cellular phenotypes. However, little is known about how ionizing radiation alters the HA-matrix and how these changes affect tumor-stroma interactions.

To investigate changes of the HA-matrix induced by ionizing radiation, mono-cultures of KYSE410 cells (KYSE) and human fibroblasts (hF) were irradiated with 2Gy. The HA matrix was analysed by qRT-PCR, ELSA and affinity-cytochemistry. Cells were observed by time lapse microscopy and cell death was assessed visually, by PARP western blotting, live cell staining with Hoechst33342/propidium iodide and sub-g1 cell cycle analysis. The role of ROS in matrix changes was assessed by the ROS inhibitors, N-acetylcysteine (NAC) and sodium selenite (SSE).

The main HAS isoform, HAS2, showed significant down-regulation in irradiated hF (0.55±0.09 fold of control). HA quantification by ELSA showed however an increase in irradiated hF, whereas irradiated KYSE showed a trend to decreasing extracellular HA. Although structural changes of the pericellular HA-matrix such as the formation of HA-cables were not observed in irradiated KYSE, less HA-cable like structures were observed in irradiated hF. To evaluate functional consequences of the altered HA-matrix for tumor-stroma interactions, fibroblasts were co-cultured with KYSE 24h after irradiation. Surprisingly increased death of KYSE was observed in co-culture with irradiated fibroblasts compared co-culture with mock-irradiated fibroblasts (16.10±4.25 fold of control) suggesting that irradiated fibroblasts contribute to tumor cell death in response to irradiation. This effect was abolished by pre-incubation of hF with ROS inhibitors NAC or SSE. PARP western blots, live cell staining and cell cycle analysis confirmed the microscopic results. Importantly, co-culturing of irradiated KYSE with siHAS2 transfected fibroblasts also led to increased cell death of KYSE mimicking the effects seen with irradiated hF (16.99±4.81 fold of control).

In conclusion, irradiation of stromal cells enhances cell death of tumor cells in a ROS dependent manner. This effect appears to be mediated by down-regulation of HAS2 and a thereby altered HA matrix.

## 363

**Clostridium difficile Toxin CDT Changes Microtubule Organization and Redirects Vesicle Traffic to Increase Bacterial Adherence****Schwan, Carsten**; Krupke, Anna S.; Nölke, Thilo; Aktories, Klaus

Institut für Experimentelle und Klinische Pharmakologie und Toxikologie, 1, Freiburg, Germany

*Clostridium difficile* causes antibiotic-associated diarrhea and pseudomembranous colitis. The Rho-glucosylating toxins A and B are the major virulence factors of the pathogen. Recently identified hypervirulent strains additionally produce the actin ADP-ribosylating toxin *Clostridium difficile* transferase (CDT). CDT depolymerizes actin and causes formation of microtubule-based protrusions. The network of CDT-induced tentacle-like protrusions increases pathogen adherence. These protrusions allow vesicle traffic and contain endoplasmic reticulum (ER) tubules. The ER is connected to microtubules via the calcium sensor Stim1. The toxin re-routes Rab11-positive vesicles from basolateral to the apical membrane in a microtubule- and Stim1-dependent manner. The vesicles contain fibronectin, which is involved in bacterial adherence.

The data yield a new model of *C. difficile* adherence: Actin depolymerization causes microtubule restructuring, ER-translocation, Stim1-dependent Ca<sup>2+</sup> signaling, vesicle re-routing and secretion of extracellular matrix (ECM) proteins to increase bacterial adherence.

## 364

**Regulation of Adipose Triglyceride Lipase (ATGL) Expression by Nuclear Estrogen Receptors****Schwanstecher, Annekatrin**; Benz, Verena; Kintscher, Ulrich; Kirsch, Sebastian; Foryst-Ludwig, Anna

Charité Universitätsmedizin Berlin, Center for Cardiovascular Research, Germany

**Aims:**

Estrogen Receptors (ERs) are known to play an important role in the metabolic functions of adipose tissue (AT). Sex-specific differences concerning lipolysis have been reported. For instance, female mice are known to mobilize energy from fat more efficiently than male littermates under exercise conditions. Also, changes in fat distribution and metabolic activity of adipose tissue during menopause are associated with an increasing risk for metabolic and cardiovascular complications in humans. The characterization of molecular mechanisms of estrogen action in AT might help to understand and treat metabolic disorders in the future.

This study investigates the impact of nuclear ERs (a and b) on the expression of Adipose Triglyceride Lipase (ATGL), the rate-limiting lipolytic enzyme in the process of triglyceride-degradation.

**Methods and Results:**

The regulatory impact of ERa and ERb on the expression of ATGL was investigated in 3T3L1-preadipocytes on promoter-, and mRNA level. Cells were transiently transfected with ERa/ERb or PSG5 and stimulated with vehicle vs. selective ERa/ERb agonists PPT/DPN (c=100nM) for 24h.

Promoter-activity of the sequence 3000bp upstream of the first exon of the ATGL-gene was assessed by performing luciferase assay. Transcription increased both ligand-independently under the overexpression of ERa/ERb (1.6-/2.5-fold, p<0.05 vs. PSG5-control), as well as under receptor overexpression and stimulation with the respective ER-agonist (2.7-/3.3-fold, p<0.05 vs. vehicle).

In accordance, bioinformatical promoter analysis performed on the murine sequence revealed 7 putative ERb- and only 1 putative ERa-binding site.

qRT-PCR-analysis demonstrated a significant increase in the amount of ATGL-mRNA by factor 1.3 under vehicle- and factor 1.5 under PPT-stimulation for cells overexpressing ERa vs. PSG5-control (both p<0.05). Similar experiments for the overexpression of ERb showed a significant increase in ATGL-mRNA-amount by factor 3.5 in DPN-stimulated cells vs. PSG5-control (p<0.05). Additionally, in cells overexpressing ERb a significant increase by factor 2.3 could be observed between vehicle- and DPN-stimulation (p<0.05). Most likely attributable to endogenous ERb, a significant 2-fold increase of ATGL-mRNA could be observed under DPN-stimulation in PSG5-control-cells (p<0.05).

**Conclusions:**

The present study demonstrates that both ERs exert positive regulatory actions on the expression of ATGL. The impact of ERb on ATGL promoter-activity and mRNA-expression appears to be stronger when compared to ERa. Further experiments will be required to determine the importance of these findings for an ER isoform-specific regulation of lipolysis.

## 365

**Phenobarbital-mediated tumor promotion in transgenic mice with humanized CAR and PXR**Gavrilov, Alina; Braeuning, Albert; **Schwarz, Michael**

Universität Tübingen, Toxikologie, Germany

The nuclear receptors CAR (constitutive androstane receptor) and, to a lesser extent, PXR (pregnane X receptor) mediate the hepatic effects of phenobarbital (PB) and similarly-acting compounds. While being potent non-genotoxic tumor promoters in rodent liver, humans appear, if at all, to be at much lower risk from PB or related substances. Species differences in the susceptibility to tumor promotion by PB might be attributed to divergent functions of the PB receptors CAR and PXR in mice and humans. Transgenic mice expressing human CAR and PXR were used to detect possible differences between wild type and humanized mice in their response to CAR activation. Two studies were performed: a 28 days study with different concentrations of PB, and an initiation/promotion experiment with a single injection of the tumor initiator N-nitrosodiethylamine preceding chronic PB treatment for 10 months.

Induction of model CAR target mRNAs did not substantially differ between wild type and humanized mice. At high PB doses, hepatic PB contents were higher in the humanized

group. Analysis of liver tumor burden revealed that PB slightly more efficiently promoted tumor growth in wild type mice. In conclusion, the present findings support the hypothesis that human CAR and PXR support tumor promotion in mouse liver to a lesser extent than the murine receptors.

### 366

#### Signaling through ATM and p53 mediates HEMA-induced apoptosis

**Schweikl, Helmut**; Petzel, Christine; Bolay, Carola; Hiller, Karl-Anton; Buchalla, Wolfgang; Krifka, Stephanie

Universitätsklinikum Regensburg, Poliklinik für Zahnerhaltung und Parodontologie, Germany

Resin monomers of dental composites like 2-hydroxyethyl methacrylate (HEMA) induce cell death via apoptosis. The induction of apoptosis is related to the availability of the antioxidant glutathione. A detailed understanding of signaling pathways, however, is unknown. The present study provides insight into the causal relation between oxidative stress, oxidative DNA damage, and the specific signaling pathway leading to HEMA-induced apoptosis in RAW264.7 mouse macrophages. The differential expression of the antioxidant enzymes superoxide dismutase, glutathione peroxidase or catalase in HEMA-exposed cells indicated oxidative stress, which was associated with the cleavage of pro-caspase 3. A 2-fold increase in the amounts of mitochondrial superoxide anions after a 24h exposure to HEMA (6-8 mM) was paralleled by a considerable decrease in the mitochondrial membrane potential. Additionally, transcription-dependent mechanisms of p53-regulated apoptosis were activated, and p53 was translocated from the cytosol to mitochondria. HEMA-induced transcriptional activity of p53 was indicated by increased levels of PUMA (p53 upregulated modulator of apoptosis) in the mitochondrial fraction. A HEMA-induced and oxidative stress-sensitive delay of the cell cycle to indicate DNA damage response occurred independent of the influence of KU55939, a potent inhibitor of ATM (*ataxia-telangiectasia mutated*) activity. However, ATM, a protein kinase which responds to DNA double strand breaks, and the signaling pathway *downstream* were still activated in HEMA-exposed cells. HEMA-induced expression and phosphorylation of the ATM targets H2AX and p53 was reduced in the presence of KU55939. The inhibition of the expression of PUMA in the presence of KU55939 further indicated a direct signaling cascade from ATM to PUMA through p53. Moreover, the percentages of cells undergoing apoptosis drastically decreased in HEMA-exposed cell cultures pre-treated with KU55939. These findings demonstrate that HEMA-induced apoptosis is mediated through the intrinsic mitochondrial pathway as a consequence of p53 activation via ATM signaling upon oxidative DNA damage. Supported by the Deutsche Forschungsgemeinschaft DFG (Schw 431/13-2)

### 367

#### Dynamic interaction between sphingolipid enzymes, S1P and inflammatory cytokine regulation in dendritic cells

**Art, Olga**<sup>1</sup>; **Schwiebs, Anja**<sup>1</sup>; Pfarr, Kathrin<sup>1</sup>; Ranglack, Annika<sup>1</sup>; Ferreirós Bouzas, Nerea<sup>1</sup>; Schreiber, Yannick<sup>1</sup>; Neuber, Corinna<sup>2</sup>; Kleuser, Burkhard<sup>2</sup>; Pfeilschifter, Josef M.<sup>1</sup>; Radeke, Heinfried H.<sup>1</sup>

<sup>1</sup>pharmazentrum frankfurt/ZAFES, Clinic of the Goethe University, Pharmacology and Toxicology, Frankfurt, Germany

<sup>2</sup>University of Potsdam, Institute of Nutritional Science, Dept. Nutritional Toxicology, Nuthetal, Germany

Sphingosine 1-phosphate (S1P) is an immune modulatory lipid mediator and has been implicated in numerous pathophysiological processes. S1P is produced by sphingosine kinase (SphK)-1 and SphK2 and is de-phosphorylated by two S1P phosphatases or irreversibly degraded by a lyase. We recently showed that toll-like receptor (TLR)-4 induced IL-12p70 is selectively counter regulated by SphK1, S1P receptor 1 and its extracellular ligand S1P. On the other hand it has also been shown that S1P acts intracellularly, for example in cell proliferation induced by PDGF. Moreover, intracellular S1P shows inhibiting activity on histone deacetylases HDAC1/HDAC2 and is enhancing the TRAF2/RIP1/NFκB signaling pathway.

To evaluate the role and importance of the action of intracellular S1P in dendritic cells (DCs) we examined the expression profile and activity of S1P lyase (sgpl1), which tightly regulates intracellular S1P levels. Importantly, sgpl1 was dramatically down-regulated on the mRNA level in a time and dose dependent manner upon TLR-stimulation in murine bone marrow-derived DCs differentiated with GM-CSF for seven days. This set of real time PCR data was further confirmed by semi-quantitative PCRs using defined exon-specific primer for murine sgpl1. Subsequent systematic analysis with dose-optimized ligands of TLR 1/2, 5, 2/6, 7/8 and TLR 9 showed a differential pattern of S1P lyase down-regulation. Recent publications suggested that complete S1P lyase deficiency may affect signaling pathways; therefore we quantified a set of relevant cytokines of murine DCs including IL-12p70, IL-23 and IL-6 on protein and mRNA level. Furthermore, due to strong down-regulation of sgpl1, the cells showed increased hexadecenal and decreased S1P concentrations after long term LPS-activation. This has crucial effects on the survival of hyperactivated DCs. In ongoing investigations we are analyzing these effects in more detail.

Given the prominent role of DCs for chronic inflammation and cancerogenesis our studies may unravel modulatory mechanisms of extra- versus intracellular S1P and the respective sphingolipid enzyme regulation, thereby providing specific targets for sphingolipid therapeutics.

### 368

#### Respiratory muscle function blocked by different organophosphorus compounds is recovered by the bispyridinium non-oxime MB327

**Seeger, Thomas**; Worek, Franz; Thiermann, Horst

Bundeswehr Institute of Pharmacology and Toxicology, Experimental Pharmacology, Munich, Germany

#### Introduction:

Oximes are rather inefficient in restoring muscle function blocked by different organophosphorus compounds (OP), e.g. soman. The bispyridinium non-oxime MB327 showed therapeutic efficacy in soman and tabun poisoned guinea pigs in vivo. In addition, positive therapeutic effect of the 4-tert butyl bispyridinium compound MB327 on soman blocked neuromuscular transmission was verified in human and rat respiratory muscles (Seeger et al., 2012). Now, the ability of MB327 to restore tabun, sarin and VX blocked neuromuscular function of rat diaphragms was investigated in vitro.

#### Methods:

In a high throughput system with 12 organ baths force generation of diaphragm hemispheres, stimulated via an indirect electrical field stimulation technique (20, 50, 100 Hz), was determined before and after exposure towards OP and subsequent application of MB327 (1-300 µM) after wash-out of OP. Muscle force was analyzed as time-force integral and expressed as percentage of the control.

#### Results:

Force production was completely blocked by 3 µM sarin, tabun or VX or by 10 µM of the pesticide paraoxon. After wash-out of the OP no recovery of muscle force could be observed. The partial restoration of muscle strength by MB327 was shown with all tested OP. The effect of MB327 was concentration-dependent with the highest activity at 300 µM. Hereby, the recovery of the muscle force was most pronounced at 20 Hz (sarin: 29 ± 8 %, tabun: 28 ± 8 %, VX: 30 ± 6 %, paraoxon: 26 ± 5 %, 300 µM, 20 Hz). At high stimulation frequencies, the restoration of the muscle generation was low to non-existent.

#### Conclusion:

This study showed that MB327 was able to restore in part neuromuscular block induced by different OP in rat diaphragms. Hence, MB327 may be considered as a potential generic antidote in poisoning by structurally different OP.

T. Seeger, M. Eichhorn, M. Lindner, K. V. Niessen, J. E. Tattersall, C. M. Timperley, M. Bird, A. C. Green, H. Thiermann, F. Worek, *Toxicology* 2012, 294 80-84.

### 369

#### Cardiac L-type calcium channel function of mtDNA mutator mice

**Seemann, Wiebke Kirsten**; Matthes, Jan; Herzig, Stefan

Universität zu Köln Institut für Pharmakologie, Germany

L-type Ca<sup>2+</sup> channels (L-VDCCs) belong to the superfamily of voltage-gated ion channels that are widely distributed in the mammalian body and control a lot of physiological functions. For example, influx of Ca<sup>2+</sup> through L-VDCC is required for the contraction of skeletal and smooth muscles as well as for hormone secretion and neurotransmitter release. In cardiomyocytes, the L-type Ca<sup>2+</sup> channel is the main route for extracellular Ca<sup>2+</sup> entry and essential for the maintenance of cardiac excitation and contraction (1). Proper channel activity is necessary for accurate cardiac function, whereas alterations in Ca<sup>2+</sup> channel activity and Ca<sup>2+</sup> homeostasis have been associated with cardiomyopathies resulting in cardiac hypertrophy and heart failure (2). In general, clinical manifestation and the prognosis of cardiac diseases worsen with increasing age. Until now, it is still a matter of debate if cardiac dysfunction is the consequence of improper calcium signalling or vice versa. To answer this question we check L-VDCC function by patch clamp experiments in murine ventricular cardiomyocytes at different stages of age. Therefore we use the mtDNA mutator mouse that expresses a proof-reading-deficient version of the mitochondrial DNA (mtDNA) polymerase PolgA. These mice possess an increased amount of point mutations and deleted mtDNA, resulting in a premature onset of ageing related phenotypes including heart enlargement (3). Beyond the patch clamp perspective, we will quantify L-VDCC expression as well as markers of cardiomyopathy and heart failure (e.g. MHC-beta, BNP) at the mRNA level. These results will be matched with the patch clamp data and might help to improve the knowledge of the pathophysiology of cardiac Ca<sup>2+</sup> handling.

(1) Triggler DJ (2006) L-type Calcium Channels, Voltage-Gated Ion Channels as Drug

Targets, Volume 29, Wiley-VCH Verlag GmbH & Co. KGaA, Weinheim

(2) Benitah JP et al. (2010) L-type Ca<sup>2+</sup> current in ventricular cardiomyocytes. *J Mol Cell Cardiol*; 48: 26-36

(3) Trifunovic A et al. (2004) Premature ageing in mice expressing defective mitochondrial DNA polymerase. *Nature*; 429:417-423

### 370

#### The cAMP dependent transcription factor CREM and its isoform ICER inhibit proliferation of vascular smooth muscle cells

**Seidl, Matthias Dodo**<sup>1</sup>; Hildebrandt, Iris<sup>1</sup>; Wolf, Christian<sup>1</sup>; Steingraber, Annika Katharina<sup>1</sup>; Endo, Shogo<sup>2</sup>; Kojima, Nobuhiko<sup>2</sup>; Schmitz, Wilhelm<sup>1</sup>; Müller, Frank Ulrich<sup>1</sup>

<sup>1</sup>Westfälische Wilhelms-Universität, Institute of Pharmacology and Toxicology, Münster, Germany

<sup>2</sup>Tokyo Metropolitan Institute of Gerontology, Japan

<sup>3</sup>Gunma University Medical School, Maebashi, Japan

The transcriptional regulation mediated by the transcription factor CREM (cAMP responsive-element (CRE) modulator) represents an important mechanism of gene control in vascular smooth muscle cells (VSMCs) and is associated with anti-proliferative effects in the vasculature. The *CreM* gene encodes several short transcriptional repressor isoforms like ICER (inducible cAMP early repressor) and the recently discovered small ICER (smICER) which are rapidly induced by intronic promoters in response to elevated intracellular cAMP levels. In this study we investigated the role of ICER and smICER for the cAMP mediated gene regulation in VSMCs with regard to the regulation of VSMC proliferation by the use of ICER-KO (IKO) mice.

Transfection of immortalized smooth muscle cells (SMC) with *Icer* or *smIcer* promoter driven luciferase reporter gene constructs led to an increased *Icer* (16.3±0.7 fold n=20) and *smIcer* (2.7±0.2 fold n=20) promoter activity after 4h stimulation with forskolin (FSK; an activator of the adenylyl cyclase). Consistently, stimulation of primary VSMCs with FSK led to a 38-fold and 19-fold increase of *Icer* and *smIcer* mRNA levels in primary VSMCs within 2 hours. Overexpression of ICER or smICER proteins in SMCs inhibited 77-84% or 30-45 % of the FSK induced *Icer* and *smIcer* promoter activity (n=4), respectively. Under basal conditions the proliferation rate of IKO VSMCs (13±1 %; 4098 cells/5 isolations) was slightly increased by 12% as compared to WT VSMCs (11±1 %; 4684 cells/5 isolations; \*P<0.05). Since ICER is induced by FSK, we studied the effects of FSK on VSMC proliferation to assess the functional role of ICER under activation of the cAMP-dependent signal transduction pathway. FSK inhibited the proliferation rate of both FSK-IKO (11±1 %, 3490 cells/5) and FSK-WT VSMCs (8±1 %, 4677 cells/5) by 15 and 30% compared to basal conditions. Still the difference between genotypes existed with a 37% higher proliferation rate in IKO.

We conclude (i) that the stimulation of the cAMP dependent signal transduction pathway induces small CREM isoforms like ICER and smICER via intronic promoters in vascular smooth muscle cells, (ii) that ICER and smICER are able to mutually inhibit their own promoters in SMCs, (iii) that ICER exhibits antiproliferative effects in VSMCs, and (iv) that induced antiproliferative effects by activation of cAMP signaling are for the most part independent from CRE-mediated ICER induction. (Supported by the DFG)

### 371

#### Functional characterization of rare and population specific genetic variants in the organic cation transporter OCT1

Seitz, Tina; Stalman, Robert; Dos Santos Pereira, Joao Nuno; Dalila, Nawar; Brockmüller, Jürgen; Tzvetkov, Mladen  
Institut für Klinische Pharmakologie, Göttingen, Germany

The organic cation transporter OCT1 is strongly expressed in the sinusoidal membrane of the human liver and mediates the uptake of drugs into hepatocytes. Common genetic polymorphisms in *OCT1* lead to reduction or even complete loss of OCT1 activity. These polymorphisms can influence the pharmacokinetic of drugs transported by OCT1. Several previously unknown rare *OCT1* polymorphisms have been recently identified by our group during a worldwide genetic analysis of *OCT1*. The aim of this project is the functional characterization of these novel and of previously known rare and population specific genetic polymorphisms.

Nine polymorphisms leading to potentially functional amino acid substitutions in *OCT1* were analyzed: Ser14Phe, Ser29Leu, Pro117Leu, Ser189Leu, Arg206Cys, Thr245Met, Glu284Lys, Gly414Ala and Ile449Thr. The analyses were performed using HEK293 cells stably transfected to overexpress the different *OCT1* variants. Transport measurements were carried out with model *OCT1* substrates (MPP<sup>+</sup>, TEA<sup>+</sup> and ASP<sup>+</sup>) and with clinically used drugs (morphine, metformin, debrisoquine and tropisetron). Cellular localization of the *OCT1* variants was analyzed using immunocytochemistry combined with confocal microscopy.

*OCT1* variants carrying the Ser29Leu and Glu284Lys substitutions lack transport activity for all substrates tested. The variants carrying the Pro117Leu and Gly414Ala substitutions showed no differences compared to wild-type. The remaining variants showed substrate dependent loss of *OCT1* activity, e.g. the *OCT1* variant carrying Thr245Met transported MPP<sup>+</sup>, ASP<sup>+</sup> and debrisoquine, but not TEA<sup>+</sup>, morphine and metformin. The *OCT1* variants carrying the complete loss-of-function polymorphisms Ser29Leu or Glu284Lys were not properly located on the cell membrane. In both cases the *OCT1* protein seems to be retained in the endoplasmic reticulum as suggested by double staining with an ER-specific antibody against calnexin.

In conclusion, this project demonstrated that a number of rare and population specific variants may lead to loss of *OCT1* function. Interestingly, a substantial part of these variants (five out of nine variants tested) showed substrate specific loss of activity that may reflect the poly-specificity of *OCT1* and suggest different substrate binding mechanisms.

### 372

#### Hyperforin is a protonophore and mediates significant H<sup>+</sup> currents

Sell, Thomas Sebastian; Belkacemi, Thabet; Flockerzi, Veit; Beck, Andreas  
Universität des Saarlandes, Experimentelle und Klinische Pharmakologie und Toxikologie, Homburg, Germany

Hyperforin is a pharmacologically active component of the medicinal plant *Hypericum perforatum* (St. John's wort). Part of its action has been attributed to TRPC6 channel activation. Using the whole-cell patch clamp technique, we found that extracellular application of hyperforin induces prominent TRPC6-independent inward and outward

currents in different cell types, including cultured mouse cortical microglia and chromaffin cells, as well as HEK-293 cells. Removal or substitution of extracellular ions does not significantly affect the current-voltage relationship of the hyperforin-induced conductance, whereas changing the extracellular pH results in prominent shifts of its reversal potential. In intact cells hyperforin induces intracellular acidification, and in voltage-clamped cells the changes of intracellular pH depends on the holding potential. Finally, lipid bilayers at the tip of a patch pipette also reveal a proton-dependent conductance upon application of hyperforin. This shows that hyperforin alone is sufficient to act as a protonophore in lipid bilayers. In addition, we show that hyperforin depletes large dense core vesicles in primary chromaffin cells, which require a pH gradient in order to accumulate monoamines. In summary the protonophore properties of hyperforin will contribute essentially to its pharmacological actions.

### 373

#### Non-catalytic subunits, p87 and p101, determine specificity of class I<sub>β</sub> PI3Kγ enzymes

Shymanets, Aliaksei; Prajwal, -; Bucher, Kirsten; Beer-Hammer, Sandra; Harteneck, Christian; Nürnberg, Bernd  
Institut für Experimentelle und Klinische Pharmakologie und Toxikologie, Abteilung Pharmakologie und Experimentelle Therapie, Tübingen, Germany

Class I<sub>β</sub> phosphoinositide 3-kinases (PI3Kγ) control a plethora of fundamental GPCR-driven cellular processes. PI3Kγ comprises one catalytic p110γ subunit, which forms two separate heterodimeric variants by binding to non-catalytic subunits, p87 or p101. Different sensitivity of p87/p110γ and p101/p110γ to stimulation by Gβγ and Ras was reported earlier (Kurig et al., *PNAS*, 2009). Growing experimental data characterizing either p87/p110γ or p101/p110γ place PI3Kγ enzymes into different signalling pathways. However, the cellular and molecular mechanisms which govern the specificity of PI3Kγ enzymes are still obscure.

In a side by side study, we analysed the impact of p87 as well as p101 non-catalytic subunits in forming of heterodimeric p87/p110γ and p101/p110γ. Analysis of interaction of p87 and p101 with p110γ discovered differences in the stability of the heterodimeric complexes. Our data argue for strong binding of p101 to p110γ and a high stability for p101/p110γ, whereas interaction of p87 with p110γ is weaker and hence p87/p110γ complex is less stable. Subsequent analysis of distribution in tissues and evaluation of the expression pattern of p87 and p101 by RT-PCR and immunoblot analysis revealed distinct and characteristic distribution of non-catalytic subunits in various tissues. Whereas p87 was detectable in nearly all tissues studied, p101 showed a more distinct expression pattern. Additionally, expression profile of p87 and p101 changed upon stimulation in human PBMCs. Whereas expression of p101 increased during activation of human PBMCs in a time-dependent manner, expression level of p87 remained unaltered. These findings point to different cellular functions of both enzymes. While the traditional view on p87/p110γ and p101/p110γ discuss both as redundant enzymes, our study provides a new sight considering p87/p110γ as a constitutively expressed and p101/p110γ as an inducibly expressed PI3Kγ. Taken together, our data argue for distinct roles of the non-catalytic subunits in still unknown PI3Kγ pathways.

### 374

#### Redox regulation of protein phosphatase-1 in cardiomyocytes

Singh, Simran; Saadatmand, Ali Reza; Vettel, Christiane; El-Armouche, Ali  
Universitätsmedizin Göttingen, Institut für Pharmakologie, Germany

**Background:** Reactive oxygen species (ROS) are currently viewed as second messengers that control signal transduction by modifying the activity of various kinases and phosphatases. In the heart, recent studies have indicated significant cross-talk mechanisms between phosphorylation and ROS-dependent signaling through redox-sensitive kinases. However, despite the fact that the predominant cardiac Ser/Thr protein phosphatase 1 (PP-1) contains a highly conserved motif with putative reactive cysteine residues in close proximity to the active site, the potential redox-sensitivity of PP-1 has not been addressed yet. In this study, we hypothesized that physiological ROS modulates the oxidation status of PP-1 which in turn affects its activity and the phosphorylation pattern of prominent downstream cardiac regulator phospho-proteins.

**Methods and Results:** The experiments were conducted using either recombinant PP-1 in vitro or in living neonatal rat cardiomyocyte (NRCM) treated with the mild oxidizing agent H<sub>2</sub>O<sub>2</sub>. Our results show that increasing concentrations of H<sub>2</sub>O<sub>2</sub> induces a significant reduction in PP-1 activity. Consistently, the reducing agent Tris (2-carboxyethyl) phosphine (TCEP), when added to recombinant PP-1, reversed H<sub>2</sub>O<sub>2</sub>-induced PP-1 inactivation. Immunoblotting revealed that the phosphorylation status of classical PP-1 downstream target proteins such as phospholamban (PLB) and cardiac myosin binding protein-C (cMyBP-C) were differentially affected by H<sub>2</sub>O<sub>2</sub>, indicating a complex layer of regulation of both redox sensitive kinases and phosphatases. Consistently, the phosphorylation status of protein phosphatase inhibitor-1 (I-1), a crossstalk protein between protein kinase A and PP-1 signaling, showed a bell-shaped phosphorylation response with maximal peak at 100 μM. In order to investigate, whether PP-1 Cys-oxidation status changes in response to ROS, we utilized biotin-conjugated iodoacetamide (BIAM) to label free cysteine thiol following exposure of NRCM cells to H<sub>2</sub>O<sub>2</sub>. Indeed, exposure of NRCM to H<sub>2</sub>O<sub>2</sub> was associated with cysteine oxidations in PP-1. The critical cysteine residues within the PP-1 active site are currently investigated via mass spectrometry.

**Conclusion:** These results demonstrate that physiologically relevant concentrations of H<sub>2</sub>O<sub>2</sub> reduce PP-1 activity, it is however difficult to allocate changes in PP-1 activity to

the phosphorylation status of downstream proteins due to a mutual effect of H<sub>2</sub>O<sub>2</sub> on kinase activity. Our data indicate that oxidative stress exerts its influence on PP-1 activity through oxidative modification of cysteine residues within the structure of PP-1.

375

#### Assessment of the Sensitization Potential of Retapamulin Using the Loose-fit Coculture-based Sensitization Assay (LCSA) in Two Different Setups

**Sonnenburg, Anna**<sup>1</sup>; Kliche, Meike<sup>1</sup>; Frombach, Janna<sup>2</sup>; Stahlmann, Ralf<sup>1</sup>

<sup>1</sup>Charité Universitätsmedizin Berlin, Institut für Klinische Pharmakologie und Toxikologie, Germany

<sup>2</sup>Charité Universitätsmedizin Berlin, Klinik für Dermatologie, Venerologie und Allergologie, Germany

Retapamulin is a pleuromutilin antibiotic used for topical treatment of infections caused by *Staphylococcus aureus* and *Streptococcus pyogenes*. The commercially available ointment contains 1% retapamulin. Some case reports suggest that sensitization from retapamulin may occur. Data from animal experiments or *in vitro* assays studying the sensitization potential of retapamulin have not been published. We have tested retapamulin in two different setups of the LCSA, a sensitization assay developed by our working group (Wanner et al., *ToxicolApplPharmacol* 2010; 245:211). In the standard setup the LCSA consists of a monolayer of primary human keratinocytes cocultured with dendritic cell-related cells (DC-rc) derived from peripheral blood mononuclear cells. Cytokine-supplemented keratinocyte growth medium (KGM-2) is used. The alternative setup uses the human keratinocyte cell line HaCaT grown in DMEM instead of primary cells. By flow cytometric measurement of the maturation marker CD86 on DC-rc the sensitization potential of xenobiotics can be assessed. The half maximal increase of the relative CD86 expression induced by the test compound is used as the main endpoint (EC<sub>50</sub>) in comparison to the control. At the same time, uptake of the viability stain 7-AAD allows an assessment of the irritative potential of the substance. Retapamulin caused a pronounced induction of the CD86 expression in both setups of the LCSA with EC<sub>50</sub> values of 9.3 µmol/l in the standard setup and 11.4 µmol/l in the alternative setup. Substances classified before as "extreme" or "strong" sensitizers, such as dinitrochlorobenzene (EC<sub>50</sub> = 3.0 µmol/l) or trinitrobenzenesulfonic acid (EC<sub>50</sub> = 40 µmol/l), had been tested positive in the alternative setup of the LCSA at similar concentration ranges. Up to a concentration of 100 µmol per liter medium retapamulin caused no significant uptake of 7-AAD. In summary, we showed that the LCSA can be improved by using HaCaT cells cultured in DMEM. Retapamulin gave comparable results with both setups. This is the first report on the effects of retapamulin in an *in vitro* assay developed to study the sensitization potential of xenobiotics.

Wanner et al., *ToxicolApplPharmacol* 2010; 245:211

376

#### The protein kinase DYRK1A phosphorylates p27<sup>Kip1</sup> and Cyclin D1: A new function in neuronal cell cycle exit and differentiation

**Soppa, Ulf**<sup>1,2</sup>; Schumacher, Julian<sup>1</sup>; Florencio Ortiz, Victoria<sup>2</sup>; Tejedor, Francisco J.<sup>2</sup>; Becker, Walter<sup>1</sup>

<sup>1</sup>RWTH Aachen University, Institute of Pharmacology and Toxicology, Germany

<sup>2</sup>Instituto de Neurociencias, Consejo Superior de Investigaciones Científicas (CSIC) y Universidad Miguel Hernandez, San Juan de Alicante, Spain

Dual specificity tyrosine-phosphorylation-regulated kinase 1A (DYRK1A) is encoded on human chromosome 21 and 1.5-fold overexpressed in Down syndrome (DS). Different reports from animal models provide strong evidence that in an altered *DYRK1A* gene dosage results in disturbed neuronal development. Therefore, *DYRK1A* is considered as a candidate gene for the DS associated altered neuronal development and brain function. Thus, normalization of the elevated *DYRK1A* kinase activity is currently investigated as a possible therapeutic option in DS. Nonetheless, the underlying cellular mechanisms how *DYRK1A* affects neuronal development remain largely unknown. Using a human neuronal cell model we therefore have analyzed the effect of *DYRK1A* overexpression on neuronal cell cycle progression and differentiation. We here show that *DYRK1A* stopped proliferation of SH-SY5Y neuroblastoma cells within 24 h dependent on the dosage of overexpression and the kinase activity. Pharmacological inhibition of *DYRK1A* kinase activity attenuated this effect. Analysis by flow cytometry revealed that *DYRK1A* overexpression induced a cell cycle arrest in G<sub>1</sub>-phase. Moreover, we provide evidence that sustained *DYRK1A* overexpression caused premature neuronal differentiation and lead to G<sub>0</sub> cell cycle exit. Furthermore, we found out that *DYRK1A* controls protein stability of Cyclin D1 and the cyclin-dependent kinase (CDK) inhibitor p27<sup>Kip1</sup>, both known to fulfill important functions in neuronal differentiation by regulation of G<sub>1</sub>-G<sub>0</sub> cell cycle transition. *DYRK1A* overexpression rapidly reduced the cellular level of Cyclin D1 by phosphorylating Thr286, which is known to induce proteasomal degradation. Additionally, *DYRK1A* increased the cellular amount of p27<sup>Kip1</sup> by Ser10 phosphorylation dependent protein stabilization. Additionally, we tested the relevance of *DYRK1A* dependent p27<sup>Kip1</sup> Ser10 phosphorylation in brain development. Pharmacological inhibition of endogenous *DYRK1A* activity decreased Ser10 phosphorylation in cultured mouse hippocampal neurons and in embryonic mouse telencephalon. Therefore, our data suggests that *DYRK1A* overexpression induces G<sub>0</sub> cell cycle exit and premature neuronal differentiation by phosphorylation of Cyclin D1 and p27<sup>Kip1</sup>.

Becker W. 2012. Emerging role of DYRK family protein kinases as regulators of protein stability in cell cycle control. *Cell Cycle* 11: 0-5.

Chen J-Y, Lin J-R, Tsai F-C, Meyer T. 2013. Dosage of Dyrk1a Shifts Cells within a p21-Cyclin D1 Signaling Map to Control the Decision to Enter the Cell Cycle. *Molecular Cell* 52: 87-100.

Hämmerle B, Ulin E, Guimera J, Becker W, Guillemot F, Tejedor FJ. 2011. Transient expression of Mnb/Dyrk1a couples cell cycle exit and differentiation of neuronal precursors by inducing p27KIP1 expression and suppressing NOTCH signaling. *Development* 138: 2543-2554.

377

#### Determination of the frequencies of rare mutations in both mitochondrial and nuclear DNA in human cell and tissue samples by random mutation capture assay

**Spielmann, Benjamin**<sup>1</sup>; Schmalbach, Katja<sup>1</sup>; Eckert, Peter<sup>2</sup>; Lehmann, Leane<sup>1</sup>

<sup>1</sup>University of Würzburg, Section of Food Chemistry, Würzburg, Germany

<sup>2</sup>Praxis Prof. Dr. med. Peter Eckert Facharzt für plastische Chirurgie, Würzburg, Germany

Besides nuclear (n) DNA, mitochondrial (mt) DNA is susceptible to mutagenesis, and its mutation frequency (MF) is generally higher. Both mutations in nDNA and mtDNA seem to be involved in pathologies such as cancer; however, little is known about the correlation of mtMFs and nMFs: up to now, the only published data has been determined by sequencing the whole mitochondrial genome and one nDNA gene, an approach, which is not applicable to rare mutations present in only one or a few cells among a lot of wildtype cells.

Thus, the aim of the present study was the determination of spontaneous MFs in both nDNA and mtDNA within the same human cell and tissue sample. A technique applicable both to mt and n DNA is the Random Mutation Capture assay (RMCA), which uses the amplification of uncleaved mutated products after *TaqI* restriction with primers flanking the *TaqI* recognition site. The calculation of MF requires the precise number of the total copies/base pairs screened.

nMF was determined with a modification of a published RMCA for intron 6 of TP53. For the determination of mtMF, an RMCA specific for mtDNA was developed. Human mammary gland tissue (MG) was derived from a healthy woman undergoing cosmetic reduction surgery and commercially available primary AGO fibroblasts were cultured according to the distributors specifications.

For the mtRMCA, the mitochondrial *cytochrome B* gene was chosen due the possibility to place adequate primers in relation to the *TaqI* restriction site and lack of nDNA amplicates indicated by data bank analysis. Reference sequences were generated by PCR, purified, and quantified spectrofluorimetrically with SYBR-Green. Total copy numbers were determined by Taqman PCR with external calibration using reference DNA. Between 9.1\*10<sup>5</sup> and 9.1 copies, the calibration was linear and of homogenous variances and the mean recovery in three independent experiments was 100.0±1.7%. The recoveries of the PCR reactions for mutant identification were 9, 12, and 12 out of 13.6 expected copies.

Applying both the nRMCA and the mtRMCA to DNA isolated from human primary cells and tissue, MFs of 6.9\*10<sup>-7</sup> (AGO cells) and 7.2\*10<sup>-8</sup> per bp (MG), respectively, were determined. In contrast, mtMFs were 6.0\*10<sup>-5</sup> (AGO) and 5.0\*10<sup>-5</sup> per bp (MG), resulting in mtMF:nMF ratios of 87 (AGO) and 694 (MG).

In conclusion, the parallel determination of spontaneous MFs both in nDNA and mtDNA derived from cultured primary cells and healthy human tissue was achieved for the first time, enabling the future investigation of the role of spontaneous and induced mtMFs and nMFs both *in vitro* and *in vivo*.

378

#### Potential Ways To Decrease Environmental Contaminations Of Antimicrobial Agents From Animal Livestock

Zessel, Katrin<sup>1</sup>; Kietzmann, Manfred<sup>1</sup>; Hartung, Jörg<sup>2</sup>; Schulz, Jochen<sup>2</sup>; **Stahl, Jessica**<sup>1</sup>

<sup>1</sup>Stiftung Tierärztliche Hochschule Hannover, Institut für Pharmakologie, Toxikologie und Pharmazie, Germany

<sup>2</sup>Stiftung Tierärztliche Hochschule Hannover, Institut für Tierhygiene, Tierschutz und Nutztierethologie, Germany

Introduction: The aim of the present study was to determine potential ways to minimize environmental contaminations by antibacterial agents, since their frequent use of antimicrobials in livestock farming poses the risk of the contamination of the environment. Therefore, the effect of different pharmaceutical formulations on the entry of the test compound sulfadiazine into the environment was investigated in pigs.

Materials and Methods: Six pigs were orally treated with two formulations (powder vs. pellets) of sulfadiazine over four days to obtain information about the effect of different formulations on the environmental contamination. To study a carry over via the environment, the treated pigs were replaced by non-treated pigs (sentinels) on day 5. Blood and urine samples of the pigs and samples of sedimented dust in the stable were analysed for sulfadiazine, as well as air filters installed apart from the housing compartment. UV/VIS-High performance liquid chromatography was used for analysis.

Results: The comparison of powder and pellet feeding results in massive differences in the environmental pollution rates, although contrastable plasma and urine levels were obtained. Pellets decrease the entry of sulfadiazine into the air. Sentinels housing in a contaminated stable after powder treatment of sulfadiazine exhibit traces of sulfadiazine in plasma and urine.

Discussion: Using pharmaceutical formulations like pellets, the environmental pollution of sulfonamides can be diminished significantly compared with powder due to a severe reduction of dust during the feeding process. Thus, the development of bacterial resistance due to the uptake of subtherapeutic dosages of antimicrobial agents can be avoided.

The study was supported by the "Deutsche Bundesstiftung Umwelt" DBU, Osnabrueck, Germany.

## 379

**DNA methyl transferase inhibition in experimental cardiomyocyte hypertrophy in engineered heart tissue leads to extensive transcriptional changes and improved contractile function**

**Stenzig, Justus**<sup>1,2</sup>; Hirt, Marc N.<sup>1,2</sup>; Hensel, Jan-Tobias<sup>1,2</sup>; Müller, Christian<sup>3,2</sup>; Hansen, Arne<sup>1,2</sup>; Eschenhagen, Thomas<sup>1,2</sup>

<sup>1</sup>Universitätsklinikum Hamburg-Eppendorf, Institut für Experimentelle Pharmakologie und Toxikologie, Germany

<sup>2</sup>Deutsches Zentrum für Herz-Kreislauf-Forschung e.V., Standort Hamburg/Kiel/Lübeck, Germany

<sup>3</sup>Universitätsklinikum Hamburg-Eppendorf, Klinik und Poliklinik für Allgemeine und Interventionelle Kardiologie, Germany

**Purpose:** Cardiomyocyte hypertrophy can be investigated in engineered heart tissue (EHT) subjected to an increased afterload for 7 days. This not only leads to cellular hypertrophy and associated functional and transcriptional alterations but also to highly dynamic DNA methylation changes in promoter regions of hypertrophy-associated genes. The hypertrophy associated impairment of contractile function can be attenuated by DNA methyl transferase (DNMT) inhibition. To assess if this treatment regulates transcription of key pathways of hypertrophy we investigated the influence of the DNMT inhibitor RG108 on the transcriptome of EHTs.

**Methods:** EHTs from neonatal rat cardiomyocytes in a fibrin matrix were cultured for 2 weeks between 2 flexible hollow silicone mountings in a 24-well cell culture format. When the EHTs displayed coherent beating activity the mounting posts were stiffened by inserting metal braces, acutely increasing the resistance in one group of EHTs ("afterload enhancement", AE), another group was left unmodified (CTR). AE and CTR EHTs were either treated with the DNMT inhibitor RG108 (80 µM) or vehicle only. Force, contraction velocity (CV) and relaxation velocity (RV) were analyzed before and after a 7-day intervention. RNA from 5 EHTs per group was subjected to gene expression micro-array analysis (Affymetrix). Data was analyzed by two-way ANOVA, adjusted for multiple testing and clustered and mapped using Partek Genomic Suite and Ingenuity software.

**Results:** Untreated AE-EHTs displayed a drop of 25% in force, 32% in CV and 43% in RV, respectively as compared to CTR. RG108 attenuated this impairment of contractile function by 40% (force), 38% (CV) and 22% (RV) respectively, but had no effect in CTR. Transcriptional changes induced by RG108 treatment map to pathways involved in energy metabolism and regulation of calcium handling, contractility and hypertrophy. Genes clustered largely independently of those regulated by afterload enhancement.

**Conclusion:** A DNMT inhibitor can ameliorate hypertrophy associated contractile dysfunction *in vitro*. RG108 treatment leads to transcriptional alterations that map to relevant pathways. Whereas a mere attenuation of AE-induced transcriptional changes could likely be caused by mechanisms other than direct transcriptional regulation, the regulation of a gene programme partially distinct from the hypertrophic gene programme suggests a specific epigenetic mechanism by which contractile function is affected.

## 380

**Protein expression profiling of TRPV6 channel proteins in adult mice**

**Stoerger, Christof**; Schalkowsky, Pascal; Bentrícia, Teqiyya; Weißgerber, Petra; Flockerzi, Veit

Universität des Saarlandes, Experimentelle und Klinische Pharmakologie und Toxikologie, Homburg, Germany

TRPV6 (TRP channel, vanilloid type 6) belongs to the TRP superfamily and is the ion-conducting subunit of a cation channel highly selective for calcium (Ca<sup>2+</sup>) ions. After overexpression of its cDNA in cell lines like HEK or COS, TRPV6 forms plasmalemmal ion channels leading to Ca<sup>2+</sup> influx as long as the intracellular Ca<sup>2+</sup> concentration is kept negligibly low by EGTA or comparable chelators. Recently TRPV6 channels have been shown to be critical for Ca<sup>2+</sup> absorption from the lumen of the epididymal duct and the prostate in mice [1, 2] indicating that TRPV6 works as an epithelial Ca<sup>2+</sup> uptake channel in these tissues. TRPV6 transcripts were identified in human syncytiotrophoblasts of placenta, pancreatic acinar cells, salivary gland cells and cancerous prostate [3], but only little is known on the TRPV6 function in these cells and tissues. In addition knowledge on the endogenous TRPV6 proteins and their expression patterns in mouse tissues is scarce, most probably because of the low abundance of TRPV6 proteins. In fact, no direct protein sequence data have been so far obtained from mouse tissues. Accordingly, a major goal of our work is to identify the TRPV6 protein in various mouse tissues and cells and to reveal the TRPV6 protein sequences present *in vivo*. Specific locations of the TRPV6 protein within the organism may show up which could generate new hypotheses about possible functions of TRPV6 in these cells/tissues.

During the last years we have generated several polyclonal and monoclonal antibodies for TRPV6. Most of these antibodies do readily recognize the TRPV6 protein in Western blots after expression of its cDNA in HEK or COS cells. However, it happened to be much more challenging to identify TRPV6 proteins using protein fractions from mouse tissues. By systematically varying protein isolation procedures we developed an antibody-based affinity purification scheme which allows TRPV6 proteins to be enriched from mouse tissues. The enriched TRPV6 protein is readily detected in Western blots by antibodies. From the enriched protein fractions we identified TRPV6 proteins by coupled mass spectrometry in various mouse tissues including epididymis, prostate, placenta and pancreas. We are currently trying to get an estimate of TRPV6 protein abundance in these tissues and to characterize in more detail its cellular and subcellular localization.

[1] Weissgerber et al. (2011) *Sci Signal*, 4(171) ra27; [2] Weissgerber et al. (2012) *J Biol Chem* 287, 17930-17941; [3] Wissenbach et al. (2001) *J Biol Chem* 276, 19461-19468

## 381

**Role of CysLT<sub>1</sub> receptors as novel mechanosensors mediating myogenic vasoconstriction**

**Storch, Ursula**; Blodow, Stephanie; Gudermann, Thomas; Mederos Y Schnitzler, Michael

Ludwig-Maximilians-Universität München, Walther-Straub-Institut für Pharmakologie und Toxikologie, Germany

G-protein coupled receptors and especially angiotensin II AT<sub>1</sub> receptors are discussed as mechanosensors in vascular smooth muscle cells (VSMCs) mediating myogenic vasoconstriction. Analyzing myogenic tone of isolated murine mesenteric arteries of AT<sub>1A</sub> and AT<sub>1B</sub> receptor double gene-deficient (AT<sub>1AB</sub><sup>-/-</sup>) mice *ex vivo* we found a hyper-reactivity of these arteries in the low pressure range up to 70 mmHg and a decreased myogenic tone at higher pressures up to 120 mmHg. Performing a gene expression array we identified high mRNA expression levels of cysteinyl leukotriene 1 receptor (CysLT<sub>1</sub>R) in AT<sub>1AB</sub><sup>-/-</sup> compared to wild-type mesenteric arteries which was verified using a qPCR approach. Pharmacological blockade of CysLT<sub>1</sub>Rs with pranlukast significantly reduced myogenic tone not only in AT<sub>1AB</sub><sup>-/-</sup> but also in wild-type arteries suggesting that these receptors are generally involved in myogenic vasoconstriction. Furthermore, in wild-type arteries additional blockade of AT<sub>1</sub> receptors with candesartan resulted in an additive reduction of myogenic tone. To analyze whether CysLT<sub>1</sub>Rs are intrinsically mechanosensitive, calcium imaging experiments were performed with Fura-2 loaded HEK293 cells over-expressing CysLT<sub>1</sub>Rs and with isolated mesenteric VSMCs. Hypoosmotically induced membrane stretch induced calcium transients that were significantly reduced by pranlukast indicating that these receptors are intrinsically mechanosensitive. Moreover, the G<sub>q/11</sub> protein inhibitor YM254890 was used to analyze the involvement of G<sub>q/11</sub> proteins in myogenic vasoconstriction and led to a severe reduction of myogenic tone to the same extent as induced by application of pranlukast plus candesartan. These findings demonstrate that myogenic tone is mainly mediated by mechanosensitive AT<sub>1</sub> and CysLTR<sub>1</sub> receptors via G<sub>q/11</sub> protein activation.

## 382

**Characterization of G<sub>i/o</sub>-coupled receptors using a cAMP-sensor based FRET and a Kir channel based electrophysiological approach**

**Straub, Julie**; Storch, Ursula; Gudermann, Thomas; Mederos Y Schnitzler, Michael; Walther-Straub-Institut für Pharmakologie und Toxikologie, München, Germany

To functionally characterize different GPCR-subtypes (G<sub>i/o</sub>, G<sub>s</sub>) in more detail we performed a fluorescent approach with a cAMP-sensitive reporter coupled to a FRET-pair, the ECFP/EYFP-flanked cAMP sensor Epac. This sensor is commonly used to measure cAMP increases upon G<sub>s</sub>PCR activation. We aimed to analyze whether this sensor might be also useful to monitor G<sub>i/o</sub>-protein activation. For this, HEK293 cells transiently over-expressing the G<sub>i/o</sub>-protein coupled adrenergic α<sub>2A</sub> receptor and the cAMP sensors EYFP-Epac1-ECFP or EYFP-Epac2-ECFP were analyzed. After incubations with either forskolin, IBMX or bromo-cAMP agonist stimulation with noradrenalin caused an increase in FRET signals corresponding to a decrease of cAMP levels. Furthermore, we replaced the ECFP by mTurquoise2, which gave higher quantum efficiency, photostability and strictly single-exponential fluorescence decay. In addition, EYFP was exchanged by mVenus to obtain less sensitivity to pH and Cl<sup>-</sup> changes. First measurements with HEK293 cells expressing the G<sub>s</sub>-protein coupled adrenergic β<sub>2</sub> receptor with mVenus-Epac1/2-mTurquoise indicate that the new sensors are functional. To substantiate these findings, we performed whole-cell measurements with HEK293 cells over-expressing G<sub>i/o</sub>-protein coupled 5-HT<sub>1B</sub> receptors and Kir3.1/Kir3.2 or Kir3.1/Kir3.4 channel complexes that are activated by β dimers of G<sub>i/o</sub>-proteins following receptor activation. Agonist stimulations with serotonin resulted in profound current increases. Altogether, our results demonstrate that a FRET based approach using the cAMP sensor Epac is as suitable to determine G<sub>i/o</sub>-protein activation as an electrophysiological approach monitoring Kir channel activation.

## 383

**Mutational analysis of A<sub>1</sub> and A<sub>2A</sub> receptor dynamics via FRET measurements**

**Stumpf, Anette Dora**<sup>1</sup>; Ziegler, Nicole<sup>1</sup>; Dang, Tu<sup>2</sup>; Schmitt, Saskia<sup>2</sup>; Zabel, Ulrike<sup>2</sup>; Lohse, Martin J.; Hoffmann, Carsten<sup>1</sup>

<sup>1</sup>Institut für Pharmakologie, Rudolf Virchow Zentrum, Bio Imaging Center, Würzburg, Germany

<sup>2</sup>Institut für Pharmakologie, Würzburg, Germany

The recently published crystal structures of the adenosine A<sub>2A</sub> receptor in the active and inactive state have revealed static endpoints of the conformational changes associated with the activation process. To investigate the activation dynamics we looked at the ligand binding behavior of two different adenosine receptor subtypes via fluorescence resonance energy transfer (FRET). Experiments were done with a modified A1 receptor (A1R) and A2AR sensor. Both sensors were designed by fusion of the cyan fluorescent protein (CFP) to the C-terminus of the receptor and insertion of the fluorescent arsenical hairpin binder (FIAsH) motif into the third intracellular loop. Next, based on the ligand binding pocket revealed from the crystal structure of the A2AR we created ten individually mutated receptor sensors for each receptor subtype. To compare the dynamic binding behavior, we established HEK293 cell lines stably expressing these receptor sensors. We investigated the changes in FRET ratio for all mutants in living

cells by generating concentration response curves for adenosine and two receptor subtype specific ligands. Based on their effects we identified three different classes of mutations. One class causes problems in membrane localization at the A1R but not the A2AR, and this effect could be rescued by 24h incubation with theophylline. A second group of mutations is involved in binding of the ribose moiety and has significantly stronger effects in the A1R compared to the A2AR. The third class consists of mutants that are involved in binding of the adenine moiety and have similar effects for adenosine and theophylline binding at the A2AR. Thus, our study provides evidence that the same amino acids serve different functions within the A1R and A2AR ligand binding pocket. In summary the different signal amplitudes are indicative for a different activation behavior of the A1R and A2AR and thus our study gives new insight into the A1R- structure.

### 384

#### Mobile phone radiation and the hematopoietic system: effects in HL-60 cells and hematopoietic stem cells

**Taichrib, Katharina**<sup>1</sup>; Hintzsche, Henning<sup>1</sup>; Rohland, Martina<sup>2</sup>; Baaske, Kai<sup>2</sup>; Kleine-Ostmann, Thomas<sup>2</sup>; Schrader, Thorsten<sup>2</sup>; Stopper, Helga<sup>1</sup>

<sup>1</sup>Universität Würzburg, Institut für Pharmakologie & Toxikologie, Germany

<sup>2</sup>Physikalisch-Technische Bundesanstalt, Braunschweig, Germany

Today, mobile phones are used worldwide to a huge amount. Therefore questions concerning electromagnetic radiation and its potential to affect biological systems at low intensity levels are of great interest. Many studies have been performed to investigate this issue but no complete consensus has been reached so far. Most of the investigations do not indicate a harmful potential of this radiation, but two questions remain open, i.e. long-term effects and specific effects on children. It has been demonstrated that in comparison to adults, children absorb far higher doses of mobile phone radiation in the skull, particularly in the bone marrow, where hematopoiesis takes place. These absorptions occasionally exceed the recommended safety limits. The aim of this study is to elucidate, whether cells of the hematopoietic system can be affected by different forms of mobile phone radiation.

As biological system, two cell types are investigated, HL-60 cells as an established cell line, and hematopoietic stem cells. Cells are irradiated with frequencies of the major technologies, GSM (900 MHz), UMTS (1.950 MHz) and LTE (2.535 MHz). LTE modulation is now commonly applied but has not been studied sufficiently so far. The exposure takes place for a short and a long period and with different intensities ranging from 0 to 4 W/kg. Studied endpoints include apoptosis, cell cycle, differentiation, DNA damage, DNA repair, epigenetics and oxidative stress.

Results of irradiated HL-60 cells did not reveal any changes in the endpoints, neither after short-term nor after long-term exposure. Investigations with hematopoietic stem cells are still in progress. These results will also be presented and discussed.

### 385

#### mRNA as a pharmacological target of platinum-containing drugs

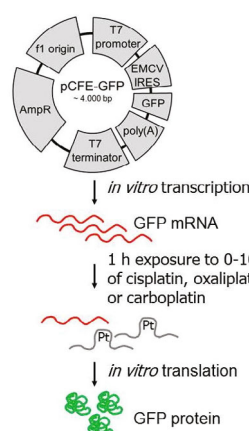
**Theile, Dirk**; Becker, Jonas Philipp; Weiß, Johanna  
Universitätsklinik Heidelberg, Abt. Klinische Pharmakologie und  
Pharmakoepidemiologie, Germany

DNA is considered the preferential target of platinum containing cytostatics such as cisplatin, oxaliplatin, and carboplatin. Despite profound knowledge on the interaction between platinum drugs and DNA, there is little data on the interaction with mRNA and even less on the potential differences among these antineoplastic agents to inhibit protein synthesis.

We therefore established an *in vitro* translation system using *in vitro* transcribed mRNA encoding green fluorescent protein (GFP) to evaluate the effects of exposure of GFP mRNA to 0 – 100  $\mu$ M of cisplatin, oxaliplatin, or carboplatin. We additionally investigated the interaction between these drugs and mRNA through evaluation of crossing-points during quantitative real-time polymerase chain reactions.

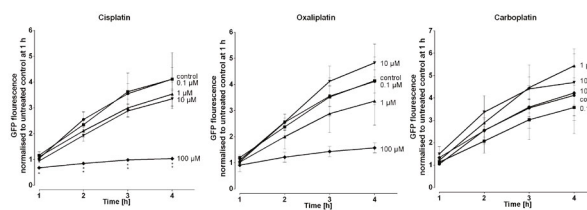
In contrast to oxaliplatin or carboplatin, 100  $\mu$ M cisplatin significantly increased crossing-points by about 3 cycles ( $p < 0.01$ ) and profoundly attenuated translation of GFP mRNA ( $p < 0.05$ ). Oxaliplatin showed a trend to reduce GFP mRNA translation, whereas carboplatin entirely failed to influence it.

In conclusion, this study for the very first time documents different effects of platinum cytostatics on mRNA translation and demonstrates mRNA to be a functionally relevant target of at least cisplatin.



#### Experimental procedure:

Scheme describing the experimental procedure



#### Translation inhibition:

Inhibition of GFP mRNA translation by cisplatin, oxaliplatin, and carboplatin.

### 386

#### Signaling via IRAG regulates platelet development in mice

**Huettnner, Johannes Philip**; **Thoma, Julia**; Schinner, Elisabeth; Schlossmann, Jens  
University of Regensburg, Pharmacology and Toxicology, Institute of Pharmacy,  
Germany

Platelets are produced primarily in the bone marrow by budding off from megakaryocytes. These megakaryocytes in turn develop from hematopoietic stem cells after stimulation with thrombopoietin and different cytokines. In this study we aimed to get insight in the role of the inositoltrisphosphate-receptor associated cGMP-kinase substrate (IRAG) for the development of platelets.

In IRAG knockout (IRAG-KO) mice we found an increased number of platelets circulating in the blood compared to wild type (WT) mice. Furthermore, spleen and bone marrow from IRAG-KO and WT mice was analysed to evaluate the number of megakaryocytes. Spleen and femuri were fixed in a 2% paraformaldehyde solution. To allow microtome sectioning of femuri, they had to be decalcified in EDTA-solution for 1 week prior to fixation and dehydration. The dehydrated organs were embedded in paraffin, cut and stained with hematoxyline and eosin. Microscopic analysis of the stained sections showed a reduced number of megakaryocytes in bone marrow and spleen of IRAG-KO mice compared to WT.

Subsequently we generated a platelet/megakaryocyte-specific IRAG-KO by crossbreeding IRAG-flox (IRAG-L2L2) with mice expressing CRE-recombinase under the platelet/megakaryocyte-specific platelet factor 4 (PF4) promoter. In these platelet/megakaryocyte-specific IRAG-KO mice we observed the same rise in platelet count and decrease in megakaryocyte number in bone marrow and spleen sections. These observations imply a direct regulating effect of IRAG on platelet formation and maturation of megakaryocytes.

### 387

#### Genotoxic properties of *Alternaria* toxins in terms of topoisomerase interactions and DNA repair mechanisms

**Tiessen, Christine**; Gehrke, Helge; Kropat, Christopher; Pahlke, Gudrun; Marko, Doris  
Universität Wien, Institut für Lebensmittelchemie, Austria

*Alternaria* toxins belong to the so-called emerging mycotoxins on account of their frequency of occurrence and gaining toxicological concern. Alternariol (AOH) and

altertoxin-II (ATX-II) possess genotoxic properties. Concerning AOH, it could be confirmed that topoisomerase poisoning is one mode of action which contributes to its genotoxicity. Additionally, it is known that the topoisomerase-specific repair factor tyrosyl-DNA-phosphodiesterase-1 (TDP1) is involved in the repair processes of damaged DNA. But so far, the whole mechanism could neither be completely clarified for both. Hence, the question was addressed whether interference with topoisomerase II might play a role for the genotoxicity of ATX-II. Additionally, the role of further DNA repair pathways for the extent of DNA damage by AOH was investigated. The decatenation assay of AOH and ATX-II showed a loss of activity of topoisomerase II in a comparable concentration range. Enhanced levels of covalent DNA-topoisomerase II complexes could also be detected for AOH in HT29 cells, thus acting as a topoisomerase poison in DNA damaging concentrations. In contrast, genotoxic concentrations of ATX-II did not exhibit any effect on the stability of these complexes, indicating that interference with topoisomerases does not play a relevant role. These differences in genotoxic mechanisms were displayed in the activation of p53. AOH increased p53 phosphorylation in DNA damaging concentrations whereas ATX-II did not affect p53 phosphorylation despite substantial increase in tail intensity in the comet assay. These results and the persistence of DNA damage after 24 h imply that DNA lesions formed by ATX-II are not detected by the DNA-repair machinery. In contrast to ATX-II, cells incubated with AOH showed a loss of tail intensity after 3 h, leading to the assumption of an activation of DNA repair pathways. However, microarray and qPCR analysis did not indicate substantial impact of AOH on the transcription of key elements of DNA repair pathways. Even so, siRNA-experiments indicate that, in addition to TDP1, the expression of other elements of the DNA repair machinery as exemplified by the 70 kDa Ku autoantigen and proliferating-cell-nuclear-antigen are relevant for AOH-mediated DNA damage. In conclusion, topoisomerase poisoning by ATX-II does not play a relevant role in genotoxicity, whereas DNA strand breaks induced by AOH after 1 h can be associated with topoisomerase poisoning, thus being a substrate to the respective DNA-repair machinery.

Tiessen, C., Gehrke, H., Kropat, C., Schwarz, C., Bächler, S., Fehr, M., Pahlke, G. and Marko, D., 2013. Role of topoisomerase inhibition and DNA repair mechanisms in the genotoxicity of alternariol and altertoxin-II. *World Mycotoxin Journal* 6: 233-244.

### 388

#### Increased function of the presynaptic inhibitory cannabinoid CB<sub>1</sub> receptors in DOCA-salt hypertensive rats

**Toczek, Marek**<sup>1</sup>; Grzęda, Emilia<sup>1</sup>; Schlicker, Eberhard<sup>2</sup>; Karabowicz, Piotr<sup>1</sup>; Malinowska, Barbara

<sup>1</sup>Medical University of Białystok, Department of Experimental Physiology and Pathophysiology, Poland

<sup>2</sup>University of Bonn, Institute of Pharmacology and Toxicology, Germany

The level of the endocannabinoid anandamide in the plasma and the expression of the cannabinoid CB<sub>1</sub> receptors in the myocardium, aortic endothelium and brain increase in hypertensive rats. Presynaptic CB<sub>1</sub> receptors inhibit the neurogenic vasopressor response. Thus, the aim of our study was to examine whether hypertension affects the sympathetic transmission to vessels via the presynaptic inhibitory CB<sub>1</sub> receptor. Hypertension (DOCA-salt model) was induced by deoxycorticosterone acetate, high salt diet and uninephrectomy. The study was performed on vagotomized and pitthed rats, in which basal diastolic blood pressure (DBP) and heart rate were significantly lower than in the control group (rats after uninephrectomy fed a standard diet). Increases in DBP were induced four times (S<sub>1</sub>-S<sub>4</sub>). Electrical stimulation (0.75 Hz, 1 ms, 50 V, 15 impulses) of the preganglionic sympathetic nerve fibers stronger elevated DBP in S<sub>1</sub> in control than in DOCA-salt rats. Intravenous injection of phenylephrine (0.01 μmol/kg) induced similar increases in DBP in both groups. The cannabinoid receptor agonist CP55940 given in increasing doses (0.01, 0.1 and 1 μmol/kg) before the three subsequent stimulations did not inhibit the increases in DBP induced by phenylephrine. In contrast, it dose-dependently inhibited the neurogenic vasopressor response. This inhibitory effect was 20, 30 and 35%, respectively in the control group and was stronger or tended to be stronger in DOCA-salt rats, amounting to 30, 55 and 50% respectively. The inhibitory influence of CP55940 was prevented by the CB<sub>1</sub> receptor antagonist AM251 (3 μmol/kg). Moreover, AM251 enhanced the electrically induced increases in DBP during S<sub>3</sub> and S<sub>4</sub> in DOCA rats, but not in control rats. Our results demonstrate that cannabinoids stronger inhibit the neurogenic vasopressor response in DOCA-salt hypertensive rats than in normotensive rats, and that this effect occurs via presynaptic CB<sub>1</sub> receptors localized on postganglionic and/or preganglionic sympathetic nerve fibers innervating resistance vessels. This phenomenon might play a protective role in hypertension.

### 389

#### Improvement and standardization of the pilocarpine model of temporal lobe epilepsy in rats

**Töllner, Kathrin**<sup>1,2</sup>; Brandt, Claudia<sup>1,2</sup>; Löscher, Wolfgang<sup>1,2</sup>

<sup>1</sup>Tierärztliche Hochschule Hannover, Institut für Pharmakologie, Toxikologie und Pharmazie, Germany

<sup>2</sup>Zentrum für Systemische Neurowissenschaften, Hannover, Germany

Diverse brain insults, including traumatic brain injury, tumors and prolonged acute symptomatic seizures, such as status epilepticus (SE), have the potential to induce the development of epilepsy, termed epileptogenesis. Epileptogenesis can be studied in post-SE models of temporal lobe epilepsy, e.g. the rat pilocarpine model [1]. The goal of anti-epileptogenesis research is to identify therapeutic interventions that prevent,

interrupt or reverse the epileptogenic process. Therefore, a potentially anti-epileptogenic drug or a cocktail of drugs can be administered after a pilocarpine-induced SE, i.e. during the latent period before spontaneous recurrent seizures (SRS) occur.

In order to reduce animal numbers, costs and labour, the ideal model has a high percentage of rats experiencing SE and a high incidence of SRS after a defined latent period. Furthermore, only a reliable SE termination after a defined SE length without recurrence of seizure activity renders animals with comparable insult severities for valuable anti-epileptogenesis studies. Different modifications of the pilocarpine model (lithium pre-treatment, repeated low-dose injection instead of pilocarpine bolus, SE termination after a defined SE length) have already resulted in reduced mortality [2; 3; 4].

We now tried a) to optimize SE induction by intraperitoneal pilocarpine, b) to standardize SE termination, and c) to determine the critical duration of SE for induction of epileptogenesis with brain damage and behavioural alterations.

Our findings were:

- A more individualized dosing scheme, i.e. intraperitoneal injection of a pilocarpine bolus plus repeated low-dose injections, renders in a higher percentage of rats with SE.
- A three-step SE termination scheme, i.e. diazepam, phenobarbital and scopolamine for acute termination and up to 8 hours later via different administration routes, results in a true and reliable SE termination.
- A pilocarpine-induced SE leads to significant neurodegeneration in the hilus of the hippocampus with a trend for reduced neurodegeneration in a shorter SE. A SE duration of 60 min is too short to induce epileptogenesis, 120 min result in a poor general health state or death, but 90 min seem to be effective rendering > 70% of spontaneously epileptic rats.

Currently, we are determining the length of the latent period in the modified lithium-pilocarpine model.

This study was supported by a grant of the Deutsche Forschungsgemeinschaft FOR 1103.

[1] TURSKI et al. 1983; *Behav Brain Res* 9:315-35

[2] JOPE et al. 1986; *Exp Neurol* 91:471-80

[3] JOPE et al. 1986; *Exp Neurol* 93:404-14

[4] GLIEN et al. 2001; *Epilepsy Res* 46:111-9

### 390

#### Human model of oxidative stress based on oral paracetamol administration

**Tretlin, Arne**<sup>1</sup>; Modun, Darko<sup>2</sup>; Madunic, Sanja<sup>3</sup>; Vukovic, Jonatan<sup>3</sup>; Radman, Maja<sup>3</sup>; Jordan, Jens<sup>1</sup>; Tsikas, Dimitrios<sup>1</sup>

<sup>1</sup>Hannover Medical School, Institute of Clinical Pharmacology, Germany

<sup>2</sup>University of Split, Department of Pharmacology, Croatia

<sup>3</sup>University Hospital Split, Department of Internal Medicine, Croatia

Reactive oxygen species (ROS) and reactive nitrogen species (RNS) react with biomolecules and alter their physiological functions in all types of cells and in extracellular spaces. Therefore, oxidative stress (OS) is central to human health and disease. OS is commonly quantified by measuring in biological samples the concentration of particular fingerprints left by ROS and RNS on biomolecules, the so called biomarkers of OS. Thus far, there is no human model of OS. Our goal was to develop a human OS model that could safely be applied in healthy subjects and in patients. In view of the favorable pharmacological and chemical properties of paracetamol, we thought that oral administration of paracetamol (e.g., 5 mg/kg) and measurement of di-paracetamol and 3-nitro-paracetamol in blood or urine may represent a suitable model of study OS in vivo in humans. Ten healthy normolipidemic, nonsmoking male volunteers (20-35 ys; BMI 24.2 ± 1.8 kg/m<sup>2</sup>) taking no medications randomly consumed either placebo or a 500-mg paracetamol tablet in a cross-over design. Paracetamol, di-paracetamol and 3-nitro-paracetamol were measured in plasma and urine samples by GC-MS/MS and LC-MS/MS methods. In the paracetamol group, we identified the occurrence of di-paracetamol and 3-nitro-paracetamol (Fig. 1) of which the pharmacokinetic profiles in plasma and urine were very similar to those of paracetamol (Fig. 2). In the paracetamol group, the molar ratios of these metabolites to unchanged paracetamol were several orders of magnitude smaller. Measurement of di-paracetamol and 3-nitro-paracetamol in plasma and/or urine upon oral paracetamol administration at t<sub>max</sub> or other time points may serve as a model of OS in health and disease.

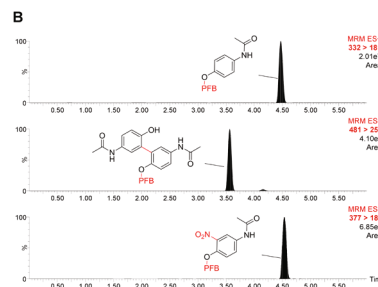


**Fig. 1:** LC-MS/MS chromatograms (positive ESI) obtained by SRM of m/z 332 to m/z 181 for APAP, m/z 481 to m/z 258 for (APAP)<sub>2</sub>, and m/z 377 to m/z 181 for NO<sub>2</sub>-APAP as pentafluorobenzyl derivatives.



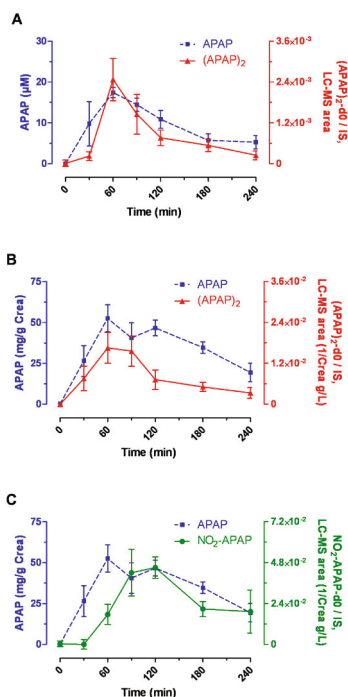


**Fig. 2:** Concentration time curves for (A) paracetamol (APAP) and di-paracetamol (APAP)<sub>2</sub> and for (B, C) 3-nitro-paracetamol NO<sub>2</sub>-APAP in plasma and urine of 10 healthy subjects taken 5-7 mg/kg paracetamol.

### 391

#### Non-targeted Metabolomics in a cell model for the Lesch-Nyhan Syndrome

**Tschirner, Sarah Kristin**<sup>1</sup>, Bähre, Heike<sup>1,2</sup>, Seifert, Roland<sup>1</sup>, Kaever, Volkhard<sup>1,2</sup>

<sup>1</sup>Institute of Pharmacology, Hannover Medical School, Germany

<sup>2</sup>Research Core Unit Metabolomics, Hannover Medical School, Germany

Lesch-Nyhan syndrome (LNS) is an X-chromosomal monogenic disorder characterized by hyperuricemia and neuropsychiatric symptoms such as severe motor handicap, intellectual disability and self-injurious behaviour. The underlying defect is a congenital deficiency of the purine salvage enzyme hypoxanthine-guanine phosphoribosyl transferase (HPRT) [1]. Whereas the occurrence of hyperuricemia can be well explained, the relationship between impaired HPRT activity and the neurological symptoms of LNS remains to be understood.

Various cell and animal models have been applied to elucidate the pathophysiology of the neurological and behavioural anomalies of LNS [2]. We have described earlier several metabolic alterations of proliferating rat B103 neuroblastoma HPRT knockout compared to wild type cells [3].

In the present study, both B103 cell lines were grown under either proliferating or resting conditions and the resulting metabolomes were compared in a non-targeted metabolomic approach by high performance liquid chromatography-coupled quadrupole time of flight mass spectrometry. Hypoxanthine, a substrate of HPRT, always accumulated in HPRT knockout cells, but in different amounts due to the culture conditions. In proliferating cells, hypoxanthine was almost exclusively detectable in the knockout cells, whereas it was found in both knockout and wildtype cells under resting conditions at about two-fold higher amounts in the HPRT knockout cells. Cytidine occurs in higher amounts in resting knockout B103 cells. In contrast, cytidine is not accumulated in proliferating knockout cells, but was even slightly elevated in proliferating wildtype cells. Further differences in resting versus proliferating cells were detected, among others for metabolites that still remain to be identified.

Our findings show that different cultivation conditions lead to different metabolic states of B103 cells, including purine and pyrimidine metabolism. This has to be considered in finding a suitable cell culture model for a certain disease like LND.

[1] Torres, R. J., Puig, J. G., Jinnah, H. A., Update on the phenotypic spectrum of Lesch-Nyhan disease and its attenuated variants. *Curr Rheumatol Rep* 14: 189-194, 2012

[2] Jinnah, H.A., Lesch-Nyhan disease: from mechanism to model and back again. *Dis Model Mech* 2: 116-121, 2009

[3] Burhenne, H., Tschirner, S.K., Kuhn, M., Kaever, A., Seifert, R., Kaever, V., Metabolic alterations in Lesch-Nyhan syndrome. *N-S Arch Pharmacol* 386 (suppl 1): S14

### 392

#### SLC22A13 catalyzes unidirectional efflux of aspartate and glutamate at the basolateral membrane of type A intercalated cells in renal collecting duct

**Tuschy, Thorsten**<sup>1</sup>; Krüger, Johanna<sup>1</sup>; Schulz, Christian<sup>1</sup>; Fork, Christian<sup>1,2</sup>; Bauer, Tim<sup>1</sup>; Golz, Stefan<sup>1</sup>; Geerts, Andreas<sup>1</sup>; Schömig, Edgar<sup>1</sup>; Gründemann, Dirk<sup>1</sup>

<sup>1</sup>Universität Köln, Pharmakologie, Germany

<sup>2</sup>Goethe-Universität Frankfurt, Kardiologische Physiologie, Germany

<sup>3</sup>Bayer Pharma AG, Global Drug Discovery, Wuppertal, Germany

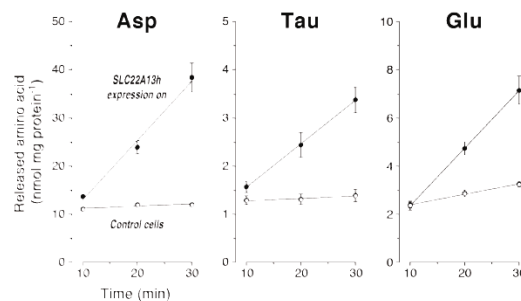
The SLC22 gene family encodes for membrane-inserted carrier proteins, which transport organic cations, zwitterions or organic anions. The precise localisation and physiological function of SLC22A13 have been unresolved. Immunohistochemistry experiments demonstrate the expression of SLC22A13 in the basolateral membrane of type A intercalated cells in rat kidney collecting duct. To identify physiological substrates of SLC22A13 we used LC-MS difference shading. We applied this technique to 293 cells in which human and rat SLC22A13 were heterologously expressed. Expression of SLC22A13 decreased the cellular content of guanidinosuccinate, aspartate, glutamate, and taurine. Time courses of uptake of <sup>3</sup>H-aspartate and <sup>3</sup>H-glutamate revealed that SLC22A13 counteracted endogenous uptake. Thus, SLC22A13 stimulates unidirectional efflux of both anionic amino acids. This substrate preference was confirmed by measuring the velocity of efflux of most standard amino acids.

After preloading of cells, the velocities of efflux of taurine and aspartate via SLC22A13 increased linearly with intracellular concentrations. We propose that in type A intercalated cells SLC22A13 serves to compensate the apical expulsion of protons by mediating the basolateral efflux of glutamate and aspartate. In this context the SLC22A13-catalyzed unidirectional efflux – without anion reentering – maintains the balance of intracellular charges. Loss of SLC22A13 function could cause distal tubular acidosis.

1. Schömig, E., Lazar, A. and Gründemann, D. (2006) Extraneuronal Monoamine Transporter and Organic Cation Transporters 1 and 2 - A Review of Transport Efficiency. In *Handbook of Experimental Pharmacology - Neurotransmitter Transporters* (Sitte, H. H. and Freissmuth, M., eds.), pp. 151-180, Springer, Heidelberg

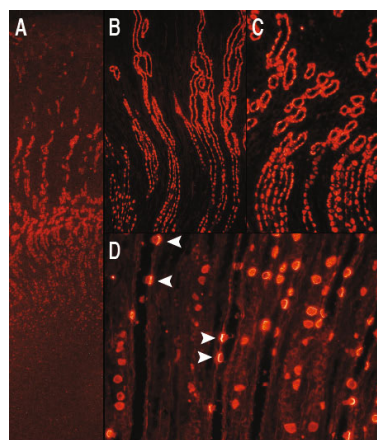
2. Fork, C., Bauer, T., Golz, S., Geerts, A., Weiland, J., Del Turco, D., Schömig, E. and Gründemann, D. (2011) OAT2 catalyses efflux of glutamate and uptake of orotic acid. *Biochemical Journal*. 436, 305-312

3. Bach, M., Grigat, S., Pawlik, B., Fork, C., Utermöhlen, O., Pal, S., Banczyk, D., Lazar, A., Schömig, E. and Gründemann, D. (2007) Fast set-up of doxycycline-inducible protein expression in human cell lines with a single plasmid based on Epstein-Barr virus replication and the simple tetracycline repressor. *FEBS Journal*. 274, 783-790



#### Efflux Asp Tau Glu:

Efflux of aspartate, taurine, and glutamate from 293 cells without or with expression of human SLC22A13



#### SLC22A13 in rat kidney :

Immunohistochemistry of rat kidney sections with an anti-rat SLC22A13 antibody

### Evaluation of the pentylenetetrazole seizure threshold test and the maximal electroshock seizure threshold test in epileptic mice as models for pharmacoresistant epilepsy

**Twele, Friederike**<sup>1,2</sup>, Töllner, Kathrin<sup>1,2</sup>, Brandt, Claudia<sup>1,2</sup>, Löscher, Wolfgang<sup>1,2</sup>

<sup>1</sup>Stiftung Tierärztliche Hochschule Hannover, Institut für Pharmakologie, Toxikologie und Pharmazie, Germany

<sup>2</sup>Zentrum für Systemische Neurowissenschaften, Hannover, Germany

The maximal electroshock seizure (MES) and pentylenetetrazole (PTZ) seizure tests are widely used models to screen drugs for anticonvulsant activity. Recently, Blanco et al. (Epilepsia, 50:824-831, 2009) reported that several clinically established antiepileptic drugs (AEDs), including phenobarbital (PB) and valproate (VPA), lost their anticonvulsant effect on PTZ-induced seizures, but not MES, when these tests were performed in rats that had developed epilepsy after a pilocarpine-induced status epilepticus (SE). The authors suggested that the PTZ test in animals pretreated with pilocarpine might constitute an effective and valuable method to screen for more effective AEDs. The aim of our study was to test whether similar results are obtained with the PTZ and MES tests in mice following a pilocarpine-induced SE.

We used the pilocarpine model to induce SE in female NMRI mice. Six weeks after SE, we determined the seizure threshold either by the timed i.v. PTZ seizure threshold test or the MES threshold (MEST) test in epileptic and control mice. The threshold for PTZ seizures was calculated in mg/kg PTZ for the first myoclonic twitch by infusion of a 1% PTZ solution into the tail vein of freely moving mice. The MEST was calculated as the median convulsive current (CC<sub>50</sub>) that induced seizures in 50% of the mice tested, using a sine-wave alternating current via corneal electrodes and taking hindlimb tonus as seizure. PB was tested at 18 mg/kg for the PTZ test and 10 mg/kg for the MEST test. VPA was tested at 300 mg/kg and 400 mg/kg in the PTZ test.

Six weeks after SE, control seizure thresholds in epileptic mice did not differ significantly from control mice in the PTZ and the MEST test. The effect of PB on seizure thresholds was not different between controls and epileptic mice in both tests. 300 mg/kg VPA was less effective to suppress seizures in epileptic mice in the PTZ test, but 400 mg/kg VPA had comparable anticonvulsant efficacy in control and epileptic mice.

In contrast to the results of Blanco et al. (2009) in rats, epileptic mice do not show a different response profile in the MEST and PTZ test when pretreated with PB, but, similar to epileptic rats in the s.c. PTZ test, VPA is less potent to suppress seizures in epileptic mice in the i.v. PTZ test. Testing of further AEDs is essential to find out whether using epileptic mice in the MEST and PTZ tests is a suitable model to investigate the mechanisms of pharmacoresistant epilepsy.

### Protection of TLR2<sup>-/-</sup> mice from myocardial ischemia reperfusion (I/R) injury depends on caspase-1-mediated improvement of mitochondrial function

**Tybl, Elisabeth**; Dröse, Stefan; Zacharowski, Kai; Scheller, Bertram; Mersmann, Jan  
Universitätsklinikum Frankfurt, Klinik für Anästhesiologie, Intensivmedizin und Schmerztherapie, Frankfurt am Main, Germany

**Objective:** Myocardial infarction, resulting from a sudden occlusion of the coronary artery is one of the main causes of death worldwide. Therapeutic treatment options focus on the limitation of injury caused by ischemia and reperfusion (I/R). A growing body of evidence indicates that oxidative stress and the inflammatory response are involved as triggers of membrane defects or enzyme damage. Toll-like receptors (TLR) are key regulators of the inflammatory response and especially TLR2-dependent mechanisms have been implicated in cardiac dysfunction. Reestablishment of mitochondrial aerobic respiration during reoxygenation results in excessive ROS production leading to cell death. Caspases play pivotal roles in apoptosis and inflammation and recently, a caspase-1 triggered reduction of mitochondrial ROS production has been reported which resulted in reduced cell death.

In the present study, we aimed to investigate the relationship between caspase-1 expression and TLR2 signaling and its impact on mitochondrial respiration during myocardial I/R.

**Methods:** Adult wildtype (WT) or TLR2<sup>-/-</sup> mice underwent experimental myocardial ischemia and reperfusion. Caspase-1 mRNA expression was investigated by real time RT-PCR. Caspase-1 activity was quantified using a fluorometric assay. I/R injury was also investigated *in vitro* using the mouse cardiomyocyte cell line HL-1, that underwent hypoxia and reoxygenation. In order to examine the effect of TLR2 and caspase-1 on mitochondrial function, oxygen consumption was assessed in a respirometer (Oxygraph). Intact mitochondria display a large respiration control rate (RCR) which implies that the mitochondria have a high capacity for ATP turnover and a low proton leak.

**Results:** Real-time RT-PCR demonstrated a significantly up-regulated caspase-1 expression upon I/R injury in TLR2<sup>-/-</sup> hearts. This was accompanied by an enhanced caspase-1 enzyme activity. In HL-1 cells we could show that TLR2 knock-down by RNA interference (RNAi) also increased caspase-1 mRNA levels. Using the synthetic TLR2-agonist Pam<sub>2</sub>CSK<sub>4</sub> we could demonstrate a "preconditioning" effect resulting in increased caspase-1 mRNA and protein expression and larger respiration rates, i.e. an improved mitochondrial function. After RNAi of caspase-1 in HL-1 cells, significant decline in respiration rates was measured in comparison to control, whereas upon TLR2-deletion respiration rates increased. Although not significant, the measured effects seemed slightly amplified upon hypoxia.

**Conclusion:** Regulation of mitochondrial respiration by a TLR-2 dependent regulation of caspase-1 activity may contribute to protection from myocardial ischemia reperfusion injury.

### Analysis of *In Chemico* and *In Silico* Methods to Predict Skin Sensitization Potentials

**Urbisch, Daniel**<sup>1</sup>; Mehling, Annette<sup>2</sup>; Kolle, Susanne<sup>1</sup>; Honarvar, Naveed<sup>1</sup>; Teubner, Wera<sup>3</sup>; Guth, Katharina<sup>1</sup>; van Ravenzwaay, Bennard<sup>1</sup>; Landsiedel, Robert<sup>1</sup>

<sup>1</sup>BASF SE, Experimental Toxicology and Ecology, Ludwigshafen am Rhein, Germany

<sup>2</sup>BASF Personal Care and Nutrition GmbH, Düsseldorf, Germany

<sup>3</sup>BASF Schweiz AG, Product Safety, Basel, Switzerland

Allergic contact dermatitis is the clinical manifestation of the immunological response resulting from repeated contact to an allergen. In the European Union, an animal testing ban now applies to ingredients and products falling under the Cosmetics Regulation. Therefore, in order to ensure the safety of cosmetic products, reliable data from predictive non-animal methods needs to be generated. Typically, chemical allergens are small-sized electrophilic molecules which need to bind to cutaneous proteins in order to become immunogenic. One non-animal method to assess the peptide reactivity of a test substance is the *in chemico* Direct Peptide Reactivity Assay (DPRA). A second approach is the analysis of relevant structural characteristics of a substance associated with protein-binding capacities and sensitization. The OECD QSAR Toolbox, an *in silico* expert system, provides two profilers based on OASIS and OECD algorithms for grouping target chemicals into six mechanistic domains regarding peptide reactivity (MA, SB, S<sub>N</sub>2, S<sub>N</sub>Ar, Ac, non-binding).

In order to determine the correlation of protein-binding properties with skin sensitization potentials, the *in silico* and *in chemico* results of 152 chemicals representing 44 non-sensitizers and 108 sensitizers were compared to *in vivo* LLNA data. The target chemicals represent a range of chemical classes, including fragrances, preservatives and dyes. It was thereby possible to identify a number of strengths and weaknesses of the investigated methods and to elucidate their applicability domains.

With an overall accuracy of 79% (sensitivity = 82%, specificity = 70%), the *in chemico* assay DPRA showed a better predictivity compared to the *in vivo* LLNA data than the two *in silico* methods. The consideration of human data for one false negative and two false positive results within the LLNA reference database would even lead to an accuracy of 81% of the DPRA.

The accuracies of both toolbox profilers were 71%. The lack of metabolically or abiotically activated structural alerts explains the poor sensitivities of 69% and 66% of the *in silico* profilers provided by OASIS and the OECD, respectively. Nevertheless, the protein-binding profiler of the OECD showed the highest specificity (84%) within this study. Based on these results, both methodologies can be used to generate reliable data. A good understanding of the strengths and limitations is necessary to interpret the data and to ensure a proper use in hazard and risk assessments.

### PRODUCTION OF NATURAL CC AND CXC CHEMOKINES, CHEMOKINE-ANTAGONISTS AND FLUORESCENT CHEMOKINES IN BACULOVIRUS-INFECTED INSECT CELLS

**Vatter, Petra**; Weiss, Carolin; Koenig, Carolin; Moepps, Barbara

Pharmacology and Toxicology, University of Ulm, Medical Center, Germany

Chemokines constitute a growing superfamily of small cytokines involved in regulating a wide array of leukocyte functions, including chemotaxis, adhesion, and transendothelial migration. Transmembrane signaling of chemokines is mediated by chemokine receptors, members of the G protein-coupled receptor (GPCR) family that signal in G protein-dependent and b-arrestin-dependent modes. Several findings indicate that inflammatory diseases are initiated or maintained by an imbalance of chemokine agonists and endogenous, naturally occurring chemokine receptor antagonists and/or by an imbalance of receptor biased signalling. The latter refers to the ability of chemically distinct receptor ligands to endue individual receptors with qualitatively different G-protein- versus b-arrestin-dependent signalling. Since biased agonists selectively stabilize a specific receptor conformation leading to a distinct signalling mode, targeting of these conformations with biased antagonists may allow to specifically inhibit pathophysiological receptor functions, while retaining physiological or even salutary functions and causing fewer side effects. To address the functional roles of peptidic chemokine agonists and/or antagonists under pathophysiological conditions, in particular in inflammatory diseases, we set out to produce and purify naturally occurring and fluorescently-labeled agonists and antagonists from baculovirus infected insect cells. We purified the proteins to near homogeneity and compared their functional and biological activity. For example, the fluorescently labeled monocyte chemoattractant protein-1 (MCP-1), the major agonist of CCR2a and CCR2b receptors, was used in comparative analysis of G-protein-regulated signalling pathways (e.g. activation of phospholipase C isoenzymes and Rho GTPases) and b-arrestin-regulated pathways (e.g. internalization of receptors and phosphorylation of extracellular-signal-regulated kinase (ERK)-kinases) in the presence or absence of small molecule antagonists. Additionally, the fluorescently labelled chemokines are currently used to identify peptidic agonists and/or antagonists from the human peptidome.

397

**Establishment of a Saline Lavage Model in the Isolated Perfused Rat Lung****Walter, Dorothee**; Fischer, Monika; Dasenbrock, Clemens

Fraunhofer Institut für Toxikologie und Experimentelle Medizin, Umwelt- und Arbeitssicherheit, Hannover, Germany

For studies on the effectiveness of new lung surfactant formulations, the rat lung lavage (RLL) model is the method of choice. Prior to the test, the rats are anesthetized, tracheostomized and pressure-controlled ventilated. Saline lavages are performed, whereupon the rats receive aerosolized surfactant. The restoration of the lung function is indicated by the recovery of oxygenation. During the test procedure, the RLL model is subject to large fluctuations within the measured parameters which are why another model for the investigation of lung surfactant formulations is desirable. In this context, the establishment of an *ex vivo* model such as the isolated perfused rat lung (IPL) should provide more constant measurement results, as the respiratory parameters can be adjusted individually. Furthermore, the use of the IPL contributes to the refinement and reduction of animal testing.

We tested the effect of different lavage procedures and various ventilation strategies using the IPL. Sprague-Dawley rats were ventilated with 100 % oxygen at a respiratory rate of 80 breaths/min, inspiration : expiration ratio of 1 : 1, and a positive end-expiratory pressure (PEEP) of 3 cmH<sub>2</sub>O. High inspiratory pressure (P<sub>insp</sub> / PEEP) of 26 / 3 cmH<sub>2</sub>O led to edema formation in less than one hour. With a P<sub>insp</sub> of up to 20 cmH<sub>2</sub>O, the lungs survived with normal respiratory values for at least three hours. Up to 6 lavages drop the O<sub>2</sub> level for at least 200 units without leading to severe edema, when pressure-controlled ventilated with a P<sub>insp</sub> of 20 cmH<sub>2</sub>O. Our results show that an imitation of moderate Acute Respiratory Distress Syndrome (100 mmHg < PaO<sub>2</sub> / FiO<sub>2</sub> ≤ 200 mmHg) in the *ex vivo* model IPL is possible. In the future, the development of a new test system for surfactant formulations shall replace the *in vivo* batch testing.

398

**The coumarin derivative daphnetin increases stress resistance and prolongs life span in the model organism *Caenorhabditis elegans*****Stolz, Stephan**; Wilke, Simone; Havermann, Susannah; Wätjen, Wim

Martin-Luther Universität, IAEW, AG "Biofunktionalität sekundärer Pflanzenstoffe", Halle (Saale), Germany

Coumarins are a group of phenolic compounds initially found in tonka bean. By today more than 1300 coumarin derivatives have been identified in a variety of plants, most prominently in spices, herbs and fruit. Due to its amiable odour, coumarin is often used in cosmetics but is also applied in pharmaceuticals due to e.g. anti-inflammatory, neuroprotective and antioxidative properties.

We have analysed the effects of coumarin and its derivatives umbelliferon (7-hydroxycoumarin) and daphnetin (7, 8-dihydroxycoumarin) on stress resistance and oxidative stress in the nematode model organism *C. elegans*. We first investigated the radical scavenging capacity of these coumarins in a cell free system (TEAC assay), demonstrating that only daphnetin is an effective direct antioxidative compound. Then we analysed the ability of the compounds to reduce the intracellular accumulation of reactive oxygen species in the nematode (fluorescent probe: DCF) under conditions of thermal stress. Daphnetin increased the tolerance of *C. elegans* to lethal thermal stress (SYTOXgreen assay) while both coumarin and umbelliferon showed no protection.

A life span analysis showed that daphnetin was able to prolong the median life span (non-stress conditions) of the nematode by 20% while neither coumarin nor its main metabolite in humans umbelliferon had no effect. To elucidate the mechanism of life prolongation, we investigated the effect of the compounds on the ageing associated transcription factors DAF-16 and SKN-1 (homologues to mammalian FoxO and Nrf2). We used transgenic strains expressing GFP-fusion proteins of DAF-16 and SKN-1 to analyse if the compounds lead to an activation of these pathways (nuclear translocation). Furthermore, we used loss-of-function mutant strains (DAF-16) or RNA-interference knockdown (SKN-1) to verify the molecular mechanism of daphnetin-induced stress resistance and life prolongation.

399

**Auxiliary functions of the cell cycle for inflammatory gene expression programs****Weber, Axel**<sup>1</sup>; Dittrich-Breiholz, Oliver<sup>2</sup>; Handschick, Katja<sup>1</sup>; Müller, Helmut<sup>1</sup>; Schneider, Heike<sup>3</sup>; Schmitz, M. Lienhard<sup>3</sup>; Kracht, Michael<sup>1</sup><sup>1</sup>Justus-Liebig-University Giessen, Rudolf-Buchheim-Institute of Pharmacology, Gießen, Germany<sup>2</sup>Medical School Hannover, Institute of Biochemistry, Germany<sup>3</sup>Justus-Liebig-University Giessen, Institute of Biochemistry, Gießen, Germany

The cytokine-regulated inflammatory gene response operates through numerous feedforward loops. It is not known if the cell cycle state *per se* contributes to this amplification program. For studying impact of the cell cycle phase on IL-1-triggered gene expression, cells were arrested and released to re-enter the G1 phase and additionally treated by a short pulse of IL-1. A comprehensive assessment of gene expression on high density microarrays showed that cell cycle release on its own induced the expression of 448 genes and sequential cell cycle release plus IL-1-treatment upregulated 532 genes, whereas IL-1 alone specifically induced 29 genes. Several IL-1-regulated genes were also regulated by G1 release and their number increased to 28, if

cells were released to re-enter the cell cycle prior to IL-1 treatment suggesting that G1 release primes and cooperates with the majority of the cytokine-driven gene response. We also found that G1 release led to much higher mRNA expression of many of these genes, raising the question for the molecular pathways underlying the cell cycle contribution to inflammatory gene expression. The activities of CDK6 and CDK4 increase during G1 phase of the cell cycle by association with D-type cyclins suggesting that these kinases might be a molecular link connecting cell cycle with cytokine response genes. Therefore, we suppressed CDK4 or CDK6 by RNAi and determined the transcriptomes in arrested and in synchronized cell cultures. These analyses showed that only 8-12% of all genes regulated by G1 release or by G1 release plus IL-1 are dependent on CDK6 or CDK4. However, 34-45% of all IL-1-induced genes required either CDK4 or CDK6. The overlapping set of IL-1-induced genes regulated by CDK4 and by CDK6 contained 7 genes including *IL8*, *IL6*, and *CCL20*. CDK6 was required for up- or downregulation of 692 genes, whereas CDK4 was required for regulation of 434 genes. The genes divergently regulated by CDK6 or CDK4 point to gene-specific functions of the kinases beyond their function in cell cycle regulation, as supported by GO analyses of differentially expressed genes. Collectively, these data identify a set of inflammatory genes that are strongly regulated by cell cycle and also by IL-1 and whose expression is modulated by CDK-dependent pathways.

400

**Sperm Evaluation by 3D Laser Scanning Microscopy (Olympus LEXT OLS4000)****Weber, Klaus**<sup>1,2</sup>; Fendl, Diana<sup>3</sup>; Hein, Felix<sup>3</sup>; König, Andres<sup>4</sup>; Kunze, Marc<sup>3</sup>; Leoni, Anne-Laure<sup>5</sup>; Ordoñez, Patricia<sup>4</sup>; Quierici, Roberto<sup>3</sup>; Riedel, Wolfram<sup>3</sup>; Rivera, Javier<sup>4</sup>; Romano, Ivano<sup>5</sup>; Takawale, Pradeep<sup>3</sup>; Waletzky, Alexander<sup>2</sup><sup>1</sup>AnaPath GmbH, Oberbuchsitzen, Switzerland<sup>2</sup>AnaPath Services GmbH, Liestal, Switzerland<sup>3</sup>BSL BIOSERVICE Scientific Laboratories GmbH, Planegg, Germany<sup>4</sup>Vivotecnia Research S.L., Tres Cantos (Madrid), Spain<sup>5</sup>Olympus Schweiz AG, Volketswil, Switzerland

Sperm analysis is one of the endpoints in reprotoxicity studies. Different methods for quantitative sperm analysis (total count of motile (live) and non-motile (dead) sperm, motility percent, motility grade profile, pH, white blood cell count, agglutination and if necessary, vitality and fructose count) have been described. For qualitative morphological sperm analysis, either such techniques, smears of sperm or histological sperm staging are in use. Any of these methods provides morphological results on a light microscopy level.

Laser scanning microscopy is a technique using a focused laser for scanning an object. The Olympus LEXT with optional possibilities of Differential Interference Contrast (DIC) provides a microscopic method for visualizing sub-nanometer micro asperities, which are far beyond the resolving power of a typical light or laser microscope.

The obtained live images are comparable to those of a scanning electron microscope under relatively low power magnifications. The Olympus LEXT was developed to evaluate technical surfaces and materials (material analysis). An attempt was made to use the Olympus LEXT technology for morphological analysis on sperm of rats, mice, rabbits and cynomolgus monkeys.

This technology was never before applied to any tissues or cells. The reason is simply that a scanning laser is always reflected by wet and/or reflecting surfaces and hence, imaging is hindered or impossible.

However, using a fixative for electron microscopy evaluation and handling dried slides of cell smears without coverslipping, the application of this technology was deemed to be possible. Sperm of rats, mice, rabbits and cynomolgus monkeys were evaluated at magnifications up to x17090. Excellent images, similar to scanning electron microscopy, could be obtained.

Measurements on sperm parameters were taken by an integrated image analysis software tool. Abnormalities were easily detectable. The application of this technology provides results within minutes once a properly prepared slide undergoes the evaluation process. The images obtained and the related image analyses capabilities, with highest measuring accuracy, are useful tools for the interpretation of induced sperm injury.

[1] Ohtani K, Yamazaki S, Kubota H, Miyagawa M, Saegusa J. (2004): Comparative investigation of several sperm analysis methods for evaluation of spermatotoxicity of industrial chemical: 2-bromopropane as an example. *Ind Health*, 42: 219-225

[2] Cummins JM, Woodall PF (1985): On mammalian sperm dimensions. *J Reprod Fert*, 75: 153-175

401

**Molecular Characterization of *Pasteurella multocida* toxin-induced deamidation of heterotrimeric G proteins****Weise, Markus**; Aktories, Klaus; Orth, Joachim

Universität Freiburg, Institut für Experimentelle und Klinische Pharmakologie und Toxikologie, Germany

*Pasteurella multocida* toxin (PMT) is a major virulence factor of *Pasteurella multocida* causing pasteurellosis in humans and animals and is responsible for atrophic rhinitis in pigs. The toxin stimulates various signaling pathways by acting on the heterotrimeric G proteins Gα<sub>q/11</sub>, Gα<sub>12/13</sub> and Gα<sub>i</sub>. The toxin activates the Gα-subunit by deamidation of an essential glutamine residue. This glutamine in the switch II region is conserved throughout all α-subunits and is crucial for the hydrolysis of the bound nucleotide. Deamidation inhibits the hydrolysis of GTP and leads therefore to a constitutive

activation of the G protein. Here, we characterized the enzymatic activity of PMT in an *in vitro* model. To this end, we determined the deamidation of  $G\alpha_2$  by PMT, utilizing deamidation specific monoclonal antibody against the  $\alpha$ -subunit.

PMT is a typical AB-type toxin, consisting of a receptor binding/ translocation domain (B) and an enzymatic active domain (A). The enzymatic activity is harboured in the very C-terminal C3 domain. Using the *in vitro* deamidation system, we tested whether additional domains contribute to the enzymatic activity. Interestingly, the catalytic center of PMT is covered by a disulfide bond between Cys<sup>1159</sup> and Cys<sup>1165</sup>. The cleavage of that disulfide bond is essential for the formation of the catalytic triad, containing Cys<sup>1165</sup>, His<sup>1205</sup> and Asp<sup>1220</sup>. Affecting the disulfide bond by reducing agents or mutagenesis of Cys<sup>1159</sup>, we studied deamidation activity. The molecular target of PMT are the  $\alpha$ -subunits of heterotrimeric G proteins, which are molecular switches, cycling between an active GTP-bound and an inactive GDP-bound state. We investigate in which step of the GTPase cycle PMT deamidates the  $\alpha$ -subunit most efficiently. Our presented data support the understanding of the interaction of PMT and G proteins on a molecular level.

## 402

### N996I mutational effects on $I_{Kr}$ current in hiPSC derived cardiomyocytes are reproduced in HEK 293 cells solely with the appropriate subunit assembly

Binder, Katrin<sup>1</sup>; Dreyer, Tobias<sup>1</sup>; Haas, Jessica<sup>2</sup>; Casini, Simona<sup>3</sup>; Bellin, Milena<sup>3</sup>; Moretti, Alessandra<sup>1</sup>; **Welling, Andrea**

<sup>1</sup>Technische Universität München, Institut für Pharmakologie und Toxikologie, Germany

<sup>2</sup>Klinikum rechts der Isar der Technischen Universität München, I. Medizinische Klinik, Molekulare Kardiologie, Germany

<sup>3</sup>Leiden University Medical Center, Department of Anatomy and Embryology, Netherlands

The rapid delayed rectifier potassium channel  $K_v11.1$  (commonly known as HERG) plays a key role in the repolarisation of cardiac action potentials. Diseased or disordered HERG channels are a major cause of the long QT syndrome 2 (LQT2), a life-threatening disorder characterized by prolonged ventricular repolarisation, a propensity to polymorphic ventricular tachycardia and sudden cardiac death in young patients. Malfunction of the channels can be caused by acquired or inherited disorders. Thus, until now about 300 mutations have been described in the gene *KCNH2* encoding the channel.

We identified a family with a yet uncharacterized heterozygous c.A2987T (N996I) mutation in the *KCNH2* gene encoding the carboxyterminal part of potassium channel. The effects of the mutation on the deduced  $I_{Kr}$ -current were analysed in transiently transfected HEK 293 cells by patch-clamp measurements. In humans, HERG channels are composed of four  $\alpha$ -subunits and several  $\beta$ -subunits. The  $\alpha$ -subunits exist in two alternative transcripts, a long HERG1a and a short HERG1b isoform, with a shorter aminoterminal. Usually, the implications of channel mutations are tested by sole expression of HERG1a. We found that HERG1a mutated channels (HERG1a\*) showed a reduced current density and a shift in the voltage-dependence of activation and inactivation compared to the wildtype HERG1a. Coexpression of the HERG1b isoform restored the current density and the voltage-dependence in mutated versus wildtype channels, but induced an acceleration of the deactivation time constants. Because the effects of the mutation were obviously dependent on the channel composition, we tested every possible subunit combination and compared the results with human induced pluripotent stem (hiPS) cell derived cardiomyocytes from a patient carrying the same mutation in the HERG channel and a corrected channel<sup>1</sup>. Identical results were found with channels assembled of a wildtype and a mutated subunit of each isoform (HERGaa versus HERGaa\*bb\*).

Supported by the DZHK (German Centre for Cardiovascular Research) and the DFG (For 923).

<sup>1</sup>Bellin M, Casini S, Davis RP, D'Aniello C, Haas J, Ward-van Oostwaard D, Tertoolen LG, Jung CB, Elliott DA, Welling A, Laugwitz KL, Moretti A, Mummery CL. Isogenic human pluripotent stem cell pairs reveal the role of a *KCNH2* mutation in long-QT syndrome. *EMBO J*. 2013 Nov 8. doi: 10.1038/emboj.2013.240. [Epub ahead of print]

## 403

### cGMP imaging in embryonic dorsal root ganglion neurons with FRET-based cGMP sensor knock-in mice

**Wen, Lai**<sup>1</sup>; Lu, Shen<sup>1</sup>; Thunemann, Martin<sup>1</sup>; Pop, Sinziana<sup>1</sup>; Schmidt, Hannes<sup>2</sup>; Feil, Robert<sup>1</sup>

<sup>1</sup>Interfakultäres Institut für Biochemie, Universität Tübingen, Germany

<sup>2</sup>Developmental Neurobiology Group, Max Delbrück Center for Molecular Medicine, Berlin, Germany

Cyclic GMP (cGMP) is an important second messenger regulating various physiological processes, including smooth muscle relaxation, platelet aggregation, and axonal bifurcation. It is generated from GTP by soluble guanylyl cyclase in response to nitric oxide (NO), or by particulate guanylyl cyclases activated by natriuretic peptides, such as ANP or CNP. cGMP is degraded by phosphodiesterases (PDEs). It is believed that cGMP signaling events are highly dynamic and can occur in subcellular compartments. To visualize cGMP signals *in vivo*, we have generated so-called cGMP sensor knock-in mice [1]. A Cre recombinase-activatable expression cassette of the fluorescence resonance energy transfer (FRET)-based cGi500 sensor driven by the CAG promoter was integrated into the Rosa26 locus. Depending on the strategy to activate sensor

expression, these mice show either ubiquitous or tissue-specific sensor expression allowing for delineation of cGMP signaling *in vivo*. cGMP was successfully imaged in isolated smooth muscle cells as well as in blood vessels of living mice [1].

In the present study, we have monitored cGMP signals in live E12.5 dorsal root ganglion (DRG) neurons. It is well known that a CNP-triggered cGMP signaling pathway regulates axonal bifurcation during embryonic development, but the molecular mechanism behind this function is not completely understood. FRET imaging experiments showed that CNP but not ANP or NO could induce a cGMP increase in DRG neurons. Through application of various PDE inhibitors we specified that PDE 1 and 2 are mainly responsible for the degradation of CNP-induced cGMP in these neurons. Notably, local application of CNP revealed that cGMP can be generated in the growth cone independently of the soma. These results suggest that the growth cone can detect CNP when projecting into the dorsal root entry zone of the spinal cord. The local elevation of cGMP in the growth cone in response to CNP may be important for sensory axon bifurcation during embryonic development.

In conclusion, these data provide novel insights into the molecular mechanism underlying axonal bifurcation of embryonic DRG neurons and demonstrate that the cGMP sensor knock-in mice are useful tools for real-time monitoring of cGMP signals with subcellular resolution. In combination with other mouse models and advanced FRET microscopy techniques, these mice should find widespread use in order to improve our understanding of cGMP signaling *in vivo*, both under physiological and pathophysiological conditions.

[1] Thunemann, M., Wen, L. et al., *Transgenic mice for cGMP imaging*. *Circ Res*. 2013;113:365-71.

## 404

### Cell-cell contacts provide resistance to ROS-induced regulated necrosis

**Wenz, Christine**; Faust, Dagmar; Frumkina, Anna; Kaina, Bernd; Dietrich, Cornelia  
Universitätsmedizin Mainz, Toxikologie, Germany

Oxidative stress is one of the most prominent inducers of cell death and DNA damage leading to the on-set of pathological processes such as inflammation, neurodegenerative diseases and cancer. While ROS (reactive oxygen species)-induced apoptosis has been intensively studied during the last decades, the molecular mechanisms of regulated necrosis, especially in response to ROS are less clear so far. Moreover, studies have been performed almost exclusively in non-confluent, exponentially growing cells despite the fact that *in vivo* most of the cells have established cell-cell contacts, which regulate proliferation and differentiation. Since previous work of our group showed that confluent cultures of murine fibroblasts are protected against ROS-induced regulated necrosis, we hypothesized that cell-cell contacts might also regulate survival. We therefore investigated the cytotoxic response of confluent versus semi-confluent (proliferating, serum-starved, U0126-treated) murine fibroblasts (NIH3T3) and human keratinocytes (HaCaT). Confluent, serum-starved and U0126-treated cultures showed similar cell cycle distribution with 70 % of cells in G0/G1-phase compared to proliferating cultures (50 %). Only the confluent cells were protected against butyl hydroxyperoxide (t-BOOH)-induced cell death. Importantly, confluent or serum-starved cultures cells were not quiescent at this stage, but still proliferated. We therefore conclude that cell-cell-contacts protect against ROS-mediated cell death. Survival of confluent cells was not triggered by upregulation of anti-oxidative capacities, or altered cytosolic ROS or ATP level. In line with these observations, the initial induction of DNA single-strand breaks was comparable under all culture conditions. While DNA double-strand breaks (DSBs) increased with time in semi-confluent cultures, no time-dependent increase in DSBs occurred in confluent cultures. Moreover, mitochondria of confluent cells were protected against t-BOOH, whereas mitochondrial vitality in semi-confluent cultures dramatically decreased. We further showed that cell death in semi-confluent cultures was independent of caspases and PARP-1, but dependent on the kinase RIP1. In conclusion, cell-cell contacts prevent t-BOOH-triggered reduction of mitochondrial vitality, the formation of DSBs and hence the induction of RIP1-dependent regulated necrosis. The data give new insights into the regulation of ROS-induced cell death.

## 405

### Brain endothelial cells but not astrocytes regulate neurovascular coupling through $G\alpha_{q/11}$

**Wenzel, Jan**<sup>1</sup>; Assmann, Julian Christopher<sup>1</sup>; Vogt, Miriam Annika<sup>2</sup>; Ridder, Dirk Andreas<sup>1</sup>; Wetschureck, Nina<sup>3</sup>; Hüttmann, Gereon<sup>4</sup>; Gass, Peter<sup>2</sup>; Offermanns, Stefan<sup>3</sup>; Schwaninger, Markus<sup>1</sup>

<sup>1</sup>University of Lübeck, Institute of Experimental and Clinical Pharmacology and Toxicology, Germany

<sup>2</sup>Medical Faculty Mannheim/Heidelberg University, Central Institute of Mental Health, Germany

<sup>3</sup>Max-Planck-Institute for Heart and Lung Research, Department of Pharmacology, Bad Nauheim, Germany

<sup>4</sup>University of Lübeck, Institute of Biomedical Optics, Germany

Cerebral blood flow (CBF) is tightly regulated to meet the high metabolic demands of the brain. Several brain disorders, such as stroke, small-vessel disease, and depression, are associated with impaired CBF regulation or endothelial dysfunction. However, the mechanisms behind the regulation of CBF are still under debate. Astrocytes are supposed to play a major role in triggering an increase of blood flow after neuronal activity, a process termed functional hyperemia or neurovascular coupling (NVC).

According to this concept, glutamate released from neurons stimulates  $G_{\alpha_{q11}}$ -coupled receptors located on astrocytes subsequently increasing intracellular calcium which induces the secretion of vasodilating gliotransmitters. To test this concept we used  $G_{\alpha_{q11}}$  knockout mice and crossed them with the *GlastCreER<sup>2</sup>* mouse line carrying a floxed  $G_{\alpha_q}$  gene. The resulting mice were deficient of  $G_{\alpha_{q11}}$  signaling in astrocytes. NVC was induced by short whisker stimulation and blood flow was monitored by laser speckle imaging. Unexpectedly, a loss of  $G_{\alpha_{q11}}$ -signaling in astrocytes had no effect on the maximal value or the area under the curve of the blood flow response after neuronal stimulation. As  $G_{\alpha_{q11}}$ -coupled receptors are known to be involved in NVC, we asked, whether  $G_{\alpha_{q11}}$  in brain endothelial cells mediate the effect. Therefore, we used the *SLCO1C1-CreER<sup>2</sup>* line to generate mice with a deficiency of  $G_{\alpha_q}$  and  $G_{\alpha_{q11}}$  in brain endothelial cells. The knockout was efficient as demonstrated by calcium imaging in primary brain endothelial cells, showing a high response upon treatment with ATP that was almost absent in endothelial cells deficient of  $G_{\alpha_{q11}}$ . After whisker stimulation the blood flow response was significantly reduced in mice lacking  $G_{\alpha_{q11}}$  in brain endothelial cells. By using two-photon microscopy we found a reduced blood cell velocity in pial arterioles but not in pial venules in  $G_{\alpha_{q11}}$  deleted mice. To examine whether these changes could affect behavior we performed different tests and found the  $G_{\alpha_{q11}}$  deficient mice to be more anxious but still able to perform memory tasks. In summary, our data indicate an important role of brain endothelial cells in the regulation of cerebral blood flow after neuronal stimulation. In contrast to previous concepts on CBF regulation, interruption of  $G_{\alpha_{q11}}$  signaling in the endothelium but not in astrocytes affected NVC. Impaired NVC led to behavioral changes in mice deficient of  $G_{\alpha_{q11}}$  in brain endothelial cells.

## 406

### Evidence for Non-Canonical Histamine H<sub>2</sub>-Receptor Signaling Pathway in Human Monocytes

**Werner, Kristin**; Neumann, Detlef; Seifert, Roland  
Hannover Medical School, Institute of Pharmacology, Germany

Histamine (HA) mediates its biological effects via four histamine receptor subtypes ( $H_2R$ ), all belonging to the superfamily of G-protein-coupled receptors (GPCRs). According to the canonical histamine  $H_2$ -receptor ( $H_2R$ ) signaling pathway, the  $H_2R$  couples to  $G_s$ -proteins. Activation of  $H_2R$  leads to adenylyl cyclase activation and cAMP accumulation [1]. However, stimulation of  $H_2R$  results in an increase of intracellular calcium [ $Ca^{2+}$ ] in HL-60 promyelocytes indicating coupling to  $G_q$ -proteins and subsequent activation of phospholipase C (PLC) [2]. Furthermore, HA, via  $H_2R$ , reduces the production of reactive oxygen species (ROS) in native myeloid cells [3].

The aim of our present study was to examine the  $H_2R$  signal transduction pathway in human monocytes. Therefore, we analyzed the effects of selective  $H_2R$  ligands on cAMP accumulation and N-formyl-L-methionyl-L-leucyl-L-phenylalanine (fMLP)-induced ROS production. Moreover, we investigated the influence of HA on [ $Ca^{2+}$ ] increase. Monocytes were isolated from peripheral blood of healthy human volunteers. ROS production was measured using the lucigenin chemiluminescence assay. cAMP levels were determined by HPLC-coupled mass spectrometry. In addition, the Fura-2-AM method was performed to assess HA induced [ $Ca^{2+}$ ] increase.

Generally, all  $H_2R$  agonists inhibited fMLP-induced ROS production and increased cAMP levels. Interestingly, dissociations occurred in the potencies and efficacies of  $H_2R$  ligands with respect to cAMP production and ROS inhibition. HA caused no increase of [ $Ca^{2+}$ ], indicating no involvement of [ $Ca^{2+}$ ] as a second messenger in the reflection of ROS production.

Our data suggest that besides cAMP accumulation, non-canonical  $H_2R$  signaling pathways are involved in the  $H_2R$  mediated inhibition of ROS. Contrary to the results obtained with HL-60 promyelocytes, we could not find any evidence for the  $H_2R$  coupling to  $G_q$ -proteins. In conclusion, it is likely that activation of  $H_2R$  leads to  $\beta$ -arrestin mediated signaling.

[1] Seifert, R., et. al.: *Trends Pharmacol. Sci.* 2013, **34**(1): 33-58

[2] Seifert, R., et. al.: *Mol. Pharmacol.* 1992, **42**(2): 235-41

[3] Reher, T. M., et. al.: *Biochem. Pharmacol.* 2012, **84**(9): 1174-85

## 407

### Inhalation toxicity of three different types of nano-size organic pigments

**Wiench, Karin**<sup>1</sup>; Simmendinger, Peter<sup>2</sup>; Ma-Hock, Lan<sup>3</sup>; Groeters, Sibylle<sup>3</sup>; van Ravenzwaay, Bennard<sup>3</sup>; Landsiedel, Robert<sup>3</sup>

<sup>1</sup>BASF SE, Product Safety, Ludwigshafen am Rhein, Germany

<sup>2</sup>BASF Schweiz AG, Product Stewardship, Basel, Switzerland

<sup>3</sup>BASF SE, Experimental Toxicology and Ecology, Ludwigshafen am Rhein, Germany

Four different organic pigments, which are nanomaterials according to the EU definition, were tested in the 5 day short term inhalation study (STIS) in rats. The STIS is a sensitive test system, which comprises a comprehensive scheme of biological effects (such as inflammatory reactions in the lung) as well as preliminary biokinetic data (such as lung burdens and potential translocation). A recovery period provides information on the persistence, progression and/or regression of effects is obtained.

The pigments represent three different chemical classes of organic pigments, the diketopyrrolopyrrol-pigments (Pigment Red 254 and DPP Orange), the arylide yellow pigments (Pigment Yellow 74) and copper phthalocyanine pigments (Pigment Blue 15). These pigments are poorly soluble particles, the average particle size distribution of these pigments are 25 – 250 nm.

The pigments were tested in the concentrations from 1 to 30 mg/m<sup>3</sup>, examination of the lung lavage as well as histopathological examinations were performed after the exposure period as well as after a recovery period of 3 weeks.

Only mild and partly reversible morphological changes were observed in lung and lymph nodes at the highest concentrations tested with the diketopyrrolopyrrol-pigments, whereas Pigment Yellow 74 showed no changes in histopathology and lavage parameter up to the highest concentration tested.

As a first result it can be concluded these nano-size organic pigments only represent a mild inhalation hazard potential.

## 408

### Development of an online-SPE-LC-MS method for the investigation of the intestinal absorption of 2-amino-1-methyl-6-phenylimidazo[4,5-b]pyridine (PHIP) and its bacterial metabolite PHIP-M1 in a Caco-2 Transwell system

**Willenberg, Ina**; von Elsner, Leonie; Steinberg, Pablo; Schebb, Nils Helge

University of Veterinary Medicine Hannover, Institute for Food Toxicology and Analytical Chemistry, Germany

2-Amino-1-methyl-6-phenylimidazo[4,5-b]pyridine (PHIP) is a heterocyclic-aromatic-amine formed during the heat processing of food. PHIP does not only undergo human metabolism but is also metabolized by the intestinal microbiota. The main bacterial metabolite is 7-hydroxy-5-methyl-3-phenyl-6,7,8,9-tetrahydropyrido[3',2':4,5]imidazo[1,2-a]pyrimidin-5-ium chloride (PHIP-M1). The aim of the present study was to develop a LC-MS method with online sample preparation for the quantification of PHIP and its metabolites and to apply it to analyze the passage of PHIP-M1 through a Caco-2 cell-monolayer.

The developed online-SPE-LC-ESI-MS proved to be a powerful tool for the rapid quantitative analysis of PHIP, *N*-hydroxy-PHIP, 4-OH-PHIP and PHIP-M1. In the Caco-2 Transwell system PHIP-M1 crossed the cell monolayer more rapid from the basolateral to the apical compartment than from the apical to the basolateral compartment. Experiments in the presence of P-glycoprotein and multiple drug resistance 2 transporter inhibitors showed that PHIP-M1 is a substrate for both transporters.

In conclusion the present study showed that the intestinal absorption of PHIP and its bacterial metabolite PHIP-M1 occurs to a similar extent and a significant absorption of PHIP-M1 has to be expected. Thus, not only the human metabolites of PHIP could contribute to its toxic effects but also the bacterial metabolite PHIP-M1 formed in the gut.

Vanhaecke et al., *J. Agric. Food Chem.* (2006), **54**, 3454-3461

## 409

### Analysis of an unknown sodium conducting protein

Beck, Andreas; Flockerzi, Veit; **Wissenbach, Ulrich**

Universität des Saarlandes, Exp. u. Klinische Pharmakologie u. Toxikologie, Homburg Saar, Germany

A protein of yet unknown function was cloned from human placenta. The open reading frame codes a ~100kDa protein with a number of hydrophobic segments indicating that the protein is most likely present in cellular membranes. Transmembrane prediction programs indicate 8-11 transmembrane domains. Overexpression of a C-terminal GFP-fused construct reveals a punctuate expression pattern indicating that most of the protein is located in intracellular compartments. Nevertheless, biotinylation experiments also indicate expression in the plasma membrane. Northern and data base analysis show that the corresponding mRNA is detectable in all tested tissues which include heart, brain, skeletal muscle, several glands and others. Using a membrane potential sensitive dye (FLIPR), cells overexpressing the 100kDa protein show a robust cytosolic fluorescence change in a sodium addition protocol. In addition, whole cell patch clamp experiments reveal a constitutive sodium conductance in cells overexpressing the protein.

## 410

### Comparison of the influence of engineered silica nanoparticles on the proliferation and signalling pathways in human gastric and colon carcinoma cells

**Wittig, Anja**; Gehrke, Helge; Fritz, Eva-Maria; Marko, Doris

Universität Wien, Institut für Lebensmittelchemie und Toxikologie, Austria

Nanostructured silica particles (SiO<sub>2</sub>-NP) are commonly used in many different scopes especially in cosmetics and food industry. Thus their environmental and health impacts are of great interest. While previous studies mainly focused on the inhalative impact of SiO<sub>2</sub>-NP, this present study aims to contribute to the rarely investigated effects on cells originating from the gastrointestinal tract. Here, the toxicological relevance of commercially available SiO<sub>2</sub>-NP with 12 nm of diameter was examined focused on proliferative effects as well as on the influence on cellular signalling pathways (MAPK/ERK1/2; Nrf2/ARE) [1].

The study was performed in different human gastrointestinal carcinoma cell lines (GXF251L - stomach, HT29 - colon). Influence on the cell growth was determined using the sulforhodamine B (SRB) assay. Furthermore, interference with the MAPK/ERK1/2 pathway was investigated by Western blot analysis, while effects on the Nrf2/ARE-driven gene  $\gamma$ -glutamate cysteine ligase ( $\gamma$ -GCL) were analysed by qPCR.

The results show that the investigated SiO<sub>2</sub>-NP stimulate cell growth, depending on incubation time and particle concentration as well as on the examined cell line. However, growth stimulation is distinctly emerged in HT29 cells compared to GXF251L cells. Further investigations in HT29 cells revealed that these effects were associated with changes in the MAPK/ERK1/2 - pathway, leading to an increased phosphorylation of ERK1/2. Additionally, interactions with the Nrf2/ARE signalling pathway were observed as significantly enhanced transcription of  $\gamma$ -GCL. This effect could be suppressed by co-incubation with a specific MEK-inhibitor, indicating a cross-link between these two pathways, both deeply involved in the regulation of cellular processes like the antioxidative defence system as well as cell cycle progression [2]. In contrast, exposure of GXF251L cells to SiO<sub>2</sub>-NP induced neither growth stimulation nor an increase of ERK-phosphorylation. Further, an increase of  $\gamma$ -GCL transcripts after 24 hours could not be determined as well.

In summary, the results of the comparative study indicate that biological responses triggered by SiO<sub>2</sub>-NP appear to be cell line specific. Whereas for HT29 cells a growth stimulus as well as interference with the MAPK/ERK1/2 and/or the Nrf2/ARE signalling pathways could be observed, none of these endpoints seem to play a significant role in GXF251L cells. This leads to the conclusion that in GXF251L cells other modes of action seem to be more prevalent.

[1] Lin, W., Huang Y., Zhou, X.-D., Ma, Y., *In vitro* toxicity of silica nanoparticles in human lung cancer cells. *Toxicology and Applied Pharmacology* 2012, 217, 252-259.

[2] Gehrke, H., Fröhmeser, A., Pelka, J., Esselen, M., et al., *In vitro* toxicity of amorphous silica nanoparticles in human colon carcinoma cells. *Nanotoxicology* 2013, 7 (3), 274-293.

## 411

### Analysis of cCMP signaling proteins

**Wolfertstetter, Stefanie**<sup>1</sup>; Schinner, Elisabeth<sup>1</sup>; Hofmann, Franz<sup>2</sup>; Schlossmann, Jens<sup>1</sup>  
<sup>1</sup>Universität Regensburg, Institut für Pharmazie, Pharmakologie und Toxikologie, Germany

<sup>2</sup>Technische Universität München, Carvas, Germany

cAMP and cGMP are well established second messengers and essential for numerous of (patho)physiological processes. These purine cyclic nucleotides activate cGK and cAK, respectively. Meanwhile a possible function of cyclic cytidine 3',5'-monophosphate (cCMP) is arising. Formation of cCMP by cytidyl cyclases is debated. cCMP induces relaxation of vascular smooth muscle and inhibits platelet aggregation via cGKI. However, functions regulated by cCMP are mostly unknown. Our aim is to elucidate whether cCMP plays a role as second messenger and to identify cCMP signaling proteins. In former studies we showed that cCMP activates the purified cyclic nucleotide-dependent protein kinases cGK and cAK. We investigated the regulation of cCMP on purified cyclic nucleotide-dependent protein kinases and on intact tissues of wildtype (WT) and cGKI-knockout (KO) mice, namely jejunum and lung. Moreover, we identified complexes of cCMP with various signaling proteins in tissue lysates. These results indicate that cCMP could play an important role in physiological processes of jejunum and lung.

## 412

### Fatty acid amide hydrolase inhibitors induce mesenchymal stem cell migration and differentiation into the osteoblastic lineage

**Wollank, Yvonne**<sup>1,2</sup>; Ramer, Robert<sup>1</sup>; Salamon, Achim<sup>2</sup>; Peters, Kirsten<sup>2</sup>; Hinz, Burkhard<sup>1</sup>

<sup>1</sup>Institute of Toxicology and Pharmacology, University of Rostock, Germany

<sup>2</sup>Department of Cell Biology, University of Rostock, Germany

Migration and differentiation of mesenchymal stem cells (MSCs) are known to be involved in various regenerative processes such as bone healing. However, little is known about the pharmacotherapeutic options aiming at the mobilization and differentiation of MSCs. In view of several reports demonstrating tissue healing properties of cannabinoids, the present study focussed on inhibitors of the enzyme fatty acid amide hydrolase (FAAH) which catalyzes the degradation of endocannabinoids (anandamide [AEA]; 2-arachidonoylglycerol [2-AG]) and endocannabinoid-like substances (N-oleylethanolamide [OEA]; N-palmitoylethanolamide [PEA]). Using Boyden chamber assays, the FAAH inhibitors arachidonoyl serotonin (AA-5HT) and URB597 were found to increase the migration of adipose-derived MSCs in a time- and concentration-dependent manner. The increase of migration by both compounds was inhibited by AM-630 (CB<sub>2</sub> receptor antagonist) and mimicked by AEA, 2-AG, OEA and PEA. Moreover, the promigratory effect of AA-5HT and URB597 was antagonized by inhibition of the p42/44 mitogen-activated protein kinase (MAPK) pathway which became activated upon treatment with both substances. A p42/44 MAPK-dependent promigratory effect was likewise demonstrated for the selective CB<sub>2</sub> receptor agonist JWH-133. Additional evidence for a functional effect of FAAH inhibitors on MSCs was provided by experiments demonstrating long-term stimulation with AA-5HT and URB597 to induce differentiation of MSCs into the osteoblastic lineage as evidenced by increased mineralization assessed by cresolphthalein complexone assay. Collectively, this study demonstrates FAAH inhibitors to promote the migration of MSCs via a CB<sub>2</sub> receptor-dependent pathway involving activation of p42/44 MAPK and to induce osteoblastic

differentiation. FAAH inhibitors may therefore recruit MSCs to sites of calcifying tissue regeneration and subsequently support bone regeneration via an osteoanabolic action on MSCs.

## 413

### Occurrence of perfluorinated compounds in human milk from Lower Saxony, Germany

**Wollin, Klaus-Michael**<sup>1</sup>; Ehlers, Susan<sup>2</sup>; Bernsmann, Thorsten<sup>2</sup>; Fürst, Peter<sup>2</sup>; Huppmann, René<sup>1</sup>; Suchenwirth, Roland<sup>1</sup>

<sup>1</sup>Niedersächsisches Landesgesundheitsamt, Hannover, Germany

<sup>2</sup>Chemisches und Veterinäruntersuchungsamt Münsterland-Emscher-Lippe (CVUA-MEL) - AöR, Germany

It is generally accepted that breastfeeding ensures the best possible health as well as the best developmental and psychosocial outcomes for the infant. However, uncertainties exist regarding the assessment of possible risks of chemical contaminants in breast milk. Perfluorinated compounds (PFCs) are a group of chemicals that are widely used in various industrial and consumer applications. They are extremely resistant towards thermal, chemical and biological degradation processes. Concerns exist due to the widespread exposure to humans, the persistence in the environment and the observed toxicity in *in vitro* studies as well as in animal models.

In this study, twelve PFCs (perfluorobutane sulfonic acid (PFBS), perfluorohexanoic acid (PFHxA), perfluoroheptanoic acid (PFHpA), perfluorohexane sulfonate (PFHxS), perfluorooctanoic acid (PFOA), perfluoroheptane sulfonate (PFHpS), perfluorononanoic acid (PFNA), perfluorooctane sulfonic acid (PFOS), perfluorodecanoic acid (PFDA), perfluoroundecanoic acid (PFUnA), perfluorododecanoic acid (PFDoA), and perfluorodecane sulfonate (PFDS)) were measured in a total of 110 human milk samples collected in 2010/2012 from Lower Saxony. Analyses of PFCs were performed by liquid chromatography-tandem mass spectrometry (LC-MS/MS). PFOA and PFOS were found to be the predominant compounds. PFOA could be quantified in 96% of all samples (mean: 38.6 ng/L, median: 30.8 ng/L, range: 12.5-270.0 ng/L, n=106). PFOS was analysed in 102 samples (93%) (mean: 32.4 ng/L, median: 24.2 ng/L, range: 12.0-141.5 ng/L, n=102). The high proportion of samples with quantified PFOA levels is noteworthy. A significant correlation between PFOA and PFOS concentrations was observed ( $|r|=0.3897 > r=0.24$  ( $f=108$ ,  $P=0.99$ )). In contrast, PFNA, PFHxS and PFDA were quantified in a subset of 11 (10%), 5 (5%) and 1 (1%) samples. PFNA and PFHxS concentrations in the positive samples ranged from 12.9 to 59.0 ng/L and 12.0 to 19.2 ng/L with median values at 15.0 ng PFNA/L and 14.0 ng PFHxS/L, respectively. The values of all other target PFCs were below the respective *Limit of Detection*.

Intake levels for exclusively breast-fed infants were estimated for three age groups (birth to <1 month, 1 to <3 months and 3 to <6 months) using the PFOS and PFOA maximum values. The calculated intake did not exceed the *Tolerable Daily Intake* for PFOS of 0.15  $\mu$ g/kg b.w./day and PFOA of 1.5  $\mu$ g/kg b.w./day as established by the European Food Safety Authority.

## 414

### Endotoxin detection in a bovine whole blood assay

**Wunderlich, Christian**; Schumacher, Stephan; Kietzmann, Manfred

University of Veterinary Medicine Hannover, Foundation, Institute of Pharmacology, Toxicology and Pharmacy, Germany

The detection of endotoxin contamination is an essential part of drug safety testing. The rabbit pyrogen test (RPT), the Limulus amoebocyte lysate (LAL) test and the monocyte activation test (MAT) are established methods for the detection of pyrogens. However, the RPT and LAL test are solely capable of identifying the presence of endotoxins whereas the use of the MAT is limited by the availability of human blood[1]. Conveniently bovine blood seems to react with lipopolysaccharide (LPS) and in addition to that it is remarkably that the bovine species reacts homologous to human species considering pathogen-associated molecular pattern (PAMP) detection via toll-like receptors (TLR)[2]. This led us to establish a method of using bovine whole blood as a tool for the detection of endotoxin contaminations.

225  $\mu$ l lithium heparin bovine blood from different donors were pipetted into 96 well cell culture plates and stimulated at least for 20 hours with 25  $\mu$ l LPS at varying concentrations derived from *Escherichia coli* 0111:B4. LPS effect was quantified by measuring PGE<sub>2</sub> concentration, using a Prostaglandin E<sub>2</sub> Express Kit following the manufacturer's instructions.

LPS (*E.coli* 0111:B4, 1.5625 pg/ml – 12.5 pg/ml final concentration) was found to induce a dose-dependent increase of PGE<sub>2</sub> (Figure 1). However, in preliminary tests, concentrations lower than 1.5625 pg/ml induced only a slight PGE<sub>2</sub> release and more than 12.5 pg/ml did not result in a distinct further increase of PGE<sub>2</sub> production suggesting a plateau was reached.

In conclusion, our work demonstrates the far reaching possibilities of using our *in vitro* bovine whole blood assay in accordance to PGE<sub>2</sub> production for endotoxin detection. In the matter of fact that there is no restriction in availability of bovine blood the assay could be a sensitive tool for endotoxin testing in larger quantities; congenial to the equal TLR equipment of humans and cattle our *in vitro* bovine blood assay seems to be at least as sensitive as the MAT.

1. Charton E, Brügger P, Spreitzer I, Golding B: *Alternatives to Animal Testing*. In: *EDQM Symposium: 16.09.2011 2011; Strasbourg, France*: EDQM, Council of Europe; 2011.

2. McGuire K, Jones M, Werling D, Williams JL, Glass EJ, Jann O: Radiation hybrid mapping of all 10 characterized bovine Toll-like receptors. *Anim Genet* 2006, 37(1):47-50.

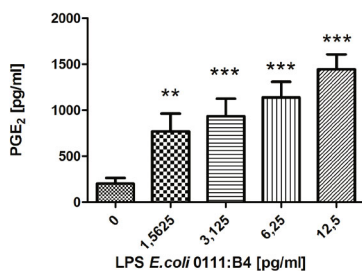


**Figure 1:** Prostaglandin E2 concentration after LPS stimulation of fresh (stored)

## 415

### CE-LIF and CE-MS for investigating adduct formation and kinetics of Pt-based anti-cancer drugs.

Zabel, Robert<sup>1</sup>; Kullmann, Maximilian<sup>2</sup>; Weber, Günther<sup>1</sup>

<sup>1</sup>Leibniz-Institut für Analytische Wissenschaften - ISAS - e.V., Systemanalyse, Dortmund, Germany

<sup>2</sup>Pharmazeutisches Institut Universität Bonn, Klinische Pharmazie, Germany

Pt-based anti-cancer drugs, such as cisplatin, are effective chemotherapeutic agents and widely used in the therapy of various types of cancer and are known to undergo several (bio-) chemical transformation steps after application. Hydrolysis and adduct formation with small nucleophiles and bigger proteins are thought to be the most relevant reactions on their way to the final reaction site (DNA), but there are still many open questions regarding the identity and pharmacological relevance of different proposed adducts and intermediates.

The aim of the project is the identification of binding partners inside tumor cells *in vitro*. CFDA-Platinum, a fluorescent cisplatin analogue with related pharmacodynamic and -kinetic properties, should help to identify binding partners. Due to the high separation power and sensitivity, capillary electrophoresis with laser induced fluorescence (CE-LIF) is the method of choice. Capillary electrophoresis with mass spectrometry (CE-MS) is used for the identification of unknown compounds. For the *in vitro* experiments we compared the cytosolic fraction of a human ovarian cancer cell line (A2780) and its corresponding cisplatin-resistant variant (A2780cis). In addition, we performed model experiments with CFDA-Platinum and potential binding partners, e.g. glutathione.

CE-LIF and CE-MS are appropriate analytical methods to detect and identify CFDA-Platinum and different complexes up to the ppb/ppm range. First results show a complex formation of CFDA-Platinum with biological molecules of interest. A comparison of human ovarian cancer cells and its cisplatin-resistant variant indicates differences in the intracellular accumulation of CFDA-Platinum.

## 416

### Prostaglandin E2 can bypass the need for AhR signaling in immunosuppressive IDO gene induction by dendritic cells

Bargen, Imke<sup>1</sup>; Kadow, Stefanie<sup>1</sup>; Zado, Katia<sup>2</sup>; Esser, Charlotte<sup>1</sup>

<sup>1</sup>IUF-Institut für Umweltmedizinische Forschung, Immuntoxikologie, Düsseldorf, Germany

<sup>2</sup>Charite, Inst. für Klinische Pharmakologie und Toxikologie, Berlin, Germany

The aryl hydrocarbon receptor (AhR) is sensor of small chemicals and orchestrates responses as diverse as xenobiotic catabolism and immune responses. We and others have shown that the inducible expression of the immunosuppressive enzyme indoleamine-2,3-dioxygenase (IDO) is absent in AhR-deficient Langerhans cells and BM-derived dendritic cells (BM-DC). IDO generates kynurenin from tryptophan. DC thus can curb availability of the essential amino acid tryptophan and thereby create an immunosuppressive micro-milieu. In addition kynurenin, as an AhR ligand, can ensure continuing AhR activity. IDO expression can be triggered by LPS via the NFkB pathway or via IFNg/STAT1. The failure of AhR-deficient DC to induce IDO is not due to a defect in the respective signalling cascades, as toll-like receptors were detectable, and LPS or IFNg could induce TNFa, IL6, CXCL10 and IRF1 or the IDO downstream enzyme kynureninase. We therefore asked whether prostaglandin E<sub>2</sub> (PGE<sub>2</sub>) signalling, which had been reported to induce IDO mRNA, cooperates with AhR-signalling in IDO mRNA induction. Treatment of wild-type bone-marrow derived DC with LPS and PGE<sub>2</sub> enhanced IDO in a synergistic fashion, while PGE<sub>2</sub> treatment alone induced IDO only moderately. Abrogation of IDO induction in AhR-deficient BM-DC could be overcome by stimulation with LPS and PGE<sub>2</sub>. Inhibition of PGE<sub>2</sub> with acetylsalicylic acid led to a

decreased IDO induction of wild-type BM-DCs and no detectable expression at all in AhR-deficient DCs. Thus, PGE<sub>2</sub> contributes to shifting DC towards IDO production and thus ultimately down-modulation of inflammation. Moreover, PGE<sub>2</sub> has a role in by-passing the need for AhR-signaling in IDO induction by DC. Our results reveal a novel cross-talk of AhR signalling with other inflammatory pathways in dendritic cells.

## 417

### Gtl2/Meg3 – a reliable marker for hepatocarcinogenesis?

Zeller, Eva; Unterberger, Elif; Braeuning, Albert; Schwarz, Michael

Institut für Experimentelle und Klinische Pharmakologie und Toxikologie, Abteilung Toxikologie, Tübingen, Germany

Carcinogenesis is a progressive multistep process comprising various genetic alterations such as mutations in tumor suppressor genes and oncogenes. Non-genotoxic carcinogens (NGCs) induce tumor formation by mechanisms other than changes in the underlying DNA sequence. Phenobarbital (PB) is a classic non-genotoxic carcinogen leading to perturbations in gene expression and DNA methylation. Recently, non-coding RNAs from the *Dlk1-Dio3* cluster were identified as potential biomarkers for mouse liver tumor promotion caused by PB. One gene within this imprinted region is named *Gtl2/Meg3*. In humans, loss of *MEG3* expression is found in various primary tumors, but not in hepatoblastoma, a malignant liver neoplasm occurring in infants and children. We noticed that *Gtl2* is overexpressed in PB-treated murine tissue ( $\beta$ -Catenin-mutated tumor and normal liver) as well as in the majority of human hepatoblastoma samples containing activating  $\beta$ -Catenin mutations. *Gtl2* overexpression meets with the activation of Wnt/ $\beta$ -Catenin signaling. Two other tumor promoters, the aryl hydrocarbon receptor (AhR) agonist PCB 126 and PCB 153, acting via activation of the constitutive androstane receptor (CAR) led to enhanced *Gtl2*-expression in murine normal liver. In contrast, rats only partially indicated an increase in *Gtl2*-expression after PB and clofibrate (CF) treatment, another NGC. In murine hepatoma cell lines, *Gtl2/Meg3* could not be detected because these cells lack the constitutive androstane receptor. *Gtl2*-knockout models in the literature are not suited for a long-term carcinogenicity experiment, because the animals die within a few weeks after birth. For this reason, mice were infected with a *Gtl2*-expressing adenovirus to study effects of *Gtl2* overexpression in hepatocytes.

In conclusion, *Gtl2* seems to be a reliable marker for hepatocarcinogenesis in mice, but the interspecies transferability to rats is limited.

## 418

### Activation of intermediate-conductance calcium-activated potassium channels by nucleoside diphosphate kinase B is required for neointimal hyperplasia in injured mouse carotid artery

Zhou, Xiao-Bo<sup>1</sup>; Feng, Yu-Xi<sup>2</sup>; Sun, Qiang<sup>1,3</sup>; Lukowski, Robert<sup>4</sup>; Qiu, Yi<sup>2</sup>; Spiger, Katharina<sup>2</sup>; Ruth, Peter<sup>2</sup>; Korth, Michael<sup>5</sup>; Skolnik, Edward Y.<sup>6</sup>; Borggreffe, Martin<sup>7</sup>; Dobrev, Dobromir<sup>1,3,8</sup>; Wieland, Thomas<sup>2,8</sup>

<sup>1</sup>Division of Experimental Cardiology, Medical Faculty Mannheim, University of Heidelberg, Germany

<sup>2</sup>Institute of Experimental and Clinical Pharmacology and Toxicology, Medical Faculty Mannheim, University of Heidelberg, Germany

<sup>3</sup>Institute of Pharmacology, Medical Faculty, University of Duisburg-Essen, Germany

<sup>4</sup>Department of Pharmacology and Toxicology, Institute of Pharmacy, University of Tübingen, Germany

<sup>5</sup>Department of Experimental Pharmacology and Toxicology, University Medical Center Hamburg-Eppendorf, Germany

<sup>6</sup>Department of Medicine and Department of Pharmacology, New York University Langone Medical Center, United States

<sup>7</sup>1st Medical Clinic, Medical Faculty Mannheim, University of Heidelberg, Germany

<sup>8</sup>DZHK (German Center for Cardiovascular Research), Partner Site, Heidelberg-Mannheim, Germany

**Rationale-**Endothelial injury stimulates proliferation of vascular smooth muscle cells (VSMCs). The intermediate-conductance Ca<sup>2+</sup>-activated K<sup>+</sup> channel (SK4 channel) is apparently required for VSMC proliferation during atherosclerosis and postangioplasty restenosis. Nucleoside diphosphate kinase B (NDPK B) has been shown to activate SK4 channels, e.g. in proliferating T-lymphocytes, via histidine phosphorylation of the channel C-terminus.

**Objective-**We intended to explore the role of NDPK B in the regulation of SK4 channels in proliferating VSMC and thus neointima formation in injured arteries.

**Methods and Results-**Functional expression of SK4 channels in VSMCs from guide-wire injured mouse carotid artery was assessed by patch-clamp and real-time PCR analysis. SK4 channel currents (I<sub>SK4</sub>) were detectable in neointimal but not in mature VSMCs. Concomitantly, a reduction in the mRNA encoding BK channels and in BK currents (I<sub>BK</sub>) occurred. Application of recombinant NDPK B into neointimal VSMCs through the patch pipette led to ~2-fold increase in I<sub>SK4</sub> amplitude, whereas application of NDPK A or NDPK C had no effect. NDPK B did not increase the membrane currents in neointimal VSMCs from mice lacking SK4 (SK4<sup>-/-</sup>), indicating that NDPK B activates specifically SK4 channels in proliferating VSMCs. Concomitant inclusion of protein histidine phosphatase 1 (PHP-1), but not the kinase-inactive mutant (PHPT-1(H53A)), into the cells prevented the effect of NDPK B. In inside-out patches, direct application of NDPK B to the intracellular side of the membrane increased SK4 channel activity. PHP-1 completely reversed the effect of NDPK B, indicating that histidine phosphorylation in the channel is responsible for the channel activation. Application of

PHPT-1 alone or genetic NDPK B deficiency (NDPK B<sup>-/-</sup>) led to ~50 % reduction of endogenous I<sub>SK4</sub>, indicating a constitutive activation of SK4 channels in proliferating VSMCs. Both, SK4-deficient and NDPK B-deficient mice were similarly protected from neointima formation in injured arteries.

**Conclusion**-NDPK B constitutively activates SK4 channels which get expressed when mature VSMCs turn into the proliferative phenotype. The NDPK-B activated SK4 channels are required for VSMC proliferation and thus neointimal hyperplasia in injured arteries.

#### 419

##### Effect of oxygen pressure and statins on ionizing radiation-induced stress response of human keratinocytes

**Ziegler, Verena**; Albers, Anne; Henninger, Christian; Fritz, Gerhard  
Heinrich Heine University Düsseldorf, Institute of Toxicology, Germany

The majority of head and neck cancer patients receiving radiotherapy suffer from ionizing radiation (IR)-induced oral mucositis which impedes the maximum tolerated radiation dose and limits effective cancer treatment. Mucositis is initiated by direct injury to epithelial cells resulting in the production of inflammatory cytokines. Radiation-induced DNA strand breaks and generation of reactive oxygen species (ROS) also contribute to the pathogenesis of mucositis. Keeping in mind the limited treatment options, we aim to identify pharmacologic strategies for the prevention and the treatment of radiation-induced oral mucositis.

To assess ionizing radiation (IR)-induced stress responses spontaneously transformed, but non-tumorigenic, human keratinocyte cells (HaCaT) were used as an *in vitro* model. Since ROS contribute to IR-induced DNA damage formation and the DNA damage response (DDR) we compared HaCaT cells that were grown under normal (21 %) or low ( $\leq 5$  %) oxygen conditions. We monitored the formation of DNA strand breaks using the comet assay and measured nuclear Ser139 phosphorylated histon 2AX (γH2AX) foci at different time points after irradiation. Alamar Blue assay allowed to examine a reduction of cell viability following irradiation. In order to determine alterations in cell cycle progression and induction of cell death (i.e. subG1 fraction) after irradiation, HaCaT cells were subjected to flow cytometric analysis. Western Blot analysis was performed to analyse expression and activity status of proteins involved in the DDR.

Based on the fact that statins protect from IR-induced cell death *in vitro* and normal tissue damage *in vivo*, we hypothesize that this might also hold true for keratinocytes. To this end, we currently test whether inhibition of Ras homologous (=Rho) small GTPases by lovastatin might modulate the signaling of HaCaT cells after IR-induced damage. Our current aim is to investigate whether statins are able to attenuate mucositis-associated pathologic processes following irradiation using the HaCaT model. The results obtained will be presented and discussed.

#### 420

##### The SILICOAT project: *In vitro* and *in vivo* toxicity screening of quartz varieties from traditional ceramics industry and approaches for an effective quartz surface coating

**Ziemann, Christina**<sup>1</sup>; Reamon-Buettner, Stella Marie<sup>1</sup>; Tillmann, Thomas<sup>1</sup>; Hansen, Tanja<sup>1</sup>; Ibañez, María Jesús<sup>2</sup>; Monfort, Eliseo<sup>2</sup>; Bonvicini, Giuliana<sup>3</sup>; Escrig, Alberto<sup>3</sup>; Creutzenberg, Otto<sup>1</sup>

<sup>1</sup>Fraunhofer Institut für Toxikologie und Experimentelle Medizin ITEM, Hannover, Germany

<sup>2</sup>Instituto de Tecnología Cerámica ITC, Castellón, Spain

<sup>3</sup>Centro Ceramico Bologna CCB, Italy

The International Agency for Research on Cancer (IARC) has classified respirable crystalline silica (RCS) in the form of quartz or cristobalite from occupational sources as human carcinogens (category 1; 1997), however, acknowledging differences depending on source, as well as chemical, thermal and mechanical history of RCS. In the traditional ceramics industry, quartz containing raw materials are indispensable for manufacture and workers exposed to higher RCS concentrations in the air are potentially at risk for lung inflammation, silicosis or even lung tumors. The SILICOAT project thus aims at increasing workers' safety by developing and implementing cost-effective RCS coating technologies into ceramic processes which should saturate reactive surface silanol groups and inhibit quartz-specific toxic effects. Initially, 25 quartz-containing or -free raw materials from four ceramic producers (bulk powders or dried after wet milling) were screened *in vitro* (primary rat alveolar macrophages, 4 h of incubation, 75 µg/cm<sup>2</sup>) and *in vivo* (intratracheal instillation, Wistar rats, 4 mg/rat, sacrifice after 3 and 28 days) for their biological activity using highly active quartz DQ12 as the positive control. Lactate dehydrogenase (LDH) screening tests ± aluminum lactate (quencher of quartz-specific effects), revealed no marked cytotoxic effect for all quartz-free (calcite, dolomite, alumina) and feldspar samples, and almost all wet milled materials. But, bulk samples exhibited variable quartz-related cytotoxic potential. Clastogenicity (comet assay) and pro-inflammatory CXCL2 gene expression (qRT-PCR) were then investigated for the samples with highest quartz content. All quartzes and kaolins, but no clay, mediated DNA damage, and all materials induced (in part quartz-independently) CXCL2 gene expression. A subsequent *in vivo* validation study, elicited lack of effect for clays, acute response for one kaolin and initially retarded, but then progressive effects for quartzes (polymorphonuclear neutrophils, LDH, β-glucuronidase, total protein). The most active quartz was subsequently used for development of promising covalent organosilane-based coating strategies. In conclusion, toxicity screening demonstrated gradually

different quartz-specific but also quartz-independent biological activities of ceramic raw materials and indicated attenuation of quartz effects by wet milling with alumina balls.

**The project has received funding by the European Union's 7<sup>th</sup> Framework Programme (FP7/2007-2013) under grant agreement n° 285787.**

#### 421

##### IL-1-triggered NF-κB activity critically depends on HDAC3-mediated p65 deacetylation

**Ziesché, Elisabeth**<sup>1</sup>; Kettner-Buhrow, Daniela<sup>1</sup>; Weber, Axel<sup>1</sup>; Wittwer, Tobias<sup>2</sup>; Jurida, Liane<sup>1</sup>; Soelch, Johanna<sup>1</sup>; Müller, Helmut<sup>1</sup>; Newel, Doris<sup>1</sup>; Kronich, Petra<sup>1</sup>; Schneider, Heike<sup>3</sup>; Dittich-Breiholz, Oliver<sup>3</sup>; Bhaskara, Srividya<sup>4</sup>; Hiebert, Scott<sup>1</sup>; Hottiger, Michael<sup>5</sup>; Li, Haiying<sup>6</sup>; Burstein, Ezra<sup>6</sup>; Schmitz, M. Lienhard<sup>2</sup>; Kracht, Michael<sup>1</sup>

<sup>1</sup>Justus-Liebig-Universität Giessen, Rudolf-Buchheim-Institut für Pharmakologie, Germany

<sup>2</sup>Justus-Liebig-Universität Giessen, Institut für Biochemie, Germany

<sup>3</sup>MHH, Physiologische Chemie, Hannover, Germany

<sup>4</sup>Vanderbilt University, Department of Biochemistry, Nashville, United States

<sup>5</sup>Universität Zürich, Institute of Veterinary Biochemistry and Molecular Biology, Switzerland

<sup>6</sup>UT Southwestern, Medical Center, Dallas, United States

Histone deacetylase (HDAC) 3, a cofactor in co-repressor complexes containing silencing

mediator for retinoid or thyroid-hormone receptors (SMRT) and nuclear receptor co-repressor (N-CoR), has been shown to repress gene transcription in a variety of contexts. To investigate the contribution of HDAC3 in cytokine signaling, its function was inhibited by various experimental approaches. Interference with HDAC3 expression or catalytic activity by RNAi-mediated knockdown in human epithelial cells, conditional gene deletion in murine embryonic fibroblasts or inhibition by the small molecule apicidin indicate a novel role for HDAC3 as positive regulator of the majority of IL-1-induced human or murine genes. This effect was independent from the gene regulatory effects mediated by the broad-spectrum HDAC inhibitor trichostatin A (TSA) and thus suggests IL-1-specific functions for HDAC3. The stimulatory function of HDAC3 for inflammatory gene expression involves a mechanism that employs binding to NF-κB p65 and its deacetylation at various lysines (K122, K123, K310, K314 and K315). NF-κB p65-deficient cells stably reconstituted to express wild-type or acetylation-mimicking forms of p65 (p65 K/Q) revealed that mutants resembling the acetylated form of p65 had largely lost their potential to regulate IL-1-triggered gene expression, implying that the co-activating property of HDAC3 involves the removal of inhibitory p65 acetylation at K122, 123, 314 and 315. Together with recent publications from others, these data reveal HDAC3 as a co-activator in inflammatory signaling pathways and help to explain the anti-inflammatory effects frequently observed for HDAC inhibitors in (pre)clinical use.

#### 422

##### Clinical lead poisonings due to drinking water – analysis of historical case descriptions

**Zietz, Björn**

Akademie für öffentliches Gesundheitswesen (Academy of Public Health), Düsseldorf, Germany

The toxic metal lead was utilized for drinking water pipes and water installations since antiquity. In the 19th century and at the beginning of the 20th century cases of lead poisonings with clinical symptoms in relation to drinking water lead pipes were frequently observed. The largest documented case clusters in the German-speaking countries occurred in Dessau in the years 1886/1887 and in Leipzig in 1930. Other case clusters were particularly reported for Calau (1888), Clausthal-Zellerfeld (1929), Diepholz and area (1886-1905), Emden (1897), Görlitz (1911), the North Sea Island of Helgoland (until 1935), Krosno on the Oder (1888), Naunhof (1913), Offenbach/Main (1884), Teplitz-Schönau (1903), Wilhelmshaven (1886), as well as for various other unspecified places. The victims showed symptoms such as lead colic and other gastrointestinal symptoms, pallor, fatigue and Burton's gum line. In some cases they also developed neurological symptoms such as peripheral paralysis. In addition to the lead pipes, several other physico-chemical conditions were reported by the examiners, which were supposed to be connected with the case clusters, too. Almost always soft or very soft water was associated with the cases. In addition one or more additional supervening factors such as presence of plenty of free carbonic acid or presence of humic acids, air/oxygen in the pipe systems, great length of lead pipes, recent pipework construction, long stagnation periods or changes in the water chemistry were mentioned in context with the poisonings. In the case clusters where lead in tap water was measured, concentrations frequently exceeded 1 mg/L and sometimes 10 mg/L in stagnation samples (usually colorimetric determination with H<sub>2</sub>S). Since the 18th century, there was a partially controversial discussion whether lead pipes were suitable for drinking water, p.r.n. necessary conditions for their use and possible lead limit values. In the 19th century this discussion was usually referred as the "lead pipe question". Due to modern water treatment and water distribution systems the nowadays measured concentrations of lead in tap water in presence of lead pipes are normally much lower than the historically observed values. Recently the lead limit value for drinking water in Germany was lowered to 0,01 mg/L, regulated by the German drinking water ordinance (effective 1st Dec. 2013).



### Identification of residues of parathyroid hormone receptors undergoing agonist-induced phosphorylation

Zindel, Diana<sup>1,2</sup>; Butcher, Adrian<sup>2</sup>; Bünemann, Moritz<sup>1</sup>; Tobin, Andrew<sup>2</sup>; Krasel, Cornelius

<sup>1</sup>Philipps-Universität Marburg, Institut für Pharmakologie und Klinische Pharmazie, Germany

<sup>2</sup>University of Leicester, MRC Toxicology Unit, Great Britain

Phosphorylation of G-protein coupled receptors (GPCRs) represents a key event in regulating receptor function and determines about subsequent signaling properties of this receptor superfamily. It has been shown previously that the activation of the human parathyroid hormone receptor 1 (hPTH1R) results in phosphorylation by PKA, PKC and GRKs (1). Although it is known that the PTHR is phosphorylated by PKC in the proximal portion of the tail and GRK2 phosphorylates the receptor more distally in the tail (2), the precise sites of ligand-induced receptor phosphorylation remain to be determined. Using a mass spectrometry-based approach we set out to map the PTH (1-34)-induced sites of phosphorylation within the human parathyroid hormone receptor in intact HEK293 cells stably expressing the receptor. We could identify a motif within the C-terminal tail being phosphorylated on serines and threonines. Furthermore this study aims to compare different PTHR ligands with regard to their potential of receptor phosphorylation. It has been reported that [Trp<sup>12</sup>, Tyr<sup>34</sup>]PTH(7-34) selectively mediates arrestin signaling (3). [Trp<sup>12</sup>, Tyr<sup>34</sup>]PTH(7-34) did not induce any phosphorylation of the receptor as determined by <sup>32</sup>P labeling. Using fluorescence microscopy we could not observe any arrestin translocation to receptors upon [Trp<sup>12</sup>, Tyr<sup>34</sup>]PTH(7-34) treatment.

1. Blind E, Bambino T, Nissenson RA. Agonist-stimulated phosphorylation of the G protein-coupled receptor for parathyroid hormone (PTH) and PTH-related protein. *Endocrinology*. 1995 136:4271-7.

2. Blind E, Bambino T, Huang Z, Blizotes M, Nissenson RA. Phosphorylation of the cytoplasmic tail of the PTH/PTHrP receptor. *J Bone Miner Res*. 1996 11:578-86.

3. Gesty-Palmer D, Flannery P, Yuan L, Corsino L, Spurney R, Lefkowitz RJ, Luttrell LM. A beta-arrestin-biased agonist of the parathyroid hormone receptor (PTH1R) promotes bone formation independent of G protein activation. *Sci Transl Med*. 2009 1:1ra1.

### Author Index

Aasland D.	311, 016
Abd Alla J.	088
Abdalla S.	243
Abdel-Aziz H.	224, 091, 090, 089, 001
Abdelaziz R.	294
Abdel-Naby D. H.	224
Abdullah S.	246
Abraham K.	002
Abt C.	247
Abu Abed M.	140
Acker-Palmer A.	085
Adam B.	096
Adam I.	285
Adawy A.	061
Adelung R.	294
Ahles A.	092
Akdeli N.	101
Aktories K.	401, 363, 242, 210, 131, 098, 057, 055, 040, 024
Albarran-Juarez J.	093
Albers A.	419
Albrecht A. E.	094
Albrecht W.	041
Alexiou C.	208
Ali N.	156, 095
Alms D.	286
Althoff T.	093
Amini M.	096
Anger L. T.	097
Apers J. A.	086
Aretz J. S.	003
Arianov R.	054
Arit O.	367
Arndt H.	315
Assmann J. C.	405
Augspach A.	098
Augustin C.	284
Aumiller V.	199
Autengruber A.	099
Autenrieth S.	123
Autschbach R.	337
Avila J.	173
Baaske K.	384
Bach A.	100, 004
Bachmann H. S.	101
Backs J.	324, 102
Bader M.	355, 304
Bähre H.	391, 276, 103, 073
Balszuweit F.	104
Bankoglu E. E.	105
Bankstahl M.	005
Baranyai D.	106
Barg M.	167

Bargen I.	416
Bartels J.	107
Barth H.	345, 134, 027, 024
Bartkuhn M.	008
Batkai S.	155
Batke M.	357, 295, 248, 178, 144, 108
Bauer T.	392
Baumann S.	114
Bäumer W.	359, 331, 068
Bayer J. K.	109
Becirovic E.	153
Beck A.	409, 372, 244, 111, 096, 034, 006
Becker J. P.	385
Becker W.	376, 322
Beer-Hammer S.	373, 123
Begher-Tibbe B.	183
Behrends S.	329, 282, 107
Bekka E.	110
Belkacemi A.	111
Belkacemi T.	372, 006
Bellin M.	402
Bellmann B. T.	180, 087
Belz M.	323
Benahmed M.	029
Bencke S.	007
Bentrcia T.	380
Benz V.	364
Benzin A.	281
Berberat P.	179
Berg K.	112, 015
Berger S.	255, 162
Bernard C.	122
Bernd A.	113
Bernsmann T.	413
Bert B.	136
Bertin A.	251
Besik V.	120
Beuerlein K.	008
Beyer A.	114
Bhaskara S.	421
Biel M.	153, 059
Bilkei-Gorzo A.	152
Bilstein A.	099
Binder K.	402
Binz T.	133
Birk B.	075
Birkhofer C.	345
Birnbaumer L.	245, 223, 078
Birtel M.	048
Bischoff R.	015
Bitsch A.	347, 295, 178, 108
Blaszkevicz M.	170, 156, 095
Blei T.	206
Blodow S.	381
Blömeke B.	190, 104
Blum M. - M.	213

Blume R.	291	Daiber A.	249, 069
Bober H.	201	Dalila N.	371
Bock A.	009	Damm G.	301
Bock G.	056	Dammann M.	125
Böckmann S.	115	Danciu C.	300
Bode C.	255, 162	Dang T.	383
Bodmann E. - L.	052	Dangwal S.	132
Boeddinghaus J.	197	Danser J.	022
Böhm A.	261, 116	Dasenbrock C.	397, 154
Böhmer K. E.	040	de Amici M.	009
Bolay C.	366	de Wit C.	075
Bolbrinker J.	354, 173	Debiak M.	048, 007
Boldt K.	045	Degen G. H.	156, 095
Bollmann F.	010	Dehelean C.	300
Bollmann P.	232	Dehn C.	133
Bondarenko A. I.	161	Deiss K.	341
Bonvicini G.	420	Del Turco D.	256
Borggrefe M.	418	Demleitner J.	134
Bormann S.	117	Deng S.	085, 019
Börnchen C.	197	Denzinger S.	341
Bos S.	288	Dewenter M.	324, 272
Bothe A.	256	Dhein S.	321
Bracher F.	322	Dick L. S.	135
Braeuning A.	417, 365, 176, 118	Dickhut C.	130
Braig S.	011	Diedrich A.	074, 037
Brand S.	361	Diel P.	206
Brandt C.	393, 389, 119	Diesler K.	311
Braun A.	229	Dietrich A.	229, 199, 134, 078
Braunschweig T.	337	Dietrich C.	404
Brede M.	340	Dietrich K.	020
Breit A.	120	Dietze S.	136
Brenneisen P.	362	Ding Z.	280
Breyer F.	213, 212	Dittmar F.	137
Brinkmann J.	045, 037	Dittrich-Breiholz O.	421, 399, 008
Brockmüller J.	371, 140, 079	Dizayee S.	223
Bröderdorf S.	330, 121	Dobrev D.	418
Broekmans K.	012	Dole W.	022
Bröer S.	122	Döring B.	138
Broschk S.	309	Dorner B. G.	238
Brosda J.	159	Dörr J.	265, 111
Brunner T.	242	Dörsam B.	139
Brunhofer G.	119	Dorweiler B.	174
Brüning T.	351	Dos Santos Pereira J. N.	371, 140
Brunskole Hummel I.	171	Douros A.	173
Buchalla W.	366	Dove S.	062
Büchele B.	021	Draheim H.	056
Bucher K.	373, 123	Drasdo D.	183, 031
Bucher P.	118	Drejjer A. R.	086
Buchholz B.	064	Dresler M.	038
Buchholz S.	004	Drexler M.	278
Büchter C.	231, 124	Dreyer T.	402
Buckpitt A.	064	Driesch D.	031
Buesen R.	241, 126, 125	Driessen T.	160
Bühler A.	081, 013	Driessen S.	185
Buhrke T.	127, 002	Dröse S.	394
Bumke Scheer M.	143	Dürr S.	208
Bünemann M.	423, 128, 092, 052, 043	Dvorak M.	285
Bünger J.	351	Eaton P.	217
Burckhardt B. C.	014	Ebert J.	141
Burckhardt G.	014	Eckert P.	377, 163
Burkhardt B.	301	Eder A.	197
Burkhardt H.	310	Edlund K.	183
Bürkle A.	048, 007	Ehlers S.	413
Buron S.	173	Ehrenmann J.	226
Burstein E.	421	Eich M.	142
Busch R.	261	Eilander W.	086
Busemann A.	221	Eirich J.	011
Busker M.	282, 107	Eisen D.	059
Butcher A.	423	El Gafaary M.	021
Büttner M.	286	El-Armouche A.	374, 324, 272
Calebiro D.	260, 168	Elbahr M.	294
Cardinaux J. - R.	277	Eldahshan A.	348
Carell T.	059	Elger D. A.	165
Carrier L.	277	El-Ghazaly M. A.	224
Cartus A.	129, 015	El-Hazek R.	224
Cascorbi I.	181	Elsässer-Beile U.	098
Casini S.	402	Emous M.	086
Cavalié A.	004	Endo S.	370
Chan A.	085	Engel A.	143
Chang Y.	096	Engel G.	076
Chatterji B.	130	Engelhardt S.	334, 327, 223, 179, 092, 049
Chhibber A.	181	Engeli S.	022
Christmann M.	311, 016	Epstein J.	085
Cicha I.	208	Erdelmeier C. A. J.	230, 161
Closs E.	249, 069	Erdogmus S.	023
Coch C.	196	Erkel G.	058
Coenen M.	196	Erker T.	119
Colnot S.	176	Ernst H.	180
Couraud P. - O.	286	Ernst K.	024
Creutzenberg O.	420, 017	Esch H. L.	302, 163, 094
Czulkies B.	131	Eschenhagen T.	379, 277, 197
Dabrowski A.	018	Escher S.	357, 352, 248, 144
Dahlke M.	022	Esrig A.	420
		Esselen M.	175, 015
		Esser C.	416, 145

Etscheid J.	146	Glatt H.	325, 275, 015
Etzrodt J.	147	Glebe D.	138
		Glei M.	339
Fabian E.	177	Glünder G.	333, 114
Fahrer J.	139, 025	Godbole A.	168
Falk C.	132	Göder A.	139, 025
Falkenstein M.	169	Gödte-Armbrust U.	106, 019
Faust D.	404	Golka K.	170, 169
Fecher-Trost C.	148	Golombek M.	084
Fedrowitz M.	319, 149, 026	Golz S.	392
Fehrmann E.	356, 150	Göpfert J.	176
Feil R.	403, 075	Görgler N.	323
Feil S.	075	Gorressen S.	280
Feldmann K.	151	Gosens R.	288
Feliszek M.	152	Gotic M.	099
Felix S.	261	Göttle M.	252, 171
Fels B.	236, 150	Götz K.	032
Fender A.	298	Goy S.	172, 030
Fender A. C.	109	Grabowski K.	173
Fendl D.	400	Graefe A.	158
Feng Y. - X.	418	Graemer M.	243, 088
Fenske S.	153	Grandoch M.	280, 189, 151, 109
Fernandes J.	348	Grechowa I.	174
Fernekoru U.	262	Grittner D.	246
Ferreirós Bouzas N.	367, 256	Groeters S.	407, 241, 222, 125, 029
Fiedler D.	251	Groh I. A. M.	175
Fiedler J.	155	Groll N.	176
Fiedler S.	134	Groothuis G.	288
Filingeri D.	013	Grosse R.	278, 033
Fink H.	159, 136	Grosshennig A.	037
Fischer J. W.	362, 316, 298, 280, 237, 189, 160, 151, 135, 109	Grube M.	202
Fischer M.	397, 179, 154	Gründemann D.	392, 239
Fischer S.	308	Grüning B.	307
Flockerzi V.	409, 380, 372, 266, 265, 244, 148, 111, 100, 096, 078, 006, 004	Grzęda E.	388
Flockerzie K.	245	Gudermann T.	382, 381, 278, 271, 229, 216, 199, 157, 134, 120, 110, 023
Florencio Ortiz V.	376	Gundert-Remy U.	296, 295, 178, 108
Flößer A.	116	Günther G.	312, 061
Foinquinos A.	155	Guo Z.	277
Föllmann W.	156	Gust R.	056
Fork C.	392	Guth K.	395, 177
Forst A. - L.	157	Gütlein M.	295, 178, 108
Förstermann U.	249, 069	Gutmann J.	179
Förtsch C.	027		
Foryst-Ludwig A.	364	Haas B.	187
Foth H.	360, 262, 219	Haas J.	402, 013
Fowler S. C.	067	Haase N.	107
Franke H.	158	Haase T.	107
Franke R. T.	159	Haastert-Talini K.	317
Freichel M.	266, 100, 078, 034, 004	Habermeier A.	249, 069
Frensch I.	028	Hackbarth A.	180, 087
Frericks M.	029	Haenisch S.	181
Freudenberger T.	237, 160	Hagemann S.	318, 317, 164, 080
Fricker G.	113	Hagos Y.	014
Friebe A.	147	Hahn S.	347, 250
Friebel A.	183	Halwachs S.	182
Friedrich R. P.	208	Hammad S.	183
Frieling C.	187	Hammelmann V.	153
Friese A.	114	Hammer H. S.	184
Fritz E. - M.	410	Hammock B. D.	064
Fritz G.	419, 240, 192, 191, 117, 038	Hampel J.	262
Frohnweiler K.	265	Han B.	185
Frombach J.	375	Han X.	075
Frumkina A.	404	Handreck A.	165
Fuchs S.	161	Handscheck K.	399, 008
Fukumura D.	075	Hansen A.	379, 197
Fürst D.	162	Hansen T.	420, 284, 017
Fürst P.	413	Häring H. - U.	287
Fürst R.	161	Harms T.	173
Fussell K. C.	029	Harteneck C.	373, 314
Futh S.	163	Hartmann G.	196
		Hartung J.	378
Gabriel M.	119	Hartung P.	193
Gajewski P. D.	169	Hartwig C.	336, 137, 084, 073
Garbers C.	280	Hasan A.	186
Gareis M.	094	Hasan N.	034
Gass P.	405	Hass M.	187
Gavrilov A.	365, 118	Hass R.	026
Gebhardt R.	031	Hassan S. I.	153
Geerts A.	392	Hausmann R.	188
Gehrke H.	410, 387	Haustein M.	308, 035
Geiger D.	241	Havenith G.	013
Geisslinger G.	256, 225, 217, 051	Havermann S.	398, 231, 036
Geminn J.	078	Hecker M.	309
Genth H.	332, 164, 030	Heidecke C. - D.	221
Genz B.	085	Heijink I. H.	306
Gergs U.	321, 269, 268, 232, 207	Hein F.	400
Gerhard R.	172, 030	Hein L.	320, 307, 255, 167, 162
Gernert M.	166, 165	Heinick A.	356, 346
Gey L.	166, 165	Heinisch N.	189
Geyer J.	138, 003	Heise T.	343, 228, 063, 018
Ghallab A.	312, 031	Heiss C.	160
Gierschik P.	081, 013	Helma C.	295, 178
Gillsbach R.	320, 307, 255, 167	Hemmasi S.	131
Glage S.	130	Hengstler J. G.	183, 170, 169, 031
Glahn F.	360, 219	Henke J.	058
		Henkel S.	031

Henkler F.	297
Hennen J.	190
Hennicke T.	191
Henninger C.	419, 192
Hensel J. - T.	379
Herbarth L.	045
Herebian D.	003
Herjigers P.	266
Hermkes E.	081
Herrmann K.	275
Herzig S.	369, 223
Heiß J.	101
Hessel S.	258, 211
Heusser K.	074, 037
Hey V.	060
Hiebert S.	421
Higley E.	309
Hildebrandt I.	370
Hill K.	193
Hiller K. - A.	366
Hiltensperger G.	094
Himmler K.	346
Hintzpete J.	194, 072
Hintzsche H.	384, 195
Hinz B.	412, 308, 115, 035
Hinz L.	092
Hinze A. V.	196
Hipp L.	050
Hirt M. N.	379, 197
Hodwin B.	049
Hoehme S.	183
Höfer T.	267
Hoffmann A.	286
Hoffmann C.	383, 340, 023, 009
Hoffmann K.	254, 198
Hoffmann L. S.	147
Hofmann F.	411
Hofmann K.	199
Höhme S.	031
Holdenrieder S.	196
Hollert H.	309
Holzgrabe U.	094, 009
Honarvar N.	395
Honnen S.	038
Honscha W.	182, 114
Hopfer C.	271, 216, 110
Horke S.	249, 200, 174, 141, 039
Hornung J.	194
Horzowski S.	251, 201
Hoshino M.	085
Hossain K.	095
Hottiger M.	421
Hubeny A.	202
Huelßenbeck S. C.	164
Huener H. - A.	309
Huettnet J. P.	386
Huhn T.	007
Hummel R.	203
Hümmert M.	077
Huppmann R.	413
Hüttmann G.	405
Hutzler C.	350, 297, 273, 204
Ibáñez M. J.	420
Ickstadt K.	170
Ignatius A.	027
Illing S.	264
Immel T.	007
Isaev R.	335, 205
Ishikawa T.	054
Jäckel S.	010
Jacobs G.	266
Jaeger M.	309
Jaffe L.	075
Jäger S.	206
Jahn T.	207
Jain R.	075
Janik T.	040
Janke C.	208
Jarek M.	008
Jatho A.	209, 041
Jebessa Z.	102
Jedliitschky G.	330, 121
Jehle D.	210
Jendrossek V.	362
Jha A.	100
Jia J.	221
John A.	211
John H.	214, 213, 212
Joos T. O.	184
Jordan J.	390, 074, 045, 037, 022
Junemann J.	215
Jung A.	038
Jung F.	285
Juretschke C.	216
Jurida L.	421, 008
Jurk K.	010
Just I.	332, 318, 317, 303, 172, 164, 130, 080, 030
Kadow S.	416
Kaever V.	391, 103
Kaina B.	404, 311, 285, 253, 142, 139, 025, 016
Kallenborn-Gerhardt W.	256, 217
Kalwa H.	218, 134
Kamalakkannan S. S.	219
Kämmerer S.	270
Kamp H.	125
Kannler M.	134
Kappenstein O.	273
Kaps S.	294
Karabowicz P.	388, 220
Kazmaier U.	011
Kecskes M.	266
Kegel V.	301
Keiser M.	221, 202
Kelber O.	091, 090, 089, 001
Keller J.	222
Keller K.	223
Keim M.	160
Kestler H. A.	013
Kettner-Buhrow D.	421
Khayyal M. T.	224
Kietzmann M.	414, 378, 333, 331, 274, 114, 068
King T. S.	225
Kintscher U.	364
Kirch W.	289
Kircher P.	278
Kirsch S.	364
Kittana N.	209, 041
Klein S.	005
Kleine-Ostmann T.	384
Kleinert H.	058, 010
Klenk C.	226
Klepper A.	112
Kleuser B.	367, 106
Kliche M.	375
Kliwer A.	227
Klussmann E.	348, 306
Knebel C.	228, 018
Knebel J.	315
Kneuer C.	018
Kniznik A.	253
Köbele C.	307
Koch D.	229
Koch E.	349, 230, 161
Koch K.	231
Koch W.	154
Kock H.	017
Kockskämper J.	305
Koenig C.	396, 050
Koesling D.	044, 012
Köhler C.	232
Köhm M.	310
Kojima N.	370
Kolb C.	090
Kolb P.	128
Kolle S.	395, 126
König A.	400, 138
Königsbauer S.	153
Königshoff M.	199
Könnecker G.	250
Korostylev A.	085
Korth M.	418
Kostenis E.	009
Köster U.	233
Kotsiou A.	234
Kracht M.	421, 399, 008
Kraehling J. R.	042
Kräenbring J.	327
Kraft K.	091, 001
Krajka V.	281
Krämer E.	285
Krämer L. K.	235
Kramer S.	295, 178, 108
Krämer U.	145
Kranick D. S.	236, 150
Krasel C.	423, 043
Kraus J. M.	013
Krawutschke C.	044
Kreja L.	027
Kretschmer I.	237
Kreutz R.	173
Krez N.	133
Kriebs U.	100, 078
Krieger K.	112
Krifka S.	366
Kroemer H. K.	330, 121
Kroetz D. L.	181
Kroh A.	238
Kroker M.	099

Kroll J.	082	Ma-Hock L.	407, 241, 222
Krome K.	250	Mahrhold S.	133, 083
Kromrey M. - L.	330	Mahringer A.	113
Kronich P.	421	Mai P.	262
Kropat C.	387	Maier L. S.	076
Kruel A. M.	238	Maihöfer N.	337
Krüger J.	392, 239, 130	Malinowska B.	388, 220
Krüger K.	240	Mali E. M.	165
Krüger M.	238	Mandel P.	263
Kruppke A. S.	363	Mandl M.	046
Kühbeck F.	179	Mangelsdorf I.	352, 248, 144, 017
Kuhlmann D.	188	Mangerich A.	048
Kuhlmann J.	127	Mann A.	264
Kuhn M.	276	Mannebach S.	265, 078, 034
Kühne R.	144	Mannebach-Götz S.	100
Kulling S.	206	Marko D.	410, 387, 353, 175
Kullmann M.	415	Markov A.	235
Kuner R.	085	Marks J. D.	083
Kunze M.	400	Marks V.	153
Kupatt C.	153	Markx D.	050
Küper J.	246	Martello R.	048
Küppers J.	116	Martin C.	337
Küttler K.	222	Martin H. - J.	194, 072
		Marx-Stoelting P.	343, 228, 063, 018
Laidig F.	045	Maser E.	294, 194, 072
Lampen A.	328, 258, 251, 211, 201, 143, 127, 002	Masuck I.	204
Landsiedel R.	407, 395, 309, 241, 222, 177, 126, 125	Mathar I.	266
Lang A.	024	Mathäs M.	020
Lang S.	242	Matka C.	004
Lang T.	054	Matthes J.	369, 223
Langer A.	243	Mauersberger R.	056
Langer S.	345	Maunz A.	295, 178
Latta L.	244	May M.	164, 164, 045, 022
Laube S. K.	059	Mayer P.	187
Laux P.	350	Mayer S.	340, 320
Lees K.	136	Mayer T.	134
Lehmann L.	377, 324, 302, 206, 163, 094	Mayr D.	046
Lehnart S. E.	071	Mazurek N.	267
Lehr S.	151	Meckert C.	328
Leiss V.	287, 245	Mederos Y Schnitzler M.	382, 381, 157, 023
Lemoine H.	246	Mehling A.	395
Lemoine L.	070	Mehling H.	074, 037
Lenhardt I.	259	Meier M.	130
Lenze D.	258	Meini W.	325
Leonhardt A.	180, 087	Meister J.	268
Leoni A. - L.	400	Melcher S.	349
Levy M.	247	Melching-Kollmuss S.	029
Lewin G.	357, 248	Mellert W.	126
Lex K.	048	Melzer A.	269
Li H.	421, 249, 069, 010	Menacher G.	104
Licht O.	250	Menke J.	058
Lichtenstein D.	251, 201	Mergia E.	012
Liebl J.	046	Mersmann J.	394
Link S.	060	Merx M.	192
Linnebacher M.	035	Metzger U.	118
Linnenbaum M.	329	Metzner K.	270
Lipp P.	100	Meurs H.	344, 288, 065
List J. H.	098	Meyer J.	271
Littmann T.	252, 062	Meyer K.	049
Loerz C.	072	Meyer-Roxlau S.	324, 272
Lohse M. J.	383, 341, 168, 077, 066	Michalakis S.	059
Lokan S.	253	Michel M.	233
Londoño J. E.	266	Michel T.	218
Lorenz J. E.	217	Mielke H.	296
Lorenz K.	341, 077	Mielke N.	273
Löscher W.	393, 389, 319, 286, 254, 166, 149, 122, 119, 026, 005	Mielke S.	274, 130
Löser K.	259	Mikhed Y.	249
Lothar A.	255, 162	Milner J. D.	013
Lou J.	083	Mishra Y. K.	294
Lu R.	256, 217, 051	Mitchell A.	197
Lu S.	403	Mizaikoff B.	212
Lübke J.	238	Mobarec J. - C.	128
Lübker C.	257	Modun D.	390
Luch A.	350, 297, 273, 204, 070	Moepps B.	396, 050
Lücke A. - C.	332	Mohr C.	138
Luckert C.	258	Mohr K.	345, 146, 009
Ludwig A.	203, 053	Monfort E.	420
Ludwig R.	326	Monien B.	325, 275
Luft F. C.	074, 037	Monzel M.	276
Lukas J.	269	Monzon Penza T.	327
Lukowski R.	418	Moretti A.	402
Lupp A.	259	Morhenn K.	277
Luther P. K.	197	Morin D.	064
Lutz S.	291, 277, 209, 082, 041	Möser C.	225, 051
Lyer S.	208	Moser M.	255, 162
Lyga S.	260	Muallem S.	100
		Mückter H.	271, 216, 110
Maalouf K.	286	Muehlich S.	278
Maarsingh H.	344, 306, 288, 185	Mueller W.	279
Maarsingh M.	065	Müller A. - L.	052
Maaß M.	223	Müller C.	379
Machann J.	287	Müller F. U.	370, 356, 346, 236, 150
Madunic S.	390	Müller H.	421, 399, 008
Magelsdorf I.	357	Müller J.	280, 135, 091, 090
Mahajan-Thakur S.	261, 047	Müller M.	196, 059
		Müller-Ehmsen J.	223
		Müller-Fielitz H.	281

Munder A.	336, 073
Nagel F.	279
Nagel G.	025
Naim H. Y.	286
Naumann S.	339
Neidhardt I.	282
Nersesyan A.	105
Nestler S.	106
Neuber C.	367
Neumann D.	406, 335, 205, 172
Neumann J.	321, 269, 268, 232, 207
Neumann M.	283
Newel D.	421
Nguyen H.	053
Nieber K.	090
Niederberger E.	225, 051
Niehof M.	284, 087
Niemann B.	251, 201
Niemann L.	343, 228, 063, 018
Nies A. T.	054
Nikolaev V.	320, 071, 032
Nikolova T.	285, 142
Nikonova Y.	305
Nilius B.	266
Noack A.	286, 149
Noack C.	299
Noack S.	286
Nölke T.	363
Nolte I.	233
Nosseck M.	278
Novakovic A.	287
Nürnberg B.	373, 287, 245, 123
Nussberger J.	022
Nüssler A.	301
Oberemm A.	328
Oenema T.	288
Oertel R.	289
Oetjen E.	277
Offermanns S.	405, 134, 093, 085
Ogrissek N.	290
Ohlig J.	192
Okpanyi S. N.	090, 089
Olbrich K.	051
Oldenburger A.	344, 306, 065
Olling A.	172
Olteanu V. S.	157
Ongherth A.	291
Ordoñez P.	400
Orth J.	401, 210, 055
Ortner N.	056
Ostermann A.	292
Oteiza P.	060
Othman A.	183
Othman E. M.	293
Otte A.	026
Ozawa T.	252, 167, 062
Pahl A.	277
Pahlke G.	387
Palavinskas R.	251
Palea S.	230
Papatheodorou P.	131, 057
Papavlassopoulos H.	294
Parasar P.	022
Partosch F.	296, 295, 178, 108
Pasch S.	291
Paschke M.	297
Patrzyk M.	221
Paulowicz I.	294
Pautz A.	058, 010
Pavic G.	298
Pavlova E.	299
Perera A.	059
Perera R. K.	071
Perez-Bouza A.	337
Pertz H. H.	159
Pesch T.	007
Peters H.	173
Peters K.	412
Petrich A.	227
Petrikat T.	176
Petrokokinos L.	234
Petzel C.	366
Pfarr K.	367, 300
Pfeifer A.	147, 100
Pfeiffer C.	239
Pfeiffer E.	301
Pfeil R.	343, 228, 063, 018
Pfeilschifter J. M.	367, 310, 300, 290
Pfenning C.	302
Philipp S.	034
Philipp S. E.	006
Pich A.	303, 283, 130
Piehl M.	355, 304
Pieper M. P.	337
Pilawski I.	122
Plackic J.	305
Planatscher H.	184
Plener J.	173
Plückthun A.	226
Pluteanu F.	305
Pohl C.	038
Pohlmann G.	017
Pöll F.	227
Ponath V.	048
Pop S.	403
Popoff M.	332
Poppinga W. J.	344, 306, 185, 065
Poth A.	309
Potkura J.	328
Pötz O.	184
Prajwal .	373
Preisenberger J.	305
Preißl S.	307
Prescott M.	022
Prokopets O.	043
Proksch P.	038
Qiu Y.	418
Queisser N.	060
Quierici R.	400
Quitterer U.	243, 088
Raasch W.	355, 304
Radeke H. H.	367, 310, 300, 290
Radman M.	390
Rajagopal C.	042
Ramba B.	291, 209, 041
Ramer R.	412, 308, 035
Ramirez T.	126
Ramirez-Hernandez T.	309
Ranglack A.	367, 310
Rauch B. H.	298, 261, 116, 047
Rauhaus K.	246
Real C. I.	256
Reamon-Buettner S. M.	420, 087
Reich T.	311
Reif R.	312, 061
Reifenberg G.	249, 069
Reinartz M. T.	062
Reinhardt C.	010
Reiss L. K.	313
Remke J.	155
Renner C.	339
Rezniczek T.	335
Rice R. H.	064
Ridder D. A.	405
Riedel W.	400
Rieg A. D.	337
Riehle M.	314
Rieke S.	343, 228, 063
Riemann K.	101
Rinne A.	128
Ritter D.	315
Rittinghausen S.	180
Rivera J.	400
Rochais F.	092
Röck K.	362, 316
Rodewald F.	092
Röhl C.	294
Rohland M.	384
Rohrbeck A.	318, 317, 303, 164, 080
Rohrer S. G.	097
Romano I.	400
Rörmann K.	319, 286, 149
Romero I. A.	286
Romero N.	218
Rommel C.	320
Roos W. P.	142
Rosenkranz N.	351
Rosenthal W.	348
Rösler U.	114
Rösner S.	320
Rothbauer U.	176
Rothkirch D.	321
Rotsch J.	164
Rozycki C.	328
Rüben K.	322
Rummel A.	238, 133, 083
Runge D.	221
Ruppert C.	077
Russe O.	225, 051
Russwurm M.	075, 044
Rustenbeck I.	358, 323
Ruth P.	418
Rüther U.	109
Rychlik M.	214

Saadatmand A. R.	374, 324, 140
Saarberg W.	230, 161
Sacher B.	219
Sachs A.	246
Sachse B.	325, 275
Sack M.	362
Sadik C.	326
Salamon A.	412
Sanders S. - J.	076
Sandner A.	360
Sarikas A.	334, 327, 179, 049
Sartoretto J.	218
Sartorius T.	287
Sawada S.	328
Schaaf S.	197
Schaefer M.	270, 193
Schäfer B.	329
Schaletzki Y.	330, 121
Schalkowsky P.	380
Schaper K.	331
Scharfe M.	008
Schaudien D.	180, 017
Schebb N. H.	408, 292, 064
Schelle I.	332
Scheller B.	394
Scheller J.	280
Schenk K.	209, 041
Scherz G.	333, 114
Scheufele F.	334
Schinner E.	411, 386
Schirmer B.	336, 335, 205, 073
Schlaudraff J.	256
Schleifer K. - J.	097
Schlenstedt G.	096
Schlepütz M.	337
Schlicker E.	388, 220, 152, 146
Schlobach da Costa C.	338, 289
Schlörmann W.	339
Schlossarek S.	277
Schlossmann J.	411, 386
Schmalbach K.	377, 206, 163
Schmalzing G.	188
Schmid B.	340
Schmid E.	341
Schmidt A.	342, 104, 048
Schmidt C.	246, 214, 213, 212
Schmidt F.	343, 228, 063
Schmidt G.	242, 098
Schmidt H.	403
Schmidt M.	344, 306, 185, 065, 001
Schmidtko A.	256, 217
Schmitt F.	123
Schmitt J.	341
Schmitt J. P.	066
Schmitt S.	383
Schmitz M. L.	421, 399, 008
Schmitz W.	370, 356, 346, 236, 150
Schmoeckel E.	046
Schneider E. H.	276, 067
Schneider H.	421, 399, 008
Schneider L.	002
Schneider S.	126, 029
Schnell L.	345
Schnick T.	307
Schober A.	262
Scholz A.	100
Scholz B.	356, 346
Scholz R.	347
Schömig E.	392
Schön I.	360
Schönlau C.	309
Schorch B.	057
Schrade K.	348
Schrader J.	280
Schrader T.	384
Schramm E.	349
Schreiber Y.	367
Schreiber I.	350
Schremmer I.	351
Schrenk D.	129, 112, 097, 015
Schröder C.	074
Schröder K.	352
Schröder S.	277
Schröder T.	337
Schroeder A.	303
Schroeder C.	037
Schroeter A.	353
Schrör K.	298, 116, 047
Schröter A.	175
Schubert S.	354, 289
Schuchard J.	355, 304
Schuhwerk H.	007
Schuler D.	160
Schulte J. S.	356, 346, 150
Schulz C.	392
Schulz F.	357
Schulz J.	378
Schulz S.	279, 264, 227
Schulze A.	193
Schumacher F.	275
Schumacher J.	376
Schumacher K.	358, 323
Schumacher M.	188
Schumacher S.	414, 359, 068
Schumann B.	360
Schupp N.	361, 263, 060
Schürmann A.	245
Schuster M.	345
Schütz D.	279
Schütze A.	362
Schüürmann G.	144
Schwab M.	054
Schwan C.	363
Schwaninger M.	405, 281
Schwanstecher A.	364
Schwarz M.	417, 365, 118
Schwede F.	283, 137
Schweikl H.	366
Schwiebs A.	367
Schwob E.	014
Schwonbeck S.	250
Seeger T.	368
Seehofer D.	301
Seeland M.	295, 178, 108
Seemann W. K.	369
Seferos N.	234
Seidel A.	211
Seidl M. D.	370, 356, 236, 150
Seifert R.	406, 391, 336, 335, 283, 276, 257, 252, 205, 186, 171, 137, 103, 084, 073, 067, 062
Seitz T.	371, 079
Selinski S.	170
Sell T. S.	372
Sentürk A.	085
Sessa W. C.	042
Sezin T.	326
Shuhaibar L.	075
Shymanets A.	373
Siddeek B.	029
Sieber S.	011
Siegmund W.	221, 202
Siffert W.	101
Simetska N.	352
Simmendinger P.	407
Simmet T.	021
Singh S.	374
Sippl W.	322
Siuda D.	249, 069
Skolnik E. Y.	418
Smit M.	288
Smrcka A.	134
Soelch J.	421, 008
Song S.	057
Sonnenburg A.	375
Soppa U.	376
Sostmann B.	047
Sostmann K.	173
Soukup S.	206
Sowa T.	076
Sowada J.	070
Spielmann B.	377
Spiger K.	418
Spillner J.	337
Sprenger J. U.	071
Srivaratharajan S.	030
Stahl F.	317
Stahl J.	378, 333, 274, 114
Stahlmann R.	375, 295, 178, 108
Stalman R.	371, 079
Stapelfeld C.	072
Stark H.	068
Stein J.	346
Steinberg P.	408, 343, 180
Steinbrecher J. H.	071
Steinemann M.	040
Steingraber A. K.	370
Steinmetz V.	253
Steinritz D.	342, 104, 048
Stellzig J.	008
Stelzer T.	336, 073
Stenzig J.	379, 197
Stephan H.	051
Stichtenoth D. O.	045
Stieber J.	203, 053
Stilgenbauer S.	081
Stitah S.	022
Stöckmann D.	099
Stoerger C.	380
Stölting I.	355, 304
Stolz S.	398, 036
Stopper H.	384, 293, 195, 105, 060
Storch U.	382, 381, 157, 134, 023





Zelarayan L.....	299	Ziesché E. ....	421
Zeller E. ....	417	Zietz B. ....	422
Zellmer S. ....	031	Zillikens D. ....	326
Zessel K. ....	378	Zimmer K. ....	155
Zhang S. ....	046	Zimmermann J. ....	244
Zhao Y. ....	181	Zimmermann K. ....	100
Zhou X. - B. ....	418	Zimmermann W. H. ....	299, 235, 076
Ziegler N. ....	383	Zindel D. ....	423, 043
Ziegler V. ....	419	Zoremba M. ....	291
Ziemann C. ....	420, 087	Zühlke K. ....	348
Ziems K. ....	121	Zwenger C. ....	027
Zierau O. ....	309		